Global Guide to Tropical Cyclone Forecasting

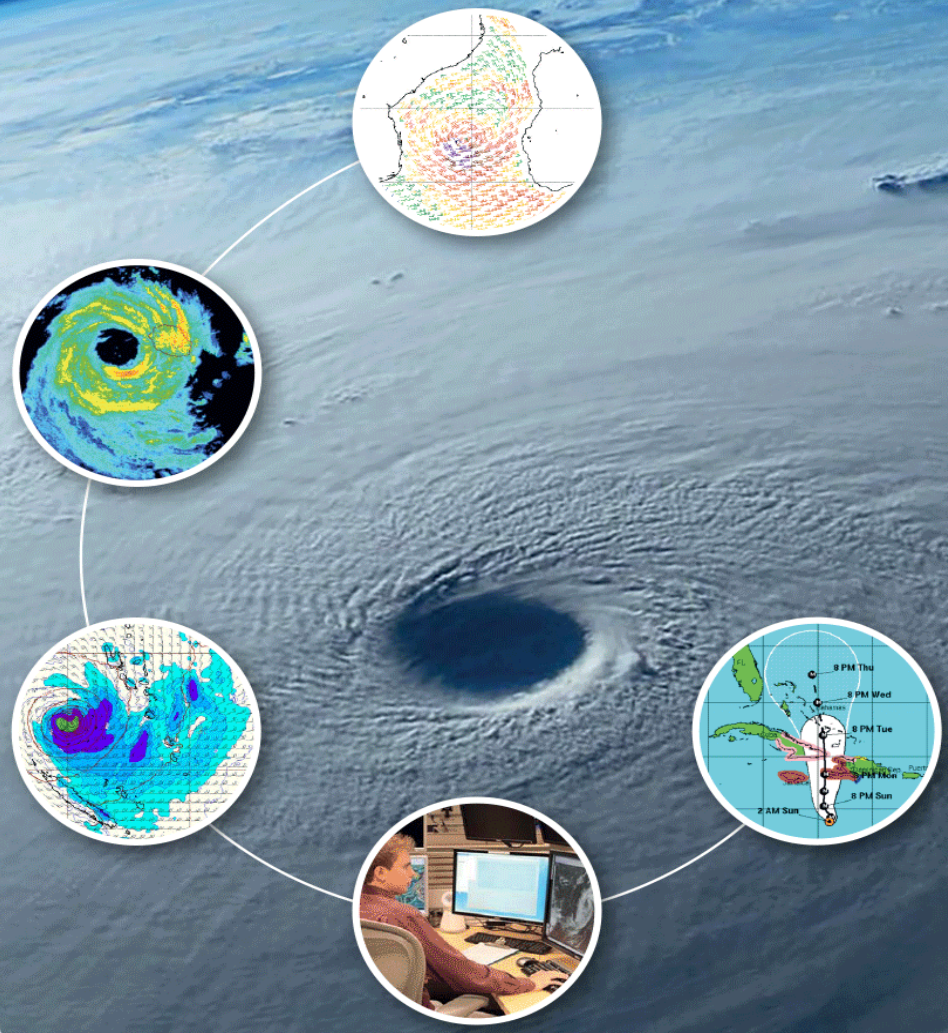

WEATHER CLIMATE WATER

WORLD METEOROLOGICAL ORGANIZATION

WMO-No. 1194

WMO-No. 1194

Chairperson, Publications Board
World Meteorological Organization (WMO)
7 bis, avenue de la Paix
P.O. Box 2300
CH-1211 Geneva 2, Switzerland

ISBN 978-92-63-11194-4

Preface

Tropical cyclones are amongst the most damaging weather phenomena that directly affect hundreds of millions of people and cause huge economic loss every year. Mitigation and reduction of disasters induced by tropical cyclones and consequential phenomena such as storm surges, floods and high winds have been long-standing objectives and mandates of WMO Members prone to tropical cyclones and their National Meteorological and Hydrometeorological Services. To this end, accurate and timely available forecasting of tropical cyclones are fundamental to enable those objectives and mandates to be materialized.

The *Global Guide to Tropical Cyclone Forecasting* is a collection of the state-of-art sciences and technologies and best practices that are available for use by operational tropical cyclone forecasters. It is both a heritage and development of forecasting techniques and warning methodologies for tropical cyclones. It serves as a series of tools and a platform for information source for operational forecasters to acquire essential skills and competencies and latest techniques in tropical cyclone monitoring, forecasting and warnings.

The *Global Guide to Tropical Cyclone Forecasting* was first compiled and edited by Dr Greg Holland in 1992, with contributions from a large number of scientists and experts. However, significant changes in many aspects of tropical cyclone forecasting have occurred since 1992, as results of advances in computing, radar and satellite capabilities, and meteorological science itself. Therefore, the *Global Guide to Tropical Cyclone Forecasting* was recommended to be updated by a group of experts and forecasters who attended the serial WMO International Workshops on Tropical Cyclones in 2006 and 2010. The updating was finally completed in 2015.

The updating of the *Global Guide to Tropical Cyclone Forecasting* includes contributions from experts from around the world. Particular thanks are due to Charles "Chip" Guard (United States of America), Chief Editor, for his leadership and scientific contributions, and the chapter authors for their time, dedication and expertise, and many others who kindly provided their advice and assistance.

The updated *Global Guide to Tropical Cyclone Forecasting* is adopting modern Web-based technology with easy access by readers. It was initially configured by a technical team led by Dr Beth Ebert of Australia Bureau of Meteorology. For this special thanks go to Dr Beth Ebert and her team.

The current e-book is reformatted following latest Web standards. It now becomes more user-friendly. I hope this e-book and its PDF version, together with other publications on tropical cyclones, will become a valuable source of information, tools, data, techniques, methodologies, and best practices in tropical cyclone monitoring, forecasting and warning services.

Petteri Taalas
Geneva, 16 May 2017

Introduction

This website of the World Meteorological Organization (WMO) is aimed to serve as a platform for the information sources for tropical cyclone forecasters to obtain data and tools which are useful for monitoring and forecasting of tropical cyclones. Forecasters may access the various sources providing conventional and specialized data/products including those from numerical predictions and remote sensing observations as well as forecasting tools concerning tropical cyclone development, motion, intensification and wind distribution. It will continue to develop along with the availability of new data and products and will also contain techniques and best practices from tropical cyclone forecast centers that could be adapted by other forecast centers. This Training manual has been developed using contributions from various authors around the world. It will be updated from time to time as the science and practice of Tropical Cyclone monitoring and forecasting evolves. The multi-author nature of this document means that both British and American spellings will appear across various parts of the document.

Figure 1 is a taste of the imagery types included in the Guide.

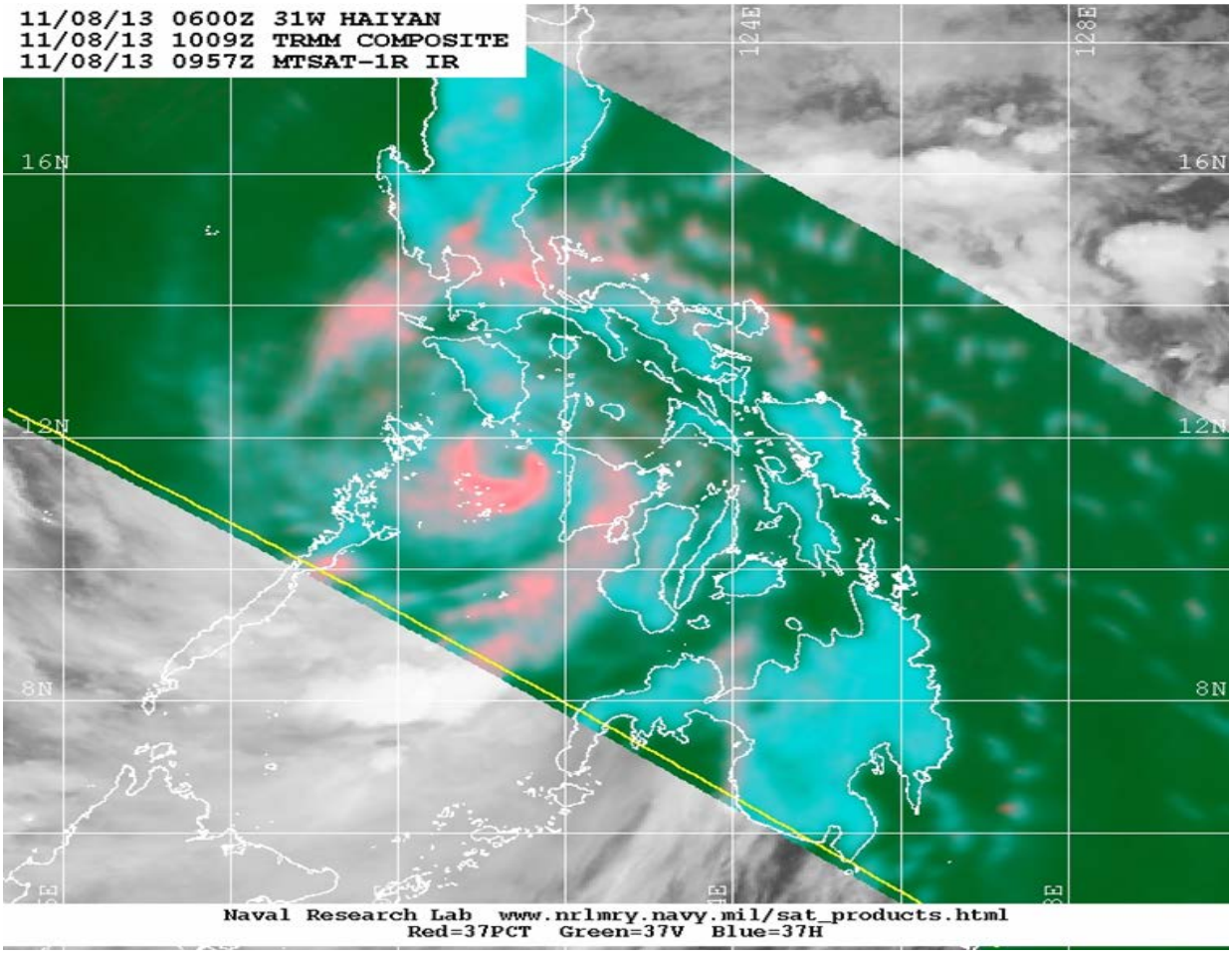

Figure 1 shows an example of a 37-GHz polarized corrected temperature (PCT) image of Super Typhoon Haiyan on 8 November 2013, where blue-green streamers indicate low cloud bands and reds and pinks indicate well-developed convective clouds. Dark green patches, represent areas that are the same temperature as the ocean surface. The green spot inside the pink ring indicates the partially cloud-free eye. Analysis of multiple images (preferably within six hours of the analysis time) can increase the chances of correctly identifying the TC center. Sequential multiple images can be animated to improve center location of poorly organized systems (Edson, personal, communication). (Image courtesy of the US Naval Research Laboratory).

Table of Contents

Chapter One

Charles J. Neumann
USNR (Retired)
U.S. National Hurricane Center
Science Applications International Corporation
Charles 'Chip' Guard
NOAA/National Weather Service Forecast Office Guam

1. Global Guide to Tropical Cyclone Forecasting Overview

1.1 Introduction and purpose

The previous (first) Global Guide to Tropical Cyclone Forecasting, heretofore referred to as the Global Guide or Guide, was compiled and edited by Dr. Greg Holland in 1992. A large number of scientists and experts contributed their expertise to the Guide. Many aspects of tropical cyclone (TC) forecasting have changed in the last two decades. For example, track forecasting is now largely accomplished through numerical weather prediction. Thus, a separate chapter on numerical weather prediction is no longer needed. Instead, numerical weather prediction is now integrated into the motion, intensity/structure change, rainfall and storm surge chapters. Advances in computer, radar and satellite capabilities have also advanced many of the aspects of TC forecasting such as intensity prediction and rainfall detection and prediction.

This Global Guide is designed primarily to assist the developing RSMCs, TCWCs and National Hydro-Meteorological Service (NHMS) Offices around the world. It may also be used to a lesser extent by large, well-established Tropical Cyclone Warning Centers (TCWCs) or Regional Specialized Meteorological Centers (RSMCs), which typically have comprehensive and well-documented procedures already in place. In fact, it is hoped that they will be able to contribute their expertise and evolving capabilities to the Guide.

Chapter 1 provides background information relevant to the more specific topics addressed in subsequent chapters. In keeping with the overall theme of the Guide, emphasis is placed on the presentation of material in tabular or graphical format for ready reference. We begin with a discussion of the WMO global TC forecasting concept, including the structure and goals of the WMO Tropical Cyclone Programme (TCP), areas of forecast responsibility, TC naming conventions, and descriptive terminology. A key issue here is to note the many procedural differences between forecast offices and ocean basins. Readers are encouraged to visit the Tropical Cyclone Programme website at www.wmo.int/pages/prog/www/tcp/ in order to view the most comprehensive and up-to-date description of the WMO program.

There are several basic components of TC forecasts. The Global Guide will address these in various chapters. However, in general, a TC warning center is involved in the following main activities:

- Monitoring (meteorological watch) of current conditions, analysis of current parameters, detection of developing or developed TCs
- Prediction of various parameters (e.g., position, intensity, size/wind distribution, storm surge, ocean waves, rainfall (flood, flash flood, mudslide/debris flow potential)
- Production of alerts, watches, warnings, and products for decision assistance
- Post-analysis and performance assessment

Various forms of guidance, tools and techniques that help a TC warning activity accomplish the above activities are covered in the various chapters of the Global Guide. Monitoring, analysis and detection of various parameters, such as position or intensity, will be covered in the same chapter that addresses the prediction of those parameters. For example, Chapter 3 will discuss analysis of the TC center and the prediction of the track. Chapter 4 will discuss analysis of intensity and size and intensity and wind distribution prediction. Storm surge and rainfall analyses and predictions are handled similarly. The following paragraphs will summarize the various chapters of the new Global Guide and highlight some of the changes from the old Guide.

1.1.2 Tropical Cyclone Climatology (Neumann)

Chapter 2 is the home of a new unique and comprehensive global TC climatology that has been developed by Dr. Charles Neumann and is now contained in its own chapter. This climatology is an updated version through 2007 of that introduced in the previous edition of the Global Guide by Dr. Neumann, and is presented in a manner that enables direct comparisons from one basin to another. Various global and ocean basin charts are presented and used to illustrate forecasting problems in the identified basins. A new chart is introduced that produces statistics based on both 1-minute and 10-minute averaged winds. There are many other tropical cyclone data sets and climatologies. Most are for individual basins (e.g., HURRDAT for the Atlantic and SPEArTC for the southwest Pacific), but a newly developed data base called iBTrACS is a global data base that incorporates data from all basins. It will likely be the follow-on data source for future updates of this Chapter.

1.1.3 Tropical Cyclone Motion (Kimberlain and Brennen)

The previous motion chapter concentrated on many manual techniques and deep-layer mean atmospheric steering relationships. In the previous version of the Global Guide, there was a separate chapter that discussed tropical cyclone numerical prediction models and their capabilities and characteristics. Since that time, knowledge learned from several tropical cyclone motion research programs, combined with enhanced computer resource capabilities, have led to greatly improved tropical cyclone numerical prediction models. In fact, the numerical prediction models have improved so much that they have become the primary method for producing tropical cyclone track forecasts. This chapter discusses the models, and concentrates on the application of ensemble and consensus forecasting techniques. It also

addresses conditions that can cause rapid changes in track motion that can often lead to large forecast errors.

While track forecasts have improved, tropical cyclone analysis is still a challenge for the forecaster. Analysis is at least as important now as it was in the past for model initialization and for short-term forecasting in land falling situations. Thus, in the new version of the Guide, we expanded our discussion of tropical cyclone analysis techniques for the forecaster.

Although the United States Joint Typhoon Warning Center (JTWC) located at Pearl Harbor, Hawaii (moved from Guam in January 2000) is not directly associated with the WMO, its near-global mission is tacitly associated with the WMO forecasting system. JTWC, established in May 1959, has a strong reputation for issuing quality TC products and a long history of TC forecast improvement and verification. The agency has routinely made its products available to official international forecasting agencies. Accordingly, JTWC's role in the global TC forecasting system is included. A historical guide to JTWC operations and systems up to the early 1990´s can be found in Guard et al. (1992).

1.1.4 Tropical Cyclone Structure (Evans)

The prediction of tropical cyclone structure/intensity change has greatly lagged that of track forecasting. This is well documented in the forecast statistics of the various warning agencies, where improvement in intensity forecasting has been virtually flat over the last 20 years. Despite this, our knowledge of several aspects of tropical cyclone structure such as extratropical transition and genesis has improved. Of particular interest is the process of rapid changes in intensity and structure of the wind field and rapid changes in the rain structure and distribution. In addition, structure and structure change has become the number one research objective for many tropical cyclone research programs. In this Chapter, we also address formation/genesis, and tropical cyclone intensity and wind structure analysis techniques, including statistical and dynamical approaches to intensity and wind distribution prediction. It considers: various intensity analysis techniques, including the most widely used one, the Dvorak TC surface wind estimation technique, and the latest modifications and improvements to the technique; other satellite intensity techniques; conventional analysis sources and techniques; and, aircraft reconnaissance.

1.1.5 Storm Surge and Open Ocean Waves (Lyons)

Chapter 5 provides ocean wave analysis and prediction techniques and storm surge and inundation prediction techniques. Potentially, the most deadly aspect of a strong tropical cyclone is the storm surge, which has killed tens-of- thousands of people, even in modern times (e.g., Cyclone Nargis, May 2008 in Myanmar). Tropical cyclone storm surge and open ocean wave forecasting has improved considerably since the last version of the Global Guide. Much of the improvement has been the result of new satellite sensors that provide improved ocean wind speed and direction coverage from scatterometers and improved open ocean wave

heights from space-based radar altimeters. In addition, high resolution Light Imaging, Detection and Ranging (LIDAR) has improved near-coastal bathymetry and elevation measurements. Unfortunately, these data are very expensive to acquire, and many locations do not have them. Nonetheless, new prediction capabilities have increased the accuracy of storm surge forecasts. The use of parametric wave models and spectral ocean wave models is discussed, as is the conversion of waves to surf and surf to coastal inundation. Despite this, the major challenge is getting people to respond and move away from the threated areas. These societal challenges will primarily be addressed in the Warning Strategy Chapter.

1.1.6 Tropical Cyclone Hydrology (Lai et al.)

Chapter 6 discusses techniques for analyzing and predicting TC induced rainfall and its contributions to flash floods, to inland and river flooding, to coastal flooding, and to mudslides/debris flows. This Chapter looks at conventional and satellite systems used for monitoring rainfall rates and accumulation, and stream flow and river flow. Next to storm surge, hydrological events associated with tropical cyclones, such as flash floods, mudslides, and river flooding are the most deadly aspects of tropical cyclones. Weather radar reflectivity data and real-time rain gauge networks are valuable tools for hydrology forecasts. New satellite techniques such e-TRaP are also very valuable for tropical cyclone rainfall forecasting. While most hydrology techniques have been in place for decades, new remote sensor and computer capabilities have made them much more effective. Flash floods and mudslides can happen very rapidly and often catch people by surprise. While they usually threaten small populations, there is little response time. Flooding, where river waters overflow the river banks, is a slower process, and evacuation is a different type of problem: a threat to large populations, but longer response times.

1.1.7 Seasonal Forecasting (Klotzbach et al.)

Chapter 7 addresses the topic of seasonal TC prediction and to some extent the effects of climate change. Seasonal tropical cyclone predictions are very popular and have made great strides since the last Global Guide. Despite the many successes of seasonal forecast programs, they have also experienced some major busts. But, these predictions are so popular that they are undoubtedly here to stay. Thus, it is important that tropical cyclone forecasters understand how these models work, their limitations, and how to interpret them. The chapter also discusses the important effects of El Nino and La Nina (the El Nino-Southern Oscillation (ENSO) cycle), the contributions of the Madden-Julian Oscillation (MJO), and other climate influences such as the Atlantic and the Pacific Decadal Oscillation (PDO) on tropical cyclone activity in the various basins.

1.1.8 Forecasting Strategy (Burton et al.)

Chapter 8 provides insight for optimizing the efficiency of a Tropical Cyclone Warning Centre (TCWC). It illustrates how to develop strategies that make the most effective use of its two most

valuable resources, its people and its technology base. It addresses such topics as forecast office design and staffing, dealing with incoming communications, workstation technology, forecast preparation and dissemination, interacting with the media, pre-season preparation, and forecast evaluation. Many new technological innovations have improved the working environment of the tropical satellite analyst and the tropical cyclone forecaster. Any good forecast strategy requires a good analysis. This chapter also addresses tropical cyclone track, intensity, storm surge and rainfall analyses, but concentrates on how to pull them together into a meaningful forecast.

1.1.9 Warning Strategy (Guard)

Chapter 9 presents information on warning strategies, that is, strategies that provide a framework of guidelines to assist decision-making required to counter the threat of an approaching tropical cyclone. The chapter deals with the primary objectives of an integrated national warning service: to promote effective community response; to avoid potential disaster; to reduce the loss of life and property, minimize environmental damage; and, reduce the community disruption to a realistic minimum. Warning strategies have changed considerably, as there has been a significant change from rural to urban coastal populations. Costs associated with tropical cyclone warnings have ballooned, and thus false alarms are costly. The societal effects of tropical cyclones are addressed in this chapter, including such items as setting Watches and Warnings and assessing human behavior in response to tropical cyclone warnings.

1.1.10 Training materials (Guard)

Great strides have been made in the availability of training materials, especially web-based ones. One of the most comprehensive locations for training materials is at the NOAA National Weather Service Learning Center's Cooperative Partner Program known as COMET Met-Ed. The Met-Ed website hosts hundreds of hours of education and training materials in the geosciences. An example of a training module is "Microwave Remote Sensing: Overview, 2nd Edition." (https://www.meted.ucar.edu/training_module.php?id=979

1.1.11 Ready Reckoner

A resource of useful information is provided in the chapter 11 ready reckoner. This has been mostly updated with the 2014 release, however some information can still become dated. Links are provided within the text to resources that are maintained up to date.

1.2 The global tropical cyclone forecasting network

Six **Regional Associations** are responsible for the coordination of meteorological, hydrological and related activities within their respective regions. Respectively, these regions (Region I

through VI) encompass the land masses of: Africa (RA I); Asia (RA II); South America (RA III); North America, Central America, and the Caribbean (RA IV); Southwest Pacific (RA V); and, Europe (RA VI), together with their surrounding islands and oceanic areas (Fig. 1.1). Information on the Regional Associations can be found at http://www.wmo.int under Governance.

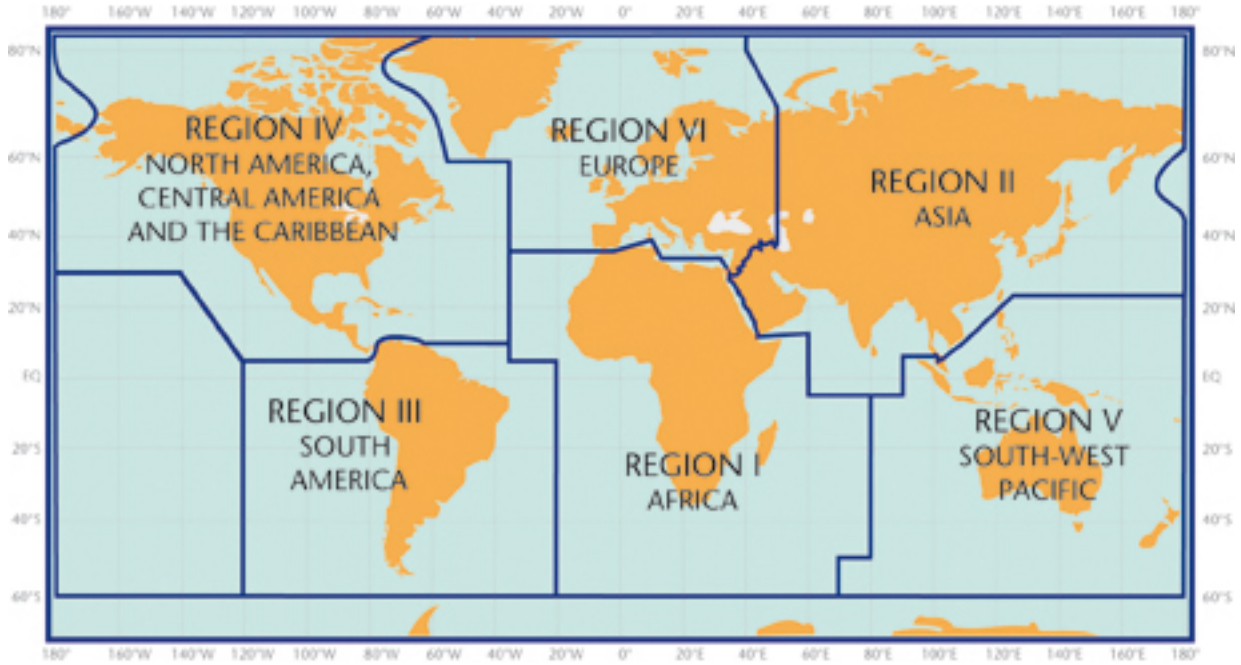

Figure 1.1. Geographical distribution of WMO Regional Associations.

The WMO Tropical Cyclone Programme (WMO/TCP) is a part of the WMO´s Weather and Disaster Risk Reduction Services Department tasked to establish national and regionally coordinated systems to ensure that the loss of life and damage caused by tropical cyclones are reduced to a minimum. The program is affected through national and regional levels through cooperative actions. It covers the activities of Members, WMO Regional Associations, other international and regional bodies, and the WMO Secretariat. The program has two main components: the **General Component** and the **Regional Component**. The **General Component** is concerned with methodology like the transfer of technology, information and scientific knowledge to Members, for meeting the Objectives of the TCP. The Objectives are available on the TCP web page. The **Regional Component** comprises the planning and implementation of the programs of the **Regional Bodies**. Each of the **Regional Bodies**has an Operational Plan or Manual, which records the agreements reached on the sharing of responsibilities for the warning services, and their infrastructures, throughout its region. The plans were designed to provide the best possible forecasting and warning services within the limits of scientific knowledge and technological developments, and of the available resources, ensuring full coordination and taking maximum advantage of the high level of cooperation, which has been achieved. These plans are regularly updated to incorporate new facilities, operational procedures, advances and developments.

Since not all Regions are affected by tropical cyclones, and the regional structure does not always coincide with tropical cyclone basins, the TCP established five Regional Bodies. The Regional Bodies are shown in Figure 1.2 and at http://www.wmo.int/ under organization. They are listed in Table 1.1. These committees also extend across the ocean basins defined in Figure 1.2. The WMO Technical Manuals referred to in Table 1.1 contain practical information, such as: station duties, addresses, telephone and other communication numbers, communication procedures, terminology, definitions, procedures, tropical cyclone naming conventions, unit conversions, coordination, analysis requirements, radar and satellite observations and dissemination, aircraft reconnaissance (where applicable), and wording of warnings. Through the efforts of the WMO/TCP there has been considerable procedural standardization among the regional bodies. However, some differences still remain, as discussed in this section. The Tropical Cyclone Programme can be found at http://www.wmo.int/ under Programmes and finally under Tropical Cyclone Programme.

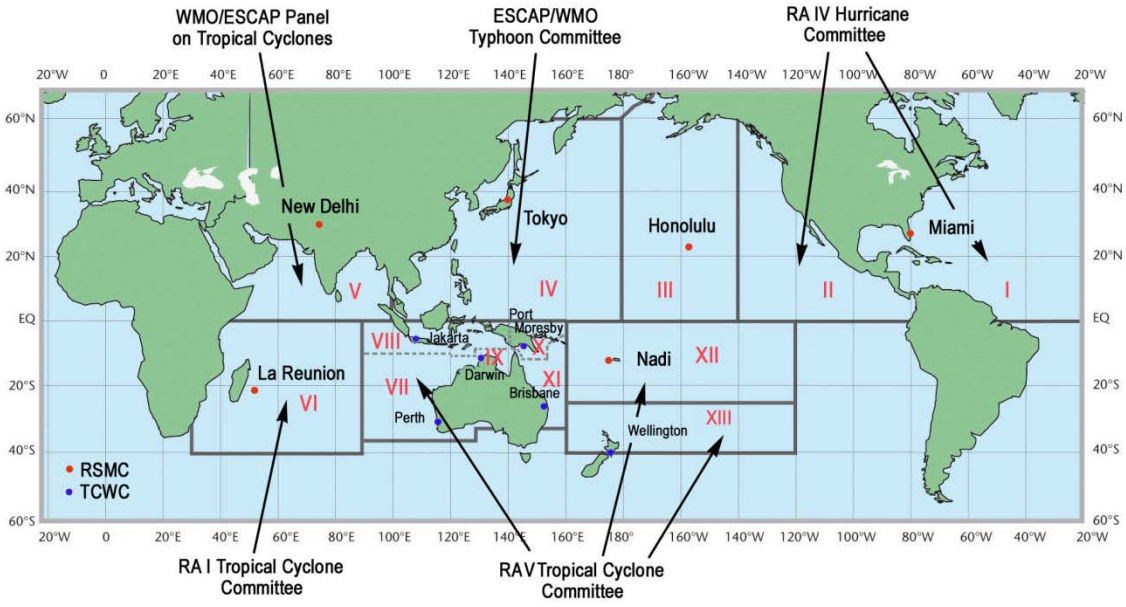

Figure 1.2. WMO map of the five Tropical Cyclone Regional Bodies.

In the Tropical Cyclone Programme, there are three main fields of activities — **Operational Meteorology, Hydrology**, and **Prevention and Preparedness**.

Operational Meteorology: Activities under this field are concerned with the provision of the required basic meteorological data, analyses and other processed products together with the application of appropriate techniques to ensure accurate tropical cyclone forecasting and timely warnings. The Operational Tropical Cyclone Plans/Manual drawn up by the TC Regional Bodies are important accomplishments in this field.

Hydrology: Activities under this field are based on the WMO Operational Hydrology Programme (OHP) and are concerned with the provision of the required basic hydrological data and the application of the appropriate techniques to ensure accurate flood forecasting and timely warnings. Within the programs of the Typhoon Committee and the Panel on Tropical Cyclones, wider accomplishments in the field, related to flood plain management and hydrological research, were achieved with the cooperation of ESCAP.

Prevention and Preparedness: Activities under this field are concerned with all other structural and non-structural measures required to ensure the maximum safety of human life and the reduction of damage to a minimum.

1.2.1 Tropical cyclone warnings

There are two general types of tropical cyclone warnings: those for land areas and coastal waters and those for the high seas (sometimes referred to as marine warnings). Each Member of a regional body is normally responsible for its land and coastal waters warnings. There are some exceptions, however, for example, the United States National Hurricane Center in Miami, Florida (NHC), issues warnings for Haiti, Aruba and the Netherlands Antilles, St. Barthelemy, St. Martin and their coastal waters. The relevant details are discussed in the appropriate WMO Manuals cited in Table 1.1.

The areas of high seas warning responsibility are defined in the manuals specified in Table 1.1 and are indicated in Figs. 1.3, 1.4, 1.5, 1.6 and 1.7. The area of responsibility for JTWC extends over several ocean basins. The full global map of zones is shown in Fig. 1.8.

Table 1.1. The five Regional Bodies of the WMO/TCP. The abbreviation ESCAP refers to the Economic and Social Commission for Asia and the Pacific.

Name	Area of Responsibility	Forecast Manual*	Basin Numbers	Map Ref.
WMO/Regional Association I (RA I) Tropical Cyclone Committee *Est: 1974*	Southwest Indian Ocean	TCP-12	5	Fig.1.3
WMO/Regional Association IV (RA IV) Hurricane Committee *Est: 1978*	North Atlantic Ocean, Caribbean Sea, Gulf of Mexico and the eastern North Pacific	TCP-30	1, 2	Fig.1.4 a & b
WMO/Regional Association V (RA V) Tropical Cyclone Committee *Est: 1985*	South Pacific Ocean and southeast Indian Ocean	TCP-24	6, 7	Fig.1.5

WMO/ESCAP Panel on Tropical Cyclones *Est: 1973*	Bay of Bengal and Arabian Sea	TCP-21	4	Fig.1.6
ESCAP/WMO Typhoon Committee *Est: 1968*	Japan, East Asia and Southeast Asia	TCP-23	3	Fig.1.7

** Latest manuals available at http://www.wmo.int/pages/prog/www/tcp/operational-plans.html*

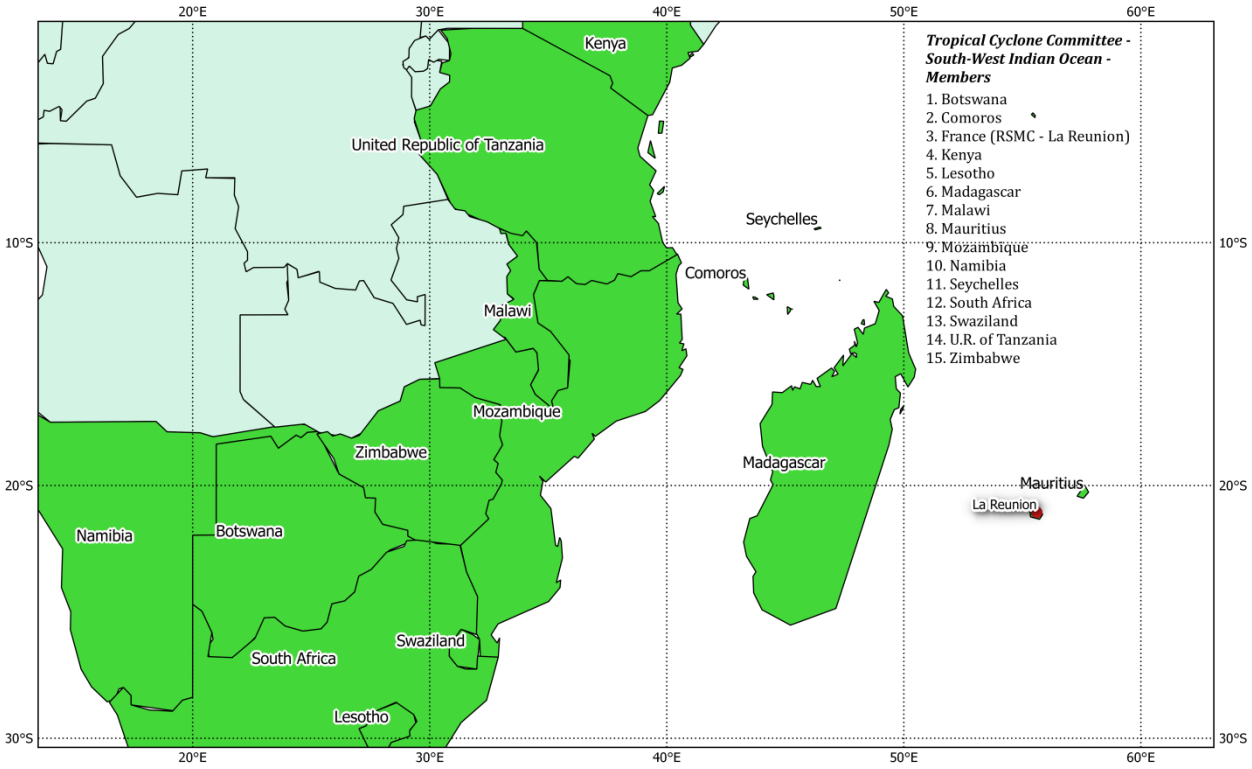

Figure 1.3: Regional Association I: International tropical cyclone warning responsibility areas for La Reunion.

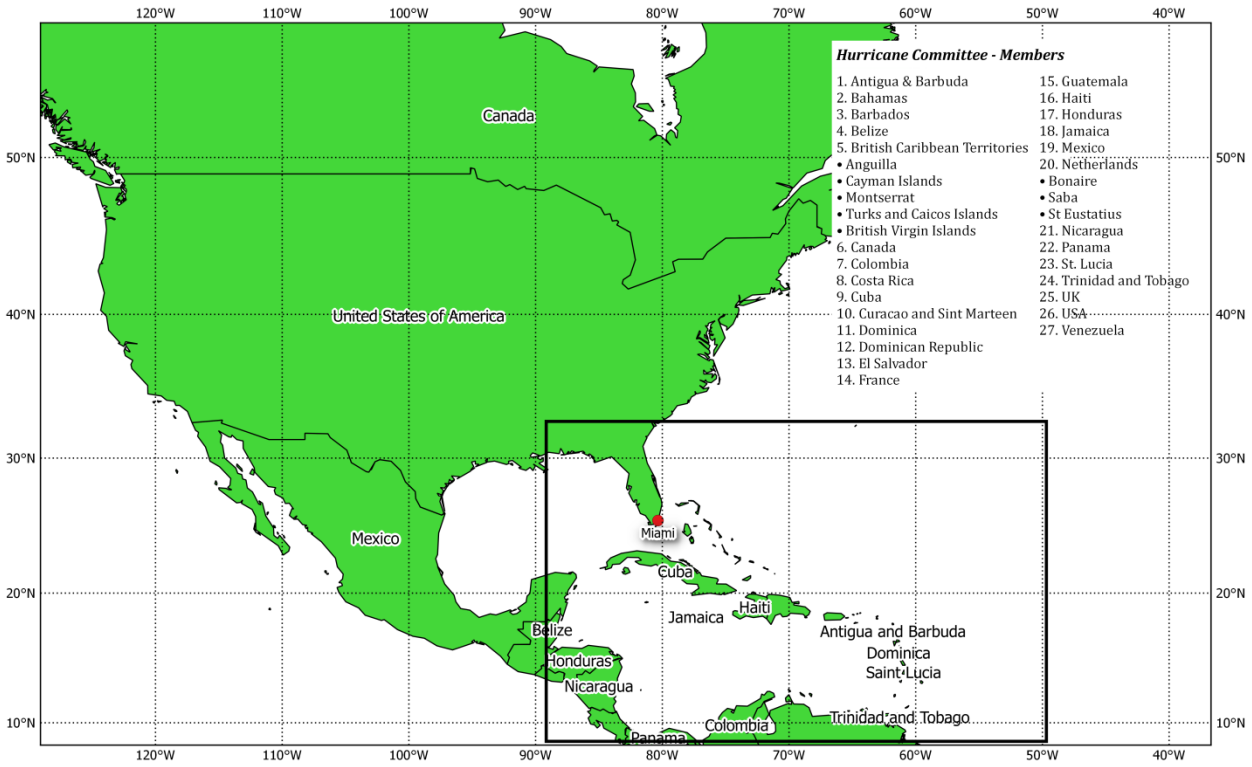
Hurricane Committee - Members
1. Antigua & Barbuda
2. Bahamas
3. Barbados
4. Belize
5. British Caribbean Territories
• Anguilla
• Cayman Islands
• Montserrat
• Turks and Caicos Islands
• British Virgin Islands
6. Canada
7. Colombia
8. Costa Rica
9. Cuba
10. Curacao and Sint Marteen
11. Dominica
12. Dominican Republic
13. El Salvador
14. France
15. Guatemala
16. Haiti
17. Honduras
18. Jamaica
19. Mexico
20. Netherlands
• Bonaire
• Saba
• St Eustatius
21. Nicaragua
22. Panama
23. St. Lucia
24. Trinidad and Tobago
25. UK
26. USA
27. Venezuela
Canada
United States of America
Mexico
Miami
Cuba
Jamaica
Haiti
Belize
Honduras
Nicaragua
Panama
Colombia
Antigua and Barbuda
Dominica
Saint Lucia
Trinidad and Tobago
120°W
110°W
100°W
90°W
80°W
70°W
60°W
50°W
40°W
50°N
40°N
30°N
20°N
10°N

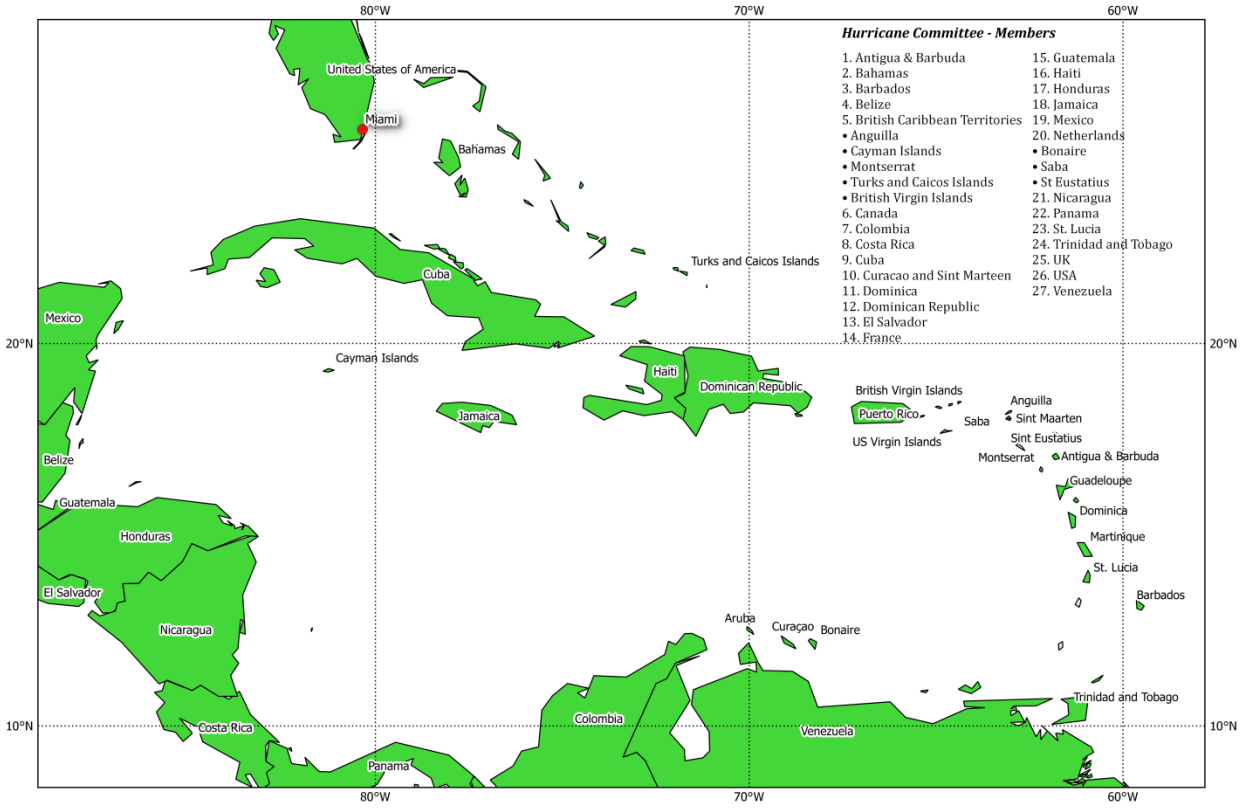

Figures 1.4a/b: Regional Association IV: International tropical cyclone warning responsibility areas for the NHC (Miami) and for the CPHC (Honolulu).

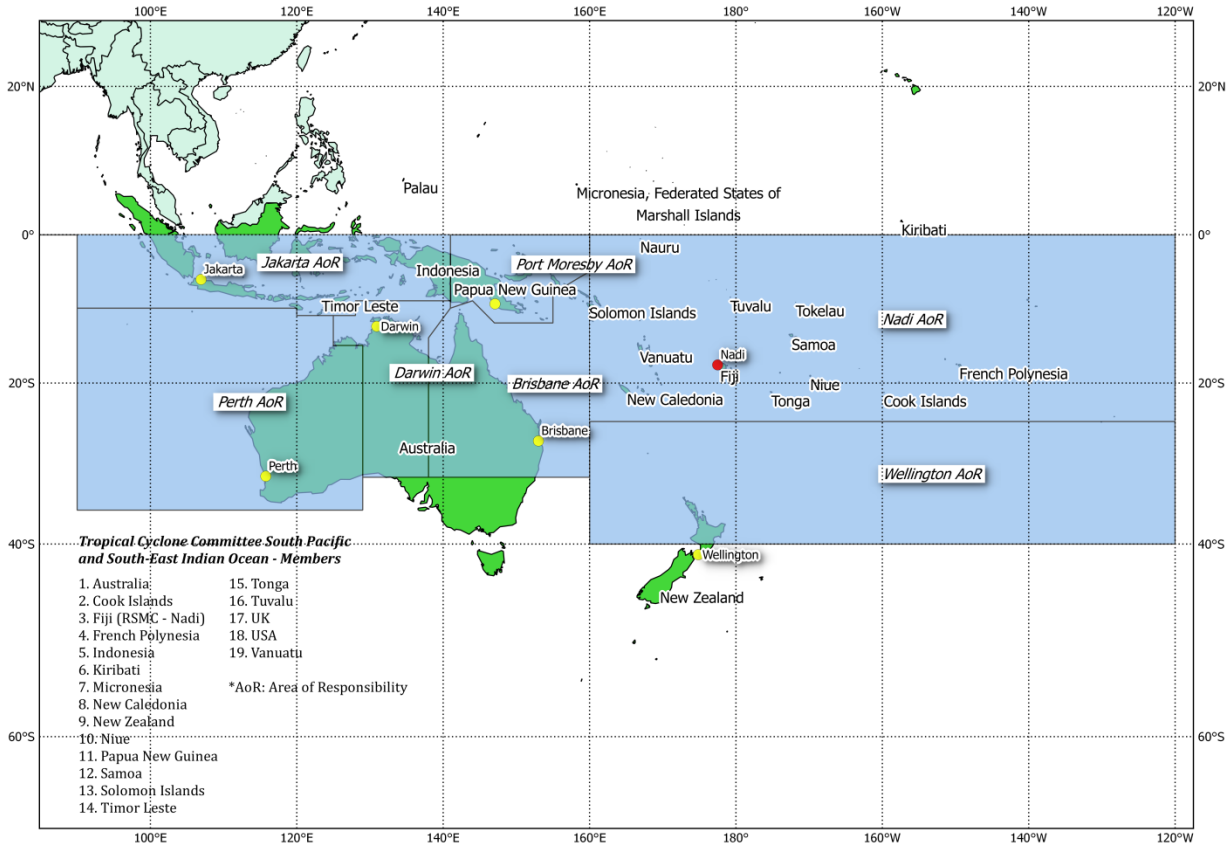

Figure 1.5: Regional Association V: International tropical cyclone warning responsibility areas for Nadi, Wellington, Brisbane, Perth, Darwin, Jakarta and Port Moresby.

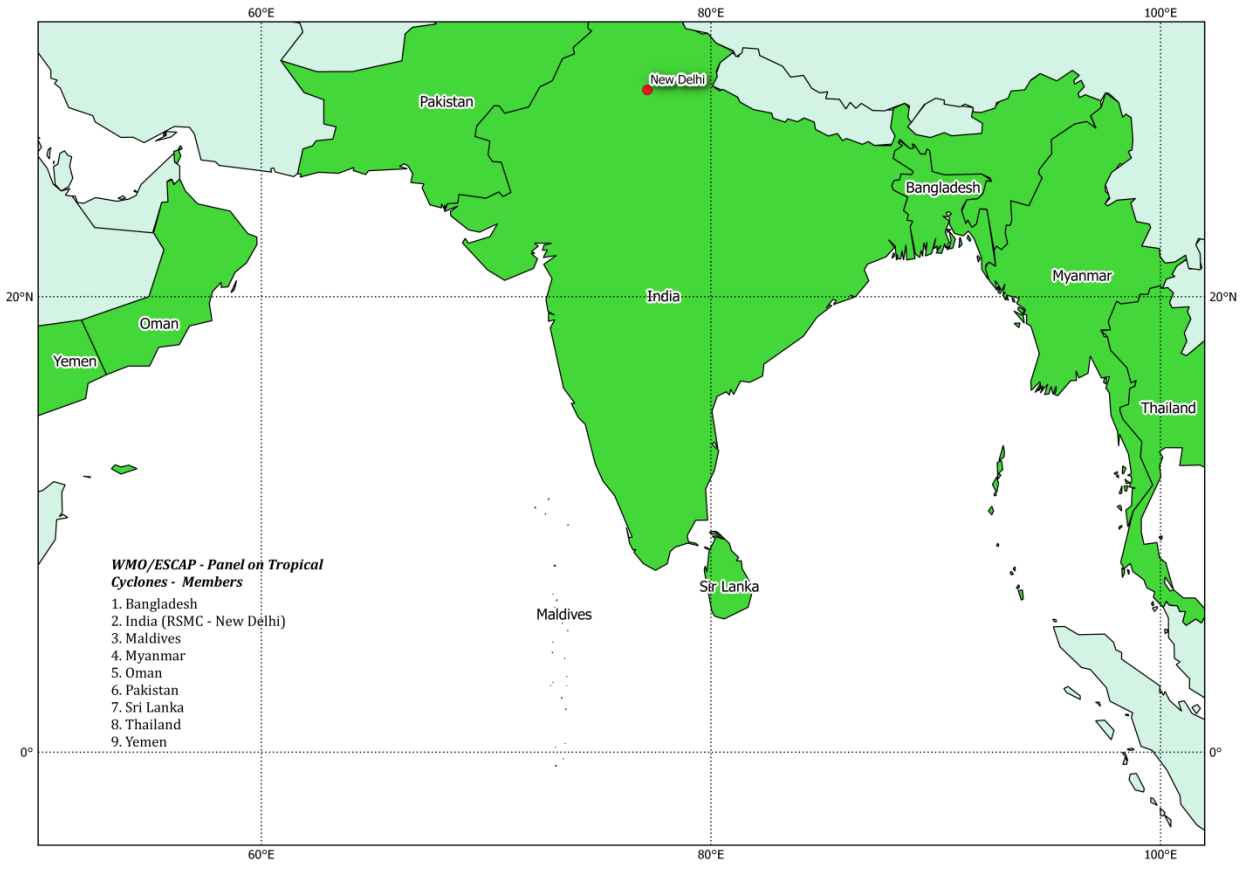

Figure 1.6: WMO/ESCAP Panel on Tropical Cyclones: International tropical cyclone warning responsibility areas for Delhi.

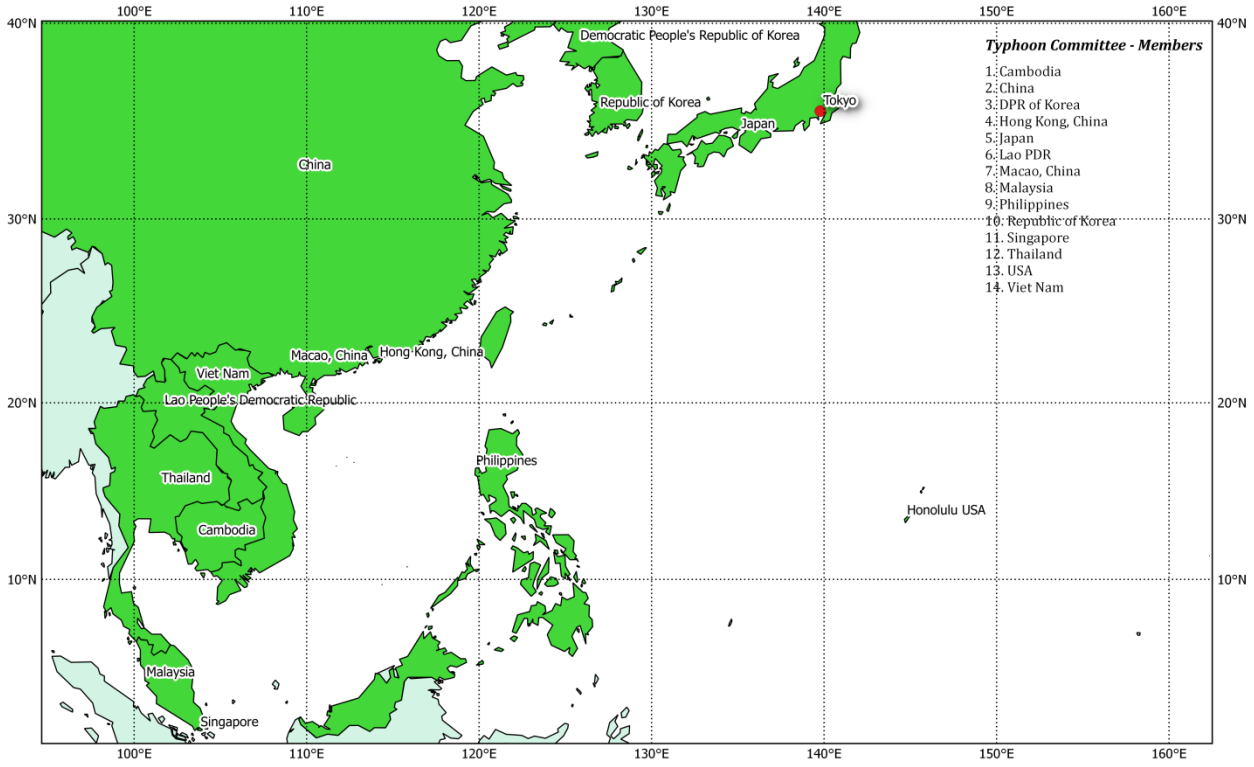

Figure 1.7: ESCAP/WMO Typhoon Committee: International tropical cyclone warning responsibility areas for Tokyo.

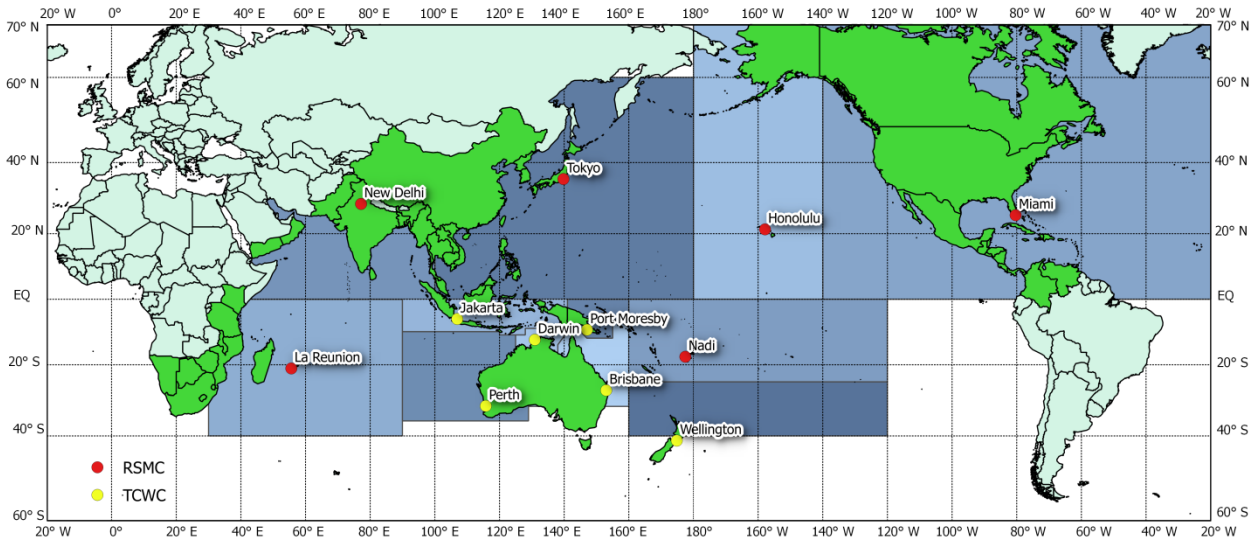

Figure 1.8: Full global map of zones.

1.2.2 Naming of tropical cyclones

The practice of naming storms (tropical cyclones) began years ago in order to help in the quick identification of storms in warning messages because names are presumed to be far easier to remember than numbers and technical terms. Many agree that appending names to storms makes it easier for the media to report on tropical cyclones, heightens intrest in warnings and increases community preparedness.

Experience shows that the use of short, distinctive given names in written as well as spoken communications is quicker and less subject to error than the older more cumbersome latitude-longitude identification methods. These advantages are especially important in exchanging detailed storm information between hundreds of widely scattered stations, coastal bases, and ships at sea. It also helps in archives.

There is a strict procedure to determine a list of tropical cyclone names in an ocean basin(s) by the Tropical Cyclone Regional Body responsible for that basin(s) at its annual/biennial meeting. There are five tropical cyclone regional bodies, i.e. ESCAP/WMO Typhoon Committee, WMO/ESCAP Panel on Tropical Cyclones, RA I Tropical Cyclone Committee, RA IV Hurricane Committee, and RA V Tropical Cyclone Committee. For instance, Hurricane Committee determines a pre-designated list of hurricane names for six years separately at its annual session. The pre-designated list of hurricane names are proposed by its members that include National Meteorological and Hydrological Services in the North/Central America and the Caribbean. Naming procedures in other regions are almost the same as in the Caribbean. In general, tropical cyclones are named according to the rules at a regional level.

Each Regional body also has a numbering system based on sequence of disturbances by season. JTWC also uses its own unique numbering system for its advices.

For more information naming the following WMO links should assist: http://www.wmo.int/pages/prog/www/tcp/Storm-naming.html

Detail on the policies and lists used by the individual Regional Bodies can be found in their respective operational plans, available here: http://www.wmo.int/pages/prog/www/tcp/operational-plans.html

The JTWC does not name tropical cyclones. JTWC uses the names determined by the World Meteorological Organization (WMO) Tropical Cyclone Program. JTWC will add the tropical cyclone name in parentheses after the JTWC-designated tropical cyclone number only after the WMO-designated Regional Specialized Meteorological Center (RSMC) or Tropical Cyclone Warning Center (TCWC) names a cyclone. If the RSMC/TCWC has not yet named a cyclone, JTWC uses its own TC number, spelled out, as a placeholder, i.e. "TS 16P (SIXTEEN)

1.2.3 Terminology

A considerable variation occurs in terminology used for the different stages of tropical cyclones (Table 1.2). Differences in wind averaging times further compound the confusion, since 1-min, 3-min and 10-min averages are used in different countries. Thus, a tropical system may acquire a name or number in one country, but not in another with the same wind criteria but different averaging times.

Table 1.2 provides an approximate summary of terminologie used across the globe. More detail can be found in the respective Regional Body Operational Plans:
http://www.wmo.int/pages/prog/www/tcp/operational-plans.html

Table 1.2. WMO classifications of tropical cyclones, tropical depressions and tropical disturbances.

	Max sustained wind (kts)					
	< 34	**34-47**	**48-63**	**64-89**	**90-115**	**> 115**
Beaufort number & descriptive term	up to 7	8.Gale 9. Strong gale	10. Storm 11. Violent storm	12. Hurricane		
SW Indian Ocean	Tropical depression	Moderate tropical storm	Severe tropical storm	Tropical cyclone	Intence tropical cyclone	Very intense tropical cyclone
Arabian Sea & Bay of Bengal	Depression or Severe depression	Cyclonic storm	Severe cyclonic storm	Very severe cyclonic storm		Super cyclonic storm
NW Pacific	Tropical depression	Tropical storm	Severe tropical storm	Typhoon		Super typhoon
NE Pacific & N Atlantic*	Tropical depression	Tropical storm		Hurricane		
S Pacific (E of 160E)	Tropical depression	Tropical cyclone (gale)	Tropical cyclone (storm)	Tropical cyclone (hurricane)		
SW Pacific & SE Indian	Tropical low	Tropical cyclone		Severe tropical cyclone		
US Saffir-Simpson Scale*	-	-	-	1	2-3	4-5
Australian Scale	-	1	2	3	4	5

* *US uses 1-minute average winds*

1.3 References

Guard, Charles P., Lester E. Carr, Frank H. Wells, Richard A. Jeffries, Nicholas D. Gural, Dianne K. Edson, 1992: Joint Typhoon Warning Center and the Challenges of Multibasin Tropical Cyclone Forecasting. *Wea. Forecasting*, **7**, 328 - 352.

Chapter Two

Charles J. Neumann
USNR (Retired)
U, S. National Hurricane Center
Science Applications International Corporation

2. A Global Tropical Cyclone Climatology

2.1 Introduction and purpose

Globally, seven tropical cyclone (TC) basins, four in the Northern Hemisphere (NH) and three in the Southern Hemisphere (SH) can be identified (see Table 1.1). Collectively, these basins annually observe approximately eighty to ninety TCs with maximum winds 63 km h^{-1} (34 kts). On the average, over half of these TCs (56%) reach or surpass the hurricane/ typhoon/ cyclone surface wind threshold of 118 km h^{-1} (64 kts). Basin TC activity shows wide variation, the most active being the western North Pacific, with about 30% of the global total, while the North Indian is the least active with about 6%. (These data are based on 1-minute wind averaging. For comparable figures based on 10-minute averaging, see Table 2.6.)

Table 2.1. Recommended intensity terminology for WMO groups. Some Panel Countries use somewhat different terminology (WMO 2008b). Western N. Pacific terminology used by the Joint Typhoon Warning Center (JTWC) is also shown.

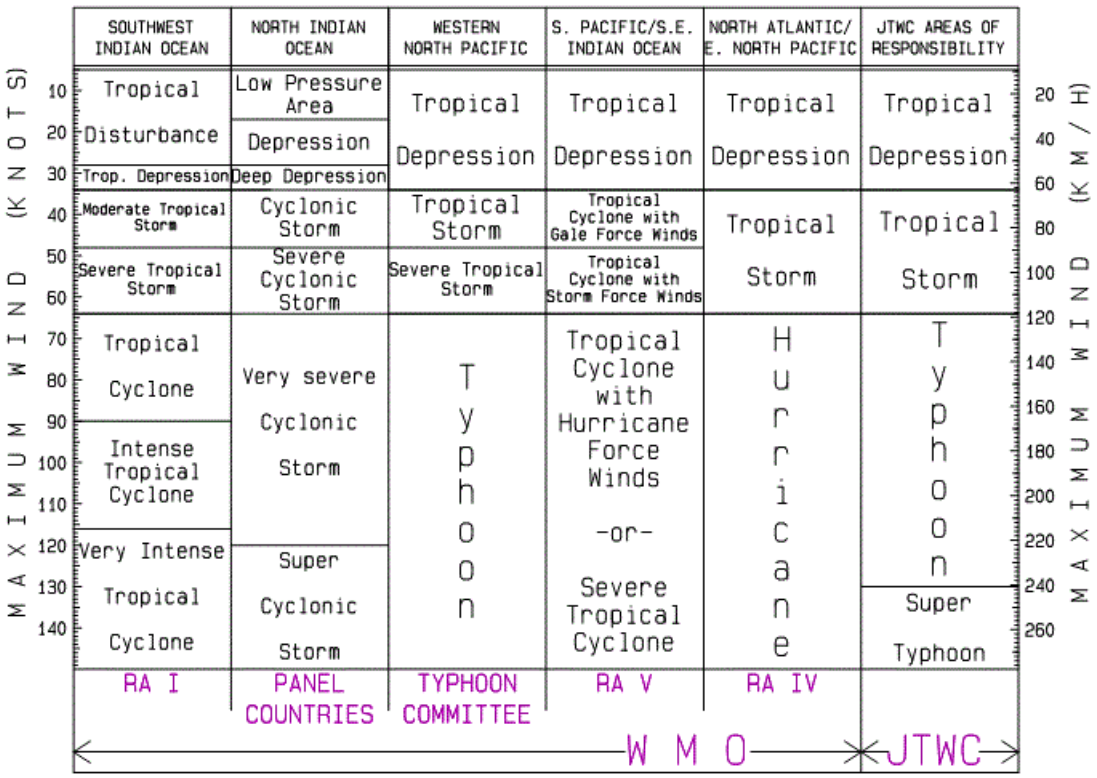

Over the years, many countries subject to these TC events have nurtured the development of government, military, religious and other private groups to study TC structure, to predict future motion/intensity and to mitigate TC effects. As would be expected, these mostly independent efforts have evolved into many different TC related global practices. These would include different observational and forecast procedures, TC terminology, documentation, wind measurement, formats, units of measurement, dissemination, wind/ pressure relationships, etc. Coupled with data uncertainties, these differences confound the task of preparing a global climatology.

While the World Meteorological Organization (WMO), through its Tropical Cyclone Programme (TCP), has taken the lead in standardizing many of these TC procedures, considerable differences remain. Some of these are relatively easy to address. Others, such as wind measurement, are not.

Throughout this chapter, measurement will be given in both English and metric units. However, differentiating between the numerous regional TC intensity (stage) terminologies in textual material is awkward and detracts from readability. Accordingly, intensity stages will be described using WMO Region IV terminology; that is, tropical depressions, tropical storms or hurricanes. Table 2.1, derived from recent WMO publications such as WMO (2008a), provides equivalent terminology for other regions. Tropical cyclones that fail to reach the tropical storm stage will not be included in any of the tables or charts that follow. The main reason for this omission is that documentation of these weaker TCs is inconsistent and highly objective among basins.

Each of the seven basins, as defined in Table 2.2 in Chapter 2.1.3, has both unique and common features that relate to TC internal structure, motion, forecast difficulty, frequency, intensity, energy, intensity, etc. The primary purpose of this Chapter is to display all but the first of the above listed features (internal structure) in such a manner that inter- and intra-basin and hemispheric differences and similarities can readily be identified. In keeping with this goal, tabular listings are avoided as much as possible. Due to measurement or estimation uncertainties as well as to different basin definitions of sustained wind, TC intensity will be discussed in other than explicit terms.

A secondary but still important purpose of this chapter is to assess the quality and quantity of the TC data utilized in the construction of the various tables and charts contained herein. It will be shown that the quality of the data is highly variable, being dependent on location and era. Other data-related issues that will be addressed are some of the afore-mentioned dissimilar operational practices at various Centers.

To fill in data voids and to make inferences about extreme values, TC climatological data are often manipulated statistically using parametric and non-parametric methods. Accordingly, with emphasis on shortcomings of the data, some statistical procedures and associated statistical pitfalls will also be discussed.

2.1.1 About historical TC data

Presentation of a global tropical cyclone (TC) climatology is necessarily based on best-track documentation. Therefore, the quality of this climatology will be commensurate with the quality of the best-track data. The amount of information contained in most current best-track formats is limited to storm location and intensity (winds and/or pressures) at 6-hourly intervals (0000, 0600, 1200, 1800 UTC). Such data make it possible to compare basin attributes insofar as they relate to those parameters.

Unfortunately, most best-tracks do not currently address other important surface features of TCs such as size, radius of maximum wind (RMW), radius of various intensity winds, landfall location and time of landfall, etc. This makes it difficult to compare basin-to- basin characteristics of those parameters. Ready availability of such parameters would also enhance TC research efforts such as lowering unexplained variance in wind/pressure relationships (Knaff and Zehr, 2007; Guard and Lander, 1996). Various research and operational interests have noted this best-track deficiency. The World Meteorological Organization (WMO) has prepared and disseminated a comprehensive best-track format, a template of which appears in the various Regional Manuals available at http://www.wmo.int/pages/prog/www/tcp/operational-plans.html.

In regard to data quantity, at least 25 years of best-track data are desirable. In the early 1990's, at which time the first edition of this WMO Guide was in preparation, no long-term global collection of creditable best-tracks, in a common format, was known to exist. Accordingly, the author of Chapter 1 (Neumann, 1993), using the United States National Hurricane Center (NHC)

best-track format, assembled such a data set based on the many existing and often conflicting local data sets available at that time. Although Northern Hemisphere (NH) data were reasonably easy to assemble, the Southern Hemisphere (SH) presented problems and these are described and addressed by Neumann (1999, 2000). Particularly troublesome were the numerous heterogeneities and track discontinuities in SH data.

The structure of the Neumann global data set is different for each hemisphere. For the NH, TC tracks are separately documented for each of the four basins. Thus, a multi-basin TC will appear in more than one set and could, inadvertently, be counted more than once in hemispheric totals. For the Southern Hemisphere portion of the data set, each TC is a single entity and, the basin it occupies is determined by the TC longitude. The U.S. Joint Typhoon Warning Center (JTWC) also treats SH best-tracks in this manner. This avoids the possibility of counting the same TC more than once in hemispheric totals. A disadvantage is that the available periods of record for the various hemispheric basins may be dissimilar.

The Neumann global data set, updated through the 2007 TC seasons, mostly with data from the U.S. Joint Typhoon Warning Center (JTWC) and NHC, is used as the basis for all charts in this study. Tabular data (tables 2.5 and 2.6) include the 2008 seasons. Also, many needed changes, particularly to the early SH data, have come to the attention of the author and these have been incorporated into the files. In the interest of eliminating at least some of the pre-satellite data, the early years (1960-1961 through 1965-1966) for the SH and 1891-1970 for the North Indian basin have not been used for any of the graphical or tabular presentations.

2.1.2 On the quality of TC data

The global warming issue has focused attention on the adequacy of archived TC data for detecting secular trends in TC frequency, intensity, landfall, length of season, etc. Data quality is a diverse issue and difficult to assess on a global scale. In general, the quality improves with time and early data is more reliable in the Northern Hemisphere. Polar orbiting weather satellites, in a research mode, were first launched by NASA in 1960 but were not declared operational until 1965. Thus, for the period, 1960-1965, satellite documentation was very fragmented. Even after the 1965 operational era began, it took many years for some Centers to take full advantage of this new TC viewing platform and to develop the expertise to associate satellite signatures with storm position and intensity. Subjectively, problems still exist in this regard.

For the North Atlantic and western North Pacific basins, aircraft TC reconnaissance began in the mid-1940's and became routine in 1946. Such reconnaissance continues and has been expanded in the Atlantic, but was discontinued for the western North Pacific in 1987. Although this platform provided needed ground-truth, early flights were made only once or twice a day, assuming the TC was within the operational range of the aircraft. Intensity changes or peak intensity could easily have been missed. In U.S. Navy Atlantic and western North Pacific aircraft reconnaissance of the 1940's and early 1950's, surface wind speed and direction were subjectively based on visual sea-state conditions, made from altitudes of 400 to 600 feet

(Neumann, 1952). In this connection, Neumann (1996) describes a 1940's era Navy reconnaissance policy of limiting maximum typhoon surface winds to 120 knots. Navigational aids of that era, particularly in the Pacific, were poor and the position of an aircraft in the eye of a TC as well as communication with ground personnel was often very uncertain. This early aircraft reconnaissance is incomplete in contrast to current capabilities.

In addition to TC observational deficiencies, there was little official interest or coordination in the TC documentation issue for the years following WW II. Even after the introduction of computers, transferring TC data to punch cards was laborious, of a low priority and lacking standardization. In the United States, the TC needs of the United States Space Program focused attention on this TC documentation deficiency and prompted Hope and Neumann (1968) to structure a best track file for the Atlantic basin, known as HURDAT. The introduction of computer graphics in the early 1970's and personal computers in the mid-1980's and the World Wide Web greatly simplified compilation and error checking of best-track files.

Before the satellite and aircraft reconnaissance eras, the location and intensity of a tropical cyclone were based largely on chance encounters with ships or populated landmasses. These observations were quite fragmented and meteorological expertise, if available, was required to "connect the dots." Some storms were not detected until several days after their formation or not at all. Thus, the data on individual storms leaves much to be desired. However, in the collective sense, there is valuable information in historical tracks.

In general, the location of a TC is more reliable than is the intensity. Indeed, early TC documentation either lacked intensity or used an *intensity code* (i.e., depression, tropical storm or hurricane). Maximum intensity is particularly uncertain and, even if accurate, may not be documented if a maximum occurred between 6-hourly synoptic times used in best-track files. Also, there is a greater chance of biases in the estimation of intensity. For this reason, other than for the distinction between storm stages (hurricanes, tropical storms, etc.), the charts contained in this chapter (Figs. 2.7 through 2.10) do not explicitly address maximum intensity.

Because of the aforementioned recent widespread intrest in global TC frequency and intensity trends, considerable effort is being focused on the improvement of historical TC best-track data. Harper, et al. (2008) conclude that maximum winds for the early years of the Neumann (1999) global data set, being based largely on early Bureau of Meteorology (BoM) and JTWC data, are too low in the Australian area. Also, a welcome new global data set, International Best Track Archive for Climate Stewardship (IBTrACS)(Kruk et al., 2008) has been assembled, see http://www.ncdc.noaa.gov/oa/ibtracs/. Additionally, Landsea, et al., (2003) describe an extensive ongoing project to revise Atlantic best-tracks back to the year 1851 (HURDAT). Efforts are also underway to re-evaluate historical satellite photos. As pointed out earlier, augmented best-tracks or best-track supplements are needed to document additional TC parameters.

2.1.3 Basin boundaries

Basin bounds used in this study are given in Table 2.2. For the NH, four clusters (see Fig 2.1) of tropical cyclone activity are clearly identifiable: the N. Atlantic, eastern N. Pacific, western N. Pacific and the North Indian (Bay of Bengal and Arabian Sea) basins. For the SH, such clustering is not obvious and the determination of a basin bound is based on other considerations.

The Cape York Peninsula at longitude 142°C is often taken as the bounds between the Australia/southeast Indian and the Australia/southwest Pacific basins. From Fig. 2.4, it can be noted that the average motion of TC's east of this longitude exhibit more of an easterly component while those to the west exhibit a westerly component. Also, from Fig. 2.2, there is somewhat of a minimum of activity at this longitude.

In regard to the bound between the southwest and the southeast Indian Ocean, given as 100°E in Table 2.2, the WMO official high seas warning area between Perth/Jakarta and RSMC La Rèunion is at 90°E. However, from Fig. 2.2, a minimum of TC activity is seen to occur 100°E to 105°E and such minima are typically used to define basin bounds. As a compromise, 100°E will be used here as the basin bound even though it differs somewhat from the WMO forecast responsibility bound of 90°E. Also, the central North Pacific (140°W, westward to 180°) is referred to as the central North Pacific basin with an RSMC in Honolulu. Although TC's, such as INIKI in 1992, do develop in this basin, it will be considered here as part of the eastern North Pacific basin.

Table 2.2. Geographical bounds of the TC basins used in this study. The Eastern and Central N.Pacific are combined into a single basin.

Northen Hemisphere

North Atlantic	Eastern N. Pacific / Central N. Pacific	Western N. Pacific	North Indian
N. Atlantic, Caribbean Sea & Gulf of Mexico	West coast of North America to 140°W 140° to dateline	Dateline to Asia	Bay of Bengal & Arabian Sea

Southern Hemisphere

SW Indian	Australian / SE Indian	Australian / SW Indian
<100°E to Africa	100°E to 142°E	142°E to 120°W

2.1.4 Wind averaging times

A major problem arises when dealing with global tropical cyclone intensity: different sustained wind averaging times are being used by various Centers. U.S. interests use 1-minute averaging while, as sanctioned by the WMO, most other interests use 10-minute averaging. (Two and three minute averaging has been used in portions of some basins.) The average wind is inversely proportional to the averaging time and a near-coastal inland wind averaged over 10

minutes (600 seconds) is about 88% (BoM, 1978, Murnane, 2004) of the wind averaged over 1-minute (60 seconds) such that $V_{600}=0.88V_{60}$ or $V_{60}=1.136V_{600}$. Thus, a hurricane having a maximum wind of 120 km h^{-1} (65 knots) in the 1-minute system, would only be a maximum wind of 106 km h^{-1} (57 knots) in the 10-minute system and would be designated as a tropical storm or equivalent rather than a hurricane or equivalent. Additional discussion on this topic can be found in Murnane (2004).

Table 2.3 provides additional insight into the wind-averaging dilemma. To simulate 10-minute averaging, all best-track sustained one-minute winds for the North Atlantic (ATL), eastern North Pacific (EPC) and western North Pacific (WPC) were multiplied by 0.88. Referring to the table, it can be noted that, over the 42-year period for the Atlantic basin, there were 470 TCs designated as tropical storms and 261 as hurricanes. However, after the simulated conversion to the 10-minute system, there were 454 TCs reaching the tropical storm threshold (a 3.4% reduction) and only 191 reaching the hurricane threshold (a 26.8% reduction) for that basin.

Table 2.3. The effect of wind averaging time on defining TC stages. Period of record is 1966-2007.

	Number of TCs			
	ATL	EPC	WPC	ALL
At least 63 km h^{-1} (34kts) in 1-min system	470	666	1120	2256
At least 63 km h^{-1} (34kts) in 10-min system	454	619	1064	2137
% difference ((1-min - 10-min)/1-min)	3.4	7.1	5.0	5.3
At least 118 km h^{-1} (64kts) in 1-min system	261	364	716	1341
At least 118 km h^{-1} (64kts) in 10-min system	191	301	615	1107
% difference ((1-min - 10-min)/1-min)	26.8	17.3	14.1	17.4

The general conclusion from the data given in Table 2.3 is that the different averaging times have a significantly greater effect on reaching the hurricane threshold than reaching the tropical storm threshold. From best-track files in the 10-minute system, it can be noted that many TCs have maximum winds of 110 km h^{-1} (60 kts) and would be designated as tropical storms or the equivalent. As pointed out earlier, these would be designated as hurricanes in the 1-min system. Other factors, such as satellite interpretation, wind-pressure relationships and measurement errors also enter into the picture. In reality, the preciseness of the various wind definitions far exceeds the ability to measure or estimate wind with that precision. Nonetheless, standardization of the timing would further clarify the TC wind issue.

2.2. Chart preparation

Excluding TC's that failed to reach an intensity of 34 kts (63 km h^{-1}), Figs. 2.1, 2.2, and Figs. 2.4 through 2.6, depict tropical cyclone frequency and/or motion on a global scale. With some exceptions, these are typically TC's named by one of the WMO Regional Specialized

Meteorological Centers (RSMC's). In some, cases, however, a post-analysis had indicated a TC did reach the tropical storm threshold and was later included in the season summary, but without a formal name. In summaries, these are often designated as not named or unnamed. For the Atlantic basin, charts also include some unnamed storms designated as sub-tropical (McAdie et al., 2008).

For Figs. 2.4, 2.5 and 2.6, the analyses are based on a 60 nm grid system having 331 points in the zonal direction and 143 meridionally. Each grid point represents a scan-circle centered on the grid-point. Thus, if the scan-circle radius is over 30 nm, the circular areas will overlap in both the zonal and meridional directions, providing some smoothing to the data. As shown by Taylor (1986), the use of circular rather than square or rectangular scan areas such as latitude/longitude "squares" is a non-biased method of areal tabulation.

For Fig. 2.2, a 75 nm (140 km) scan-radius was used. For a typical TC landfall, this distance approximates the extent of at least minimal damage or concern. For the other global charts involving motion, the scan distance was increased to twice this amount so as to provide additional sample sizes and smoothing. As illustrated by Xue and Neumann (1984a and 1984b), TC's from each basin were passed through the global grid system and counts or sums of various TC parameters were made. For this purpose, the 6-hourly best-track anchor points were interpolated to 1-hourly points using the method of Akima (1970). If more than one hourly point was contained within a grid-zone, only a single average value was retained. This prevents a bias toward slower moving TC's.

2.2.1 Tropical cyclone tracks

Figure 2.1 presents a 10-year display of global TC tracks and considerable variation in track characteristics is evident. Some of these differences are due to different documentation procedures at the various Centers. For example, NHC best-tracks include early portions of the TC extratropical stages (dashed tracks on Fig. 2.1). Other track differences are due to environmental factors such as sea-surface temperature (SST), steering patterns, topography, etc. Additional detail on global tropical cyclone motion is provided by Elsberry (1987).

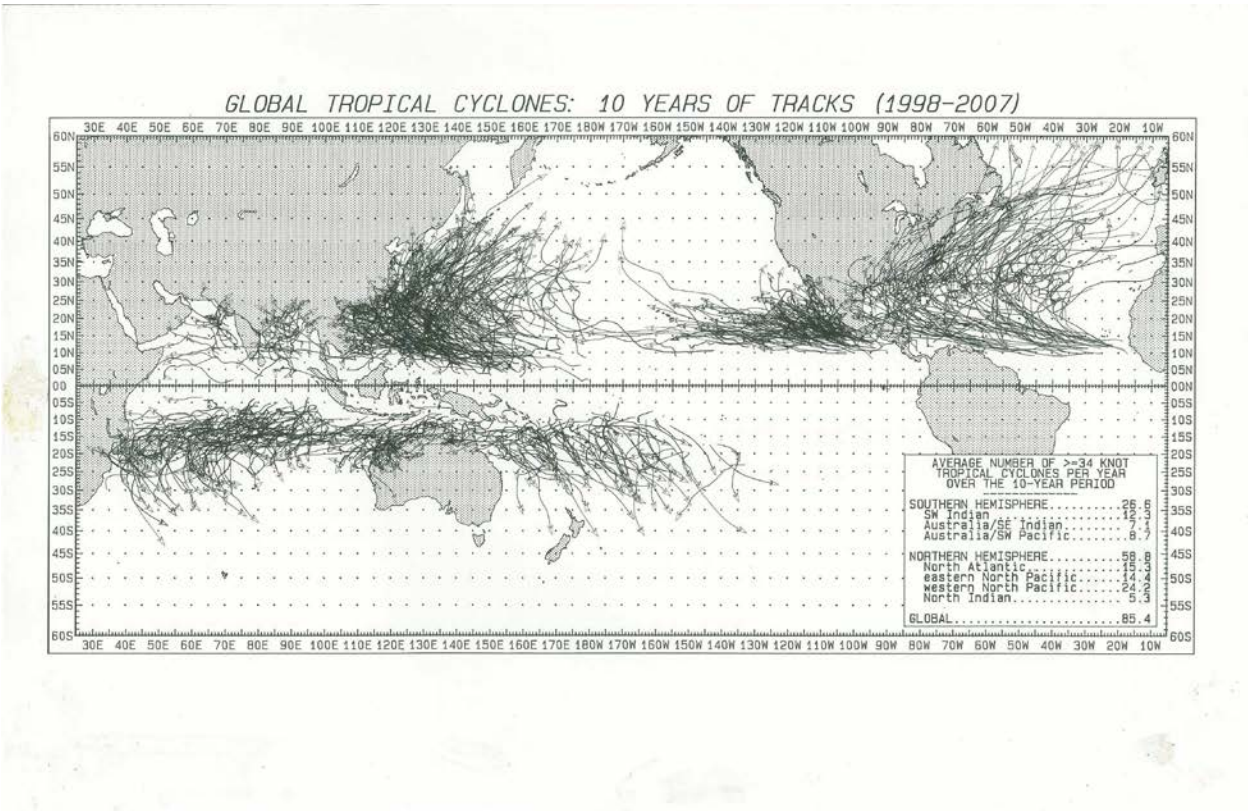

Figure 2.1. Global TC tracks 1998-2007. (click image for full size in new window).

The inset to Fig. 2.1 gives the 10-year totals for each basin and hemisphere. By far the biggest change in these totals from the 10-year 1980-1989 period used in the previous edition of this Guide was for the N. Atlantic where the average annual number of TC's increased from 9.3 to 15.3.

In the eastern North Pacific, TC's typically encounter cold SST's (less 22.5°C) at low latitudes (Frank, 1987) and dissipate before recurvature into the westerlies. By comparison, relatively warm SST's in the western N. Pacific and the N. Atlantic allow many TC's to be sustained well poleward, even after recurvature into the westerlies.

Southern Hemisphere SST's, on the average, are lower than those for given latitudes in the NH. This, together with the more equatorward extent of the SH westerlies, typically result in poleward moving tropical cyclones losing their warm-core characteristics at lower latitudes than for otherwise similar systems in the NH.

All basins observe TC tracks that are anomalous in regard to location, intensity or duration. On rare occasions, for example, eastern North Pacific TC's affect the extreme southwestern portions of the United States (Chenoweth and Landsea, 2004). Other anomalous TC's for other basins include 1989 typhoon GAY that brought extreme damage to both Thailand and India; North Indian 2008 Cyclone NARDIS that devastated southern Myanmar; 1974 Cyclone TRACY that hit Darwin, Australia; and Cyclone LEON-ELINE that brought considerable damage to

Madagascar, Mozambique and Zimbabwe in 2000. Still other examples would be the 33-day duration of North Atlantic Hurricane GINGER in 1971, the 870 hPa surface pressure of Typhoon TIP in the western North Pacific in 1979 or the development of Hurricane INIKI, 1992 in the central North Pacific. Numerous other examples of anomalous and noted TC's could be cited.

TC's are sometimes evaluated according to their destruction potential and several indices have been introduced. One such index (Bell, 2000) is referred to as Accumulated Cyclone Energy (ACE) and is a function of all of the 6-hourly sustained winds (v) ≥ 34 kts (63 km h^{-1}) over the life of the storm: [$ACE=10^{-4}\Sigma(v^2)$]. Multiplying by 10^{-4} reduces the sum to a more manageable level. Since ACE is dependent on the size of the basin, its use, without size normalization, is mainly for evaluating damage potential in single basins.

Table 2.4 gives average ACE values for the 10-year period used in Fig. 2.1. ACE does not address other destructive factors such as landfall frequency or storm surge. For example, even though the North Indian basin has the lowest ACE average, it has the highest death rate from storm surges. In this connection, Powell and Reinhold (2007), with comments by Hsu and Blanchard (2008), suggest an integrated kinetic energy (IKE) index that addresses this deficiency. *For additional information on ACE, see http://models.weatherbell.com/tropical.php*

Table 2.4. Average ACE values 1988-2007.

North Indian	Aus/SE Indian	Aus/SW Pacific	Eastern N.Pacific	SW Indian	North Altanic	Western N.Pacific
20	40	63	100	104	158	297

2.2.3 Tropical cyclone track density

Visual inspection of the TC tracks displayed in Fig. 2.1 suggest that both the eastern and western N. Pacific have the largest local TC concentration (number per unit area) for a given time interval. Figure 2.2 quantifies this parameter where the unit of measurement is the number of tropical storms or hurricanes per 100 years passing within 75 nmi (140 km) from any point. As previously mentioned, this distance approximates the extent of at least minimal damage from an average TC making landfall. The contours on Fig. 2.2 are based an objective analysis of the 60 nmi (331 x 143) grid, each grid point being an overlapping 75 nmi radius scan circle (Taylor, 1986; Xue and Neumann, 1984a, 1984b).

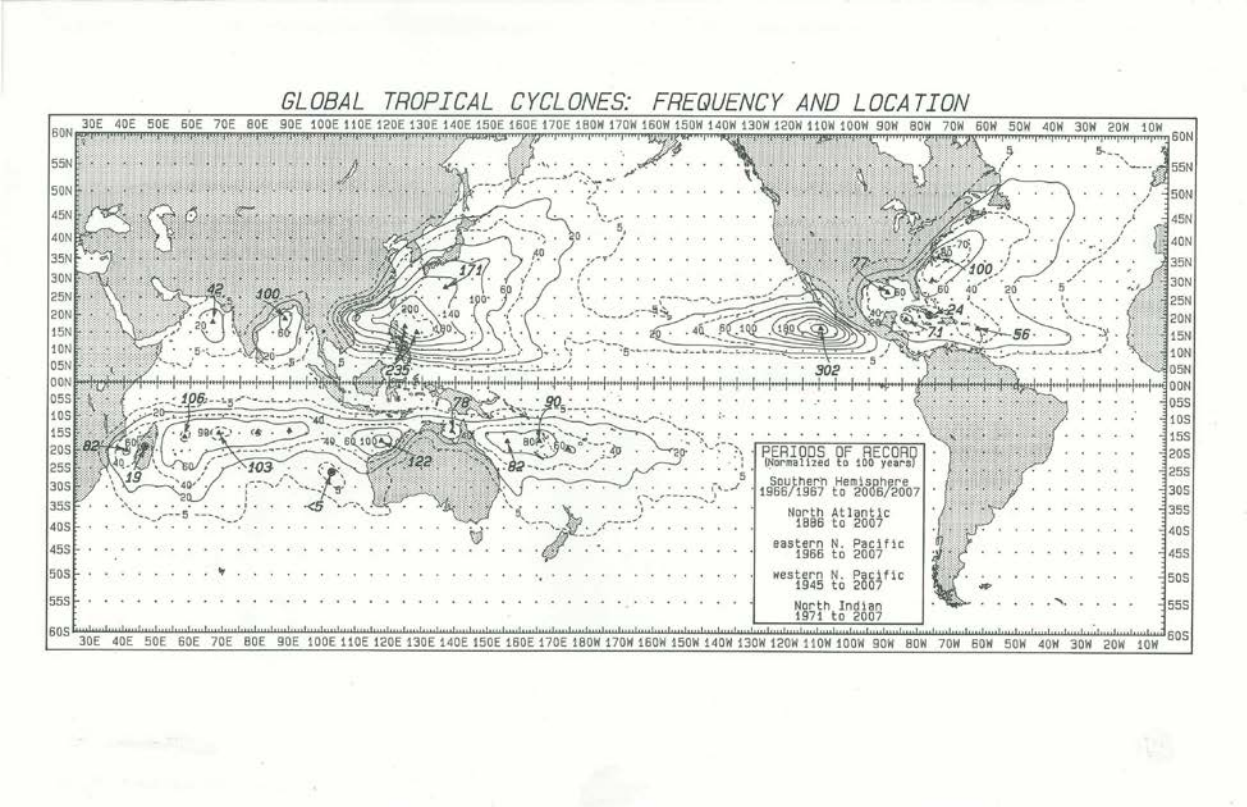

Figure 2.2. Global TC frequency (storms per hundred years). (click image for full size in new window)

The maximum climatological TC density (302 per 100 y or 3.02 per year) occurs in the eastern N. Pacific near 17.2°N, 109.5°W. This is near Isla Socorro (18.8°N, 111.0°W). Another substantial concentration occurs east of Luzon in the Philippine Sea. The highest SH frequency (122 per 100 y) is located off northwestern Australia. Local minima (dark circles on the figure) occur over Madagascar, over eastern Cuba and off the central west coast of Australia. These maximum/ minimum values are somewhat dependent on the grid-point interpolation and smoothing methodology.

The use of a 100-year statistic, as was done in Fig. 2.2, has a number of advantages. It allows combining different periods of record for different basins. Also, it provides convenience in using the Poisson distribution (see Section 2.6.1) to estimate probability of discrete events such as the probability of no TC's passing within 75 nmi of the location of the eastern N. Pacific maximum in any given year. Using the procedure described in Xue and Neumann (1984a), the percent probability of this event is $e^{-3.02}$ x 100 = 4.9% of the 42 years (1966-2007) or 2.05 event occurrences. This is in agreement with observations since the event did not occur for the years 1970 and 1993.

2.2.4 Motion parameters

Before introducing global charts of TC motion, a discussion of motion terminology as used on the charts will be presented. TC motion, being a vector quantity, is difficult to describe in the univariate sense. This is illustrated in Fig. 2.3. The figure compares motion characteristics of 22 TC's passing within two of the scan-circles described in section 2.2.1. The upper panel uses data from a region where motion can be described as highly variable while the lower panel does likewise for a region where motion is relatively consistent.

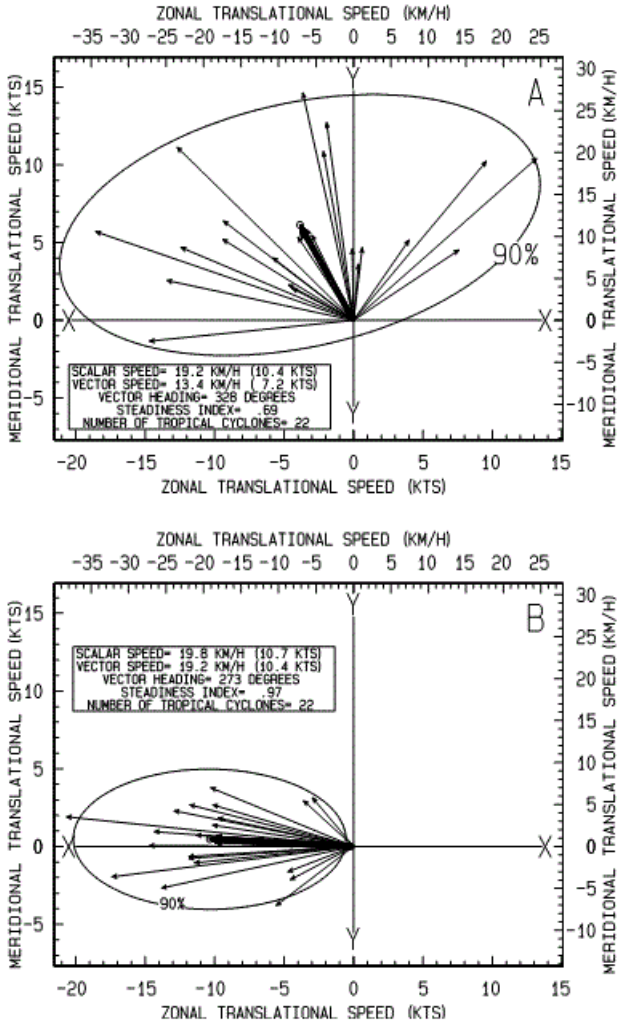

Figure 2.3. Illustration of motion parameters discussed in text. Examples are from two areas with contrasting motion: (a) recurvature zone of western N. Pacific basin and (b) southern portion of eastern N. Pacific basin.

In the X, Y coordinate system, the small arrows depict the end points of each individual motion vector as the TC passes through one of the grid point scan-circles. The average length of these 22 individual vectors, regardless of direction, is defined as the average scalar speed. A *centroid* (small circle on the charts) is obtained by summing and averaging the mathematically signed individual u- and v-components of motion. The length of the bold vector, extending from the X, Y origin to the centroid represents the mean vector speed and the angle (measured

clockwise from north) is the mean *vector direction* or heading. Collectively, they are referred to as mean *vector motion*.

The bivariate normal distribution (Crutcher et al., 1982) is often used to describe bivariate quantities such as wind, tropical cyclone motion, TC forecast errors, etc. Using this distribution at the two contrasting TC motion sites, Fig. 2.3 displays the theoretical elliptical envelope containing 90% of the vector end-points. The size and shape of the elliptical area reflects the standard deviation of the components of motion as well as the linear correlation between the (X, Y) components. The latter become zero along a new rotated (X', Y') ellipse axes (not shown) through the centroid and random selections from the two marginal distributions can be made along this rotated system.

The ratio of the vector speed divided by the scalar speed provides a measure of motion variability, often referred to as steadiness or a steadiness index (Hope and Neumann, 1971; Crutcher and Quayle, 1974). The higher the ratio, the steadier will be the motion and the highly unlikely value of 1.0 would only be attained if all TC's moved with the same speed and direction. Somewhat arbitrarily, steadiness indices of <0.75, 0.75 to 0.90 and >0.90, are defined here, respectfully, as highly variable, intermediate and relatively steady motion. These values are somewhat different than previously used and were based on the desire to contain about the same number of cases in each of the three motion classification bins used on the global charts. With these criteria, the upper panel in Fig. 2.3, having a steadiness value of 0.69 is described as highly variable and the lower panel, having a steadiness index of 0.97, is described as relatively steady.

2.2.5 TC vector direction

Continuing with a discussion of the global motion charts, the arrows in Fig. 2.4, as illustrated in Fig. 2.3, only represent the average vector direction of TC motion. This is a reflection of the large-scale atmospheric steering patterns. In some areas, these patterns are modified by local influences such as topography (Brand and Blelloch, 1974; Yeh and Elsberry, 1993; Zehnder, 1993). Although the scale of Fig. 2.4 is too crude to show these mesoscale features near Taiwan, they are identifiable around mountainous Madagascar and the extreme southwestern Gulf of Mexico where TC's are deflected to the left by the Sierra Madre mountains of Mexico.

Mean vector motion, by itself, is a rather frail statistic in that it fails to address speed or motion variability. The length of the arrow could be made proportional to speed as is done on Figs. 2.7 through 2.10 but this is difficult to display on such a small-scale map and does not address the motion variability issue.

The colored shading in Fig. 2.4 does provide some insight into motion variability. In the previous section, it was pointed out that steadiness indices of <0.75 are associated with highly variable motion; 0.75 to 0.90 with intermediate motion and >0.90 as relatively steady motion. On Fig. 2.4, it can be noted that the Southern Hemisphere contains little of the "relatively steady" motion. Indeed, much of the motion is designated as "highly variable". In the Northern

Hemisphere, highly variable motion is primarily confined to the recurvature zones. Mostly "relatively steady" motion is noted in the eastern North Pacific basin.

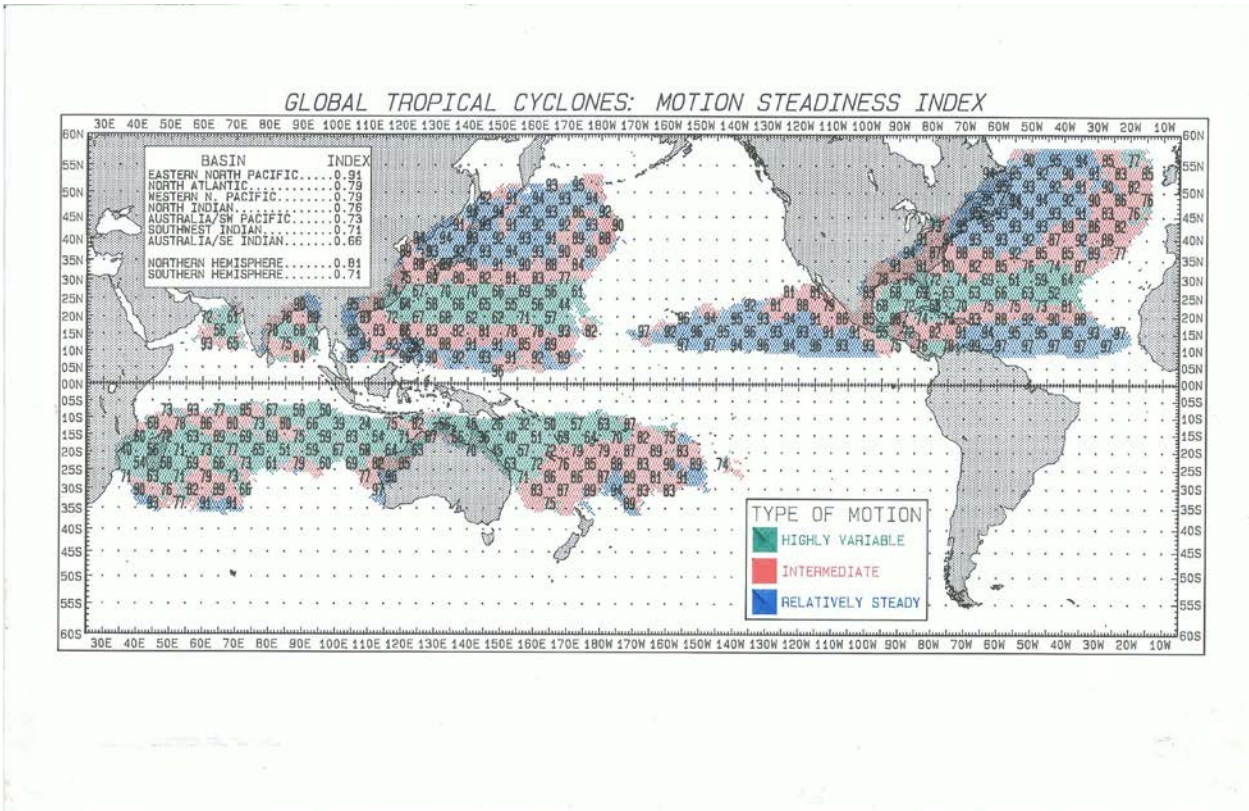

Figure 2.4. Motion steadiness index. (click image for full size in new window)

2.2.6 Vector and scalar speeds

Fig. 2.5 gives global vector and scalar translational TC speeds. These are presented in the "steadiness index" mode (vector speed divided by scalar speed). Three classes of scalar speeds are somewhat arbitrarily defined as slow, medium and fast with specific delimiting values being defined in the figure inset. Slower translational speeds are noted over the SH. As discussed in section 2.2.2, the limited poleward penetrations of Southern Hemisphere TC's contribute to the lack of "fast" motion in that hemisphere. Also noted are the "slow" speeds over the North Indian basin. Both the North Atlantic and the western North Pacific basins exhibit a classical pattern of slower translational speeds during recurvature with much higher speeds poleward and somewhat higher speeds equatorward.

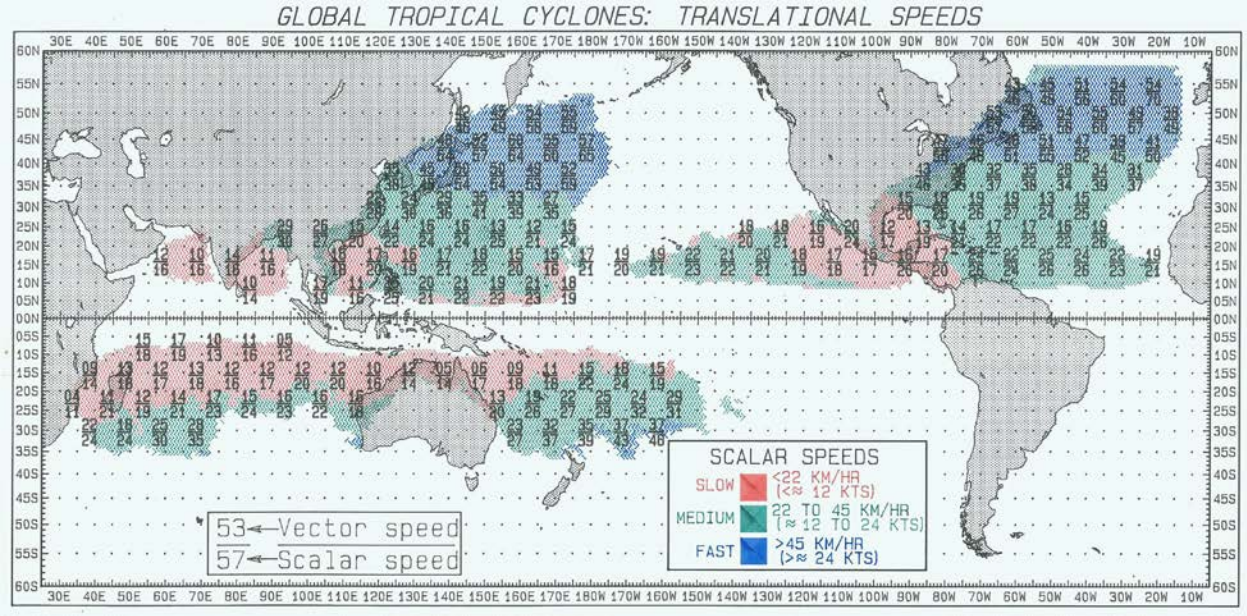

Figure 2.5. Translational TC speeds (vector speed divided by scalar speed).

2.2.7 Global values of the steadiness index

Fig. 2.6 gives global values of the steadiness index (SI) multiplied by 100 and wide variability can be noted. Compared to the NH, many more low values of the SI are noted in the SH, particularly in the Coral Sea area east of Queensland, Australia and off the northwestern coast of Western Australia, where some values are <50. In the NH, highest SI values are found over the eastern N. Pacific basin with some values being as high as 97. The upper left inset gives average steadiness indices for each basin and hemisphere. As would be expected from visual inspection of Fig.2.6, lowest values are found over the SH in the vicinity of Australia and the highest steadiness values are found over the eastern N. Pacific.

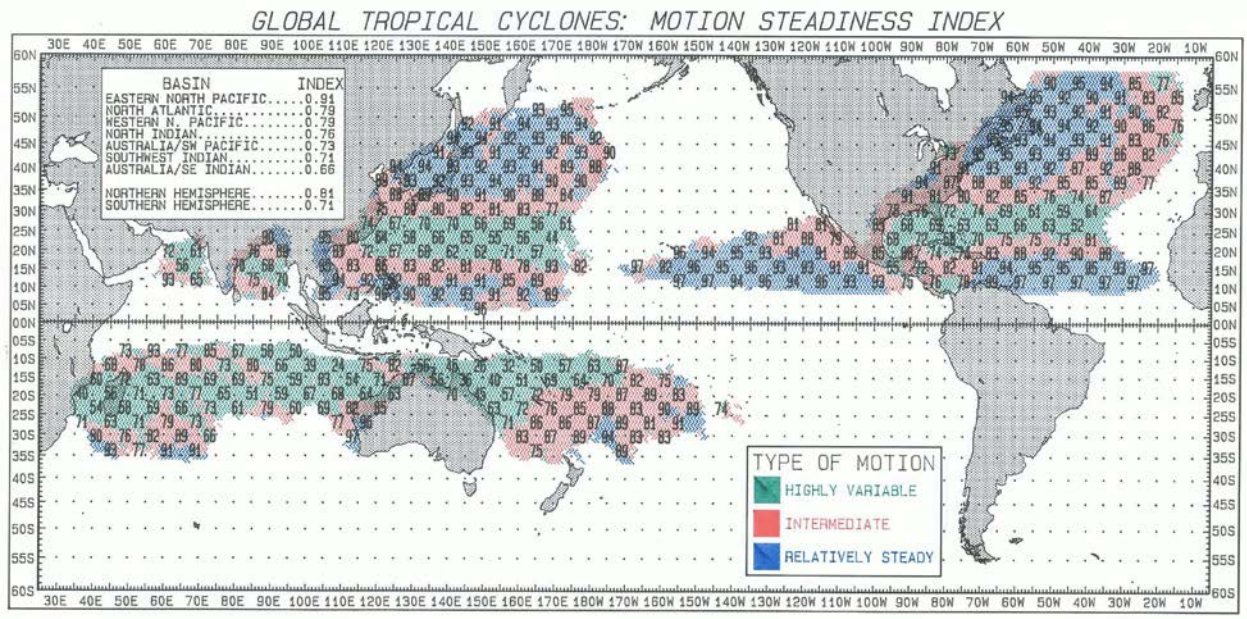

Figure 2.6. Steadiness index (SI) multiplied by 100. (click image for full size in new window)

Neumann (1981), defines a *forecast difficulty* index (FDI) based on residual errors from the CLIPER (Neumann, 1972) model. Pike and Neumann (1987) developed ad hoc CLIPER models to rank forecast difficulty for the various basins and their rankings are very similar to those given in the Fig. 2.6 table. Thus, both being a function of TC motion variability, the steadiness index is closely related to FDI. Forecast difficulty is mainly applicable to errors in statistical models. Recent error statistics (personal communication, M. Fiorino, 2008) on numerical model errors suggest that they are becoming more independent of the forecast difficulty concept.

2.3 Tabular data

2.3.1 Seasonal summaries

For the 30-year period, 1979-2008, Table 2.5 gives the number of tropical cyclones per season having maximum sustained winds of ≥34 kts (63 km h^{-1}) and ≥64 kts (118 km h^{-1}). Preparation of this table was problematic. In the previous edition of this Guide, the analogous table was based on a mixture of 1- and 10- minute averaged wind data. However, as stated in the introduction to this revised chapter, one of the goals is to present basin-comparable statistical data and the earlier wind-mixture is not consistent with that goal.

Thus, the decision was made to present two tables — one based on the 1-minute system (Table 2.5) and another on the 10-minute system (Table 2.6). Since 10-minute winds are not available for some basins, a decision was further made to multiply the best-track winds used in the construction of Table 2.5 by the usual factor 0.88 (see section 2.1.4) to estimate the 10-minute

winds. Errors introduced by this approximation are commensurate with the errors and uncertainties in specifying a representative surface wind.

Table 2.5. Based on 1-minute averaging, left cell entry gives seasonal totals of TC's with maximum winds ≥34 kts (63 km h^{-1}) and parenthetical entry with maximum winds ≥64 kts (118 km h^{-1}). Southern Hemisphere seasons begin and end 6-months prior to Northern Hemisphere seasons. Because some TC's traverse more than one basin, global totals (last column) are always less than or equal to the sums of the individual basins.

NH Season	North Atlantic	Eastern North Pacific	Western North Pacific	North Indian	Southwest Indian	Australia/ Southeast Indian	Australia/ Southwest Pacific	All Basins
1979	9(6)	10(6)	23(14)	5(2)	14(4)	7(2)	11(3)	74(37)
1980	11(9)	14(7)	24(15)	4(0)	14(9)	9(6)	10(4)	81(47)
1981	12(7))	15(8)	28(16)	3(2)	15(5)	9(5)	10(4)	89(47)
1982	6(2)	23(12)	26(19)	5(2)	14(7)	13(3)	7(5)	91(50)
1983	4(3)	21(12)	23(12)	3(0)	7(4)	4(2)	15(11)	77(44)
1984	13(5)	21(13))	27(16)	4(2)	17(7)	10(6)	9(3)	99(52)
1985	11(7)	23(13)	26(17)	6(0)	15(6)	12(8)	13(6)	102(56)
1986	6(4)	17(9)	28(19)	3(0)	15(8)	9(4)	10(6)	86(50)
1987	7(3)	20(10)	24(18)	8(0)	9(3)	6(4)	13(7)	87(45)
1988	12(6)	15(7)	26(14)	5(1)	13(7)	1(0)	7(5)	76(40)
1989	11(7)	17(9)	31(21))	3(1)	15(8)	6(4))	14(6)	95(56)
1990	14(8)	21(16)	31(21	2(1)	15(10)	7(5)	7(4)	93(64)
1991	8(4)	14(10)	30(20)	4(1)	10(6)	6(2)	4(3)	74(45)
1992	7(4)	27(16)	32(21)	11(3)	13(5)	6(4)	15(9)	105(60)
1993	8(4)	15(11)	30(21))	2(2)	13(4)	4(0)	13(8)	83(50)
1994	7(3)	20(10)	36(21)	5(1)	17(11)	9(4)	6(4)	96(53)
1995	19(11)	10(7)	26(15)	4(2)	12(7)	4(3)	5(3)	80(48)
1996	13(9)	9(5))	33(21)	8(4)	13(8)	10(5)	7(2)	89(54)
1997	8(3)	19(11)	31(23)	4(2)	18(11)	6(3)	16(9)	100(61)
1998	14(10)	13(9)	18(9)	8(5)	13(2)	7(3)	18(12)	90(50)
1999	12(8)	9(6)	24(11)	5(3)	15(5)	10(7)	11(3)	83(41)
2000	15(8)	19(6)	24(15)	4(1)	13(8)	10(7)	9(4)	89(46)
2001	15(9)	15(8)	29(20)	4(1)	10(7)	8(3)	5(2)	84(49)
2002	15(8)	12(6)	26(18)	5(0)	15(9)	4(1)	7(2)	83(42)
2003	16(7)	16(7)	22(17)	4(1)	14(9)	5(2)	10(7)	85(49)
2004	19(11)	15(9)	31(20)	5(2)	12(9)	5(3)	4(2)	84(51)
2005	28(15)	15(70	24(18)	6(0)	12(6)	9(2)	7(6)	99(53)
2006	10(5)	19(11)	22(14)	6(1)	9(3)	8(3)	8(5)	79(41)

2007	16(7)	11(4)	22(16)	6(3)	10(8)	5(3)	8(4)	78(45)
2008	16(9)	16(7)	26(12)	6(1)	14(7)	7(3)	7(4)	91(43)
Sums	355(196	491(271)	803(514	148(44)	396(203)	216(107	286(153)	2623(1469)
Average	11.8(6.5)	16.4(9.0)	26.8(17.1)	4.9(1.5)	13.2(6.8)	7.2(3.6)	9.5(5.1)	87.4(49.0)
Std Dvn	4.8(2.9)	4.5(3.1)	4.0(3.5)	1.9(1.3)	2.5(2.3)	2.7(1.9)	3.7(2.6)	8.5(6.4)
Percent	13.2(13.2)	18.2(18.2)	29.8(34.5)	5.5(3.0)	14.7(13.7)	8.0(7.2)	10.6(10.3)	100.(100.)

Table 2.6. Same as Table 2.5 except winds averaged over 10 minutes.

NH Season	North Atlantic	Eastern North Pacific	Western North Pacific	North Indian	Southwest Indian	Australia/ Southeast Indian	Australia / Southwest Pacific	All Basins
1979	9(6)	10(6)	23(14)	5(2)	14(4)	7(2)	11(3)	74(37)
1980	11(9)	14(7)	24(15)	4(0)	14(9)	9(6)	10(4)	81(47)
1981	12(7))	15(8)	28(16)	3(2)	15(5)	9(5)	10(4)	89(47)
1982	6(2)	23(12)	26(19)	5(2)	14(7)	13(3)	7(5)	91(50)
1983	4(3)	21(12)	23(12)	3(0)	7(4)	4(2)	15(11)	77(44)
1984	13(5)	21(13))	27(16)	4(2)	17(7)	10(6)	9(3)	99(52)
1985	11(7)	23(13)	26(17)	6(0)	15(6)	12(8)	13(6)	102(56)
1986	6(4)	17(9)	28(19)	3(0)	15(8)	9(4)	10(6)	86(50)
1987	7(3)	20(10)	24(18)	8(0)	9(3)	6(4)	13(7)	87(45)
1988	12(6)	15(7)	26(14)	5(1)	13(7)	1(0)	7(5)	76(40)
1989	11(7)	17(9)	31(21))	3(1)	15(8)	6(4))	14(6)	95(56)
1990	14(8)	21(16)	31(21	2(1)	15(10)	7(5)	7(4)	93(64)
1991	8(4)	14(10)	30(20)	4(1)	10(6)	6(2)	4(3)	74(45)
1992	7(4)	27(16)	32(21)	11(3)	13(5)	6(4)	15(9)	105(60)
1993	8(4)	15(11)	30(21))	2(2)	13(4)	4(0)	13(8)	83(50)
1994	7(3)	20(10)	36(21)	5(1)	17(11)	9(4)	6(4)	96(53)
1995	19(11)	10(7)	26(15)	4(2)	12(7)	4(3)	5(3)	80(48)
1996	13(9)	9(5))	33(21)	8(4)	13(8)	10(5)	7(2)	89(54)
1997	8(3)	19(11)	31(23)	4(2)	18(11)	6(3)	16(9)	100(61)
1998	14(10)	13(9)	18(9)	8(5)	13(2)	7(3)	18(12)	90(50)
1999	12(8)	9(6)	24(11)	5(3)	15(5)	10(7)	11(3)	83(41)
2000	15(8)	19(6)	24(15)	4(1)	13(8)	10(7)	9(4)	89(46)
2001	15(9)	15(8)	29(20)	4(1)	10(7)	8(3)	5(2)	84(49)
2002	15(8)	12(6)	26(18)	5(0)	15(9)	4(1)	7(2)	83(42)
2003	16(7)	16(7)	22(17)	4(1)	14(9)	5(2)	10(7)	85(49)
2004	19(11)	15(9)	31(20)	5(2)	12(9)	5(3)	4(2)	84(51)
2005	28(15)	15(7)	24(18)	6(0)	12(6)	9(2)	7(6)	99(53)
2006	10(5)	19(11)	22(14)	6(1)	9(3)	8(3)	8(5)	79(41)
2007	16(7)	11(4)	22(16)	6(3)	10(8)	5(3)	8(4)	78(45)
2008	16(9)	16(7)	26(12)	6(1)	14(7)	7(3)	7(4)	91(43)
Sums	355(196)	491(271)	803(514	148(44)	396(203)	216(107	286(153)	2623(1469)
Average /td>	11.8(6.5)	16.4(9.0)	26.8(17.1)	4.9(1.5)	13.2(6.8)	7.2(3.6)	9.5(5.1)	87.4(49.0)
Std Dvn	4.8(2.9)	4.5(3.1)	4.0(3.5)	1.9(1.3)	2.5(2.3)	2.7(1.9)	3.7(2.6)	8.5(6.4)
Percent	13.2(13.2)	18.2(18.2)	29.8(34.5)	5.5(3.0)	14.7(13.7)	8.0(7.2)	10.6(10.3)	100.(100.)

Other than the use of the 0.88 conversion factor, there are several reasons why the data listed in these tables may differ from data maintained by other groups. Pre-1990 Table 2.5 data are a composite (Neumann, 1999) of best-tracks from various RSMC's and the Australian Bureau of Meteorology; later data are from JTWC and NHC. Another reason for differences between Table 2.5 data and that maintained by the various Centers could be related to basin bounds as stated in Table 2.2. Still other reasons could be related to local counting procedure. For example, the 1999 JTWC Annual TC Report lists 12 tropical storms and 12 typhoons or super typhoons in the western North Pacific for that year, whereas the Neumann data set gives only 11 typhoons or super-typhoons. Perhaps this is due to a different interpretation of 1999 TC DORA's intensity as it moved northwestward across the dateline from the central North Pacific basin to the western North Pacific basin.

2.3.2 Other comments on seasonal summaries

In addition to basin frequencies, Table 2.5 and 2.6 give global totals and it might be noted that these totals are typically less than the sum of individual basin totals. As mentioned in the table heading, this is due to some TC's traversing more than one basin. For example, 1999 DAMIEN, in the Australia/SE Indian Ocean basin moved westward and was renamed BIRENDA by the Mauritius Meteorological Service. This is only counted as a single TC. Another example was hurricane DORA, cited in the previous paragraph. The annual average number of TC's having maximum winds at least 34 kts (63 km h^{-1}) and summed in this manner is given as 87.4 in Table 2.5 and 79.7 in Table 2.6. (For the same 30-year period (1979-2008) and based on 10-min wind averaging, IBTrACS (Kruk et al., 2008) gives a seasonal average of 78.2 (37.4) TC's.) Before making further interpretations of data given in these tables, it should be noted that the beginning and ending times of SH seasons are 6-months prior to NH seasons.

The standard deviation of global totals is considerably higher than that of individual basins. Also, as would be expected, the western North Pacific TC basin is the largest contributor to the global totals while the North Indian basin is the smallest.

From Table 2.5, it is noted that the annual number of global tropical cyclones shows wide variation. In 1991, only 74 TC's were identified worldwide, while, for the following year, the count rose to 105. As noted earlier, the global standard deviation (8.5 TC's) of seasonal totals is greater than the standard deviation for individual basins.

2.4 Meridional profiles

Meridional profiles of zonally averaged TC parameters for each of the seven basins defined in Table 2.2 are presented in Figs. 2.7 through 2.10. The data for each basin were averaged zonally for 2-degree latitude bands centered at odd latitudes from 1° to 55°N. The total number of TC's included in the analysis are given in the inset as "NSTMS=nnn", while the number of cyclones passing within each latitude band is given in the column labeled "number of cyclones". Thus, for

the North Atlantic basin (Fig. 2.7) there were 1145 TC's used in the analyses and 240 of them passed through the 12°-14°N latitude band. Only those bands having at least 10 cases were included in the analyses.

The meridional profiles show average **u** (zonal speed component), **v** (meridional speed component) and **s** (scalar speed) within each latitude band while arrows depict vector heading with length proportional to scalar speed. In general, all increase with increasing latitude. However, there are some exceptions in the more polar and equatorial regions. In the Atlantic or example, south of about 22°N, average scalar speeds increase equatorward and, at high latitudes, there is some decrease in the u-component. Over the eastern North Pacific, recurving and accelerating TC's often make landfall over Mexico and rapidly dissipate. This feature shows up as somewhat of a discontinuity near 29°N. Because of fewer TC movements into the more poleward latitudes, SH cyclones, on average, have lower translational speeds than those of the NH. Other features can be noted on individual charts.

2.4.1 Translational motion

The inset on each figure gives the latitude of zero zonal motion (U_0).In basins that exhibit a classical recurvature pattern such as the North Atlantic, the western North Pacific and, to some extent, the southwest Indian Ocean basin, this can be interpreted as the average latitude of recurvature into the westerlies. However, the two Australian basins lack the classical recurvature pattern and U_0 has no significant meaning in that regard.

Also specified on each chart is the average wind (WBAR), here defined as the basin-wide average of all 34 kt (63 km h<sup-1< sup="">) six-hourly best-track winds. For a number of reasons, this is a rather frail statistic. However, when used in conjunction with the same statistic for each two-degree latitude band (W_j), it provides a *maximum wind index* (W_j/WBAR), where some of the fragility cancels out. For the Atlantic basin, this index varies from 0.71 at the lowest latitude band to 1.05 at the latitude band centered at 27°N. The maximum wind zone for this basin is located just equatorward of the average recurvature latitude (U_0), 27.6°N. A similar relationship between recurvature latitude and maximum wind zone can be noted for the other basins having the classical recurvature pattern (western North Pacific and southwest Indian Ocean) but not for the other basins. For the western North Pacific, this relationship was pointed out by Riehl (1972). Later investigators (Evans and McKinley, 1998; Knaff, 2009) also point out that the relationship, on the average, is valid in some basins but not in others and that it is somewhat dependent on the TC intensity.</sup-1<></sup-1<>

2.4.2 Meridional values of steadiness index

As previously discussed and portrayed in Fig. 2.6, Figs. 2.7 through 2.10 also give meridional values of the steadiness index as was displayed globally on Fig. 2.6. For basins having the classical recurvature pattern, steadiness values are lowest in the recurvature latitudes. As pointed out earlier, steadiness values are lower in the SH than in the NH. For the

Australia/southeast Indian basin (Fig. 2.9), SI values are particularly low with averages of 0.40 being noted between latitudes 10° to 12°S.

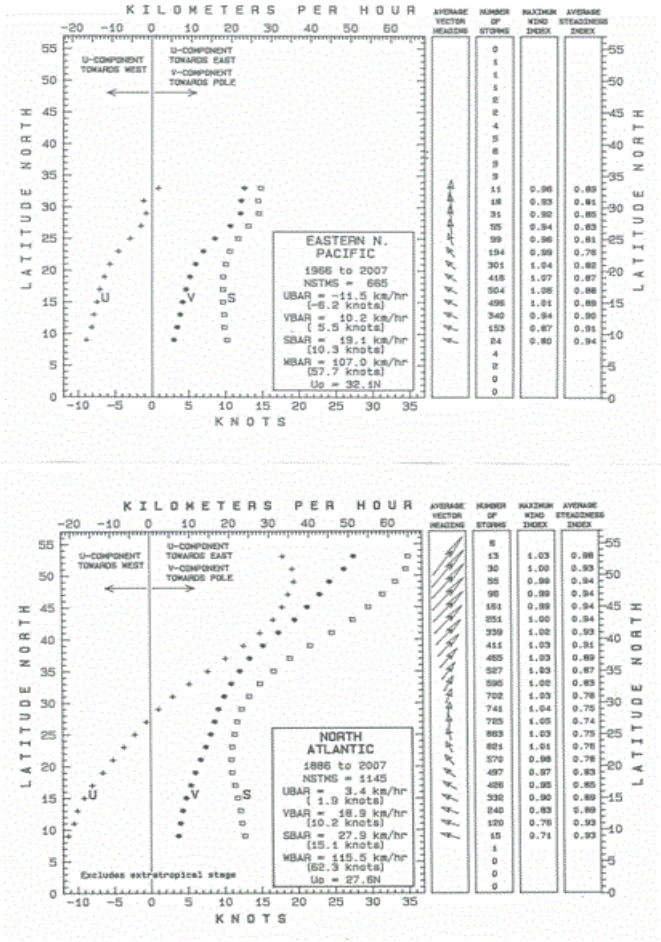

Figure 2.7. Meridional values of the steadiness index for the E. North Pacific and North Atlantic basins

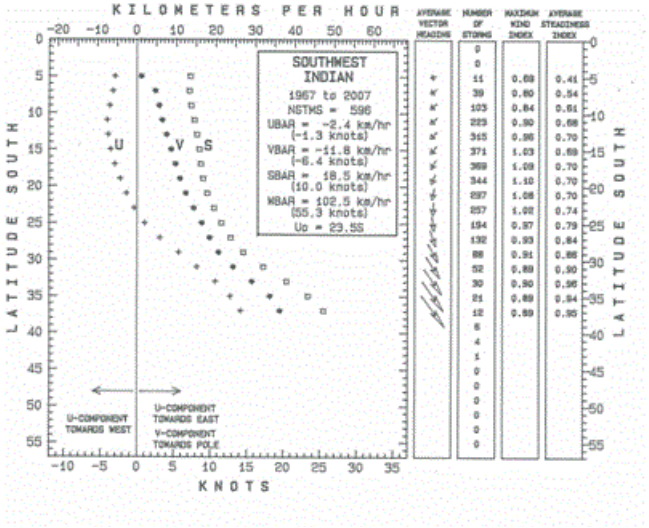

Figure 2.8. Meridional values of the steadiness index for the Southwest Indian basin.

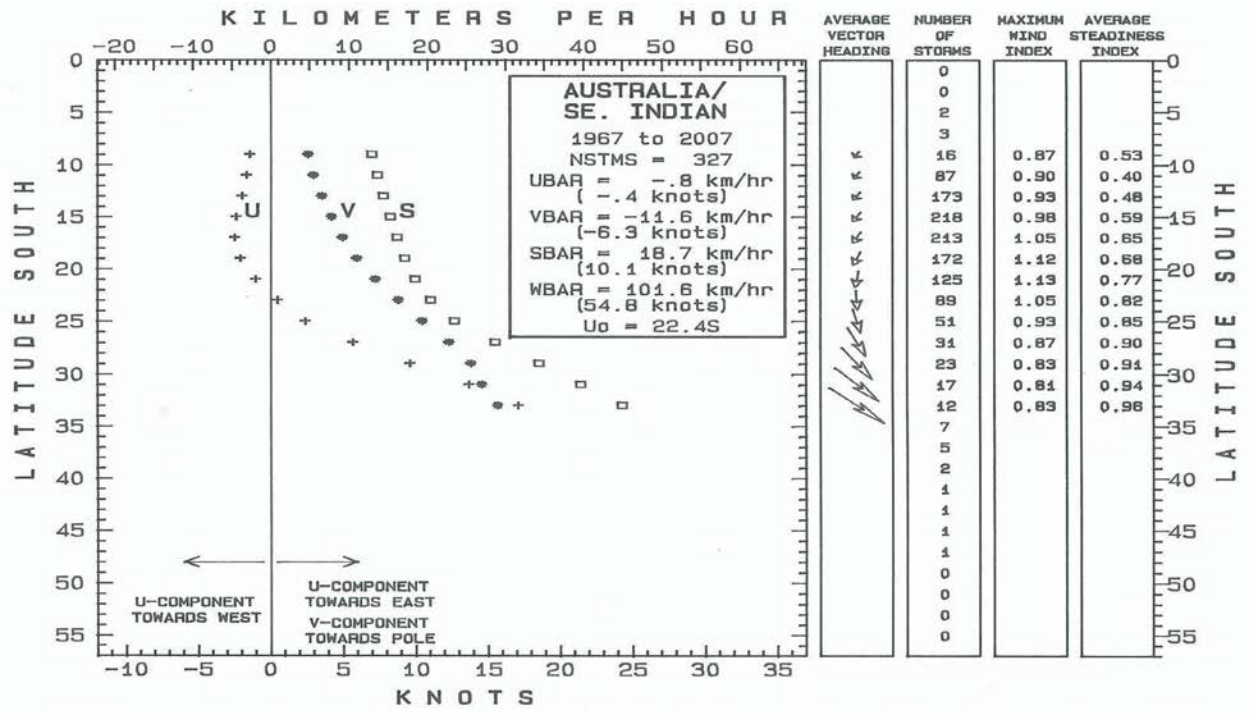

Figure 2.9. Meridional values of the steadiness index for the Australia / SE Indian basins.

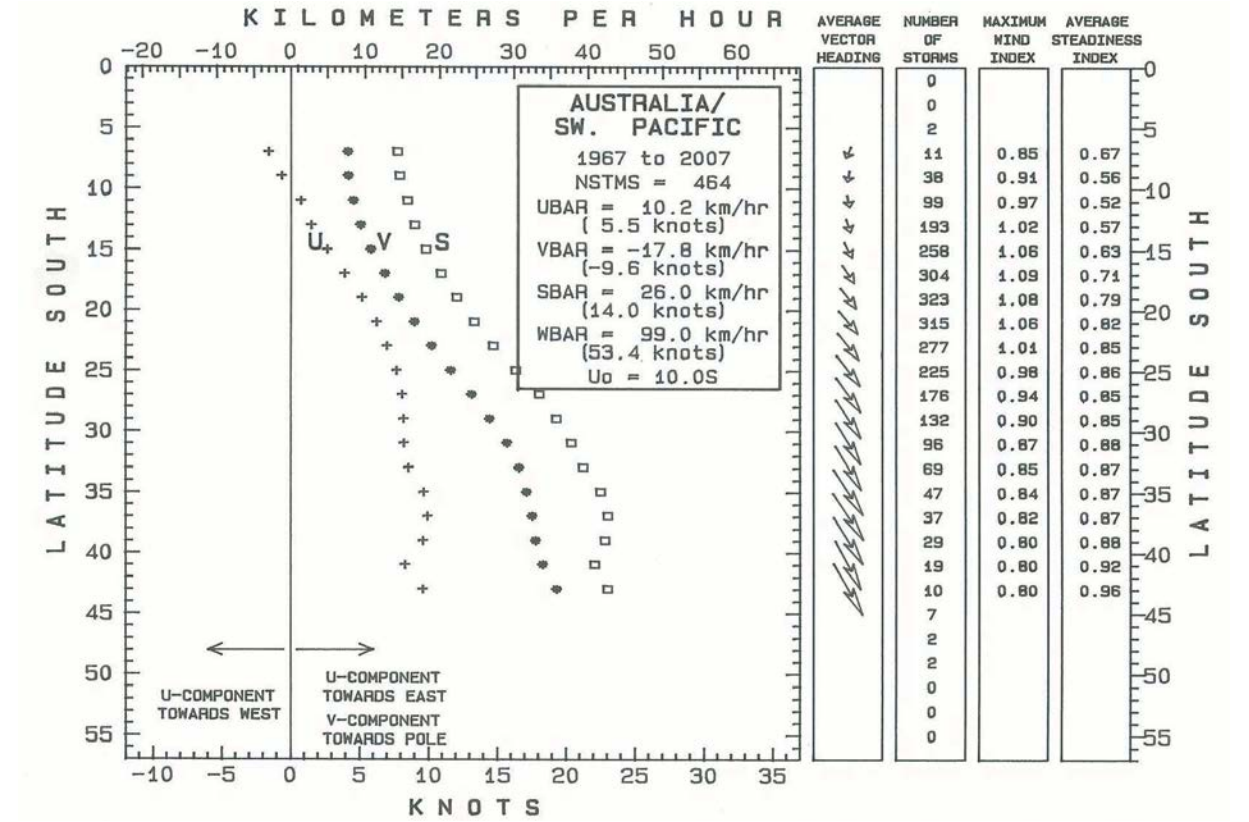

Figure 2.10. Meridional values of the steadiness index for the Australia / SW Pacific basins.

2.5 Intra-seasonal TC occurrence

Using the same global data set described earlier, Figs. 2.11 through 2.13 (shown on the next page) address the average day-to-day variation in tropical cyclone occurrence. Several authors (Holland, 1981; Murphy, 1988; Harper et al., 2008; Landsea, 1993) point out that not all TC's were detected in the pre-satellite era and that their intensities were under- or even over-estimated. Accordingly, there may be somewhat more tropical storm or hurricane area than shown on these charts. The data were smoothed using a moving-average period of 15-days. For very long periods of record, McAdie et al. (2008) find that, for charts of this type, a 9-day period is optimal for removing random data fluctuations while preserving known seasonal variations. However, the longer 15-day moving average used here is more applicable to relatively short period of records for the SH. The unit of measurement is *number of tropical cyclones per 100 years*. Use of this unit bypasses the problem of dealing with dissimilar periods of record.

In preparation of these figures, multiple TC occurrences on single days were included in the overall totals. Thus, the occurrence of three TC's on a given date and year would yield the same average as a single TC on the same date for each of three years. This counting methodology needs to be considered when making further interpretations of these data.

The Poisson probability function is useful in estimating the probability of, 0, 1, 2,...n, TC's occurring on single days (Xue and Neumann, 1984a). The Poisson distribution is given by $P(x) = e^{-m}m^x/x!$, where m is the mean occurrence over the desired period and x is the number of occurrences. For example, for the Australia/SW Pacific basin, the number of TC's per 100 years on 27 February is given on Fig. 2.12 as 55.9. According to the Poisson distribution*, this gives the theoretical probability ($0 \leq p \leq 1$) of 0, 1, 2 and ≥1 TC's on this date as 0.57, 0.32, 0.09 and 0.43, respectively.

These figures reveal much of the temporal character of the tropical cyclone activity over the various basins. Obviously, the seasonal shift between the two hemispheres is clearly shown. The western North Pacific is the only basin showing activity throughout the year but with a distinct minimum in mid-February. The season is also quite lengthy over the southwest Indian basin. The North Atlantic shows a sharp maximum near 10 September and another weak maximum around 10 October caused by the activation of a separate genesis region over the western Caribbean area. Other basins such as the North Indian exhibit more of a bimodal pattern caused by seasonal migration of the monsoon trough. Other than the above, it is uncertain whether some of the small-scale patterns are real or are due to an insufficient period of record. Additional details are provided by Frank (1987).

By summing individual basin daily values, Fig. 2.13 shows the global tropical cyclone daily occurrence pattern. The maximum near 10 Sept. is related to the greater NH activity while the

secondary maximum centered about 10 February is due to lessor SH activity. As would be expected, the two peaks are exactly six months apart. Minimum global activity is noted in late April/early May. In Fig. 2.13, there is also a suggestion that the percentage of tropical cyclones reaching the 64 kt threshold is somewhat greater in the Northern Hemisphere. More details for the Atlantic can be found in McAdie et al. (2008) and for the Australian area in BoM (1978).

$P(x) = e^{-m}.m^{x}/x!$, where m is mean occurrence over desired period and x is number of occurrences.

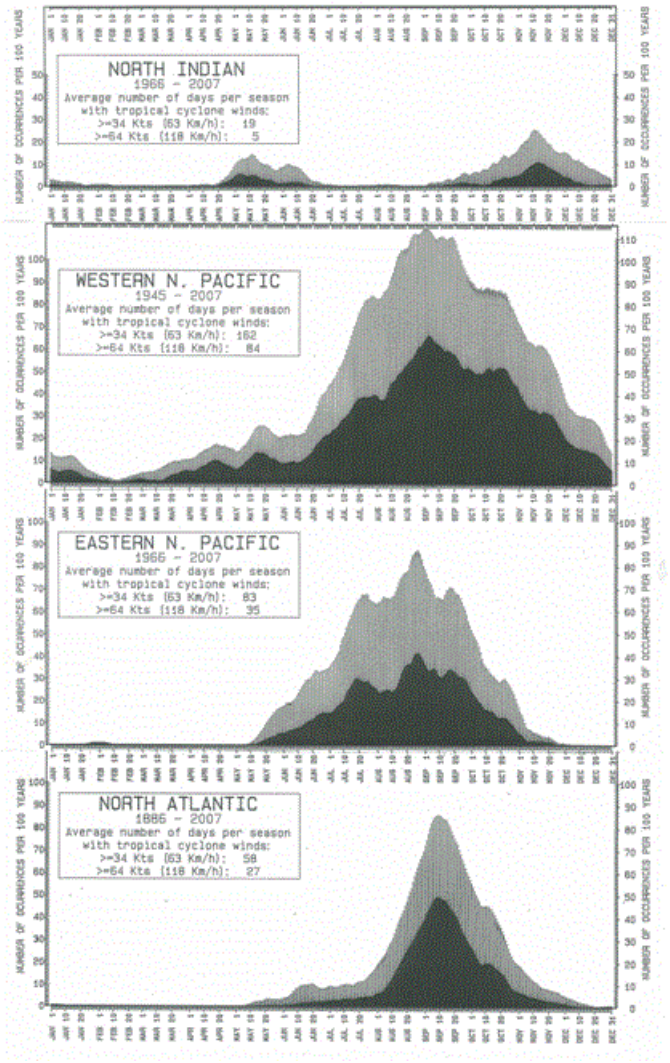

Figure 2.11. Average day-to-day variation in tropical cyclone (TC) occurrence for Northern Hemisphere basins. Gray area indicates TCs >34 kt (>63 km/hr) and black area indicates TCs >63 kt (>118 km/hr).

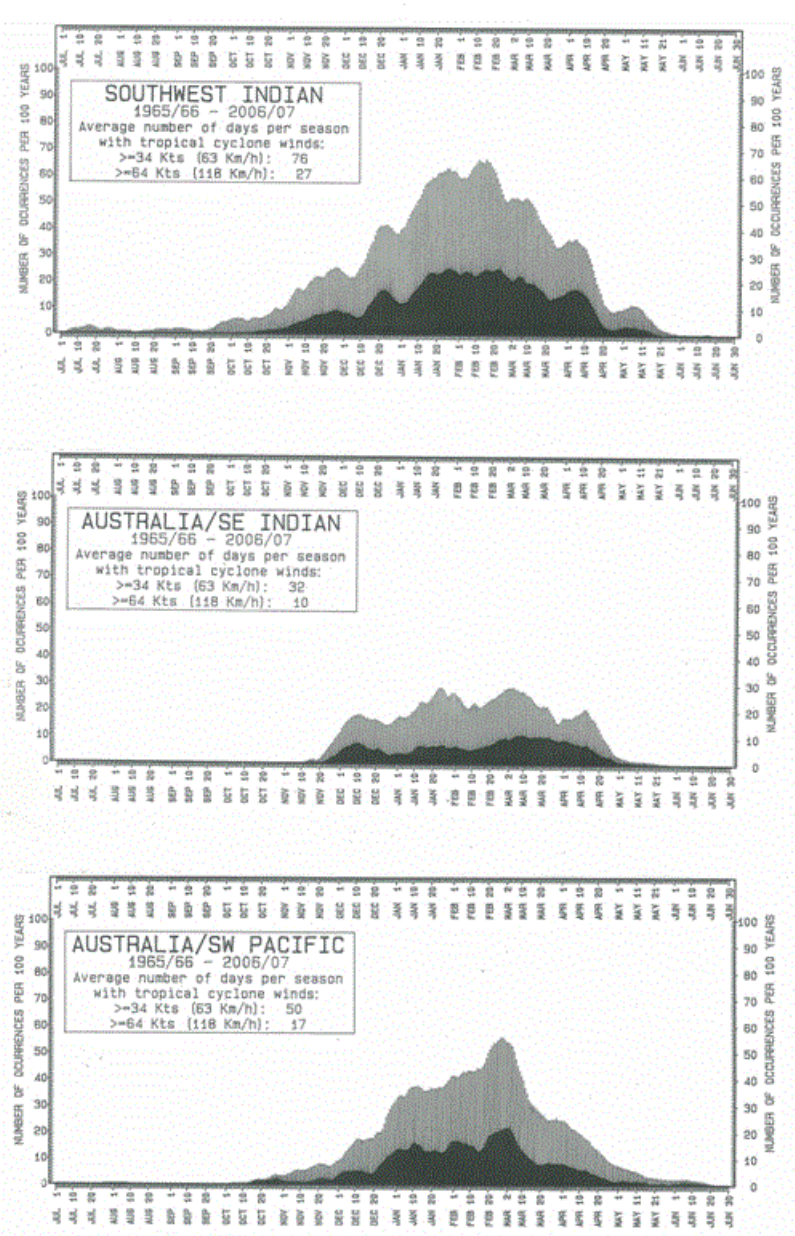

Figure 2.12. Average day-to-day variation in tropical cyclone (TC) occurrence for Southern Hemisphere basins. Gray area indicates TCs >34 kt (>63 km/hr) and black area indicates TCs >63 kt (>118 km/hr).

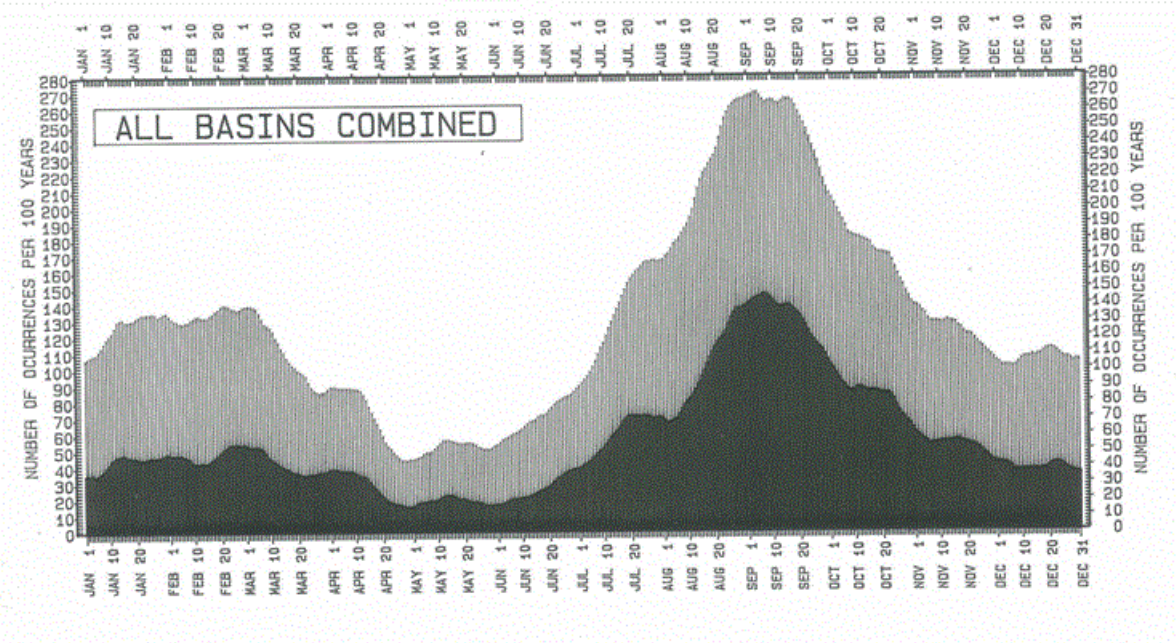

Figure 2.13. Average global day-to-day variation in tropical cyclone (TC) occurrence for all basins combined. Gray area indicates TCs >34 kt (>63 km/hr) and black area indicates TCs >63 kt (>118 km/hr).

2.6 Some statistical considerations

Further interpretation of climatic data often involves fitting to parent probability distributions or mathematical functions. This allows inferences to be made about gaps in the data or in making inferences beyond the range of the observational evidence. However, there are many pitfalls here. There is always the danger of selecting the wrong mathematical relationship or of trying to fit a multimodal set of data with a unimodal function. As stated by the pre-computer-age statistician Mills (1955), fitting of data to a mathematical function or distribution is often done on the grounds of "practicality or expedience". To this could be added: on the grounds of "convention" (Wilks, 2008, personal communication). If the parent distribution is difficult to identify and a long period of some event is available, it may be profitable to use empirical rather than mathematical probabilities.

Detailed discussion of statistical applications is well beyond the scope of this chapter. Only some of the more important issues, as they relate to TC's, will be discussed here. Readers are referred to the above authors for a more in-depth discussion.

2.6.1 Binomial and Poisson distributions

Building codes are often based on *n*-year wind events where *n* is often taken as 50- or 100-years. For structures with a high degree of hazard, such as nuclear power plants, much longer periods for some components of the construction are used. An *n*-year wind event is a wind

value that is equaled or exceeded on the average every *n* years. A closely related statistic is the recurrence interval or return-period, defined as the average number of years between an event. If this average is 50 years, then it is a 50-year event.

If, over a 50-year period, an event occurs for the first three years and not at all for the next 47 years or if it occurs at 25-, 15- and 10-year intervals, the average return year period of 50/3 or 16.7 years would be the same. Thus, *n*-year events need not occur every *n* years.

For randomly occurring events, it can be shown exactly by the binomial distribution and to a close approximation by the Poisson distribution that the percentage probability of an *n*-year event occurring at least once in *n* years is 63.4%; in 2*n* years, 86.6%; in 5*n* years, 99.3%. The chance of the event not occurring would be 100% minus those values. Meteorological events are often associated with large-scale atmospheric periodicities, which tend to lock in specific atmospheric patterns, such that the randomness requirement may be somewhat invalidated. However, experience has shown that the Poisson distribution gives reasonable TC event estimates.

2.6.2 Mixed distributions

2.6.2.1 TC motion (bivariate normal distribution)

One of the more useful distributions in tropical cyclone work is the bivariate normal. Five parameters are needed to define the distribution: the means of the x and y components, their standard deviations and the linear correlation coefficient between x and y components. The distribution was illustrated and briefly discussed in section 2.2.4. It is often used to describe tropical cyclone motion, forecast errors and strike probabilities (Sheets, 1984). A pitfall often ignored when fitting bivariate data thereto is the possibility that the data are bimodal rather than unimodal (Crutcher and Joiner, 1977).

A good example of the latter problem is given by Crutcher et al. (1982). The authors show that tropical cyclone forecast errors for the Atlantic basin come from more than one bivariate normal distribution. They also show that clustering algorithms can be used to sort the data into homogeneous sets.

Another example of this mixture problem can be found in areas where tropical cyclone tracks tend to diverge in a bimodal pattern. In the Atlantic, this occurs east of Barbados where tracks tend to move either with more of a poleward component north of the Leeward Islands or to continue westward into the Caribbean Sea. To a lesser extent, this same divergent pattern occurs off the northwest coast of Australia where some TC's continue westward or recurve southward.

2.6.2.2 TC wind (Weibull distribution)

The Weibull distribution (Tsokos, 1972; Abernethy et al., 1983) can be used to describe tropical cyclone maximum winds (Georgiou, 1985). However, one problem to be addressed in fitting TC maximum winds to this distribution (Neumann, 1987) is that the right tail extends to infinity whereas there are environmental constraints for TC maximum sustained winds going beyond certain limits. This concept of maximum possible intensity (MPI) is discussed by Emanuel (1986).

In the previous section, the problem of mixed data being fitted to the bivariate normal distribution was discussed. The same potential problem exists in fitting to other distributions such as the Weibull. This is illustrated in Fig. 2.14 where maximum wind data at three sites are fitted to this distribution. In the top panel, the fit is visually quite good and the mathematical probabilities can be used in place of the empirical values. At this coastal site, intensity data is reasonably reliable and the slight wind misfit could well have been within wind estimation error. Here, TC's make landfall from a unimodal direction distribution.

The Miami wind data depicted in the center panel of Fig. 2.14 are also quite reliable and the data suggest a secondary maximum wind peak in the class-intervals near 100 knots. This bimodal maximum wind distribution is probably related to the fact that the TC approach direction at this location mid-July through mid-September is from the south to east and more from the southwest in the early and late portions of the North Atlantic season. Making random selections from this distribution, as is often done in risk analysis, would underestimate winds in the 84 to 124 kt (156-230 km h^{-1}) range. Here, it might be necessary to make seasonal fits to the wind data.

In the lower panel of Fig. 2.14, for whatever the reason, the fit is completely unsatisfactory. Without further analyses, the Weibull function could not be used for a wind analysis at this site.

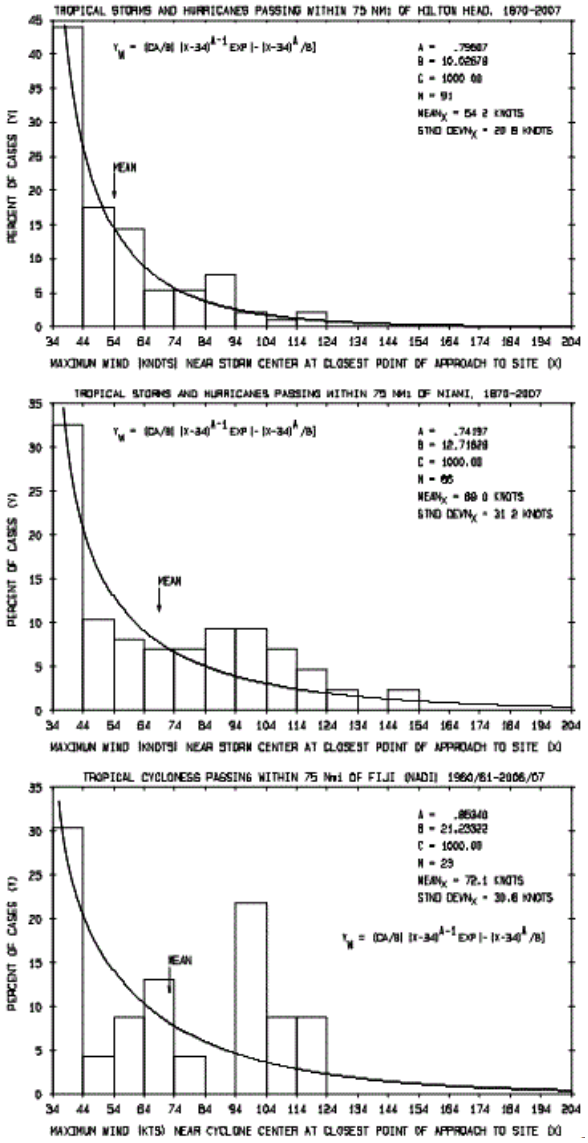

Figure 2.14. Example of good (top), marginal (center) and poor (bottom) fits of TC maximum wind to a Weibull distribution.

2.6.3 Other TC related distributions

Insofar as TC's are concerned, radius of maximum winds (RMW) data are often fitted to a log-normal distribution (Neumann, 1987; Georgiou, 1985; Batts et al., 1980). On the average, RMW is directly proportional to latitude and inversely proportional to TC intensity. Although the explained variance is rather small, RMW is often taken as an empirical function of these two TC parameters (Neumann, 1987).

Finally, the Gamma distribution (Hahn and Shapiro, 1967) is often used to describe variables bounded on one end by zero but unbounded on the other end. Thus, the distribution is often

used to describe rainfall amounts. As discussed by Neumann (1987), it could also be used in place of the Weibull distribution for TC winds.

2.6.4 Additional remarks

Many statistical applications require specification of the sample size. Because of serial correlation in meteorological time series, the true (uncorrelated) sample size is typically much less than the apparent sample size. Some of the TC aspects of this problem are discussed by Neumann (1979). However, the issue is quite complex and recommended references are to an old textbook on statistical methods in the social and economic sciences (Mills, 1955) and a new textbook on statistical methods in the atmospheric sciences (Wilks, 2006).

In the pre-computer age, fitting of large masses of data to mathematical functions and statistical distributions was tedious. However, the process was associated with a close scrutiny of the data and errors, inconsistencies and biases were often noted. TC data, now typically estimated or remotely sensed, are particularly vulnerable to these data problems and with modern computer technology, are easily overlooked. Accordingly, many of the discussions in this Chapter called attention to the data issue. As stated by the pre-computer age statistician Mills, (1955), "Wisdom in the selection of functions, time-units, strategic periods, etc., requires some understanding of the ground plan of nature in the particular field of study, as well as competence in the application of statistical techniques. The task of analysis is never purely mechanical."

The chapter is concluded with a blank section for inclusion of regional climatologies by local forecast offices.

2.7 References

Abernethy, R.B. J.E. Breneman, C.H. Medlin and G.L. Reinman, 1983: *Weibull Analysis Handbook*, AFWAL-TR-2079,USAF, Aero Propulsion Laboratory, Wright-Patterson AFB, 228 pp.

Akima, H., 1970: A new method of interpolation and smooth curve fitting based on local prodedures.*J. Assoc. Computing Mach.* **17**, 589-602.

Batts, M.E., M.R.Cordes, L.R. Russell, J.R. Shaver and E. Simiu, 1980: Hurricane wind speeds in the United States. *NBS Building Science Series* 124 , 41 pp.

Bell, G. D., M. S. Halpert, R. C. Schnell , R. W. Higgins, J. Lawrimore, V. E. Kousky, R. Tinker, W. Thiaw , M. Chelliah, and A. Artusa, 2000: Climate Assessment for 1999. *Bull. Amer.* Met. Soc., June 2000, pp. S1-S50.

Brand, S. and J.W. Blelloch, 1974: Changes in the Characteristics of Typhoons Crossing the Island of Taiwan. *Mon. Wea. Rev.,* **102**, 708-713

BoM, 1978: *The Australian Tropical Cyclone Forecasting Manual.* (Ed. A. B. Neal & G. J. Holland) Bureau of Meteorology, Melbourne, Australia, 274 pp.

Chenoweth, M. And C. Landsea, 2004: The San Diego hurricane of 2 October, 1858. *Bull. Amer. Meteor. Soc.*, **85**, 1689-1697.

Crutcher .H. L. and R. L. Joiner, 1977: Separation of Mixed Data Sets into Homogeneous Sets, *NOAA Technical Report* EDIS 19, Asheville, NC., 167 pp.

Crutcher, H. L., C. J. Neumann and J. R. Pelissier, 1982: Tropical cyclone forecast errors and the multinormal bivariate normal distribution. J. *Appl. Meteor*, **21**, 978-989.

Crutcher , H, L. and R. G. Quayle, 1974: *Mariner's worldwide guide to tropical storms at sea*. National Climatic Center and U. S. Navy, Asheville, NC., 114 pps. + 312 charts

Elsberry, R. L, 1987: Tropical Cyclone Motion. *A global view of tropical cyclones*. (ED. R.L. Elsberry), ONR Marine Meteorology Program, Arlington, VA, 91-128.

Emanuel, K.A., 1986: An Air-sea Interaction Theory for Tropical Cyclones. Part I. *J. Atmos. Sci.* **42**, 586-604.

Evans, J. L. and K. McKinley, 1998: Relative Timing of Tropical Storm Lifetime Maximum Intensity and Track Recurvature. *Meteorol. Atmos. Phys.,* **65,** 241-245.

Frank, W. M., 1987 : Tropical Cyclone Development. *A global view of tropical cyclones.*(Ed. R. L. Elsberry), ONR Marine Meteorology Program, Arlington, VA, 53-90

Georgiou, P.N., 1985: Design Wind Speeds in Tropical Cyclone Prone Regions. University of Western Ontario *Research Report* BLWT-2-1985, London, Ontario, Canada, 295pp.

Guard, C. P. and M. A. Lander, 1996: A wind-pressure relationahip for midget TC's in the western North Pacific. *Annual Tropical Cyclone Report (ACTR), JTWC*, page 311.

Hahn, G.J. and S.S. Shapiro, 1967: *Statistical Models in Engineering*. John Wiley & Sons, New York, NY, 354 pp.

Harper, B. A., S. A. Stroud, M. McCormick and S. West, 2008: A review of historical tropical cyclone intensity in Northwestern Australia and implications for climate change trend analysis. Aust. Met. Mag . 59, 121-141. .

Holland, G. J., 1981: On Quality of the Australian Tropical Cyclone Data Base. *Aus. Met. Mag.,* **29**, 169-181.

Hope, J. R., and C. J. Neumann, 1968: Probability of Tropical Cyclone Induced Winds at Cape Kennedy. *ESSA Technical Memorandum* SOS-1. 67 pp.

Hope, J. R. and C. J. Neumann, 1971: Computer methods applied to Atlantic area tropical cyclone climatology. *Mariner's Wea. Log*, **15**, 272-278.

Hsu, S.A., and B.W. Blanchard, 2008: Tropical Cyclone Destructive Potential by Integrated Kinetic Energy. *Bull. Amer. Meteor. Soc.*, **89**, pp. 1575-1576.

Kruk, M. C., K. R. Knapp, D. H. Levinson and J. P. Kossin (2008), National Climatic Data Center Global Tropical Cyclone Stewardship. *Preprints*, 28th Conference on Hurricanes and Tropical Meteorology, Orlando, AM S

Knaff, J.A., and R. M. Zehr, 2007: Re-examination of tropical cyclone wind-pressure relationships. *Wea. And Fcstng.*, 22, 71-78.

Knaff, J. A., 2008: Knaff, J. A. 2009, Revisiting the maximum intensity of recurving tropical cyclones. *Int. J. Climatol.,* **29** 827-837.

Landsea, C. W., C. Anderson, N. Charles, G. Clark, J. Dunion, J. Partagás, P. Hungerford, C. Neumann and M. Zimmer, 2003: "The Atlantic hurricane database re-analysis project." Chapter 7, *Hurricanes and Typhoons, Past, Present and Future*, R.J. Murnane and K. B. Liu, Editors, CLandsea, C. W., 1993: A Climatology of Intense (or Major) Hurricanes. *Mon. Wea. Rev.*, **121**, 1703-1713.

McAdie, C. J., C. W. Landsea, C. J. Neumann, J. E. David, E. S. Blake and G. R. Hammer 2008: Tropical cyclones of the North Atlantic Ocean, 1851-2006. *Historical Climatology Series 6-2*. NOAA, National Climatic Data Center,

Mills, F.C., 1955: *Statistical Methods*. Holt, Rinehart and Winston, New York, NY, 842 pp

Murnane, R. J., 2004: Chapter 9, page 252 of *Hurricanes and typhoons, past, present and future*. Richard J. Murnane and Kam-Biu Liu, editors. Columbia University Press, 462 pps.

Murphy, K., 1988: Correspondence, Aust. *Met. Mag.*, **36**, 227-228.

Neumann, C. J.,1952: *Wind estimations from Aerial Observations of Sea Conditions*. USN Weather Squadron Two (VJ-2), NAS, Jacksonville FL., 26 pp. (limited distribution)

Neumann, C. J., 1972: An alternate to the HURRAN tropical cyclone forecast system. *NOAA Technical Memorandum* NWS SR-62., 24 pp.

Neumann, C.J., 1979: *Operational techniques for forecasting tropical tyclone tntensity and movement.*, Chapter 4, World Meteorological Organization No. 528, pp. 4.21- 4.25 + appendices.

Neumann, C.J., 1981: Trends in forecasting the tracks of Atlantic tropical cyclones. *Bull. Amer. Met. Soc.*, **62**, 1473-1485.

Neumann, C. J., 1987: The National Hurricane Center risk analysis program (HURISK).*NOAA Technical Memorandum* NHC38, 56 pps.

Neumann, C.J., 1993: A global guide to tropical cyclone forecasting, Chapter 1.WMO *TD/560, pps. 1.1-1.42*

Neumann, C.J., 1996: *Minutes of the 50th Indepartmental Hurricane Conference*, U.S. Department of Commerce, NOAA, pp 1-2, Research presentations.

Neumann, C.J., 1999: The HURISK model: an adaptation for the Southern Hemisphere. SAIC Contract Report N00014-96-C-6015., Science Applications International Corporation, Monterey, CA, 53 pp.

Neumann, C.J., 2000: The Atlantic HURISK model: Adaptation to other tropical cyclone basins. Preprints, 24th Conf. on Hurricanes and Tropical Meteorology, Ft. Lauderdale, FL., Amer. Meteor. Soc., 549-550.

Pike, A.C. and C. J. Neumann, 1987: The variation of track forecast difficulty among tropical cyclone basins. *Wea and Fcstng.*, Vol. 2, No. 3, 237-241.

Powell, M.D. and T.A. Reinhold, 2007: Tropical cyclone destructive potential by integrated kinetic energy. *Bull. Amer. Meteor. Soc.*, **88**, 513-526.

Riehl, H. , (1972): Intensity of recurved typhoons. J. *Appl. Met.*, **11**, 613-615.

Sheets, R.C., 1984: The National Weather Service Hurricane Probability Program. *NOAA Technical Report* NWS 37, 70 pp.

Taylor, K.E., 1986: An analysis of the biases in traditional cyclone frequency maps. *Mon. Wea. Rev.*, Vol. 114, No. 8, 1481-1490

Tsokos, C.P. 1972: Probability Distributions: An Introduction to Probability Theory with Applications. Belmont, CA: Duxbury Press

Wilks, D. S. , 2006: *Statistical Methods in the Atmospheric Sciences*. 2nd Edition, Academic Press, 627 pp.

Xue, Z., and C.J. Neumann, 1984a: Frequency and motion of western North Pacific tropical cyclones. *NOAA Technical Memorandum NWS* NHC23, 84 pp.

Xue, Z., and C. J. Neumann, 1984b: A new frequency and motion climatology of western North Pacific tropical cyclones. Preprints, AMS 15th Conf. On Hurr. and Trop. Meteor., pp.107-114.

Yeh, T,-C. and R. L. Elsberry, 1993: Interaction of typhoons with the Taiwan orography. *Mon. Wea. Rev.*, **121**, 3193-3212.

Zehnder, J. A., 1993: The influence of large-scale topography on barotropic vortex motion. *J. Atmos. Sci.* **50**, 2519-2532.

Chapter Three

Todd B. Kimberlain and Micheal J. Breman
National Hurricane Center
NOAA/NWS/NCEP, Miami, Fl

3. Tropical Cyclone Motion

3.1 Introduction

While the prediction of tropical cyclone (TC) track remains a challenging problem, new tools to observe TCs have emerged in recent years to facilitate locating the TC center and estimating TC motion. The advent of new technology has coincided with remarkable progress in numerical weather prediction, which has helped to reduce typical TC track errors by half in the Atlantic basin at all lead times since 1990 (Rappaport et al. 2009). Similar improvement has been seen in the western North Pacific by the Japan Meteorological Agency and by the Joint Typhoon Warning Center. In fact, there has been dramatic improvement in all of the basins. This success is partially due to a tremendous increase in satellite data, which are particularly valuable in data-sparse regions such as the Tropics. The increase in observations and advances in data assimilation techniques have greatly improved the quality of initial condition analyses for regional and global dynamical models. The development of ensemble and consensus methods has also contributed to improvements in track forecasting. As a result of these advances, the performance of the regional and global dynamical models has far surpassed that of statistical and simple dynamical models.

This chapter describes contemporary approaches to analyzing TC position and forecasting TC track. The first section focuses on position analysis and the various observational platforms used in this task. A discussion of numerical model guidance applications and TC forecasting techniques follows in the second section, with particular emphasis on "ensemble" and "consensus" forecasting. The chapter concludes with a description of verification methods and their uses in an operational setting.

3.2 Position analysis

Construction of a best track

Operational best track

Locating the center of the TC is the first step in forecasting TC track, as it establishes the current motion of the cyclone. In an operational environment observations arrive from a wide array of platforms at different times. These observations contain errors, vary in spatial and temporal coverage, and can be unrepresentative and contradictory. This makes the

determination of the actual TC position and motion difficult. An accurate current motion estimate is important for diagnosing the interaction of the TC with the surrounding environment, evaluating the quality of the current forecast, and initializing some computer models.

A center "fix" can be obtained by using any or all of the observational platforms described in the sections that follow. As a forecaster examines the fixes, determining the current position depends on the confidence in the observations and the forecaster's judgment. For example, when the current position uncertainty is high (i.e., in the case of a poorly defined system or a system at night), a heavy reliance should be given to the previous positions established with greater confidence (i.e., during the daytime or when the center was better defined). Position estimates made with high confidence may also be helpful in revising the best track during the previous 24-hour period.

After determining a preliminary position, the TC motion can be computed. The time period over which the current motion is calculated depends on the steadiness of the motion and the confidence in the accuracy of the center fix, with the goal of minimizing unrepresentative short-term motions such as trochoidal motion or other wobbles (Lawrence and Mayfield 1977).

The track should be smoothed over this time period, and the re-analysis can be extended further in time if new data become available. A typical smoothing period for estimating the initial motion might be 18 hours, somewhat longer when uncertainty with regard to initial position is high (e.g., a poorly-defined IR fix) and somewhat less when the uncertainty is low (e.g., a good radar fix). Then, the bearing and speed of the TC are computed, and the new motion estimate is compared to that from the previous forecast cycle to ensure realistic values. Striking a balance between the high and low confidence scenarios described above is key to the process of maintaining an operational best track. When late satellite or synoptic data arrive, that data should be assessed, and if necessary, appropriate adjustments should be made to the working best track in order to improve the TC motion vector.

Construction of a final best track

A post-analysis review of operational track positions with data from a wide variety of sources should be conducted to optimally re-construct the best track of a TC. This type of analysis is generally not possible in real-time, since the "working best track" is developed under tight time constraints, when some data may not be available. The final product should satisfy the basic components of an accepted "best track" definition such as the one currently in place at the NHC:

"A subjectively-smoothed representation of a TC's location and intensity over its lifetime. The best track contains the cyclone's latitude, longitude, maximum sustained surface wind, and minimum sea-level pressure at six-hourly intervals. Best track positions and intensities, which are based on a post-storm assessment of all available data, may differ from values contained in storm advisories. They also generally will not reflect the erratic motion implied by connecting individual center fixes."

A major consideration is the degree of detail to furnish when preparing the "best track." A fundamental part of NHC's "best track" definition is the six-hourly representative estimates of the cyclone's center location. Plotted raw fix data often reveal a series of irregular movements, which do not generally persist for more than a few hours (refer to the short-term motion section below). Short-term track wobbles are not representative of the overall TC motion, and a subjectively-smoothed "best track" that does not focus on these short period, transient motions is ideal.

Some forecasters have interpreted this to mean that, if a TC is, in fact, located at a given position at 0600 UTC, the "best track" need not lie exactly at that location in post-analysis. From a sampling perspective, the re-positioning that results from the smoothing process is part of a filtering procedure that could be administered to avoid aliasing small-scale noise. For a time series with data points ΔT apart, the smallest wavelength which can be depicted accurately is about 4 x ΔT. Since the typical advisory analysis times are six hours apart, the smallest periods which can be adequately represented are on the order of 24 hours. Thus the analyst might try to avoid analyzing oscillations with a period less than 24 hours.

The final best track estimate often differs a little from the real time advisory estimate because the former is meant to represent a particular time, while the latter is meant to be *valid* at a particular time.

Satellite fixes

The most common method of fixing a TC's location is through the use of geostationary satellite imagery. These satellites provide high temporal resolution visible and infrared (IR) imagery and are the primary tool for TC center fixing. Geostationary images can also be animated and modified with color enhancements that correspond to various brightness temperatures to help determine the location and motion of a TC center. In many cases, animating visible satellite imagery to examine low cloud motions is a reliable way to identify a TC center. However, if available, ocean vector wind data and 37 GHz microwave data can help refine the surface center position.

At night it is often difficult to distinguish between low and high clouds in IR imagery, complicating the center fixing of weaker TCs. Nighttime "visible" imagery (Ellrod 1995) was developed to supplement conventional IR imagery for TC center fixing (Jiann-Gwo Jiing, personal communication). This imagery is created by merging the shortwave IR (3.9 micron) and longwave IR (11 micron) windows. The radiative properties of the shortwave window allow for the identification of low cloud features, while the longwave channel is more sensitive to the tops of deep convective clouds.

Therefore, the merged product is useful for locating the center of sheared or poorly-organized TCs. However, its utility is limited if the low cloud pattern is obscured by cirrus. If available, 37 GHz microwave imagery can reveal the low-level center of sheared systems, even though the center is obscured by overlying cirrus.

A major consideration is the degree of detail to furnish when preparing the "best track." A fundamental part of NHC's "best track" definition is the six-hourly representative estimates of the cyclone's center location. Plotted raw fix data often reveal a series of irregular movements, which do not generally persist for more than a few hours (refer to the short-term motion section below). Short-term track wobbles are not representative of the overall TC motion, and a subjectively-smoothed "best track" that does not focus on these short period, transient motions is ideal.

Some forecasters have interpreted this to mean that, if a TC is, in fact, located at a given position at 0600 UTC, the "best track" need not lie exactly at that location in post-analysis. From a sampling perspective, the re-positioning that results from the smoothing process is part of a filtering procedure that could be administered to avoid aliasing small-scale noise. For a time series with data points ΔT apart, the smallest wavelength which can be depicted accurately is about $4 \times \Delta T$. Since the typical advisory analysis times are six hours apart, the smallest periods which can be adequately represented are on the order of 24 hours. Thus the analyst might try to avoid analyzing oscillations with a period less than 24 hours.

The final best track estimate often differs a little from the real time advisory estimate because the former is meant to represent a particular time, while the latter is meant to be *valid* at a particular time.

Satellite fixes

The most common method of fixing a TC's location is through the use of geostationary satellite imagery. These satellites provide high temporal resolution visible and infrared (IR) imagery and are the primary tool for TC center fixing. Geostationary images can also be animated and modified with color enhancements that correspond to various brightness temperatures to help determine the location and motion of a TC center. In many cases, animating visible satellite imagery to examine low cloud motions is a reliable way to identify a TC center. However, if available, ocean vector wind data and 37 GHz microwave data can help refine the surface center position.

At night it is often difficult to distinguish between low and high clouds in IR imagery, complicating the center fixing of weaker TCs. Nighttime "visible" imagery (Ellrod 1995) was developed to supplement conventional IR imagery for TC center fixing (Jiann-Gwo Jiing, personal communication). This imagery is created by merging the shortwave IR (3.9 micron) and longwave IR (11 micron) windows. The radiative properties of the shortwave window allow for the identification of low cloud features, while the longwave channel is more sensitive to the tops of deep convective clouds.

Therefore, the merged product is useful for locating the center of sheared or poorly-organized TCs. However, its utility is limited if the low cloud pattern is obscured by cirrus. If available, 37 GHz microwave imagery can reveal the low-level center of sheared systems, even though the center is obscured by overlying cirrus.

Rules for locating the TC center with satellite imagery are contained in the Enhanced Infrared (EIR) version of the Dvorak (1984) technique. Figure 3.1 illustrates the typical cloud pattern evolution of TCs and how using pattern recognition can help the analyst determine the cloud system center (CSC). In addition to using the pictographs in Figure 3.1, several other methods such as drawing lines to visualize the curvature of bands and looping images at different speeds can also be used (Dvorak (1984, 1995). In the Dvorak technique, an accurate intensity analysis often requires an accurate center position. In fact, the Dvorak technique "assumes" that you "know" where the center is located.

Using satellite imagery to identify the CSC does have limitations. For example, it is possible to mistake a mid-level center for the low-level center in weak or sheared systems. Also, mid- or high-level clouds may obscure the low-level center. The presence of multiple centers, especially within a broad monsoon disturbance, can also be a complicating factor. In this situation, the analyst should estimate a centroid location of the overall circulation and not focus on a single center.

While conventional satellite imagery is vital to operational TC forecasting, aircraft reconnaissance data, if available, are nearly always favored over these satellite observations since aircraft fixes are in situ and are generally more accurate than satellite-based fixes. A National Hurricane Center (NHC) study showed that about a quarter of all satellite position estimates were in error by at least 20 nm, while aircraft reconnaissance position estimates had smaller errors when compared to final best track data. (Of course, aircraft data, when available, are somewhat more heavily weighted in the production of the best track.)

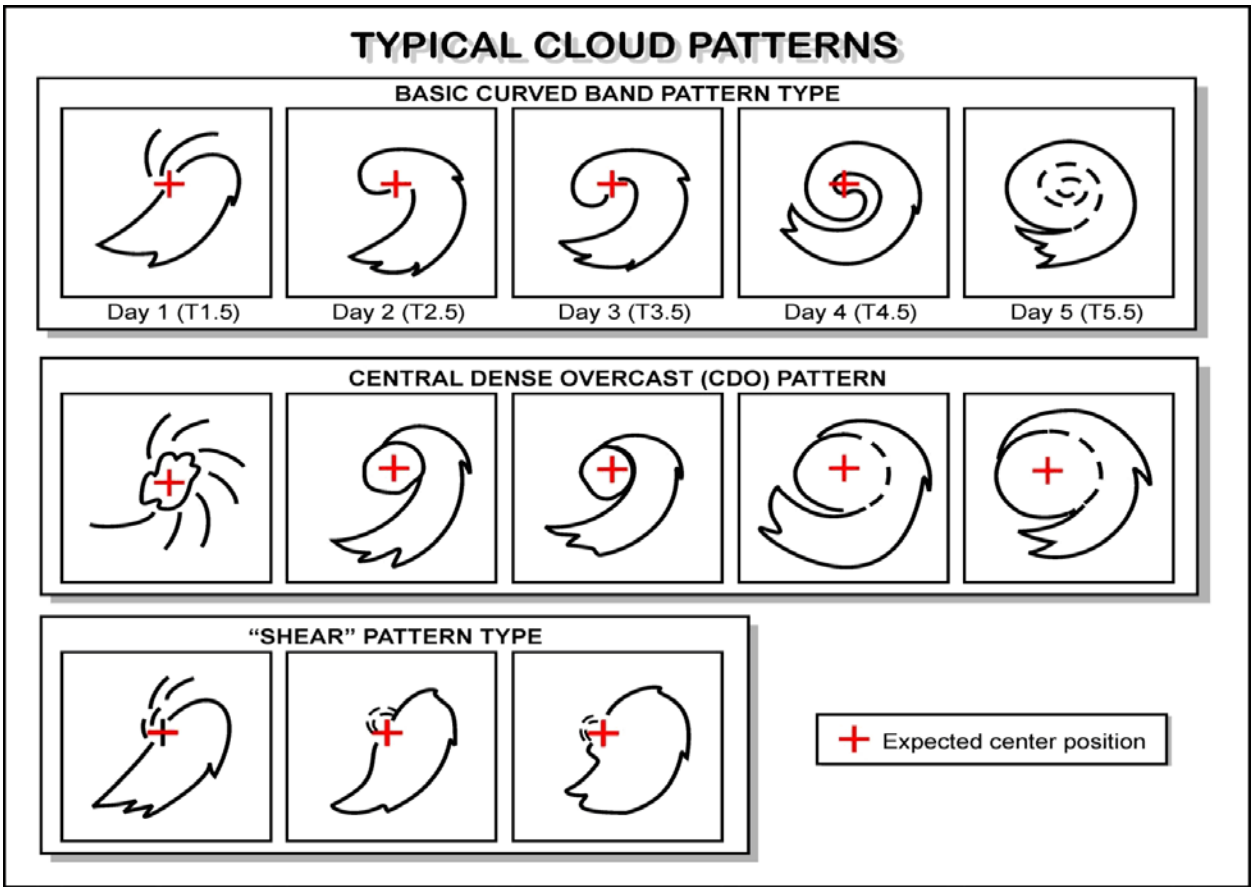

Figure 3.1. Typical cloud pattern evolution of an idealized TC, using the EIR Dvorak technique. The basic curved band (top row), CDO (middle row), or "shear" pattern types (bottom row) with a standard developmental curve from left to right can be used to determine the CSC. Reproduced from Dvorak (1995).

Proper application of the Dvorak technique requires considerable training and practice. The original visual Dvorak technique has different application rules than the EIR technique. Intensity aspects of the technique are discussed in Chapter 4.

Microwave satellite data

The availability of microwave data for TC center fixing from low-earth orbiting satellites has increased in recent years. Passive radiometers sense emitted microwave radiation over a wide range of wavelengths, enabling them to see through clouds and discern structures difficult to observe using visible and infrared satellite imagery.

Instrumentation

As of 2010, a total of 13 low Earth orbiting (LEO) satellites were operational (Table 3.1)
.

Table 3.1. Current suite of microwave polar orbiting instruments and the associated satellite.

Satellite	Instrument	Operating Since	Scan Strategy/ Type	Frequency (GHz)	No. of Channels	Resolution (km)	Swath Width (km)
NASA/DoD Coriolis	Windsat	2003-	conical, imager	6.8-37[1]	22	11-55	1025
NASA/JAXA TRMM	TRMM (TMI)	1997-	conical, imager	10.65-85.5	9	5-50	780
Metop-A[%]	AMSU-A AMSU-B ASCAT	2006-	cross-track, sounder scatterometer	23.8-89 85-183.31 5.25	15 5	48 16 50(25)	1650 1650 2520
F-15 F-18	SSM/T2 SSM/I	1987- 2009-	cross-track, sounder	92-183	5	*309 (85-213)[#]	1400
DMSP(F-16, F-17, F-18)	SSMIS	2004-	conical, imager & sounder	19-183	24	12-55	1700
Aqua	AMSR-E	2002-	conical, imager	6.9-89	14	5-50	1600
NOAA-15 NOAA-16 NOAA-18	AMSU	1998- 2000- 2005-	cross-track, sounder	50-183	20	**50 (16)[@] **150 (50)[#]	2200

1 WindSat channels at 10.7, 18.7, and 37 GHz are fully polarimetric
@ at nadir
# at limb
$ pulse, fixed-point radar
% METOP-B to be launched in 2012

A description of selected instruments is provided below:

- The Tropical Rainfall Measuring Mission (TRMM) flies in a near-equatorial orbit, measuring rainfall and other rainfall-related parameters using two different sensors. The passive TRMM Microwave Imager (TMI) detects rainfall by measuring the intensity of backscattered radiation at five frequencies between 10.7 and 85 GHz. As a consequence of its lower orbital altitude, the satellite has smaller footprint sizes and higher resolution (6 km). The TMI is frequently used for TC observation because its mid-Earth orbit is confined to the region between 35°N and 35°S.
- The Advanced Microwave Sounding Unit-B (AMSU-B) is a passive instrument on the NOAA series of polar-orbiting satellites. The AMSU instrument looks cross-track and therefore its scan angle varies with distance from nadir.
- METOP-A is the first in a series of three polar-orbiting satellites flown by the European Space Agency (ESA) carrying a high-resolution microwave imager similar to the AMSU-B found on the NOAA satellites.
- The Special Sensor Microwave Imager (SSM/I) is a microwave instrument onboard Defense Meteorological Satellite Program (DMSP) satellites.
- The SSMIS instrument is a follow-on and replacement for to the SSM/I. SSMIS is a passive, conically-scanning radiometer that has more spectral channels and a wider swath width than the SSM/I (1700 km compared to 1400 km).
- WindSat is one of two payloads aboard the U.S. Navy's Coriolis satellite launched in 2003. It can measure wind speed and direction, although not reliably in the heavy rain environment of a TC's inner core. The multi-frequency polarimetric radiometer passively measures emitted microwave radiation at five frequencies from 6.8 to 37 GHz. WindSat is a conical scanner with resolution about three times higher than the SSM/I.
- The Advancing Microwave Sounding Radiometer — Eos (AMSR-E) is a passive conically-scanning instrument flying on the NASA Aqua research satellite. It senses microwave radiation at 12 different channels at six frequencies from 6.9 to 89 GHz.

The analyst can obtain a myriad of real-time and archived microwave imagery from the U.S. Navy's NRL located at: http://www.nrlmry.navy.mil/tc_pages/tc_home.html.

Interpretation of microwave imagery

Data obtained at 85 to 91 GHz are primarily used to observe deep convective clouds, especially in the TC core. Within this region of the electromagnetic spectrum, cloud water droplets near the freezing level deplete upwelling microwave radiation. Since non-precipitating cirrus has

little effect on radiation at this wavelength, the remaining upwelled radiation is released to space, where satellites can observe it. The effects of scattering and absorption reduce the net microwave radiation aloft, making satellite brightness temperatures appear cold.

An example of deep convective and cirrus clouds obscuring the center of developing eastern North Pacific Tropical Storm Georgette at 0411 UTC 27 August 2004 is shown in Figure 3.2. While the center is not apparent in the geostationary IR imagery (Fig. 3.2a,b), 85-GHz imagery from the SSM/I (Fig. 3.2c,d) clearly shows the exposed low-level center of the developing TC at the edge of the convective canopy.

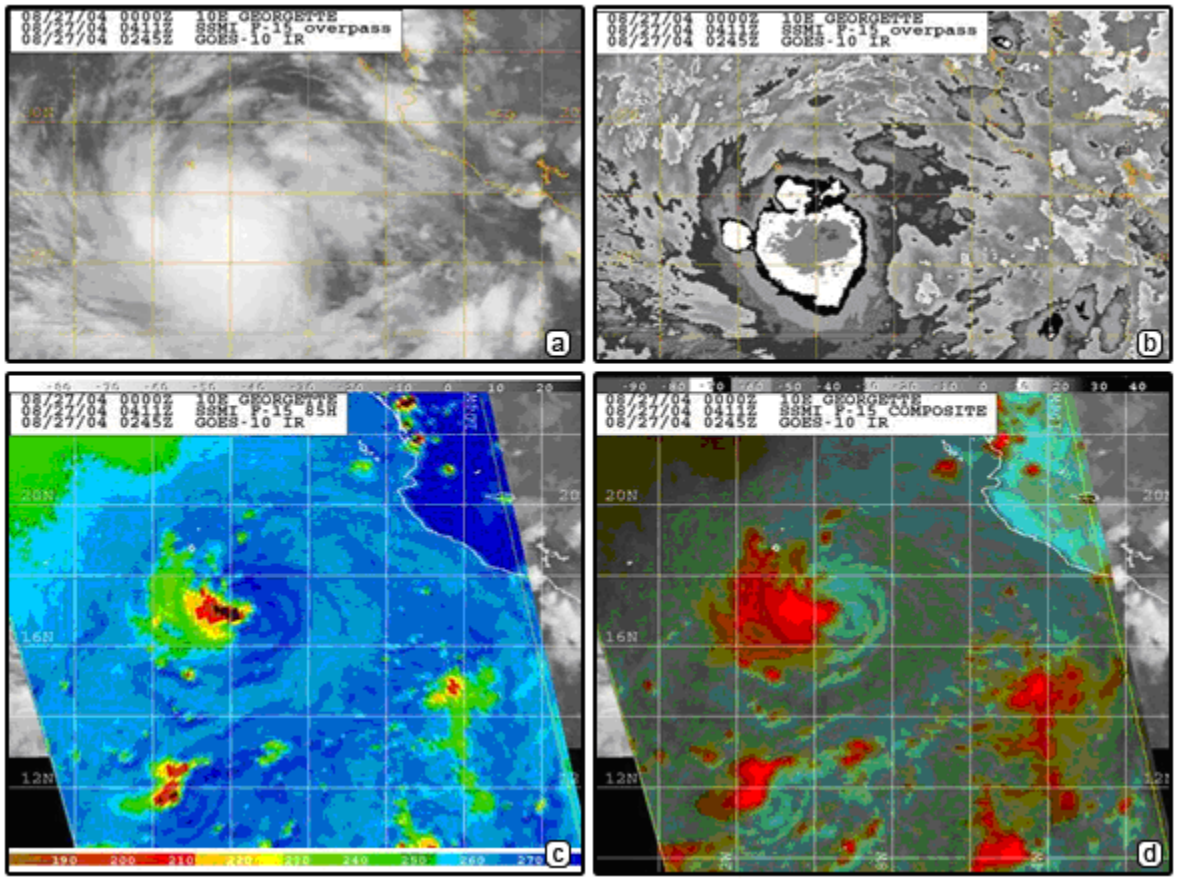

Figure 3.2. (a and b) IR satellite imagery of Tropical Storm Georgette from 0245 UTC 27 August 2004, with no enhancement in (a) and the standard BD Dvorak curve in (b). (c) SSM/I 85 GHz H pass from 0411 UTC over Georgette and (d) the composite image for the pass, illustrating the exposed low-level center located near 16.8N 109.1W.Data at lower frequencies (e.g., 37 GHz) are used to identify low cloud features. Emission and absorption of microwave radiation by hydrometeors near and below the freezing level is minimal at this frequency, making observed brightness temperatures in areas of low clouds and precipitation appear warm.

Comparing data from 85-91 GHz and 37 GHz can help determine if the TC is experiencing vertical wind shear. Imagery at 85-91 GHz reveals features at middle- to upper-levels and can show the location of a mid-level center while imagery from 37 GHz can reveal low cloud features indicative of the low-level center position. Therefore, center fixes from these two channels may not be in agreement if the TC is sheared. The 37-GHz imager is better suited for

center fixes in weaker or sheared TCs, even though it is of lower resolution than the higher frequency channels on most satellites.

Microwave radiation emitted from the Earth's surface and elsewhere in the atmosphere is initially unpolarized but its interaction with different atmospheric or Earth constituents can cause it to become partially polarized. This makes it possible to determine certain characteristics of the environment through which it is passing. For example, land and water differences become apparent when comparing horizontally polarized emissions at low microwave frequencies. The contrast between land, water, low clouds, or the ocean is more distinct when comparing composite microwave images of both horizontal and vertical polarizations against those from high and low frequency channels and can help to distinguish important features (as discussed next).

Analysts should examine multiple channels/frequencies, polarizations, and composite images to determine the TC center location. Combining and cross-referencing center fixes obtained from multiple images can increase confidence in the TC position estimate. A brief, step-by-step procedure providing center fixes from an analysis of microwave images follows.

A good starting point is to evaluate high and low frequency single polarization images. The 85-91 GHz images are easy to interpret because the cloud liquid water in low clouds (warm rain processes) at outer radii appears warm (darker blue in Fig. 3.3), while significantly colder brightness temperatures (yellows and red) depict radiometrically cold convective tops at a much higher level surrounding the eye. Next, lower frequency polarized images (e.g., Figs. 3.4-3.5) should be evaluated. Condensate in low clouds and rainbands appear warm relative to the radiometrically cold ocean surface at lower frequencies (Fig. 3.4). The warmest brightness temperatures are coincident with the greatest concentration of low-level cloud liquid water in the inner core. The center of incipient systems can sometimes be difficult to locate since increasing low-level convergence of cloud liquid water near the vortex can mask the center.

Finally, the analyst should evaluate both high and low frequency color composite images, which use the Polarization Correction Temperature (PCT) solution to discriminate intense convection from both single polarized images. On the PCT image, one should focus on the blue-green colors, which primarily denote low-level clouds. In stronger storms, the TC center can be located by looking for a dark spot on the low frequency composite image, which should be the rain-free dry region.

Figure 3.5 shows an example of a 37-GHz PCT image, where blue-green streamers indicate low cloud bands and reds and pinks indicate well-developed convective clouds. A dark green spot, representing an area that is the same temperature as the ocean surface, indicates the cloud-free eye. Analysis of multiple images (preferably within six hours of the analysis time) can increase the chances of correctly identifying the TC center. These sequential multiple images can be animated to improve center location of poorly organized systems (Edson, personal communication).

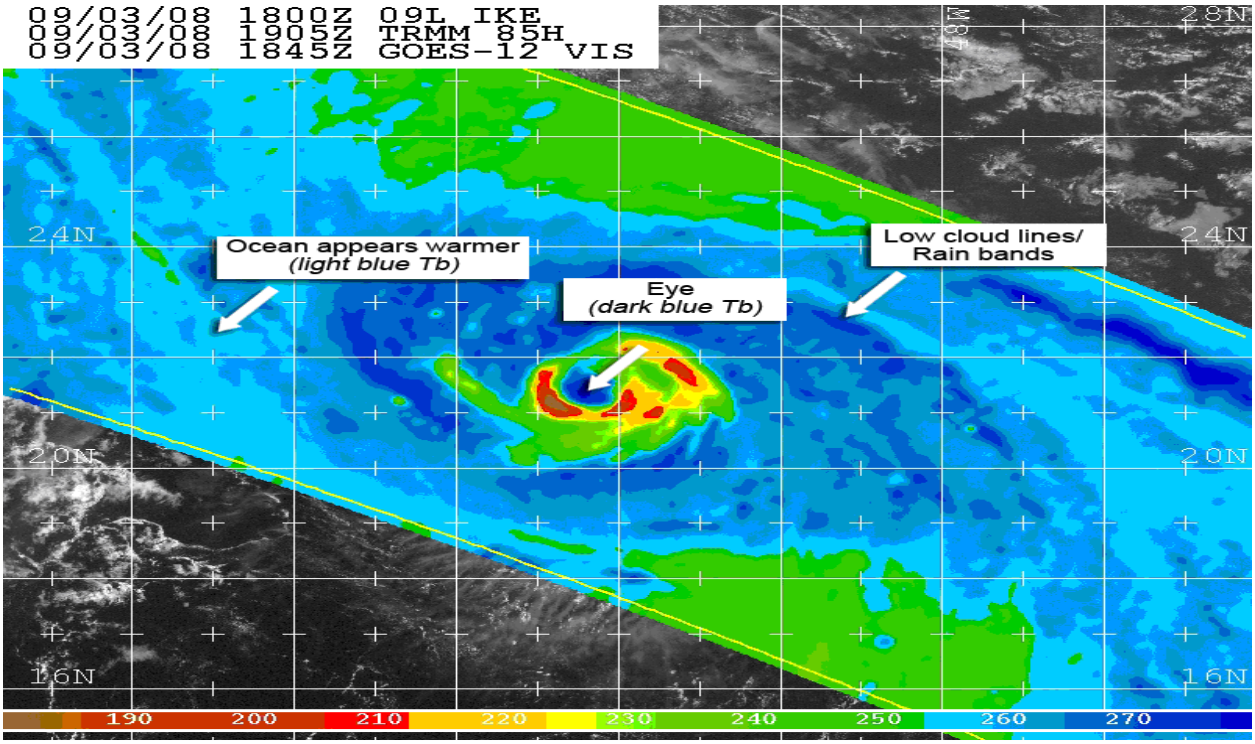

Figure 3.3. TRMM 85-GHz H-pol image over Hurricane Ike at 1905 UTC 3 September 2008. Brightness temperature (K) is indicated by the scale at the bottom of the figure. Image courtesy of the U.S. Naval Research Laboratory.

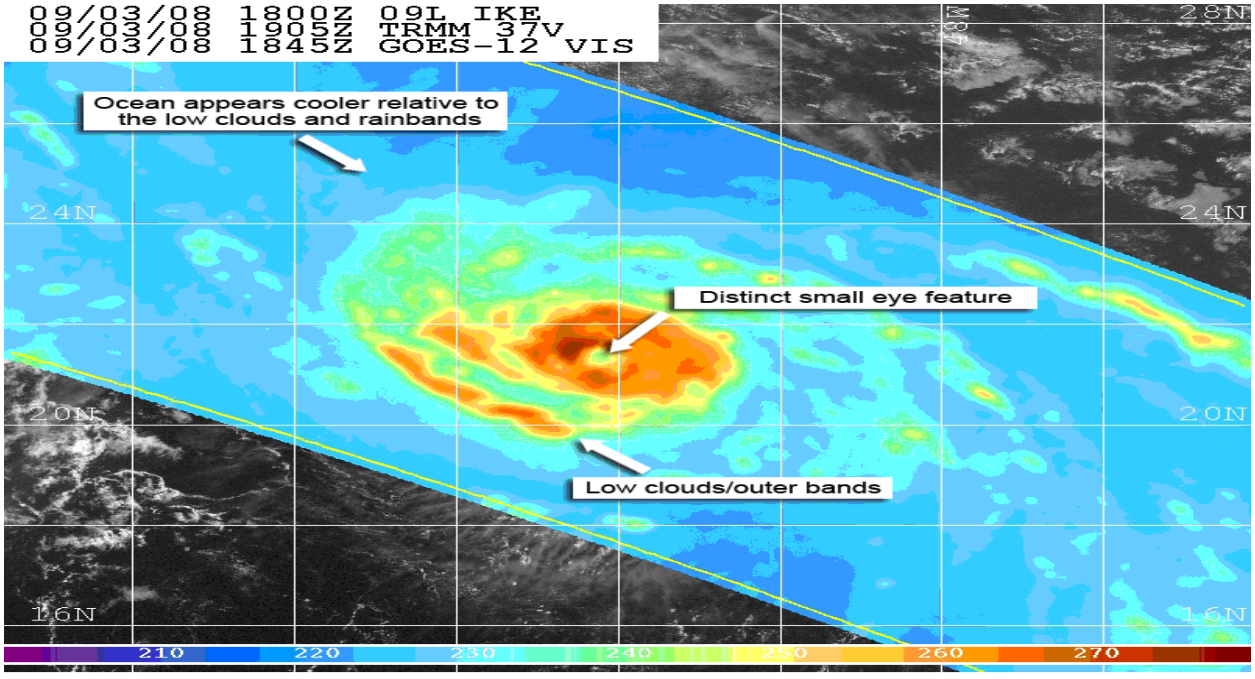

Figure 3.4. As in Fig. 3.3, except TRMM 37-GHz V-pol image. Image courtesy of the U.S. Naval Research Laboratory.

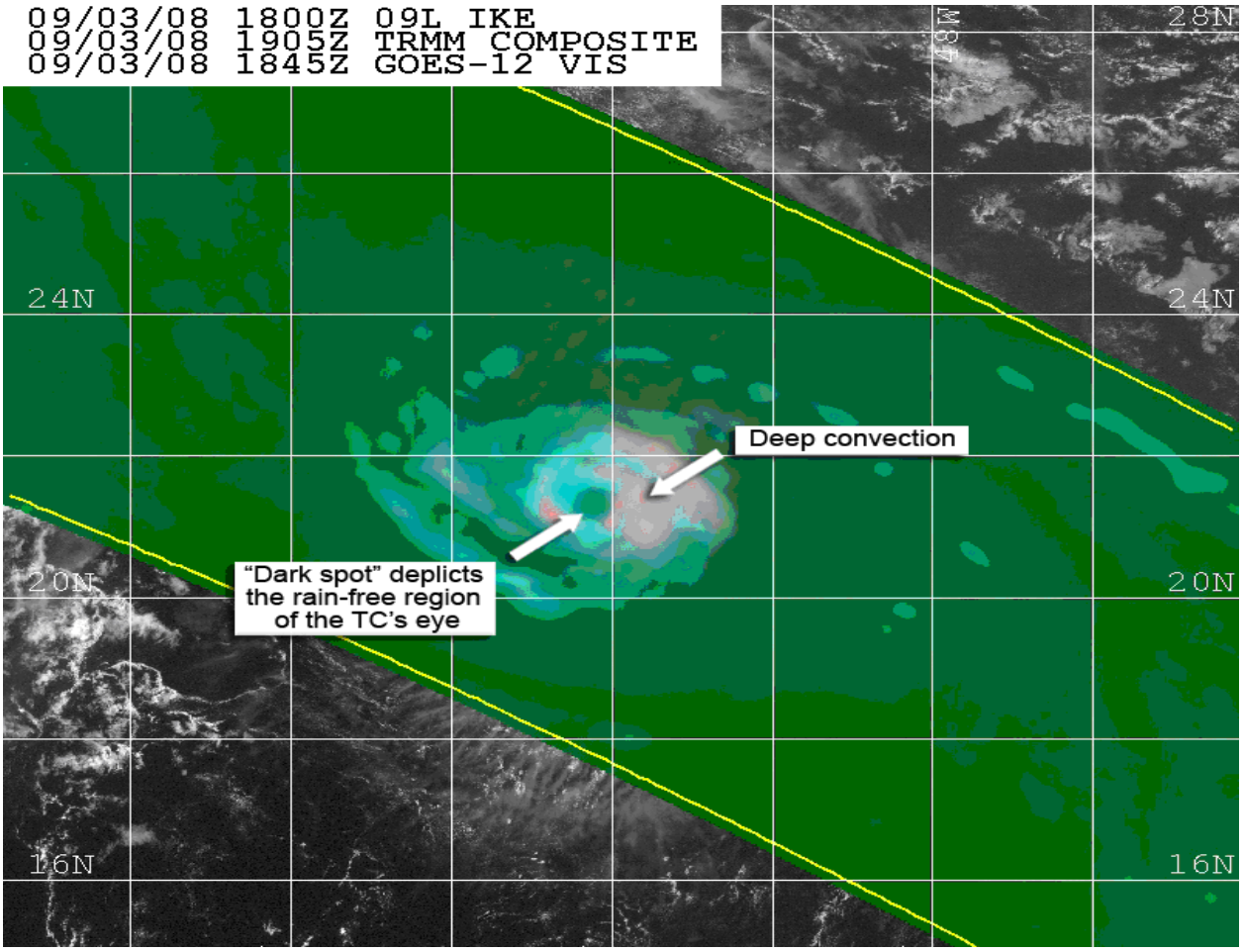

Figure 3.5. As in Fig. 3.3, except TRMM 37-GHz Polarization Correction Temperature (PCT) image. Image courtesy of the U.S. Naval Research Laboratory.

Scanners onboard the various low earth-orbiting satellites are either cross-track or conical. Conical-scanning instruments look forward at a fixed angle with a rotating antenna, and footprints of equal size provide the same resolution across the entire swath (Fig. 3.6a). Cross-track instruments scan at varying angles as the instrument points away from nadir. As a result, these imagers have degraded resolution near the edge of the scan, where the footprint size is larger (Fig. 3.6b).

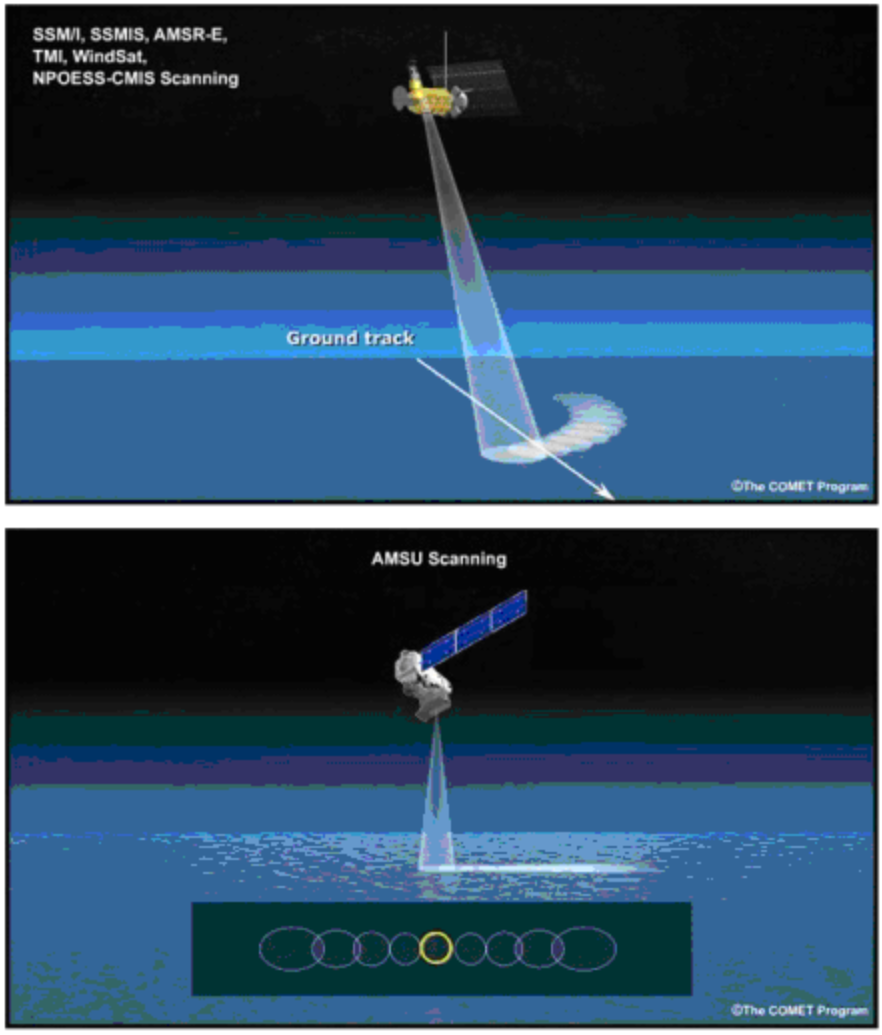

Figure 3.6. Illustration of (a) a conical scanner, which has a fixed viewing angle and a constant-sized footprint size across the swath, and (b) a cross-track scanner, which scans at varying angles with higher resolution in the middle of the swath and lower resolution on the edges (courtesy of UCAR/COMET).

The difference between the two scanning techniques is apparent over western Pacific Super Typhoon Podul (Figs. 3.7-3.9). The AMSU-B 89-GHz image at 0246 UTC 25 October 2001 captures Podul at the edge of the swath, where the limitation of larger footprint size and a coarser resolution leads to an enlargement of the pixel size and a distortion of the image (Fig. 3.7). This distortion can severely hamper TC center fix estimates. The higher resolution 2228 UTC 24 October 2001 SSM/I image (Fig. 3.8) from a few hours earlier allows for a more precise TC center fix, demonstrating the superior quality of the conical scanner. Figure 3.9, an SSM/I image of Podul from 1036 UTC 25 October 2001, illustrates the high resolution of the SSM/I pass, even at the edge of the swath.

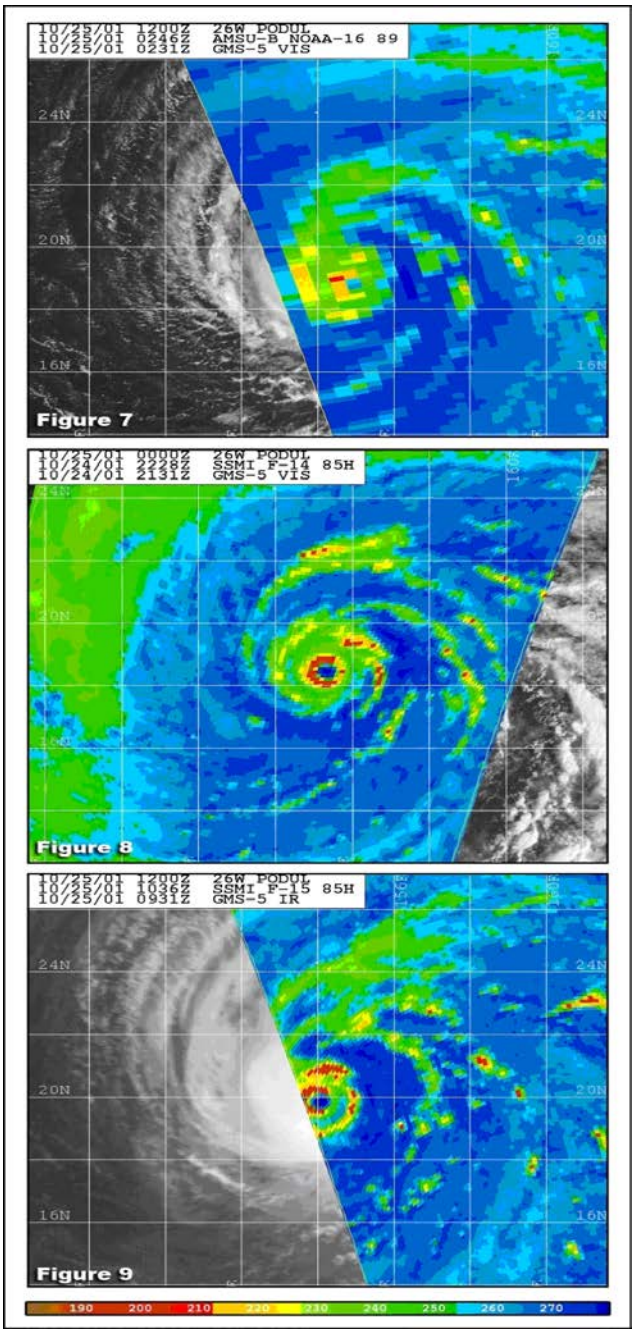

Figure 3.7. AMSU-B 89-GHz image of Super Typhoon Podul at 0246 UTC 25 October 2001, illustrating the poor resolution of the cross-track scanner at the edge of the swath. Colors correspond to brightness temperatures (K) in the legend.

Figure 3.8. SSM/I 85-GHz H-pol image of Super Typhoon Podul from 2228 UTC 24 October 2001, illustrating the superb resolution of the conical scanner across the entire swath. Colors correspond to brightness temperatures (K) in the legend.

Figure 3.9. SSM/I 85-GHz image of Super Typhoon Podul from 1036 UTC 25 October 2001, illustrating the high resolution of conical scanner at limb. Colors correspond to brightness temperatures (K) in the legend.

Cautionary considerations

Microwave estimates of TC location should be used with some caution since the slanted viewing geometry of microwave polar-orbiting satellites displaces features slightly askew of their actual location (i.e., parallax error). Figure 3.10 illustrates the typical parallax error in the 85-GHz channel, where scattering of microwave radiation by ice particles is dominant and in the 37-GHz channel which mainly senses microwave radiation emitted from cloud water droplets in low clouds. Paired with the schematic drawings (Fig. 3.10a,c) are two nearly simultaneous microwave images over Typhoon Jelawat on 8 August 2000, which reveal the discrepancy in TC position between the two frequencies. Figure 3.10b shows Jelawat in 37 GHz imagery, with the red circle indicating the general location where the analyst might place the center. The 85-GHz imagery (Fig. 3.10d) reveals a much broader eyewall surrounding the center, with the yellow circle corresponding to a possible center fix. While parallax error is present in both images, the 15- to 20-km error in the 85-GHz channel is much larger than the 5-km error in the 37-GHz image. Smaller (greater) parallax error is typically observed in the 37-GHz (85-GHz) imagery because the particles sensed at this frequency are emitted from a lower (higher) altitude, reducing (increasing) the distortion caused by the viewing geometry.

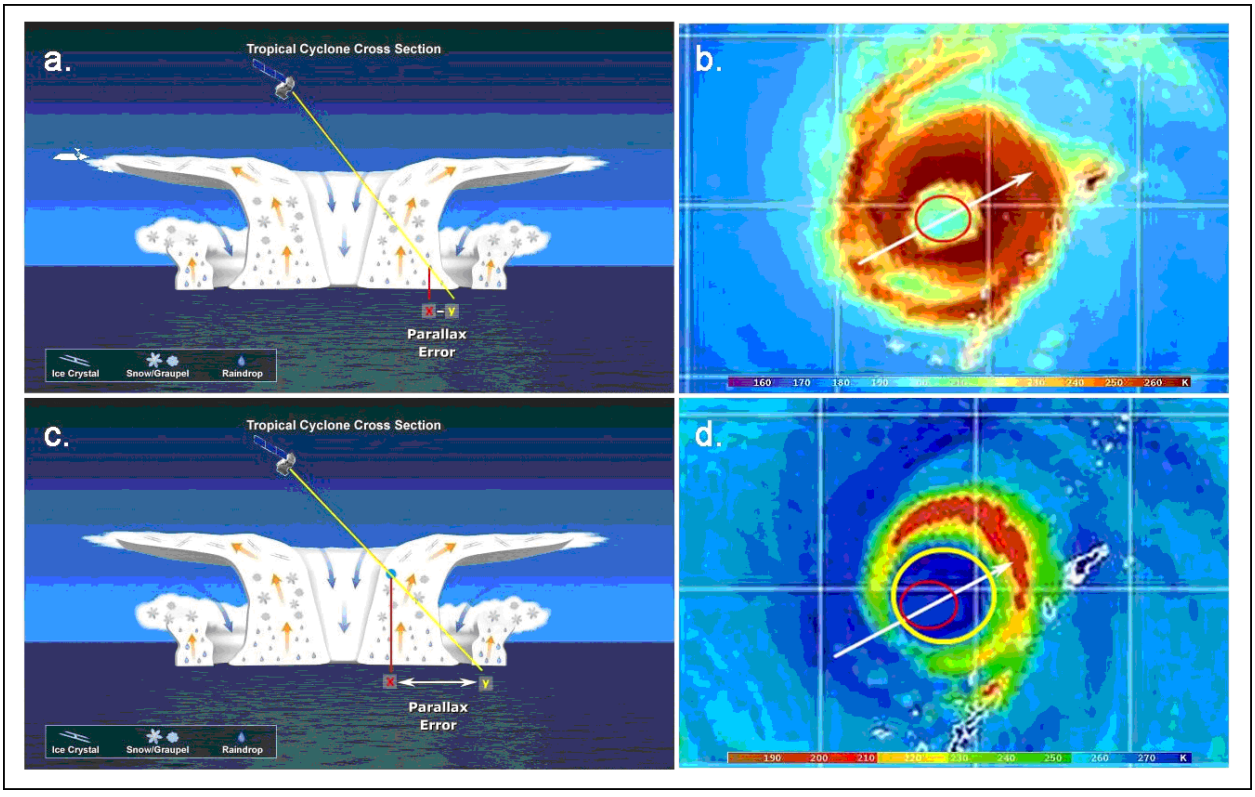

Figure 3.10. Illustration of typical parallax error associated with two microwave channels. (a) shows an exaggerated cross-section of the parallax error from the 37-GHz channel, while (c) shows the parallax error associated with the 85-91-GHz channels. (b) and (d) show parallax error observed in microwave imagery, with (b) showing minor parallax error at 37-GHz and (d) showing more substantial parallax error at 85-GHz. Figure courtesy of UCAR/COMET.

Microwave imagery presents a "snapshot" of the TC at a point and time. Since microwave imagery has relatively low temporal resolution, it may be difficult to determine if a feature in a single image is the true TC center. In Figure 3.11a, the forecaster may focus on the curved

convective clouds in the 89-GHz channel to fix the center of Tropical Storm Kevin. Comparing the microwave fix to the corresponding color composite image (Fig. 3.11b) could help confirm its accuracy. In some cases, however, errors may still occur, especially for weak TCs or pre-TC disturbances. For example, the actual center of Tropical Storm Kevin was located almost a degree farther south at this time (not shown).

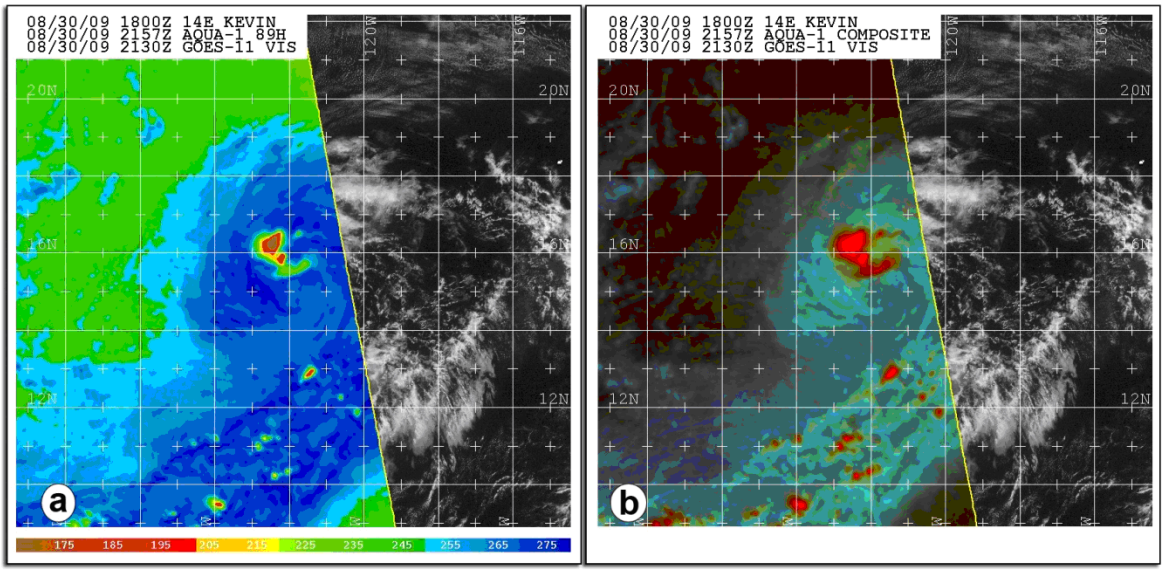

Figure 3.11. (a) AMSR-E 89 GH-z image of Tropical Storm Kevin at 2157 UTC 30 August 2009. (b) AMSR-E Color Composite image of Tropical Storm Kevin at the same time.Image navigation can also be problematic.If possible, a forecaster should inspect geographic features within the image to ensure that they are properly located.However, it is not possible to identify image navigation errors for TCs over the open ocean because there is no land in the image.

Data latency, the time between a satellite overpass and the successful transmission of its data to a ground receiving station for processing can result in a significant delay in the arrival of data for operational analysis. Figure 3.12 indicates the fraction of data available as a function of data latency. On average, nearly 80% of all data are available within five hours of overpass, but there are occasions when data arrive even later. The next generation of U.S. low earth orbiting satellites is expected to greatly reduce data latency with additional ground receiving sites and with 95% of all data likely available within 30 minutes of overpass (see NPOESS COMET module).

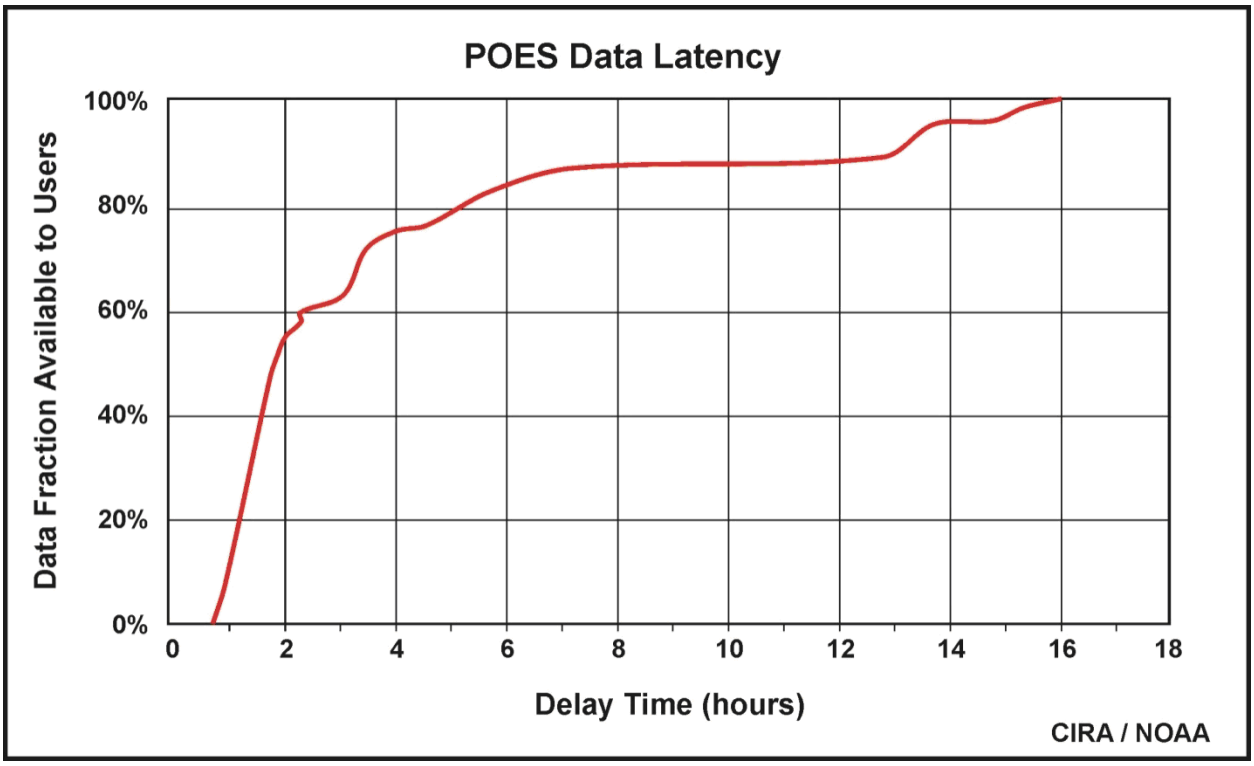

Figure 3.12. Plot of the fraction of microwave polar-orbiting data available to users in real time as a function of time. The x-axis or delay time is in hours, while the y-axis or data fraction available to users is in %. Figure courtesy of UCAR/COMET.

Scatterometry

Scatterometers estimate near-surface wind speed and direction over the ocean surface by measuring the backscatter variations from small-scale roughness elements (capillary waves) on the ocean surface. The European Space Agency's Advanced Scatterometer (ASCAT) onboard the METOP satellite series will be described here. Although the NASA SeaWinds instrument onboard the QuikSCAT failed in late 2009, it will be discussed briefly as well, since there is a possibility that data from scatterometers similar to QuikSCAT will become available for TC analysis in the coming years.

ASCAT is an operational scatterometer currently flying on the METOP satellite series (three missions are planned through 2020). ASCAT has two 550-km wide swaths and a 720-km nadir gap. Due to this swath configuration, ASCAT only provides about 60% of the coverage that was provided by QuikSCAT (Fig. 3.13), and the nadir gap results in few passes that sample the entire circulation of a TC. ASCAT wind retrievals are available at 50- and 25-km resolution and are noticeably smooth, as they were designed primarily for assimilation into numerical models. ASCAT exhibits a notable low wind bias at wind speeds above 30 kt compared to QuikSCAT and other observations (Cobb et al. 2008). Since ASCAT is a C-band scatterometer, its retrievals are less sensitive to rain than those from QuikSCAT were, which results in improved retrieval quality, particularly in weaker TCs.

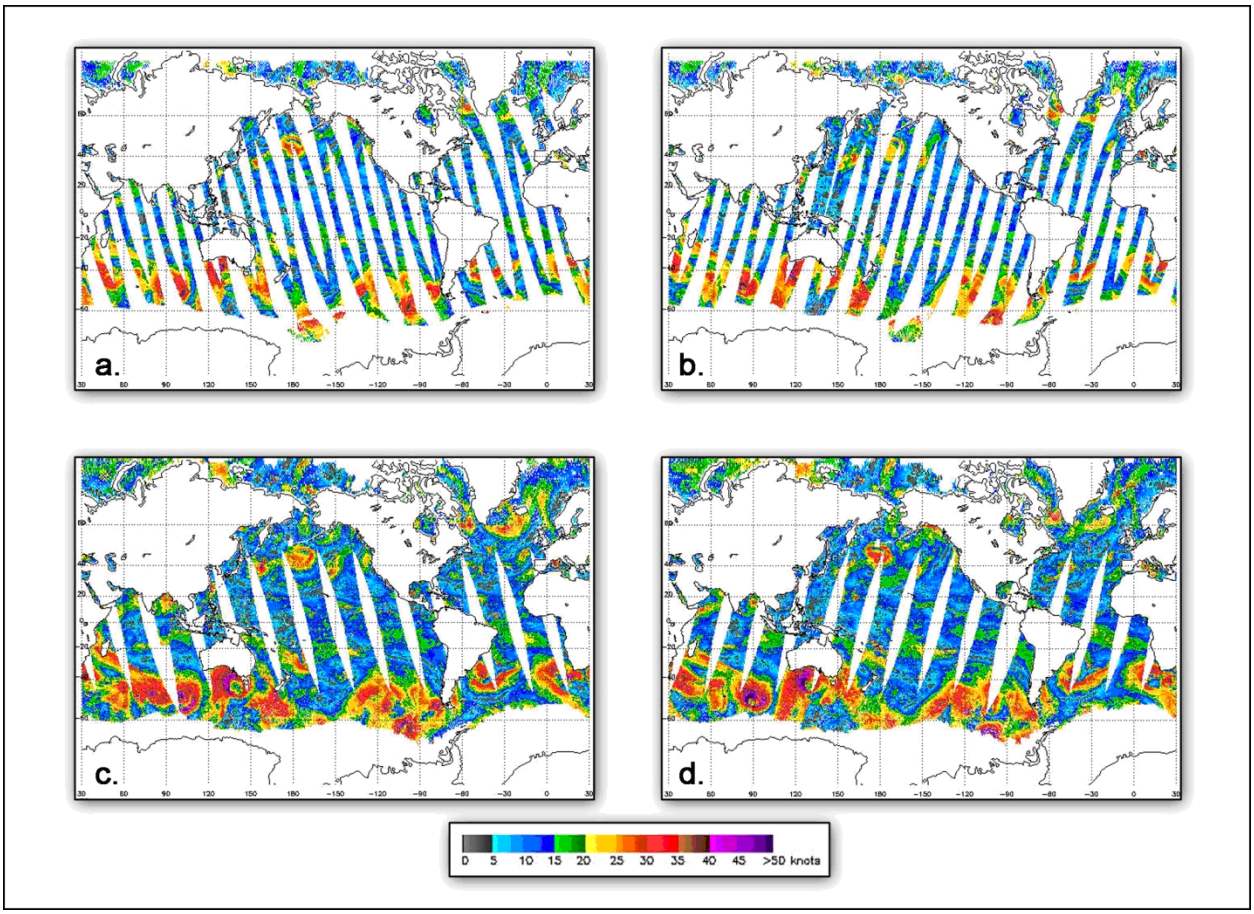

Figure 3.13. Image showing typical, daily coverage of ASCAT (top) and QuikSCAT (bottom). Note the wider QuikSCAT swaths compared to ASCAT, with large gaps in coverage from both sensors over the Tropics.

Aerial reconnaissance data

Aerial weather reconnaissance provides the best source of data to determine the center location of TCs. Even though aerial reconnaissance data have been used in TC forecasting since 1944 in the Atlantic, it is not used in most other global basins due to its prohibitive cost. In the Atlantic and sometimes in the Eastern and Central North Pacific basins, specially modified and equipped aircraft of the U.S. Air Force Reserve (AFRES) and the National Oceanic and Atmospheric Administration's Aircraft Operations Center (NOAA/AOC) are used to investigate TCs.

A typical mission consists of the plane flying at 10,000 ft (700 hPa) for hurricanes and 5,000 ft (850 hPa) for tropical storms. For pre-TC disturbances (i.e., "invest" missions), the typical flight altitude is 1,500 ft (457 m). The plane flies a figure four or "alpha" pattern through the system (Fig. 3.14). Missions can last from 10 to 12 hours, with two to six center fixes possible. Aircraft observations from within the TC are generally restricted to locations along and near the flight path.

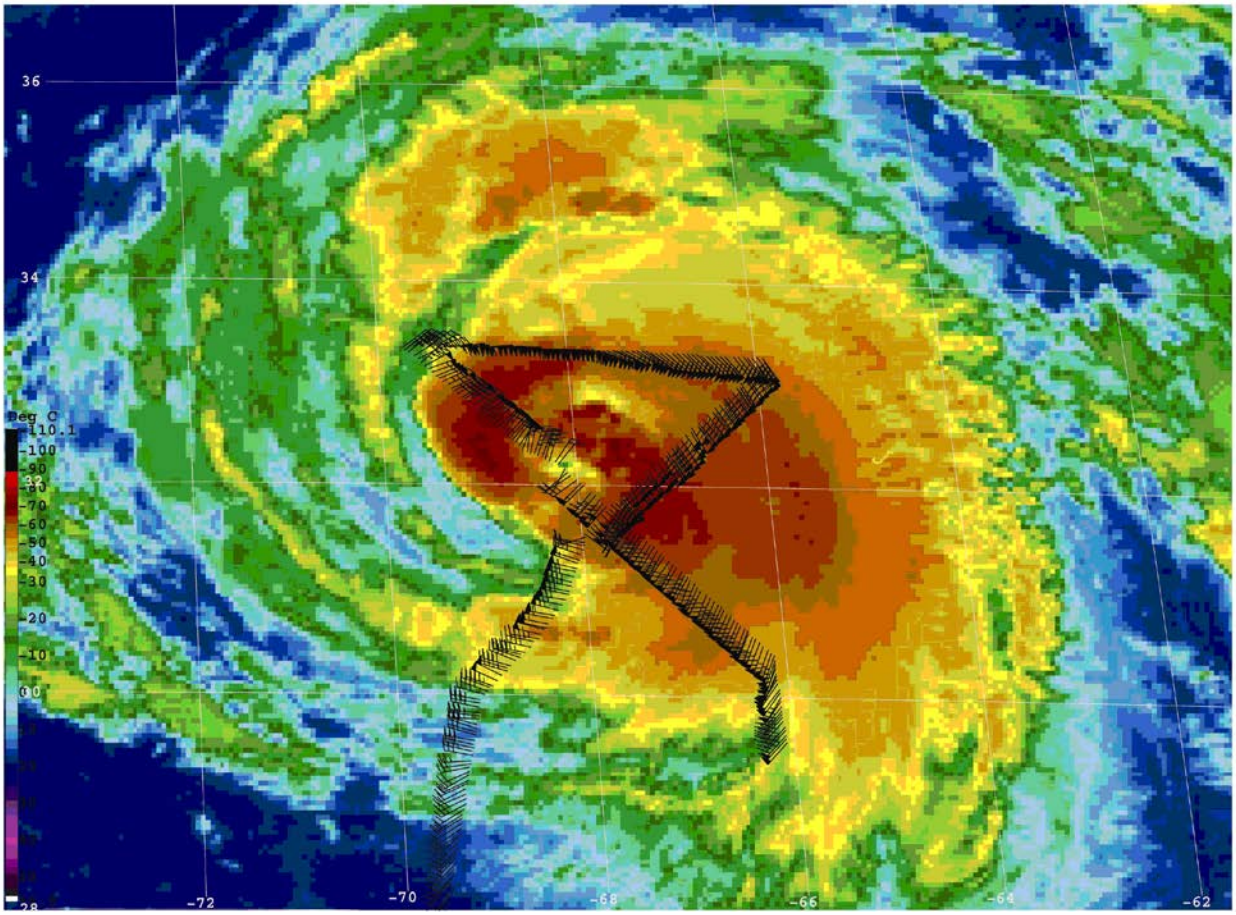

Figure 3.14. Illustration of the standard figure four or alpha pattern flown by aerial reconnaissance aircraft into TCs. This image shows the flight track from a mission into Hurricane Bill from 22 August 2009 at around 0300 UTC.

Sometimes the flight-level center is not coincident with the surface center, as in the case of a sheared system, and this will be noted in the remarks section (section P) of the vortex message. Figure 3.15 shows a vortex message from Atlantic Tropical Storm Ernesto in 2006, where the meteorologist on board noted that the surface and flight-level centers were not coincident.

The center fix listed in the vortex message identifies the location of the wind speed minimum or wind shift encountered along the flight path. The actual location of the center at flight-level could have been missed by several miles. Examining the individual high-density observations can help determine whether the flight-level center and reported center fix are coincident. Also, successive center fixes can be found at large distances from each other in poorly organized or weak systems (e.g., Atlantic Tropical Storm Frances in 1998 had consecutive center fixes around 50 n mi apart at times, as the cyclone had a large, central area of light winds).

```
000
URNT12 KNHC 271756
VORTEX DATA MESSAGE
A. 27/17:54:50Z
B. 17 deg 45 min N
   073 deg 52 min W
C. 700 mb 3143 m
D. 35  kt
E. 135 deg 015 nm
F. 186 deg 030 kt
G. 136 deg 075 nm
H. EXTRAP 1007 mb
I. 10  C/ 3046 m
J.  14 C/ 3052 m
K.   3 C/ NA
L. NA
M. NA
N. 12 45/ 7
O. 0.02 / 10 nm
P. AF302 0605A ERNESTO      OB 07
MAX FL WIND 30 KT SE QUAD 16:49:20 Z
SFC CNTR 191 / 21 NM FROM FL CNTR
SLP EXTRAP FROM 700 MB
RADAR BANDING EVIDENT
```

Figure 3.15. Vortex message from Atlantic Tropical Storm Ernesto (2006). In Section P, the on-board meteorologist notes that the surface center is displaced 21 nm south of the flight-level center.

Aircraft reconnaissance data can often improve track forecasts. For example, NHC track forecast error was decreased out through 72 hours when aircraft data were available in a sample from 1989-2002 (Fig. 3.16).

The increase in forecast error when aircraft data are not available is largest near the beginning of the forecast period and slowly diminishes at later times. This trend is likely due to the fact that many track forecast errors in the first few hours are primarily dependent upon accurately locating the center, while track forecast errors later in the forecast period are more influenced by errors in the large-scale steering pattern.

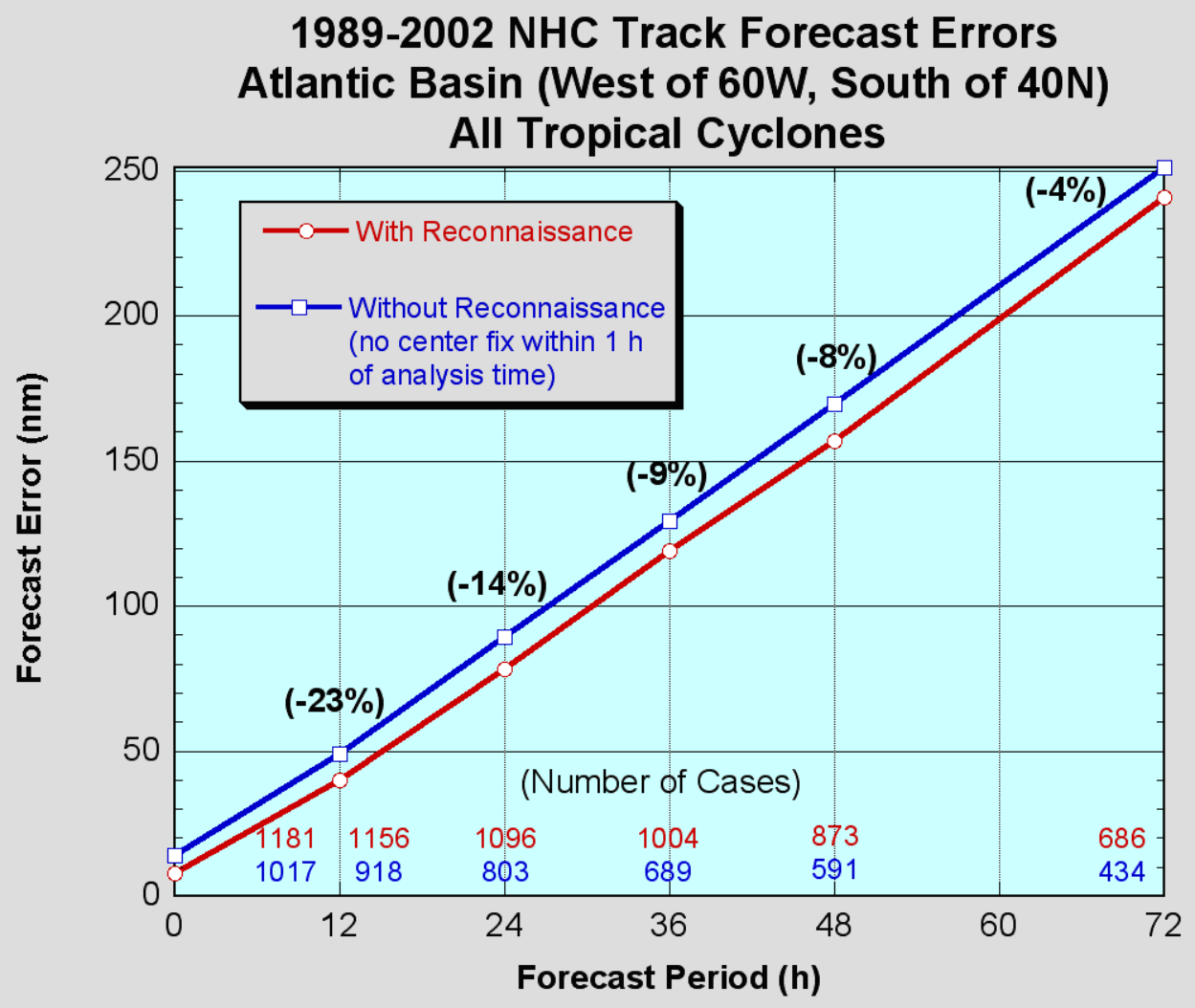

Figure 3.16. NHC official forecast errors with and without reconnaissance data, 1989-2002. The percent improvement in track error when aircraft data were available is indicated in parentheses.

urveillance missions

An accurate representation of large-scale steering features in the TC environment and their interaction with TCs is critical to TC track forecasting. Acquisition of wind, geopotential height, and thermodynamic observations in the often data-sparse TC environment is helpful in accomplishing this goal. Air Force reconnaissance aircrews often flew "synoptic" missions from at least from 1974 to 1987 in the western North Pacific to assess mid-tropospheric ridge structure in order to ascertain the likelihood of recurvature or non-recurvature (Guard, personal communication). NOAA's Hurricane Research Division (HRD) flew a large number of "synoptic flow" missions near and around TCs in the Atlantic between 1982 and 1996, and these data resulted in significant reductions in forecast errors (Burpee et al. 1996). Improvements depend greatly on the amount of data coverage but have been on the order of 10-15% in critical watch/warning situations from 1997-2006 (Aberson 2010). These research flights led to

operational "synoptic surveillance" missions for TCs threatening land areas in the western part of the Atlantic basin (Aberson 2002).

Figure 3.17 illustrates a typical flight path in the near-storm environment of Hurricane Dolly (2008). Note that the flight path is designed to gather data ahead of and on the periphery of a TC to augment the routine radiosonde network. The impact of these data is largest in the first 48 hours of the forecast and decreases at later forecast times (Aberson 2010) (Fig. 3.18).

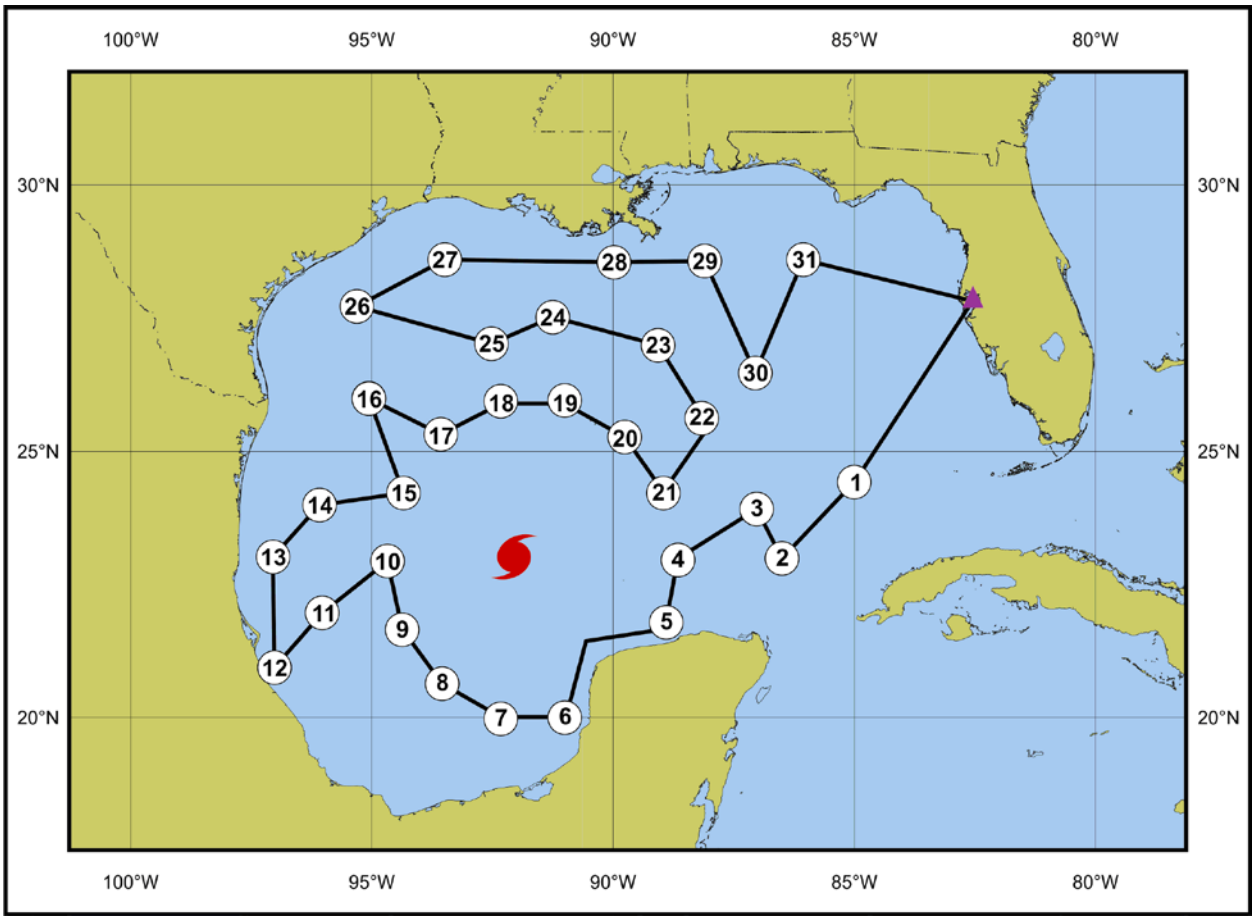

Figure 3.17. Flight path for the synoptic surveillance mission at 0000 UTC 22 July for Hurricane Dolly. Solid white dots indicate the flight path of the NOAA G-IV aircraft around Dolly, starting at observation 1 and ending at observation 31. The pink triangle indicates where the mission originated.

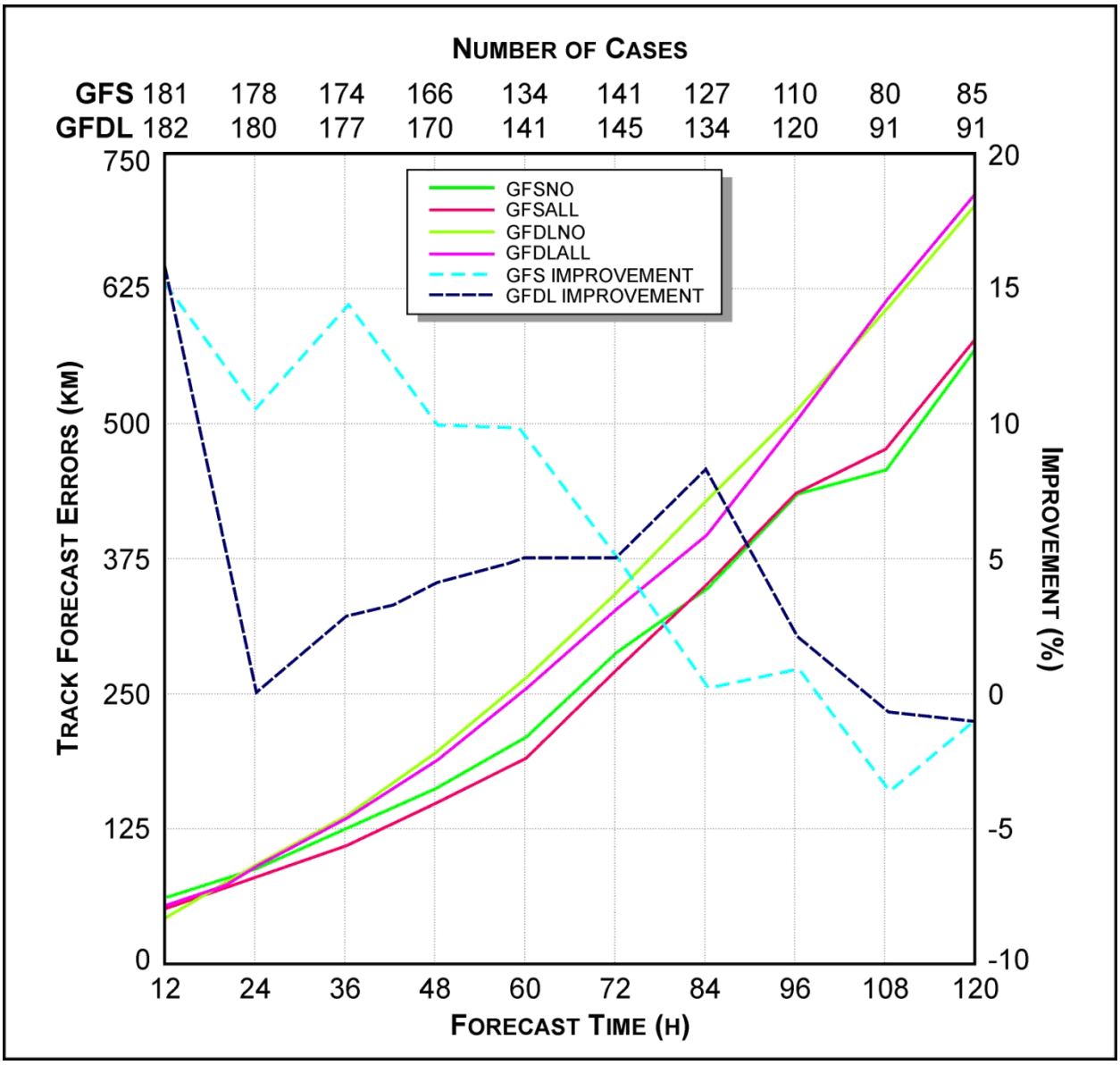

Figure 3.18. Average track errors (km) for a homogeneous sample of GFS model runs and a homogeneous sample of GFDL model runs, with (ALL) and without (NO) surveillance data initialized only at mission nominal times, and improvements over the former and not the latter (%). Sample sizes for each model at each forecast time are provided above the graph. Reproduced from Aberson (2010).

Radar fixes

The use of radar provides another data source to fix the center of TCs nearing land. As a TC approaches a radar site, outer rainbands, some of which move ahead of and at roughly the same speed and direction as the cyclone, appear first. While determining an accurate center location by radar is not possible at this stage, fitting logarithmic curves with a constant crossing angle of 10°-20° can provide an initial indication of the cyclone center once significant lengths of spiral band are observed (Senn and Heiser 1959). Once an eye or distinct circulation center appears, radar can provide center fixes with high temporal frequency. The accuracy of these

fixes can approach or exceed those of aircraft reconnaissance. However, the precision of the center fixes varies with the range and intensity of the TC due to the Earth's curvature and greater uncertainty associated with interpreting reflectivity patterns at long ranges from the radar site.

Figure 3.19 shows a scatter of radar fixes at a distance from the radar, when Tropical Storm Fay was poorly organized between Cuba and south Florida. As Fay intensified and the center became better defined, the scatter in fix positions decreased. Radar images can be animated to maximize the utility for centering fixing. Due to refraction of the radar beam and the Earth's curvature, considerable resolution and information are lost as the distance from the radar increases. The effect of the increase in height of the beam with increasing range is illustrated in Figure 3.20, where it appears that little deep convection exists on the southwest side of the eyewall. However, the lack of deep convection southwest of the eye is likely a result of the radar beam overshooting the largest hydrometeors associated with the convection in that area.

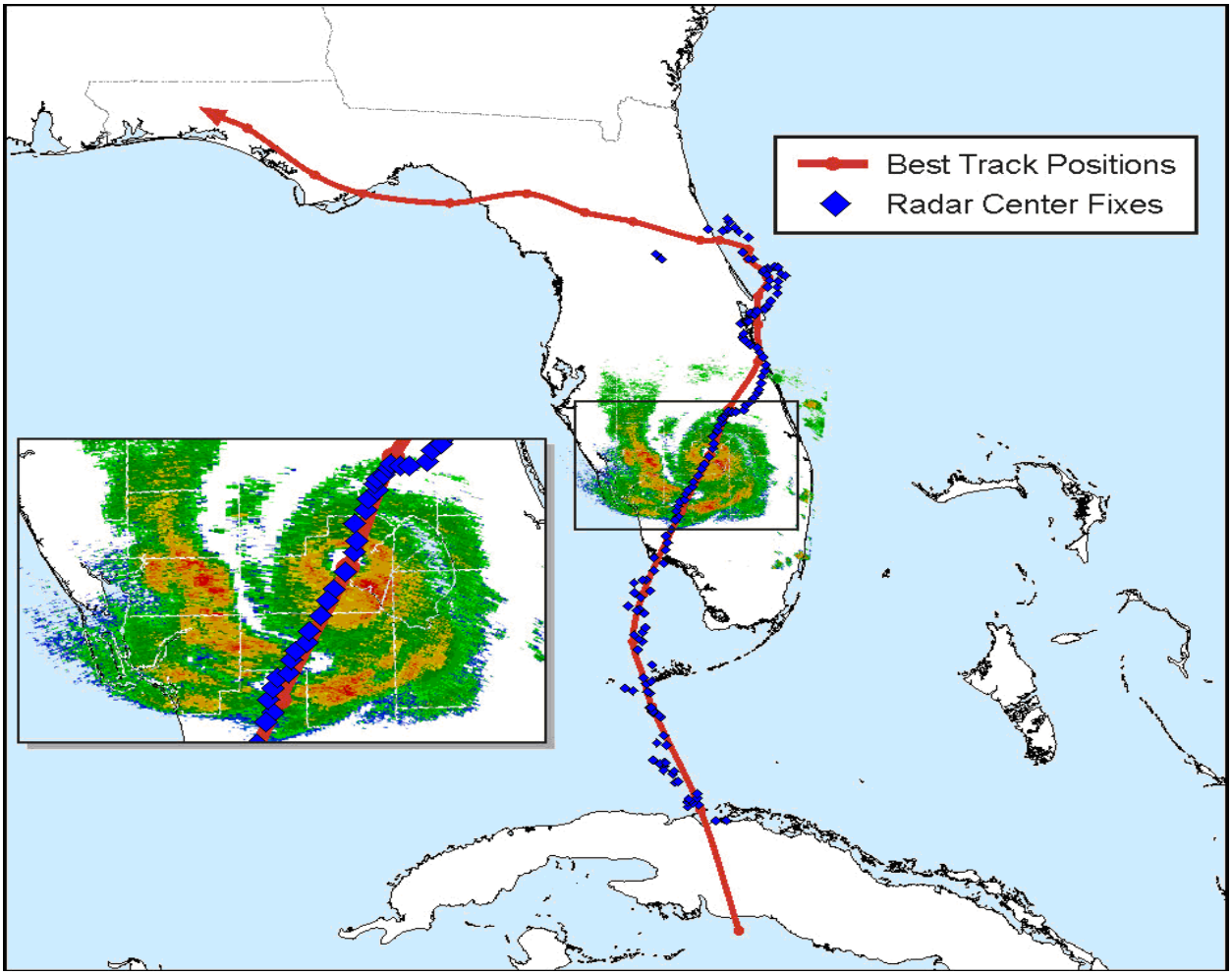

Figure 3.19. Operational radar center fixes plotted for Atlantic Tropical Storm Fay (18-21 Aug 2008) as it traversed the Florida peninsula. Scatter in the early land-based radar fix positions is strongly a function of distance from the radar and strength of the system. Smoothed best-track positions are overlaid, along with a radar image from the Key West WSR-88D (KBYX) from 1811 UTC 19 Aug.

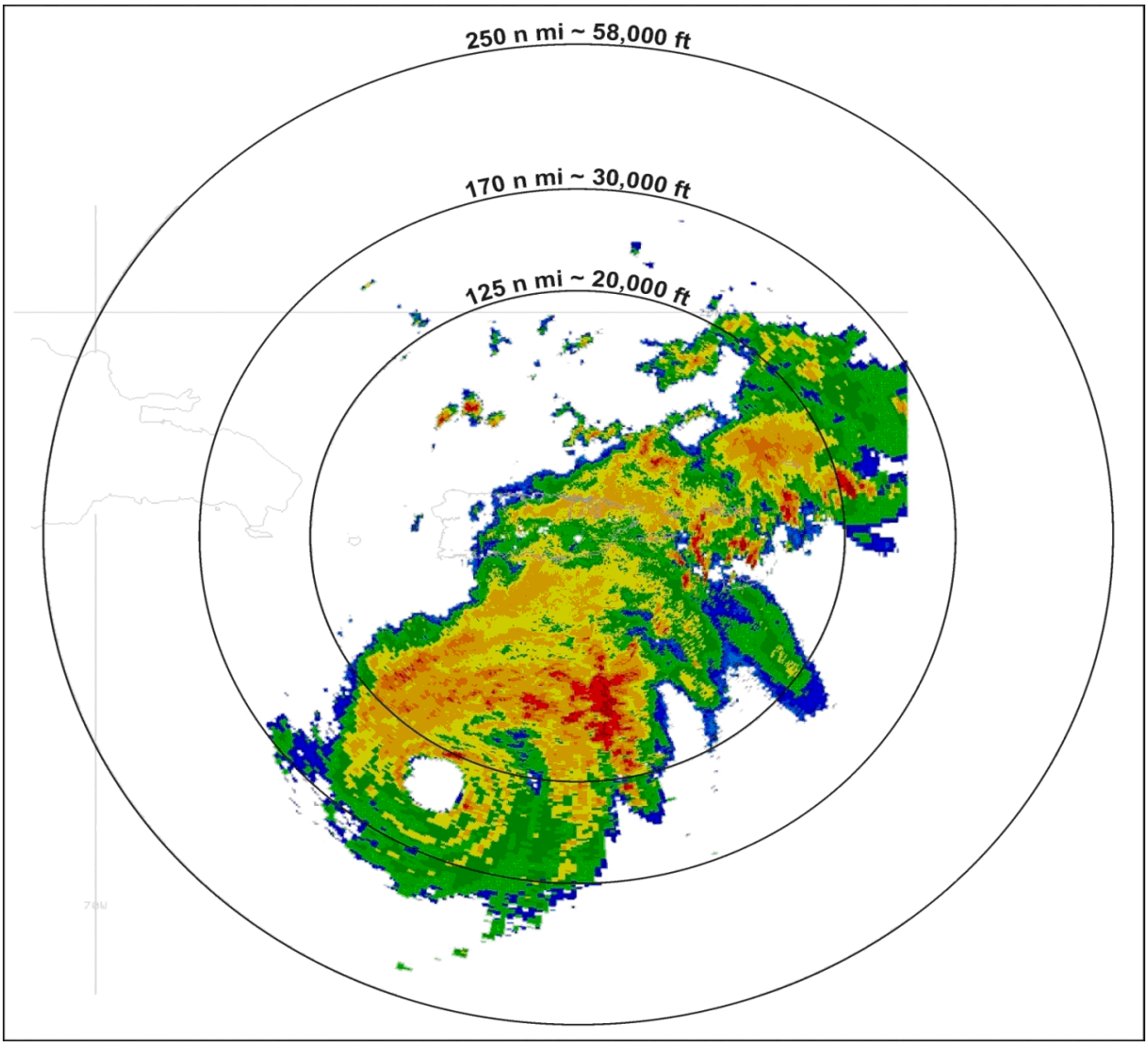

Figure 3.20. Atlantic Hurricane Lenny (0212 UTC 17 Nov 1999) south of Puerto Rico. The effect of the increased height of the beam above the surface with increasing range is demonstrated. Range rings indicate the height of the center of the radar beam above the surfac

The basic center-fixing technique is to find the geometric center of the eye (which may be circular or elliptical). Significant errors can occur when the eye is ragged or only formed on one side (Meighen 1987). In these circumstances, the eye wall feature should be found by animating the radar images and maintaining a conservative size and shape of the eye over several hours. In addition to reflectivity data, Doppler radar can measure whether backscattering particles are moving towards or away from the radar (i.e., radial velocity). Two Doppler radars in close proximity can provide full three-dimensional winds in regions where their beams overlap at an appropriate angle. An airborne Doppler radar can also obtain a full wind field by sampling the same volume from different locations.

The use of single-Doppler velocities in conjunction with the reflectivity (Fig. 3.21a) can greatly increase the accuracy of a radar-determined center fix. The zero isodop (Figure 3.21b), indicating particle motion normal to the beam, establishes the bearing of the TC center from the radar. The wind center will lie on or near the zero isodop, assuming that the component of TC motion towards or away from the radar is small. Although the TC center will be found between the inbound and outbound radial velocity maxima, the center observed by radar is at some distance above the surface. If data from adjacent radars are also available, multiple estimates of zero-isodops can help to refine or confirm a center fix, particularly in weaker systems. A reflectivity mosaic from multiple radar sites can also be helpful in identifying the center.

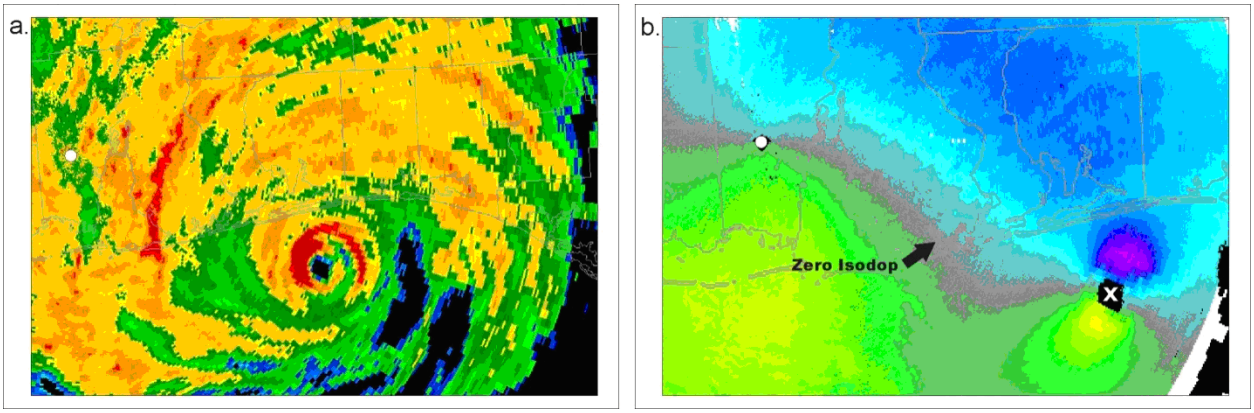

Figure 3.21. Radar reflectivity image of Hurricane Dennis at 1835 UTC 10 July 2005, as it approaches the Gulf coast of Florida. The radar location is indicated by white dot. b) corresponding velocity image, with "x" indicating center fix. Note inbound velocity maximum (dark blue) and outbound maximum (yellow) falling on either side of the zero "isodop" (gray) (counter-clockwise flow, northern hemisphere). Maximum velocity in this image is 56 ms-1 (109 kt) inbound at an altitude of about 2400 m (8000 ft).

Land observations and ship reports

Surface observations are not dense enough to accurately track a TC center, especially over the open oceans. However, surface observations can be important, particularly if they are located near the TC center. For example, an unexpected ship report can sometimes confirm the presence or location of a TC center in an otherwise data-void area. The wind speed and direction from surface observations give some indication of how far from and in what direction the TC lies from the observing site, while the pressure tendency helps to determine whether the TC is moving toward or away from the site. A time series of surface observations updated with regular frequency is more valuable than a single observation. Veering or backing of the wind direction with time indicates whether the TC center is approaching or moving away from a location, respectively. Unfortunately, most ship reports are made only at 3- or 6-hourly time intervals. First-order land sites and mesonets, coastal stations, and buoys report hourly, but some stations may have data interruptions due to power outages, communication failures, and even station destruction in more severe TCs. Also, the representativeness of surface

observations should be considered to ensure that transient features within the TC circulation have not contaminated the data.

There has been an expansion of land and ocean observations in recent years from a variety of new sources. For example, the number of coastal mesonets and other buoy networks over different parts of the globe has rapidly increased. Figure 3.22 shows the relatively high density of observations in the vicinity of the Florida peninsula. Some university research groups coordinate the deployment of observing networks in the path of a TC to supplement observations available at a TC la

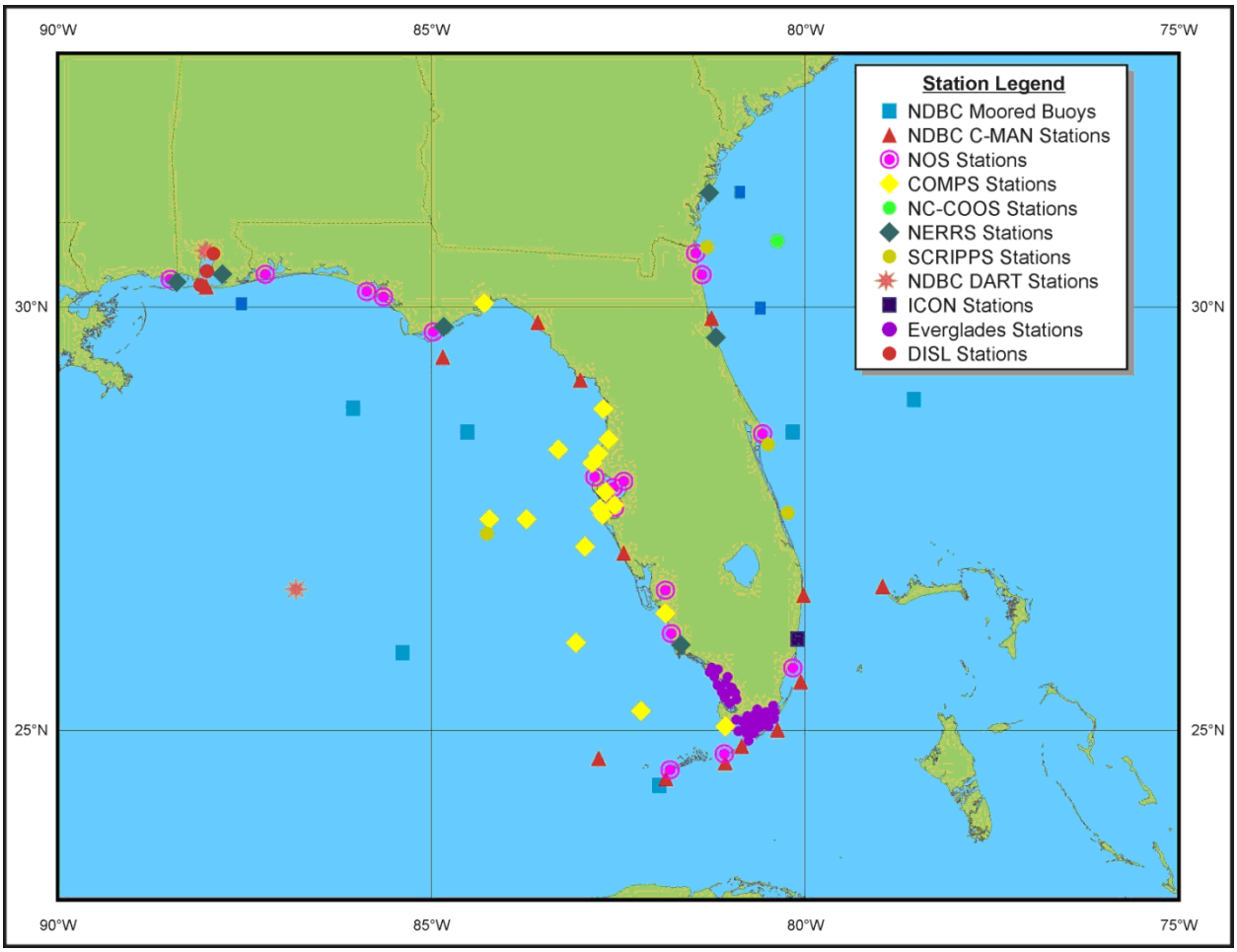

Figure 3.22. Map showing a subset of the large number of coastal observations in the vicinity of the Florida peninsula in the southern United States.

Sustained winds are greatly influenced by exposure and surface roughness characteristics. A better measure of tropical cyclone sustained wind is frequently obtained by using the observed gust and then converting it to an associated sustained wind as determined from a general relationship that better pertains to winds observed in tropical storms and hurricanes (e.g., Krayer and Marshall 1992; Harper et. al. 2010).

An observed coastal, island, buoy or ship wind is often interpreted as the "'maximum' maximum" wind at that distance from the center (e.g.,radius of maximum wind, or radius of 15 ms^{-1} wind). However, it should be interpreted as the "minimum maximum" wind. Why? Because there is very little chance that the sampled wind is located exactly at the point of the peak wind at that distance.

While there are various geometric techniques that can be used to estimate the location of the TC center from synoptic data at various locations, satellite techniques are now more accurate and render these techniques obsolete. Techniques for operationally combining and weighting various types of data are covered by Powell (XXXX).

3.3 TC track forecasting

Factors influencing TC motion

Large-scale flow

Fundamentally, TC motion is governed by two mechanisms: advection of the relative vorticity associated with the TC by the environmental flow, and advective processes that involve multi-scale interactions on different scales with the environmental flow, the planetary vorticity gradient, and the TC vortex. In the first mechanism the TC is analogous to a "cork moving in a stream," where the layer-averaged winds over the depth of the troposphere correlate well with the actual storm motion, indicating the dominance of the environmental steering mechanism. A forecaster can develop a simple estimate of the deep-layer steering, which could serve as a proxy for the actual TC motion. The calculation for this parameter is known as the deep-layer mean (DLM) wind and is simply the mass-weighted average wind through some layer of the troposphere. For example, if the vertical layer extends from 850 hPa to 200 hPa, the vertical integration can be approximated by the following expression:

$$[(U_{850}+U_{500})/2 * 350\ mb + (U_{500}+U_{200})/2 * 300\ mb)] / (650\ mb)$$

Neumann (1979) examined the relationship between deep-layer mean heights and TC motion and determined that geopotential height works equally well as using layer winds. He also discovered that layer-averaging was more preferable than using a single layer and determined that a mass-weighted average extending from near the surface to 100 hPa explained the greatest variance of short-term TC motion.

An empirical relationship exists between the intensity of the TC and the vertical depth of its vortex in the troposphere (Velden & Leslie 1991 and Velden 1993). Therefore, a forecaster should consider the intensity of a TC before determining the appropriate steering layer to consider. Figure 3.23 indicates that stronger TCs typically extend through the depth of the troposphere and are steered by a DLM wind. Weaker storms typically have less vertical depth, and a shallower layer of average winds should be examined to assess the potential TC motion.

The forecaster can use this concept to compare the vertical depth of the vortex in model output to ensure that the model has the proper representation of the TC. If a TC is sheared to the point that the low-level circulation center and the deep convection become decoupled, the sheared low-level center will generally be steered by the 850 hPa or 850-700 hPa mean flow.

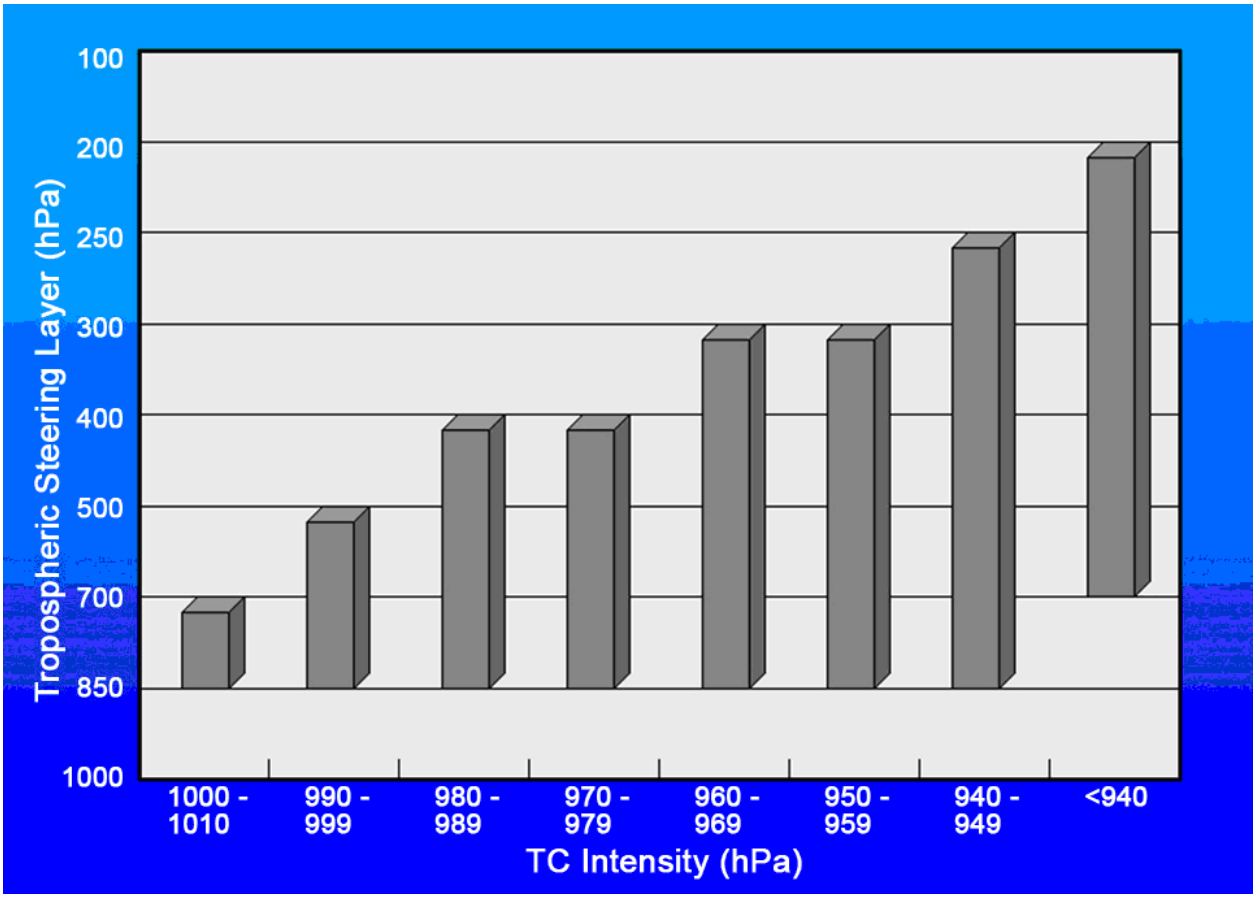

Figure 3.23. Relationship between TC intensity and TC environmental steering from Velden (1993). Bars indicate the depth of the steering layer in hPa (y-axis) and TC intensity is given on the x-axis.

Figure 3.24 shows the forecast scenario at 0600 UTC 5 September 2008, when Hurricane Ike was centered well east of Florida. A majority of the track guidance at that time indicated that Ike would turn from a west-southwest course north of Puerto Rico to a west-northwest or even northwest course later in the forecast period.

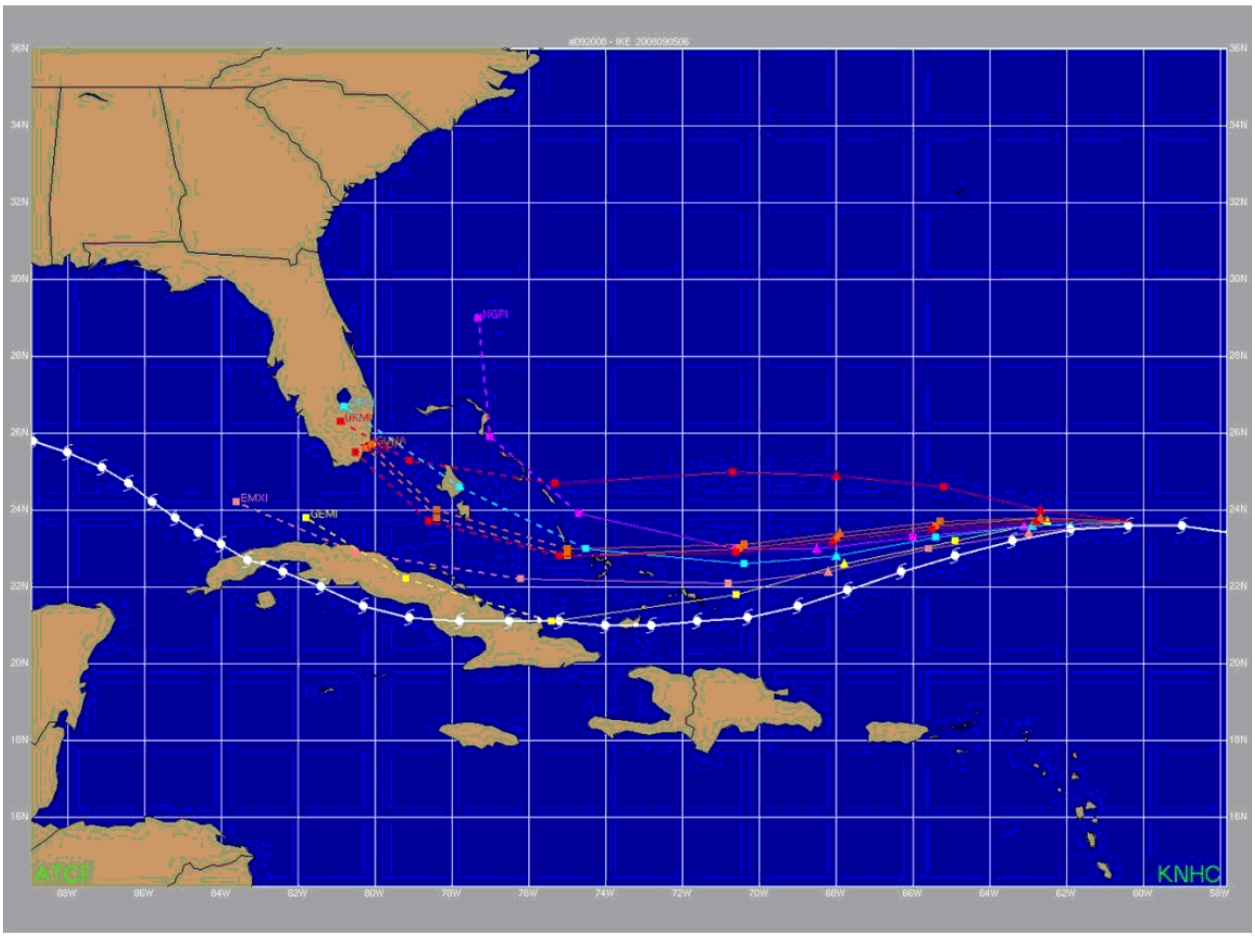

Figure 3.24. Model track guidance for Hurricane Ike at 0600 UTC 5 September 2008. The solid white line with hurricane symbols represents the best track, while the multi-colored lines represent individual track model forecasts out to 3 days; multi-colored, dashed lines represent individual track model forecasts from 3 to 5 days. The cyan track is the official forecast, the black line is the GFS model, and the orange line is the ECMWF model.

A series of cross-sections from the GFS, one of the models forecasting a northwesterly course beyond 72 hours, appears in Figure 3.25a. These cross-sections show that the GFS depicts Ike as a shallow vortex, with little circulation evident above about 500 hPa, even though Ike was a hurricane at the initial time. Many of the other models also forecasting a northwesterly course suffered from poor model representations of the TC vortex, indicating a weak TC throughout the forecast period (not shown). In contrast, the ECMWF (Fig. 3.25b) shows a deeper TC vortex consistent with a mature hurricane. The ECMWF model, with its more accurate depiction of Ike's vortex, consistently forecast the hurricane to remain farther south, closer to the eventual track. This result suggests that Ike was being steered by a deep layer mean (DLM) flow from the northeast around a strong subtropical high to the north (Fig. 3.26b). The GFS, however, steered its weaker representation of Ike in shallower flow around the low- to mid-level Atlantic ridge (Fig 3.26a).

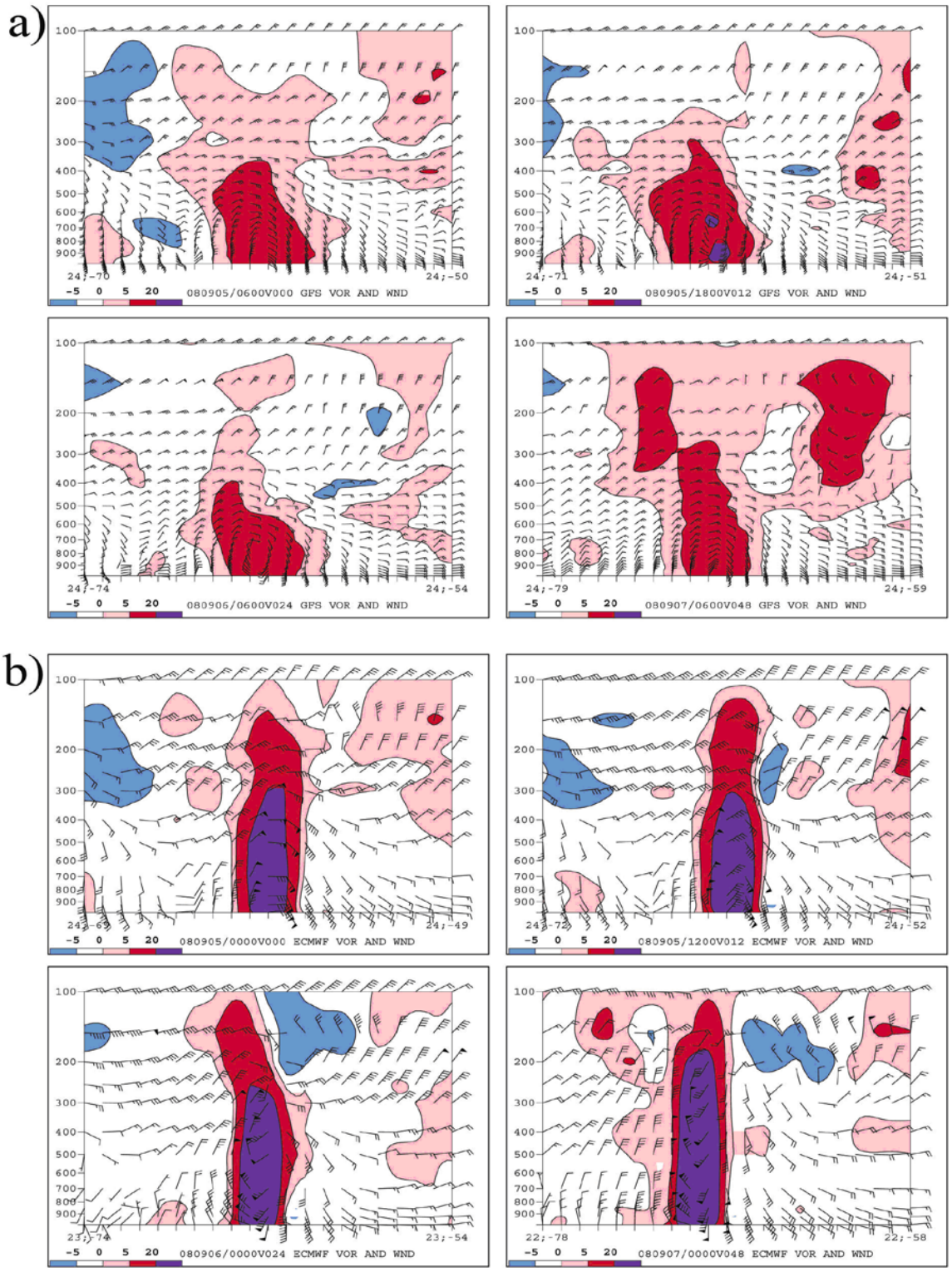

Figure 3.25. Forecast east-to-west model cross-sections for Hurricane Ike. GFS's (a) and ECMWF's (b) analyses and forecasts through 48 h of relative vorticity and horizontal winds (every 6 hours) associated with Hurricane Ike from model cycles at 0600 UTC 6 September and 0000 UTC 6 September, respectively. A horizontal distance across the TC is on the x-axis, while pressure (in hPa) is indicated on the y-axis. Vorticity is shown in units of x 10^{-5} m^{2} s^{-2}, with the red and purple shading indicating positive vorticity and blue shadings indicating negative vorticity. Forecast wind barbs are displayed in knots.

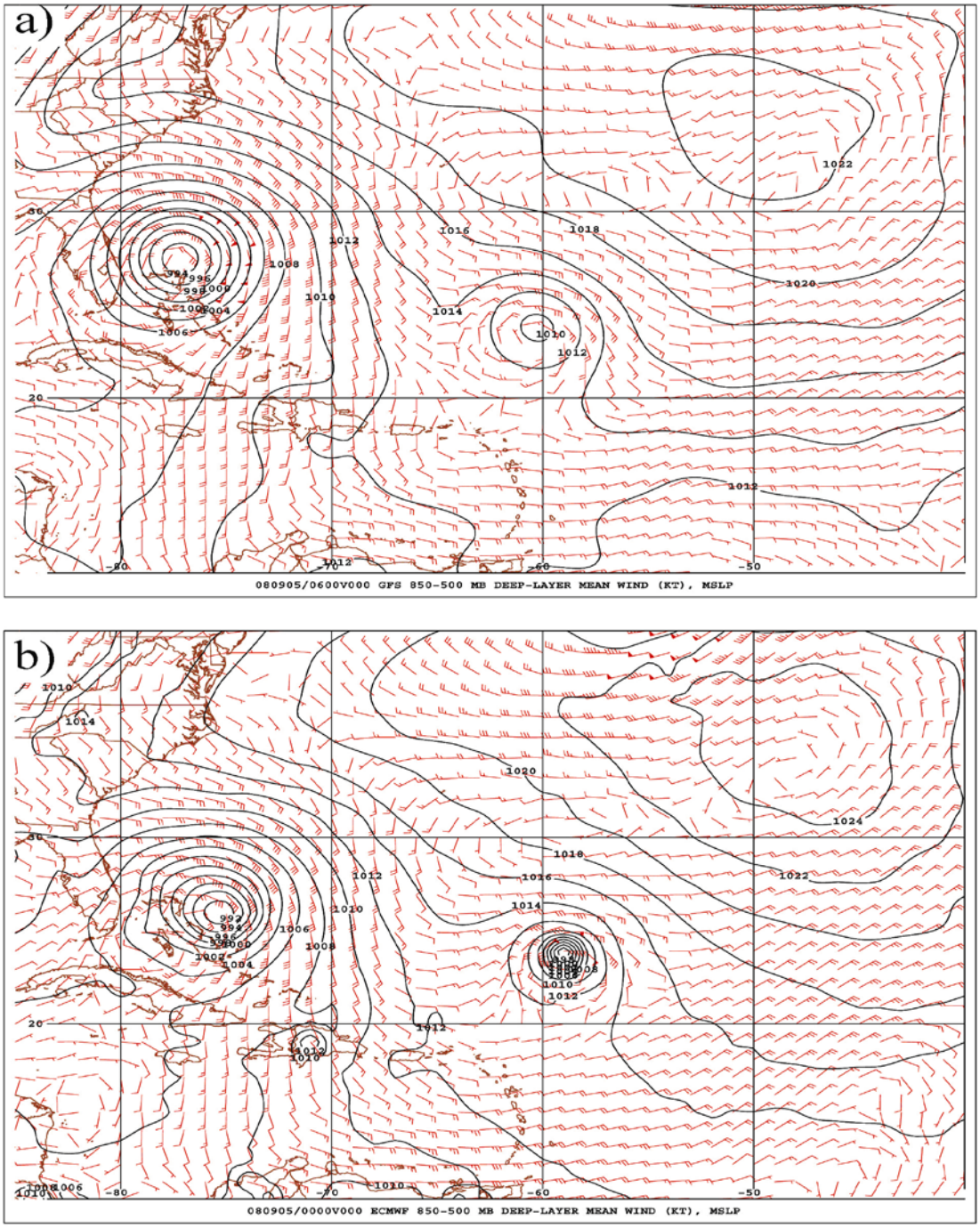

Figure 3.26. Analysis at 0000 UTC 9 September 2008 from (a) GFS showing sea level pressure (contours, hPa) and 850-500-hPa layer average wind (barbs, kt), and (b) ECMWF showing sea level pressure (contours, hPa) and 850-200-hPa deep layer mean (DLM) wind (barbs, kt).

Beta-gyres

The beta effect represents a form of self-advection and results from differential advection of planetary vorticity on either side of the TC circulation. The differential advection induces weak

secondary circulations known as “beta gyres” on either side of the TC, which cause a net westward and poleward drift of about 1-2 ms^{-1}. Observing beta gyres in nature is virtually impossible, as their effects are manifest as a subtle modification to the large-scale steering flow. The beta effect is dependent on the outer wind structure of the TC, a part of the storm that is often poorly sampled even by reconnaissance aircraft (Carr and Elsberry 1997). The Beta and Advection Models (BAMs) are simple, two-dimensional trajectory models that contain vertical layer-averaged horizontal winds in addition to a correction term that accounts for the beta effect. In fact, most contemporary dynamical models incorporate the effects of beta-gyres. Thus, while forecasters should be aware of this contribution, under most conditions, they need not calculate it.

Binary interaction

The interaction of two or more closely-spaced TCs can lead to what is known as the Fujiwhara effect (Fujiwhara 1921, 1923, 1931; Brand 1970) or binary interaction (Dong and Neumann 1983). Fujiwhara (1921, 1923, 1931) explains how similar-sized cyclones are mutually attracted to one another and orbit cyclonically about a mid-point. Brand (1970) showed that TCs begin to interact significantly when their centers come within 700-800 nm (1125-1290 km) of each other. The degree of interaction increases rapidly as the distance between the cyclones decreases. The details of the interaction also depend on storm size, intensity, and the ambient steering flow, with storms of unequal sizes likely to have a greater interaction than two of the same size (Prieto et al. 2003).

Once two TCs come into proximity, there are several possible outcomes: the two TCs could move in a stable, cyclonic orbit about their centroid; one cyclone could escape the interaction of the other; or one of the cyclones could dissipate via capture and merger. The absorption of one TC by another is relatively rare and is most likely to occur when one cyclone is much larger and stronger than the other (Lander and Holland 1993). For example, Tropical Storm Henriette in the eastern North Pacific in 2001 dissipated after coming within 85 km of Tropical Storm Gil, after having already rotated about 540 degrees around their centroid (Prieto et al. 2003). Ritchie and Holland (1993) found that vortices must come within 150-300 km of each other before a "shearing-out" process can occur which can ultimately lead to dissipation of the smaller of the two vortices.

Binary interactions are most prevalent in the western North Pacific since TCs there are in relative greater abundance of multiple cyclones and the characteristics of the monsoon trough environment favor multiple opportunities for TCs to encounter one another (Dong and Neumann 1983). Atlantic TCs generally form from individual perturbations (African Easterly Waves) outside of the ITCZ and have fewer chances to undergo binary interaction (Dong and Neumann 1983). Dong and Neumann (1983) also found that the expected annual number of binary interactions in the western North Pacific is 1.5, considerably higher than the 0.33 expected annually in the Atlantic. When normalized with respect to total storm numbers, however, the western North Pacific experiences about the same amount as most other global basins, except for the Atlantic basin, which experiences the lowest amount.

Track forecasting becomes more difficult when considering the interactions of two or more TCs (Dong and Neumann 1983). Carr and Elsberry (1998) presented a detailed conceptual model that classifies binary interaction events by the degree of interaction between storms (direct, semidirect, and indirect), the dominance of one system over another, a cyclone's interaction with neighboring steering features, or the mean steering flow. Unfortunately, the scheme is qualitative in practice and can fail to detect binary interaction or delay its detection. From the forecaster's perspective, binary interaction can be masked by the influence of the environmental flow, making its onset difficult to determine.

Contemporary numerical models can better resolve TCs and handle binary interaction better than they did a decade or two ago, although no systematic study has assessed model forecast skill in these cases. Model forecasts should be evaluated to determine if they properly analyze the location, intensity, and size of the TCs involved in binary interaction, since a failure to correctly analyze any of these parameters could result in a degradation of details of the binary interaction depicted in the model forecast. All of the parameters are critical to properly resolve the timing and degree of binary interaction. Differences between various models can be compared to see if the interaction shown in the model is consistent with previous studies.

TC interaction with surrounding environment

Interactions between a TC and the surrounding environment are also important to TC motion (Ross and Kurihara 1995). Large, strong TCs have a more significant effect on the surrounding environment than smaller, weaker ones, and this environmental modification could influence TC motion. One example is the transport of heat by upper-level outflow poleward of a TC, which could enhance a mid- to upper-level anticyclone and keep the TC on a general westward heading. The Beta Effect discussed above is another example of a TC environmental interaction.

TC motion can also be affected by terrain interaction; however, the details of this interaction vary with the strength of the TC, the strength and direction of the actual environmental steering, and the characteristics of the terrain. Observational and numerical studies have demonstrated that an acceleration and significant poleward track deflection can occur upstream of a rugged land mass (e.g., like Taiwan) for westward-moving TCs (Brand and Blelloch 1974; Chang 1982; Bender et al. 1987; Yeh and Elsberry 1993). These same studies also show that stronger TCs tend to have more continuous tracks across mountainous islands while weaker TCs tend to "jump" or reform a secondary circulation on the lee side of elevated terrain through the conservation of potential vorticity. Similar track deflections have also been observed in TCs passing over other islands such as Cuba, Hispañiola, Puerto Rico, and Luzon in the Philippines (Lin et al. 2006). The low-level circulation center of TCs approaching the north-south oriented Sierra Madre mountain range of eastern Luzon in the Philippines tends to: 1) cross the mountain range if the environmental steering has a greater westward than northward component; or 2) move northward east of the mountain range if the environmental steering has a greater northward component than westward component (Guard, personal communication).

TC core processes that influence motion

Several "secondary" mechanisms also produce TC track oscillations. Holland and Lander (1993) discuss how TCs tend to oscillate about a mean path, even if they are in a particularly well-defined steering current. Willoughby (1988) demonstrated that a mass source and sink couplet exhibited trochoidal oscillations along the cyclone path, such as those documented in Atlantic Hurricane Belle in 1976 by Lawrence and Mayfield (1977). Willoughby (1984, 1990) and Holland and Lander (1993) further discuss the role that convective asymmetries, such as mesoscale convective systems rotating within the core of the TC, can have on short-term TC motion. Ritchie and Elsberry (1993) acknowledge the possibility that significant track changes on the order of tens to even hundreds of kilometers over several days could result from the interaction of a TC and a persistent MCS rotating within its circulation. Even in cases of land interaction, changes in TC motion are sometimes related to convective asymmetries within the storm due to asymmetric surface fluxes and frictional effects (Wong and Chan 2006).

Models and forecasters have not been able to routinely predict convectively-related "jumps" or reformations of the center observed in TCs. In the case of Tropical Storm Claudette on 12 July 2003, the center, which was located over the central Gulf of Mexico, unexpectedly jogged north of the forecast track. Claudette was embedded in a persistent southwesterly shear environment, which caused the bulk of the convective activity to be distributed asymmetrically north and northeast of the center. This is consistent with Ritchie and Elsberry (1993) who found that a persistent burst of convection, especially in an asymmetric pattern, can cause a localized pressure fall through latent heat release and an increase in the vertical vorticity through the divergence term in the vorticity equation, resulting in a "jump" or reformation of the center. In the case of Claudette, the convective asymmetry appeared to tug the center northward throughout the day, with the center eventually reforming closer to the deepest convective cells several hours later. Neither forecasters nor the track guidance anticipated this motion, and the likelihood of being able to forecast short-term track motion with a time scale of this type of convective asymmetry is low.

If an asymmetric convective pattern is expected to persist, the forecaster may be able to deviate from the track guidance (Ritchie and Elsberry 1993), however, extrapolating a short-term motion too far into the future, especially after the initial forcing agent has dissipated, is not advisable. The important aspect for the forecaster is to recognize the potential for a change in motion so that when it occurs, he or she does not go into an extended period of denial (i.e., not believing what they are seeing).

Tools for TC track forecasting

Climatology

There are some motion characteristics of TCs that occur regionally and seasonally. For example, late season TCs in the Atlantic basin tend to form over the western Caribbean Sea and accelerate northward or northeastward. Storm-specific information such as the location, current motion, day of the year, and intensity of a TC can be compared to historical TCs with similar characteristics through linear regression to develop a "climatology-persistence" (CLIPER)

model that identifies a "typical" storm behavior. As forecasts from dynamical models have improved, the operational use of simple statistical models such as CLIPER for track forecasting has declined sharply. Since the CLIPER technique contains no information about the current state of the atmosphere, its use, especially at longer time ranges, is rather limited and it is no longer an effective forecast tool, but such information could be used as a long-term planning tool.

Apart from its limited use in an operational setting, CLIPER or similar methods serve as a benchmark against which the performance of dynamical models can be evaluated (Aberson 1998, Bessafi et al. 2002). Since CLIPER contain no information about the current state of the atmosphere, it represents a "no skill" forecast. Forecasts from other techniques, including the official forecast, can be evaluated against CLIPER to quantify the amount of skill they have. In addition, if CLIPER errors for a particular TC or an entire season are low (high), the interpretation can be made that the storm(s) were inherently easier (more difficult) to forecast than normal. This concept of forecast difficulty has been normalized to rank basins according to their general forecast difficulty (Pike and Neumann, 1987).

Persistence

TC motion is determined mostly by the large-scale steering flow. If the flow in which a TC is embedded is gradually evolving, persistence can be important in forecasting TC track in the first 12 to 24 hours. At these short time periods, extrapolation of the TC's past track can be used to determine future position. Beyond that time, steering mechanisms and their non-linear interactions become complex and TC track is best predicted using dynamical model guidance.

In order to use persistence, a forecaster must determine a representative estimate of TC motion. The initial motion is typically computed with an averaging period over the past 6, 12, 18, or even 24 hours. An interval of 6 to 12 hours is best if known changes in the track are occurring (e.g., recurvature), but a longer interval may be chosen if the center location is uncertain. In general, the time interval for averaging can be thought of as a smoothing factor, with more smoothing and a longer averaging time necessary for TC centers that are difficult to fix.

Continuity

Maintaining continuity with the previous forecast should be a priority in the forecast process. Small, incremental changes are typically made to the forecast from cycle to cycle in an attempt to avoid following the sometimes abrupt changes in track model guidance (e.g., Figs. 3.29-3.32). If forecast changes are not constrained by continuity, large changes in one direction may have to be adjusted significantly back in the other direction shortly thereafter. It is important to avoid large changes to the forecast track since they could cause the public and other users to lose confidence in the official forecast. The forecaster should instead strive for gradual changes from one forecast to the next following trends in the guidance. However, there are occasionally situations when large changes to the forecast track are required, such as the reformation of the center or a significant, unexpected deviation from the previous forecast motion.

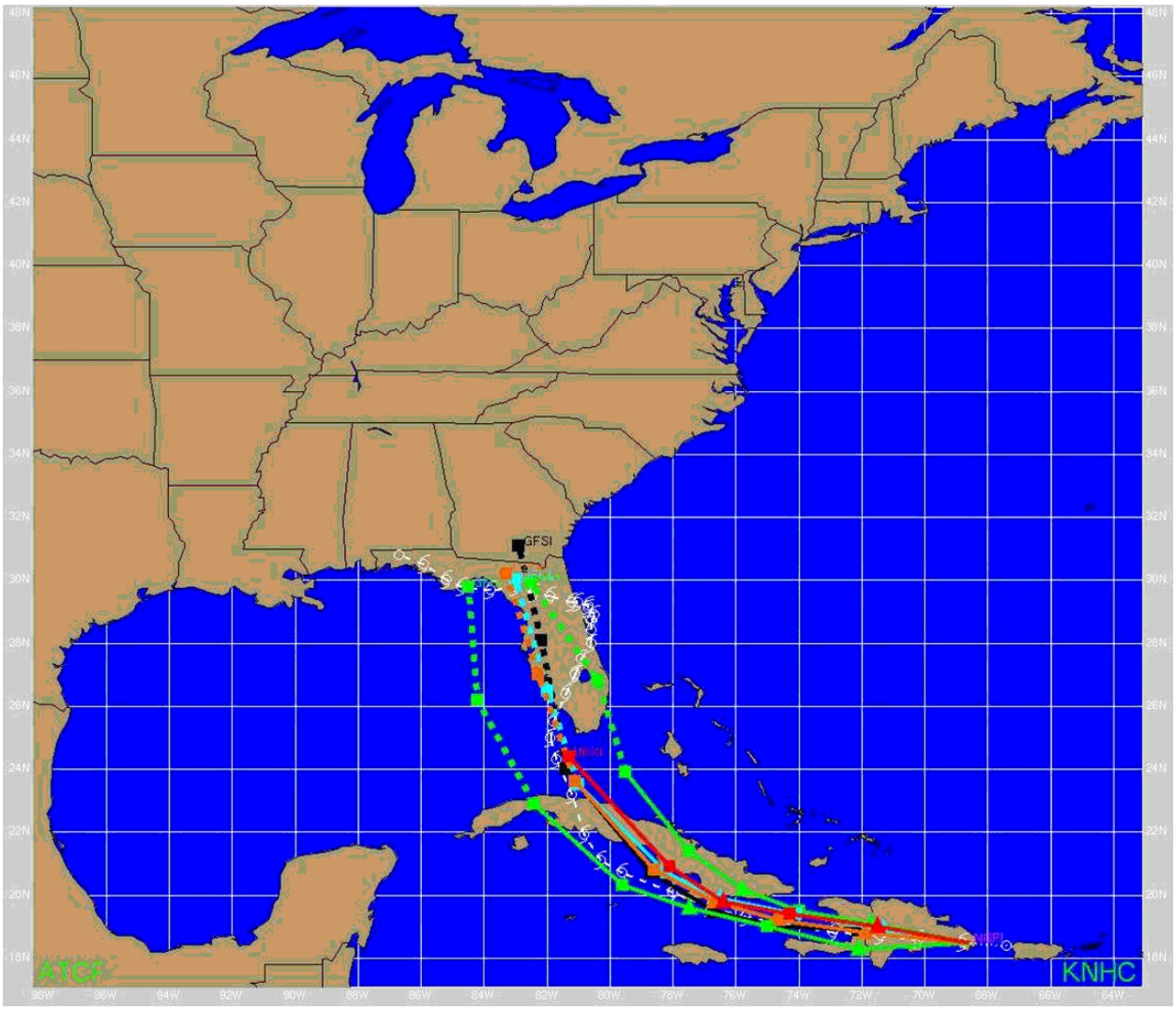

Figure 3.27. Numerical model guidance at 1800 UTC 15 August 2008 for Tropical Storm Fay, centered over the eastern tip of the Dominican Republic. The white line with hurricane symbols represents the final best track of the storm. The cyan line represents the official NHC forecast track, and the multi-colored lines represent other forecast models. Dashed lines represent the forecast from 72 h to 120 h.

The example of Atlantic Tropical Storm Fay in the Atlantic (2008) demonstrates the advantages of maintaining continuity. Figure 3.27 shows numerical model output at 1800 UTC 15 August 2008, when Tropical Storm Fay was centered over the eastern tip of the Dominican Republic. The official forecast (in cyan) is in the middle of the guidance envelope, very close to the TVCN model consensus (an average of at least two of the following models: the GFS, UKMET, NOGAPS, GFDL, HWRF, GFDN, or ECMWF. During the next forecast cycle (Fig. 3.28) several of the leading models and the model consensus shifted their tracks westward. Knowing that model guidance varies from cycle to cycle, particularly at long lead times, the forecaster nudged the official forecast track slightly westward, placing the official NHC forecast track on the eastern edge of the guidance envelope. One benefit of following continuity is that it allows the forecaster to make incremental adjustments toward a particular solution once the guidance

begins to consistently predict a given scenario, while avoiding drastic changes. The track models shifted back toward the east (Fig. 3.29) at 0600 UTC 16 August, closer to the original set of guidance from 12 hours before, and the forecaster made only a minor adjustment to the official forecast track.

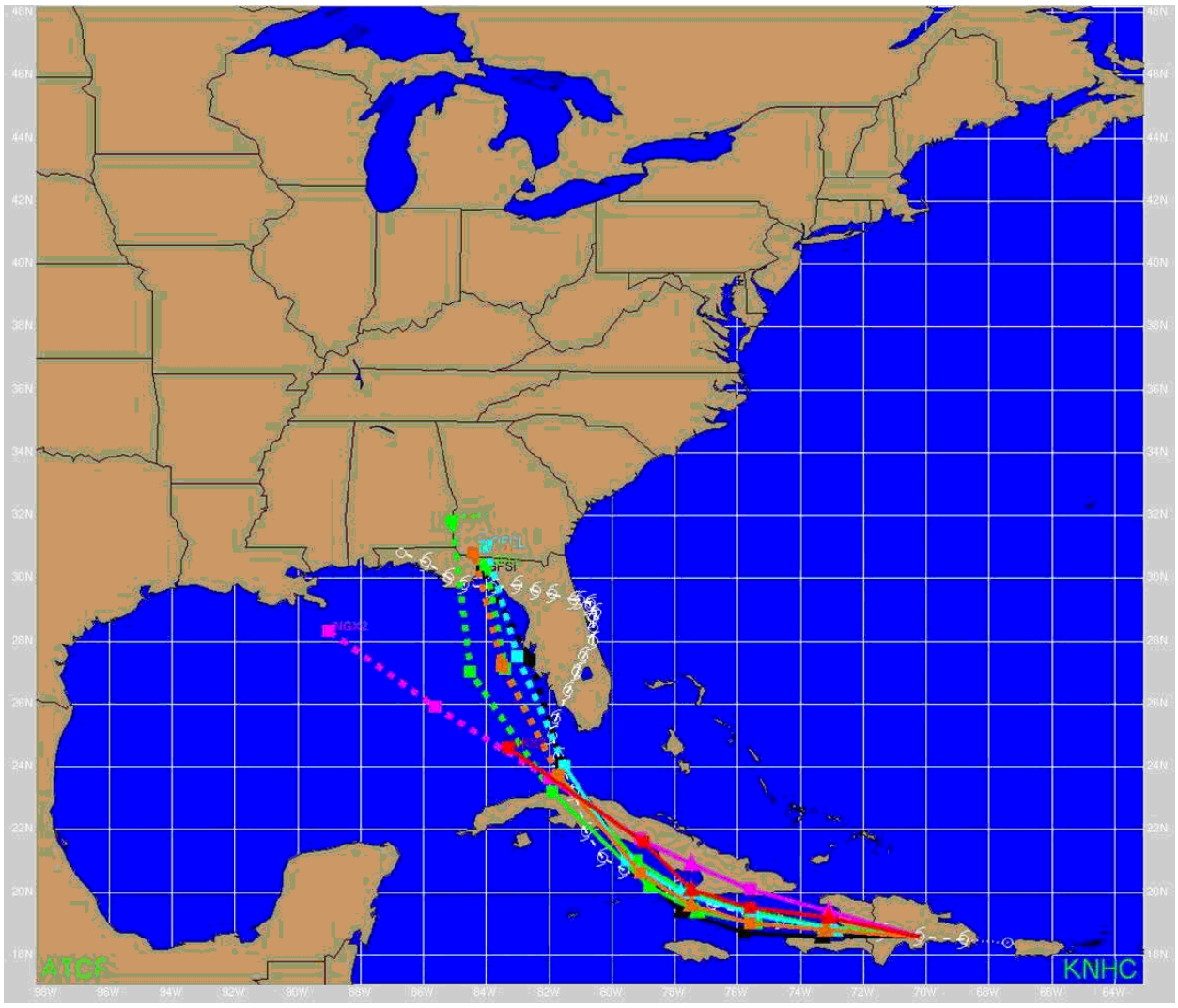

Figure 3.28. As in Fig. 3.27, except for 0000 UTC 16 August 2008, when Tropical Storm Fay was near Santo Domingo, Dominican Republic.

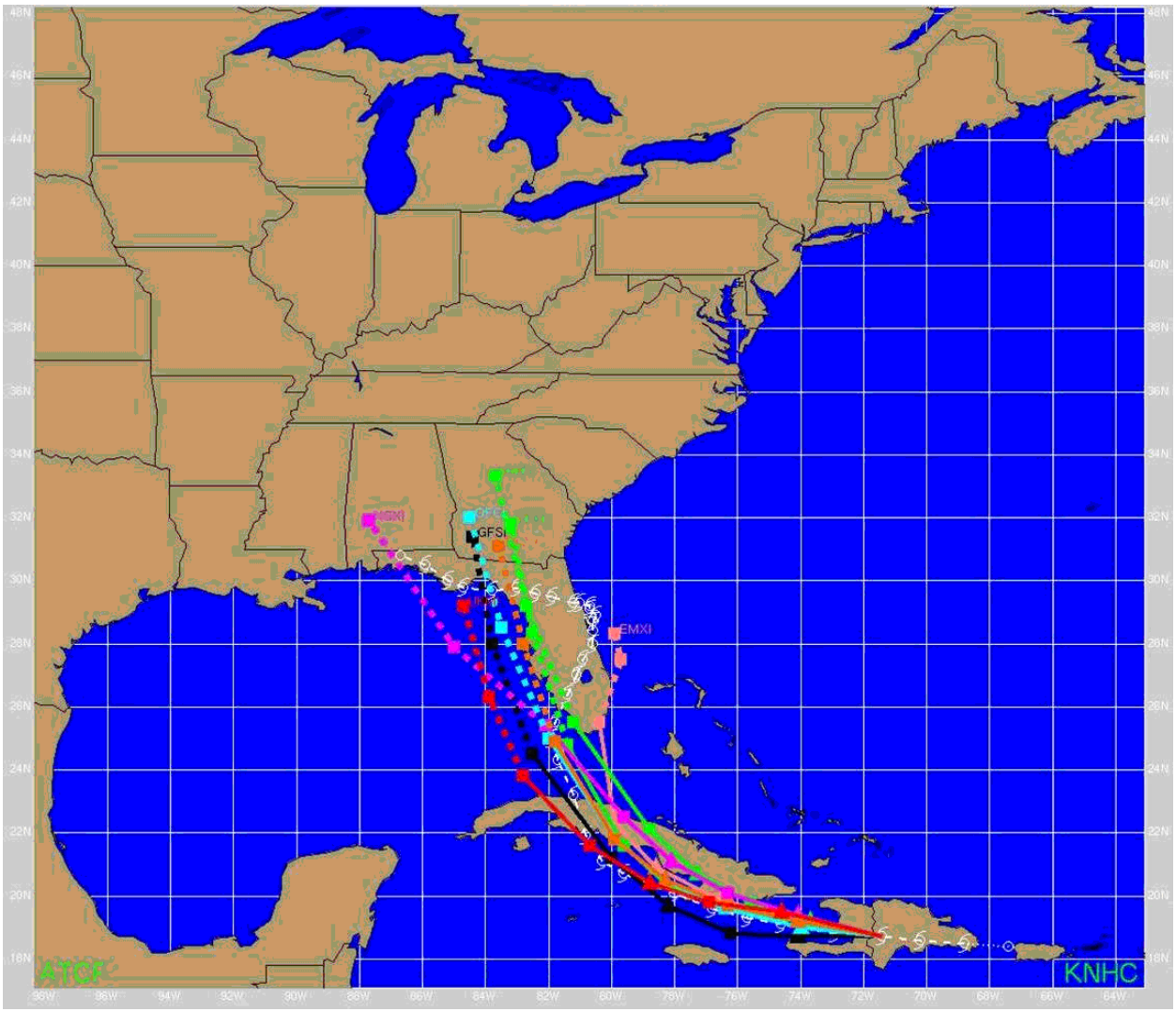

Figure 3.29. As in Fig. 3.27, except for 0600 UTC 16 August 2008.

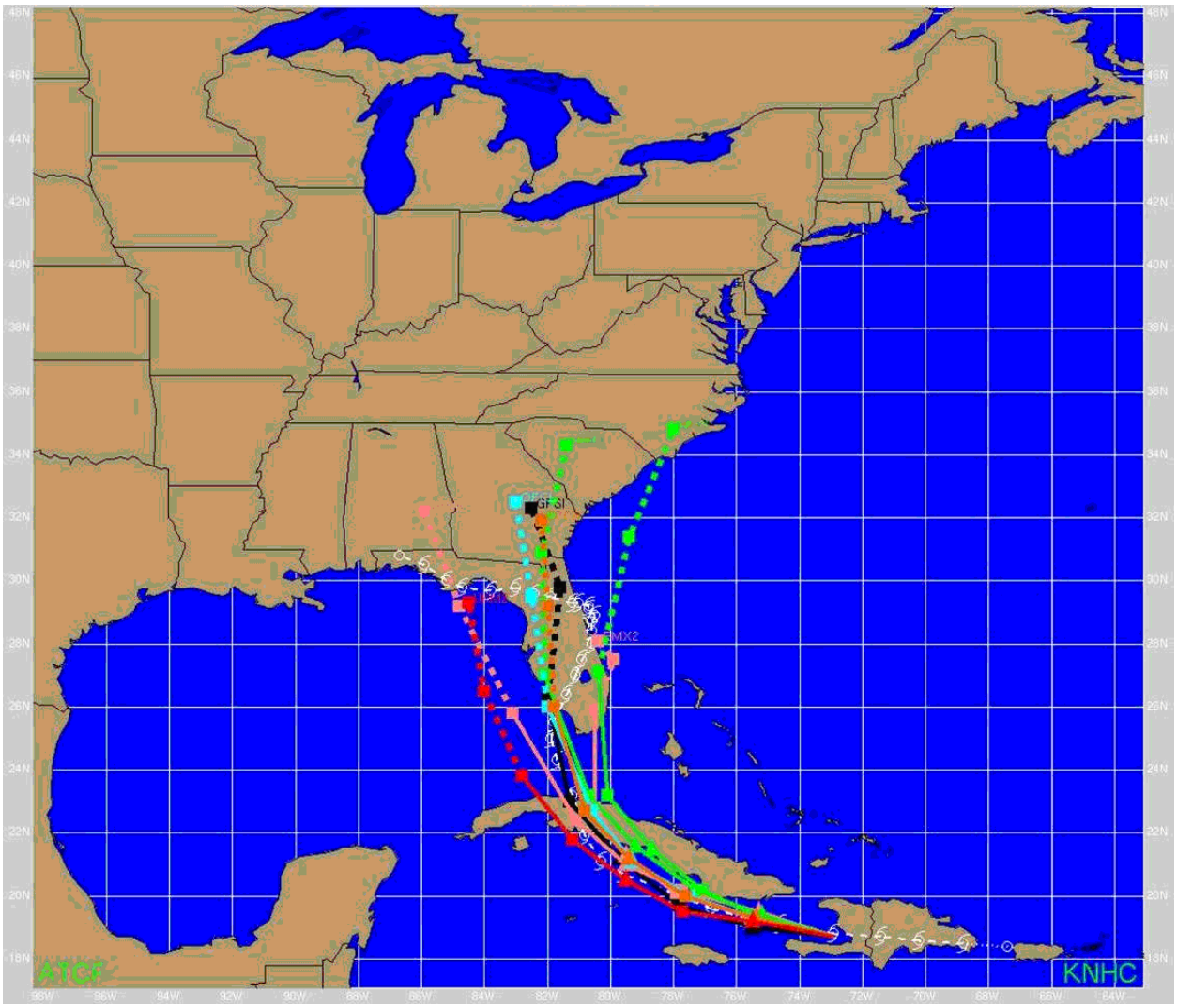

Figure 3.30. As in Fig. 3.27, except for 1200 UTC 16 August 2008.

Model guidance continued shifting eastward at 1200 UTC 16 August (Fig. 3.30), and the forecaster, now detecting a possible trend, shifted the track more significantly eastward. The official NHC track deviated little from the 1200 UTC forecast track during the next several cycles as the model guidance converged on a solution. In this case, if the forecaster had not considered continuity and had shifted the track farther westward at 0000 UTC 16 August, the eastward shift in the model guidance at subsequent forecast times would have required major changes to the forecast.

Beta and Advection Models (BAM)

BAM refer to a class of simple trajectory models that use vertically-averaged horizontal winds to produce TC trajectories, while adding a beta correction term to account for the Earth's rotation. These models use different layer means and can be used to assess likely storm motion in different situations: BAM shallow (850-700 hPa), BAM medium (850-400 hPa), and BAM deep

(850-200 hPa), known as BAMS, BAMM and BAMD, respectively. For example, for a weak or severely sheared system the BAMS output would be a better indicator of TC motion than BAMD, especially when the environmental flow is simple and baroclinic forcing is weak.

Global models

Many forecasting agencies such as the European Center for Medium-Range Weather Forecasts (ECMWF), the U.S. National Weather Service (NWS), and the U.K. Met Office (UKMET) operate central facilities that run numerical weather prediction models at least twice daily out to as long as 15 days. While global dynamical models were not designed to explicitly predict TC track, they have demonstrated increasing skill in this area due to improved forecasts of the large-scale steering flow that controls TC motion. Also, their lack of lateral boundary conditions in global models means that their performance at longer ranges is more skillful than regional models. In fact, global models are the best TC track forecast guidance, especially beyond 48-72 h.

A significant challenge to TC modeling has been developing a method by which the relatively small-scale TC vortex can be properly analyzed by relatively coarse models in regions with little data. In the NOGAPS and UKMET global models, a method to construct a TC vortex by using "bogus" or synthetic observations is utilized. Another scheme known as "vortex relocation" is utilized in the GFS model, which does not modify the analyzed TC vortex but repositions it to the official position estimate, resulting in more accurate forecasts by that model. Elsberry (2005) found that the GFS model 72-hour average track error decreased considerably, to 193 nm after the inclusion of this procedure from 2000-2003; an astonishing increase in forecast skill of 42% with respect to CLIPER. However, the ECMWF global model, which uses neither scheme, has emerged as one of the more skillful track models in the Atlantic in recent years. For additional information on the vortex relocation procedure, refer to Liu et al. (2000), Gao et al. (2010) or Hsiao, et al. (2010).

Regional models

Dynamical models designed specifically for TCs (e.g., GFDL, GFDN, and HWRF) are known as limited-area or regional models. Their limited areal coverage means that they can have higher horizontal and vertical resolution, which is an important factor in the accurate depiction of TC structure for intensity forecasts. In the GFDL, the vortex is "spun up" in a separate model and inserted into the model analysis at the initialization time. The more explicit representation of the TC also means that regional models can handle interactions better between the TC and its environment, which can result in improved short-term track forecasts. However, a disadvantage to the limited model domain is that critical upstream weather features may initially be located outside the model domain and may be handled poorly in the model forecast (M. Bender, personal communication). As a result, the skill of regional models for track beyond a few days is less than that of the global models (Franklin 2009). For example, the GFDL model performs well through 48 h followed by a severe degradation in forecast skill by 120 h (Fig 3.31).

Ensembles

An ensemble is a collection of model forecasts verifying at a common time. Ensembles are generally composed of multiple model forecasts, typically from the same model using small changes (i.e., perturbations) in the initial conditions to represent the uncertainty in the analysis. These initially small perturbations grow with time and in a perfect ensemble, the truth would always lie within the envelope of possible ensemble solutions. Most global ensemble systems are run with 20 or more member forecasts with somewhat coarser resolution than their global deterministic model counterparts. Other ensembles are created by varying the formulation of the model itself. Also, a collection of forecasts from different models is another way to construct an ensemble.

While global model ensembles are most frequently used for large-scale pattern forecasting, they can be useful for longer-term TC track forecasting, particularly for diagnosing trends in the large-scale circulation patterns that can govern TC motion. However, up to this time, the average forecast skill of the ensemble mean of both the U.S. Global Ensemble Forecast System (GEFS) and the ECMWF ensemble system through five days has not surpassed that of their counterpart deterministic global models in the Atlantic or East Pacific (Franklin 2010).

More detailed overview of the use of ensembles in TC track forecasting can be found at Heming & Goerss (2010). Further examples are presentations at ITWC VII by Foley (2010) and Nakazawa (2010).

Table 3.2 presents basic model specifications and other characteristics. Heming & Goerss (2010) provides a detailed description of specific global models and descriptions of individual ones primarily used for TC track prediction.

Note that NWP development is ongoing, these specifications were current about 2009.

Table 3.2. Operational models in use at NHC. Timeliness is given as "E" for early and "L" for late. & Canadian GEM model uses a 4D-VAR scheme that makes use of in situ flight data.

Name/Description	ATCF ID	Type	Resolution	Vortex Specification	Timeliness
NWS/Geophysical Fluid Dynamics Laboratory (GFDL) model	GFDL	Multi-layer regional dynamical	Inner grid 5°x5° at 1/12° spacing, intermediate grid 11°x11° at 1/6° spacing, outer grid 75°x75° at 1/2° spacing, 42 vertical levels	Synthetic vortex	L
NWS/ Hurricane Weather Research and Forecasting Model (HWRF)	HWRF	Multi-layer regional dynamical	9x9km, 42 vertical levels	Synthetic vortex	L
NWS/Global Forecast System	GFS	Multi-layer global	T382L64, (~35 km horizontal resolution)/td>	Vortex relocation	L

(GFS)					
National Weather Service Global Ensemble Forecast System (GEFS)	AEMN	Consensus	T190L28 (0-180h)	Vortex relocation	L
United Kingdom Met Office model (UKMET)	UKM	Multi-layer global dynamical (Grid point)	0.5°x 0.4° (~40 km at mid-latitudes)	Bogussing	L
Navy Operational Global Prediction System (NOGAPS)	NGPS	Multi-layer global dynamical (Spectral)	T239L30(approximately 55 km horizontal resolution)	Bogussing	L
Navy version of GFDL	GFDN	Multi-layer regional dynamical	Inner grid 5°x5° at 1/12° spacing, intermediate grid 11°x11v at 1/6° spacing, outer grid 75°x75° at 1/2° spacing, 42 vertical levels	Synthetic vortex	L
European Center for Medium-range Weather Forecasts (ECMWF) Model	EMX	Multi-layer global dynamical	T1279L91 (approximately 16 km horizontal resolution)	No vortex specification	L
Environment Canada Global Environmental Multiscale Model	CMC	Multi-layer global dynamical	33 km (~45°N) horizontal resolution, 58 vertical levels	4-D VAR scheme[&]; no bogus	L
Beta and advection model (medium layer)	BAMM	Single-layer trajectory	T25 resolution	No vortex specification	E
Beta and advection model(deep layer)	BAMD	Single-layer trajectory	T25 resolution	No vortex specification	E
Beta and advection model (shallow layer)	BAMS	Single-layer trajectory	T25 resolution	No vortex specification	E
NCEP North American Model	NAM	Multi-layer regional dynamical	12km horizontal, 60 vertical levels	No bogus	E

Consensus-based approach

No single model is consistently the best at forecasting TC track. The relative reliability of the models fluctuates from season to season due to changes in resolution, physical paramterizations, or data assimilation schemes. Fluctuations in model performance can also be seen from one run to the next due to errors in model initial conditions and how individual models handle critical features, including the TC itself.

A forecast derived from inputs from different models is often referred to as a "consensus" forecast. The simplest consensus is just an average (or mean) of the forecasts from the individual member models. Grouping several independent models together to form a multi-model ensemble can provide a more skillful forecast than an individual model. Goerss (2000) illustrated the value of a consensus-based approach by forming a simple model consensus of three global models and another consensus of two regional models. The track errors of both consensus models were significantly smaller than those from the best individual models. The addition of new models to the consensus generally leads to minor but steady gains in skill, especially if the number of models in the consensus is small since the effectiveness of a model consensus relative to each individual member is a function of the independence or effective degrees of freedom of the models forming the consensus. In fact, the inclusion of a model that is less skillful than the other consensus members can still yield a positive contribution. Sampson et al. (2006) showed that the inclusion of a relatively simple barotropic model in the consensus produced a large positive impact in spite of that model's generally larger errors. A larger consensus produces smaller mean errors by reducing the influence of large errors from any individual model, especially when the degree of independence is high.

The error reductions that occur when different models are combined are demonstrated in Figure 3.31 where the GUNA consensus, an average of the GFDL, UKMET, NOGAPS, and GFS models, outperforms not only all of the models it comprises but also the GEFS ensemble mean. Rappaport et al. (2009) note that the GUNA consensus outperformed the most skillful of all the GUNA constituents, the GFDL model, by 18% between 2004 and 2006. A dynamical model consensus is often an excellent starting point in the preparation of the track forecast and is difficult to beat as a final forecast, after accounting for continuity.

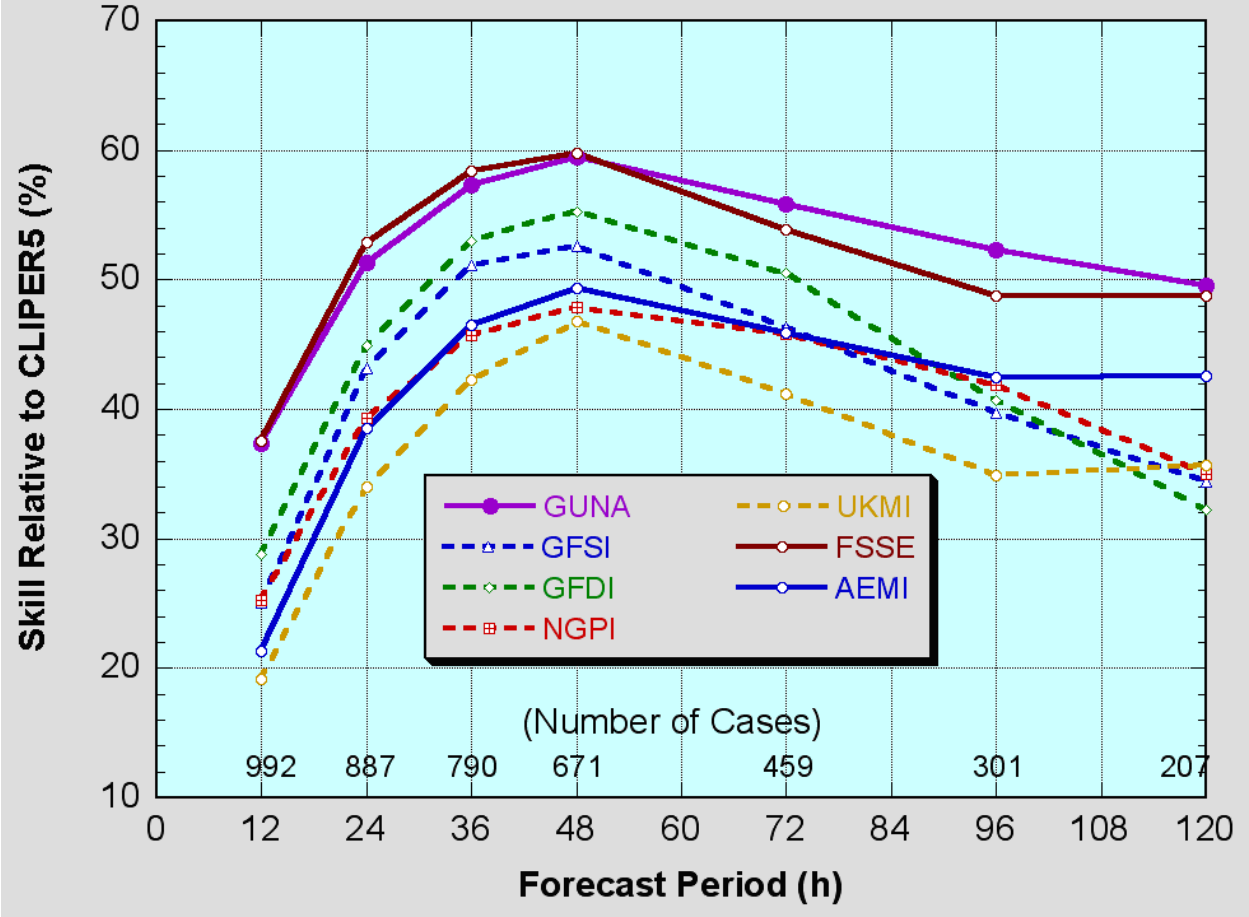

Figure 3.31. Skill of individual and consensus models for TC track in the Atlantic from 2005-2009 relative to CLIPER. The number of cases is indicated in black at each time interval.

The building of a consensus must take into account model availability, which can differ considerably from model to model. "Fixed" consensus solutions require that all members of the consensus be available before computing the model consensus (e.g., GUNA); others, like the "variable" consensus models require a minimum of two available members (e.g. TVCN, an average of at least two of the GFS, ECMWF, NOGAPS, UKMET, GFDL, GFDN, and HWRF). The greater number of consensus members increases the chance of having the minimum number of models available to generate a consensus forecast for a variable consensus model. However, this can lead to consistency issues, when, for example, the 120-hour forecast in a variable consensus may be based on a different set of models than the 96-hour position.

Corrected consensus scheme

Another technique is the "corrected" consensus, which is formed by computing statistical correctors for the member models based upon parameters that are known at the time the forecast is made. These correctors come from regressing model tracks against the "best track" and then assigning weights to each member model solution based on that model's past performance (Vijaya Kumar et al. 2003). Corrections can be based upon the previous model

biases, current model spread, the initial TC position, intensity, and the forecast track. The corrected consensus can be computed in real time or updated annually (Weber et al. 2003). The FSU Superensemble is an example of the corrected consensus technique.

The corrected consensus approach requires a large sample of retrospective runs to develop robust statistics for the bias correction. However, since models are updated frequently, the bias corrections developed may not be applicable to modified versions of the model or the corrections may not be drawn from a large enough sample. Drawing conclusions about storm behavior from an insufficient number of cases is not advisable, since meteorological conditions in small sample are not varied enough to be representative (Franklin 2009). As a result of this limitation, the corrected consensus approach has not shown improvement over the simple consensus methods.

Sustained winds are greatly influenced by exposure and surface roughness characteristics. A better measure of tropical cyclone sustained wind is frequently obtained by using the observed gust and then converting it to an associated sustained wind as determined from a general relationship that better pertains to winds observed in tropical storms and hurricanes (e.g., Krayer and Marshall 1992; Harper 2010).

Selective consensus

Another consensus approach in which the forecaster subjectively forms a consensus is known as a selective consensus. The selective consensus gives the forecaster the opportunity to reject a particular solution or set of solutions if they appear to be an outlier. The Systematic Approach Forecast Aid (SAFA) was introduced in 2000 at the Joint Typhoon Warning Center (JTWC) to help forecasters determine error characteristics for the available track models (Carr et al. 2001). Elsberry et al. (2000) demonstrated that eliminating a model suspected of underperforming improved the consensus in nearly all of the cases they examined (in these cases, forecast errors were large). The operational use of this method yielded mixed results, however, with many more cases where little to no appreciable improvement to the forecast was noted. Consequently, the use of selective consensus remains challenging.

The use of a selective consensus can sometimes produce positive results, but the forecaster must recognize when it use is appropriate. Sampson et al. (2007) suggested that model improvements in recent years have made it unlikely that a selective consensus can outperform a consensus of dynamical models, especially when model spread is small. In these cases, the skill gained by attempting to exclude “bad” guidance from the consensus comes with the risk of mistakenly eliminating “good” guidance. When the model spread is large, however, there is an opportunity for the forecaster to increase forecast skill by eliminating one or more clearly unrealistic scenarios from consideration.

Estimating forecast uncertainty

Goerss (2007) demonstrated that it is possible to predict the errors of a consensus model forecast by examining predictors such as the spread of the consensus members, the initial and

forecast intensity, the initial TC position, TC speed and motion, and the number of members available in the consensus model. The most significant predictor was the spread of the consensus members, followed by the initial and forecast TC intensity. A stepwise linear regression model and the most skillful predictors can be used to forecast the consensus model error at all forecast times. The technique, known as Goerss Prediction of Consensus Error (GPCE), was able to predict 15-20% of the forecast variance at shorter lead times and up to 45-50% of the variance at the longest lead times (Goerss 2007). Operationally, the GPCE technique produces circular radii based upon the predicted errors around each of the consensus model forecast positions at NHC, CPHC, and JTWC. These radii are constructed so that they will contain the verifying observed forecast positions 70-75% of the time (Fig. 3.32). Since the predicted GPCE radii are positively correlated with the model consensus spread, the size of the radii can be used to determine how much confidence to assign to the consensus model forecast. Making a forecast outside a GPCE circle would require a strong signal that the model consensus forecast is in error.

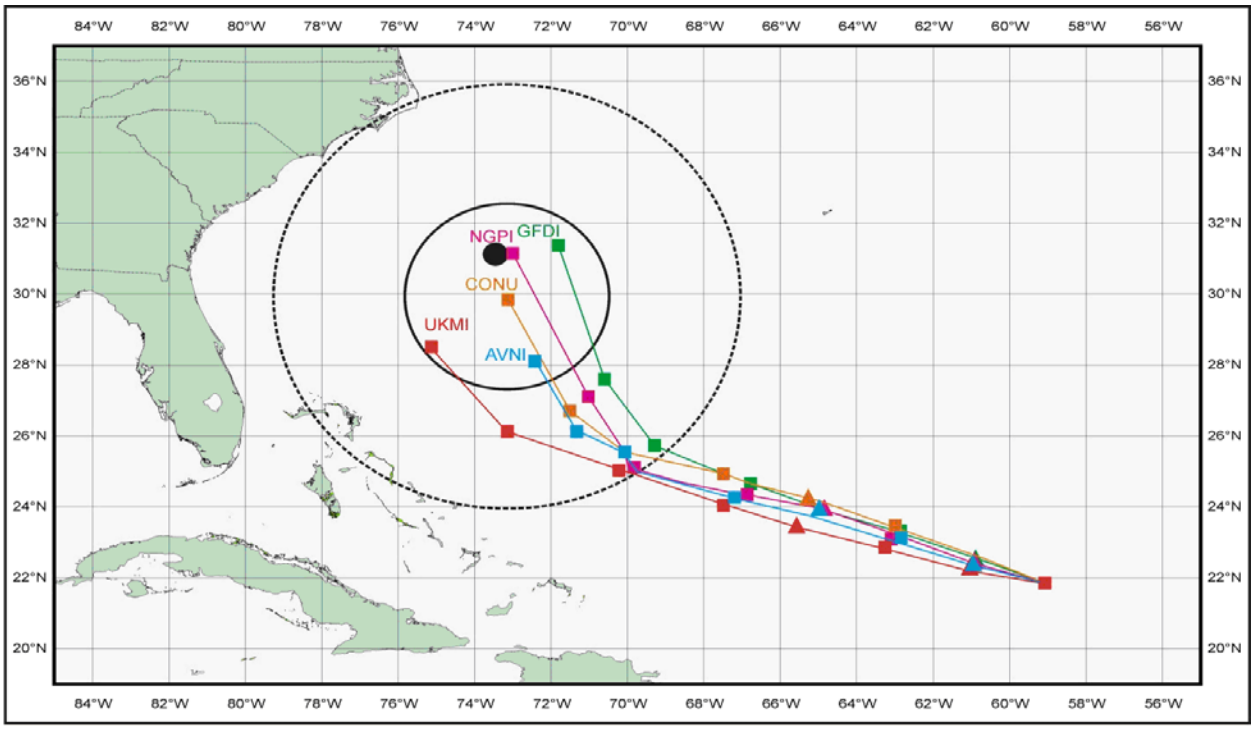

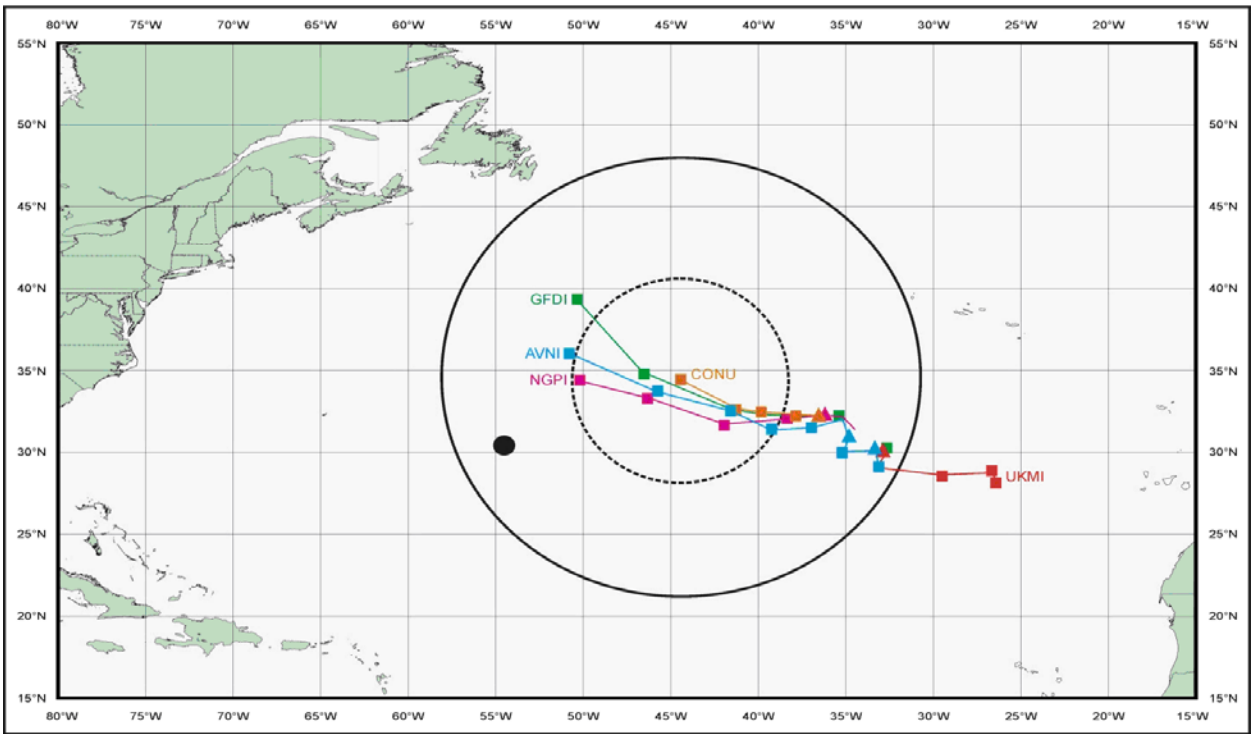

Figure 3.32. Predicted 72% confidence radius (solid circle) surrounding the 120-h CONU (consensus model computed when track forecasts from at least two of the following five models are available: GFDI, AVNI, NGPI, UKMI and GFNI) forecast for (a) Hurricane Isabel, 0000 UTC 13 Sep 2003 and (b) Hurricane Kate, 0000 UTC 30 Sep 2003. The individual model tracks used to create the CONU track are shown along with the 120-h radius (dotted circle) used by the NHC potential day 1-5 track area graphic. (Reproduced from Goerss (2007)).

The forecast process

Early vs. late models

All global TC warning centers issue an "official" forecast of position and intensity for operationally-designated TCs. Forecasts are issued every 6 hours at or around the standard synoptic times of 0000, 0600, 1200, and 1800 UTC but at varying forecast time intervals. Table 3.3 indicates the time intervals at which the main Regional Specialized Meteorological Centers (RSMCs) for tropical cyclones issue forecasts.

Table 3.3. Time intervals at which the global RSMCs issue official forecasts. "X" indicates that a forecast is made for that forecast time.

RSMCs for TCs	06	12	18	24	30	36	42	48	54	60	66	72	96	120
NHC Miami		X		X		X		X				X	X	X
CPHC Honolulu		X		X		X		X				X	X	X
RSMC Toyko		X		X		X		X				X	X	X
RSMC Reunion		X		X		X		X		X		X	X	X
RSMC Australia		X		X		X		X		X		X		
RSMC Fiji		X		X		X		X						
RSMC New Delhi, India	X	X	X	X	X	X	X	X	X	X	X	X		

Models are characterized as either early or late, depending on their availability to the forecaster during the regular 6-hourly forecast cycle. Consider the forecast cycle at the NHC that begins at 1200 UTC and ends with the issuance of the forecast at 1500 UTC. After assimilating 1200 UTC observational data, the GFS analysis and model integration take several hours. As a result, GFS model forecasts through 120 hours are not accessible until 1600 UTC, after NHC's forecast deadline. The unavailability of GFS model fields in time for the forecast deadline makes it a late model. On the other hand, the BAMS models are available within minutes of their initialization and are therefore early models. Model timeliness is given in Table 3.2.

To increase the utility of late models, the latest available run of a model can be adjusted to the current synoptic time and initial conditions. For example, the forecast from the 0600 UTC run of the GFS can be smoothed and then adjusted so that the 6-hour forecast position of the TC matches the observed 1200 UTC position. This adjustment process creates an early version of the GFS model that can be viewed with other model data for the 1200 UTC cycle. Although the interpolation process generally mitigates the problem of a poor initial analysis and six-hour forecast, errors in both of these can still lead to large errors later in the forecast.

Making a TC track forecast

Initialization

An inspection of the model analysis is necessary to determine how well the model captures the initial state of the atmosphere and the location, intensity, and structure of the TC. In some cases, model initialization errors are obvious, such as during the genesis stage of Hurricane Gordon at 1200 UTC 11 September 2006 where the GFS analysis of sea-level pressure and 10-m winds is too weak, showing only an inverted trough and little cyclonic vorticity in the wind field when the cyclone is already a 35-kt tropical storm (Fig. 3.33). In addition, microwave imagery at the time showed evidence of a closed low-level circulation (Fig. 3.34). Even though the GFS did not depict a closed circulation at the surface, its track forecast was still somewhat realistic since its forecast of the steering flow was accurate.

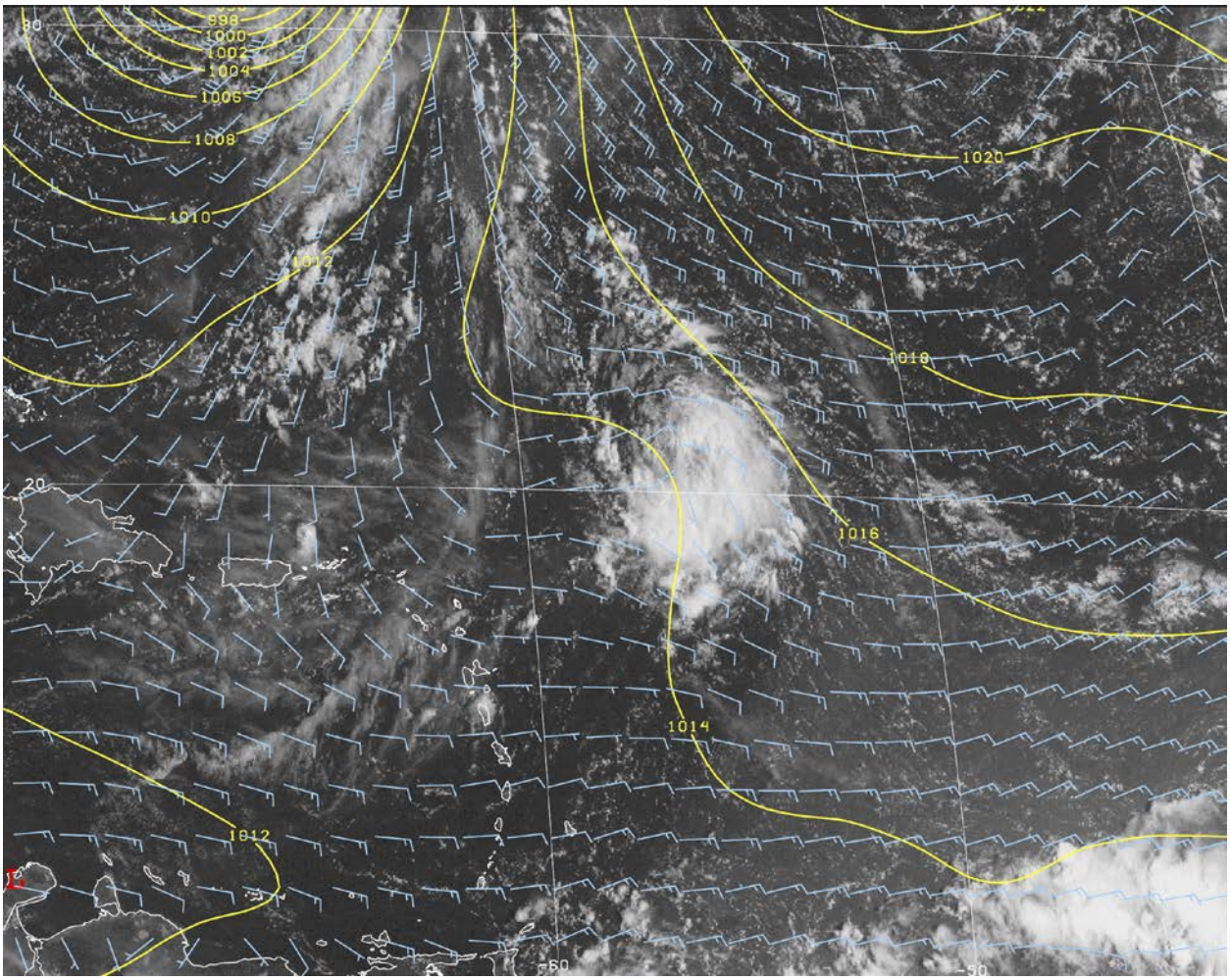

Figure 3.33. An example of a poor GFS model analysis of 10-m wind (in kt) and surface pressure (mb) at 1200 UTC 11 September 2006. Newly upgraded Tropical Storm Gordon is evident a few hundred miles northeast of the northern Leeward Islands.

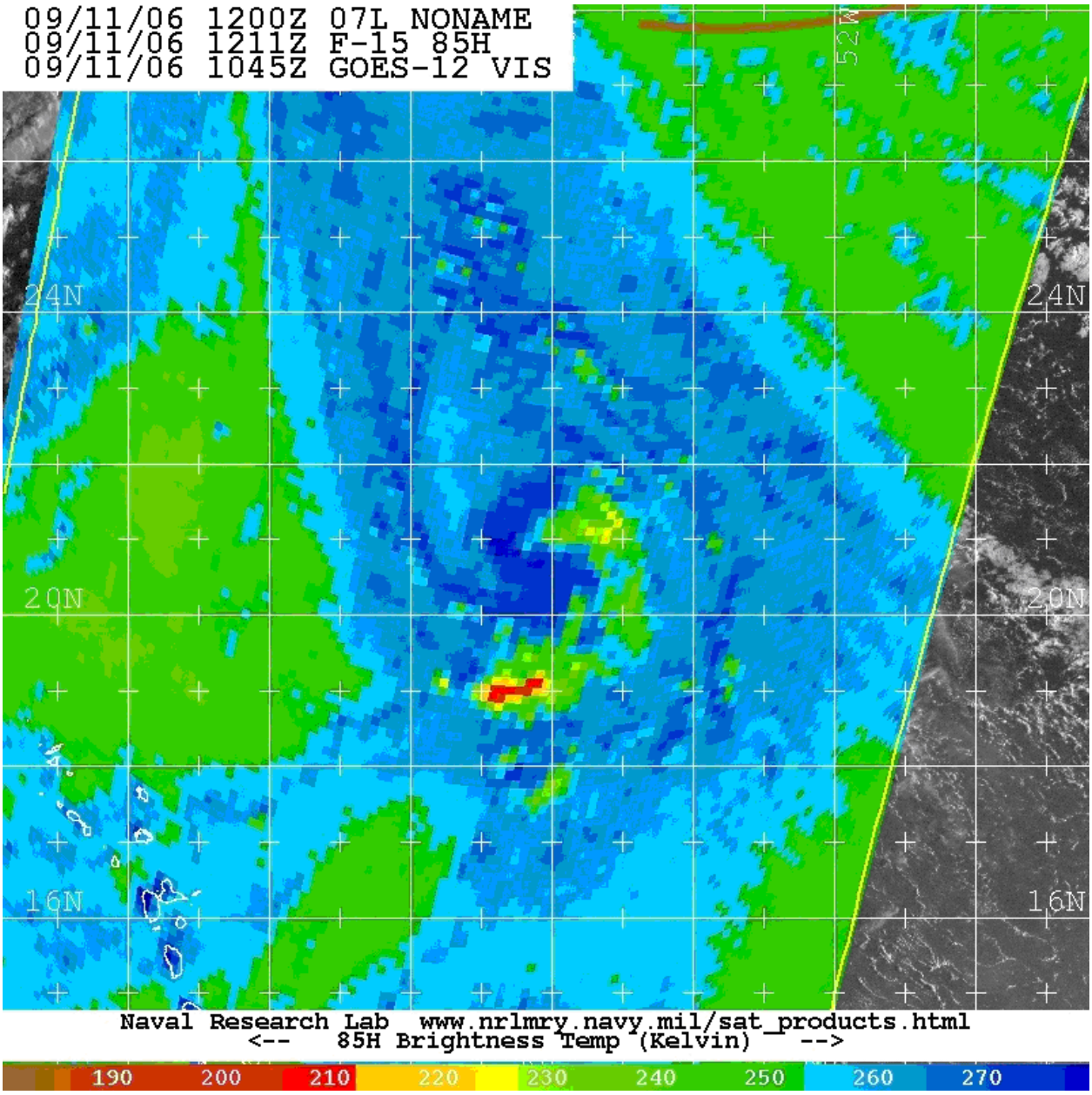

Figure 3.34. SSM/I 85-GHz H-pol image over Tropical Storm Gordon at 1211 UTC 11 September 2006. Brightness temperature (K) is indicated by the scale at the bottom of the figure.Image courtesy of the U.S. Naval Research Laboratory.

Another example of model initialization problems is from 0000 UTC 14 September 2004, where three TCs are analyzed by the GFS: Hurricane Javier and Tropical Storm Isis in the eastern North Pacific and Hurricane Ivan in the Yucatan Channel (Fig. 3.35). While Javier was nearly as intense as Ivan, the model only analyzes Javier as a weak tropical cyclone.

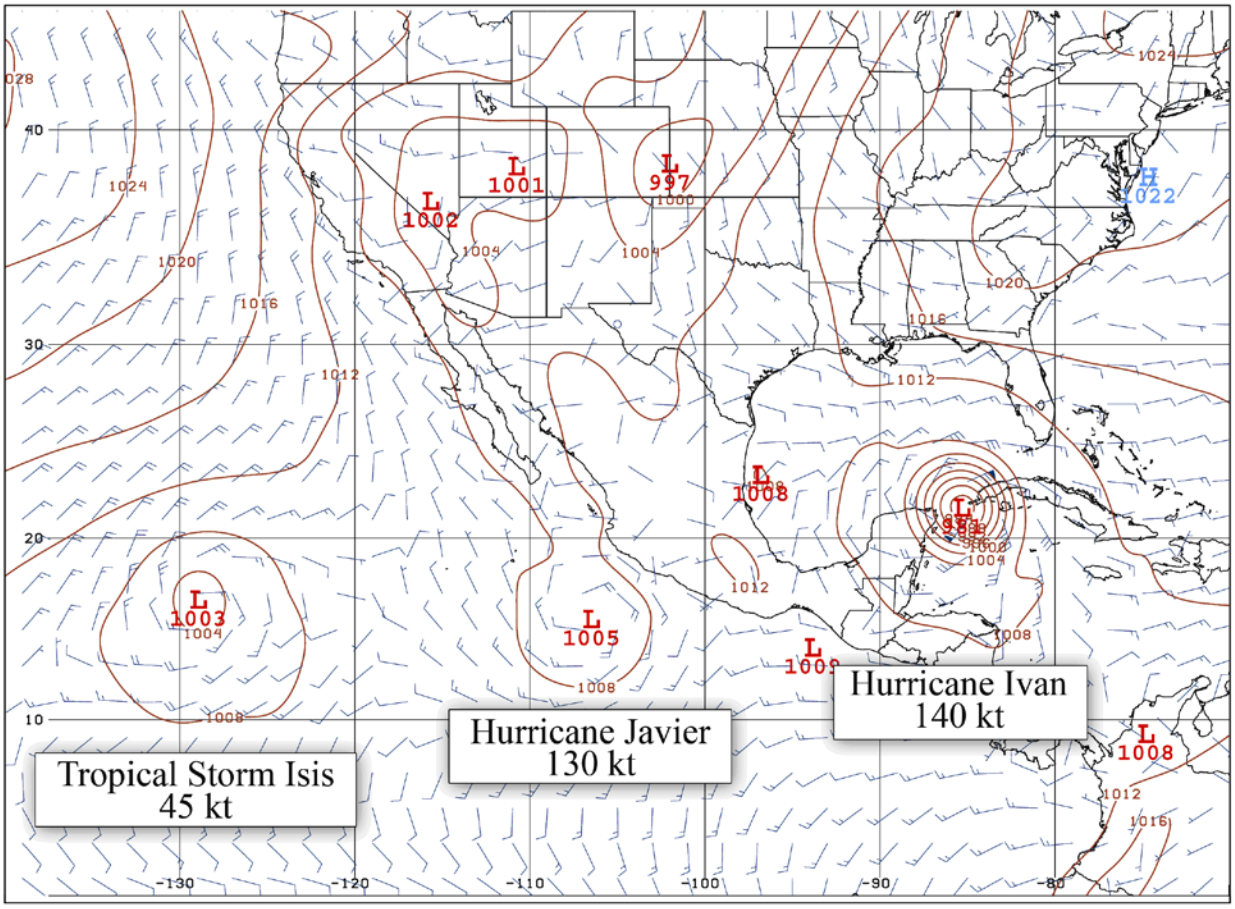

Figure 3.35. GFS model analysis of 10-m winds (in knots) and surface pressure (brown contours, hPa) at 0000 UTC 14 September 2004. The wind speed in each box for each cyclone is the best track intensity of the corresponding cyclone at the analysis time.

Satellite imagery, surface observations, and cloud-tracked winds should be examined when assessing the quality of a model analysis. Using software packages that enable the analyst to overlay these real-time data with the model analysis allow for a more detailed comparison. Models can then be ranked in terms of how far out of tolerance they are with respect to observations. In the example of Javier, the GFS analysis is so poor that the model forecast was poor beginning almost immediately. Although models with poor analyses should be viewed with suspicion, some useful information might still be obtained from them.

Forecasters should evaluate model initializations using a multi-step approach. The forecaster can first qualitatively compare the model analysis with an analysis of available observations to help familiarize the forecaster with the current data and synoptic pattern and identify critical differences that could affect the evolution of the TC. Assessing the significance of initialization errors in the context of the current forecast scenario can be difficult, especially since their identification does not necessarily reveal the ultimate impact on the model forecast. In general, the forecaster should primarily focus on initialization errors upstream of a TC since their effects will likely propagate downstream during the forecast cycle, possibly altering the large-scale

steering flow in the near-storm environment. On occasion data may be modified or deleted from the analysis by a central authority, and forecasters reviewing model analyses should realize when either action is taken and why. However, no analysis scheme will exactly match a given set of observations, and quality control routines in sophisticated data assimilation schemes make locating errors of substantial importance a more difficult task.

Short-term forecasts

Short-term forecasts (i.e., those out to 72 hours) are critical to the issuance of watches and warnings and can serve as the basis for making evacuation decisions. The regional dynamical models, such as the GFDL, GFDN, and HWRF, tend to be better performers in the short-range track forecasts due to their high spatial resolution and efforts to properly initialize the TC vortex. Fine-tuning the forecast for TCs approaching land can be done using more frequent and precise fixes from radar and aircraft. Observations of short-term oscillatory movement or trochoidal motion are not uncommon but should not be confused with a longer-term trend. In cases where a TC approaches the coast at an oblique angle, differences between short-term, oscillatory track behavior and longer-term trends can lead to large changes in the locations that experience tropical storm and hurricanes conditions and the location of landfall. As a TC moves to within a few hours of landfall, short-term trends ultimately determine when and where hazardous conditions will occur.

Extended-range forecasts

Extended-range forecasts (i.e., beyond 72 hours) rely most heavily on dynamical models and consensus model approaches. Global dynamical models have demonstrated increasing skill due to improved forecasts of the large-scale steering flows that control TC motion. However, significant differences can be seen in the large-scale pattern depicted by various global models at three days and beyond that can result in large differences in TC track.

Of the global dynamical models, those of the highest resolution like the ECMWF are generally consistent, better performers at longer ranges. One measure of global model forecast skill is the correlation between forecast and actual 500 hPa geopotential height anomalies. The skill of the ECMWF degrades more slowly compared to other global models (Fig. 3.36), indicating that the model better predicts the large-scale circulation features that can affect TC motion, especially at longer time ranges. While there is a tendency for some models to outperform others in a given year, no global model consistently performs best with TC track forecasting from year to year.

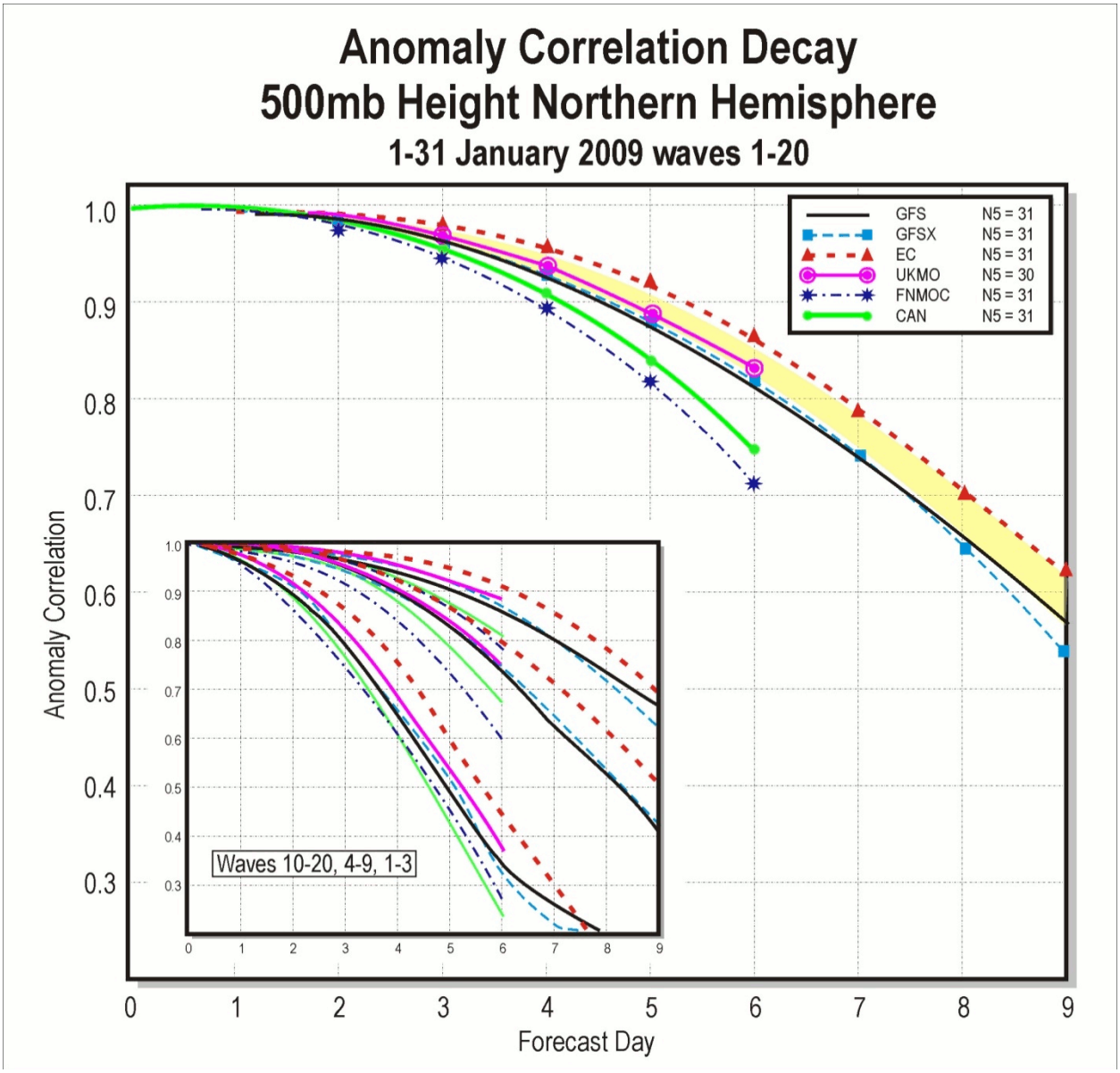

Figure 3.36. Plot of anomaly correlation 500-hPa geopotential height for various global models in the Northern Hemisphere from 1-31 January 2009.

Comparing several consecutive runs of a particular model or group of models over a period of time can reveal trends in the predictability of a forecast scenario. An example is shown from Hurricane Wilma in 2005 where three GFDL solutions generally show Wilma recurving off of the U.S. East coast in a few days, although they suggest significant uncertainty with regard to the forward speed during recurvature (Fig. 3.37). However, the 1200 UTC GFDL solution is an outlier, as it forecasts Wilma to remain in the Caribbean for the next five days. The lack of consistency in these model solutions suggests low predictability with the interaction of Wilma and the trough that may cause recurvature.

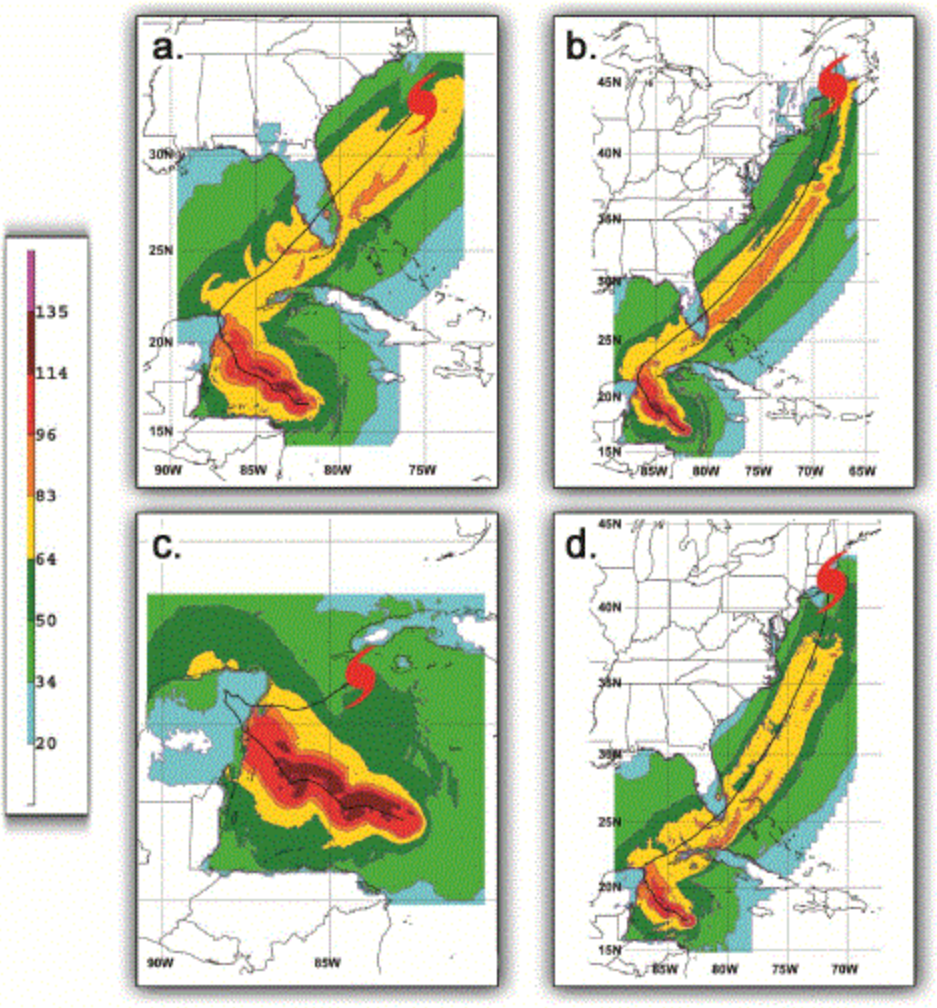

Figure 3.37. GFDL model output for Hurricane Wilma on 19 October 2005, from the (a) 0000 UTC, (b) 0600 UTC, (c) 1200 UTC, and (d) 1800 UTC cycles. The 5-day forecast track is given as a solid black line.

Challenges in the extended-range period include situations when TCs encounter poorly defined steering flows or interact with complex mid-latitude, sub-synoptic-scale flow, possibly resulting in sharp turns or loops in the track. Several examples of these situations are presented next.

No model correctly forecast the counter-clockwise loop made by Atlantic Tropical Storm Hanna in the vicinity of the southeastern Bahamas (Fig. 3.38b). In this case, each model handled the development of a deep-layer ridge near the U.S. East coast differently, resulting in large variations in Hanna's predicted track. Despite these differences, there were signals in the guidance that Hanna's forward speed would decrease and that a motion toward the west-southwest or southwest was possible. In this situation, evaluating the models over a longer period of time could lend more confidence to a particular solution or trends not apparent in a single cycle of track guidance.

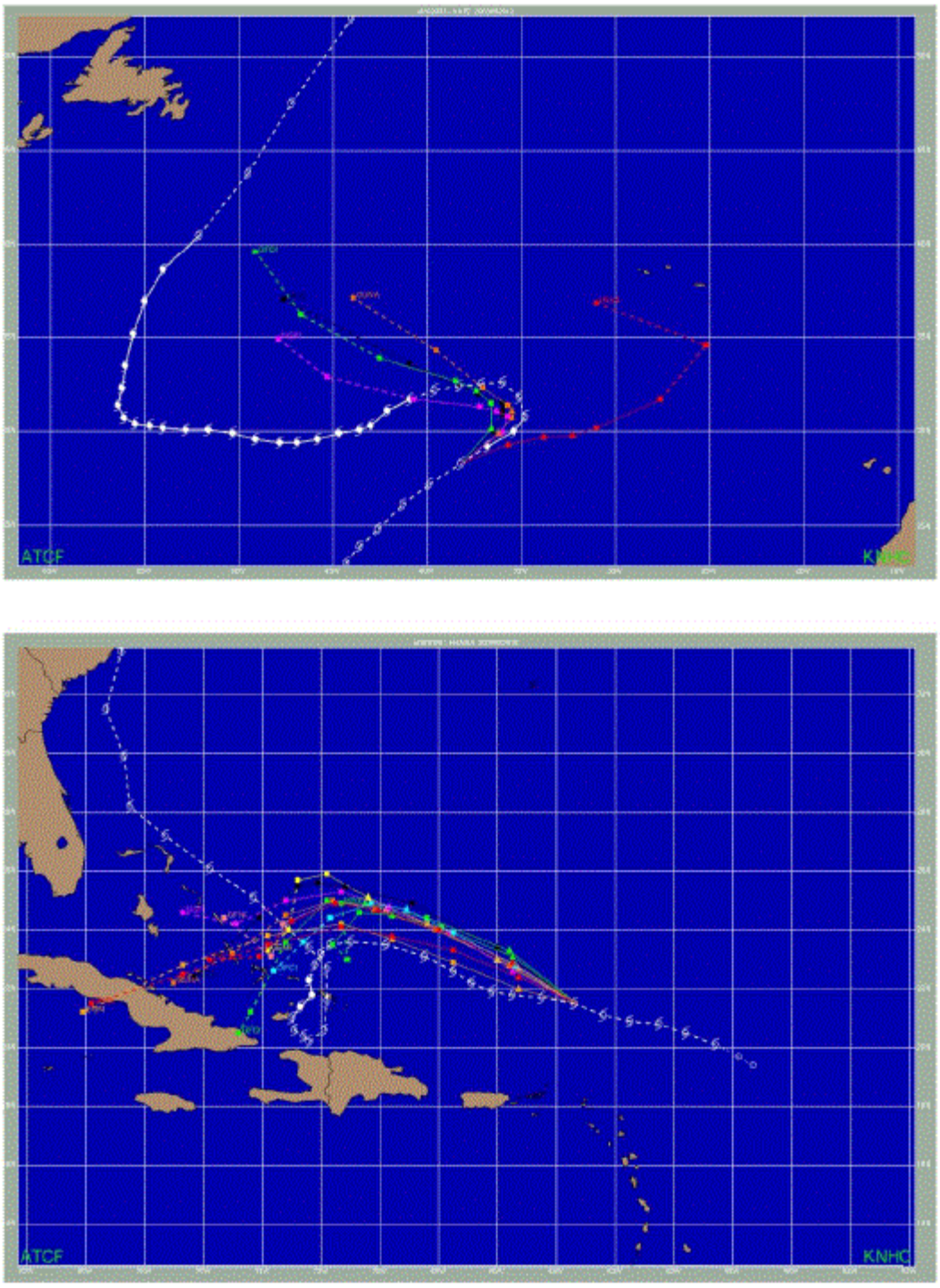

Figure 3.38. (a) Numerical model guidance at 1200 UTC 29 September 2003 Hurricane Kate over the central North Atlantic. The verifying track is given in solid white, while the individual models are color-coded. (b) As in (a), except at 1800 UTC 29 August 2008 for Tropical Storm Hanna.

Other complicated forecast scenarios involved Atlantic Hurricane Kate (2003), which stalled a few hundred miles southwest of the Azores (Fig. 3.38a) and Atlantic Tropical Storm Jeanne (2004), which stalled north of Hispaniola (Fig. 3.39). In these cases, the very large spread of the

model guidance makes forecasting a track near any one model ill-advised. The most prudent action is to closely follow the model consensus in the latter part of the forecast period until the guidance begins to converge on a solution. Another possible strategy is to form a selective consensus if some of the model solutions can be dismissed as unreasonable. However, this determination of a selective consensus is often difficult to make in real time.

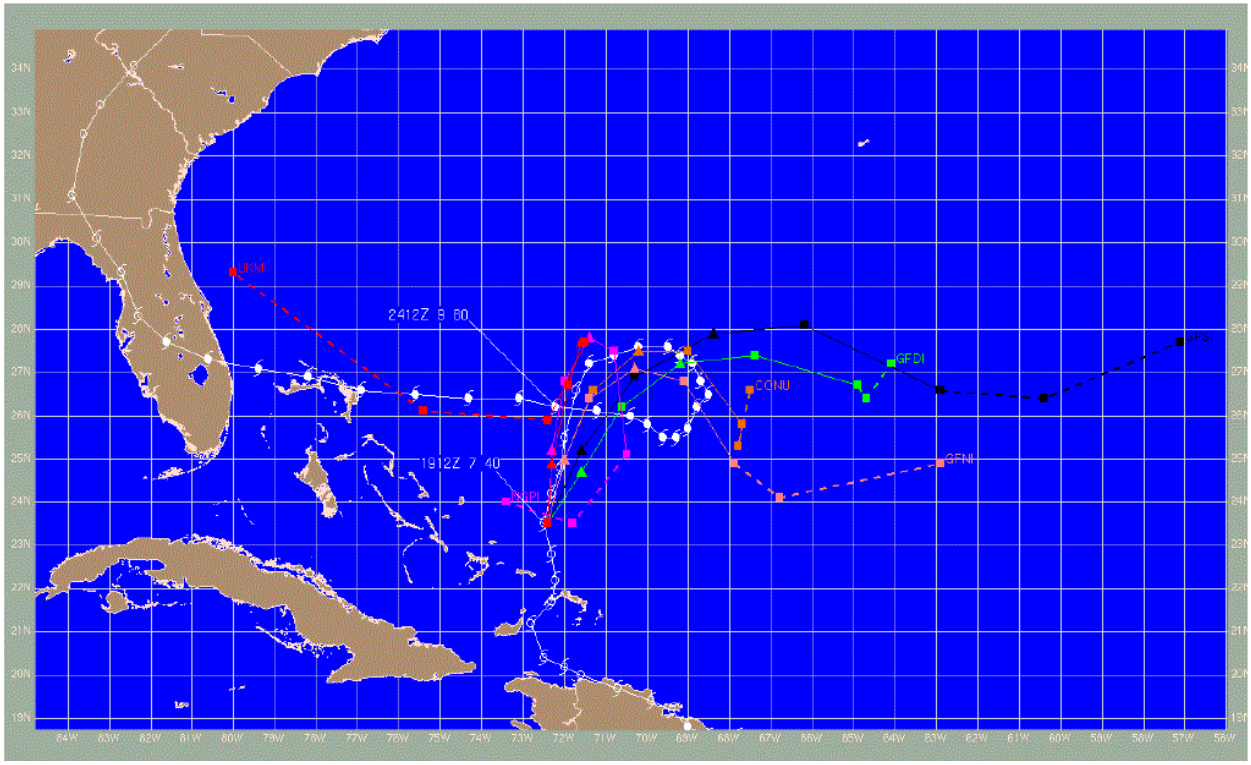

Figure 3.39. As in Fig. 3.38, except for Hurricane Jeanne at 1200 UTC September 19, 2004.

3.4 Summary and conclusions

This chapter describes current methods for estimating TC location and motion and forecasting TC track. The primary tools used to observe TCs are geostationary satellites, but the proliferation of polar-orbiting satellites with microwave sensors and scatterometers has provided other resources for analyzing TC location. In situ surface observations are of secondary importance, since their spatial coverage often severely limits their utility. All of these tools are supplementary to observations provided by aerial reconnaissance aircraft when TCs threaten land areas (in the Atlantic and occasionally the eastern and central North Pacific). Optimally, the TC center location should be determined using data from all of these platforms.

Improvements in TC track prediction have been constant over the last 15 to 20 years as numerical model resolution, computational resources and data sources greatly increase, and data assimilation methods have become more sophisticated. Multi-model consensus methods have become the most skillful predictors of TC track.

Future work in numerical modeling is expected to lead to continued improvements in TC track prediction. Advances will be made through applied research, increased observations through existing platforms and new observing technologies, increases in computer power and improvements to dynamical models and data assimilation schemes.

3.5 Acknowledgements

The authors are grateful for the comments and other support provided by Chip Guard, Jeff Hawkins, Jim Goerss, James Franklin, Jack Beven, Richard Pasch, Dan Brown, Eric Blake, Robbie Berg, John Cangialosi, and Chris Landsea. The authors are especially appreciative of the advice and other useful comments submitted by David P. Roberts regarding the Microwave section and from Jim Goerss concerning the model consensus section. We also are in debt to Colin McAdie who helped develop the radar section and to Joan David who either created or reproduced the images in this publication. Special recognition is also given to UCAR COMET for allowing the publication of several figures from COMET modules and to the Naval Research Laboratory in Monterrey, CA, for the use of archived microwave imagery for several TCs.

3.6 References

Aberson, S.D., 1998: Five-day TC track forecasts in the north Atlantic basin, *Wea. Forecasting*, **13**, 1005-1015.

Aberson, S.D., 2002: Two years of Operational Hurricane Synoptic Surveillance. *Wea. Forecasting*, **17**, 1101-1110.

Aberson, S.D., 2010: Ten years of hurricane synoptic surveillance. Mon. *Wea. Rev*., **138**, 1536-1549.

Bender, M.A., R.E. Tuleya, and Y. Kurihara, 1987: A numerical study of the effect of island terrain on tropical cyclones. *Mon. Wea. Rev.*, **115,** 130-155.

Bender, M.A, Ginis, I., B. R. Tuleya, B. Thomas, and T. Marchok, 2007: The operational GFDL coupled-hurricane ocean prediction system and a summary of its performance, Mon. Wea. Rev., **135**, 3965-3989.

Bessafi, M., A. Lasserre-Bigorry, C.J. Neumann, F. Pignolet-Tardan, D. Payet, and M. Lee-Ching-Ken, 2002: Statistical prediction of TC motion: An analog-CLIPER approach, Wea. *Forecasting*., **17**, 821-831.

Burpee, R.W., J.L. Franklin, S. J. Lord, R.E. Tuleya, and S.D. Aberson, 1996: The impact of Omega dropwindsondes on operational hurricane track forecast models. *Bull. Amer. Soc.*, **77**, 925-933.

Brand, S, 1970: Interaction of binary TCs in the western Pacific ocean, *J. Appl. Meteor.*, **9**, 433-431.

Brand, S., and J. Blelloch, 1974: Changes in the characteristics of typhoons crossing the island of Taiwan. Mon. *Wea. Rev*., **102**, 708-713.

Carr, L.E., III and R.L. Elsberry, 1997: Models of tropical cyclone wind distribution and Beta-effect propagation for application to TC track forecasting, Mon. *Wea. Rev*., **125**, 3190-3208.

Carr, L.E., III and R.L. Elsberry, 1998: Objective diagnosis of binary TC interactions for the western North Pacific basin, *Mon. Wea. Rev*., **126**, 1734-1740.

Carr, L.E., III, R.L. Elsberry, and J.E. Peak, 2001: Beta test of the systematic approach expert system prototype as a TC forecasting aid. *Wea. Forecasting*, **16**, 355-368.

Chan, J.C.L., F.M.F. Ko, and Y.M. Lei, 2002: Relationship between potential vorticity tendency and TC motion, *J. of Atmos. Sci*., **59**, 1317-1336.

Chang, S. W., 1982: The orographic effects induced by an island mountain range on propagating tropical cyclones. *Mon. Wea. Rev.*, **110**, 1255-1270.

Cobb, R. Knabb, P. S. Chang, and Z. Jelenak, 2008: Preliminary assessment of the utility of ASCAT ocean surface vector wind (OSVW) retrievals at the Tropical Prediction Center/National Hurricane Center. Preprints, *28th Conf. on Hurricanes and Tropical Meteorology,* Orlando, FL, Amer. Meteor. Soc., **15B.4**

Dong, K. and C.J. Neuman, 1983: On the relative motion of binary TCs, *Mon. Wea. Rev*., **111**, 945-953.

Dunn, G.E., and B.I. Miller, 1964: Atlantic hurricanes. Louisiana State Press, pp. 326.

Dvorak, V.F., 1984: TC intensity analysis using satellite data. NOAA Tech. Report NESDIS 11. Available from NOAA/NESDIS, 5200 Auth Rd., Washington, D.C., 20233, 47 pp.

Dvorak, V.F., 1995: Tropical clouds and cloud systems observed in satellite imagery: Tropical cyclones. Workbook Vol. 2, 359 pp. [Available from NOAA/NESDIS, 5200 Auth Rd., Washington, D.C., 20333.]

Ellrod, G. P., 1995: Advances in the detection and analysis of fog at night using GOES multispectral infrared imagery. *Wea. Forecasting*, **10**, 606-619

Elsberry, Russell L., and Les E. Carr III, 2000: Consensus of dynamical TC track forecasts – errors versus spread. *Mon. Wea. Rev.*, **128**, 4131-4138.

Elsberry, R.L, 2005: Achievement of USWRP Hurricane Landfall Research Goal, *Bull. of Amer. Met. Soc*., **86**, 643-645.

Foley G., 2010: TC Probabilistic Forecasting & Related Product Development Issues & Applications for User Risk Assessment, *Keynote presentation to ITWC-VII*, (http://www.wmo.int/pages/prog/arep/wwrp/tmr/otherfileformats/documents/KN2.pdf accessed 9 July 2014)

Franklin, J.L., cited 2009: 2008 National Hurricane Center Forecast Verification Report. [Available online at http://www.nhc.noaa.gov/verification/pdfs/Verification_2008.pdf.]

Franklin, J. L., 2010: Tropical cyclone forecast verification at the National Hurricane Center. Preprints, *20th Conf. on Probability and Statistics in the Atmospheric Sciences,* Atlanta, GA, Amer. Meteor. Soc., 6.2.

Fujiwhara, S., 1921: The natural tendency toward symmetry, etc., *Quart. J. Roy. Meteor. Soc*., **47**, 287-293.

Fujiwhara, S., 1923: On the growth and decay of vortical systems, *Quart. J. Roy. Meteor. Soc*, **49**, 75-104.

Fujiwhara, S., 1931: Short note on the behavior of two vortices. *Proc. Phys. Math. Soc. Japan, Ser*. 3, **13**, 106-110.

Gao, F., P.P. Childs, X.-Y. Huang, N.A. Jacobs, and J. Min, 2014: A relocation-based initialization scheme to improve track-forecasting of tropical cyclones. *Advances in Atmospheric Sciences*, **31**, 27-36,

George, J.E. and Gray, W.M, 1976.: TC motion and surrounding flow relationships, *J. Appl. Meteor*., **15**, 1252-1264.

Goerss, J.S., 2000: TC track forecasts using an ensemble of dynamical models. *Mon. Wea. Rev.*, **128**, 1187-1193.

Goerss, J.S., 2007: Prediction of Consensus TC Track Forecast Error. *Mon. Wea. Rev.*, **135**, 1985-1993.

Harper, B.A.,, Kepert, J.D. and Ginger, J.D., 2010: Guidelines for converting between various wind averaging periods in tropical cyclone conditions. World Meteorological Organization, TCP Sub-Project Report, WMO/TD-No. 1555.

Heming, J., and Goerss, J., 2010: Track and Structure Forecasts of Tropical Cyclones. Global Perspectives on Tropical Cyclones: pp. 287-323. doi: 10.1142/9789814293488_0010

Hoffman, R.N., and S.M. Leidner, 2005: An Introduction to the Near Real-Time QuikSCAT data, *Wea. Forecasting*, **20**, 476-493.

Holland, G.J., and M. Lander, 1993: The meandering nature of TC tracks, *J. Atmos. Sci*., **50**, 1254-1266.

Hsiao, Ling-Feng, Chi-Sann Liou, Tien-Chiang Yeh, Yong-Run Guo, Der-Song Chen, Kang-Ning Huang, Chuen-Teyr Terng, Jen-Her Chen, 2010: A Vortex Relocation Scheme for Tropical Cyclone Initialization in Advanced Research WRF. *Mon. Wea. Rev.,* **138,** 3298–3315.

Krayer, W.R., and Marshall R.D., 1992: Gust factors applied to hurricane wins, *Bull. Am. Meteorol. Soc.***73(5)**, 613-617.

Lander, M.A. and G.J. Holland, 1993: On the interaction of tropical-cyclone scale vortices. I: Observations, *Quart. J. Roy. Meteor. Soc*., **119**, 1347-1361.

Lander, M.A., 1995: The merger of two TCs, *Mon. Wea. Rev.*, **123**, 2260-2265.

Lawrence, M.B., and B.M. Mayfield, 1977: Satellite observations of trochoidal motion in hurricane Belle 1976. *Mon. Wea. Rev*., **105**, 1458-1461.

Lin, Y.L, N.C. Witcraft, and Y.H. Kuo, 2006: Dynamics of track deflection associated with the passage of TCs over a meso-scale mountain. *Mon. Wea. Rev*., **134**, 3509-3538.

Liu, Q.,T. Marchok, H. Pan, M. Bender, and S. Lord, 2000:Improvements in Hurricane Initialization and Forecasting at NCEP with Global and Regional (GFDL) Models, *NOAA Technical Procedures Bulletin* **472**.

Nakazawa, T., 2010: THORPEX/TIGGE Applications to TC Motion & Forecasting , *ITWC-VII*, (http://www.wmo.int/pages/prog/arep/wwrp/tmr/otherfileformats/documents/SF-2a.pdf accessed 9 July 2014)

Neumann C. J., 1979 On the use of deep-layer mean geopotential height fields in statistical prediction of tropical cyclone motion. *6th Conference on Probability and Statistics in Atmospheric Sciences*, Banff, Canada. Amer. Meteor. Soc., 32-38.

Neumann, C.J., 1983: The National Hurricane Center NHC83 Model. *NOAA Technical Mem. NWS NHC 41*, pp.44.

Pike A.C.,and Neumann C.J., 1987: The variation of track forecast difficulty among tropical cyclone basins, *Wea. Forecasting* **2** 237-241.

Powell, M.A., XXXX:

Prieto, R., B.D. McNoldy, S.R. Fulton, and W.H. Schubert, 2003: A classification of binary TC-like vortex interactions, *Mon. Wea. Rev.*, **131**, 2656-2666.

Rappaport, E.N., J.L. Franklin, L.A. Avila, S.R. Baig, J.L. Beven. E.S. Blake, C.A. Burr, Jiann-Gwo Jiing, C.A. Juckins, R.D. Knabb, C.W. Landsea, M. McInerney-Mainelli, B.M. Mayfield, C.J. McAdie, R.J. Pasch, C. Sisko, S.R. Stewart, and A.N. Tribble, 2009. Advances and challenges at the National Hurricane Center, *Wea. Forecasting*, **24**, 395-419.

Ritchie, E.A., and R.L. Elsberry, 1993: Simulated impacts of a mesoscale convective system on the track of Typhoon Robyn in TCM-93. *Mon. Wea. Rev*., **128**, 2232-2251.

Ritchie, E.A., and G.J. Holland, 1993: On the interaction of two TC scale vortices. II: Discrete vortex patches. Quart. *J. Roy. Meteor. Soc.*, **119**, 1363-1379.

Ross, R.J., and Y. Kurihara, 1995: A numerical study on influences of Hurricane Glorida (1985) on the environment. *Mon. Wea. Rev*., **123**, 332-346.

Sampson, C.R., J.S. Goerss, and H.C. Weber, 2006: Operational performance of a new barotropic model (WBAR) in the Western North Pacific Basin. *Wea. Forecasting*, **21**, 656-662.

Sampson, C.R., J.A. Knaff, and E.M. Fukada, 2007: Operational evaluation of a selective consensus in the western North Pacific basin. *Wea. Forecasting*, **22**, 671-675.

Senn, H.V, and H.W. Hiser, 1959: On the origin of hurricane spiral rain bands. *J. Atmos. Sci*., **16**, 419-426.

Velden, C.S.: The relationship between tropical cyclone motion, intensity and the vertical extent of the environmental steering layer in the Atlantic basin. *20th Conf. Hurr. and Trop Meteor.*, San Antonio, TX, May, 1993.

Velden, C.S., and L.M. Leslie, 1991: The basic relationship between TC intensity and the depth of the environmental steering layer in the Australian region. *Wea. Forecasting*, **6**, 244-253.

T. S. V. Vijaya Kumar, T. N. Krishnamurti, Michael Fiorino, and Masashi Nagata, 2003: Multimodel Superensemble Forecasting of Tropical Cyclones in the Pacific. *Mon. Wea. Rev.,* **131**, 574-583.

Weber, H. C. (2003): Hurricane track prediction using a statistical ensemble of numerical models,*Mon. Weather Rev.*, **131**, 749-770.

Williford, C.E., T.N. Krishnamurti, R.C. Torres, S. Cocke, Z. Christidis, and T.S. Vijaya Kumar, 2003: Real-time multimodel superensemble forecast of Atlantic tropical systems in 1999, *Mon. Wea. Rev*., **131**, 1878-1894.

Willoughby, H.E., 1988: Linear motion of a shallow-water barotropic vortex. *J. Atmos. Sci*., **45**, 1906-1928.

Willoughby, H.E., 1990: Temporal changes of the primary circulation in TCs. *J. Atmos. Sci*., **47**, 242-264.

Willoughby, H.E., F.D. Marks, and R.J. Feinberg, 1984: Stationary and moving convective bands in hurricanes. *J. Atmos. Sci*., **41**, 3189-3211.

Wong, M.L. and J.C.L Chan, 2006: Tropical cyclone motion in response to land surface friction. *J. Atmos. Sci.,* **63,** 1324-1337.

Yeh, T.C., and R.L. Elsberry, 1993: Interaction of typhoons with the Taiwan orography. Part I: Upstream track deflections. *Mon. Wea. Rev.,* **121,** 3193-3212.

Chapter Four

Jenni L. Evans
Department of Meteorology
The Pennsylvania State University, University Park, PA, USA

Notice

This chapter contains many references to the COMET/UCAR Met-Ed program. You may be requested to login to view these pages.

Login requires registration into the training program; however this registration is **free of charge**. The following links provide guidance on the Met-Ed program:

- Met-Ed Home Page: https://www.meted.ucar.edu/
- Met-Ed FAQ: https://www.meted.ucar.edu/resources_faq.php

4. Tropical Cyclone Intensity, Structure, and Structure Change

4.1 Introduction[1]

The evolution of a tropical cyclone through its lifecycle from genesis to decay provides constant forecasting challenges. In this chapter, we review the key drivers and limitations on tropical cyclogenesis; processes leading to tropical cyclone intensity and structure changes (including tropical cyclone intensity classification conventions around the world); and extratropical transition (ET) of a tropical cyclone.

Tropical cyclogenesis

Operationally, tropical cyclogenesis is said to have occurred when mean[2] surface winds in excess of tropical storm force (17 m s^{-1}; 33 knots) are observed. Implicit in this operational genesis criterion is the expectation that the tropical storm has become self-sustaining and can continue to intensify without help from its environment.

Since only around 90 tropical cyclones are observed annually around the globe, it is clear that special conditions are required for tropical cyclogenesis. In the remainder of this section, we will review the necessary conditions for tropical cyclogenesis and the sources of the incipient disturbances.

[1] Much of the material in this chapter is drawn from the chapter on tropical cyclones in *An Introduction to Tropical Meteorology*, a COMET/UCAR online textbook co-authored by myself (lead author Dr. Arlene Laing). The complete textbook is available at http://www.meted.ucar.edu/tropical/textbook/index.htm.

[2] Averaging time for surface winds varies by region; details of the different regional averaging times and intensity classifications are given below. "Surface" is defined as 10 meters above the ground.

4.2 Necessary ingredients for tropical cyclogenesis

Necessary ingredients for tropical cyclogenesis

Gray (1968) identified six features of the large-scale tropical environment that were necessary ingredients for tropical cyclogenesis:

1. *sufficient ocean thermal energy [SST > 26°C to a depth of 60 m],*
2. *moist mid-troposphere [measured by 700 hPa relative humidity],*
3. *conditionally unstable atmosphere to support deep convection,*
4. *a maximum in lower troposphere relative vorticity,*
5. *weak vertical shear of the horizontal winds at the genesis site, and*
6. *location at least 5 latitude away from the equator.*

Conditions *(i)-(iii)* capture the likelihood of deep convection in the region. These thermodynamic constraints capture variations in genesis activity on seasonal and intraseasonal (for example, due to the Madden Julian Oscillation) timescales. In contrast, conditions *(iv)-(vi)* track the daily likelihood of genesis (McBride and Zehr 1981); these conditions identify the presence of a weak incipient disturbance (Figure 4.1) and measure how favorable the environment is for intensification: given that the thermodynamics are favorable, genesis is much more likely in an environment with weak vertical wind shear.

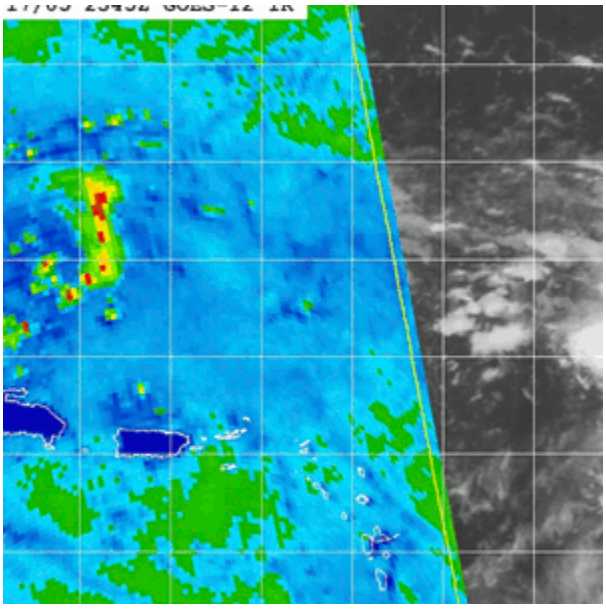

Figure 4.1. Example of an incipient disturbance (to the left of the image) in the North Atlantic: Tropical Invest 96L, which developed into Hurricane Rita (2005). Image is combined infrared and SSM/I satellite images about 0000 UTC 18 Sep 2005. Minimum surface pressure was estimated as 1012 hPa and peak surface winds were around 12 ms-1 at this time.

As observing systems have improved, we have begun to record tropical cyclones that can spend large fractions of their lifetimes within 5 of the equator. These are typically small tropical cyclones (or midget typhoons) and never cross the equator. Often these systems will form from equatorial waves, maybe even a pair of tropical cyclones straddled across the equator. All of this means that restriction on latitude identified by Gray (1968) must be relaxed. We will discuss the different sources for these incipient disturbances in each ocean basin below.

As we've seen then, Gray's (1968) necessary conditions for genesis can be summarized as (1) environmental support for active deep convection [moist free troposphere and weak shear] and (2) in the presence of a low-level absolute vorticity maximum (Evans 2011).

While all of these conditions for genesis must be present before tropical cyclogenesis can occur, even if all of these conditions are met tropical cyclogenesis may not occur. So in that sense, these are necessary, but not sufficient conditions for genesis. The additional factor that guarantees that genesis will occur has yet to be identified, so genesis remains a challenging forecast problem.

4.3 Tropical cyclone structure needed for genesis and intensification to continue

The persistence (and possible intensification) of a weak tropical disturbance depends on its structure. We can use two concepts to understand how a tropical disturbance can survive and grow: inertial stability tells us what a system needs in order to survive in an environment that is not ideal for development; and Rossby radius of deformation tells us if a system has "the right stuff" to sustain itself without help from its environment.

Inertial stability, I

The resistance of a symmetric vortex to changes in its structure can be measured through its inertial stability. Inertial stability indicates the "stiffness" of a cyclone and is calculated as the product of the absolute vorticity and the absolute rotation rate of a symmetric storm, so we see that the *inertial stability varies with radius and height in the storm*[3] (Figure 4.2). This means that the storm can have "weak spots" where adverse environmental influences can have a big impact. In fact, even an intense tropical cyclone has its Achilles' heels in the upper level outflow anticyclone and at the surface (Figure 4.2).

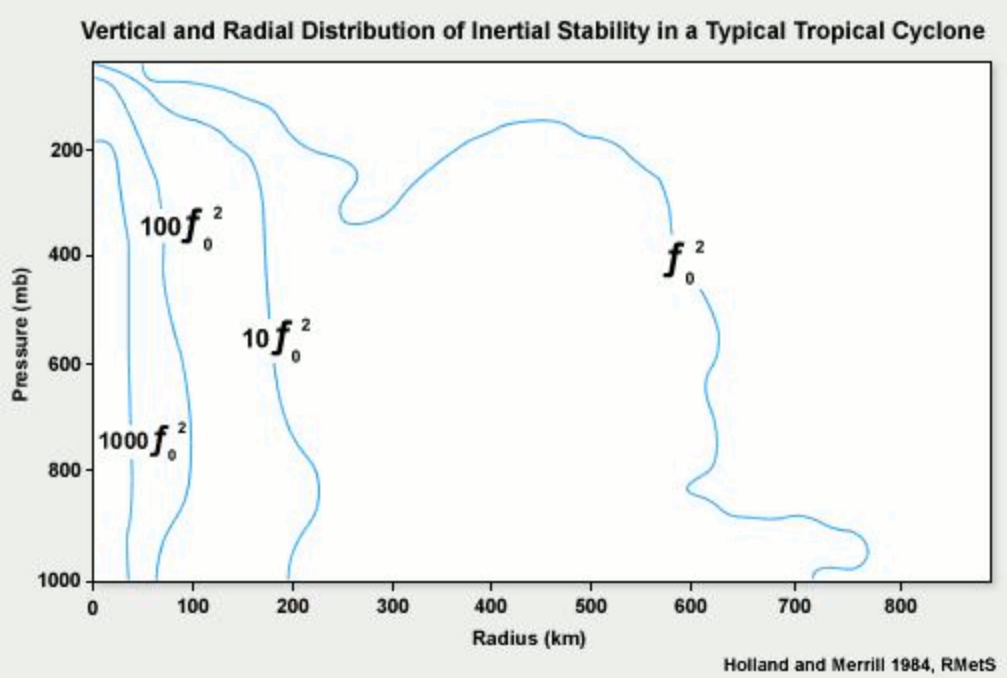

Figure 4.2. Vertical and radial distribution of the inertial stability in a typical tropical cyclone. To illustrate the contribution to inertial stability of the storm winds compared to its environment, the inertial stability values have been scaled by *f0*, the value of the Coriolis parameter at the storm center. Figure adapted by COMET from Holland and Merrill (1984) and obtained from http://www.meted.ucar.edu/tropical/textbook/ch10/tropcyclone_10_2_2_2.html.

While all of these conditions for genesis must be present before tropical cyclogenesis can occur, even if all of these conditions are met tropical cyclogenesis may not occur. So in that sense, these are necessary, but not sufficient conditions for genesis. The additional factor that guarantees that genesis will occur has yet to be identified, so genesis remains a challenging forecast problem.

3Inertial stability is calculated as $I = \sqrt{(\zeta + f_o)\left(f_o + \frac{2v}{r}\right)}$ where ζ is the relative vorticity calculated from the symmetric rotating winds (*v*), *f0* is the Coriolis parameter and *v/r* is the rotation rate of the storm. Therefore, inertial stability increases as relative vorticity, rotation rate and latitude increase, and as radius decreases. As a result, even if a storm has constant intensity, if it is contracting it will increase its inertial stability. This will make the storm more resistant to any negative forcings in its environment.

Rossby radius of deformation, L_R

The Rossby radius of deformation is a length scale that indicates whether convection will force changes in the windfield or if the winds will adapt to the convection — it is the critical length scale at which rotation becomes as important as buoyancy.

Whether a convective system lies above or below the Rossby radius line will determine its future: a disturbance that is larger ($L > L_R$) will persist, but a system that is smaller than L_R will

disperse (Figure 4.3). L_R depends on the vorticity, stability and depth of the system[4] and is inversely proportional to latitude; this latitudinal dependence means that it is typically very large in the tropics. However, the high vorticity in tropical cyclones reduces the Rossby radius and enables tropical cyclones to develop and even to last for many days to weeks. Dynamically, the low-level vorticity maximum reduces the local Rossby radius of deformation focusing the convective heating locally (Simpson et al. 1998). This means that the tropical cyclone can intensify more efficiently.

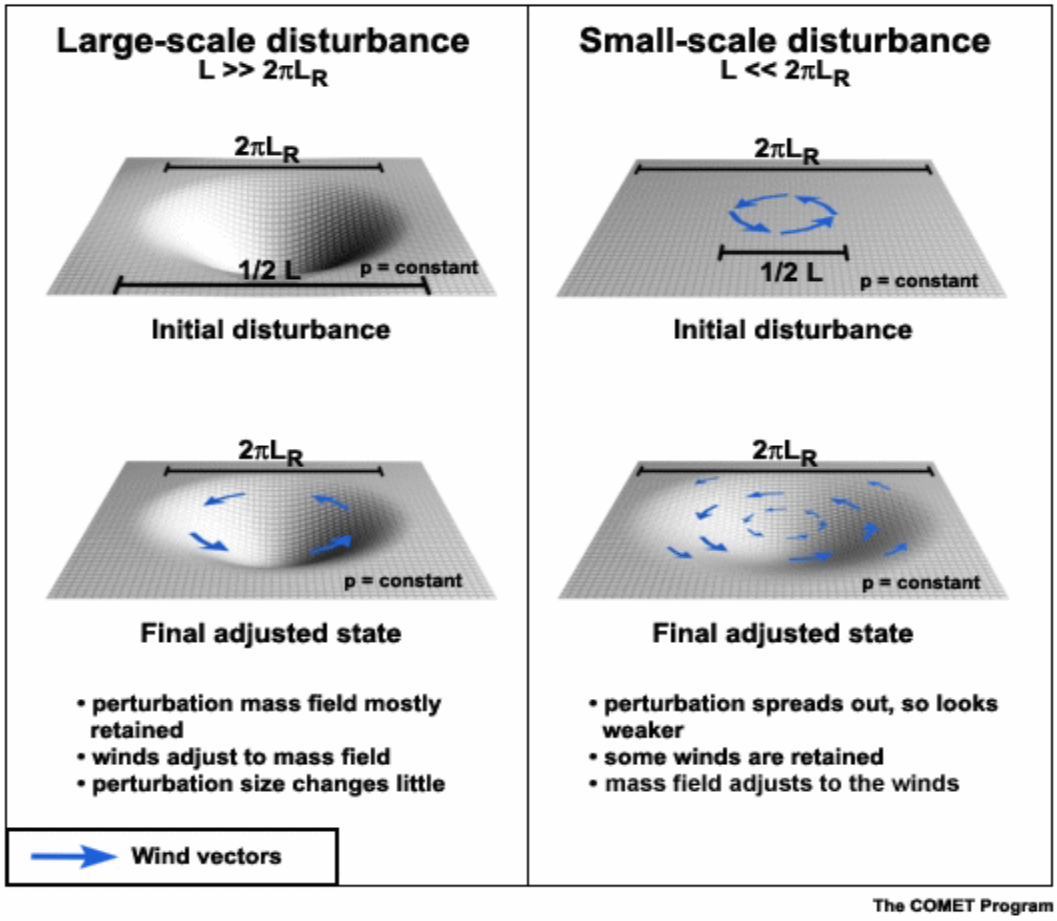

Figure 4.3. Adjustments of the wind and mass (pressure, geopotential height) fields based on the size of the disturbance relative to the Rossby radius of deformation, LR. A small convective disturbance will decay, but a disturbance that is larger than LR can develop and grow.

4The Rossby radius of deformation for a continuously stratified fluid, $L_R = \frac{N H}{f_o}$, where *N* is the Brunt Väisäla frequency, *H* is the depth of the system and *f0* is the Coriolis parameter; if a weather system has large relative vorticity (e.g. a tropical cyclone!), the vorticity of the system has to be included and LR is calculated as $L_R = \frac{N H}{\zeta + f_o}$ where ζ is the vertical component of the relative vorticity. For more information on the Rossby radius of deformation, see the COMET module, The Balancing Act of Geostrophic Adjustment, http://www.meted.ucar.edu/nwp/pcu1/d_adjust/.

4.4 Regional sources of disturbances that can develop into tropical cyclones

The environments in the eastern North Pacific and North Atlantic are quite different from the other basins where tropical cyclones occur, so some of the sources of the tropical disturbances also differ across basins. In this section we'll review the sources for the tropical disturbances that ultimately become tropical cyclones that are well known (Figure 4.4, bottom panel) and newly identified in the last twenty years or so (top panel).

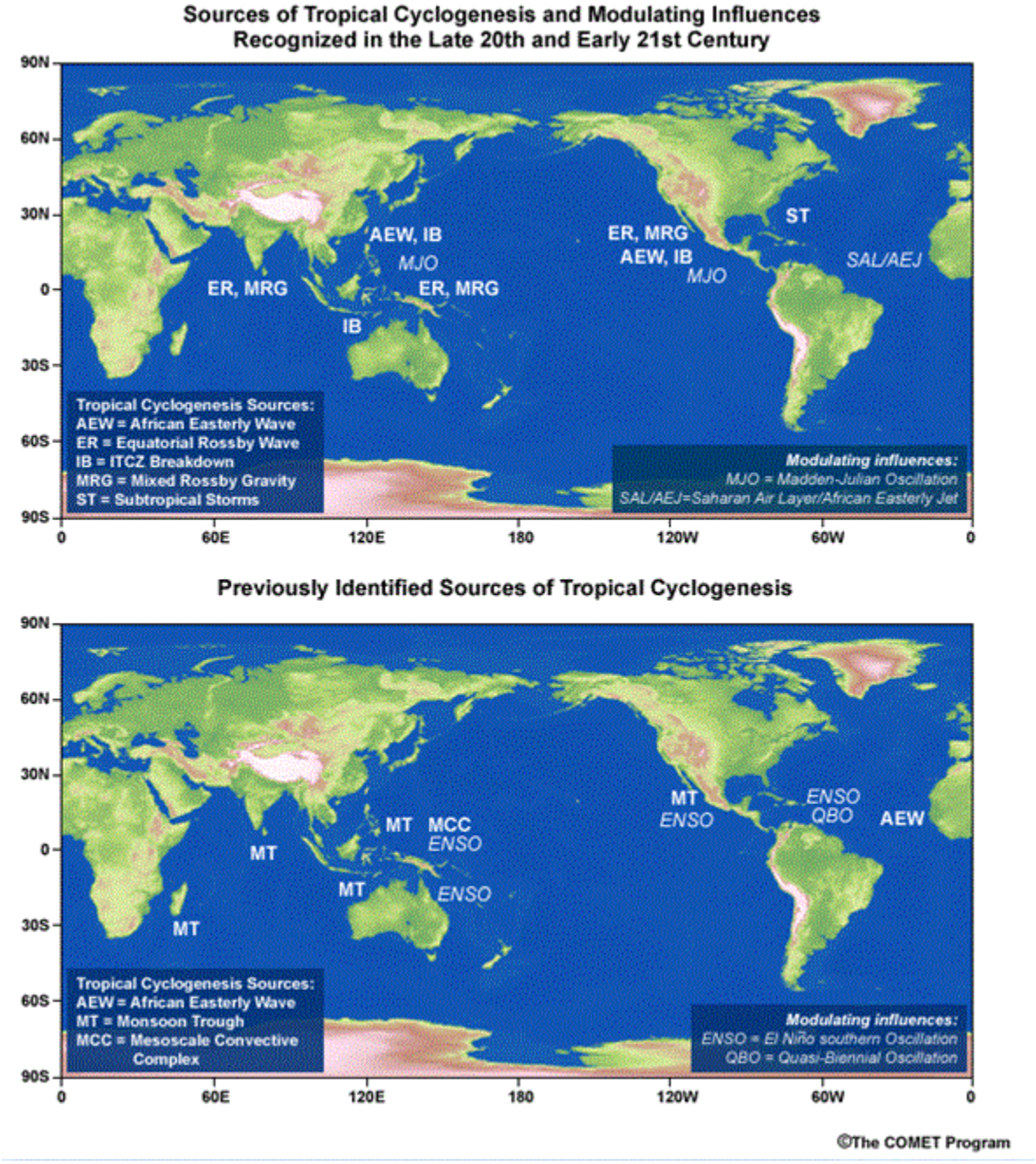

Figure 4.4. Mechanisms for formation of tropical disturbances in each ocean basin. Figures from An *Introduction to Tropical Meteorology* (COMET/UCAR), available from http://www.meted.ucar.edu/tropical/textbook/ch10/tropcyclone_10_3_5.html.

The following mechanisms (shown in Figure 4.4) are currently thought to provide most of the initial tropical disturbances that eventually become tropical cyclones in each basin:

Eastern North Pacific

Tropical storms in the eastern North Pacific mainly form from either instabilities in the ITCZ (Schubert et al. 1991; Ferreira and Schubert 1997) or easterly waves that cross Central America from the Atlantic (Zehnder 1991).

Western Pacific and Indian Oceans

For the West Pacific and Indian Oceans, the summer monsoons are the major source for disturbances that evolve into tropical cyclones (McBride and Keenan 1982; Briegel and Frank 1997). However, recently equatorial Rossby waves (Frank and Roundy 2006) and mixed Rossby gravity waves (Dickinson and Molinari 2002) have also been demonstrated to be other locations for tropical cyclogenesis in these oceans. Finally, some genesis events in the western North Pacific can result from (i) easterly waves from the North Atlantic and (ii) merger of a number of weak mesoscale convective systems into a stronger disturbance (Simpson et al. 1997).

North Atlantic Ocean

Easterly waves forming in the West African monsoon are the major source of Atlantic tropical cyclogenesis. An average of around 1-2 tropical cyclones per year from an initially subtropical cyclone (Guishard et al. 2009).

South Atlantic Ocean

Historically it was thought that the cool SST,lack of a true seasonal monsoon and strong shear in this region meant that tropical cyclones could not form. However, one tropical cyclone has been observed in the South Atlantic, Hurricane Catarina in 2003. Catarina (named after the region in Brazil where it made landfall) evolved from a subtropical cyclone much further from the equator than is typical in other basins.

4.5 Mechanisms for generation of tropical disturbances

We'll now take a very quick look at how each of these mechanisms lead to the formation of the tropical disturbances that eventually becomes tropical cyclones.

The monsoon trough

Convection can strengthen the monsoon trough, progressively lowering the surface pressure and strengthening the winds.At some point, the trough becomes too strong and narrow, and

the monsoon can break apart into a set of cyclonic disturbances that may evolve into tropical cyclones (Ferreira and Schubert 1997, Figure 4.5). An isolated monsoon gyre forming in this environment can also provide the seed for a tropical cyclone.

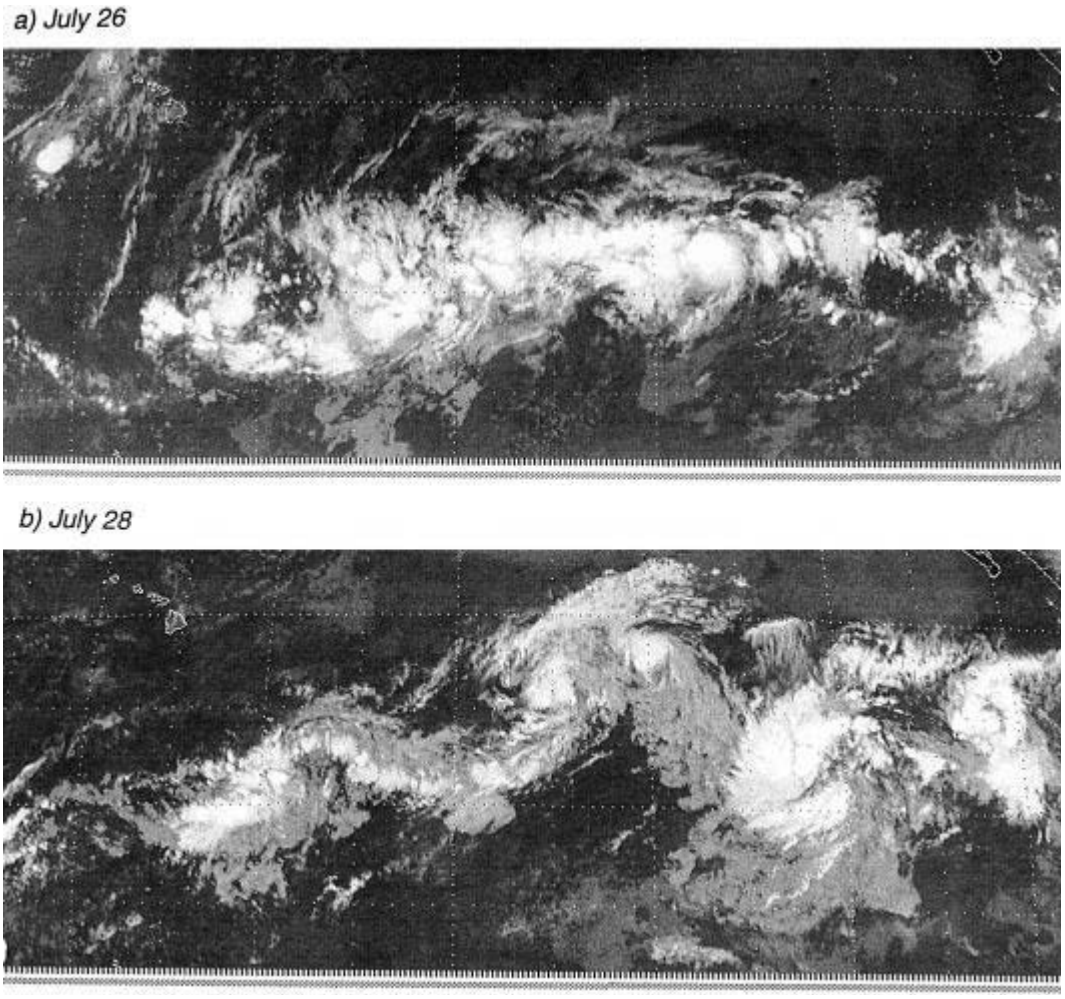

Figure 4.5. Observed breakdown of the continuous monsoon trough (top) into three tropical cyclones (3rd panel) over a period of a week (Ferreira and Schubert 1997) and the beginning of the reformation of the trough structure (bottom panel).

Equatorial waves: Rossby waves and mixed Rossby-gravity waves[5]

Two kinds of atmospheric waves that propagate along the equator have been identified as favorable regions for tropical cyclogenesis: equatorial Rossby waves (Frank and Roundy 2006) and mixed Rossby gravity waves (Dickinson and Molinari 2002). Because of convection, their real structure is different from theory, so it is only recently that we've been able to track these waves reliably and to observe their impact on tropical cyclone formation (Kiladis and Wheeler 1995; Frank and Roundy 2006).

Equatorial Rossby waves are symmetric about the equator, so the cyclonic (clockwise) flow in the wave south of the equator will be mirrored by the (counterclockwise) cyclonic flow to the north of the equator. In an equatorial Rossby wave, these cyclone pairs alternate east-west with pairs of anticyclones. The low pressure centers are regions of active convection, another reason why equatorial Rossby waves are favorable sites for genesis (e.g. Nitta 1989 and also see figure 4.6).

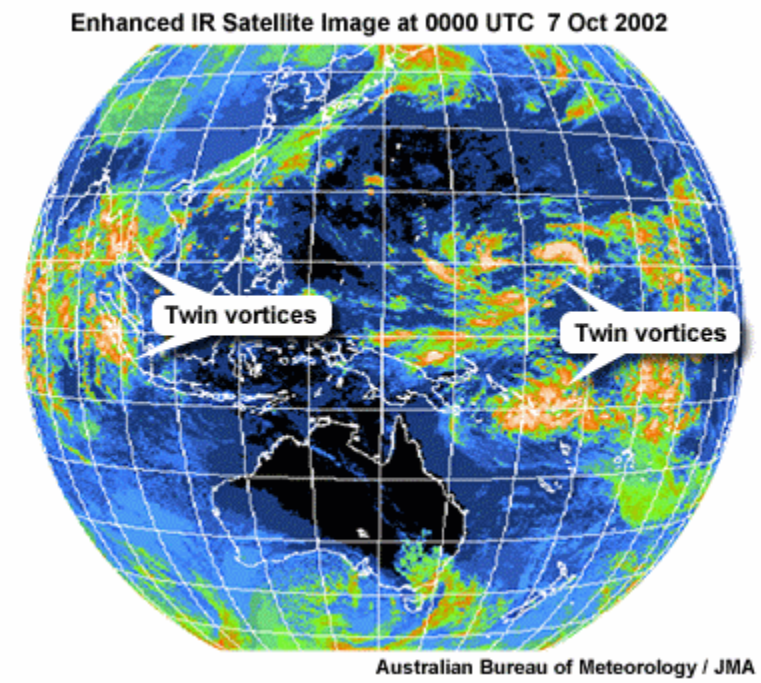

Figure 4.6. An equatorial Rossby wave is characterized by pairs of convective cyclonic regions (favorable for tropical cyclogenesis) alternating around the equator with clear zones of the similar scale. Figure obtained from http://www.meted.ucar.edu/tropical/textbook/ch5/tropvar_5_1_2_2.html.

Mixed Rossby-gravity waves are much shorter than equatorial Rossby waves and only persist for a few days instead of weeks. Even so, they have been shown to be another important source region for tropical cyclogenesis (Dickinson and Molinari 2002, Figure 4.7).

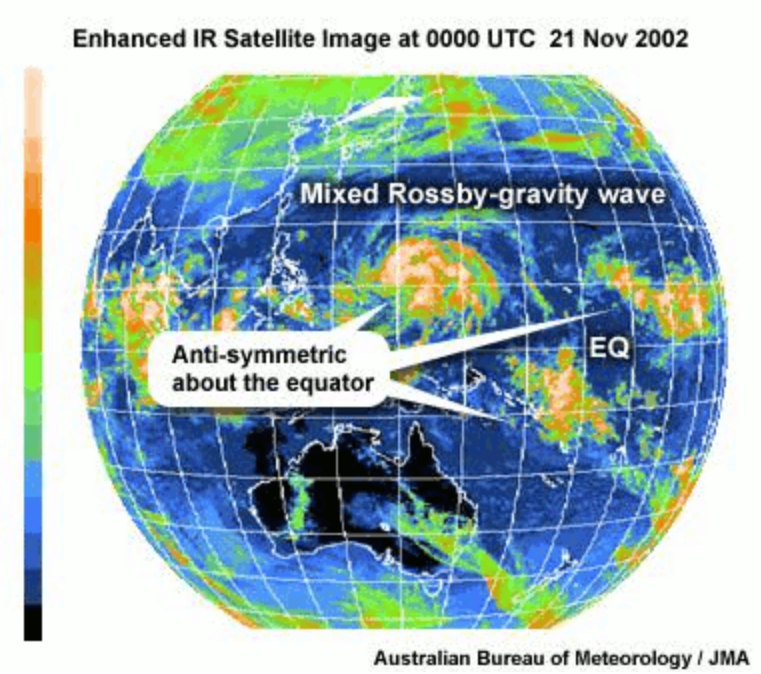

Figure 4.7. An equatorial mixed Rossby-gravity wave observed in the enhanced IR imagery from the GMS satellite at 0000 UTC 21 November 2002. Notice the convective maxima in the cyclonic flow regions and the cyclone-anticyclone pairs straddling the equator (leading to a "sawtooth" pattern of convective cyclonic centers alternating across the equator). Figure obtained from http://www.meted.ucar.edu/tropical/textbook/ch5/tropvar_5_1_2_3.html.

[5] More information on equatorial waves can be found at Matthew Wheeler's excellent operational website http://www.cawcr.gov.au/staff/mwheeler/maproom/OLR_modes/ or from Chapter 5 (Tropical Variability) the COMET textbook site at http://www.meted.ucar.edu/tropical/textbook/ch5/tropvar_5_1_2.html.

Tropical cyclogenesis from an equatorial wave does not have to occur right near the equator, although it often does. The wave also sees the ITCZ as a "vorticity equator" and will propagate along the ITCZ until it reaches the easternmost point of the monsoon trough. This is another particularly favorable region for tropical cyclogenesis to occur in the western North Pacific since low-level convergence is persistent here, making this an active region of deep convection.

African easterly waves (AEW)

African easterly waves are generated in the monsoon region in western equatorial Africa. They form as instabilities on the African Easterly Jet (AEJ) and will develop if they can form persist convection once they move over the tropical Atlantic Ocean. The development of the AEW from the jet is somewhat similar to the monsoon trough breakdown mechanism we discussed in association with Figure 4.4.

Easterly waves are strongest around 700 hPa (about the height of the AEJ). They have periods of roughly 3-5 days and scales of about 1000 km; AEW typically move westward at about 7-8 m s^{-1}. If an AEW does not develop into a tropical storm close to the African coast, strong vertical wind

shear in the central equatorial Atlantic will usually suppress its development until it nears the Caribbean Sea. It may either form a tropical storm here, or just gain energy to continue to move into the eastern Pacific (Molinari et al. 1997)

Mesoscale convective systems (MCS) as sources of tropical disturbances

Mesoscale convective systems (MCS) are organized clusters of convection. Individual MCS are usually too small (compared to the Rossby radius of deformation) to continue to develop into a tropical storm. They are also too weak (low values of inertial stability) to resist the negative influences of their environment. So to become a tropical storm, MCS must band together and merge into a stronger system (larger low-level relative vorticity). At this stage, the Rossby radius (L_R) of the developing storm has reduced so the system can strengthen further through the feedback of convective heating on the rotating winds as depicted in Figure 4.3 (Ritchie and Holland 1999).

Subtropical storms

Although they are listed now and then in the North Atlantic historical database (HURDAT), the role of subtropical storms in tropical cyclogenesis received little attention. Their regular occurrence as a seed disturbance for tropical cyclones has been documented over the last decade (e.g. Davis and Bosart 2003, 2004; Evans and Guishard 2009) and, as a result, the US National Hurricane Center (NHC) began naming those storms and recording them in HURDAT in 2002.

A subtropical cyclone evolves into a tropical cyclone via a process of tropical transition when the shallow, subtropical system (strongest winds in the lower to mid troposphere) evolves into a deep tropical cyclone with strongest winds at the surface). For tropical transition to occur the subtropical cyclone must be in a moist, low-shear environment; it must either be over warm ocean waters (SST > 26°C or more) or in a region of strong warm (and moist) air advection. All of these conditions will force deep convection in this initially baroclinic storm, allowing it to develop the deep warm-cored structure with strongest winds at the surface — a tropical cyclone!

So we see that the development of a subtropical storm into a tropical cyclone requires weak vertical wind shear in a moist, convective environment and in the presence of a relative vorticity maximum. Thus, the necessary but not sufficient conditions for tropical cyclogenesis must still be satisfied in this tropical transition path to tropical cyclogenesis!

4.6 Favorable conditions for the evolution of a tropical disturbance into a tropical storm

No matter how the tropical disturbance develops, it needs a favorable environment (Gray 1968) to continue developing and to intensify. As we've discussed above, this weak tropical system

will generally weaken and die in regions of even low to moderate vertical wind shear if it cannot sustain active convection since the shear will tilt the vortex away from the vertical, suppressing vertical motion in the cyclone core – and so suppressing convection that provides the engine for the cyclone. However, sometimes a little shear can be a good thing: in causing the vortex to tilt, it will generate upward motion downstream of the center (under the "upper" vortex) and (if there is enough moisture in the atmosphere) deep convection can become active there. This convection can form a new center and capture the original vortex (Molinari et al. 2004) in the same way as we discussed above for the MCS path to genesis.

Increasing study of variability in the large-scale tropical environment has highlighted the importance of the *Madden-Julian Oscillation* (MJO; Madden and Julian 1994) in modulating deep convection on intraseasonal timescales.

We've repeatedly emphasized the need for active deep convection to feed the engine of tropical cyclogenesis and development, so the impact of the MJO on tropical cyclogenesis is hardly surprising: the active convection phase of the MJO enhances the chances of genesis, while the suppressed phase of the MJO minimizes the likelihood that genesis will occur (Liebmann et al.1994; Molinari and Vollaro 2000; Maloney and Hartmann 2001; Aiyyer and Molinari 2008). This effect is seen in all ocean basins, even the North Atlantic (Evans and Jaskiewicz 2001), where the convective signature of the MJO itself is not readily identified.

One message comes out of our discussion of tropical cyclogenesis: each one of Gray's (1968) necessary conditions for tropical cyclogenesis is present, no matter which path to genesis (monsoon, equatorial wave, subtropical storm, MCS) the storm takes.

4.7 Tropical cyclone intensity and mechanisms of intensity change

Intensity and structure are the key characteristics of a tropical cyclone that determine its impact on society.Together they describe the maximum winds experienced and the distribution of dangerous winds and other significant weather associated with the storm.

To understand and forecast the intensity of a storm,it is helpful to understand the maximum possible intensity that a storm could achieve in its environment: its *potential intensity (PI)*. Having gauged the upper bound on the destructiveness of that storm, a review of the environmental constraints limiting its development provide guidance on the actual intensity it could achieve; the effects of storm structure changes on intensity will also be discussed. Finally, methods for observing, estimating, and classifying storms based on their intensity will be reviewed.

How strong can it possibly get? The potential intensity (PI) of a tropical Cyclone

While the actual intensity attained by a tropical cyclone is a critical measure of its societal impact, the potential intensity of a storm tells us what the "worst case" outcome of that storm could be. Potential intensity is the maximum possible surface wind speed or minimum central

pressure attainable by an individual storm given the constraints imposed on it by the thermodynamics of its environment.So potential intensity can help to guide a forecast since it provides a situation-dependent limit on the forecasted intensity (De Maria et al. 2005). Potential intensity is also of interest as an indicator of the possible impacts of climate changes on these storms (Emanuel 1988).

Two theories have been advanced to explain potential intensity,one that links intensity to the characteristics of the moist boundary layer (CISK; Ooyama 1963, 1982; Charney and Eliassen 1964; Fraedrich and McBride 1989) and the other that ties intensity more directly to the underlying ocean (WISHE; Emanuel 1986,1995). In both theories, the latent heat released in the eyewall convection is the energy source needed to maintain the winds. Each theory is summarized here.

Conditional Instability of the Second Kind (CISK), an early theory of potential intensity

(1958) proposed a theoretical model for the maximum intensity of a tropical cyclone dependent on (i) SST at the center of the storm,(ii) relative humidity of the surface air in the storm; (iii)lapse rates in the environment of the storm, and (iv) potential temperature at the top of the storm and its height above the surface. The first three conditions combine to give the moist instability of the air, and so the vigor and depth of the convection in the core. Miller (1958) calculated the hydrostatic pressure drop due to the potential temperature anomaly aloft due to the eyewall convection; his analyses demonstrated that subsidence warming in the eye must also be included to attain the range of observed minimum central pressures.

Conditional instability of the second kind (CISK) is a formal mathematical theory[6] for tropical cyclone maintenance and intensification (Ooyama 1963, 1982; Charney and Eliassen 1964; Fraedrich and McBride 1989) that is consistent with Miller's (1958) conceptual model of a tropical cyclone as a moist, frictionally-driven convective "chimney". In CISK, warm, moist (high θ_e) air converging in the tropical cyclone boundary layer provides all of the moisture available to the eyewall convection. Condensation of rain in the convective eyewall provides the latent heat source that is converted to mechanical energy, driving the winds of the tropical cyclone (Figure 4.8).

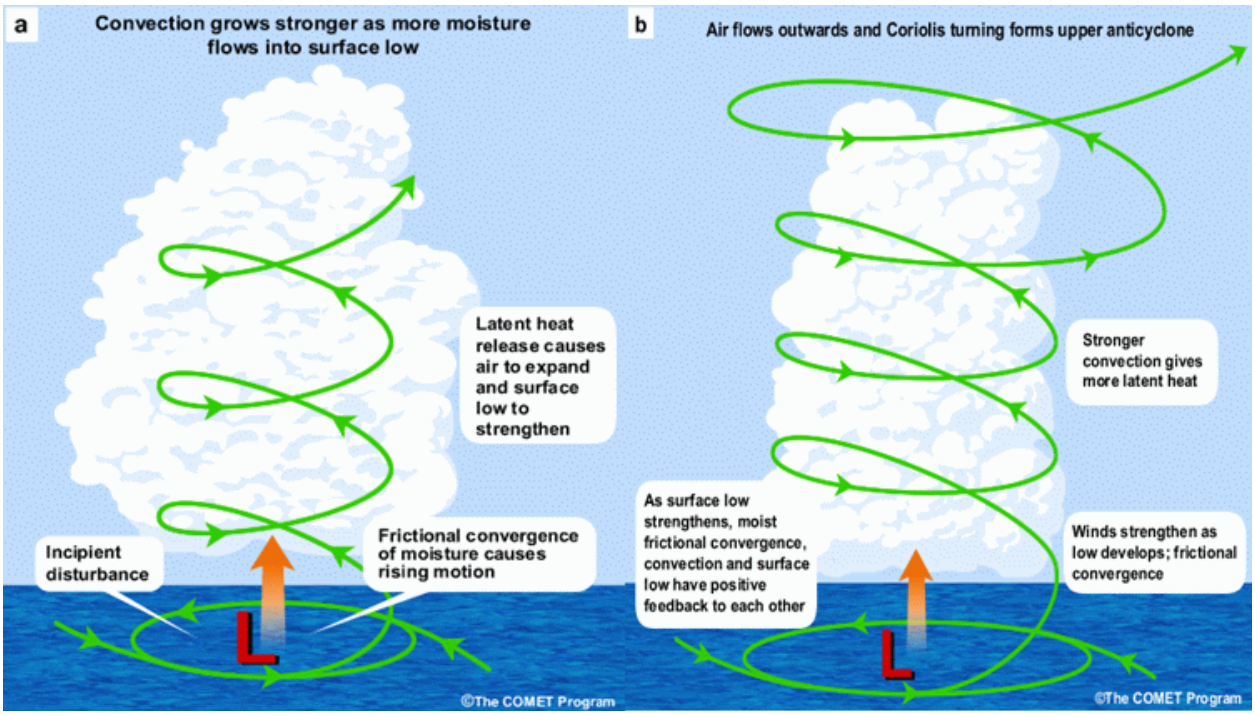

Figure 4.8. Schematic of CISK: (a)given an incipient low-level cyclone with a moist boundary layer, frictional convergence of moisture, and forced ascent drive convection; (b)latent heating due to convection reduces surface pressure, strengthens the low-level cyclone, and enhances moisture convergence and convection in a positive feedback loop. Obtained from http://www.meted.ucar.edu/tropical/textbook_2nd_edition/navmenu.php?tab=9&page=4.1.1.

6Our discussion of these two theories (CISK and WISHE) will be descriptive. Complete mathematical discussions of these theories are available in the source papers; many of these are listed in the references.

Friction in the tropical cyclone boundary layer breaks the gradient wind balance between the inward pressure gradient force and the outward Coriolis and centrifugal forces leads to the boundary layer convergence that imports the moist, boundary layer air needed to maintain the eyewall convection: *so according to CISK, friction is necessary to maintain a tropical cyclone*. Thus, the energy from the latent heat release must at least balance the energy lost to surface friction for a tropical cyclone to maintain its current intensity. If the mechanical energy due to latent heat release *exceeds (is less than)* the energy lost to surface friction, the tropical cyclone will *intensify (weaken)*.

Wind-Induced Surface Heat Exchange (WISHE), a Carnot engine theory of PI

In a Carnot engine, heat energy is converted to mechanical energy. Since tropical cyclones are built on latent heat release from active deep convection, perhaps a Carnot engine could be a good model for a tropical cyclone. The Carnot engine is a closed system in which the temperature difference across the layer provides the thermal energy available to drive motion.[7] A real tropical cyclone is not a closed system,but part of the complicated structure of

the atmospheric weather. To get around this, Emanuel (1986, 2005) assumed that the air in the upper tropospheric outflow sinking to the surface far from the storm to complete the circuit (Figure 4.9; from C to A). In spite of this and many other simplifying assumptions, the Carnot cycle PI theory provides a reasonable estimate of the upper limit for tropical cyclone intensity in a given environment, although not for the actual intensity at any given time.

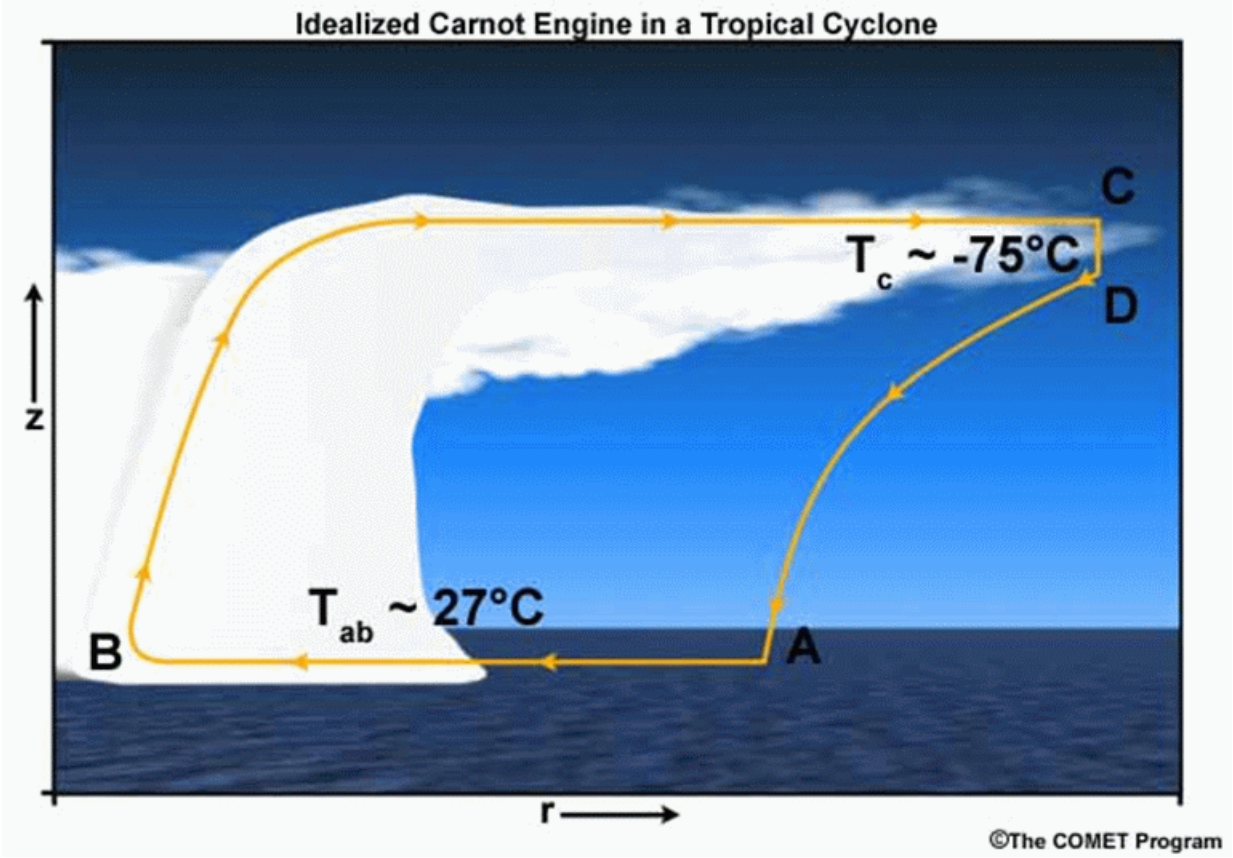

Figure 4.9. Schematic of the heat energy flow in an idealized "Carnot engine" tropical cyclone. Air in the atmospheric boundary layer flows in isothermally (AB), rises adiabatically in the eyewall convection (BC), diverges isothermally near the tropopause in the outflow anticyclone(CD). To close the circuit, this air must sink far from the storm (DA). Obtained from http://www.meted.ucar.edu/tropical/textbook_2nd_edition/navmenu.php?tab=9&page=4.1.2.

7For example, the heating element below a pot of boiling water is much warmer than the air above and the water moves turbulently — in a similar way, the radiative cooling at the top of a cloud drives turbulent motions in the vertical. The strong rotation in a tropical cyclone organizes the motions driven by the latent heat release.

Changes in thermal energy around the Carnot cycle provide the source for the mechanical energy sustaining the winds. Let's follow a parcel around the cycle depicted in Figure 4.9.

Air converging into the tropical cyclone boundary layer (AB) is warmed by (i)sensible heat flux from the ocean surface and (ii)frictional heating due to the deceleration of the winds (Bister and Emanuel 1998); this heating is balanced by (iii) adiabatic expansion as the air flows towards the

low pressure center and (iv) diabatic cooling due to evaporation(latent heat flux from the ocean). In WISHE, these four processes are assumed to balance, so there is no temperature change for air in the boundary layer inflow branch of the cycle. For calculations in the Carnot cycle model,the temperature of this isothermal inflow is taken to be the SST (Emanuel 2005).

Air rising in the eyewall convection (BC; the upward branch of the Carnot engine) rises along a moist adiabat, so the air at the top of the convective tower has the same saturation equivalent potential temperature[8] as the air feeding these clouds. However, air in the convection becomes increasingly dry as it rains and, in combination with the pressure drop in the vertical, this results in much cooler temperatures in the outflow layer (just below the tropopause) than in the boundary layer inflow. This temperature difference between the ocean surface and the tropopause provides the thermodynamic energy available to be converted into wind energy.

The Carnot engine that approximates our tropical cyclone is not perfectly efficient; only some of the thermal energy is available to be converted into motion. Typical values for a tropical cyclone are SST~27°C and tropopause temperatures about -75°C. Using these we calculate the efficiency, ε, of the Carnot engine[9] to be around one third, meaning that one third of the thermodynamic energy in our Carnot engine tropical cyclone is available to drive the winds.

8Equivalent potential temperature, θe, is defined as $\theta_e = T_e\left(\frac{p_0}{p}\right)^{\frac{R_d}{c_p}}$ where $T_e = \left(T + \frac{L_v r}{c_p}\right)\left(\frac{p_0}{p}\right)^{\frac{R_d}{c_p}}$ is the equivalent temperature corresponding to (T, p, r) at that location; T (K) and p (hPa) are the temperature and pressure of the parcel, r is the water vapor mixing ratio of the parcel (in units of kg kg-1) and Lv, the latent heat of evaporation (J kg), which varies with temperature. The constants appearing in this equation are: $p0$, the reference pressure (1000 hPa); Rd, the gas constant for dry air (287 J kg-1 K-1); and cp, the specific heat at constant pressure (1004 J kg-1 K-1)

9 $$\varepsilon = \left(\begin{matrix} T_{IN} - T_{OUT} \\ T_{IN} \end{matrix}\right) \cong \left(\begin{matrix} SST - T_{TROP} \\ SST \end{matrix}\right) = \left(\begin{matrix} 300 - 200 \\ 300 \end{matrix}\right) = \begin{matrix} 1 \\ 3 \end{matrix}$$

The climatological values of potential intensity derived from this theory agree quite well with the distribution of the most intense tropical cyclones observed (Figure 4.10), so we have some confidence that it can provide guidance on the upper limit for the intensity of an individual tropical cyclone (e.g. De Maria et al. 2005).

However,this WISHE theory is not predictive: it does not tell us what the actual intensity will be for any storm. The evolution of the intensity of an individual tropical cyclone is governed by its complete environment, not just the thermodynamics. Next, we will look at all of the other factors that go into determining the intensities achieved by a real tropical cyclone.

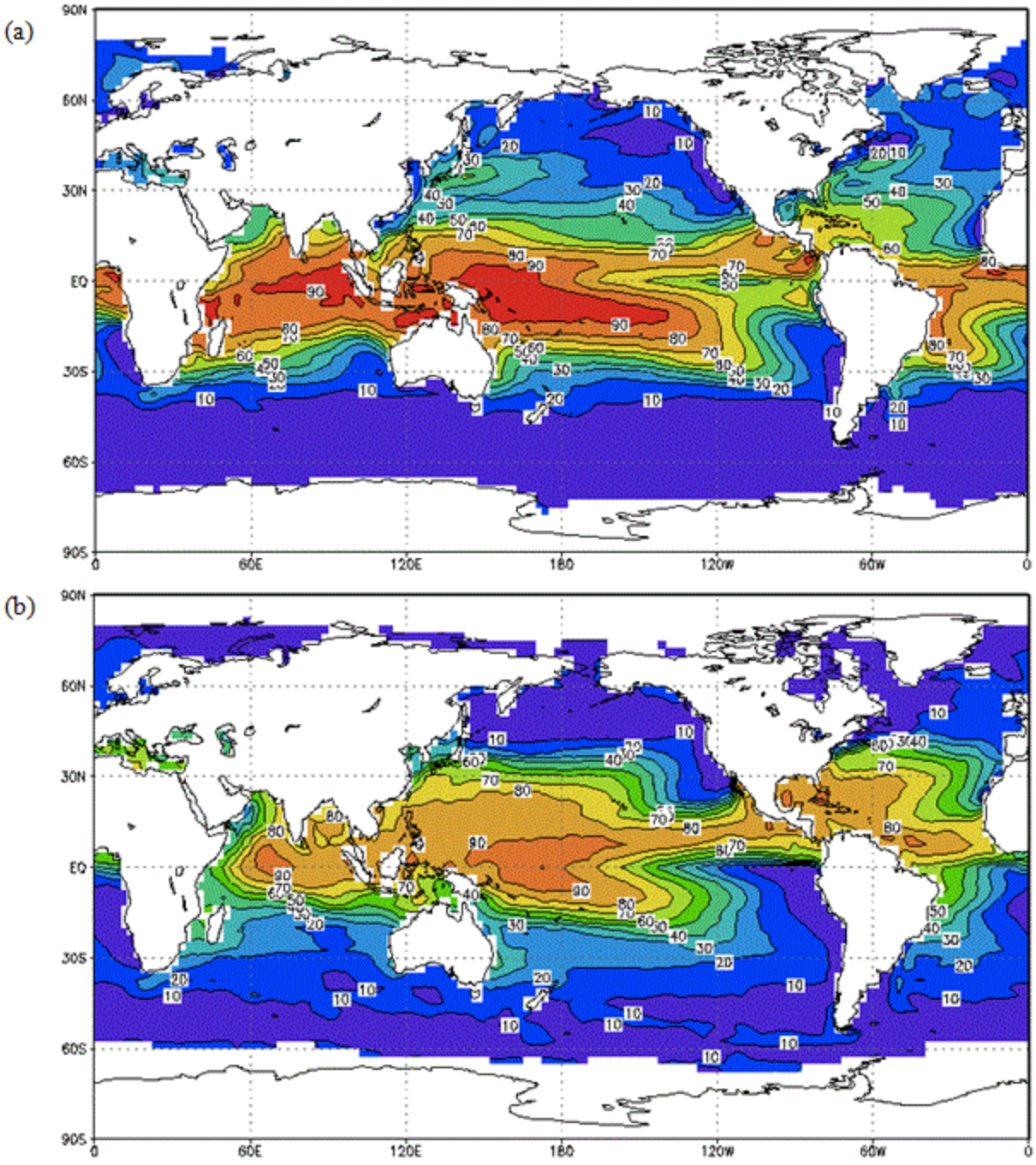

Figure 4.10. Monthly mean maximum surface winds (ms-1) calculated from the WISHE Carnot cycle model using 1982-1995 daily SST and tropopause temperatures: (top) February and (bottom) September. Note the change in color scale between the panels. Maps obtained from http://wind.mit.edu/~emanuel/pcmin/climo.html.

Observed relationships between tropical cyclone intensity and ocean temperatures

CISK and WISHE theories assume that warm ocean waters,much cooler outflow temperatures, boundary layer convergence of very moist tropical air in an environment supportive of deep convection are readily available to a developing tropical storm. If this were true for all tropical cyclones, tragedies like the Bhola (1970) and Chittagong (1990) tropical cyclones; Typhoon Vera (1959, known as Isewan Typhoon in Japan), Tropical Cyclone Tracy (1974), Hurricanes Mitch (1989) and Katrina (2005) would be the norm. Since these are rare events, it is clear that the large-scale environment of the developing tropical cyclone must interfere with the processes captured in these two theories. What does this mean? It means that the environment must somehow disrupt the deep convection in the evolving tropical cyclone, particularly near its core. Environmental conditions limiting the convection,and so limiting the intensity,of a storm include insufficient moisture (either boundary layer air or relatively dry free troposphere), cool SST,or a region of strong baroclinicity (shear and temperature gradients). While each of these environmental characteristics can inhibit intensification, taking these factors to the other extreme, for example, no vertical wind shear and very warm waters, does not guarantee that a storm will reach its PI. We'll return to this conundrum below.

"Potential" intensity is only achievable when these factors combine favorably. This is demonstrated in a study that compares the observed distribution between intensity and SST (Figure 4.11, reproduced from Evans 1993). A 20-year period chosen (1967-1986) began with the satellite era and ended with the end of aircraft reconnaissance in the western North Pacific.The complete recorded lifecycle for every tropical storm observed was included in the analyses, so these results should be interpreted in terms of the storm lifecycle. The first impression from these analyses is that the two basins with reconnaissance (panels (a) and (b)) show a dramatic increase in intensities for "tropical" SST > 25°C or so, while the strongest storms are restricted to a smaller, warmer range of SST as expected from both the CISK and WISHE theories discussed above. However, we also see that tropical cyclones can achieve any intensity for storms over SST > 25°C.

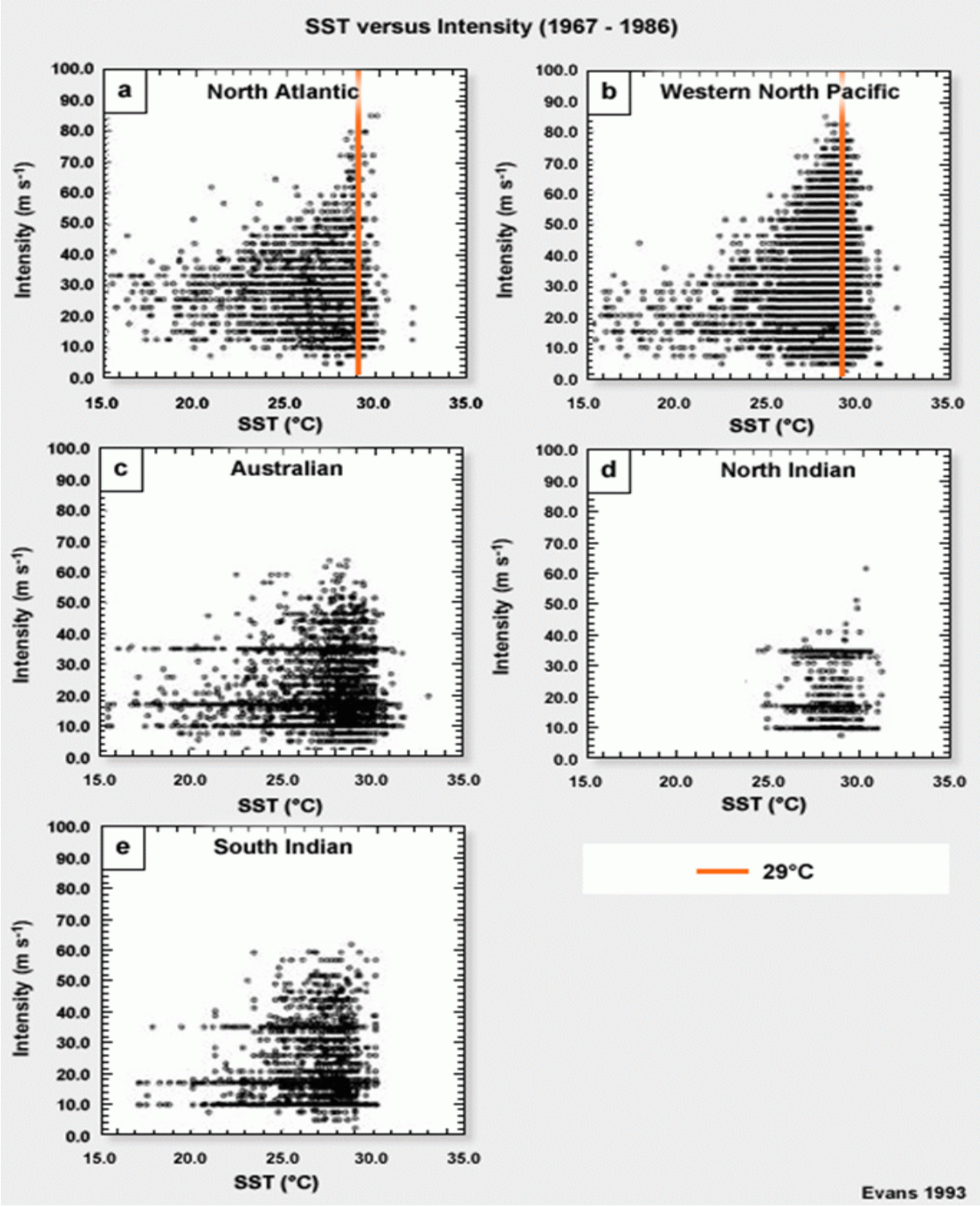

Figure 4.11. Intensity (ms-1) against SST (°C) for all tropical storm times in the 20 year period 1967-1986 for (a) North Atlantic, (b) western North Pacific,(c) Australian,(d)North Indian, and (e) South Indian Ocean basins (Evans 1993, her Fig. 1).

So what about the tropical ocean basins without regular reconnaissance flights (panels (c)-(e))? We see that the intensity distributions in these regions emphasize key intensity threshold values (likely reflecting a dependence on satellite-based algorithms to estimate intensity). Evans (1993) went on to analyze these data further and demonstrated the expected decrease in intensity with time after genesis, as storms move away from their tropical genesis environment and into cooler waters. When she compared only the peak intensity of each storm against SST, no pattern was evident. These results combined provide strong evidence that warm SST are not sufficient on their own to explain the intensity of a tropical cyclone-reinforcing the role of these two theories in identifying the peak possible intensity, not the actual intensity of a storm.

One more word on SST before we move on. The warm near-equatorial SST is unfavorable for tropical cyclone development since this is also a region of vanishing Coriolis parameter and a region where cyclonic potential vorticity changes sign. As a result, it is difficult to create a balanced, cyclonic incipient disturbance that will intensify into a tropical cyclone. As satellites have improved, storms forming very near the equator (within 5° or so), but never on the equator, have been observed. These are usually very small ("midget") cyclones while they are close to the equator (Harr et al. 1996). Hence, the Earth's vorticity (Coriolis) governs intensity and structure, not just genesis.

Based on these results, we conclude that the organization of the wind field must also be important in determining tropical cyclone intensity. We'll first look at the effects of the environmental winds on intensity, then return to the role of storm structure on its intensity.

Environmental factors limiting tropical cyclone intensity

Interaction of a tropical cyclone with a region of strong environmental vertical wind shear usually leads the storm to begin to weaken, since the storm structure must change as it adjusts to this new environment (Jones 1995, 2000a). Interaction with strong environmental wind shear will initially make the convection of the storm asymmetric (discussed further below). As a result of strong shear,the storm will either (i) reintensify as a tropical system, having generated sufficient convection to retain its tropical structure in the sheared environment; or (ii) begin to recurve, when it will initially weaken (Riehl 1972; Evans and McKinley 1998). Once it begins recurvature, this tropical cyclone will either decay or undergo extratropical transition (discussed in the structure section).

Strong vertical wind shear does not have the same impact on tropical cyclones of different intensities. As we discussed above, as the intensity of a tropical cyclone increases, its inertial stability increases. Since inertial stability is a measure of the resistance of a tropical cyclone to external influences, more intense tropical cyclones are more resilient in adverse environments. For example, a storm rotating with peak surface windspeeds of 50 ms^{-1} would be less disrupted by strong vertical wind shear than a storm of 20 ms^{-1}. A larger tropical cyclone (with strong winds far from its center) will also survive strong shear more easily since it has large values of inertial stability out to larger radius (Merrill 1984).

Two places where even the strongest tropical cyclone is susceptible to its environment are the ocean surface and the outflow anticyclone. Inertial stability in the upper-tropospheric anticyclone is weak, so the tropical cyclone is susceptible to weakening caused by upper-tropospheric weather systems (Hanley et al. 2001). Further, no matter how intense a tropical cyclone is, inertial stability will not protect it from the negative influence of cool SST. Cool ocean waters cut off the deep convection needed for a tropical cyclone to sustain itself (e.g., Figure 4.11).

Now that we've established that strong vertical wind shear limits the intensity of a tropical cyclone, can we conclude that the best environment for a tropical cyclone to intensify is no vertical wind shear? We cannot. Some vertical wind shear is needed to advect the storm along (Frank and Ritchie 1999, 2001). Without this advection, a storm will move very slowly (Chan and Williams 1987); a slow-moving storm will mix cooler ocean water from below the thermocline, cooling the SST below. (Storm rainfall may also contribute to these cooler SST, but this is a small additional effect.) By cooling the underlying SST, the storm weakens the convection in its core, so limiting its own peak intensity. While the shear associated with storm advection may delay intensification, if all other factors are favorable the storm may still reach its PI (Kimball and Evans 2002).

Impacts of tropical cyclone structure on intensity change

As we have discussed,the key to a storm maintaining its current intensity or intensifying further is the maintenance of the deep convection surrounding its core.

As mentioned above, vertical wind shear initially causes the convection in a tropical cyclone to become asymmetric (e.g., Corbosiero and Molinari 2002; Jones 2000b; Molinari et al. 2006). If the convection becomes asymmetric,this lowers the inertial stability of the storm, making it more susceptible to negative effects from its environment.If the shear persists, it can eventually lead to the decay of the tropical storm, as evident with the majority of tropical cyclones that move into the midlatitude baroclinic zone.

As we've said repeatedly, a consistently moist boundary layer is required to feed the tropical cyclone convection; even the convective downdrafts have to be saturated for the convection to be as vigorous as possible in its environment. Evaporation from the ocean must act too for the boundary layer to recover from injection of subsaturated and cool downdraft air; this will take a number of hours before intensification can resume. Intrusions of dry air advected from nearby land masses will also weaken the storm convection. In the North Atlantic,the Saharan Air Layer (SAL) (Carlson and Prospero 1972) also weakens the tropical storm convection (Karyampudi and Pierce 2002; Dunion and Velden 2004) and constrains its motion.

Rapid intensity change: Warm ocean eddies and eyewall replacement cycles

Rapid intensification or weakening are critical challenges when forecasting tropical cyclone intensity evolution. These situations arise predominantly from cyclone passage over a warm ocean eddy or eyewall replacement cycles.

Movement of a tropical cyclone over a warm ocean eddy invigorates the deep convection of the system and so provides extra latent heat energy that is available to intensify the storm.

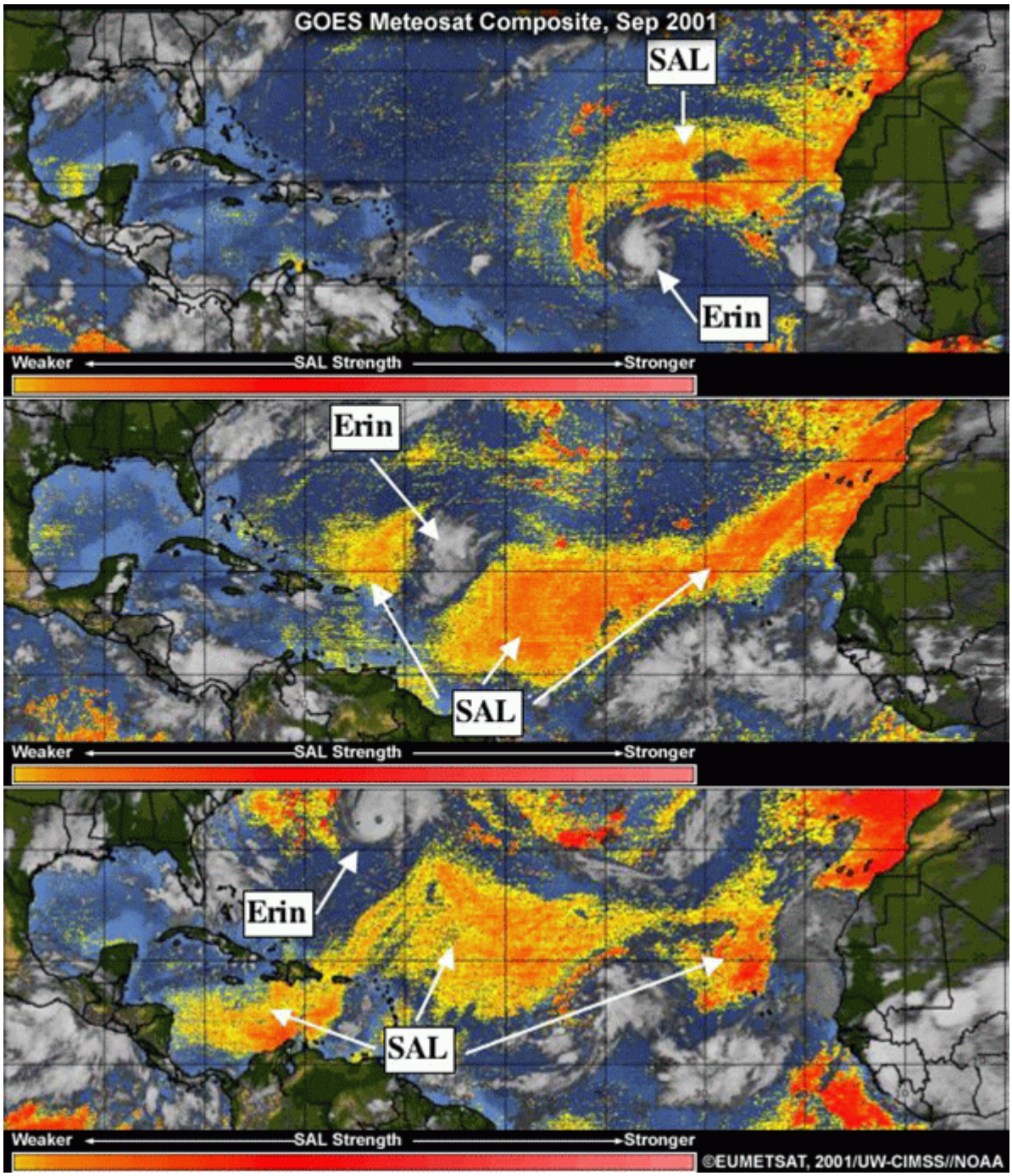

Figure 4.12. GOES SAL-tracking imagery for the interaction of Hurricane Erin (2001) with a SAL outbreak. Time goes down: (a) 0000 UTC 2 Sep, (b) 1800 UTC 5 Sep, (c) 1800 UTC 9 Sep. Image from http://www.meted.ucar.edu/tropical/textbook/ch10/tropcyclone_10_3_4.html. Real-time diagnostics of the SAL such as these are available from http://tropic.ssec.wisc.edu/

Eyewall replacement cycles occur when an outer eyewall develops, choking off the moist boundary layer inflow needed for the original eyewall to maintain itself; the existing eyewall dissipates and, as a consequence, the central pressure rises (so the surface pressure field of storm relaxes) and the tropical cyclone weakens (Willoughby et al. 1982; Willoughby 1990). At this stage, the outer eyewall contracts gradually and the tropical cyclone regains its original intensity or even becomes more intense (Figure 4.13). Eyewall replacement cycles are most commonly observed during periods of rapid intensification or weakening of intense tropical cyclones (peak winds exceeding 50 ms^{-1}).

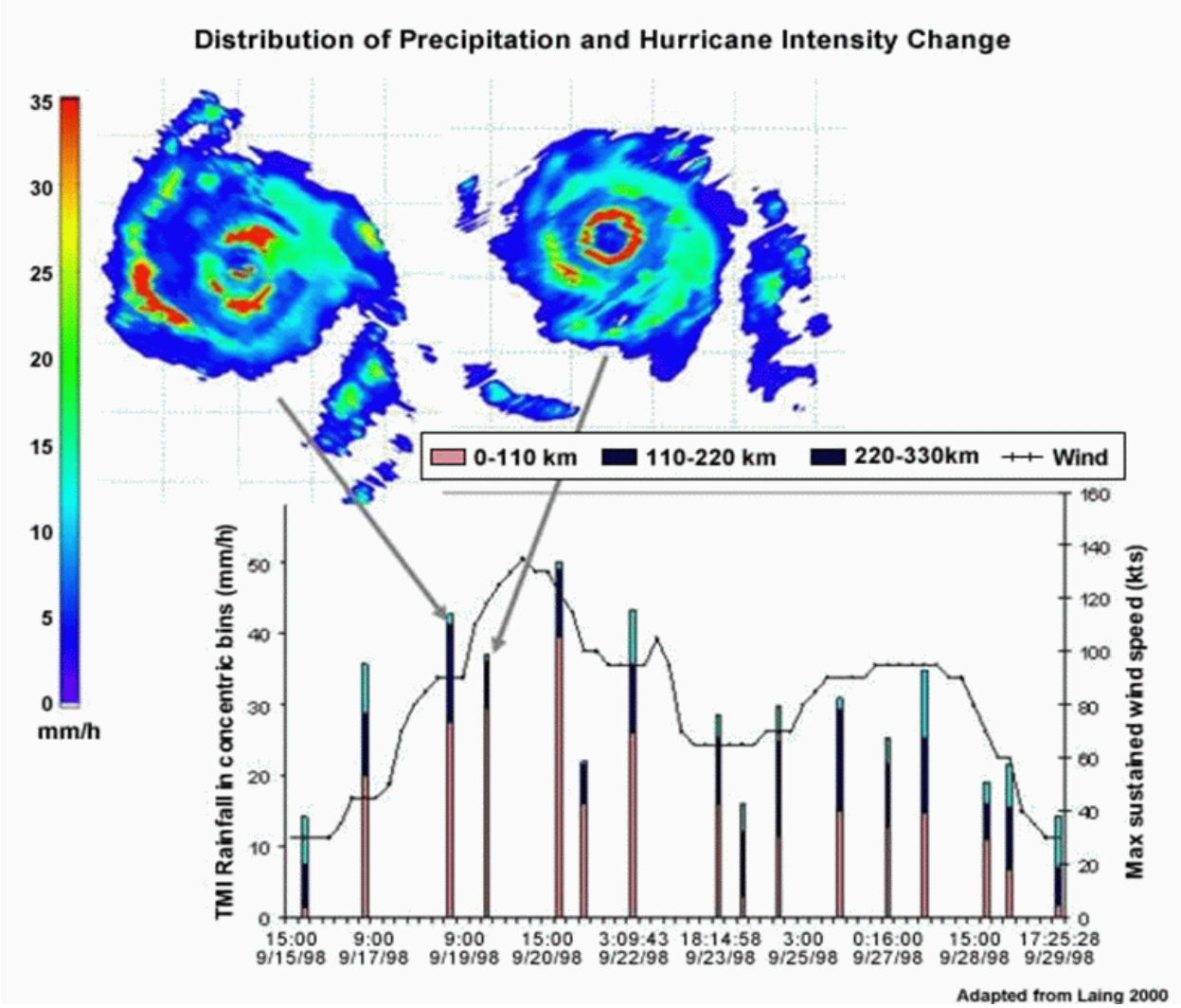

Figure 4.13. Spatial distribution of surface rain rates (mm hr-1)in Hurricane Georges via TRMM TMI, best track maximum sustained wind speed (knots, solid black line), and rainfall in concentric bins around the center of the cyclone (mm h-1, vertical bars). Laing and Evans (2012).

Concentric eyewalls and eyewall replacements are most common in the western North Pacific because this largest of the ocean basins has very warm waters, meaning that storms typically have longer to intensify before they encounter adverse environmental conditions (such as strong shear,land or cool SST). Some intense tropical cyclones can undergo multiple eyewall replacement cycles.

In summary, intensity change is affected by the current structure and intensity of the tropical cyclone, as well as its environment. Processes leading to intensity change feed back on each other.

Operational monitoring of tropical cyclone intensity

While it is a standard metric of a tropical cyclone and provided in all storm advisories or reports, tropical cyclone intensity is most often deduced via remote sensing[10]. Instruments used for inferring tropical cyclone intensity and structure characteristics include satellite radiometers (IR, visible, and microwave), scatterometers and radars, as well as ground-based radars. Outside special field experiment opportunities, airborne remote sensing of tropical cyclones is only routinely available in the North Atlantic and the eastern North Pacific; in these basins NOAA Hurricane Hunter[11] aircraft are equipped with Doppler radar and stepped frequency microwave radiometers (SFMR). Each of these observing platforms samples different volumes of the atmosphere at different resolutions and accuracy. Thus, different instruments are better suited to measuring different aspects of the storm wind field.

In terms of societal impacts,the peak wind at any single location gives the "worst possible" feature of the storm, so a single wind estimate or small region of intense winds are often be used to determine the observed tropical cyclone intensity (Avila 2010, personal communication).

10A comprehensive discussion of remote sensing applications to tropical cyclone structure and intensity is available from http://www.meted.ucar.edu/tropical/textbook/ch10/tropcyclone_10_4_5.html.

11http://www.aoc.noaa.gov/

Assumptions about the temporal and spatial scales relevant for characterization of intensity are implicit in the calculation of intensity. *The WMO standard definition of intensity is the maximum 10-minute sustained wind at 10 m above the surface.* However, while 10 m above the ground is the standard reference height used for intensity estimation, most operational forecast centers — including WMO regional forecast centers (RFC) — use different time averages. Critical wind speed thresholds — for example, from typhoon to supertyphoon — also differ across basins, as do the names assigned to the storms[12]. These various averaging periods, local classifications and wind speed thresholds are summarized in Tables 4.1 through 4.3 below.

Table 4.1. Intensity classifications and wind speed thresholds for the western North Pacific and Indian Ocean basins.

Western North Pacific	North Indian	South Indian	m s^{-1}	km h^{-1}
Tropical Storm	Tropical Storm	Tropical Storm	17-33	60-119
Typhoon	Severe Cyclonic Storm	Tropical Cyclone	> 34	> 120

Table 4.2. Intensity categories and windspeed thresholds for the North Atlantic and Eastern North Pacific Oceans and the Australian Region. See Table 4.3 for the averaging times used for estimating intensity in each basin.

Storm Category	North Atlantic and Eastern North Pacific			Australian Region	
	m s^{-1}	km h^{-1}	mph	m s^{-1}	km h^{-1}
1	33-42	119-153	74-95	< 34	< 125
2	43-49	154-177	96-110	34-47	125-165
3	50-58	178-209	111-130	47-63	165-225
4	59-69	210-249	131-155	63-78	225-280
5	70+	250+	156+	>78	>280

[12] See http://www.wmo.int/pages/prog/www/tcp/Storm-naming.html for background on naming conventions in each basin and lists of upcoming tropical cyclone names by region.

Table 4.3. Intensity averaging times, key wind speed thresholds and naming conventions for all ocean basins impacted by tropical cyclones.

Region	Wind Averaging Time[13]	Special Intensity Threshold		Naming Convention
		m s^{-1}	km h^{-1}	
Australia	10 minutes	>35	>125	Tropical Cyclone
		>46	>165	Severe Tropical Cyclone
North Atlantic and Eastern North Pacific	1 minute	>33	>120	Hurricane
		>50	>180	Major Hurricane
Western North Pacific	10 minutes	>63	>227	Super Typhoon
North Indian Ocean	10 minutes	>33	>120	Severe Cyclonic Storm
South Indian	10 minutes	>63	>227	Severe Tropical Cyclone

13A new WMO report http://www.wmo.int/pages/prog/www/tcp/documents/WMO_TD_1555_en.pdf discusses the implications of these various averaging times.

4.8 References

Aiyyer, A., and J. Molinari, 2008: MJO and tropical cyclogenesis in the Gulf of Mexico and eastern north Pacific: Case study and idealized numerical modeling. *J. Atmos*. Sci., **65**, 2691-2704.

Bister, M., and K. A. Emanuel, 1998: Dissipative heating and hurricane intensity. *Meteor. Atm. Phys.*, **52**, 233-240.

Briegel, L. M., W. M. Frank, 1997: Large-scale influences on tropical cyclogenesis in the western North Pacific. *Mon. Wea. Rev.*, **125**, 1397-1413.

Carlson T. N., and, J. M. Prospero, 1972: The large-scale movement of Saharan air outbreaks over the north equatorial Atlantic. *J. Applied. Meteorol.*, **11**, 283-297.

Chan, J. C. L., and R. T. Williams, 1987:Analytical and numerical studies of the beta-effect in tropical cyclone motion. Part I: Zero mean flow. *J. Atmos. Sci.*, **44**, 1257-1265.

Charney, J. G., and A. Eliassen, 1964: On the growth of the hurricane depression. *J. Atmos. Sci.*, **21**, 68-75.

Corbosiero, K. L., and J. Molinari, 2002: The effects of vertical wind shear on the distribution of convection in tropical cyclones. *Mon. Wea. Rev.*, **130**, 2110-2123.

Davis, C. A., and L. F. Bosart, 2003: Baroclinically induced tropical cyclogenesis. *Mon. Wea. Rev.*, **131**, 2730-2747.
Davis, C. A., and L. F. Bosart, 2004: The TT problem. *Bull. Amer. Meteor. Soc.*, **85**, 1657-1662.

DeMaria, M., M. Mainelli, L. K. Shay, J. A. Knaff, and J. Kaplan, 2005: Further improvement to the Statistical Hurricane Intensity Prediction Scheme (SHIPS). *Wea. Forecasting*, **20:4**, 531-543.

Dickinson, M., J. Molinari, 2002: Mixed Rossby-gravity waves and western Pacific tropical cyclogenesis. Part I: Synoptic evolution. *J. Atmos. Sci.*, **59**, 2183-2196.

Dunion J. P., and C. S. Velden, 2004: The impact of the Saharan Air Layer on Atlantic tropical cyclone activity. *Bull. Amer. Meteor. Soc.*, **85**, 353-365.

Emanuel, K. A.., 1986: An air-sea interaction theory for tropical cyclones. Part I: Steady-state maintenance. *J. Atmos. Sci.*, **43**, 585-604.

Emanuel, K. A., 1988: The maximum intensity of hurricanes. *J. Atmos. Sci.*, **45**, 1143-1155.

Emanuel, K. A., 1995: Onb thermally direct circulations in moist atmospheres. *J. Atmos. Sci.*, **52**, 1529-1534.

Emanuel, K. A., 2005: Increasing destructiveness of tropical cyclones over the past 30 years. Nature, **436**, 686-688.

Evans, J. L., 1993: Sensitivity of tropical cyclone intensity to sea surface temperature. *Journal of Climate*, **6**, 1133-1140.

Evans, J. L., 2001: Hurricanes, Typhoons and Tropical Storms: A Theoretical Review. In Encyclopedia of Global Environmental Change, T. Munn, M. C. MacCracken and J. S. Perry (Eds), John Wiley and Sons, London UK.

Evans, J. L., and McKinley, 1998: Relative timing of tropical storm lifetime maximum intensity and track recurvature. *Meteorological and Atmospheric Physics*, **65**, 241-245.

Evans, J. L., and M. P. Guishard, 2009: Atlantic Subtropical Storms. Part I: Diagnostic Criteria and Composite Analysis. *Monthly Weather Review*, **137**, 2065-2080, DOI: 10.1175/2009MWR2468.1.

Evans, J. L., F. A. Jaskiewicz, 2001: Satellite-based monitoring of intraseasonal variations in tropical Pacific and Atlantic convection. *Geophys. Res. Lett.*, **28**, 1511-1514.

Ferreira, R. N., W. H. Schubert, 1997: Barotropic aspects of ITCZ breakdown. *J. Atmos. Sci.*, **54**, 261-285.

Frank, W. M., and E. Richie, 1999: The effects of environmental flow upon tropical cyclone structure.*Mon. Wea. Rev.*, **127**, 2044-2061.

Frank, W. M., and E. Richie, 2001: Effects of vertical wind shear on the intensity and structure of numerically simulated hurricanes. *Mon. Wea. Rev.*, **129**, 2249-2269.

Frank, W. M., and P. E. Roundy, 2006: The role of tropical waves in tropical cyclogenesis. *Mon. Wea. Rev.*, **134**, 2397-2417.

Fraedrich, K. and J. L. McBride, 1989: The physical mechanism of CISK and the free-ride balance. *J. Atmos. Sci.*, **46**, 2642-2648.

Gill, A. E., 1980: Some simple solutions for heat-induced tropical circulation. *Q. J. R. Meteorol. Soc.*, **106**, 447-462.

Guishard, M. P., J. L. Evans, R. E. Hart, 2009: Atlantic Subtropical Storms. Part II: Climatology. *Journal of Climate*, **22**, 3574-3594, DOI: 10.1175/2008JCLI2346.1.

Gray, W. M., 1968: Global view of the origin of tropical disturbances and storms. *Mon. Wea. Rev.*, **96**, 669-700.

Hanley, D., J. Molinari, and D. Keyser., 2001: composite study of the interactions between tropical cyclones and upper-tropospheric troughs. *Mon. Wea. Rev.*, **129**, 2570-2584.

Harr, P. A., M. S. Kalafsky and R. L. Elsberry, 1996: Environmental conditions prior to formation of a midget tropical cyclone during TCM-93. *Mon. Wea. Rev.*, **124**, 1693-1720.

Jones, S. C., 1995: The evolution of vortices in vertical shear. I: Initially barotropic vortices. *Q. J. R. Meteorol. Soc.*, **121**, 821-851.

Jones, S. C., 2000a: The evolution of vortices in vertical shear. II: Large-scale asymmetries. *Q. J. R. Meteorol. Soc.*, **126:570**, 3137-3159.

Jones, S. C., 2000b: The evolution of vortices in vertical shear. III: Baroclinic vortices. *Q. J. R. Meteorol. Soc.*, **126:570**, 3161-3185.

Karyampudi, V. M., and H. F. Pierce, 2002: Synoptic-scale influence of the Saharan Air Layer on tropical cyclogenesis over the eastern Atlantic. *Mon. Wea. Rev.*, **130**, 3100-3128.

Kiladis, G. N., and M. Wheeler, 1995: Horizontal and vertical structure of observed tropospheric equatorial Rossby waves. *J. Geophys. Res.*, **100**, 22981-22998.

Kimball, S. K., and J. L. Evans, 2002: Idealized numerical simulations of hurricane-trough interaction.*Mon. Wea. Rev.*, **130**, 2210-2227.

Knaff, J. A., C. R. Sampson, and M. DeMaria, 2005: An operational statistical typhoon intensity prediction scheme for the western North Pacific. *Wea. Forecasting,* **20**, 688-699.

Laing, A., and Evans, J.L., 2012: Introduction to tropical meteorology, 2nd Edition. Chapter 8: Tropical Cyclones. Produced by the COMET Program. Available at "http://www.meted.ucar.edu/tropical/textbook_2nd_edition/" (in Spanish and English).

Liebmann, B., H. H. Hendon, and J. D. Glick, 1994: The relationship between tropical cyclones of the western Pacific and Indian Oceans and the Madden-Julian oscillation. *J. Meteor. Soc. Japan*, **72**, 401-411.

Madden, R. A., P. R. Julian, 1994: Observations of the 40-50-day tropical oscillation—A review. *Mon. Wea. Rev.*, **122**, 814-837.

Maloney, E. D., and D. L. Hartmann, 2001: The Madden-Julian Oscillation, barotropic dynamics, and North Pacific tropical cyclone formation. Part I: Observations. *J. Atmos. Sci.*, **58**, 2545-2558.

McBride, J. L., T. D. Keenan, 1982: Climatology of tropical cyclone genesis in the Australian region.*Int. J. Climatol.*, **2**, 13-33.

McBride, J. L., R. Zehr, 1981: Observational analysis of tropical cyclone formation. Part II: Comparison of non-developing versus developing systems. *J. Atmos. Sci.,* **38**, 1132-1151.

Merrill, R. T., 1984: A comparison of large and small tropical cyclones. *Mon. Wea. Rev.,* **112**, 1408-1418.

Miller B.I., 1958: On the maximum intensity of hurricanes, *J. Met.* **15**, 184-195

Molinari, J., P. Dodge, D. Vollaro, K. l. Corbosiero and F. Marks, 2006: Mesoscale Aspects of the Downshear Reformation of a Tropical Cyclone. *J. Atmos. Sci.*,**63,** 341-354.

Molinari, J., D. Knight, M. Dickinson, D. Vollaro, and S. Skubis, 1997: Potential vorticity, easterly waves, and eastern Pacific tropical cyclogenesis. *Mon. Wea. Rev.,* **125**, 2699-2708.

Molinari, J., and D. Vollaro, 2000: Planetary-and synoptic-scale influences on eastern Pacific tropical cyclogenesis. *Mon. Wea. Rev.,* **128**, 3296-3307.

Molinari, J., D. Vollaro, and K. L. Corbosiero, 2004: Tropical cyclone formation in a sheared environment: A case study. *J. Atmos. Sci.,* **61**, 2493-2509.

Nitta, T., 1989: Development of a twin cyclone and westerly bursts during the initial phase of the 1986-87 El Niño. *J. Meteor. Soc. Japan,* **67**, 677-681.

Ooyama, K., 1963: A dynamical model for the study of tropical cyclone development. *Geophys. Int.,* **4**, 187-198.

Ooyama, K. V., 1982: Conceptual evolution of the theory and modeling of the tropical cyclone. *J. Meteoro. Soc of Japan,* **60**, 369-380.

Riehl, H., 1972: Introduction to the atmosphere. McGraw-Hill, New York, N. Y.,pp. 516.

Ritchie, E. A., G. J. Holland, 1999: Large-scale patterns associated with tropical cyclogenesis in the western Pacific. *Mon. Wea. Rev.,* **127**, 2027-2043.

Schubert, W. H., P. E. Ciesielski, D. E. Stevens, and H. C. Kuo, 1991: Potential vorticity modeling of the ITCZ and the Hadley Circulation. *J. Atmos. Sci.,* **48**, 1493-1509.

Simpson, J., E. Ritchie, G. J. Holland, J. Halverson, and S. Stewart, 1997: Mesoscale interactions in tropical cyclone genesis. *Mon. Wea. Rev.,* **125**, 2643-2661.

Simpson, J., J. B. Halverson, B. S. Ferrier, W. A. Petersen, R. H. Simpson, R. Blakeslee, and S. L. Durden, 1998: On the role of “hot towers” in tropical cyclone formation. *Meteor. Atmos. Phys.,* **67**, 15-35.

Willoughby, H. E., J. A. Clos and M. G. Shoreibah, 1982: Concentric eye walls, secondary wind maxima, and the evolution of the hurricane vortex, *J. Atmos. Sci.,* **39**, 395-411.

Willoughby, H. E., 1990: Temporal changes of the primary circulation in tropical cyclones, *J. Atmos. Sci.,* **47**, 242-263.

Zehnder, J. A., 1991: The interaction of planetary-scale tropical easterly waves with topography: A mechanism for the initiation of tropical cyclones. *J. Atmos. Sci.,* **48**, 1217-1230.

Chapter Five

Dr. Steve Lyons
U.S. National Weather Service

5. Tropical Cyclone Storm Surge and Open Ocean Waves

5.1 Introduction

There has been some misunderstanding about the forecasting of tropical cyclone (TC) waves. In fact, some centers that forecast tropical storm and hurricane/typhoon waves have collocated the radius of 12-ft (4-m) seas with the radius of 34-kt (64 km/h) winds (tropical storm force winds). I am uncertain where this methodology came from, but it is a completely unfounded and an incorrect practice. It is very possible to get 12-ft (4-m) seas more than 1500 miles (~2400 km) away from a TC and I am unaware that tropical storm winds have ever had such a radial extent! So what practices are useful for forecasting TC waves? Part of the problem lies in the fact that very few numerical models actually represent the correct magnitude of TC winds in their analysis, let alone in their forecasts, especially for very strong TCs. These model wind deficiencies very often result in large underestimates of wave heights in and around a TC, especially for strong ones.

5.2 Wave growth

The physics of waves in and around a TC are no different than they are for any other oceanic wind system. The elements that dictate wave growth are three, namely;

1) Wind speed
2) Wind fetch (distance the wind blows over the ocean)
3) Wind duration (how much time wind of a given speed blows)

Wind speed is fairly straight forward assuming one has good measurements of it in and around a TC. Unfortunately, ships sortie away from strongest winds in a tropical cyclone in most cases. In fact, most ship captains try to keep their ships well outside the 34-knot (64 km/h) wind radius of a TC. Satellite winds most typically represent elevations near cumulus cloud base and can be used and adjusted to the surface (the standard is a 10 meter wind), but this requires some knowledge of atmospheric stability in the lowest few thousand feet and some knowledge of the vertical profile of wind change with height. Neither is routinely well known in and around a TC from direct measurements, hence reasonable physical assumptions are often applied which can and do have uncertainty and error. Microwave/scatterometer winds can see through deep layers of clouds and are excellent wind sources, but can become smoothed near small tight eyes of TCs where averaging of near calm eye winds and fast eyewall winds and strong tight

gradients of wind within the and just outside the eyewall can occur. The signature of scatterometer winds becomes poor for very high winds making estimates of wind speeds above 80 knots (129 km/h) very difficult. But for winds below that, they provide excellent surface (10-m) winds except where land contamination can make them unusable in coastal waters and in bays. I will not detail how to determine the best wind estimates, but sound meteorological reasoning and excellent synoptic weather analysis skills are essential. These techniques are discussed in Chapters 3 and 4.

What makes wave forecasting even more challenging is the fact that the magic three parameters (above) controlling wave growth are NOT "linearly" related to wave growth. Instead wave growth is related to them as follows:

1. **Wave growth is proportional to wind speed squared**
2. **Wave growth is proportional to the 3/2 power of wind duration**
3. **Wave growth is proportional to the square root of wind fetch distance**

So if one is to make error in the estimates of these parameters the most sensitive is wind speed, followed by wind duration; the least sensitive is fetch distance. Obviously one would want to be as accurate as possible estimating all three parameters. The fact that it is very possible for a knowledgeable meteorologist to determine current wind speed within a TC better than a numerical model can determine it begs for a simple wave model that allows direct wind inputs by the forecaster. This may not be the case for wind "forecasts."

Fortunately, because TCs are generally small compared to typical synoptic scale oceanic weather features, and because they are either short lived or meander and loop along contoured tracks, both the wind fetch and/or the wind duration are huge limiting factors for wave growth in TCs that typically produce very high winds. If it were not for this fact, we could see ocean waves routinely in the 100- to 150-foot (30- to 45-m) range from strong TCs!

The most fortunate aspect of TC wave forecasting is that wave growth is controlled by the time integrated wind speed and wind fetch. This means that we can get a fairly close approximation to wave heights without knowing the "exact" local value and spatial distribution of wind, but rather the ensemble effect of wind integrated through time. We know this by the fact that model wind nowcasts and forecasts compared to local observations have a much lower correlation than do model wave forecasts compared to local wave observations. This aspect of wave forecasting is NOT by itself obvious to many forecasters! By getting the integrated picture correct we can very often get a close estimate of wave heights and wave periods, but the exact spectrum of waves generated can be less accurate and can result in significant errors.

5.3 Wave spectrum

The nature of wind blowing on the ocean results in not a single wave height and wave period, but rather a spectrum of wave heights and wave periods. For TCs where we have very large changes in wind speed over very short distances (eye wall to eye and eye wall to circulation edge), that spectrum can become even broader than in a typical oceanic storm. The result can often be a very tumultuous sea state in and near a TC. What we actually attempt to forecast is the "significant wave height" which statistically is the average of the highest 1/3 of waves, referred to as H1/3 or H_s. This convention is used in buoy wave measurements as well as in wave forecasts for the simple reason that a ship at sea reporting a single wave height will provide a number very close to the average of the highest 1/3 of waves. So, measurements, models and forecasters attempt to measure or predict what the customer typically reports as the dominant sea state. A simple diagram, showing averages from a spectrum of waves, is shown below with significant wave height (H_s) marked.

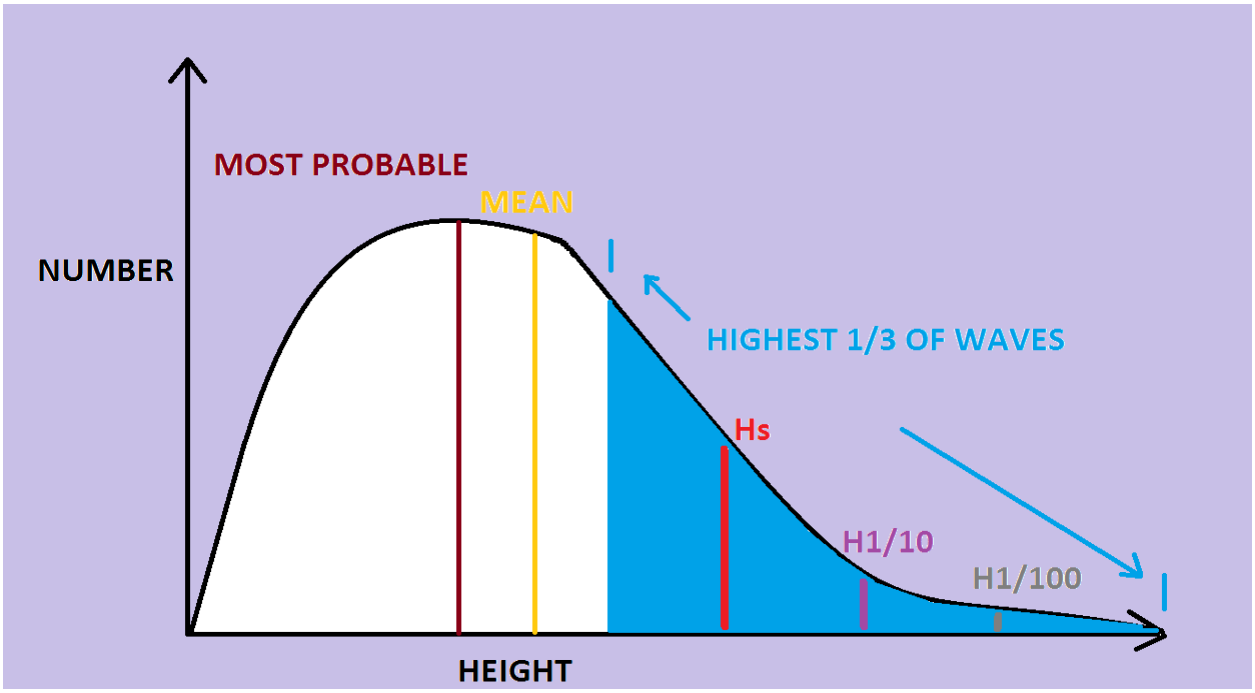

Figure 5.1. Diagram of the spectrum of waves or number versus height, where Hs is the significant wave height, H1/10 is the "maximum wave height" or the highest 10th wave, and H1/100 is the highest 100th wave. The diagram shows the relationship between the most probable wave height, the mean wave height, and the highest 1/3 of waves.

The statistical character of waves allows us to also estimate not only the average of the highest 1/3 but the average of the highest 1/10, 1/100 or single maximum wave likely to occur within a large sample. Those numbers are approximately related to $H_{1/3}$ or H_s as follows:

$H_{max} = 2.00 \times H_s$
$H_{1/100} = 1.67 \times H_s$
$H_{1/10} = 1.27 \times H_s$
$H_{1/3} = 1.00 \times H_s$

When more than one group of waves is occurring at the same time the combined H_s is typically given by

H_s combined = sqrt (w*w + s1*s1 + s2*s2 + s3*s3 + etc.)

Namely, the square root of the sum of the squares of the wind wave and each swell group within a given area. In the case of a TC this can get complicated as the circular rotation of winds around a tight center generates waves basically spreading out in all directions, some superimposing upon others temporarily as they race away from the wind wave generation source.

The maximum combined sea would then be approximated by 2.0 x H_s combined. As you can see individual very large waves can and have occurred within or near a TC. The rare "rogue wave" is basically nothing more than a very temporary, local superposition of waves of varied height and period. In some rarer cases, the "maximum single wave" recorded has been closer to 3-4 times $H_s$combined!

5.4 Wind fetch length

With a relatively small (in most cases) and circular TC, ideally there is only a single point around the circulation that is pointing in the same direction that might be considered a wind fetch distance. As the cyclone circulation becomes larger this “point” effectively becomes an area that grows with decreasing curvature (increasing cyclone size). **For all practical purposes a fetch that appears to work best is that area where wind directions are within about 20 degrees of a center line of interest. Thus an area with wind directions that span about a 40 degree region most often provide the best input to determining wind fetch length.** Hence, for example, along a line directed toward west (270 degrees), all winds within a range of approximately 250 degrees and 290 degrees would be considered within a fetch generation area pointing toward west (270 degrees). A very simple schematic is shown below of a fetch distance marked out by my time-trusted "40 degree rule" (shown in green) along a line directed from right to left.

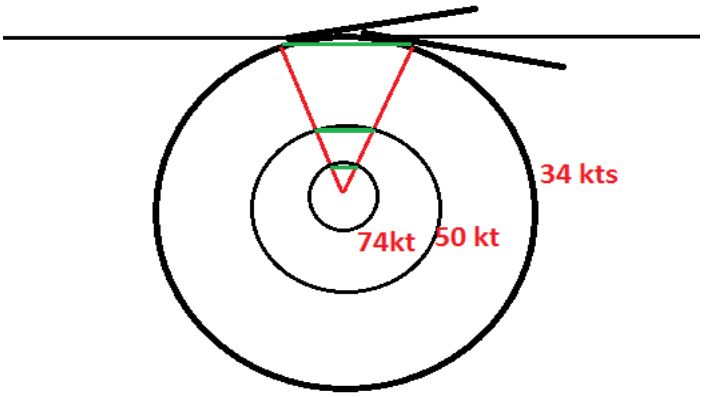

Figure 5.2. Relationship between wind speed and fetch length in a tropical cyclone. The green line shows the fetch length for a 34-knot wind, a 50-knot wind, and a 64-knot wind.

This fetch length could be for a 34-kt (64-km/h) wind, a 50-kt (93-km/h) wind, a 64-kt (119-km/h) wind or any other wind speed that might be known or estimated (as shown in Fig. 5.2).Immediately obvious is the fact that the distance of this green line increases quickly as the size of a TC increases. It is for this reason that large TCs generate much higher waves than do small TCs, many times even when the small TC is much more intense!

The net wind within a fetch can then be averaged to include the fraction or percent of wind of known speed added to those of other speeds. The net result is a wind fetch length of specific size with an averaged wind speed within it. Hence rather than have a highly changing wind speed across a short distance of a TC sector which is rarely known with great certainty, one uses a weighted wind (based on % of distance) across a larger simpler wind radius. Some reasonable assumptions using this methodology can be used to build a very simple TC wave forecast model that can be tuned using observations from a number of TC wave observations. Ideally this would be tuned initially with a TC(s) that is stationary for some length of time (not too many samples to choose from). A very accurate forecast of Hs and the period of those waves can be gotten in this manner. There can be some underestimate of maximum wave heights using this methodology when the fetch of maximum winds is very small (i.e. very small TCs), fortunately in those cases wave heights are severely limited by wind fetch and wind duration. It turns out that because the weaker winds (e.g. tropical storm winds) around the TC always cover a larger area than hurricane or strong hurricane winds, they can at times be the dominant wave generation area from a TC, especially when the strong wind area is tiny. **The exact spectral characteristics of the wave group cannot be gotten using the simple methodology described here, but if the dominant waves and wave periods are forecast, this information will be by far the most important information about any TC wave set for most purposes, especially for mariners at sea and for coastal impacts.** As noted above the "wind fetch" is the least sensitive input parameter to wave growth, that does not mean you can get it wrong and still get the correct wave answer, but the **errors from incorrect wind fetches are more forgiving and will result in far less wave forecast errors than errors in wind speed or wind duration**.

Obviously, a two dimensional wave model can be used with excellent success IF one knows the 2-D wind field through time within the model with great detail. This is sometimes known with some certainty "after" the TC event; hence it is a very valuable post-storm analysis/hindcast tool. Maximum wave climates (or wave height return periods) for specific ocean areas are often estimated in this way which aid in decisions made about coastal development among other things. A significant problem comes in real-time events with forecasts of wind waves by the wave model out in time using model wind forecasts. **Poor wind forecasts can obscure/blur the more accurate wind wave forecasts generated by initial wind conditions and/or short term wind forecasts that are more accurate.** There is no way to separate the more accurate portions of modeled waves from the highly uncertain portions of modeled waves within any numerical wave model forecast. These forecast errors can also infect the initial conditions in the wave model as no wave models that I am aware of use wave observations or "wave analyses" as input to wave model initial conditions. First guesses all come from model wave 6 hour or 12 hour forecasts based on wind forcing.

For example, an atmospheric model forecasts the TC to turn toward NW in 36 hours and strengthen, but in reality the cyclone continues on a more WNW track and does not intensify. The short term wave forecast may be accurate, but the wave forecast during the time the wind forecast was incorrect is completely erroneous. There is no way to separate the good wave forecasts from the bad ones within that model. The resultant impact at a distant coast is then a combination of an accurate swell forecast by initial conditions mixed with completely erroneous wind waves possibly affecting that coastline! Because model forecasts of TC rapid intensity change are very poor, the most sensitive wave model input (wind speed) completely overwhelms in a negative way the accuracy of the wave model forecast. Human interaction with simpler wave models allows for portions of poor wind/wave forecasts to be excluded or immediately reworked with new or more accurate winds at any time that information becomes known.

5.5 Wind duration

You know about the dangerous "right-front quadrant" of a TC in the Northern Hemisphere, it would be the "left-front quadrant" in the Southern Hemisphere. Most tropical meteorologists attribute this to the fact that this quadrant typically has the highest winds due to the forward motion of the TC being added to the winds from cyclostrophic balance or gradient wind balance (based on the rotation direction around the circulation center). However, it may be a surprise to you that the asymmetry in winds around a TC, rarely are a major cause for wave asymmetries shifted toward the cyclone's right-front quadrant!

Let's look at a few examples. The first is a stationary TC with winds exactly symmetric around the circulation. This does not mean a symmetric pressure field/gradient, as the Coriolis parameter changes with latitude and hence causes wind asymmetries around a TC for a symmetric pressure gradient due to latitudinal changes in Coriolis force. This changing Coriolis force across a TC from equator to pole leads to "Beta Drift", which alters the TC track forecasts

also. Assuming no currents or shallow water, and the same ocean temperature, waves everywhere around the TC would be identical as the wind forcing on the ocean would be symmetric (Fig. 5.3). Only the increases in winds nearing the eyewall would cause radial wave height changes, but those too would be symmetric.

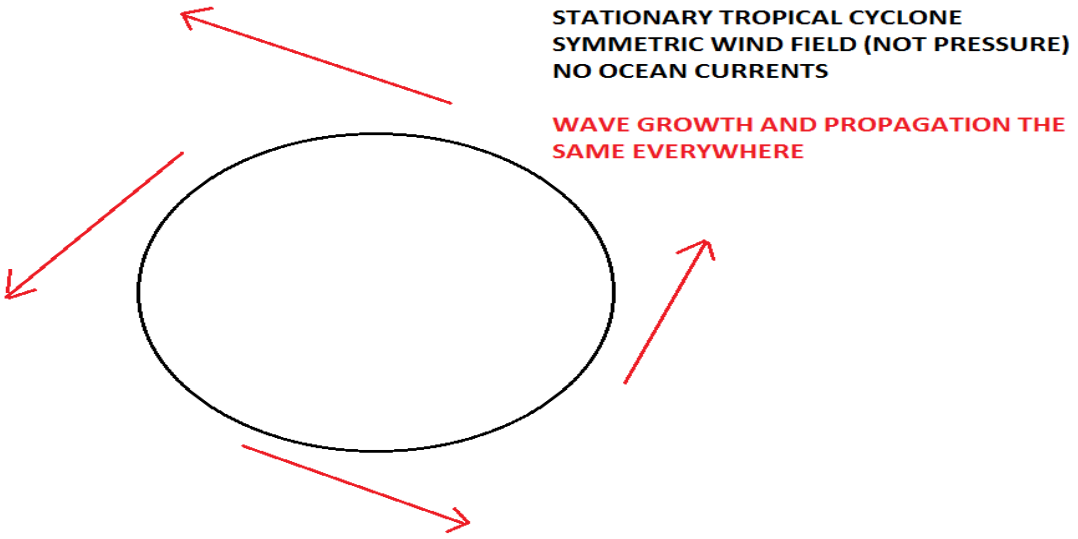

Figure 5.3. The circle represents a stationary tropical cyclone with symmetric wind field and no ocean currents. The red arrows indicate that the wave growth and propagation are the same everywhere.

Now let us add a forward motion vector (green arrow below not drawn to scale) (Fig. 5.4) to the TC as depicted below (the specific direction is irrelevant just change the direction vector to one you desire and the result relative to that direction will be unchanged).

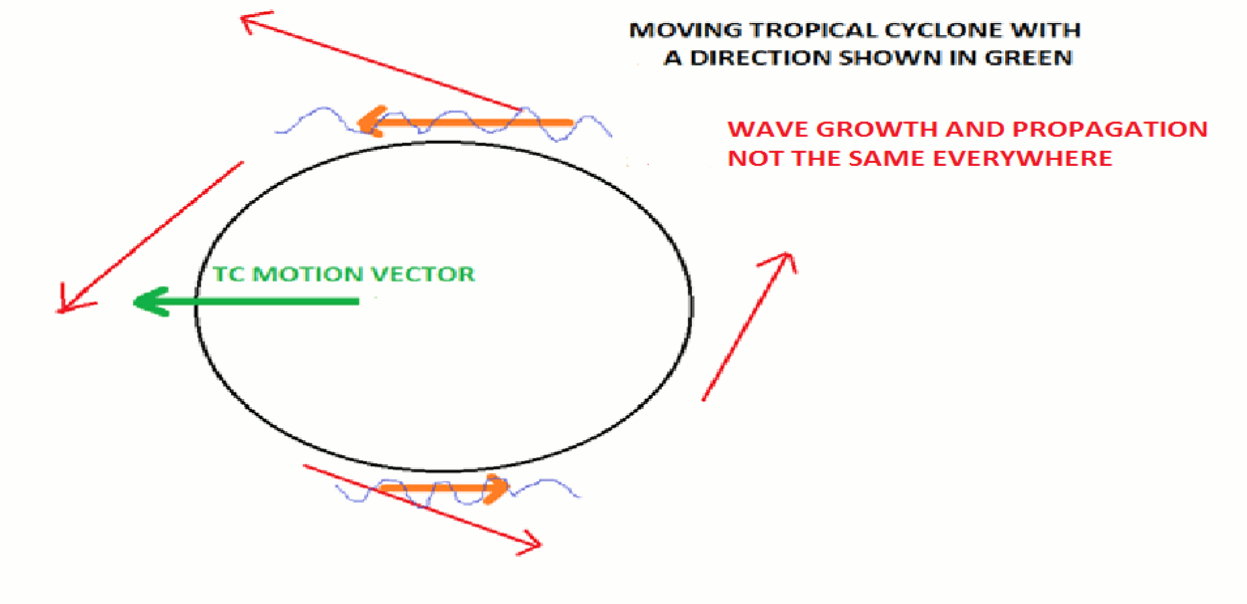

Figure 5.4. The circle represents a tropical cyclone (TC) moving in a direction and at a speed as indicated by the green TC motion vector. Orange arrows indicate the speed and direction of the wind in the direction of TC movement and opposite the TC motion. Red arrows indicate the relative winds around the TC. The blue irregular lines indicate the waves being generated by the TC in the direction of motion and opposite the direction of motion.

Two things now happen:

1) Winds on the north (top) side of this diagram become stronger (orange arrow pointing west/left) than those on the south (bottom) side of the diagram (orange arrow pointing east/right) because you are now adding the storm forward motion vector to east winds at the top, but are subtracting the forward motion vector from west winds at the bottom. This results in a wind asymmetry which can result in higher waves where winds are stronger. But this is the much smaller affect of the two.

2) Waves (blue) at the top of the diagram move to the west/left in the same direction the wind is blowing and in the same direction the TC is moving. Waves at the bottom of the diagram move to the east/right in the opposite direction the wind is blowing and in the opposite direction the TC is moving. In a relatively short time, waves moving east/right find themselves well removed from the TC wind field, while waves moving west/left continue to be within the TC wind field and depending upon the speed of the waves and the speed of the TC could remain in that wind generation area for a long time!

So 12 to 24 hours later we find that waves, which remain in the wind generation area, have grown significantly, while waves that have been left behind and are moving away from the TC, had only a short time to grow and are now decaying as swell (see Fig. 5.5). This is an example of the significant influence ﷺwind durationﷺ has on wave growth in a TC. That duration can be very short for small TCs moving quickly in quadrants other than the ﷺright-front quadrantﷺ where waves move with the TC and have more wind duration to generate waves.

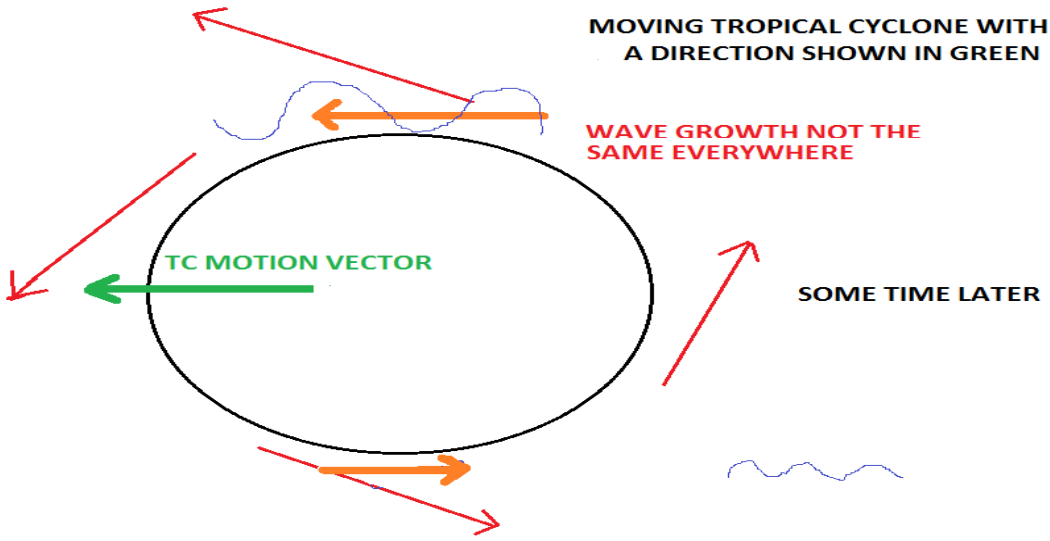

Figure 5.5. Same as Figure 5.4 but for "some later time". Blue lines show the large wave growth where waves remain in the wave generation area (top) and large wave decay where waves leave the wave generation area (bottom).

It turns out that waves spend the least amount of time in the left (right) rear quadrant in the Northern (Southern) Hemisphere and are routinely smallest there, that time dependent upon TC speed and size. Waves spend more time in the quadrants perpendicular to the TC's motion than in the left-rear quadrant, that time is dependent upon TC speed and TC size. Times (wind durations) are the same in both quadrants perpendicular to motion. Waves spend the most time in the quadrant moving in the same direction as the waves generated by the wind and that time is dependent upon how fast wave energy moves compared to how fast the TC moves. **Because wave energy speed is directly proportional to the wave's period, it is possible to generate waves with wave periods that move waves at exactly the same speed as the TC, thus keeping waves beneath the wind generation area for long periods of time (for a straight moving TC) resulting in astoundingly high wave growth.**

For TCs of typical size and of hurricane intensity wave periods that allow them to stay with the TC correspond to a TC forward motion of "about" 18-22 mph (29-35 km/h). **For small and/or weak TCs generating shorter period, slower moving waves, the optimal speed is slower. For large and strong TCs this optimal wave growth speed is faster.** Note that the optimal speed can and does change because early on waves are just beginning to form while later they become much larger. Hence, ideally maximum wave growth will occur from a TC that steadily increases in forward speed along a straight (great circle) track up to about 18-22 mph (29-35 km/h). The "trapped fetch" scenario is discussed in more detail in section 5.10.1.

If a TC moves very fast (typical for those transitioning to non-TCs in the mid-latitudes), it leaves behind most of the waves it generates, not allowing them to continue to grow. If a TC moves too slowly, generated waves move away from the TC and are no longer able to grow (the most typical scenario).

The track of the TC is very important for wind duration and hence wave generation. For a TC moving along a track that has large turns in it (e.g., Fig. 5.6), wind duration can be determined in pieces for each segment with persistent motion (e.g. the 5 segments shown below along a highly varying TC track). For a straight mover, one only has to calculate wave speed versus TC speed, determine wind fetch length and calculate the time wind remains over the waves it is generating.

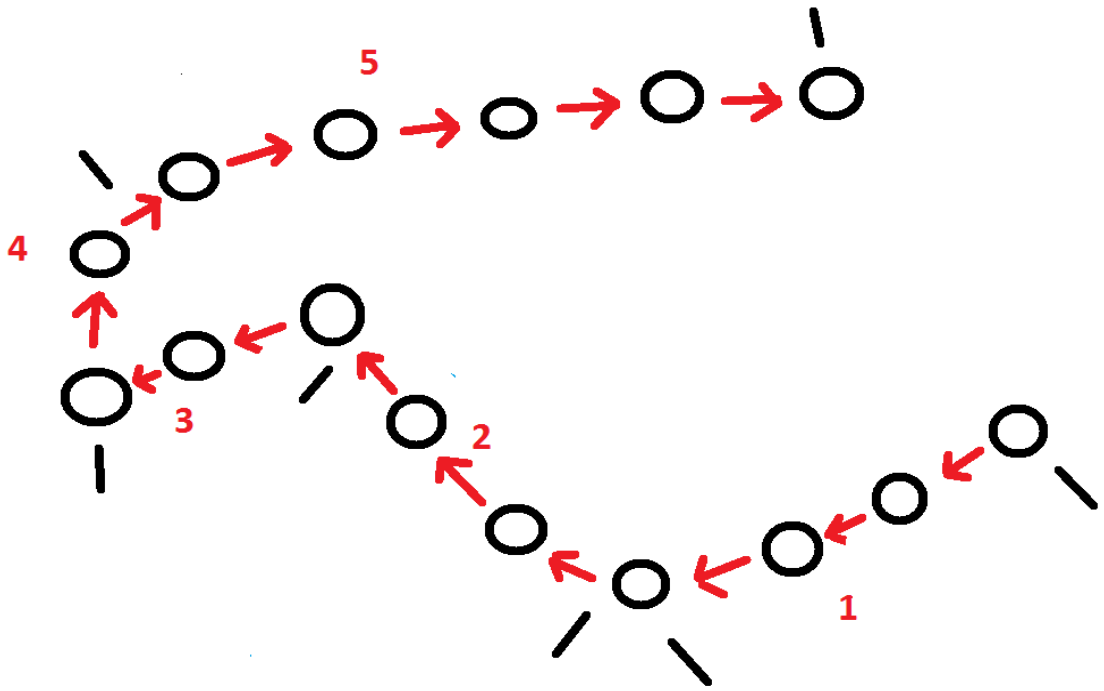

Figure 5.6. Irregular tropical cyclone track that must be split into segments (1 to 5) in order to calculate the wind duration and the resulting wave generation.

In summary, the PRIMARY reason for waves being so much larger in the right-front (left-front) quadrant of a TC in the Northern (Southern) Hemisphere is due to the duration winds have to generate waves in that sector!

5.6 Tropical cyclone swells

So far we have talked about waves generated within a TC wind area. These wind waves, do not just stop when they exit or leave the wind generation area, instead they continue to move/propagate as "swell" (waves that have left the wind generation area) away from the TC in all directions, and they will usually propagate until they reach land! The wind waves have been generated and with asymmetric heights dependent on wind speed, wind fetch length and wind duration asymmetries around the TC. **Four things happen to these swells, namely:**

1. **They move along great circle tracks with some spreading laterally along those tracks;**
2. **They undergo wave dispersion, that is they attempt to separate into swells of like wave period, the longer period swells racing away faster than the shorter period swells because swell speed increases as swell period increases (Speed in meters is approximately equal to 1.56 times wave period squared). The farther from the TC the swells go, the more ordered into like wave periods they become;**

3. **They decrease in height (they decay) due to swell dispersion and due to angular spreading of the swell away from the TC;**
4. **Because of swell dispersion, the dominate wave period associated with significant wave heights "increases" the farther away from the TC the swells move.**

By using great circles, one can determine direction changes and final destinations of swells of like initial propagation direction. An example of some great circle tracks ending in the Hawaiian Islands is shown in Figure 5.7 (courtesy National Weather Service Pacific Region Headquarters). They represent the shortest distances between two points on a sphere (in the case of Earth an oblate spheroid) and the track along which swells must move in order to reach Hawaii. Wind directions and speeds are overlaid on these great circles in order to determine whether wind fetch areas are pointed in a direction that will allow swells generated by distance winds to move to the Hawaiian Islands (the red polygon identifies those winds in this example.

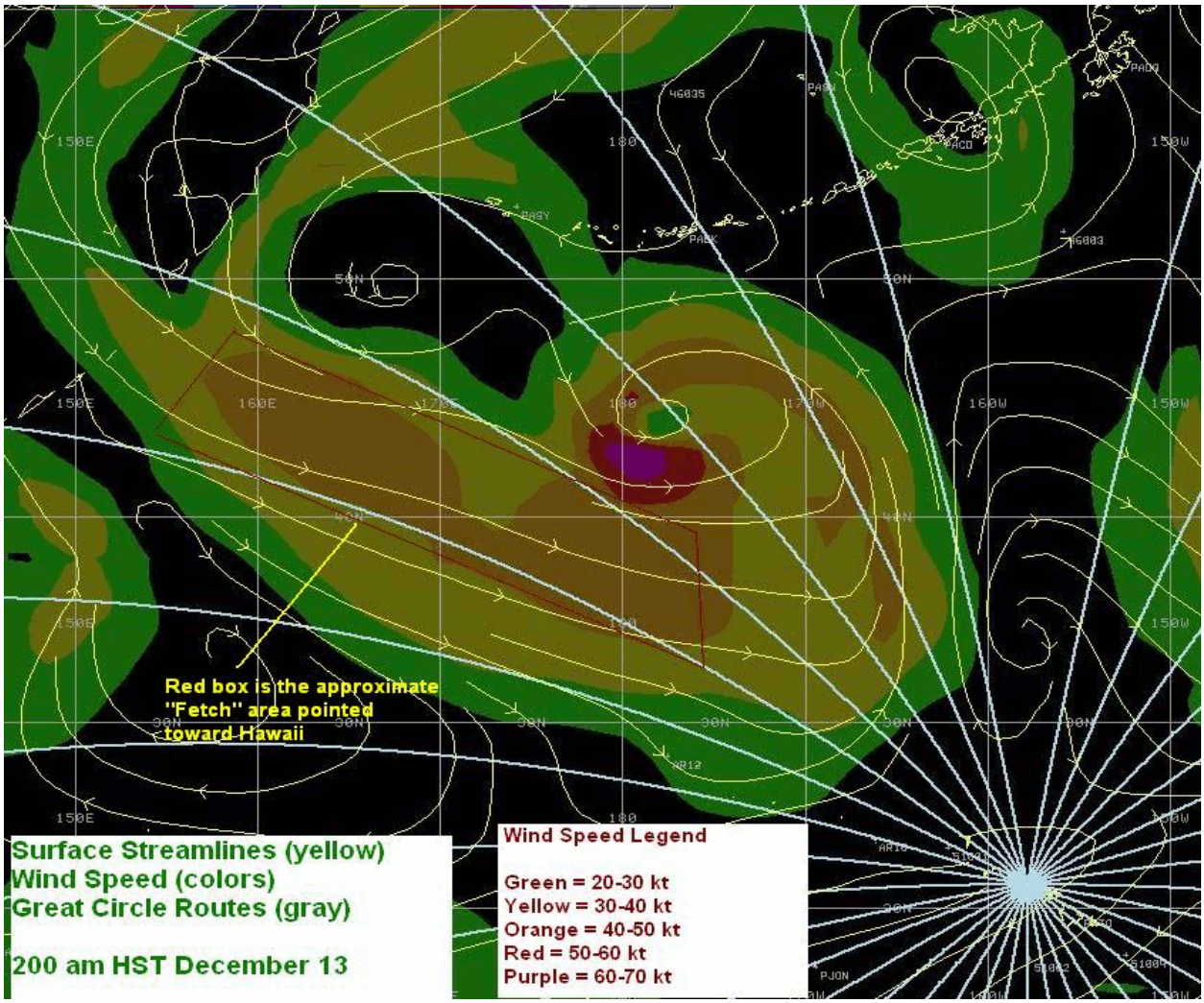

Figure 5.7. Diagram illustrating the great circle tracks that end in the Hawaiian Islands. The red box indicates the fetch area for the indicated low-level wind flow northwest of Hawaii.

The amount of wave dispersion and the rate and amount of swell decay along any great circle can be calculated by knowing the travel distance along the great circle to the destination of interest. One key element of swell decay is related to the width of the fetch that generates the initial wind waves. **The wider the initial wind generation area, the slower/less the swell decay rate will be to any point along the great circle.** It turns out that because wave dispersion occurs quickly, about 50% of wave decay occurs the first 100-200 nm (185-370 km) along the swell travel route. The next 50% of decay can take as many as 3000 nm (~5500 km) to occur (depending on fetch width and initial wave period) and is nearly all related to angular spreading of wave energy away from the great circle track of interest.

As swell steepness decreases, swell decay rates lessen; that is steep waves/swells decay faster than long period less steep, flatter swells. There are numerous equations available to calculate swell decay, the end result does not differ very much among the various methods assuming the correct initial wave significant wave height and wave period are known. A very simplified example (not suggested for operation use) of swell decay rates is shown in Table 5.1. These numbers represent the fraction of wave height remaining after a specific decay distance for shown fetch widths.

Table 5.1. Fraction of wave height remaining as a function of decay distance (nm) from wave generation area and fetch width (nm) of wave generation area.

Decay Distance (nm)	**Fetch Width (nm)**				
	50	100	200	500	1000
	Fraction of Wave Height Remaining				
100	0.45	0.55	0.65	0.74	0.83
200	0.35	0.45	0.52	0.62	0.71
500	0.24	0.33	0.42	0.50	0.58
1000	0.15	0.22	0.32	0.40	0.46
3000	0.09	0.14	0.20	0.25	0.32
5000	0.04	0.08	0.13	0.18	0.23

For example, a wave of 10 feet (3.0 m) generated in a wind fetch with a width of 200 nm (370 km) would be about 5.2 ft (1.6 m) high after 200 nm (370 km) of travel and about 2 ft (0.6 m) after 3000 nm (5500 km) of travel. These fractions multiplied by initial wave/swell height would give the swell decay height at the stated decay distance. Note that wave/swell HEIGHT does not have anything directly to do with decay rate!

There is typically more error involved in determining the final significant wave height at the start of swell motion than there is in the decay methodology, unless there are obstacles (islands) in the way. Numerical wave models obviously have decay physics in them. In numerical wave models that do not have high angle resolution, it is possible to lose wave energy in the decay process and/or dump energy from one direction bin into a nearest model direction bin that does not match reality. The result is erroneous swell heights at the end of decay and erroneous swell final destinations due to direction-bin jumping! In the case of more simple man interacting models, this problem does not exist assuming you have the correct initial wave direction and hence great circle track!

5.7 Radius of 12 foot seas vs coastal wave heights

The oceanic forecast of 12 foot (4-m) seas has been a number used by some TC prediction centers as a critical number, likely because below these heights most vessels in the high seas will survive, but above this, some can begin to have problems and have to slow their forward progress potentially delaying arrival to a final destination. Hence the radius of 12 foot (4m) seas may be seen attached to TC advisories. The 12 foot (4m) seas should NEVER be assumed to be collocated with the radius of 34 knot (64 km/h) winds (or any other wind radii) as heights are solely determined by the height of wind waves generate by winds in the TC and the decay of those waves as swell to a height of 12 feet (4m). Neither has anything directly to do with the radius of 34 knot (64 km/h) winds! 12 foot (4m) seas in the form of swell can routinely occur hundreds of miles away from a TC, even one that has generated waves along that great circle track and subsequently turned away from it and is dissipating! **Hence one has to keep track of all waves/swells moving toward a point of interest throughout the life of a tropical cyclone and beyond that. Heights must be calculated by initial wave height forecasts measured within the TC and wave/swell decay methods.**

5.8 Coastal surf

When it comes to coastal surf caused by a TC, whether making landfall or from surf generated by a TC hundreds or thousands of miles away and never striking land, many additional shallow water effects become important and can cause very large breaking wave/swell heights even when the deep water wave/swell heights are very modest. **"Wave shoaling" and "wave refraction" are the two key shallow water effects of interest. Both of these effects are highly dependent upon wave/swell period, not dependent on wave/swell height.** Long period waves/swells (typically found in TCs) result in much greater wave shoaling and wave refraction than do common low wind day to day short period wind waves. **The effect of both shoaling and refraction is to increase breaking surf heights at the coastline.**

Wave shoaling is an increase in wave height due to slowing of wave/swell in shallow water while wave/swell period is conserved. The effect is to increase wave/swell height as it moves into shallow water and finally breaks because wave energy is concentrated into smaller areas. Shoaling can enhance breaker heights between about 10% and 100% (a doubling in

height). **The amount of shoaling can be determined if one knows the wave period and near coastal bathymetry.**

Wave refraction is the bending of wave/swell energy by asymmetries in shallow water/coastal bathymetry. Waves/swells will ALWAYS bend toward shallow water due to a slowing of wave/swell speeds as they move into shallower and shallower water. Refraction can enhance breaker heights between about 10% and 100% (a doubling in height). **It too can be calculated if one knows wave period and the 2-dimensional distribution of near coast bathymetry.**

The result of these shallow water effects can be in cases of longer period TC swells nearly a quadrupling of breaking surf heights compared to wave/swell heights measured by a deep water buoy not far from shore! **It is for this reason that nearly always breaking waves from TCs along a coastline will be higher than deep water waves associated with the same tropical cyclone.**The result of this is that even a swell of 4 ft (1.2 m) in deep water can result in breaker heights along an exposed beach that may approach 16 ft (4.9 m)!

In this simple example above the coastline is exposed to surf higher than 12 feet (4 m) (e.g., 16 ft/4.9 m) and deep water waves of 12 ft (4 m) if collocated with TC 34-kt (64 km/h) winds hundreds of miles offshore would be a terrible indicator of what actually happens at the coastline! Obvious the 12-ft (4-m) seas in deep water and the radius of them collocated with a 34-kt (64 km/h) wind around a TC far at sea is a worthless assessment of beach impacts from that same TC hundreds of miles away. **No meteorologist or oceanographer should use deep water wave/swell heights as a proxy to breaking wave heights, or their impacts in the form of beach erosion and rip current threats they can cause. They must apply the correct relationships between deep water and shallow water waves.**

5.9 Tropical cyclone wave/swell setup & run-up

For many TC forecasters who leave coastal water rise to a wind driven surge model, surge is NOT the whole story! **It turns out where surge can be extreme, breaking waves are typically not a big problem, but where surge potential is not as high, waves/swells are a big threat. This is primarily because surge is large in shallow coastal waters while surf potential is high near deep coastal water.** No matter the coastal water depths, if you do not include coastal water rise from the action of breaking waves you will not only forecast water rise that is too low, but you will also potentially incorrectly forecast the time of water rise onset, its peak and its demise. A classic example of a coastline with a high wave threat and a modest surge threat is along the western Florida panhandle. In 1995 Hurricane Opal struck that coastline. Surge models including the National Weather Service SLOSH model indicated surge values that would be in the 8 foot range. However, very large waves had been generated in the right-front quadrant of that northward moving large hurricane; some waves offshore approached 45 ft (13.7 m)! The diagram below (from the National Hurricane Center) shows high water marks associated with Hurricane Opal along that Florida coast near landfall. The surge forecast of 8 ft (2.4 m) was a good one, but water rose in some locations to as high as 25 ft (7.6

m), taking out coastal homes and toppling some high rise buildings on the coastline into the sand and surf!

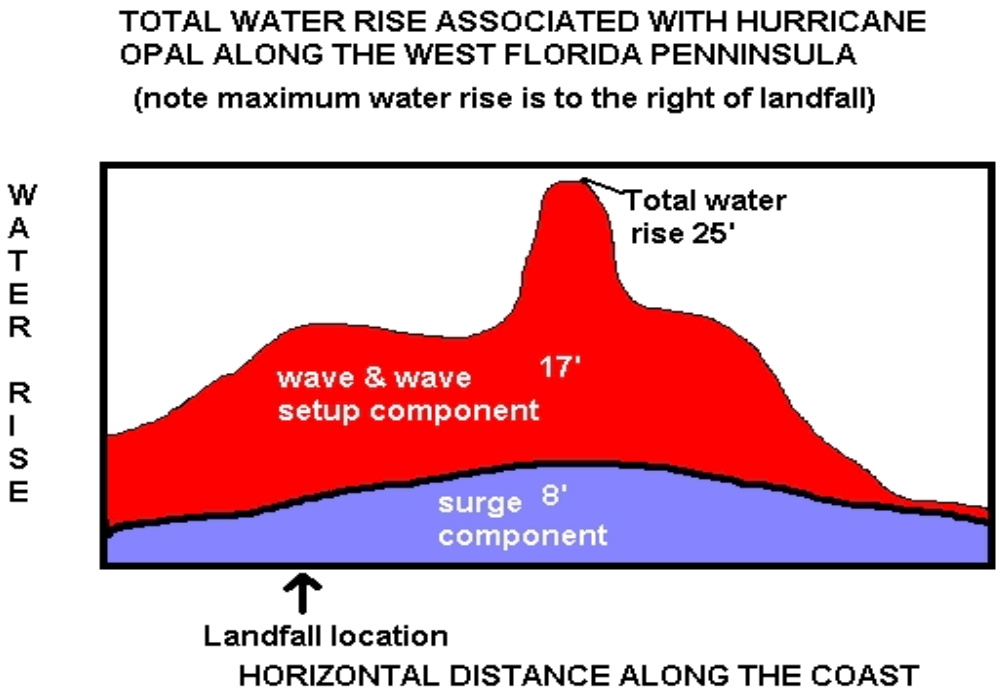

Figure 5.8. Diagram illustrating the distribution of total coastal water level rise associated with Hurricane Opal along the west Florida Peninsula as a function of horizontal distance along the coast. The purple area shows the surge component and the red area shows the wave and wave setup component.

This clearly shows the importance of water rise associated with wave action alone and how omitting it will contribute to, at times, a huge underestimate of coastal water rise. So what is wave setup? It is the water rise associated with breaking wave energy on a coastline. A very simple approximation can be estimated by 12% of the coastal breaking surf depth.

A slightly more sophisticated estimate of wave setup is given by:

$S = (\text{sqrt}(g) * H_s^2 * P) / (64 * \pi * BD^{3/2})$

Namely, the square root of gravity (g) times significant wave height (H_s) squared times wave period (P) divided by 64 times π (3.14159) times breaker depth (BD) to the 3/2 power. **Large waves with long periods breaking in shallow water provide the greatest wave setup. Small waves with short periods breaking in deeper water provide the least wave setup.**

Wave run-up, the water rise up the beach face associated with individual waves racing landward and then retreating to sea also contributes to water rise in a semi-transient way with an interval consistent with the dominant wave period. It contributes to the water rise and is approximately given by:

$R = 1.38 * H_b * E^{0.77}$,

where H_b is breaker height, and E = beach slope/squareroot (breaker height/wave length). This expression for E doesn't make sense to me. Also, are breaker height and breaker depth (prev page) the same thing?

Maximum wave run-up for a large sample of waves is approximately 1.7 times R.

As you can see coastal breaking surf heights (not deep water wave heights) are critical to forecast in order to determine wave setup, wave run-up and hence water rise associated with breaking wave action on any beach. Surge on the other hand is related only to the onshore component of wind and some elevation due to lower pressure (hydrostatic effect or inverse barometer effect). The coastal bathymetry waves/surf is excluded! Channeling by local bathymetry, and reflections from the coast also contribute to substantially amplify the surge height.

Some confusion exists between storm tides and storm surges. In this report a storm surge is the elevation of water generated by a tropical cyclone above or below the normal astronomical tide. A storm tide, on the other hand, is the total elevation (including the astronomical tide) above or below a standard datum. The storm tides are predicted water heights issued in TC advisories. The generic term "surges" is often used interchangeably according to context. It is important to identify the expected inundation, where salt water will penetrate into what is normally dry land. Storm surge and surf can be computed with modeling efforts, but the storm tide is difficult because of phasing uncertainties with the astronomical tides. **Because there are frequently two high tides during a 24-hour period, the rule of thumb to convey to emergency managers is to always plan for high tide.**

Because very often large long period swells outrun a TC to the coastline by hours or even days, water rise from breaking wave action can and often does begin well before any TC winds near the coastline and surge begins. Obviously surf-induced water rise can occur even when a TC never makes it to land!**This means that water rise can be large and significant well before TC arrival at a coastline. These rising waters can and have prevented timely coastal evacuations ahead of high winds and surge as exit routes have become impassible before winds even begin to increase.** The result can lead to coastal residents trapped by water rise well before the TC wind threat and surge begin! With proper calculation of coastal breaking surf, wave setup and wave run-up, the meteorologist should never be caught with a water rise forecast that waits for the wind, nor will he/she underestimate the total water rise by only including "surge."

On coral atolls and islands surrounded by a fringing reef, the reef flat can act to help dampen out the breaking waves. Thus, given two locations with similar bathymetry, the wider the reef, the more the waves will be dampened (by turbulence), and the smaller the waves and run-up will be. Conversely, the narrower the reef, the less effect the reef will have on dampening the waves and run-up. For very strong storms, where the water level is 30 ft (10 m) or more across the reef, the reef has little effect on dampening the waves. But, usually, where the reefs are wide, the damages will be less than where the reefs are narrow.

5.10 Some specific forecast problems

5.10.1. Trapped fetch (contributed by Mr. Jeff Callaghan)

Cyclone Heta was a powerful Category 5 cyclone that caused catastrophic damage to Tonga, Niue (Figure 5.9), and American Samoa in late December 2003 and early January 2004. Heta formed on December 25, 2003, and reached its maximum intensity of 160 mph (260 km/h) and estimated minimum sea level pressure of 915 hPa. As Heta developed, it became a large system, which is ideal for developing large waves.

(a)


0 3 6 km
0 3 6 mi
reef
Mutalau
Hikutavake
Lakepa
reef
Liku
ALOFI
Avatele
South Pacific Ocean
reef

(b)

Figure 5.9. (a) Map of Niue and (b) the main centre on Niue, Alofi, which is located on top of 20m elevated Coral Cliffs.

Heta then accelerated southwards, passing to the west of Niue with an extensive fetch of 60-kt (111-km/h) sustained winds (Figure 5.10). The speed of Heta could be accurately calculated due to it having a clear eye.

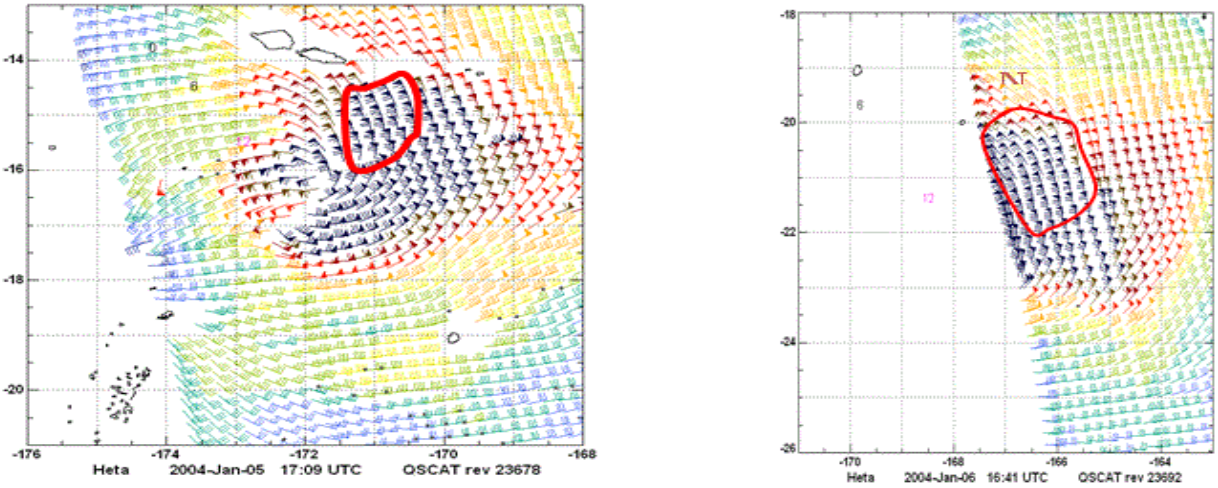

Figure 5.10. Scatterometer observations with areas highlighted where wind has a component of 330/60 knots, e.g., wind of 010/80 knots equivalent to 330/60 knots.

The development and movement of a wave train through the 60-kt (111-km/h) fetch of *Heta* is shown in Figure 5.11. The last analyses at 0425UTC 6 January 2004 was just before seawater surged into Alofi. Niue was under the eastern eye wall from the IR image at 0514UTC 6 January 2004.

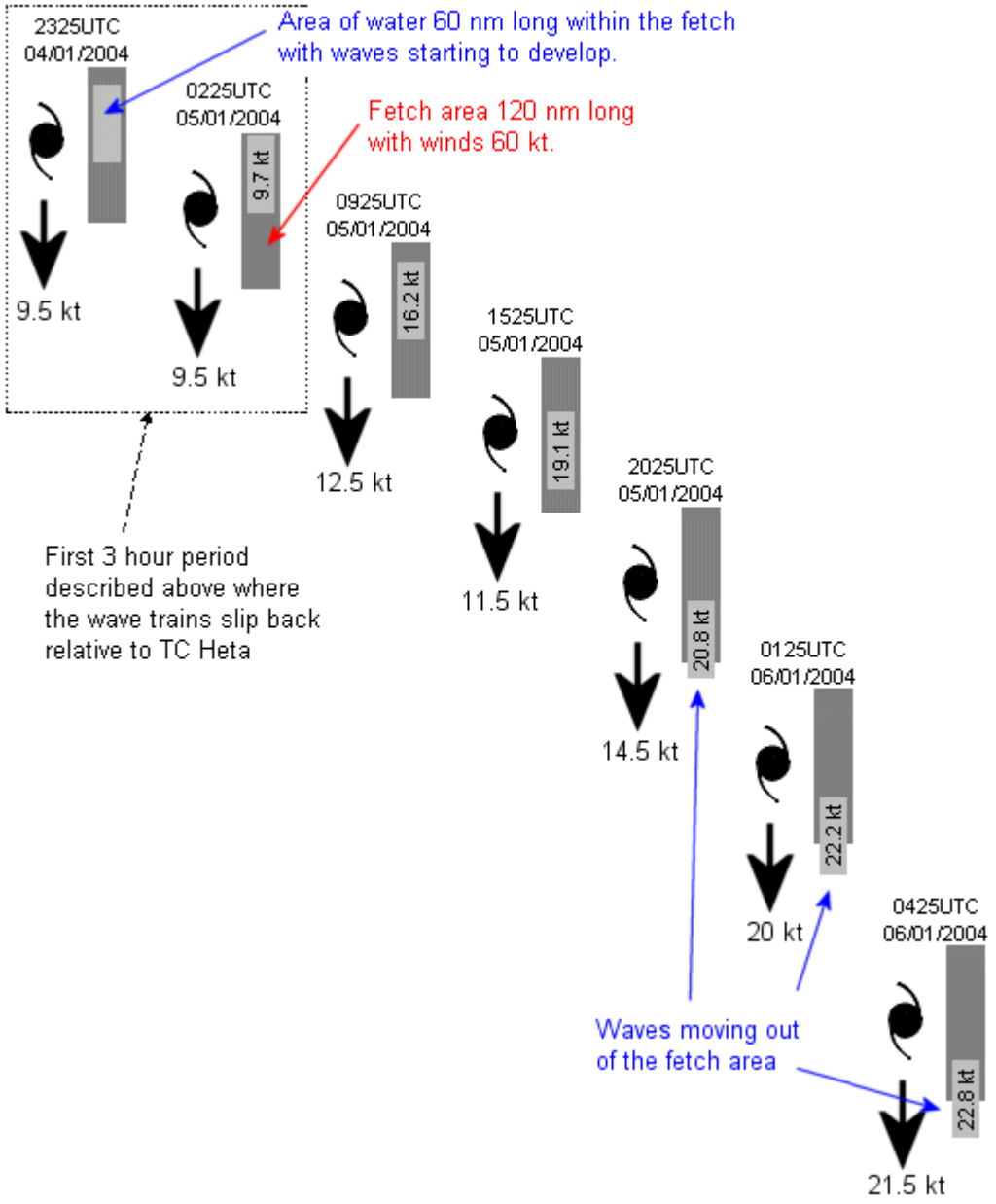

Figure 5.11. Development of wave train moving through the 60-kt (111-km/h) fetch of *Heta*.

The wave speeds in Figure 5.12 were calculated from the WMO manual on wave forecasting (WMO No.702) nomogram. From the nomogram, after 29 hours in the 60-kt (111 km/h) fetch zone, the significant wave height is just over 52 ft (16 m) and the period is 15.2 seconds.

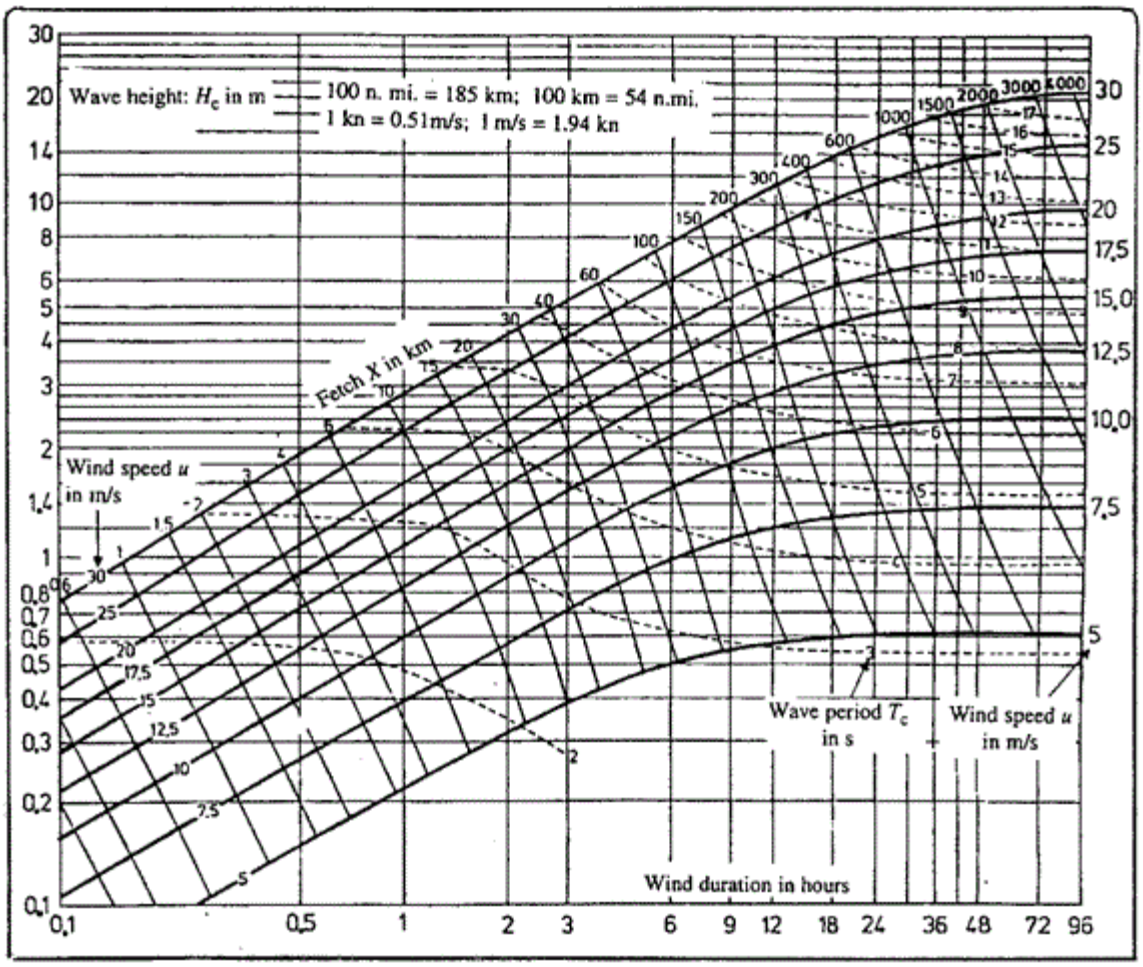

Figure 5.12. Calculation of wave train speed from a WMO manual forecasting nomogram.

Figure 5.13 shows the forerunner waves reaching Alofi at 2239UTC 5 January 2004 and the severe wave damage caused by the waves around 0500UTC 6 January.

Figure 5.13. (top) Forerunner waves at Alofi at 2239 UTC 5 January 2004; (bottom) damage at Alofi after the passage of the storm.

To illustrate that these events can be forecast, below is a note from the Brisbane Tropical Cyclone Warning Centre attached to a SATELLITE ANALYSIS BULLETIN at 2317 UTC 5 January 2004.

Heta appears to have moved around 170 nmi (315 km) over the past 12 hours or around 14 kts (26 km/h). This is fast enough for significant fetch enhancement to be occurring leading to exceptionally large waves moving with the storm."

The following calculations show how the waves grow with minimal decay in a trapped fetch scenario.

For a wind speed of 60 kts (111 km/h) after 1h period (T) = 4.5 sec as long as fetch is at least 6 nmi (11 km).

The group velocity (C_g) associated with this period = 1.5 period (in knots) = 6.8 knots. Therefore average velocity over hour = (0+6.8)/2 = 3.4 knots.

After 2h T = 5.6 s, C_g = 8.4 knots and average speed = (6.8+8.4)/2 = 7.6 knots

Similarly, average speed over third hour = 9 knots and at the end of the third hour C_g = 9.7 knots and waves are now moving slightly faster than *Heta*. However over the 3 hours, waves travelled 20 nm and *Heta* travelled 3 times 9.5 knots = 28.5 nm.

5.10.2 Storm surge probabilities

Tropical cyclone storm surge probabilities (2 - 25 feet) produced by the US National Hurricane Center can be found at http://www.nhc.noaa.gov/aboutpsurge.shtml.

5.10.3 Summary

Things to remember when forecasting tropical cyclone waves:

1) Accurately determine the "time integrated" wind, fetch and duration, don't sweat the details.

2) Time integrated wind speeds are most important to get correct.

3) Larger tropical storm wind areas can often be more important for wave growth than tiny areas of very strong hurricane winds.

4) Concentrate on wind duration for the TC quadrant of most interest to you.

5) Wind duration within a quadrant is more important to access accurately than is fetch length.

6) The PRIMARY reason for waves being so much larger in the right-front (left front) quadrant of a TC in the Northern Hemisphere (Southern Hemisphere) is due to the duration winds have to generate waves in that quadrant.

7) Fetches and fetch lengths should be done in pieces for highly varying tracks; make sure that a fetch lies along a great circle to the destination of interest.

8) NEVER use any specific wind radii as a proxy to forecasting wave heights.

9) Coastal surf can be much larger than deep water waves/swells at buoys, NEVER use buoy heights as a proxy to breaking wave heights without applying coastal wave modification processes that include shoaling and refraction.

10) Do not forget waves/swells have a spectral character both wave height and wave period. Significant wave height is routinely used as a single height identifier but the majority of waves have lower heights, while some waves can be double the significant wave height.

11) Remember that you must include wave setup and wave run-up when forecasting coastal water rise; surge alone will be an underestimate in most cases and a huge underestimate in many cases!

Chapter Six

Mr. Edwin Lai
Hong Kong Observatory

6. Tropical Cyclone Rainfall and Flood Forecasting

6.1 Introduction and basic hydrology

Tropical cyclones (TCs) are one of Mother Nature's most destructive forces. Coastal and island communities in the tropical and sub-tropical areas around the world are particularly vulnerable to their furies. Dangerous winds and storm surges can create significant damage to property and loss of lives. After landfall, TCs will begin to weaken due to lack of moisture and land interaction. Therefore, winds usually are not the primarily concern for inland communities farther away from the coast. Instead, torrential rains will be the major problem for inland areas along the path of the cyclone. Factors such as orographic lifting and interaction with cold fronts and other sub-tropical weather systems can further enhance the chance for locally heavy rainfall.

Forecasting flooding during the passage of a TC involves both meteorology and hydrology. The use of local radar, satellite imagery and mesoscale computer models can aid on predicting where the heavy rainfall will occur, and which areas will have the higher potential for flooding. Understanding the hydrological conditions of these areas beforehand can provide clues on the type, severity and duration of flooding.

Once rain has fallen on land, much of it will infiltrate into the soil and eventually become groundwater, being stored in aquifers. The rest of it will move across land as runoff to streams and rivers, which flow into larger bodies of surface water such as ponds, lakes and oceans at discharge points. Runoff includes water that flows on land surfaces known as surface runoff and also beneath the soil surface, called interflow. Since runoff is the main contributor of excessive water near the ground surface as well as into streams and rivers during a rain event, it is the most important component of flood forecasting.

6.1.1 Surface runoff

The amount of rain turning into surface runoff is determined by the characteristics of the surface or soil. Larger soil particles such as gravel and sand contain large pores which allow a higher infiltration rate. On the other hand, smaller soil particles such as silt and clay contain small pores which create a lower infiltration rate. However, smaller soil particles contain more pores in a given volume compared to larger soil particles. Therefore, the total void space in a

given volume is higher in silt and clay than sand and gravel. This gives silt and clay a higher infiltration capacity, the ability to hold a larger volume of water.

During a short but heavy downpour, surface runoff will likely occur on top of soil with a high content of silt and clay. For a long period of moderate rain, surface runoff will start to accumulate on top of gravelly and sandy soil first. Human activity, including urbanization, deforestation and forest fires, can have an important effect on surface runoff as well. Concrete and asphalt surfaces commonly found in urban areas can create rapid surface runoff due to both low infiltration rate and low capacity. Deforestation and forest fires both drastically change the soil properties of affected areas, making them more subject to surface runoff than the surrounding unaffected areas.

6.1.2 Interflow

After being absorbed into the soil just beneath the surface, water tends to travel toward a lower elevation due to gravity. As a result, interflow will move from higher areas or ridges toward lower areas or valleys in a basin. Streams or tributaries can form along these local valleys as interflow from the surrounding high ground merges and continues to flow toward the bottom of the basin. Once it has reached the bottom of the basin, the accumulated water will become a river and keep surging into the lowest point of the basin, which is known as a discharge point.

Interflow tends to travel faster in soil with larger pores such as sand and gravel, while the opposite occurs in silt and clay with smaller pores. Pre-existing voids and tunnels created by both biological and human activity underneath the ground surface can greatly enhance interflow; this process is called transmissivity feedback. In areas where a shallow layer of soil is on top of bedrock, concrete or another layer of low-permeable soil such as compact clay, saturation will happen more quickly and horizontal water movement will also increase.

6.1.3 Basin properties

Basins have different sizes, shapes and characteristics, which contribute to various volumes and rates of runoff. For basins with identical size but different shapes, water will need to travel a longer distance from the highest to the lowest point in a long and narrow basin. Also, water entering the basin closer to the discharge point will arrive there sooner. This creates a more gradual increase in flow volume and a lower peak flow, as compared to round and wider basins. For basins that are similar in shape but different in size, the distance between the highest point and lowest point is much shorter for a small basin. On top of this, a rain storm will likely cover an entire small basin but only a portion of a large basin. As a result, flow volume will rise more rapidly and yield a higher peak flow in the smaller basin.

Gravity will cause water to move much faster in a steep basin than a flat one, resulting in a faster flow volume and higher peak flow as well. Basins with streams and tributaries that are either denser or less meandering or both will also produce a higher peak flow. Surface

conditions of a stream or river can affect its runoff to the discharge point. A smooth stream or river bed will allow a more efficient runoff, while a rough bottom will hinder the movement of water and decrease its flow rate and volume.

6.1.4 Pre-event water

Except under extreme drought, a certain amount of water is always present in the soil above the aquifers. The amount depends on the frequency of rainfall and type of soil. Pre-event water is defined as water already existing in the soil and later being displaced into streams and rivers by interflow from newly fallen rain. After frequent rainstorms, most soil will become saturated or nearly saturated regardless of soil type. However, as mentioned earlier, soil with high silt and clay content can hold a higher volume of water. Therefore, streams and rivers with such soil properties will receive a higher amount of interflow during a rain event and rise faster and higher. When rain occurs infrequently, soil moisture content will be lower in gravelly and sandy soil with a higher infiltration rate, as most pre-existed water has infiltrated deeper into the aquifers below over time. This causes part of the new rainfall to be absorbed into the soil until saturation is reached. Only after this point will interflow begin to travel into the streams and rivers so that the rise is slower and not as high.

6.2 Types of flooding

The combination of the speed, intensity, and size of a tropical cyclone, along with soil properties, pre-existing moisture and local topography, will determine what kind of flooding will occur first and sequentially.

6.2.1 Flash flooding

Flash floods are rapidly occurring events. This type of flood can begin within a few minutes or hours of excessive rainfall. The rapidly rising water can reach heights of 30 feet or more and can roll boulders, rip trees from the ground, and destroy buildings, bridges and roads.

A fast moving intense cyclone with strong convection is likely to produce locally heavy downpours in its path. If a high amount of pre-event water is present in the soil, it will quickly be transferred into streams and rivers. Due to soil saturation, surface runoff will also form rapidly and add to the flow. Water levels in streams, rivers and storm drainage systems can rise very quickly to significant heights and overflow the banks, leading to flash floods. Since the amount of rainfall is limited by the fast speed of the cyclone, the flash flood will only last from several hours to a perhaps a day.

The worst case scenario is a large, slow-moving intense cyclone, bringing long lasting and widespread heavy rain. With saturated ground, flash floods will occur as described above but will then be followed by widespread inland flooding. Eventually, flash flooding streams and

rivers will transform into long-term river flooding in large areas, but on relatively small islands, flood waters will reach the ocean in a matter of hours.

6.2.2 Area and inland flooding

Area and inland floods are also rapid events although not quite as rapid or locally severe as a flash flood. Still, streets can become swift-moving rivers and basements can become death traps as they fill with water. A primary cause is the conversion of fields or woodlands to roads and parking lots.

After short-term heavy rain events created by fast moving storms, area and inland floods are usually found in areas with low infiltration rates such as urban communities with concrete and asphalt, and rural communities with compact silt and clay. Nearly 100 percent of the rainfall will convert into surface runoff instantly and travel toward streams, rivers, storm drains and other low-lying areas. Minor to moderate flooding can then take place in low-lying areas as surface runoff collects. Once downpours have stopped, excessive surface runoff will diminish rapidly. However, it can still take several days to a few weeks for flooded low-lying areas to dry out.

For long periods of moderate to occasionally heavy rain caused by slow and weakening cyclones, area and inland floods will probably be found in low-lying areas with low infiltration materials and/or poor drainage. Surface runoff is expected to gradually accumulate in these areas and cause water levels to rise steadily. Once areas have become flooded, it might take several days for the water to drain out after the last measurable rain.

6.2.3 River flooding

River floods are longer term events and occur when the runoff from torrential rains, brought on by decaying tropical cyclones, reaches the rivers. A lot of the excessive water in river floods may begin as flash floods. River floods can occur in just a few hours and also last a week or longer. After pre-event water in the soil has been displaced into streams and rivers by newly-fallen rain, this infiltrated rain water will follow on its way to the same streams and rivers. For a small basin, it can take as little as a few hours to a day for this water to reach its destination. However, due to limited amounts of rain from the fast moving storm, and the lower quantity of rain water collected by the small basin, water levels tend to drop after a few days. For a large basin, water levels can remain at flood stage from several days to a week.

Instead of bursts of torrential rain, decaying storms with a slow pace will likely produce continuous moderate rain for several days. The potential for flash flooding is low but water levels in streams and rivers will steadily rise above flood levels and remain so for a few weeks. On the other hand, if the intensity of a storm is much stronger, rain may be heavy for several days. Under these circumstances, flash flooding will become long term flooding and can last for weeks.

The sizes of storms can also affect the severity of river flooding, mainly in large basins. A small storm over a large basin will create moderate flooding since only parts of the basin will be receiving rainfall. With a large storm, it is likely that most or the whole basin will be subject to rainfall, leading to more serious flooding. Regardless of storm sizes, small basins will likely receive near 100 percent rain coverage.

Small mountainous islands have both small basins and rivers/streams with relatively short distances to the discharge points, namely the ocean. On these islands, the main threat is the flash flood, which can occur rapidly as a TC approaches and end rapidly as it moves away. Very high rain rates can occur in the eyewall cloud of a TC. On Guam (an island of 212 sq mi/3139 sq km with an elevation of 1313 ft/400 m), during Typhoon Pongsona (December 2002), rain rates as high as 7.22 in/hr (183 mm/hr) were measured.

6.2.4 Mudslides and debris flows

Mudslides or debris flows kill thousands of people each year. Those initiated by tropical cyclones account for about 25 percent of all fatalities. Mudslides/debris flows occur in hilly or mountainous areas of saturated, low permeability soils such as clays, where relatively heavy rains continue after saturation is attained. The greatest chance of mudslides occurs where the slope of the face of a hill or mountain made of clay or similar material has an angle from the vertical of 10° to 40°. Here, gravity is most likely to overcome the chemical bonding of the water molecules that surround the clay molecules. The most likely areas for mudslides are: (1) clay areas where vegetation has been removed; clay areas where mudslides occurred before but bedrock is not yet exposed; steep clay areas at least 20 ft (6 m) high. The Weather Service Office on Guam has determined the critical elements needed for mudslides to occur on the high islands of Micronesia in the Northwest Pacific (see Table 6.1). The forecast requirements are also shown that enable the islands time to warn and evacuate the threatened populations (Table 6.1). Figure 6.1 shows (a) a model of the saturated clay molecule and (b) a diagram of the terrain slopes most vulnerable to mudslides.

Table 6.1. Critical parameters for mudslide occurrence in the mountain islands of Micronesia. Parameters for issuing warnings for mudslides in Micronesia. All islands have long-chain clay molecules except for Palau, which has short-chained clay molecules. Rainfall is in inches and millimeters.

	Long-Chain Clay Molecules (All High Islands but Palau)	**Short-Chain Clay Molecules (Palau only)**
Angle from Vertical	10°-40°	10°-40°
Rain Required for Slides	24-hr Rain 10 inches (254 mm)	24-hr Rain 7 inches (178 mm)

Rain Required for Slides	36-hr Rain 15 inches (381 mm)	36-hr Rain 10 inches (254 mm)
Rain Required for Warnings	24-hr Rain 7 inches (178 mm)	24-hr Rain 5 inches (127 mm)
Rain Required for Warnings	36-hr Rain 10 inches (254 mm)	36-hr Rain 7 inches (178 mm)

(a)

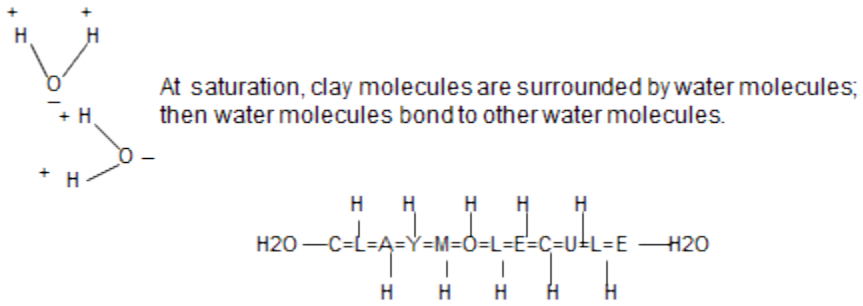

(b)

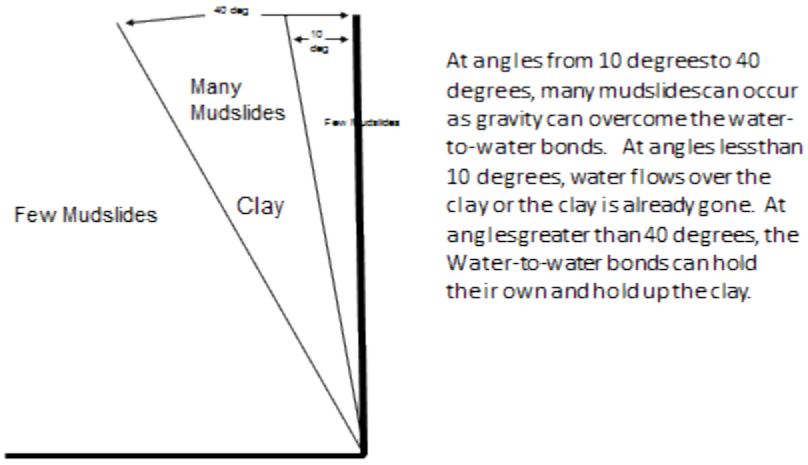

Figure 6.1 (a) Schematic of clay molecule surrounded by water molecules at saturation and chemical bonding of water molecules; and (b) relationship between mudslide occurrence likelihood and vertical angle of the clay surface.

6.3 Satellite techniques

6.3.1 Technological advances

Nowadays, space-borne instruments, such as visible/infrared (IR) imagers in geostationary satellites, Advanced Very High Resolution Radiometer (AVHRR), passive microwave sounders, infrared sounders, and precipitation radars, have high resolutions that can provide remote sensing data for meteorological and hydrological monitoring. Products include cloud characteristics, humidity sounding and wind vectors. An example of a spaceborne passive microwave sensor is WindSAT. WindSAT is a conically-scanning duel-polarimetric (vertical and horizontal) radiometer specially designed for sensing near-surface winds over the ocean (Adams et al. 2008). Its multi-frequency design also allows retrieval of multi environmental parameters, such as precipitation, at the same time.

Many TC rainfall estimation techniques have been developed using either single or combined instruments. Table 6.2 summarizes the techniques reported in Levizzani et al. (2002).

Table 6.2. Tropical cyclone satellite rainfall estimation techniques.

Instrument	Technique	Details
Satellite (visible & thermal infrared)	Cloud Indexing Methods	Assign rain rate to each cloud type
Satellite (visible & thermal infrared)	Bispectral Methods, e.g., RAINSAT (Lovejoy and Austin 1979; Bellon et al. 1980)	Derive and use the relationship between cold and bright clouds and probability of precipitation
Satellite (visible & thermal infrared)	Life History Methods, e.g., Griffith-Woodley technique (Griffith et al. 1978), Negri-Adler Wetzel (NAW) scheme (Negri et al. 1984), NOAA-NESDIS (National Environmental Satellite Data and Information Service) technique, combined NAW with radar data (Porcù et al. 1999)	Analyze clouds' life cycle
Satellite (visible & thermal infrared)	Cloud model-based techniques, e.g., cumulus convection parameterization (Gruber 1973), cloud model (Wylie 1979), Convective	Use cloud physics in the retrieval process

	stratiform technique (CST) (Adler and Negri 1988; Anagnostou et al. 1999)	
Satellite (passive microwave imagers)	Enhance precipitation signal by minimizing the effects of surface emissivity on MW measurements (Grody 1984), determine the polarization corrected temperature (PCT) and criteria for rain/no-rain boundary (Kidd 1998)	Use the strength of precipitation signal and emissivity of hydrometeors
Satellite (passive microwave sounders)	An algorithm that based on scattering indices (Grody et al. 1999)	Derive atmospheric sounding
Precipitation radar (PR)	An algorithm to get Z-R/Z-A relationship (R = rain rate, A = radar attenuation, Z = reflectivity) (Iguchi et al. 2000)	Get the vertical distribution of rainfall
Satellite (infrared and microwave)	Statistical probability matching between precipitation levels from the Special Sensor Microwave/Imager (SSM/I)+TMI algorithms and brightness temperature (TB) from geostationary satellites (Turk et al. 1998, 2000). Microwave IR Rainfall Algorithm (MIRA) (Todd et al. 2001), Microwave/Infrared Rain Rate Algorithm (MIRRA) (Miller et al. 2000), Precipitation Estimation from Remotely Sensed Information using Artificial Neural Networks (PERSIANN) (Hsu et al. 1997; Sorooshian et al. 2000), Auto-Estimator technique (Vicente et al. 1998)	
Satellite (passive microwave) and PR	Multispectral data from GOES and Tropical Rainfall Measuring Mission (TRMM) PR data (Bellerby et al. 2000)	Estimate rain profile using PR reflectivity (Haddad et al. 1997)
Lightning detection	Combine cloud-to-ground lightning and satellite IR data.	Lightning positively correlates with ice scattering intensity in

		high frequency microwave radiometry.

Looking to the future, efforts to support the development of satellite remote sensing techniques are pursued under the following two projects:

1) Hurricane Imaging Radiometer (HIRAD) by NASA MSFC/NOAA HRD

It is a C-band passive microwave radiometer, an extension of the Stepped Frequency Microwave Radiometer (SFMR), deployed for tropical cyclone measurements. It will produce imagery of ocean surface wind parameters and rain rates under high winds and heavy rain conditions that often hamper the observational capabilities of higher frequency passive microwave radiometers or scatterometers (Hood et al. 2008, El-Nimri et al. 2008).

2) Geostationary Synthetic Thinned Aperture Radiometer under the "Precipitation and All-weather Temperature and Humidity" mission (GeoSTAR/PATH) by NASA JPL

A microwave sounder in a geostationary orbit under the mission PATH, GeoSTAR will provide measurements including hemispheric 3-D temperatures, humidity and cloud liquid water fields, rain rates and totals, tropospheric wind vectors, sea surface temperatures, and parameters associated with deep convection and atmospheric instability (Lambrigtsen et al. 2008).

6.3.2 Quantitative precipitation estimation (QPE)

Satellites provide means to monitor tropical cyclones and collect information for data assimilation and tropical cyclone rainfall climatology formulation. QPE can be obtained by processing satellite data and conventional surface observation together (Chen et al. 2006). Many QPE techniques using satellite data have been developed around the world. Techniques involve model forecasts, ensemble methods, empirical models, statistical schemes, or combined statistical-dynamical approaches. Some products are available online for references. Examples are Climate Prediction Center (CPC) morphing method (CMORPH) (Joyce et al. 2004), and inversion-based algorithm using TRMM TMI and PR data (Jiang et al. 2006). Table 6.2 also includes techniques used for QPE.

Four techniques*, namely CMORPH, PERSIANN, NOAA/NESDIS Hydro-Estimator and GPM, are highlighted below.

1) NOAA CPC MORPHing method (CMORPH)

CMORPH is a technique based on geostationary satellite cloud motion winds that advect microwave-derived precipitation retrieved at irregular hours forward and backward in time, in order to yield a spatial-temporal consistent precipitation analysis. Meanwhile, precipitation

features are "morphed" during the forward and backward propagation (Figure 6.2). CMORPH allows precipitation estimate inputs from any microwave satellite. Products from CPC have resolutions from 8 km to less than 30 km (1/4 degree). However, there is a latency problem for CMORPH. Products are only available about 18 hours from the observation time. A similar product called QMORPH has since been developed. QMORPH has no morphing and can be available within three hours from the observation time (http://www.cpc.noaa.gov/products/janowiak/cmorph_description.html). A study by Joyce et al. (2004) showed that in terms of spatial correlations and equitable threat scores for cases in Australia and the United States, outputs using CMORPH performed better than those using other techniques, such as IR-derived precipitation when there was no passive microwave data available, and MWCOMB (a daily average of all available microwave-derived precipitation estimates without morphing).

2) Precipitation Estimation from Remotely Sensed Information using Artificial Neural Networks (PERSIANN)

PERSIANN has been developed at the University of Arizona using an artifical neural networks (ANN) model with a resolution of 0.25 degree (Hsu et al. 1997). The model estimates rainfall rates based on infrared satellite imagery and using ground-based data to update the ANN parameters. Hsu et al. (1997) demonstrated that the model was able to provide insights into the nature of the physical processes and the diverse precipitation characteristics in response to such processes.

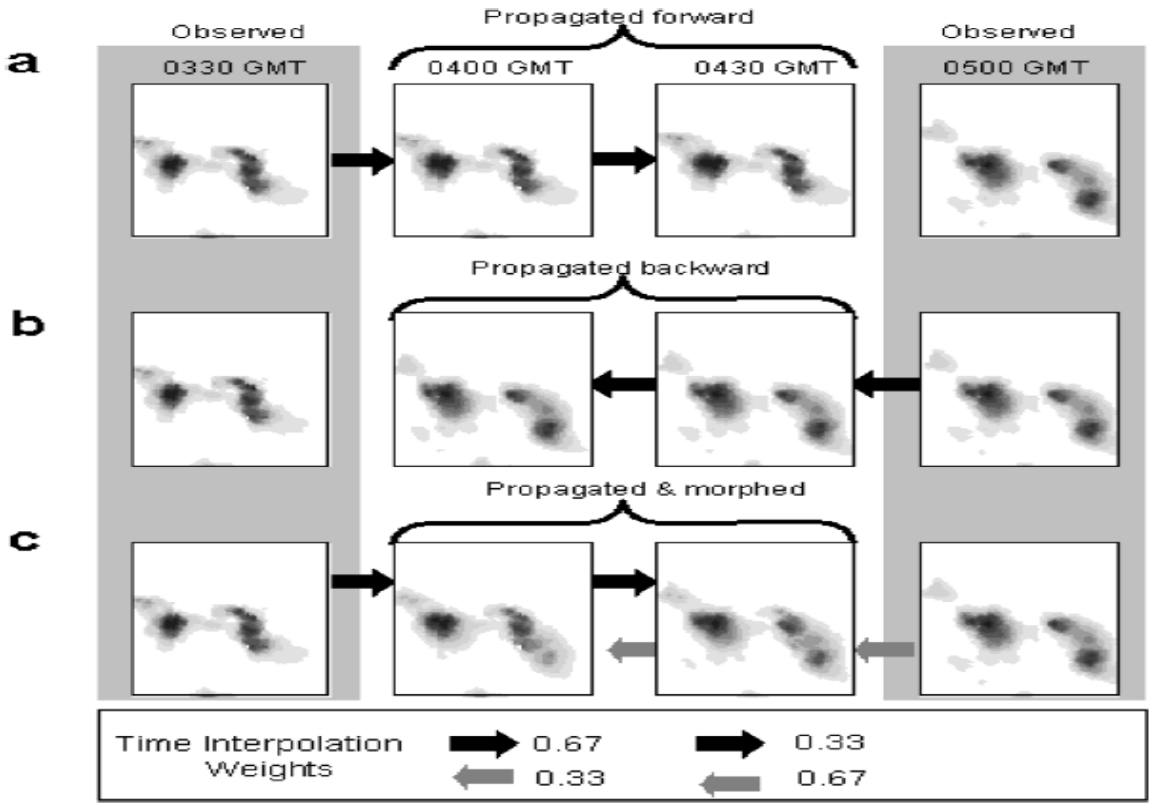

Figure 6.2 Schematic of the morphing process: analyses at 0330 and 0500 UTC are actual passive microwave rainfall estimates; (a) forward propagation from 0330 UTC with linearly decreasing weighting; (b) backward propagation from 0500 UTC with linearly decreasing weighting; (c) derived morphed rainfall fields for 0400 and 0430 UTC (extracted from Joyce et al. (2004)).

** Other notable satellite-based rainfall analyses include (i) TRMM Multi-satellite Precipitation Analysis (TMPA) by NASA; (ii) the blended satellite technique by NRL and (iii) GSMaP by JAXA. Pls. refer to Chan & Chan (2010) for the references.*

3) NOAA/NESDIS Hydro-Estimator

This algorithm outputs rainfall rate and rainfall estimate for the United States only. It is developed based on the auto-estimator algorithm using the brightness temperatures of geostationary satellites and NWP models.

4) Global Precipitation Measurement (GPM) mission

The Global Precipitation Measurement, or GPM, mission will be launched in 2014. It will use an international constellation of satellites to study global rain, snow and ice to better understand

climate, weather, and hydrometeorological processes. The GMI instrument, a multi-channel, conical-scanning, microwave radiometer, will measure Earth's atmospheric moisture with near-global coverage. The GMI Flight Unit 2 is planned to fly on a GPM partner-provided spacecraft in a low-inclination orbit as part of the GPM constellation with a targeted launch date of 2014. It will contribute to GPM by enhancing monitoring of TCs and mid-latitude storms and improving estimates of rainfall accumulation.

To validate the satellite rainfall estimates, the International Precipitation Working Group (IPWG) provides a portal on the inventory, reports, information on validation and training on its website (http://www.isac.cnr.it/~ipwg/). It carries out a project that compares and validates daily outputs of different satellite algorithms. Forecasters can make use of the information and choose the appropriate algorithm outputs. Details of the project, information about resources and materials on the techniques and performances of different algorithms can be accessed through the website: http://ipwg.isac.cnr.it/algorithms/inventory/docs/MiRS_Algorithm_Desc_IPWG.doc

6.3.3 Flood monitoring

Other than the meteorological aspects, satellites are also used to monitor flooding, with products available at different spatial and temporal resolutions. Landsat Enhanced Thematic Mapper Plus (ETM+) is able to provide information on the flooded areas which can be differentiated from other types of land cover. However, it has a poor temporal resolution (16 days) and its monitoring capability can be compromised by clouds. Flooding events that last less than two weeks could well be missed (Sandholt et al. 2003). ERS Synthetic Aperture Radar instrument (SAR) can penetrate clouds and produce maps at a local to regional scale. However, similar to Landsat ETM+, its temporal resolution is poor (35 days). As such, neither Landsat ETM+ nor ERS SAR can be used to monitor flood propagation.

NOAA AVHRR images can provide better temporal coverage for flood mapping and analysis of flood propagation at the expenses of the spatial resolution. To address the problem of limited spatial resolution of satellite images, Buckley et al. (2009) used NASA Advanced Microwave Precipitation Radiometer (AMPR) to detect surface water and flooding. The study investigated three flooding events associated with TCs. It was found that that AMPR demonstrated high resolution detection of anomalous surface water and flooding in many situations with sufficiently detailed analyses.

MODIS data can be used in flood analysis and monitoring using different algorithms and techniques (Brakenridge and Anderson 2006). For example, to identify water pixels, a threshold approach and NDVI band ratio [(band2-band1) / (band2+band1)] values can be applied. The water discharge can then be correlated with the radiance threshold to trigger flood alarm (Figure 6.3). In addition, MODIS data can be readily used in GIS to facilitate disaster reduction and mitigation efforts.

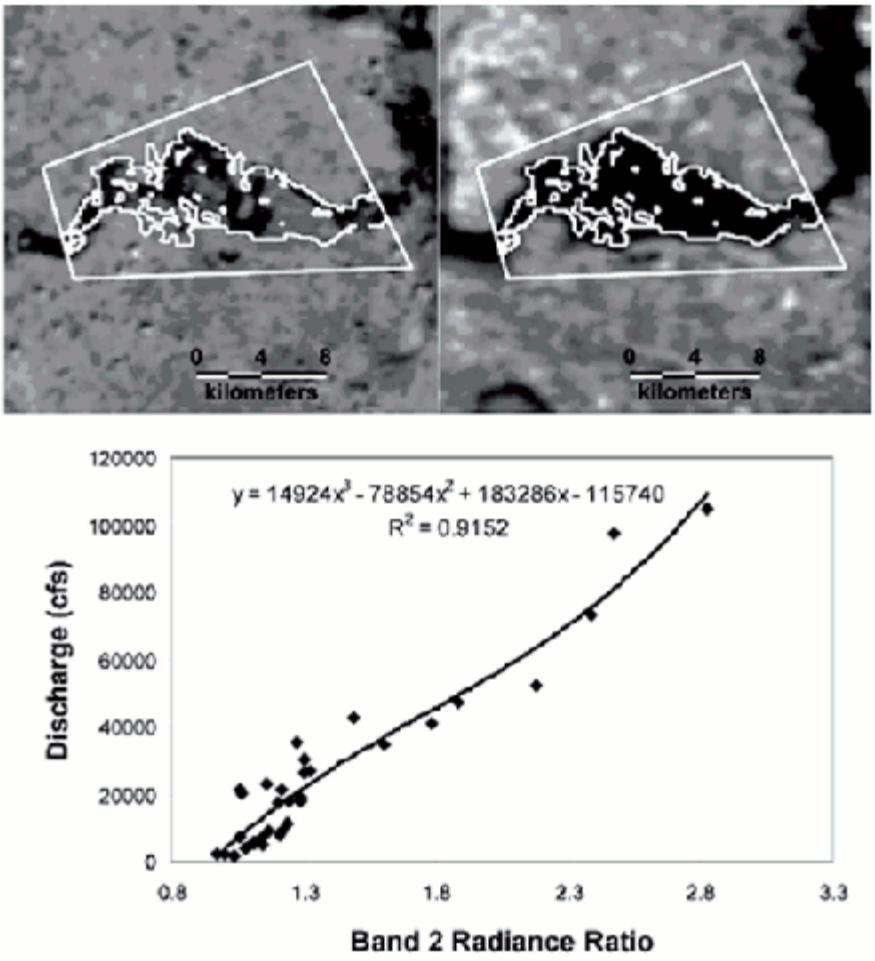

Figure 6.3 Top: MODIS band 2 images during minor flooding (left) and major flooding (right); bottom: MODIS band 2 calibrated radiance ratios versus the water discharge (extracted from Brakenridge and Anderson (2006)).

6.4 Radar techniques

6.4.1 Overview

To improve the understanding of TCs and their rain distribution, radars bearing various functions and techniques have been developed, including the U.S. National Oceanic and Atmospheric Administration (NOAA) WP-3D tail airborne Doppler radar, the Weather Service Radar (WSR) 1988-Doppler (WSR-88D) radar network and portable Doppler radars (Marks 2003). The WSR-88D is now a Dual Polarity (Dual-Pol) radar that has expanded capabilities in better discerning heavy rain, hail, and tornado debris. Along with space-borne radar systems such as NASA TRMM, land-based and satellite-based radar data can be used together for enhanced analyses of temporal as well as spatial rain variability.

Keeping pace with the evolution of radars, different algorithms have been developed to provide better rain estimates using radar signals, to study the rain characteristics, and to facilitate the design of nowcasting tools.

6.4.2 Radar quantitative precipitation estimates (QPE)

Radar QPE algorithms can be categorized into two types, the linear/non-linear regression methods and the probability matching methods. Medlin et al. (2007) studied the rainfall associated with a stationary weak hurricane Danny using WSR-88D system and the WSR-88D precipitation rate algorithm. It was found that the radar estimate with capping maximum precipitation rate and a static Z-R relationship would lead to an under-estimation of rainfall. Li and Lai (2004) adopted a dynamic update of Z-R relations using real-time raingauge measurements. This dynamic approach allowed the Z-R calibration process to evolve as the rain event unfolded, hence leading to more realistic rainfall assessment for nowcasting applications. Figure 6.4 illustrates the dynamic radar-raingauge rainfall re-analysis process.

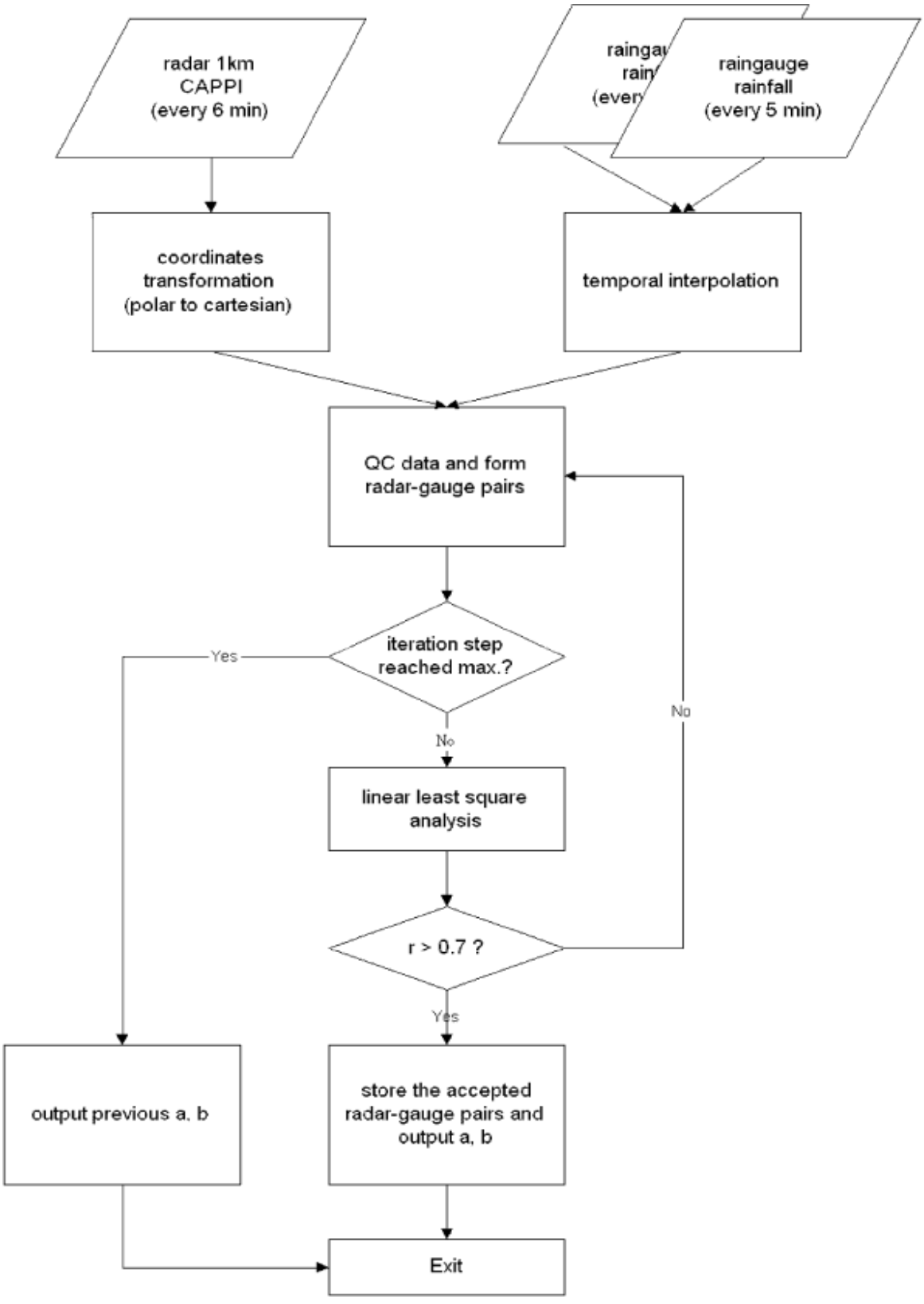

Figure 6.4 Flowchart of dynamic Z-R update process (extracted from Li and Lai 2004).

6.4.3 Rain characteristics

On the NOAA WP-3D, there are Stepped Frequency Microwave Radiomater (SFMR), tail radar, lower fuselage radar and the Knollenberg Particle Measurement System Optical Array Spectrometer Probe (Jiang et al. 2002). Data from different instruments allow the study and validation of precipitation and rainband characteristics inside TCs, and facilitates the analysis of the evolution of cyclones' kinematic structure. Such studies greatly facilitate the understanding of the weather associated with landfalling TCs. Findings can also be used for the HIRAD data mentioned in Section 6.3.1.

6.4.4 Future development

The development of NEXRAD in Space (NIS), a sophisticated Doppler precipitation radar at Ka-band frequency mounted on a GEO satellite platform, can provide observations and better understanding of rain microphysics and kinematics within tropical cyclones (Smith et al. 2008).

To provide better radar-based QPF, data assimilation techniques incorporating radar QPE, cloud analyses from radars and satellite observations are being developed for mesoscale non-hydrostatic models (e.g., assimilation of radar QPE in JMA JNoVA-4DVAR) and mesoscale ensemble prediction system.

Regional mobile X-band dual-polarimetric radars have the capacity to provide more reliable QPE. Data so derived can also be used to validate models and improve QPE.

6.5 Raingauge networks and techniques

6.5.1 Gauge-based statistical models

TC rainfall rates and distributions can be derived from raingauge/satellite climatology and persistence, and used as input for forecast models.

Rainfall Climatology and Persistence (R-CLIPER) is a gauge-based statistical model with radial distributions of rainfall, assuming symmetric rainfall pattern. Raingauge data are first grouped into annuli around the cyclone centre. The mean rainfall rate of each annulus is calculated and taken as the climatology. Rainfall associated with the cyclone was deduced according to its intensity. R-CLIPER rainfall can then be used to validate numerical outputs and improve the models.

Marks et al. (2002) refined the gauge-based R-CLIPER model by using the microwave imager (TMI) rainfall estimates from the NASA TRMM satellite, i.e. a satellite-based R-CLIPER model, on the basis that the satellite-based climatology and the gauge-based climatology had similar mean rainfall rates in the radial direction. TMI data provide a global coverage and overcome the

problem of sparse gauge data near the cyclone centre. Lonfat et al. (2004) further investigated the cyclone rainfall rates and distributions using the 3-year TMI data. A conditional (only when raining) probability density function (PDF) of rain rate occurrence (area) was constructed for each annulus within 500 km of the cyclone centre (Figure 6.5). Combining PDFs of different annuli, a contoured frequency by radial distance (CFRD) diagram was produced (Figure 6.6). Lonfat et al. (2004) re-calculated the PDFs by "weighing each rain estimate by the corresponding rain rate" and then "normalized to the total amount of rain" to get the rainfall flux. A CFRD for rainfall flux is shown in Figure 6.7. In the CFRD, a broader PDF indicates higher degree of asymmetry.

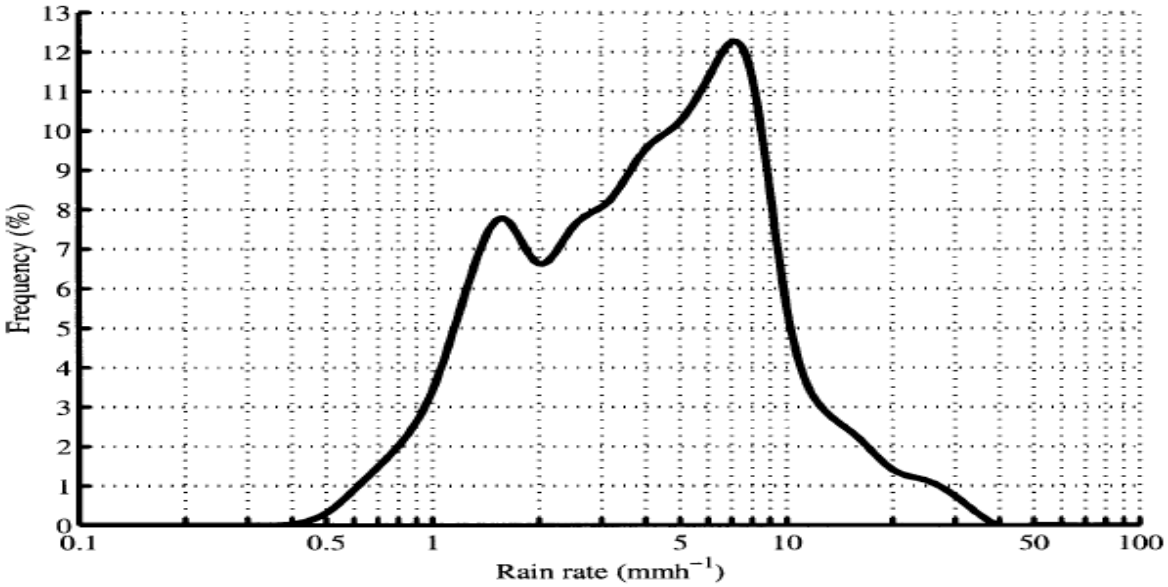

Figure 6.5. PDF of rainfall for Hurricane Dennis within 300 km from the storm center (extracted from Lonfat et al. 2004).

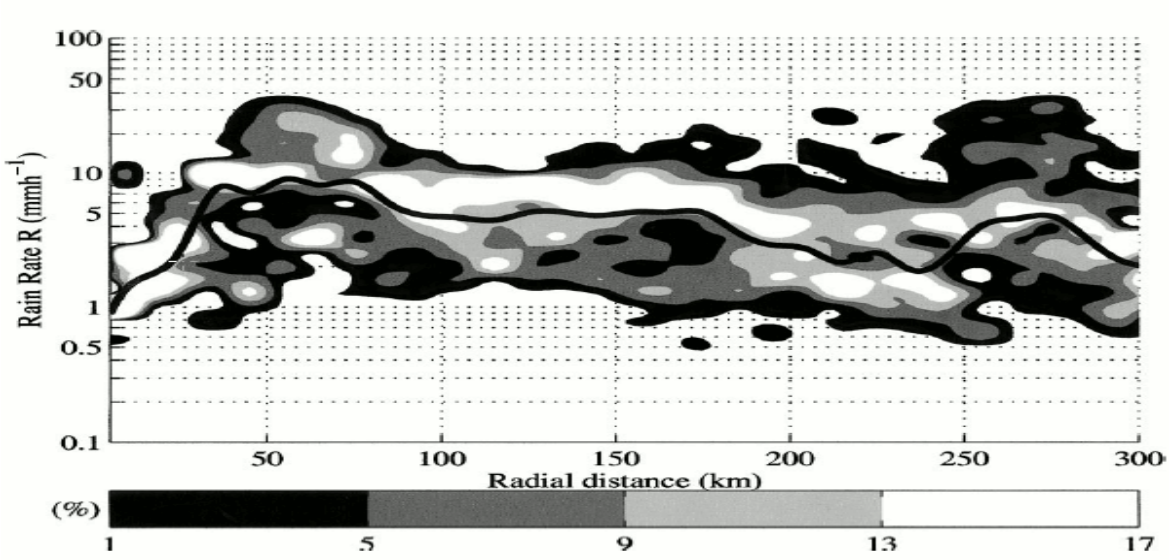

Figure 6.6. Rain rate CFRD for Hurricane Dennis. (extracted from Lonfat et al. 2004)

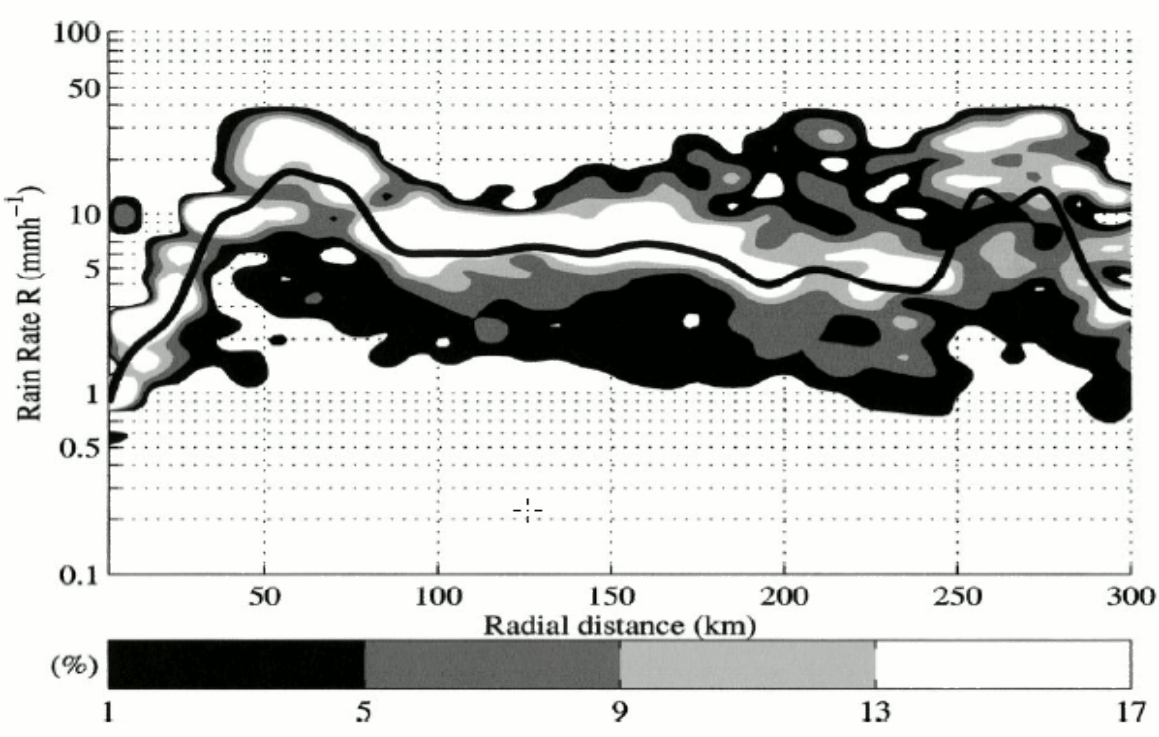

Figure 6.7. CFRD for rainfall flux for Hurricane Dennis (extracted from Lonfat et al. 2004)

CFRDs can be constructed according to cyclone intensities. Lonfat et al. (2004) found that for cyclones with higher intensity, the mean rain rate increased, location with peak rainfall rate became closer to the cyclone centre, and the spread of the PDF narrowed. This refined R-CLIPER model can predict rainfall rate of a particular time step, which can be integrated along the cyclone track and used to produce the accumulated rainfall.

6.5.2 Asymmetry and topographic effects

To forecast the change of rainfall rates after landfall, an inland decay model was proposed by Marks et al. (2002):

$$R(r,t) = (ae^{-\alpha t} + b)\, e^{-(r-r_m)/r_e}$$

where r is radius and t is time; a and α are defined by fitting raingauge data in time; b is defined by fitting rain gauge data by radius; r_m = radius of maximum rainfall; r_e = 500 (km)

Tuleya *et al*. (2007) proved that the gauge data and TMI data radial profiles for tropical storms and category 1 and 2 hurricanes had remarkable agreements. Correlation coefficients between them were more than 0.95. The R-CLIPER model with TMI climatology can be represented by equations below:

$R(r) = R_0 + (R_m - R_0)\,(r/r_m)$ $\quad r < r_m$

$R(r) = R_m \exp(-(r - r_m)/r_e)$ $\quad r \geq r_m$

where R_0 and R_m are the mean rainfall rates at r = 0 and r_m (radial extent of the inner-core rain rate) respectively; r_e (radial extent of the tropical system rainfall).

As it is based on climatological values, the R-CLIPER model generally fails to give extreme values. Tuleya et al. (2007) adjusted the TMI rain rate in the R-CLIPER model as a function of radius and maximum wind speed and incorporated the modified R-CLIPER model into the operational version of the Geophysical Fluid Dynamics Laboratory (GFDL) hurricane model.

The modified R-CLIPER model was capable of forecasting higher rainfall amount as it took the maximum wind speed into account. Forecast rainfall from the modified R-CLIPER model proposed by Tuleya et al. (2007) were verified against 32,784 daily gauge observations from 25 TC cases. The modified R-CLIPER model performed slightly better with a smaller mean absolute error than using the GFDL model. However, the modified R-CLIPER model still under-estimated the total rainfall amount while GFDL model tend to over-estimate and had high biases at all thresholds.

TC rainfall distribution depends on various factors, such as cyclone intensity, location, translation speed, wind shear (Lonfat et al. 2004) and topography (Lonfat et al. 2007). The R-CLIPER model assumes azimuthally symmetric rainfall distribution, which is one of its limitations. Lonfat et al. (2004) investigated the asymmetric component by using the first-order Fourier decomposition of the annulus rainfall estimates. It was found that higher rainfall rate was generally located ahead of the TC center. Quadrants with higher rainfall rates shifted from the front-left to front-right with increasing cyclone intensity. **Geographically, TCs in the Northern Hemisphere had rainfall rate peaking in the front-right quadrant, while those in the Southern Hemisphere peaked in the front-left quadrant.**

Lonfat et al. (2007) improved the R-CLIPER model further by parameterizing shear and topography to form the Parametric Hurricane Rainfall Model (PHRaM).

$R_{PHRaM} = R_{R\text{-}CLIPER} + R_{shear\ mod} + R_{topography}$

Impact of vertical shear is represented by wavenumber-1 and -2 Fourier coefficients:

$R_{shear\ mod}(r,\alpha) = \Sigma c_i(r)\cos(i\alpha) + \Sigma d_i(r)\sin(i\alpha)$

where r is the radial distance and α is the azimuthal angle.
Rainfall amount forecast in the R-CLIPER model is re-distributed spatially in the PHRaM model to reflect the asymmetry.

Topography effect is parameterized by using: $R_{topography} = c\vec{V}_s \bullet \nabla h_s$

where c is a constant, V_s is the surface (10m) wind field; and h_s is the ground elevation.
It is found that PHRaM model outputs have higher equitable threat score than the R-CLIPER model outputs. Both the mean cyclone total rainfall and the rain flux PDF from the PHRaM model are closer to the observation.

Instead of PHRaM, Cheung et al. (2008) used another statistical method based on rainfall climatology in Taiwan as the rainfall pattern and amount in Taiwan were found to be highly related to the topography. Climatology rain rate distribution maps corresponding to the cyclone locations in the vicinity of Taiwan were constructed (Figure 6.8).

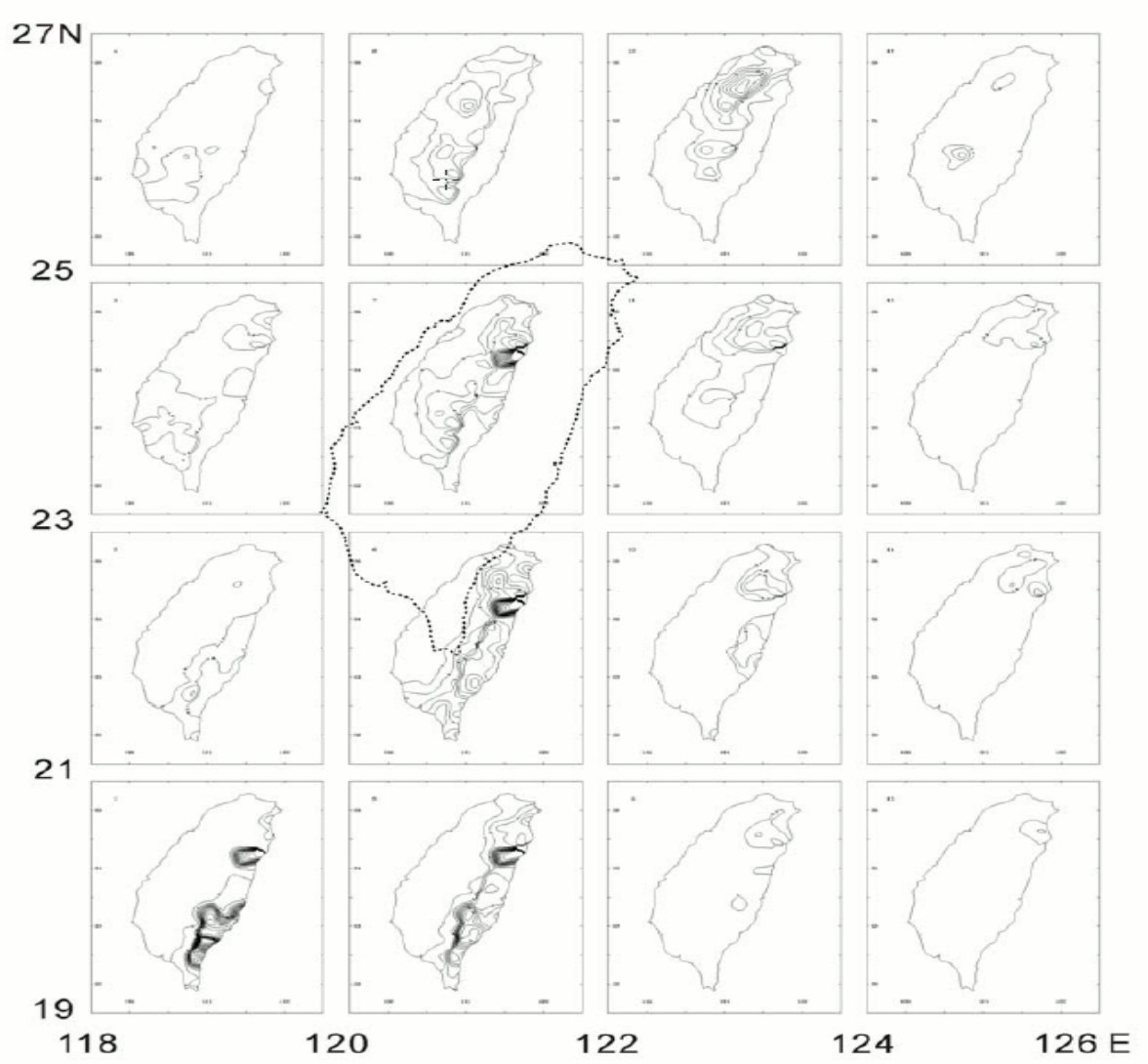

Figure 6.8. TC rainfall climatology in the Taiwan area (contours shown are hourly rain rate with interval 2 mmh-1). Each 2°x2° latitude/longitude panel represents the rain distribution when the TCs are located in that panel relative to the central Taiwan map (extracted from Cheung et al. 2008).

Temporal characteristics of rainfall were studied by Cheung et al. (2008) using cluster analysis. Results of the study showed that the clusters were geographically related. As a result, there was a reasonably good performance in terms of correlation coefficients (> 0.6) for the estimation of accumulated rainfall amount up to a duration of six hours. Equitable threat scores for 24-hour rainfall were higher (0.4 - 0.5) in northwestern Taiwan than those in the southern part. However, there was serious under-estimation of 24-hour rainfall amounts that exceeded 130 mm.

6.6 Synoptic and climatological techniques

6.6.1 Climatological patterns

Cerveny and Newman (2000) suggested that by constructing climatological relationships between TC parameters and rainfall, "seasonal predictive climatic parameters" could be identified. Based on historical rainfall data categorized into a 2.5°x 2.5° grid, two databases were generated for study: (a) total tropical cyclone rainfall aggregated over the nine grids surrounding the averaged daily cyclone positions; and (b) inner core rainfall from the central grid over the averaged daily cyclone positions. Linear relationships were found between cyclone intensity and rainfall amount for TCs over the North Pacific and the Atlantic basins. More intense cyclones generally produced more rain. The daily rainfall accumulation, as well as the ratio of inner core rainfall to the total rainfall, were both related to the cyclone's daily maximum surface wind speeds. Such relationships could potentially be used as forecast aids for operating heavy rain and flood warnings.

Rodgers et al. (2000 and 2001) used the derived mean monthly rainfall amounts of the SSM/I instruments onboard of the DMSP satellite to study the spatial and temporal features of TC rainfall over the western North Pacific and the North Atlantic. From these studies, it was found that TC rainfall (within four degrees of cyclone centres) generally increased during the El Niño years over the North Pacific but decreased over the North Atlantic. In the North Pacific, increase of rainfall in the eastern part was attributed to the higher SSTs, but the rainfall increases in the western and central parts were apparently not as closely related to the relative changes in SSTs and were probably more the result of corresponding changes in the general circulation patterns such as the migration of ITCZ. Jiang and Zipser (2010) used the TRMM data instead for studying TC rainfall (within 500 km of cyclone centres) over six basins around the globe. Similarly, **rainfall increases were observed over the North Pacific during the El Niño years.** Changes in TC rainfall were nearly neutral over the south Indian Ocean and the South Pacific, but decreased over the North Atlantic and the north Indian Ocean.

Spatially, rainfall associated with the cyclone's inner core was generally representative of the cyclone's total rainfall (Cerveny and Newman 2000). Moisture availability in the subtropics might explain the latitudinal variation of rainfall based on the combined data for the North

Atlantic and North Pacific basins. TC rainfall zonal maxima were located poleward (5°-10°) of non-TC rainfall maxima over both basins (Rodgers et al. 2000 and 2001).

Temporally, TC rainfall in the North Pacific reached a maximum in late summer and early autumn (Rodgers et al. 2000). The lag behind the months of maximum insolation was more pronounced in the western part than in the central and eastern parts. The lag was attributed to the maximum warming of the SSTs and the favourable general circulation patterns in early autumn for cyclogenesis and cyclone intensification. However, Cerveny and Newman (2000) found that TCs in the North Pacific in November and December would bring more rain as they generally occurred in the low latitudes with higher SSTs. They also showed that rainfall usually peaked around six days after cyclone formation.

6.6.2 Rainfall patterns in and around the cyclone

TC rain can generally be separated into two types: stratiform and convective rain. Yokoyama and Takayabu (2008) investigated the stratiform rain ratio (SRR) and rain type spatial structures in TCs using the TRMM data. In the study, SRR was defined as "the ratio of the stratiform rainfall to the total rainfall" and rain-top height (RTH) was defined as "the highest altitude with a threshold of 0.3 mm/h in the rain-detected pixels". The mean SRR for TCs (52%) was found to be larger than the equatorial oceanic mean (44%). RTH of TCs was concentrated in the range of 7-9 km; RTH of stratiform and convective rain at ~7.5 km and ~8.5 km respectively contributed most to TC rainfall.

The spatial distribution of stratiform and convective rain was also analyzed. The "inner core", i.e., 0-60 km from the cyclone centre, had small SRR and high RTH. Rain was mainly associated with convective activity with RTH around 8-12 km in the mature cyclone stage. Rain in the "rainband", i.e., 60-500 km from the cyclone centre, had large SRR and relatively large rain yield, suggesting large rainfall amount with moderate convective activity. Rain mainly came from regions with RTH around 6-9 km in the mature cyclone stage. An "inner rainband", situated between 80 and 230 km (90 and 140 km) from cyclone centres, also had large SRR for tropical cyclones with the maximum sustained winds greater than 64 kt/119 km/h (128 kt/237 km/h). Between the "inner core" and the "inner rainband" was a mixed zone of eyewalls and rainbands, depending on the eyewall radius, and at times, eyewall-replacement cycles.

While significant rainfall occurs invariably close to or in the vicinity of TCs, less attention is paid to enhanced rainfall while a TC is still far away or when it is dissipating. Interactions between TCs, which act as moisture suppliers, and other synoptic systems would also bring significant indirect precipitation to remote areas. Wang et al. (2009) used the Advanced Research version of the Weather Research and Forecast (WRF) model to simulate Typhoon Songda (2004) at high resolution to investigate the cyclone's influence on the environment circulation, as well as its effect on precipitation in far-away places such as Japan. While Songda was still southeast of Okinawa, heavy precipitation already occurred over parts of Japan and the adjacent seas. The numerical experiments demonstrated that Songda's outer circulation helped to enhance the southerly winds. Moisture was advected polewards and resulted in moisture flux convergence

further downstream. Wang et al. (2009) found that at one stage Songda contributed more than 90% of the rainfall over the area under study.

As a TC dissipates, its remnant will interact and become increasingly affected by large-scale weather systems. Spatial differences in rainfall patterns and amounts can be quite large. For TCs from 1992 to 2004 studied by Ritchie and Szenasi (2006), those that fully interacted with mid-latitude systems had rainfall patterns that appeared similar to those produced by mid-latitude troughs. ain would be brief but heavy. In the absence of mid-latitude troughs in the vicinity, rainfall patterns varied. A slow-moving cyclone remnant could bring persistent and widespread rain.

Environmental forcing, such as vertical wind shear, can affect the rain rate and rainfall asymmetry. Quinlan (2008) decomposed the shear vector into u- and v-components and analyzed the rain rate for Hurricane Emily (2005). There was "significant positive correlation" between the u-component of the shear vector and rain rate over the northwestern and northeastern quadrants in the vicinity of the cyclone. Lonfat et al. (2004) further analyzed the azimuthal rainfall distribution of Hurricane Dennis (1999) using TRMM observation. **It was found that rainfall rates increased on the left and front-left of the cyclone centre in the inner 150 km (81 nmi). Outside the 150 km (81 nmi) region, the outer rainbands concentrated on the front and front-right of the cyclone centre**. Gao et al. (2009) examined the vertical wind shear effect on asymmetric rainfall distributions using the mean wind difference between 850 hPa and 200 hPa over a 200-800 km (108-432 nmi) annulus from the centre of Typhoon Bilis (2006). **Rainfall was found to increase downshear right in the outer rainbands.** The study explained the phenomenon using vortex tilting and vorticity balance.

6.6.3 Orographic effect and landfall

Hurricane Dean brought heavy rain to the mountainous island of Dominica in the West Indies in 2007. Smith et al. (2009) used rain gauges, MODIS images, and radar scans to study the terrain's effect on precipitation. Assuming typical trade-wind inversion and through a Froude number assessment, it was considered that high wind speeds within the hurricane environment would not be conducive to convection triggering by terrain. As such, enhanced convection that brought twice as much rainfall to the mountainous region was apparently induced by orography through a local seeder-feeder mechanism.

Wu et al. (2009) studied a heavy rain event in the Taiwan area associated with the interaction between Typhoon Babs (1998), the East Asia winter monsoon and terrain using a series of numerical sensitivity experiments. While the interaction between Babs and the winter monsoon gave rise to enhanced low-level convergence, it was found that the terrain of Taiwan played a key role in shaping the low-level convergence patterns. Removal of the terrain also led to different rainfall distribution in the absence of orographic lifting.

To study the potential role played by cyclone motion in modulating the topographic rain, rainfall distributions corresponding to different cyclone track scenarios were thoroughly

analyzed by Harville (2009). Cyclone tracks approaching the east coast of the United States towards the southern central Appalachian mountain range were stratified into four types. Rainfall patterns corresponding to different track scenarios provided useful guidance in assessing flooding risks. Similar techniques can potentially be adopted for use in other regions.

Chan et al. (2003) investigated the convection asymmetry of four TCs making landfall along the south China coast in 1999 using radar, satellite and NCEP wind shear data. It was suggested that asymmetric convection first developed in the mid to lower troposphere west of the cyclone. It was then advected to the southward side by the cyclonic flow and rising motion in the upper troposphere.

Rainfall associated with a TC can become asymmetric after landfall. The asymmetry can be due to frictional effect in the boundary layer (maximum convergence in the forward flank right of a translating vortex), vertical wind shear (asymmetric patterns of rainfall closely related to cyclone intensity, magnitude of vertical shear and distance of rain area to the cyclone centre), and topography.

Atallah *et al.* (2007) examined hurricanes making landfall over the United States by separating them into two types: (a) those with precipitation predominantly to the left of their tracks and (b) those with precipitation mostly to the right of their tracks. Evolution of precipitation in these hurricanes were studied using the potential vorticity and quasigeostrophic frameworks. For (a), most of the hurricanes were undergoing extratropical transition. For (b), the hurricanes were interacting with downstream ridges. The contrast was attributed to potential vorticity re-distribution through diabatic heating.

Gao *et al.* (2009) analyzed the mechanism for heavy rainfall associated with Severe Tropical Storm Bilis (2006) after its landfall in China. The study divided the rain events into three stages based on timing and location. Rain during the first stage was directly induced by the inner-core circulation. Moisture, instability and lifting were all important elements for the deep moist convection that took place during the second stage when heavy rain occurred. The third stage was the interaction between Bilis and the South China Sea monsoon, enhanced by topography. Vigorous vertical motion was triggered and sustained by strong vertical shear, warm-air advection, frontogenesis and topography. Since diagnoses of the omega equation, vertical shear, vortex tilting and frontogenesis could be easily applied to any gridded observational analysis or forecast field in real time, they could also be used as forecast guidance on heavy rainfall as the TC moved inland.

6.7 QPF products

6.7.1 Numerical and satellite-based products

Unless a TC comes close to land and is within land-based radar coverage, rainfall assessment has to rely mostly on numerical and satellite-based QPF products. QPF outputs can be in the form of deterministic accumulated rainfall, probabilistic rainfall forecast, rainfall rate and precipitable water.

Increasingly, more and more QPF products are being made available online. They have different spatial coverage, spatial resolution and updated frequency. The NOAA Environmental, Satellite and Data Information Service (NESDIS) has a comprehensive website (http://www.ospo.noaa.gov/Products/atmosphere/rain.html), and two of the products are highlighted below:

1) *Tropical Storm Risk*

Tropical Storm Risk (TSR) of University College London has a graphical quantitative and probabilistic rainfall forecasting application (accessible through the website http://www.tropicalstormrisk.com). It provides forecasts up to five days ahead and updates twice a day for active TCs worldwide. Data for the precipitation forecast comes from the UK Met. Office global model. There are altogether 20 output files for each run: forecast accumulated rainfall for the next 24, 48, 72, 96, and 120 hours and probability forecasts for three rainfall thresholds.

2) *Ensemble Tropical Rainfall Potential (eTRaP)*

This is an ensemble product using POES satellite observations and different cyclone track forecasts. The spatial resolution is 4 km, updated every six hours. Products include deterministic and probabilistic accumulated rainfall forecasts. There are altogether 25 output files for each run: 0 - 6 hr, 6 - 12 hr, 12- 18 hr, 18 - 24 hr, 24 hr total rainfall and probability forecasts for four rainfall thresholds.

eTRaP, a technique derived from Tropical Rainfall Potential (TRaP - Kidder et al. 2005; Ferraro et al. 2005), basically consists of rain rate estimates using data of different microwave sensors. Rain rate estimates from satellites are propagated forward along the forecast TC track assuming both the rain rate and forecast track are accurate. To reduce errors arising from various assumptions, ensemble TRaP (eTRaP) has been brought into operation. Figure 6.9 shows the steps introduced by Ebert et al. (2009). eTRaP consists of TRaPs initialized at various observation times and along different track forecasts. Weights corresponding to sensors and latency are assigned to ensemble members. Both deterministic and probabilistic forecasts are produced. Ebert et al. (2009) compared the performances of eTRaP and TRaP for 6-hours and 24-hour accumulated rainfall. Predicted maximum rainfall, RMSE and correlation coefficient corresponding to eTRaP products were all better than those from TRaP.

Attempts were also made elsewhere to deploy satellite-based QPE for generation of TC QPF, using a method similar to TRaP or eTRaP. For example, QMORPH precipitation estimates, which are similar to CMORPH estimates (Section 6.1.2) except that there is no morphing and the microwave precipitation features are propagated forward in time only

(http://www.cpc.noaa.gov/products/janowiak/cmorph_description.html), can be used together with a subjective forecast cyclone track to produce rainfall forecasts. Chan & Chan (2010) advected the 0.25-degree hourly QMORPH rain estimates along the Hong Kong Observatory's subjective forecast cyclone track to obtain a point forecast of the hourly rainfall at the Observatory, as well as daily rainfall over the coast of Guangdong and the northern part of the South China Sea for the next three days. Forecasts are updated every hour and become available about three hours after observation time. The QPF results and products so derived are found to be particularly useful if the cyclone motion deviates from the NWP model forecast.

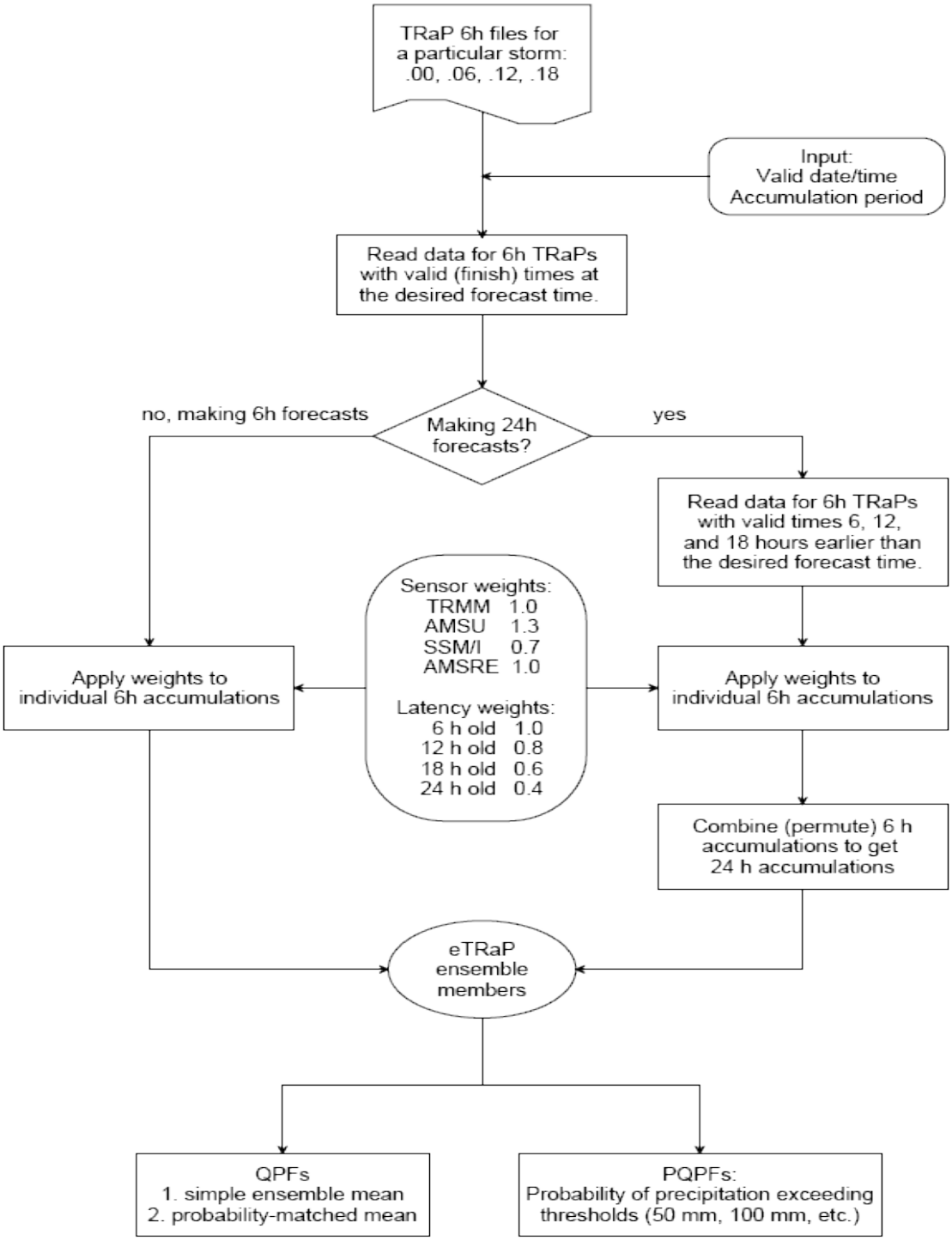

Figure 6.9. Steps in the generation of 24-hour eTraP forecasts (extracted from Ebert et al. (2009))

6.7.2 Multi-model ensemble

Even though NWP models are increasingly becoming the main prognostic tool in operational TC forecasting, model-based QPF guidance is, as yet, not reliable enough for deterministic applications. Useful information is mostly in terms of qualitative trends and probabilistic assessment utilizing a variety of ensemble techniques.

Krishnamurti et al. (2009a and 2009b) used a consensus multi-model forecast product called the FSU super-ensemble for rainfall prediction. The FSU super-ensemble rainfall forecasts were superior to individual members' forecasts and their ensemble mean (Mishra and Krishnamurti 2007, Krishnamurti et al. 2009a and 2009b).

The FSU super-ensemble strategy consisted of two phases: training and forecast phases. The training phase used outputs from ten different models to calculate the statistical weights for each prognostic variable at each grid (both horizontal and vertical), at different time steps and for different member models. "These weights (arose) from a statistical least squares minimization using multiple regressions" (Krishnamurti et al. 2009a), so that a minimum error term *G* was obtained:

$$G = \sum_{i=1}^{N_{train}} \left(S_i' - O_i'\right)^2$$

where N_{train} was the number of time samples in the training phase, and S_t' and O_t' were the super-ensemble and observed field anomalies respectively at training time *t*.

However, only the temporal anomalies of prognostic variables, not the full field, were used. The super-ensemble forecast was constructed as:

$$S = \overline{O} + \sum_{i=1}^{N} a_i \left(F_i - \overline{F_i}\right)$$

where $\overline{O}$ was the observed climatology; a_i was the weight for the *i*th member in the ensemble; and F_i and $\overline{F_i}$ were the forecast and forecast climatological values for the training period respectively for the *i*th model's forecast.

The statistical weights were then used in the forecast phases. Outputs from the same member model were fed into the super-ensemble to obtain the super-ensemble forecasts.

Mishra and Krishnamurti (2007) showed that the FSU super-ensemble forecast provided a robust forecast product up to Day 5 of the rainfall forecasts over the tropics during June-September 2007 in terms of root-mean-square errors, anomaly correlations and equitable threat scores. The equitable threat scores and bias scores both improved further over the Indian monsoon region with the use of downscaling (Krishnamurti et al. 2009a). The FSU super-ensemble products were also found to be very useful for precipitation forecasts for post-landfall heavy rain and flood events in China up to Day 10 (Krishnamurti *et al*. 2009b).

6.7.3 Radar-based now casting application

Nowcasting techniques using radar QPE can provide radar-based Quantitative Precipitation Forecast (QPF). Li and Lai (2004) and Li et al. (2000) used the Tracking Radar Echoes by Correlations (TREC) technique to track rain echoes (Figure 6.10) and provide QPF in the next three hours using a simple linear advection scheme. The results were found to be generally reliable for TC rainbands that were predominantly driven by the advective process.

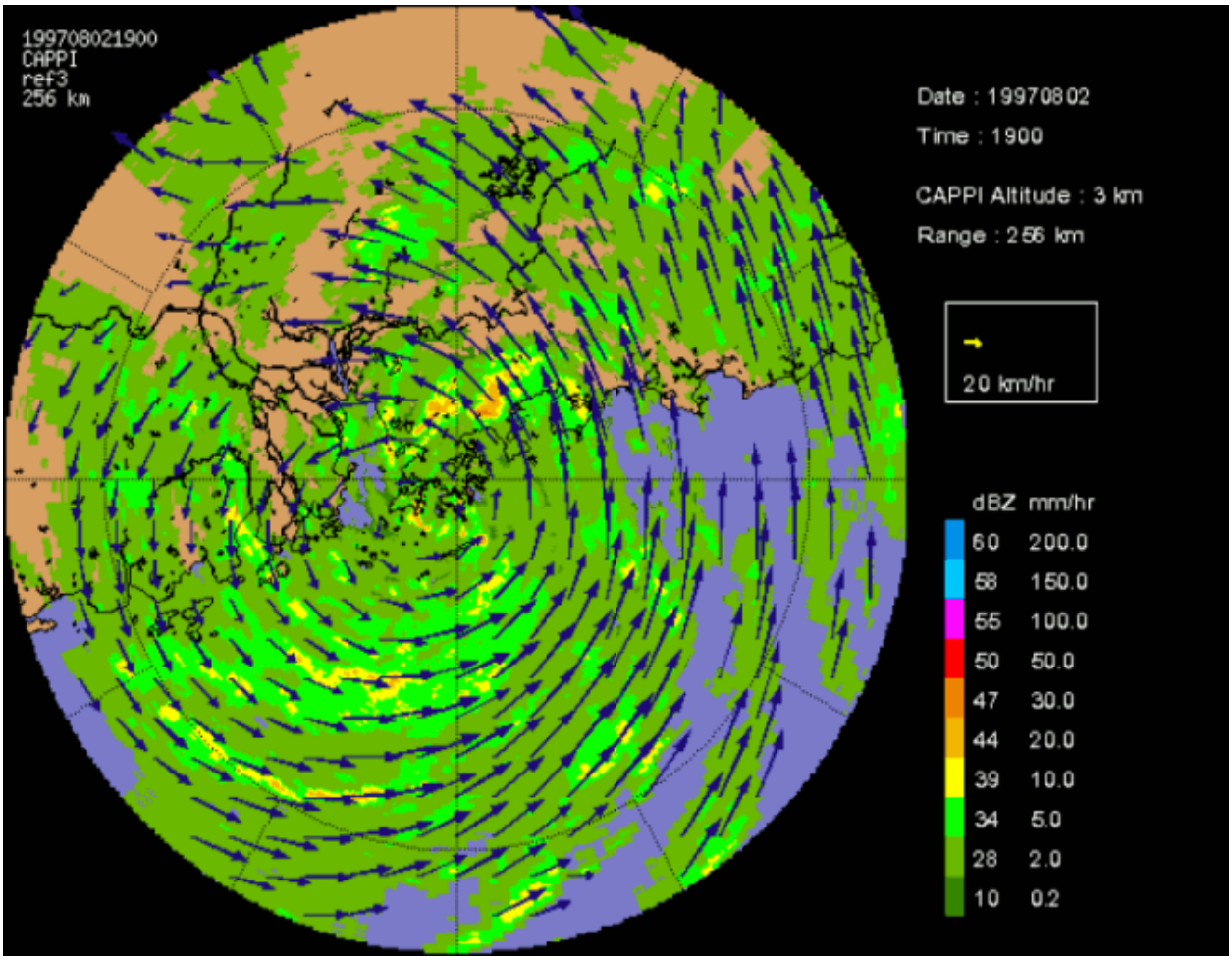

Figure 6.10. TREC vector fields of Typhoon Victor over Hong Kong at 1900 HKT on 2 August 1997 (extracted from Li *et al*. 2000).

Nowcast and NWP blending technique can also be used. Lai and Wong (2006) adopted a modified semi-Lagrangian advection scheme to replace the TREC technique for echoes advection. QPF outputs using the modified advection scheme were then blended with numerical model outputs.

6.7.4 Verification

Given the QPF limitations, well-validated performance assessment and verification statistics allow forecasters to apply the QPF products judiciously and intelligently. Marchok *et al*. (2007) developed a scheme for validating QPFs for landfalling TCs. Cyclone-total rainfall forecasts by the NCEP operational models, i.e. the Global Forecast System (GFS), the Geophysical Fluid Dynamics Laboratory (GFDL) hurricane model, the North American Mesoscale (NAM) model, and the Rainfall Climatology and Persistence (R-CLIPER) model were studied and compared for all landfalling TCs affecting the United States from 1998 to 2004. In the study, three attributes were used for verification: (1) ability to match the observed rainfall patterns; (2) ability to match mean values and amounts of observed rainfall; and (3) ability to produce extreme amounts of rain. They found that GFS performed the best among all studied models for all attributes. Other models tend to over-predict heavy rain or under-forecast rain at a distance away from the cyclone track. Marchok *et al*. (2007) implemented a technique in the verification exercise to remove the impact of track errors on QPF skill. It was found that R-CLIPER, GFDL and NAM models all had QPF skill improvements. Skills of the GFDL and NAM models became comparable to GFS. Armed with such information, forecasters could assign weights on various QPF products according to their operational assessment.

Brennan *et al*. (2008) demonstrated improvement in QPF skill when forecasters' experience was included. Verifications were conducted for 24-hr (Day 1) QPF guidance from GFS, NAM, ECMWF and the National Weather Service's Hydrometeorological Prediction Center (HPC) for TCs bringing rainfall impact upon continental United States under HPC's advisory responsibility during the 2005-2007 hurricane seasons. It was found that, in general, HPC provided better forecasts than raw model QPF, especially for heavy rain events. Brennan *et al*. (2008) attributed this to more accurate track forecasts and forecasters' experience. Results from locally conducted research might also be a factor for better HPC's value-added QPF.

6.8 Flood forecasting

6.8.1 Hydrological tools and models

One of the life-threatening damages induced by TCs is flooding, which is related to rainfall intensity and distribution, as well as the geographical and hydrological characteristics of the flood plain. However, uncertainty on forecast track, QPF and inadequacy of the precipitation network will adversely affect the accuracy of the rainfall amount and distribution pattern, which in turn, interacting with the topography and environmental flow features in the flood models, will affect the flood forecast.

A pre-requisite for flood plain management is the development of a package of hydrologic and hydraulic simulation tools to simulate the catchment responses to extreme storm events in a river basin. The package of simulation tools should be capable of incorporating the critical characteristics of tides (astronomical spring tides, sea level rises), waves, storm/typhoon surges at the estuarine end of the river. The tool should also be able to reflect the increase of flood

peak due to urbanization, and changes in flood discharges and stages associated with various structural and non-structural developments.

Once calibrated, the tools can be used for assessing potential hazards associated with flood events and for evaluating alternative mitigation measures. These simulation models, together with the established flood hazard data (maps, profiles, and flood stages) can then be used to correlate flood discharge, flood stage, flood probability and damages in the flood prone areas. The tools can be readily extended to other flood-prone areas with comparable hydro-geophysical and land-use developmental settings.

Mathematical hydrological models can be used for flood forecasting. Chen (2004) proposed a statistical model for river flood prediction. Predictors in the model included precipitation intensity that could be traced back to a few days, prevailing water level, vegetation and land surface properties, and the presence of river branches and tributaries.

Some of the hydrological models incorporate the use of Geographic Information System (GIS) and digital elevation model (DEM) data, that help "delineating basin boundary, estimating basin area, generating Thiessen Polygons of the raingauge network, calculating areal-mean rainfall, and computing watershed parameters" (Shong 2006). Tang and Xie (2008) employed the Agricultural Non-Point Source Pollution Model (AGNPS) to investigate the hydrological responses in the Tar Pamlico River basin and successfully simulated the peak flow. AGNPS, with watershed hydrology and a water quality model, topography data, and land use and soil type data, could predict surface runoff and sediment yield for flood modeling.

Results from one model can be used as input for triggering another model. This allows different configurations or suites of models to be set up to suit the local environment. For example, hydraulic model results were used in Australia to refine the operational flood hydrological model for generating a variety of flood forecast products, such as temporal and spatial variability of rainfall and runoff (Shong 2006). Hossain (2004) combined rainfall-runoff modules, a hydrodynamic model, and a flood routing model for flood forecasting in Bangladesh.

6.8.2 Operational products

The Global Flood Alert System (GFAS), under the International Flood Network (IFNet; http://www.internationalfloodnetwork.org/index.html) established in March 2003, utilizes satellite-based rainfall for flood forecasting and warning. It provides rainfall maps, text data, and heavy rain information by precipitation probability estimates. E-mail notification service is available for official hydrological services on request.

The International Center for Water Hazard and Risk Management (ICHARM), under the auspices of United Nations Educational, Scientific and Cultural Organization (UNESCO), is operating a comprehensive software package named Integrated Flood Analysis System (IFAS), accessible through http://www.icharm.pwri.go.jp/. IFAS is a tool kit implementing the "GFAS-Streamflow"

concept with satellite-based rainfall data for flood runoff analysis and forecasting in developing countries (Yamashiki and Tsujimura, 2009). It consists of five modules: the main module, the rainfall data input module, GIS data input and analysis module, runoff calculation engine module, and calculation results output module (Fukami et al. 2006). The main module is for initiating and managing the various IFAS functions. The rainfall input module handles the satellite-based and ground-based rainfall data. The GIS data input and analysis module facilitates the import of external GIS data, geophysical data analysis and estimation of hydrological model parameters. The runoff calculation engine module enables the selection of different runoff analysis engines, which are either conceptual or mesh-based distributed-parameter hydrologic models. The output module displays results graphically in different ways. As a result, even in poorly-gauged region with insufficient hydrological and geophysical data, IFAS can still produce effective and efficient flood forecasts (Sugiura et al. 2010).

6.8.3 A forecast technique for diagnosing areas of extreme rainfall

Tropical Cyclone Guba tracked south of Port Moresby in November 2007. The Port Moresby TC warning centre issued flood warnings for provinces adjacent to the track but not for the Oro Province which lay some distance from the track. The death toll from the floods in the Oro Province has been put at more than 200. With training, the extreme rainfall region in Oro Province could have been identified from the warm air advection wind profile over the region in conjunction with microwave data. We relayed this information to PNG forecasters and they asked that this diagnostic technique be included in the literature or in the Global Guide for forecasters.

The turning of winds with height, mostly between the 850hPa and 500hPa levels, has been used by forecasters for decades to diagnose likely regions of thermal advection and thus ascent and descent, but due to its roots in geostrophic theory, the diagnostic is generally not applied in the tropics. An exception is the staff at the Severe Weather Section in the Brisbane office of the Australian Bureau of Meteorology. After more than ten years of use, forecasters there have found the anti-cyclonic turning of winds with height to be an important indicator for extreme tropical and sub-tropical rainfall (Bonell and Callaghan 2008; Bonell et al. 2005; Callaghan and Bonell 2005a&b) see also the numerous rainfall event reports at: http://www.bom.gov.au/qld/flood/fld_reports/reports.shtml

Kevin Tory (2015) shows that in a vortex, where the gradient wind balance approximation is valid, warm air advection may also be equated to ascent.

To show the universal application of the diagnostic, we will examine several other major tropical cyclone-related flood events from various tropical regions.

6.8.3.1 Typhoon Bilis

Typhoon Bilis was the second deadliest event in China since 1983 and the deadliest since 1994. Significant damage occurred in Hunan where heavy flooding and mudslides destroyed over

31,000 homes and caused 526 deaths. Most of the damage and fatalities occurred in the village of Zixing. In all, Bilis was responsible for 843 deaths and 208 people reported missing.

The Chenzhou sonde station is very close to Zixing. The heaviest rain in the whole event (24h to 12Z 15 July) was greater than 250mm near Chenzhou and Zixing. From reports, the heavier rain began around 1600UTC 14th, and according to Gao et al. (2009), this rainfall was not forecast very well, with predicted 24-hour totals less than 100mm in the Zixing area.

Chenzhou winds at 00Z 15 July 2006 were 925hPa 330/31knots, 850hPa 345/33knots, 700hPa 010/23knots and 500hPa 050/29knots, which have the warm air advection pattern in the Northern hemisphere of winds turning clockwise with height. We have quantified this to be strong and equivalent to wind profiles producing extreme rainfall in the Queensland (Australia) sub-tropics.

The warm air advection zone generating extreme rainfall has been found to be best shown on 700hPa charts. The analysis in Figure 6.11 uses the 700hPa winds, 850hPa to 500hPa shears and thickness contours from actual observations to depict a warm air advection zone between Changsha through Chenzhou down to near Qing Yang. Figure 6.12 shows the 6-hourly rainfall, and evident is the N to S band of heavy rain through Chenzhou that developed in the warm air advection zone region early on the 15th.

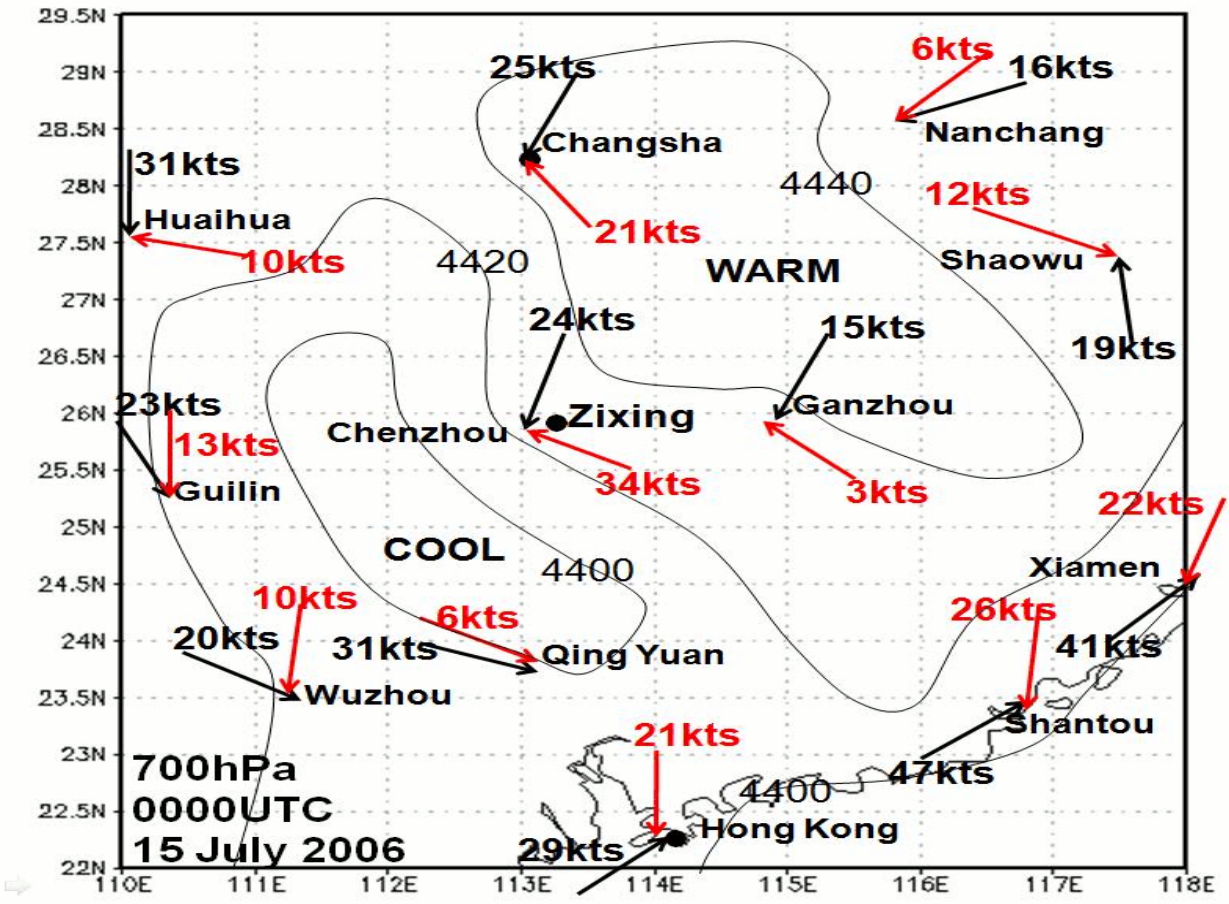

Figure 6.11. 700hPa analysis at 0000UTC 15 July 2006 from actual observations. Red arrows 850 to 500hPa shears (knots), black arrows 700hPa winds (knots), and contours 850 to 500hPa thickness (gpm).

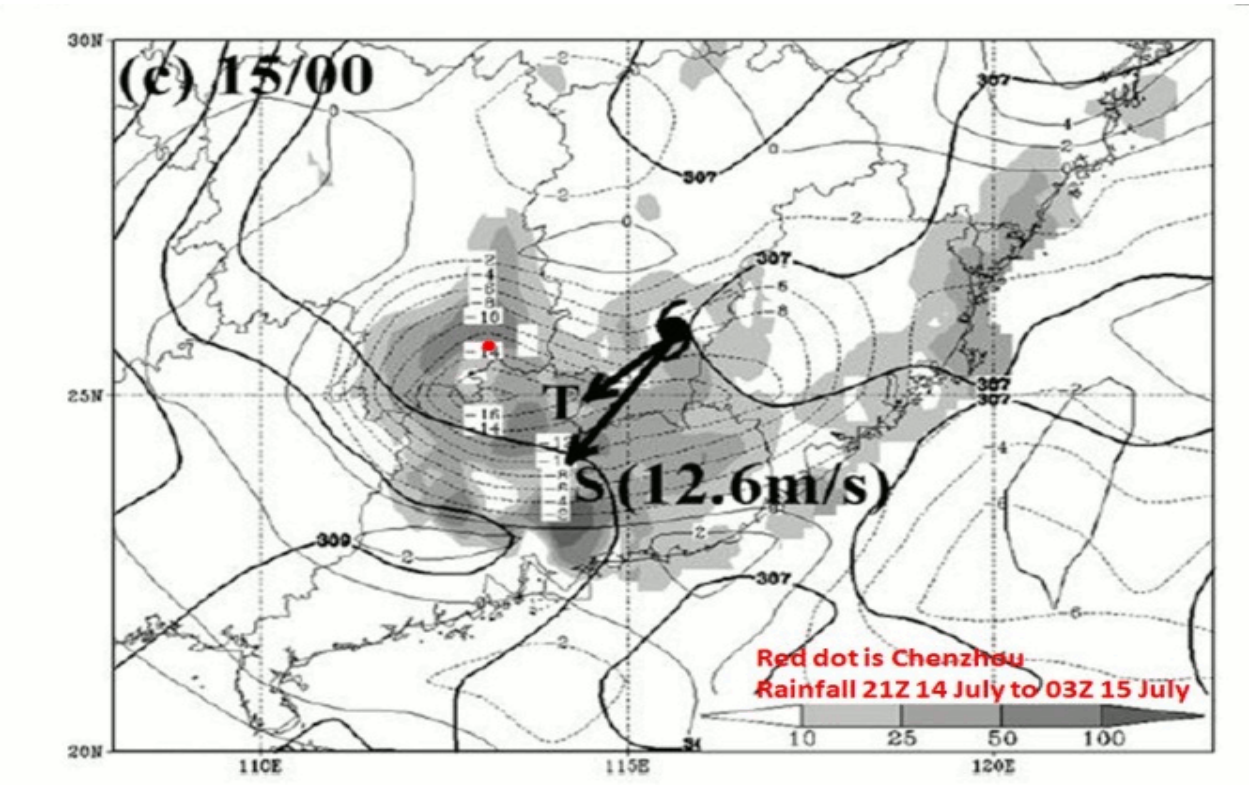

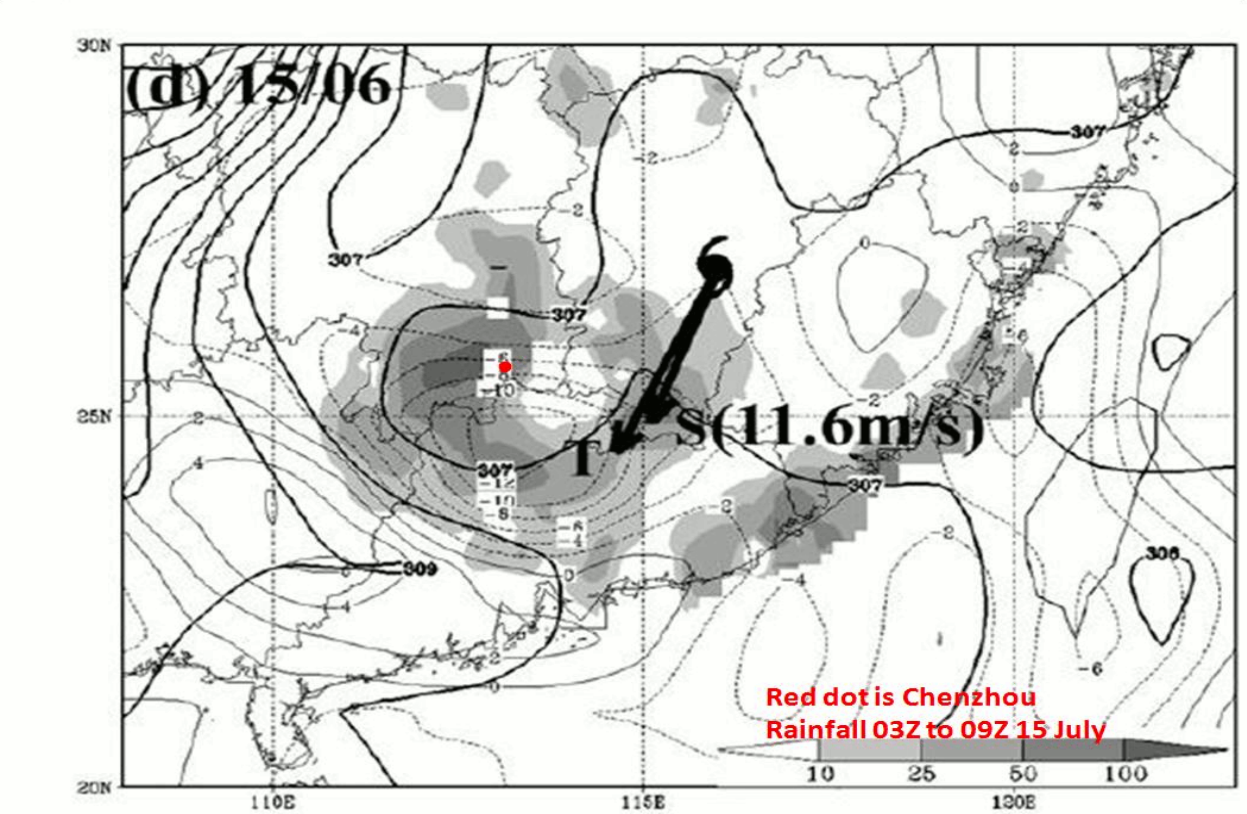

Figure 6.12. Taken from Gao et al. 2009 but focussing on the 6-hourly rainfall near Chenzhou (shown by red dot).

6.8.3.2 Hurricane Mitch

After making landfall as a major hurricane in Honduras, Hurricane Mitch slowly moved over land dropping historic amounts of rainfall in Honduras, Guatemala and Nicaragua with unofficial reports of up to 75 inches (1900 mm). Deaths due to catastrophic flooding made it the second deadliest Atlantic hurricane in history. As of 2008, the official death toll from Mitch was placed at 19,325, with thousands more unaccounted for. Additionally, around 2.7 million people were left homeless as a result of the hurricane.

First, and surprisingly, the highest recorded rainfall over the period from 25 to 31 October 1998 (912 mm) was from Choluteca near the Pacific Coast in Honduras. The maximum 24-hour total there was 467 mm (18.4 in) on 31 October 1998. The highest report from the north coast of Honduras (where landfall occurred and the heaviest totals would normally be expected) was at La Ceiba where 877 mm (34.5 in) was recorded from the 25th to the 31st and 24-hour totals reached 284 mm (11.2 in). Choluteca is close to the Casito Volcano in Nicaragua, which was the scene of a major disaster. Intense, near stationary, rain bands between 0157 UTC 29 October 1998 and 0025 UTC 31 October 1998 produced the exceptional rainfall near the Pacific Coast. In Figure 6.13, we show the microwave imagery with an associated warm air advection pattern at 700hPa, derived from NCEP/NCAR reanalysis data, during the heaviest rainfall. The crater lake

atop the dormant volcano filled and parts of the wall collapsed. The resulting massive mud flows covered an area 16 by 8 km (8.6 by 4.3 nmi). At least four villages were totally buried.

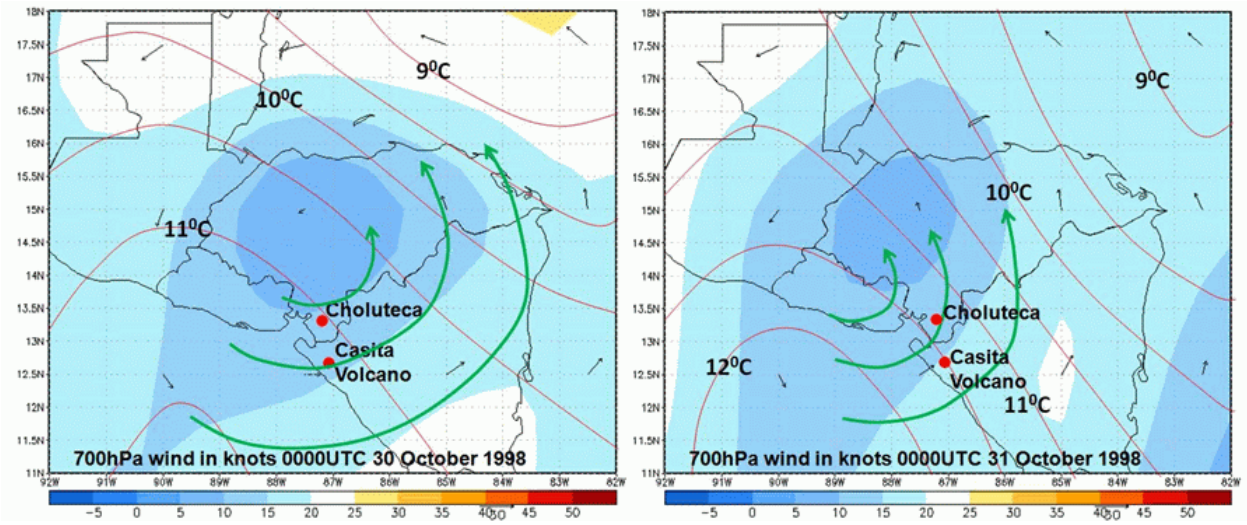

Figure 6.13. The top frames show the stationary heavy rain area near the border of Honduras and Nicaragua from microwave imagery. The lower frames, created from the National Centres for Environmental Prediction/ National Centre for Atmospheric Research (NCEP/NCAR) Reanalysis Project, show the warm air advection (green streamlines) at 700hPa near the border of Honduras and Nicaragua around the same time as the microwave images.

Over 2000 of the dead were from the areas around the volcano. Figure 6.13 shows how the heavy rainfall in the Choluteca and Casito Volcano area was associated with warm air advection at 700hPa.

6.8.3.3 Vietnam floods of November 1999

The floods of November 1999 in Vietnam were the worst in a century, and in total, 793 people lost their lives and 55,000 were made homeless. The floods brought $290 million (US) of damage to the region and caused a further $490 million (US) of economic losses. It is estimated that 1.7 million people in the central Provinces of Vietnam were affected by the floods. From Figure 6.14, the extreme rainfall occurred in a warm air advection region at 700hPa.

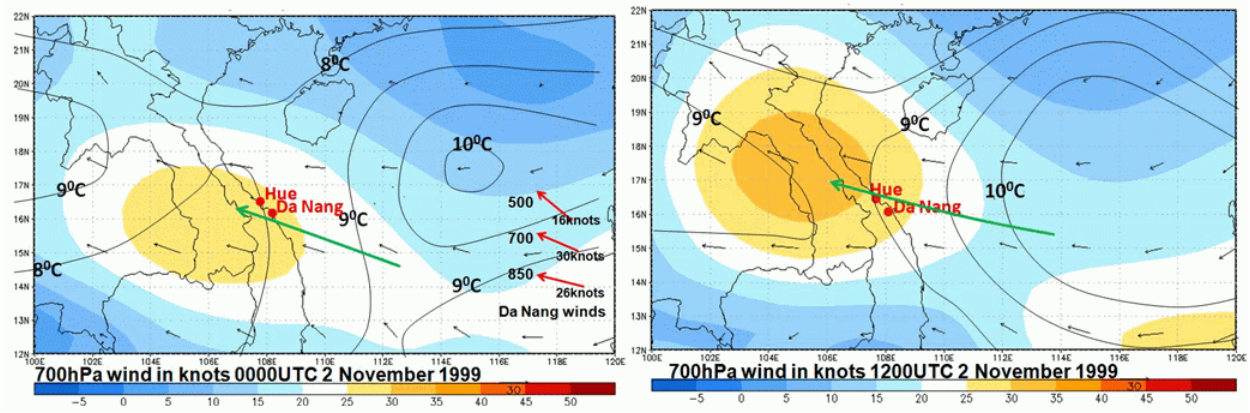

Figure 6.14. From NCEP/NCAR data the warm air advection at 700hPa through Hue and Da Nang is evident during the extreme rainfall. The clockwise turning with height wind profile at Da Nang at 0000UTC 2 November is also shown.

The rainfall at Hue was **88mm (3.46 in)** in the 24hours to 0000UTC 1 November 1999, **864mm (34.0 in)** in the 24 hours to 2 November 1999, **978mm (38.5 in)** in the 24 hours to 3 November 1999, and **272mm (10.7 in)** in the 24 hours to 4 November 1999.

At Da Nang **93mm (3.66 in)** fell in the 24 hours to 0000UTC 1 November 1999, **126mm (4.96 in)** in the 24 hours to 2 November 1999, and **593mm (23.35 in)** in the 24 hours to 3 November 1999. Da Nang winds showed the warm air advection wind profile during the heaviest rainfall as below:

Da Nang winds 0000UTC 1 November 1999

850hPa 055/18knots

700hPa 085/26knots

500hPa 090/30knots

Da Nang winds 0000UTC 2 November 1999

850hPa 100/26knots 1515.00

700hPa 110/30knots 3155.00

500hPa 135/16knots 5890.00

Da Nang winds 0000UTC 3 November 1999

875hPa 065/18knots

730hPa 090/20knots

633hPa 110/14knots

606hPa 140/14knots

6.8.3.4 Mumbai Floods

A recent example of extreme tropical rainfall occurred when Mumbai (Latitude 19.10N) recorded 944.2mm (37.2 in) in the 24-hour period ending 0330UTC 27 July 2005, which was one of the highest daily totals ever recorded in India. There were 405 fatalities and adding to the chaos apparently was the lack of public information. Radio stations and many television stations claim that they did not receive any weather warnings or alerts by the civic agencies.

The available winds at Mumbai had a warm air advection profile over this period, with strong low level westerly winds veering to north-northwesterly winds at middle levels. This warm air advection profile could easily be seen at the 700 hPa level (Figure 6.15), where northwesterly winds flowed over Mumbai and a strong 700hPa temperature gradient orientated southwest to northeast. Due to icing, the radiosonde balloon at Mumbai only ascended as far as 641hPa.

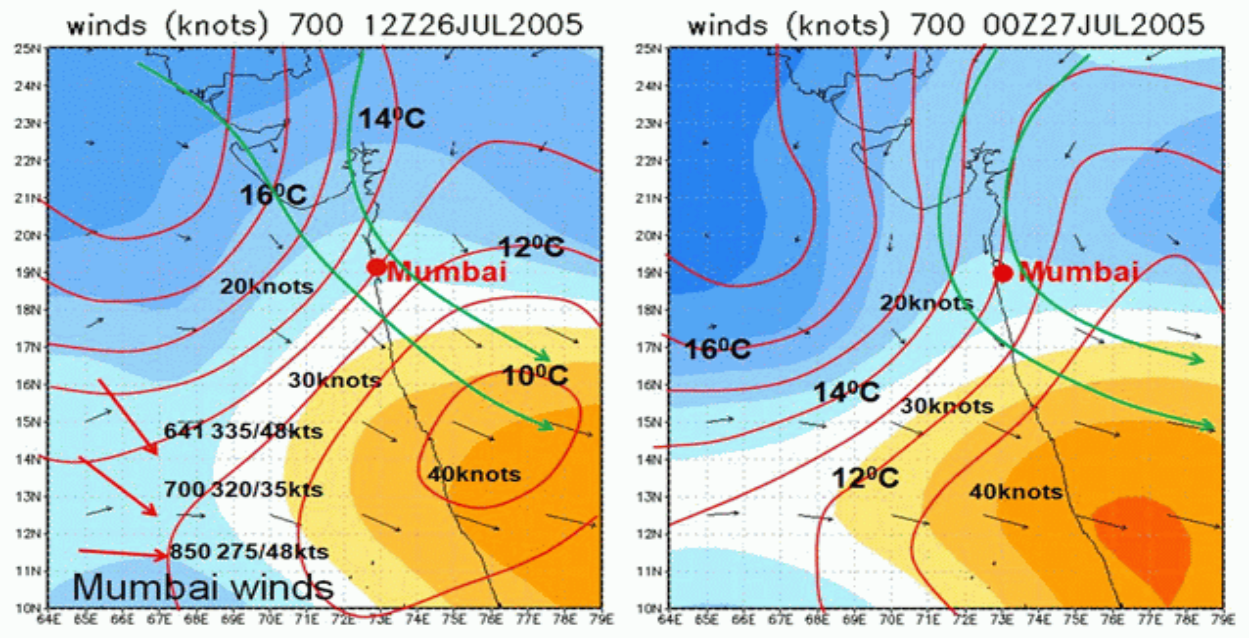

Figure 6.15. From NCEP/NCAR data the warm air advection at 700hPa through Mumbai is evident during the extreme rainfall. The warm air advection wind profile at Mumbai at 1200UTC 26 July 2005 is also shown.

6.8.3.5 Typhoon Chata'an disaster in the Chuuk Lagoon Islands, FSM

Typhoon Chata'an eventually reached super typhoon status; however, its major impact occurred during its early life when it was a tropical storm. The torrential rains of Tropical Storm Chata'an were particularly devastating to the lagoon high islands of Chuuk. A report dated from the Chuuk chapter of the Micronesian Red Cross Society indicated that the death toll was 48 with 73 persons injured. Over 1300 people were left homeless and 130 houses were completely destroyed. Heavy rain unleashed a total of 62 landslides, which caused much of the devastation. Some ranged up to 400-500 metres (1312-1640 ft) in length and were from 200-300 metres (656-984 ft) wide.

Figure 6.16 (top frames) covers the period of heavy rain and shows an area of warm air advection ascent on the western flank of Chata'an, which was aligned with the area of deep convection in the sector of Chata'an (lower frames). Over 500mm of rain was recorded at Chuuk as the area of convection on the western side of the storm passed over the islands. Figure 6.17 shows the clockwise turning with height wind profile at Chuck International airport as the convective complex moved over the island.

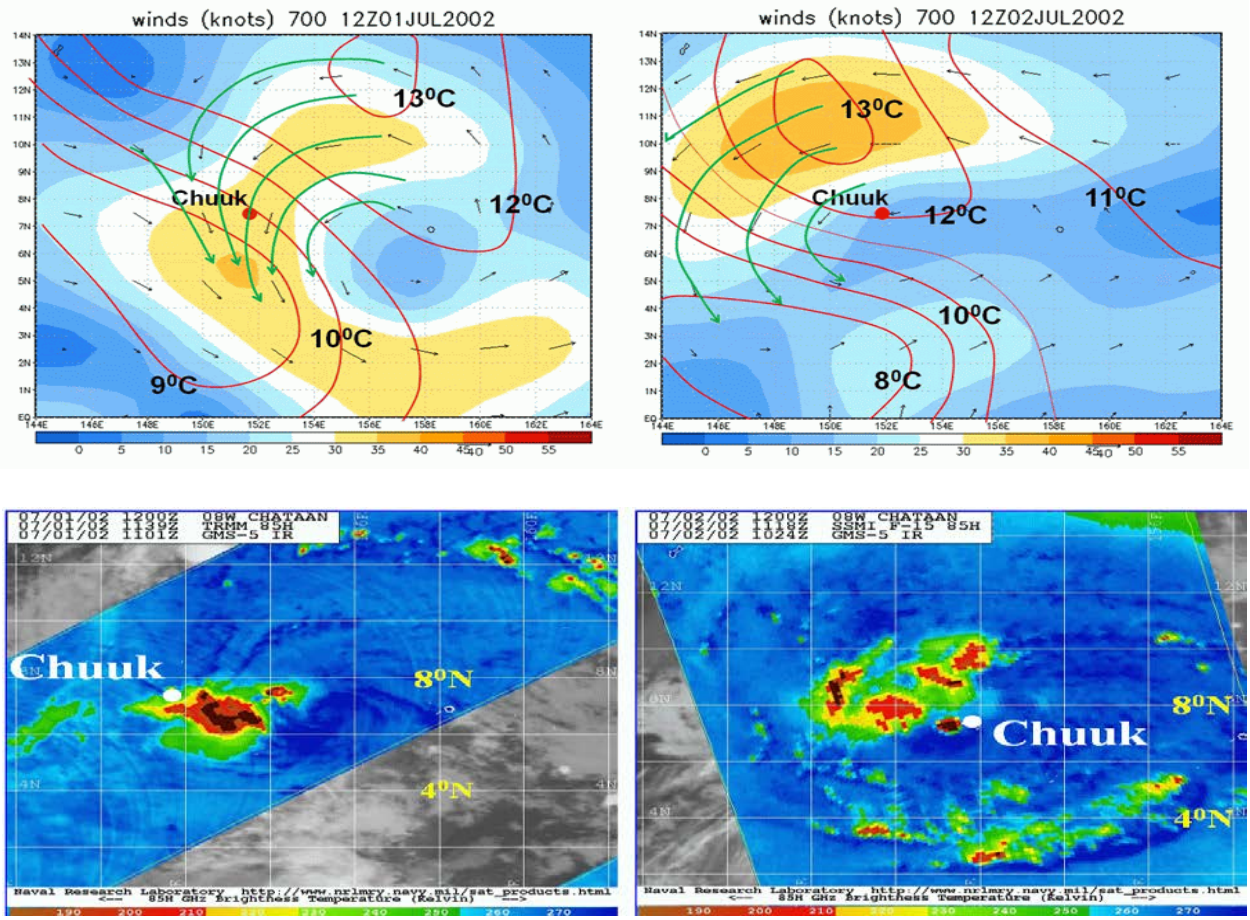

Figure 6.16. NCEP/NCAR 700hPa analysis of warm air advection (top) and corresponding horizontally polarised microwave images at 85GHz for 1139 UTC 1 July 2002 and 1118UTC 2 July 2002.

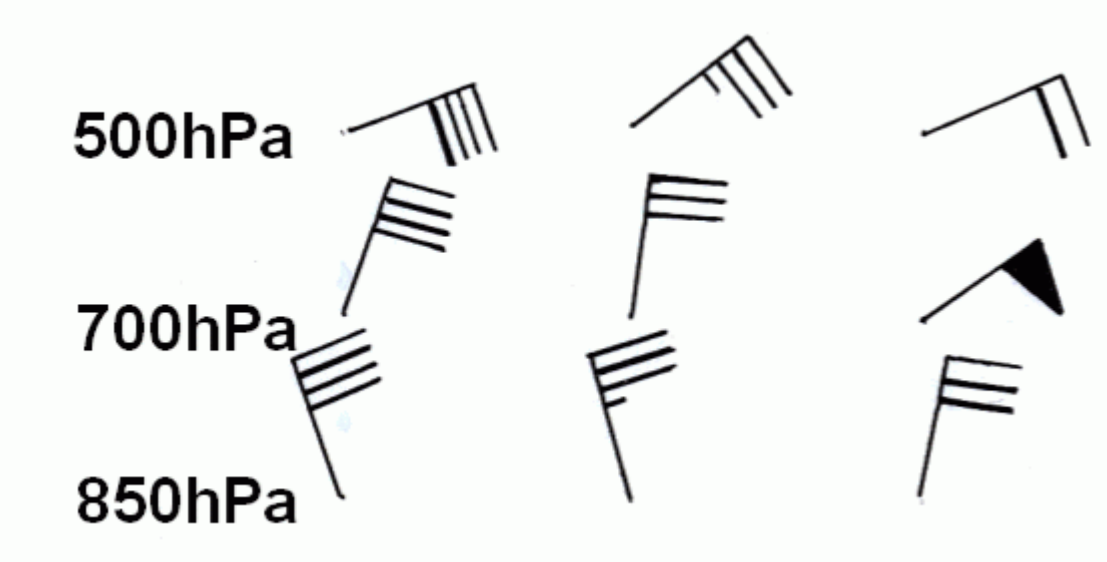

Figure 6.17. Upper winds at Chuuk Meteorological Office for 0600UTC, 1200UTC and 1800UTC 1 July 2002.

6.8.3.6 World record rainfall La Reunion

Finally, Figure 6.18 illustrates the warm air advection pattern during the world record 6-hourly rainfall event of 688mm (27.1 in) at La Reunion in 1993 (Barceló et al. 1997).

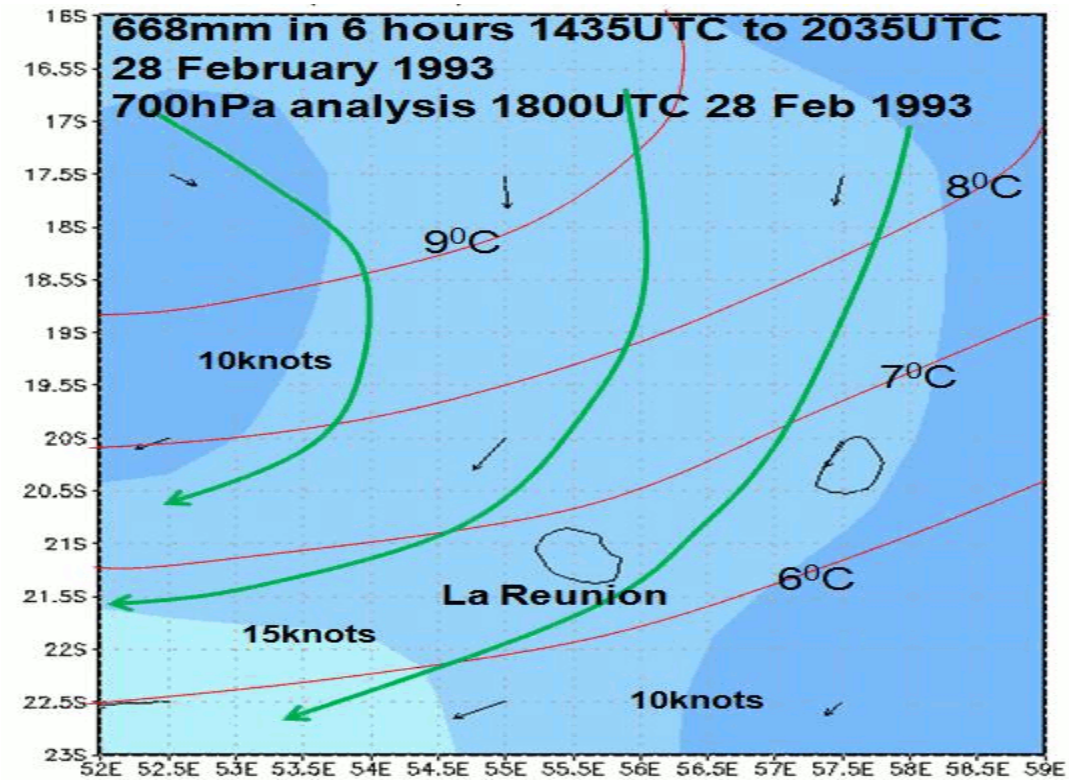

Figure 6.18. NCEP/NCAR 700hPa analysis of warm air advection during world record 6-hourly rainfall at La Reunion in 1993.

6.8.4 Some still pertinent forecast hints from the previous Global Guide

6.8.4.1. Quantitative prediction of tropical cyclone rainfall difficult for four reasons:

1. Rainfall itself is difficult to measure accurately, which hinders both operational analysis of rainfall and the development of improved forecasting aids;
2. Current errors in track prediction mean that accurate rainfall estimates cannot necessarily be transformed into precise predictions, this is especially a problem when a cyclone is moving near regions of significant orography;

3. Interactions between TCs and other weather systems are themselves complicated and poorly understood, so that heavy rain in areas of large-scale ascent and high humidity are difficult to predict;
4. Even within clearly defined threat areas, mesoscale processes, which are poorly understood and difficult to monitor, may determine the distribution of heavy rainfall.

6.8.4.2. Rainfall analysis and forecasting

Because of the meteorological complexity, measurement limitations, and lack of objective aids, analysis and forecasting of heavy rain associated with TCs can at best be indicative of likely outcomes. A suggested mode of operation is to first classify the situation as **uncomplicated** or **complicated**.

1. The TC is relatively well developed;

2. The TC is a day or less from landfall and is moving rapidly enough such that its precipitating region will pass over a given point completely within a day or less;

3. There are no topographic features within the path of the TC, which are significant enough to appreciably alter the rainfall;

4. There are no significant nearby weather systems, including frontal zones, jet streams, or upper-level cut-off lows, which are likely to interact with the TC during its passage inland.

Unfortunately, the majority of forecast situations near landfall involve rapid changes in the character and structure of the precipitation as the system moves inland and interacts with orography and other weather systems. Simple extrapolation procedures will not work very well and the situation is therefore **complicated**. About the best the forecaster can do in advance is to identify a general threat area based on the locations of the TC and surrounding weather systems. The actual locations of heavy rain must then be identified as the event proceeds in order to identify areas, which are accumulating dangerous amounts of rainfall. In the absence of dominating terrain, mesoscale processes such as the development of new convective cells at the merger of old convective outflow boundaries generally determine where within the threat area the heavy rain actually falls. If these mesoscale focusing mechanisms are quasi-stationary, extremely heavy rain may fall even though the convective elements are moving quickly.

6.8.4.3. Determining threat areas

Heavy rain threat areas should be revised at least every 12 hours. Threat areas can change. New threat areas can develop.

The heavy rain threat area for the time (analysis or prognosis) of interest is defined as the intersection of areas defined by surface and 850, 500, and 200 hPa features as listed below:

Satellite: The threat area always includes areas of current heavy convection.

Surface: The upstream edge of the threat area (relative to the surface flow) is one or more of the following: the edge of the coastal plain or beginning of terrain gradient, a frontal boundary, an outflow boundary from previous convection, or the upstream end of a surface convergence zone. The downstream edge is the 15oC isodrosotherm, or a mountain ridge line (beginning of downslope flow).

Tropical Cyclone Track: Add to the threat area the area along the forecast TC track and extending outward to the width of the current central dense overcast (CDO).

850 hPa: The threat area is a corridor 100-200 km (54-108 nmi) on either side of where the low-level jet crosses the surface threat area.

500 hPa: The threat area is beneath and upstream of the upper ridge and bounded to the west by the trough or upper low center.

200 hPa: Threat areas are in regions of jet streak divergence (left-front and right-rear of speed maxima in the northern hemisphere) and streamline diffluence.

The more of the above features present in a region, the greater the threat of heavy rain. The surface features should receive the maximum emphasis.

6.8.4.4. Monitoring the event

Use the rainfall rates every 1-2 hours or as often as imagery or measurements are available. Be especially alert for small, rapidly expanding cells as they typically produce much higher rain rates than large, impressive cloud shields, which are often mostly stratiform. Maintain a single map with positions of active cells from each estimate as this will indicate:

1) where large accumulations are probably occurring, and
2) preferred areas of redevelopment, which in conjunction with surface analyses, can help refine the threat areas.

6.9. References

Adams, I. S., M. H. Bettenhausen, and P. W. Gaiser, 2008: Passive Microwave Remote Sensing of Tropical Cyclones. *28th AMS Conference on Hurricanes and Tropical Meteorology*, Paper 14B.6.

Adler, R. F., and A. J. Negri, 1988: A satellite infrared technique to estimate tropical convective and stratiform rainfall. *J. Appl. Meteorol.*, **27**, 30-51.

Anagnostou, E. N., A. J. Negri, and R. F. Adler, 1999: A satellite infrared technique for diurnal rainfall variability studies. *J. Geophys. Res.*, **104**, 31477-31488.

Atallah, E.H., Bosart, L.F., and Aiyyer, A.R., 2007. Precipitation distribution associated with landfalling tropical cyclones over the eastern United States. *Mon. Weather Rev.* **135**, 2185-2206.

Barceló A., René Robert and Jean Coudray 1997. Major Rainfall Event: The 27 February-5 March 1993 Rains on the Southeastern Slope of Piton de la Fournaise Massif (Reunion Island, Southwest Indian Ocean). *Mon. Wea. Rev*.,**125**, 3341-3346

Bellerby, T., M. Todd, D. Kniveton, and C. Kidd, 2000: Rainfall estimation from a combination of TRMM Precipitation Radar and GOES Multispectral Satellite Imagery through the use of an artificial neural network. *J. Appl. Meteorol.*, **39**, 2115-2128.

Bellon, A., S. Lovejoy, and G. L. Austin, 1980: Combining satellite and radar data for the shortrange forecasting of precipitation. *Mon. Wea. Rev.*, **108**, 1554-1556.

Bonell, M., M. M. Hufschmidt, and J. S. Gladwell (editors), 2005: Hydrology and Water Management in the Humid Tropics: *Hydrological Research Issues and Strategies for Water Management*. Cambridge University Press, Cambridge, UK., 590 pp.

Bonell, M. and J. Callaghan, 2008: The synoptic meteorology of high rainfalls and the storm runoff response in the Wet Tropics, *Living in a Dynamic Tropical Forest Landscape*. N. Stork and S. Turton, Eds. Blackwell Press, 448 pp.

Brakenridge, R, and E. Anderson, 2006: MODIS-based Flood Detection, Mapping and Measurement: The Potential for Operational Hydrological applications. Transboundary Floods: Reducing Risks Through Flood Management, *NATO Science Series: IV: Earth and Environmental Sciences*, **72**, pp. 1-12.

Brennan, M. J., J. L. Clark, and M. Klein, 2008: Verification of Quantitative Precipitation Forecast Guidance from NWP Models and the Hydrometeorlogical Prediction Center for 2005-2007 Tropical Cyclones with Continental U.S. Rainfall Impacts. Poster Session P2H.9, *28th Conference on Hurricanes and Tropical Meteorology, American Meteorological Society*, Orlando, Florida, April 28-May 2.

Buckley, C. D., R. E. Hood, and F. J. LaFontaine, 2009: Application of Airborne Passive Microwave Observations for Monitoring Inland Flooding Caused by Tropical Cyclones. *J. Atmos. Oceanic Technol.*, **26** 2051-2070. doi: http://dx.doi.org/10.1175/2009JTECHA1273.1

Callaghan, J. and M. Bonell 2005a. Synoptic and mesoscale rain producing systems in the humid tropics. *Forests, Water and People in the Humid Tropics International Hydrological Series*, M. Bonell, and L. A. Bruijnzeel, Eds., Cambridge University Press, 925 pp.

Callaghan, J. and M. Bonell 2005b. An overview of the Meteorology and climatology of the humid tropics: *Forests, Water and People in the Humid Tropics International Hydrological Series*, M. Bonell, and L. A. Bruijnzeel, Eds., Cambridge University Press, 925 pp.

Chan, Johnny C. L. and Liang, X, 2003: Convective Asymmetries Associated with Tropical Cyclone Landfall. Part I: f-Plane Simulations. *J. Atmos. Sci.*, **60**, 1560-1576. doi: http://dx.doi.org/10.1175/1520-0469(2003)60<1560:CAAWTC>2.0.CO;2

Chan, S. T., and M.Y. Chan, 2010: applications of Satellite Rain Rate Estimates to the Prediction of Tropical Cyclone Rainfall. *42nd Session of ESCAP/WMO Typhoon Committee*, Singapore, 25-29 January 2010.

Chen, H., 2004: Extended Least Square Algorithm for Nonlinear Stochastic Systems. *ACC2004*, Boston. June 30-July 2, pp. 4758-4763.

Chen, S. S., J. A. Knaff, and F. R. Marks JR., 2006: Effects of Vertical Wind Shear and Storm Motion on Tropical Cyclone Rainfall Asymmetries Deduced from TRMM. *Mon. Wea. Rev.*, **134**, 3191-3208.

Cerveny, R. S., and L. E. Newman, 2000: Climatological Relationships between Tropical Cyclones and Rainfall. *Mon. Wea. Rev.*, **128**, 3329-3336. doi: http://dx.doi.org/10.1175/1520-0493(2000)128<3329:CRBTCA>2.0.CO;2

Cheung, K. K. W., L.-R. Huang, and C.-S. Lee, 2008: Characteristics of rainfall during tropical cyclone periods in Taiwan. *Nat. Hazards Earth Syst. Sci*.,**8**, 1463-1474. http://www.nat-hazards-earth-syst-sci.net/8/1463/2008/nhess-8-1463-2008.html doi:10.5194/nhess-8-1463-2008.

Ebert, E., A.E. Salemi, M. Turk, M. Spampata, S. Kusselson, 2009: Validation of the ensemble tropical rainfall Potential (e-TRaP) for landfalling tropical cyclones. *16th Conference on Satellite Meteorology and Oceanography*, AMS 89th Annual Meeting, Phoenix, AZ, 12-15 January 2009.

El-Nimri, S., S. AlSweiss, W. L. Jones, J. Johnson, and E. Uhlhorn, 2008: Hurricane Imaging Radiometer Wide Swath Simulation for Wind Speed and Rain Rate, *Proc. IEEE IGARSS-08*, Jul. 6 - 11, 2008, Boston, MA.
Also see: El-Nimri, Salem F., W. Linwood Jones, Eric Uhlhorn, Christopher Ruf, James Johnson, and Peter Black, An Improved C-Band Ocean Surface Emissivity Model at Hurricane-Force Wind Speeds over a Wide Range of Earth Incidence Angles, *IEEE Geosci. & Remote Sens. Letters*, **7 (4)**, pp. 641-645, Oct 2010.

Ferraro, R., P. Pellegrino, M. Turk, W. Chen, S. Qiu, R. Kuligowski, S. Kusselson, A. Irving, S. Kidder, and J. Knaff, 2005: The Tropical Rainfall Potential (TRaP) Technique. Part II: Validation. *Wea. Forecasting*, **20**, 465-475.

Fukami, K., N. Fujiwara, N. Fujiwara, M. Ishikawa, M. Kitano, T. Kitamura, T. Shimizu, S. Hironaka, S. Nakamura, T. Goto, M. Nagai, and S. Tomita, 2006: Development of an integrated flood runoff analysis system for poorly-gauged basins. *7th International Conference on Hydroinformatics (HIC)*, Nice, France, September 2006.

Gao, S., Z. Meng, F. Zhang, and L. F. Bosart, 2009: Observational analysis of heavy rainfall mechanisms associated with severe Tropical Storm Bilis (2006) after its landfall. *Mon. Wea. Rev.*, **137**, 1881-1897.

Griffith, C. G., W. L. Woodley, P. G. Grube, D. W. Martin, J. Stout, and D. N. Sikdar, 1978: Rainestimation from geosynchronous satellite imagery - Visible and infrared studies. *Mon. Wea. Rev.*, **106**, 1153-1171.

Grody, N. C., 1984: Precipitation monitoring over land from satellites by microwave radiometry. *Proc. IGARSS' 84 Symposium*, Strasbourg, 27-30 August.

Grody, N. C., F. Weng, and R. R. Ferraro, 1999: Application of AMSU for obtaining hydrological parameters. *Microwave Radiometry and Remote Sensing of the Environment*, P. Pampaloni and S. Paloscia Ed., VSP Int. Sci. Publisher, Utrecht (The Netherlands), 339-351.

Gruber, A.,1973: Estimating rainfall in regions of active convection. *J. Appl. Meteorol.*, **12**, 110-118.

Haddad, Z., E. A. Smith, C. D. Kummerow, T. Iguchi, M. Farrar, S. Darden, M. Alves, and W. Olson, 1997: The TRMM 'Day-1' radar/radiometer combined rain-profile algorithm. *J. Meteor. Soc. Japan*, **75**, 799-808.

Harville, S. L., 2009: Effects of Appalachian topography on precipitation from landfalling hurricanes.*MS thesis, North Carolina State University*, 320pp. (Available from http://repository.lib.ncsu.edu/ir/handle/1840.16/2849)

Hood, R. E., R. Atlas, P. Black, S. S. Chen, C. C. Hennon, J. W. Johnson, L. Jones, T. L. Miller, C. S. Ruf, and E. W. Uhlhorn, 2008: An overview of the Hurricane Imaging Radiometer (HIRAD). *28th AMS Conference on Hurricanes and Tropical Meteorology*, April 28 - May 2, 2008, Orlando, FL. Also see: Hood, R. Amarin, M. Bailey, P. Black, M. James, J. Johnson, L. Jones, B. Lim, C. Ruf, K. Stephens, and V. Rohwedder, 2007: Development of the Hurricane Imaging Radiometer (HIRAD) Using a Systems Engineering Approach. *61st Interdepartmental Hurricane Conference*, March 5-9, 2007, New Orleans, LA.

Hossain, A.N.H. Akhtar, 2004: Flood Management: Issues and Options. Presented in the *International Conference organized by the Institute of Engineers*, Bangladesh.

Hsu, K., X. G. Gao, S. Sorooshian, and H. V. Gupta, 1997: Precipitation estimation from remotely sensed information using artificial neural networks. *J. Appl. Meteor.*, **36**, 1176-1190.

Iguchi, T., T. Kozu, R. Meneghini, J. Awaka, and K. Okamoto, 2000: Rain-profiling algorithm for the TRMM precipitation radar. *J. Appl. Meteorol.*, **39**, 2038-2052.

Jiang, H., G. Feingold, and W. R. Cotton (2002), Simulations of aerosol-cloud-dynamical feedbacks resulting from entrainment of aerosol into the marine boundary layer during the Atlantic Stratocumulus Transition Experiment, *J. Geophys. Res.*, **107(D24)**, 4813.

Jiang, H., P. G. Black, E. J. Zipser, F. D. Marks Jr., and E. W. Uhlhorn, 2006: Validation of Rain-Rate Estimation in Hurricanes from the Stepped Frequency Microwave Radiometer: Algorithm Correction and Error Analysis. *J. Atmos. Sci.*, **63**, 252-267. doi: http://dx.doi.org/10.1175/JAS3605.1
Also see: Jiang, J. H., B. Wang, K. Goya, K. Hocke, S. F. Eckermann, J. Ma, D. L. Wu, and W. G. Read, 2004: Geographical distribution and interseasonal variability of tropical deep convection: UARS MLS observations and analyses. *J. Geophys. Res.*, **109**.D03111, doi:10.1029/2003JD003756.

Jiang, H., and E. J. Zipser, 2010: Contribution of Tropical Cyclones to the Global Precipitation from Eight Seasons of TRMM Data: Regional, Seasonal, and Interannual Variations. *J. Climate*, **23**, 1526-1543. doi: http://dx.doi.org/10.1175/2009JCLI3303.1

Joyce, R. J., J. E. Janowiak, P. A. Arkin, and P. Xie, 2004: CMORPH: A method that produces global precipitation estimates from passive microwave and infrared data at high spatial and temporal resolution, *J. Hydrometeorol.*, **5**, 487-503.

Kidd, C., 1998: On rainfall retrieval using polarization-corrected temperatures. *Int. J. Remote Sensing*, **19**, 981-996.

Kidder, S. Q., J. A. Knaff, S. J. Kusselson, M. Turk, R. R. Ferraro, and R. J. Kuligowski, 2005: The tropical rainfall potential (TRaP) technique. Part I: Description and examples. *Wea. Forecasting*, **20**, 456-464.

Krishnamurti, T. N., T. N., A. K. Mishra, A. Chakraborty, and M. Rajeevan, 2009a: Improving global model precipitation forecasts over India using downscaling and the FSU superensemble. Part I: 1-5-day forecasts. *Mon. Wea. Rev.*, **137**, 2713-2735.

Krishnamurti, T. N., A. D. Sagadevan, A. Chakraborty, A. K. Mishra, A. Simon, 2009b: Improving multimodel weather forecast of monsoon rain over China using FSU superensemble. *Advances in Atmospheric Sciences*, **26**, pp 813-839.

Lai, E. S. T., and W. K. Wong, 2006: Quantitative Precipitation Nowcast of Tropical Cyclone Rainbands Case Evaluation in 2006. Hong Kong Observatory.

Lambrigtsen, B., T. Gaier, P. Kangaslahti, and A. Tanner, 2008: A Geostationary Microwave Sounder for NASA and NOAA. Jet Propulsion Laboratory, California Institute of Technology. https://cimss.ssec.wisc.edu/itwg/itsc/itsc16/proceedings/B31_Lambrigtsen.pdf

Levizzani,V., R. Amorati, and F. Meneguzzo, 2002: A Review of Satellite-based Rainfall Estimation Methods. MUltiple-Sensor Precipitation Measurements, Integration, Calibration and Flood Forecasting (MUSIC) Project. EVK1-CT-2000-00058 Deliverable 6.1 04/02/2002.

Li, P.W., W.K. Wong, K.Y. Chan, and Edwin S.T. Lai, 2000: SWIRLS - An Evolving Nowcasting System.*Hong Kong Observatory Technical Note, No.100*.

Li, P. W., and E. S. T. Lai, 2004: Short-range quantitative precipitation forecasting in Hong Kong, *J. Hydrology*, **288**, 189-209.

Lonfat, M., F. D. Marks, and S. S. Chen, 2004: Precipitation Distribution in Tropical Cyclones Using the Tropical Rainfall Measuring Mission (TRMM) Microwave Imager: A Global Perspective. *Mon. Wea. Rev.*, **132**, 1645-1660.

Lonfat, M., R. Rogers, T. Marchok, and F. D. Marks, Jr., 2007: A parametric model for predicting hurricane rainfall. *Mon. Weather Rev.*, **135**, 3086- 3097. doi:10.1175/MWR3433.1.

Lovejoy, S., and G. L. Austin, 1979: The delineation of rain areas from visible and IR satellite data from GATE and mid-latitudes. *Atmos.-Ocean*, **17**, 77-92.

Marchok, T., R. Rogers, and R. Tuleya, 2007: Validation schemes for tropical cyclone quantitative precipitation forecasts: Evaluation of operational models for US landfalling cases. *Wea. Forecasting*, **22**. DOI: 10.1175/WAF1024.1

Marks, F. D., G. Kappler, and M. DeMaria, 2002: Development of a Tropical Cyclone Rainfall Climatology and Persistence (R-CLIPER) Model. Reprints of the *25th Conference on Hurricanes and Tropical Meteorology*, AMS, San Diego, CA.

Marks, F. D., 2003: State of the Science: Radar View of Tropical Cyclones. *Meteorological Monographs*, **30**.

Medlin, J. M., S. K. Kimball, and K. G. Blackwell, 2007: Radar and rain gauge analysis of the extreme rainfall during hurricane Danny's (1997) landfall. *Mon. Wea. Rev.*, **135**, 1869-1888.

Miller, S. W., P. A. Arkin, and R. J. Joyce, 2000: A combined microwave/infrared rain rate algorithm.*Int. J. Remote Sens.*, **22**, 3285-3307.

Mishra, A. K., and T. N. Krishnamurti, 2007: Current status of multimodel Superensemble and operational NWP forecast of the Indian summer monsoon. *Journal of Earth System Science*, **116(5)**, 369-384.

Negri, A. J., R. F. Adler, and P. J. Wetzel, 1984: Rain estimation from satellite: An examination of the Griffith-Woodley technique. *J. Climate Appl. Meteorol.*, **23**, 102-116.

Porcù, F., M. Borga, and F. Prodi, 1999: Rainfall estimation by combining radar and infrared satellite data for nowcasting purposes. *Meteorol. Appl.*, **6**, 289-300.

Quinlan, K. R., 2008: Conditions influencing Hurricane Emily's (2005) precipitation patterns, convection, and upper tropospheric outflow. *M.S. thesis, Department of Atmospheric Science, University of Alabama in Huntsville*, 116 pp.

Randall S. Cerveny and Lynn E. Newman, 2000: Climatological Relationships between Tropical Cyclones and Rainfall. *Mon. Wea. Rev.*, **128**, 3329–3336.

Ritchie, E. A., and D. Szenasi, 2006: The Impact of Tropical Cyclone Remnants on the Rainfall of the North American Southwest Region. Preprints, *27th Conf. on Hurricanes and Tropical Meteorology* P2.4, Monterey, CA. Amer. Meteor. Soc.

Rodgers, E. B., R. F. Adler, and H. F. Pierce, 2000: Contribution of tropical cyclones to the North Pacific climatological rainfall as observed from satellites. *J. Appl. Meteor.*, **39**, 1658-1678.

Rodgers, E. B., R. F. Adler, and H. F. Pierce, 2001: Contribution of Tropical Cyclones to the North Atlantic Climatological Rainfall as Observed from Satellites. *J. Appl. Meteor.*, **40**, 1785-1800. doi: http://dx.doi.org/10.1175/1520-0450(2001)040<1785:COTCTT>2.0.CO;2

Sandholt, I., L. Nyborg, B. Fog, M. Lô, O. Bocoum, and K. Rasmussen, 2003: Remote sensing techniques for flood monitoring in the Senegal River Valley, *Danish Journal of Geography*, **103 (1)**, 71-81.

Shong, 2006: Shuanzhu Gao, Zhiyong Meng, Fuqing Zhang and Lance F. Bosart, 2009: Observational Analysis of Heavy Rainfall Mechanisms Associated with Severe Tropical Storm Bilis (2006) after its Landfall. *Mon. Wea. Rev.*, **137**, 1881-1897.

Smith, R. K., M. T. Montgomery, and S. Vogt, 2008: A critique of Emanuel's hurricane model and potential intensity theory. *Q. J. R. Meteorol. Soc.*, **134**, 551-561.

Smith, R. B., P. Schafer, D. Kirshbaum, and E. Regina, 2009: Orographic Enhancement of Precipitation inside Hurricane Dean. *J. Hydrometeor*, **10**, 820-831. doi: http://dx.doi.org/10.1175/2008JHM1057.1

Sorooshian, S., K.-L. Hsu, X. Gao, H. V. Gupta, B. Imam, and D. Braithwaite, 2000: Evaluation of PERSIANN system satellite–based estimates of tropical rainfall. *Bull. Am. Meteor. Soc.*,**81**, 2035–2046.

Sugiura, T., Fukami, K., Fujiwara N., Hamaguchi, K., Nakamura, S., Hironaka, S., Nakamura, K., Wada, T., Ishikawa, M., Shimizu, T., Inomata, H., Itou, Z., 2010 (2009 in text): "Experimental application of flood forecasting system (IFAS) using satellite-based rainfall." *Ninth International Conference on Hydroingormatics*. Tianjin, China: HIC2010. 1786-1793.
Also see: Sugiura, A., S. Fujioka, S. Nabesaka, T. Sayama, Y. Iwami, K. Fukami, S. Tanaka and K.Takeuchi, 2013: Challenges on modelling a large river basin with scarce data: A case study of the Indus upper catchment. *20th International Congress on Modelling and Simulation*, Adelaide, Australia, 1-6 December 2013. http://www.mssanz.org.au/modsim2013

Tang, Q., and L. Xie, 2008: Modelling inland flooding due to tropical cyclones. *28th Conference on Hurricanes and Tropical Meteorology, American Meteorological Society*, Orlando, Florida, April 28-May 2, 2008.

Todd, M. C., C. Kidd, D. Kniveton, and T. J. Bellerby, 2001: A combined satellite infrared and passive microwave technique for estimation of small-scale rainfall. *J. Atmos. Oceanic Technol.*, **18**, 742-755.

Tory, K., 2015: (in press). *Australian Meteorological and Oceanographic Journal*

Tuleya, R. E., M. DeMaria, and R. J. Kuligowski (2007): Evaluation of GFDL and simple statistical model rainfall forecasts for U.S. landfalling tropical storms. *Wea. Forecasting,* **22**, 56-70

Turk, F. J., F. S. Marzano, and E. A. Smith, 1998: Combining geostationary and SSM/I data for rapid rain rate estimation and accumulation. Prepr. *9th Conf. Satellite Meteorology and Oceanography*, AMS, 462-465.

Turk, F. J., J. Hawkins, E. A. Smith, F. S. Marzano, A. Mugnai, and V. Levizzani, 2000: Combining SSM/I, TRMM and infrared geostationary satellite data in a near-realtime fashion for rapid precipitation updates: advantages and limitations. *Proc. The 2000 EUMETSAT Meteorological Satellite Data Users' Conference*, 452-459

Vicente, G. A., and R. A. Scofield, 1996: Experimental GOES-8/9 derived rainfall estimates for flash flood and hydrological applications. *Proc. The 1996 EUMETSAT Meteorological Satellite Data Users' Conf.*, EUMETSAT, 89-96.

Wang, Y., Y. Wang, and H. Fudeyasu, 2009: The Role of Typhoon Songda (2004) in Producing Distantly Located Heavy Rainfall in Japan. *Mon. Wea. Rev.,* **137**, 3699-3715.

Wu, C.-C., K. K. W. Cheung, and Y.-Y. Lo, 2009: Numerical study of the rainfall event due to the interaction of Typhoon Babs (1998) and the northeasterly monsoon, *Mon. Weather Rev.,* **137**, 2049-2064, doi:10.1175/2009MWR2757.1.

Wylie, D. P., 1979: An application of a geostationary satellite rain estimation technique to an extra-tropical area. *J. Appl. Meteorol.*, **18**, 1640-1648.

Yamashiki, Y., Tsujimura, M., 2009: Special Issue: Japan Society of Hydrology and Water Resources - Annual Issue VIII. *Hydrological Processes,* **23 (4)**, pp. 523-647. ISSN0885-6087 DOI10.1002/hyp.7181.

Yokoyama, C., and Y. N. Takayabu, 2008: A statistical study on rain characteristics of tropical cyclones using TRMM satellite data. *Mon. Wea. Rev.,* **136**, 3848-3862.

Chapter Seven

Phillip J. Klotzbach
Department of Atmospheric Science, Colorado State University,
Fort Collins, CO, USA
E-mail: philk@atmos.colostate.edu
Anthony Barnston
Suzana Camargo
Lamont-Doherty Earth Observatory, The Earth Institute at Columbia University,
Palisades, NY, USA
E-mail: suzana@ldeo.columbia.edu
Johnny C. L. Chan
Laboratory for Atmospheric Research and Guy Carpenter Asia-Pacific Climate Impact Centre
Kowloon, Hong Kong, China
E-mail: johnny.chan@cityu.edu.hk
Adam Lea
Tropical Storm Risk, University College London,
London, United Kingdom
E-mail: al@mssl.ucl.ac.uk
Mark Saunders
Tropical Storm Risk, University College London,
London, United Kingdom
E-mail: mas@mssl.ucl.ac.uk
Frédéric Vitart
European Centre for Medium-Range Weather Forecasts
Reading, United Kingdom
E-mail: frederic.vitart@ecmwf.int

7. Seasonal Forecasting of Tropical Cyclones

7.1 Introduction

Not long ago, scientists only dreamed of making confident and reliable seasonal hurricane forecasts. These dreams are now a reality, thanks to tremendous technological increases over the last thirty years along with an improved knowledge of the global climate system. The first seasonal hurricane forecasts for the North Atlantic basin were issued in 1984 (Gray 1984b), and by 2007, seasonal forecasts had expanded to include every major hurricane region in the world (see Table 7.1, adapted from Camargo et al. 2007a). Several of the seasonal forecasts are discussed in this chapter, while the others are briefly discussed in Camargo et al. (2007a).

Table 7.1. Agencies that issue forecasts for various tropical cyclone basins.

	North Atlantic	Eastern North Pacific	Central North Pacific	Western North Pacific	Australia Region	North Indian Ocean	South Indian Ocean	South Pacific Ocean
City University of Hong Kong, China				x Statistical				
Colorado State University, USA	x Statistical							
Cuban Meteorological Institute, Cuba	x Statistical							
European Centre for Medium-Range Weather Forecasts, England	x Dynamical	x Dynamical		x Dynamical	x Dynamical	x Dynamical	x Dynamical	x Dynamical
International Research Institute for Climate and Society, USA	x Dynamical	x Dynamical		x Dynamical	x Dynamical			x Dynamical
Macquarie University, Australia					x Statistical			x Statistical
National Meteorological Service, Mexico		x Statistical						
National Climate Centre, China				x Statistical				
NOAA Climate Prediction Center, USA	x Statistical	x Statistical	x Statistical					
Tropical Storm Risk, England	x Statistical			x Statistical	x Statistical			

Several technological advances were needed before seasonal hurricane forecasts could become widespread. One advance came in the form of a major reanalysis project carried out in 1996 by the U.S. National Atmospheric and Oceanic Administration (NOAA) and the National Center for Atmospheric Research (NCAR) (Kalnay et al. 1996). The NCEP/NCAR reanalysis project, utilizing a sophisticated global climate model, produced homogeneous and global datasets of wind, pressure, and temperature at 6-hourly intervals dating back to 1948. For the first time, the available climate record was no longer plagued by discontinuities that occurred each time an improved data analysis package and numerical forecast model was implemented.

Another major advance came with the development of global climate models which were used not only to do the reanalysis but also to provide near real-time updates of global climate conditions. Now, ever-improving technologies such as satellites, computers, land-based observation systems, and model-based forecasts and analyses are routinely used by forecasters and researchers throughout the world.

But more than just better data and technology were needed before a seasonal hurricane outlook could be made. Fundamental breakthroughs in our understanding of the dominant climate factors influencing seasonal hurricane activity were also needed. The first major breakthrough came in 1984 with the pioneering research of Dr. William Gray, who discovered that the El Niño / Southern Oscillation (ENSO) strongly influenced year-to-year fluctuations in Atlantic hurricane activity (Gray 1984a,b). Using this research, Gray made the first seasonal Atlantic hurricane outlook in that same year at Colorado State University (CSU), and his team has been issuing outlooks ever since.

Another breakthrough came in the 1990's when scientists established that multi-decadal fluctuations in Atlantic hurricane activity were more than simply a random collection of above-normal or below-normal seasons. Instead, they were explained by predictable, large-scale climate factors that included multi-decadal fluctuations in Atlantic SSTs (called the Atlantic Multi-decadal Oscillation, Gray et al. 1996, Landsea et al. 1999) and the West African monsoon system (Hastenrath 1990, Gray 1990, Landsea and Gray 1992, Landsea et al., 1992, Goldenberg and Shapiro 1996).

Utilizing the reanalysis dataset, Bell and Chelliah (2006) showed that inter-annual and multi-decadal extremes in Atlantic hurricane activity resulted from a coherent and inter-related set of atmospheric and oceanic conditions associated with the leading modes of tropical climate variability. These modes were shown to be directly related to fluctuations in tropical convection, thereby linking Atlantic hurricane activity, West African monsoon rainfall, and Atlantic sea-surface temperatures, to tropic-wide climate variability. Based on this work, NOAA's Climate Prediction Center (CPC) began issuing seasonal Atlantic hurricane outlooks in August 1998, followed by seasonal East Pacific outlooks in 2004. At the same time, forecasters throughout the world were developing seasonal hurricane predictions for other major hurricane regions (Table 7.1).

Seasonal hurricane outlooks are based on either statistical, dynamical, or a blend of statistical and dynamical, procedures. Both the statistical and dynamical approaches bring a wide spectrum of forecast techniques to bear on the seasonal hurricane forecast problem. Some techniques are purely objective. Others are a subjective blend of selected statistical and dynamical techniques. Regardless of the technique or the way the forecast is communicated, seasonal hurricane forecasts are all probabilistic in nature. Forecasters try to give the best estimate of the likely (most probable) upcoming activity, while at the same time recognizing there are uncertainties inherent in all seasonal forecast techniques.

Three main statistical techniques are presently in use. One approach first utilizes statistical regression equations to predict the likely strength of key atmospheric and oceanic anomalies. This is done by either directly predicting their strength, or by first predicting the dominant climate patterns that strongly control their strength. A second set of regression equations is then used to predict the likely seasonal activity associated with the expected anomalies.

A second and complementary statistical approach utilizes a climate-based binning technique, wherein the historical distribution of activity associated with the predicted climate conditions is isolated. This climate-based analog approach allows the forecaster to focus only on those seasons having similar climate conditions, and differs from the pure regression equations that are often derived using all seasons and therefore all sets of climate conditions.

A third statistical approach developed by NOAA for use in their 2008 forecasts utilizes regression equations that relate coupled ocean-atmosphere dynamical climate model forecasts of key atmospheric and oceanic anomalies to the observed seasonal activity. In this way, dynamical predictions can be utilized to forecast the upcoming seasonal activity without a direct count of the exact number of named storms and hurricanes produced by the model. A second dynamical approach is to directly count the number of named storms a given climate model predicts (e.g., Vitart et al. 1997, Camargo et al. 2005).

Although seasonal hurricane forecasts have expanded greatly in recent years, there are many long-term challenges ahead. Some challenges are related to the observed hurricane data itself. In many regions, accurate hurricane records do not exist before satellites became widespread in the 1970s. In the Atlantic, more accurate records date back to the late 1940s with the beginning of aircraft reconnaissance.

Other challenges involve developing long-term statistical regression equations from reanalysis data that extends back only to 1948. Also, there are biases within the Reanalysis itself, which are related to the evolution of observing systems in recent years (Ebisuzaki et al. 1997, Kistler et al. 2001). These include global satellite coverage, extensive buoy placements in the Pacific and Atlantic Ocean, and an expanded radiosonde network in tropical regions.

Still other forecast challenges are related to accurate dynamical seasonal predictions of the key circulation and sea-surface temperature anomalies. While dynamical models have improved tremendously in recent years, they all contain large biases and errors that limit their use. For example, one major forecast uncertainty inherent to all climate models is tropical convection.

Yet, two dominant climate factors influencing seasonal Atlantic hurricane activity (ENSO and the Multi-decadal signal), which are also leading modes of tropical variability, are both intimately linked to changing large-scale patterns of tropical convection. ENSO predictions are especially critical, as ENSO has been shown to have a dramatic impact on tropical cyclone activity around the globe. As a result, ENSO predictions remain a main source of uncertainty for seasonal hurricane forecasts.

Another uncertainty common to all forecast techniques is weather patterns that are unpredictable on seasonal time scales, yet can sometimes develop and last for weeks or months, possibly affecting seasonal hurricane activity. A third source of forecast uncertainty is that the numbers of named storms and hurricanes can sometimes vary considerably for the same set of climate conditions. For example, one cannot know with certainty whether a given set of climate conditions will be associated with several short-lived storms or fewer longer-lived storms with greater intensity.

Making seasonal hurricane landfall forecasts is perhaps the most sought-after goal of seasonal hurricane forecasters. Unfortunately, an ongoing consequence of these challenges and uncertainties is the present very limited ability to make such forecasts accurately, confidently, and reliably. Compounding the challenge is the fact that hurricane landfalls are largely determined by the weather patterns in place at the time the hurricane approaches, which are generally not predictable more than 5-7 days in advance.

Hurricane experts and emergency management officials throughout the world know that hurricane disasters can occur regardless of the activity within a season. They encourage residents, businesses, and government agencies of coastal and near-coastal regions to prepare for every hurricane season regardless of the seasonal outlook. It only takes one hurricane (or even a tropical storm) to cause a disaster.

In the next few sections, several of the seasonal forecast methodologies currently in use for forecasting tropical cyclone activity in various basins around the globe are discussed in detail. Several other forecast methodologies are also discussed in Camargo et al. (2007a).

7.2 Colorado State University seasonal hurricane outlooks

Colorado State University (CSU) has been issuing seasonal predictions of Atlantic basin tropical cyclone activity since 1984 (Gray 1984a, b). These forecasts are issued at four lead times prior to the active part of the Atlantic basin hurricane season: in early December, in early April, in early June and in early August. Real-time forecasts of named storms in early June have correlated at 0.57 with observations over the period from 1948-2007. The statistical models utilized by the CSU forecast team to make their predictions have undergone considerable modifications in recent years. Instead of attempting to individually hindcast indices such as named storms, named storm days, major hurricanes, etc., they have developed a technique that shows significant skill at hindcasting Net Tropical Cyclone (NTC) activity (Gray et al. 1994) and then empirically deriving these other indices from the NTC prediction. Also, for the early April, June

and August techniques, earlier seasonal forecasts are weighted at 50%, 50% and 40%, respectively when developing the final forecast (Figure 7.1). In the next few paragraphs, each forecast will be briefly discussed, with references provided for more extensive discussion.

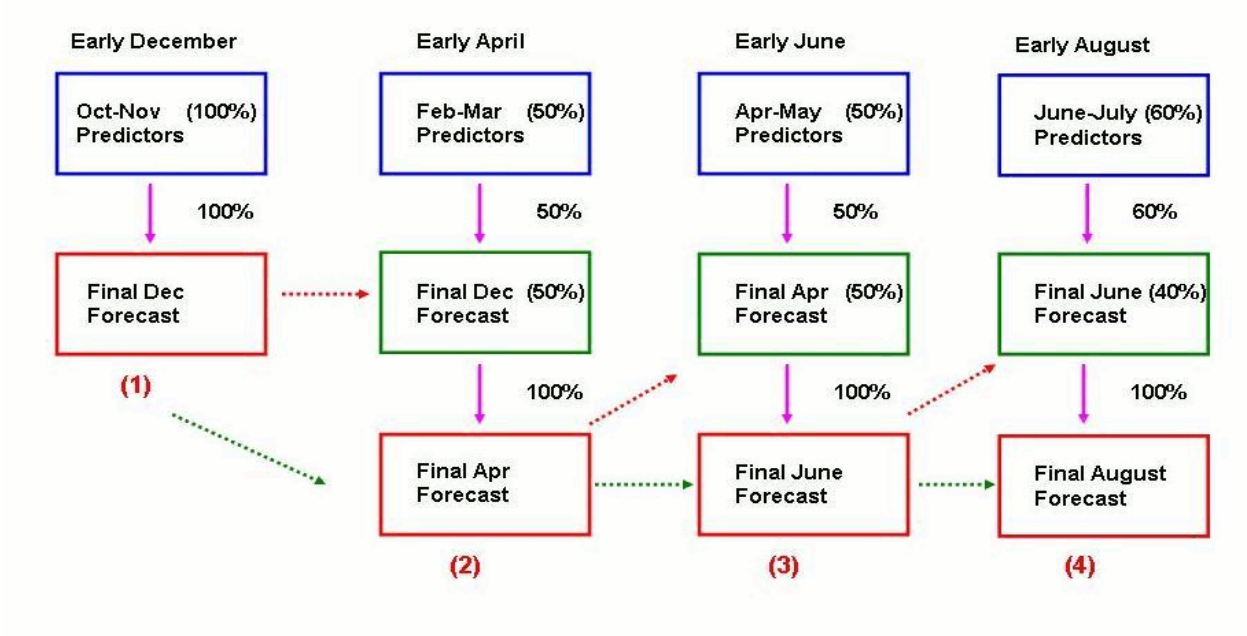

Figure 7.1. The new methodology utilized by CSU in calculating statistical forecasts of seasonal NTC.

December forecast

Initial predictions of seasonal hurricane activity from early December were issued by Gray and colleagues in December 1991 for the 1992 hurricane season (Gray et al. 1992). This model has undergone significant revisions since it was initially developed (Klotzbach and Gray 2004). Following the unsuccessful seasonal hurricane forecasts of the past few years, a new December forecast model has been developed (Klotzbach 2008). This model, as is done with the April, June and August models, was built over the period from 1950-1989 and then the equations developed over the period from 1950-1989 were tested on the years from 1990-2007 to determine if the model showed similar levels of skill in the more recent period. Table 7.2 displays the current predictors utilized in the new December statistical model.

Table 7.2. Listing of current early December predictors. A plus (+) means that positive values of the parameter indicate increased hurricane activity during the following year.

Predictor	Location
1) October-November SST (+)	(55-65°N, 60-10°W)
2) November 500 hPa geopotential height) (+)	(67.5-85°N, 50°W-10°E)
3) November SLP (+)	(7.5-22.5°N, 175-125°W)

The forecast is created by combining the three December predictors using least-squared linear regression over the period from 1950-2007. The resulting hindcasts are then ranked in order from 1 (the highest value) to 58 (the lowest value). The final NTC hindcast was obtained by taking the final December NTC hindcast rank and assigning the observed NTC value for that rank. For example, if the final December NTC hindcast rank was 10 (the 10th highest rank), the NTC value assigned for the prediction would be the 10th highest observed rank, which in this case would be 166 NTC units. Final hindcast values are constrained to be between 40 and 200 NTC units. When the rank prediction model is utilized, 54% of the variance in NTC is hindcast over the period from 1950-2007.

April forecast

April forecasts are currently issued using a similar methodology to what was used in early December (Klotzbach and Gray 2008a). Two February-March predictors were selected that explained a considerable amount of variability in NTC (Table 7.3). These predictors were then ranked and combined with the early December prediction to come up with a final seasonal NTC hindcast. 64% of the variance in NTC is hindcast over the period from 1950-2007 using the April hindcast model.

Table 7.3. Listing of current early April predictors. A plus (+) means that positive values of the parameter indicate increased hurricane activity.

Predictor	**Location**
1) February-March SST Gradient (+)	(30-45°N, 30-10°W) - (30-45°S, 45-20°W)
2) March SLP (-)	(10-30°N, 30-10°W)
2) Early December Hindcast (+)	

June forecast

Early June forecasts are currently issued using two April-May predictors combined with the early April hindcast values (Klotzbach and Gray 2008b) (Table 7.4). 66% of the variance in NTC is hindcast over the period from 1950-2007 using the June hindcast model.

Table 7.4. Listing of current early June predictors. A plus (+) means that positive values of the parameter indicate increased hurricane activity.

Predictor	**Location**
1) Subtropical Atlantic Index (+): April-May SST (+) & May SLP (-)	(20-50°N, 30-15°W) (10-35°N, 40-10°W)
2) April-May 200 hPa U (-)	(5-25°S, 50-90°E)
3) Early June Hindcast (+)	

August forecast

A final seasonal forecast update is issued in early August, prior to the climatologically most active part of the Atlantic hurricane season. The new August statistical model utilizes a combination of four predictors which show significant skill back to the start of the 20th century (Table 7.5) (Klotzbach 2007). When these predictors are combined with the early June hindcast, approximately 65% of the post-1 August variance in NTC activity can be explained. Brief descriptions of how each predictor likely impact Atlantic basin hurricane activity follow.

Table 7.5. Listing of current early August predictors. A plus (+) means that positive values of the parameter indicate increased hurricane activity.

Predictor	Location
1) June-July SST (+)	(20-40°N, 35-15°W)
2) June-July SLP (-)	(10-20°N, 60-10°W)
3) June-July SST (-)	(5°S-5°N, 150-90°W)
4) Before 1 August Tropical Atlantic Named Storm Days (+)	(South of 23.5°N, East of 75°W)
5) Early June Hindcast (+)	

Discussion

The revised statistical models developed by CSU over the past several years put more of an emphasis on understanding physical links between individual predictors and Atlantic tropical cyclone activity. Also, the new models have been developed over the period from 1950-1989, leaving aside the past 18 years for quasi-independent testing. The more concrete physical links combined with increased statistical rigor should lead to improved skill in future years.

7.3 NOAA seasonal hurricane outlooks

NOAA began issuing probabilistic seasonal outlooks for the North Atlantic hurricane region in 1998 and for the East and Central North Pacific regions in 2004. The Atlantic and East Pacific outlooks are an official product of the Climate Prediction Center, made in collaboration with the National Hurricane Center and Hurricane Research Division. The Central Pacific outlook is an official product of the Central Pacific Hurricane Center, made in collaboration with the CPC. The Atlantic hurricane seasonal outlook is issued in late May, and updated in early August to coincide with the onset of the peak months (August-October, ASO) of the season. A single seasonal outlook is issued in late May for the East and Central North Pacific regions.

NOAA's seasonal hurricane outlooks indicate the likely (approximately a two-thirds chance) seasonal range of named storms, hurricanes, and major hurricanes, along with the most probable season type. The Atlantic and East Pacific outlooks also indicate probabilities for each season type (above-, near-, or below-normal), along with the likely range of total seasonal activity as measured by the ACE (Accumulated Cyclone Energy) index which is a measure of the combined number, intensity, and duration of tropical storms, subtropical storms and hurricanes (Bell et al. 2000). The outlooks are designed to provide the public with a general

guide to the expected overall nature of the upcoming hurricane season. They are not seasonal hurricane landfall forecasts, and do not imply levels of activity for any particular region.

NOAA's seasonal hurricane outlooks are based primarily on predicting the combined impacts of three dominant climate factors: ENSO (Gray 1984a), the Atlantic multi-decadal oscillation (Gray et al. 1996, Landsea et al. 1999), and the tropical multi-decadal signal (Bell and Chelliah 2006). Each of these factors has strong links to recurring rainfall patterns along the equator, and together they produce the inter-related set of atmospheric and oceanic conditions typically associated with both seasonal and multi-decadal fluctuations in Atlantic hurricane activity (Fig. 7.2). For the August update, additional predictive information is also used, such as anomalous early season activity, and atmospheric and oceanic anomalies that may have developed which are not related to the dominant climate predictors.

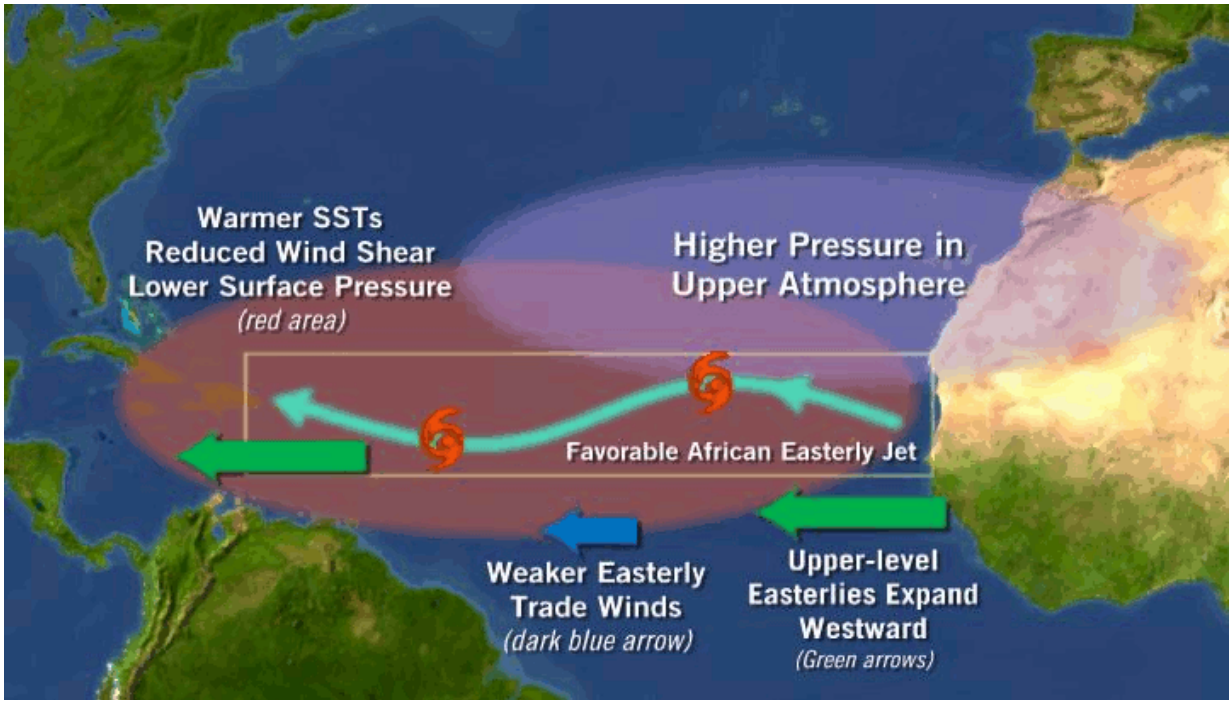

Figure 7.2. Schematic of atmospheric and oceanic anomalies during August-October (ASO) associated with active Atlantic hurricane seasons and eras.

ENSO reflects year-to-year fluctuations in tropical convection across the equatorial Pacific Ocean, and mainly influences hurricane activity for a single season at a time. The Atlantic multi-decadal oscillation reflects changes in Atlantic SSTs in both the tropics and high latitudes, and is associated with both above-normal and below-normal active hurricane eras that historically last 25-40 years. The tropical multi-decadal signal is the leading multi-decadal mode of tropical convective variability (Bell and Chelliah (2006), and captures the observed link between the Atlantic multi-decadal oscillation and an east-west seesaw in anomalous convection between the West African monsoon region (Hastenrath 1990, Gray 1990, Landsea and Gray 1992, Landsea et al., 1992, Goldenberg and Shapiro 1996), and the Amazon Basin (Chen et al. 2001, Chu et al. 1994).

NOAA's seasonal Atlantic hurricane outlooks reflect a subjective blend of three main statistical forecasting techniques. One technique utilizes regression equations for the period 1971-2007 to first establish the relationship between seasonal activity and the combined effects of ENSO, the tropical multi-decadal signal, and tropical Atlantic sea-surface temperatures. Then, forecasts of these climate factors are used to predict the upcoming seasonal activity. Such a procedure inherently assumes the climate forecast is perfect, which is generally not the case of course. Therefore, in practice the forecaster uses a regression-based contingency table for each parameter (shown here for ACE, Table 7.6), which yields a likely range of activity given reasonable uncertainties in the climate prediction itself.

Table 7.6. Contingency table showing regressed seasonal ACE (Accumulated Cyclone Energy) values associated with an active Atlantic phase of the tropical multi-decadal signal for varying strengths of ENSO and tropical Atlantic sea-surface temperature anomalies.

Tropical Atlantic Sea-surface Temperature Anomalies (°C)							
		-0.50	**-0.25**	**0**	**0.25**	**0.50**	**0.75**
El Niño	Strong	5.7	33.0	60.3	87.6	114.9	142.2
	Moderate	22.2	49.5	76.8	104.1	131.4	158.7
	Weak	38.7	66.0	93.3	120.6	148.0	175.3
	Neutral	55.2	82.6	109.9	137.2	164.5	191.8
La Niña	Weak	71.8	99.1	126.4	153.7	181.0	208.3
	Moderate	88.3	115.6	142.9	170.2	197.5	224.8
	Strong	104.8	132.1	159.4	186.8	214.1	241.4

A chart showing the historical distribution of regression errors (Fig. 7.3) is used to quantify uncertainties in the regression technique itself. For example, the regression equation explains 67% of the seasonal ACE variance.The absolute regression error in ACE is less than 20 percent of the median (meaning a highly accurate forecast) in 27% of seasons, and less than 40 percent of the median in two-thirds (67%) of seasons. Therefore, in practice NOAA assigns a range of at least ±40 percent of the median to the predicted seasonal ACE.

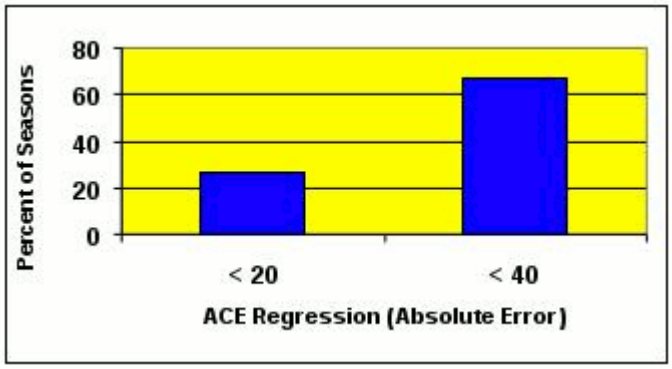

Figure 7.3. Percentage of seasons with an absolute error in the regressed seasonal ACE (Accumulated Cyclone Energy) less than 20 and less than 40 percent of the median. The absolute error is less than 20 percent of the median in about one-fourth of the seasons, and less than 40 percent of the median in about two thirds of the seasons. The regression period is 1971-2007. The predictors are ENSO, the tropical multi-decadal signal, and tropical Atlantic sea-surface temperatures.

The regression results also help the forecaster to better quantify the usefulness of the technique through an error analysis of the predicted season types. It is found that perfect predictions of the above climate factors correctly predict the Atlantic hurricane season type approximately 80% of the time. However, a one-category forecast error in season type (e.g., an above-normal season is predicted but a near-normal season is observed) is seen on average every 5-6 years. A two-category forecast error (e.g., a below-normal season is predicted but the season is above-normal) is seen on average every 12 years. Therefore, for the May outlook, the highest probability assigned to any season type is roughly 80%, and lowest probability is roughly 10%.

A second prediction technique is the climate-based analogue approach, whereby the forecaster focuses on the distributions of activity associated with past seasons having comparable climate signals to those being predicted. This approach also allows the forecaster to quickly and accurately determine the historical probabilities of the three season types associated with the predicted climate factors.

Another prediction technique (Wang et al. 2009) utilizes regression equations to first establish the relationship between the seasonal hurricane activity and dynamical model forecasts of atmospheric and oceanic conditions during ASO. The regression period is 1982-2007.The predictors in the regression equations are 60-member ensemble mean forecasts for each ASO period of vertical wind shear and Atlantic sea-surface temperatures, which are obtained from NOAA's coupled ocean-atmosphere climate model called the Global Forecast System (GFS). In practice, this technique is utilized to obtain the ensemble mean predicted seasonal activity, and the forecasted range of activity using the individual ensemble members. Using the individual members,the model probabilities of an above-, near-, and below-normal season are also derived. This technique is particularly appealing, because it avoids some of the very significant challenges associated with counting the actual number of named storms and hurricanes produced by a given climate model.

7.4 City University of Hong Kong seasonal hurricane outlooks

Introduction

Since 2000, the Laboratory for Atmospheric Research at City University of Hong Kong has been issuing real-time predictions of annual tropical cyclone (TC) activity over the western North Pacific (WNP)1. The predictands include the annual number of tropical storms and typhoons and the annual number of typhoons. These forecasts are issued in early April and early June prior to the active TC season, the latter serving as an update of the April forecast based on information in April and May. Verifications of the predictions have shown that the predictions are mostly correct within the error bars. These are all statistical predictions with predictors drawn from a large pool of indices that represent the atmospheric and oceanographic

conditions in the previous year up to the spring of the current year. Details can be found in Chan et al. (1998, 2001) and Liu and Chan (2003).

April forecast

a. Predictors related to ENSO

Many studies have shown that El Niño/Southern Oscillation (ENSO) has an effect on TC activity in the year the ENSO event develops and the year after the ENSO event (Chan 2000; Wang and Chan 2002). Therefore, indices that can be used as proxies of ENSO may be good predictors of TC activity. In this forecast scheme, a few predictors are used to represent the ENSO status prior to the TC season and to predict the possible status during the TC season.

Predictor 1. Niño3.4 index

Niño3.4 index is the mean sea surface temperature anomalies in the NINO3.4 region (5°S-5°N, 170°-120°W) and is commonly used to represent the status of ENSO. In the April forecast, the Niño3.4 index from December of the previous year to January of the current year is included to reflect the ENSO status in the winter preceding the TC season. A winter associated with an El Niño (a La Niña) condition is generally followed by a less (more) active TC season. The Niño3.4 index in March of the current year is used to represent the current ENSO status.Subsequent changes of the Nño3.4 index also give the possible ENSO status during the TC season. If an El Niño (a La Niña) event develops during the TC season, the TC season tends to be more (less) active especially for the number of typhoons. This partly explains that the skill of prediction for the number of typhoons is higher than that of the number of tropical storms and typhoons using this predictor.

Predictor 2. Equatorial Southern Oscillation Index (Equatorial SOI)

The Equatorial Southern Oscillation Index (Equatorial SOI) is defined as the standardized anomaly of the sea-level pressure difference between the equatorial eastern Pacific (80°W-130°W, 5°N-5°S) and an area over Indonesia (90°E-140°E, 5°N-5°S). This predictor also acts as a proxy of ENSO and the principle involved is similar to that of Niño3.4 index. Note that this predictor is only used in the prediction of the number of typhoons.

b. Predictors related to atmospheric circulation

Indices that represent the conditions in winter and spring prior to the TC season are used. The changes in these conditions are related to subsequent changes during the TC season so that the indices can be proxies of the summertime environment. The indices considered include the westward extension of the 500-hPa subtropical ridge and the West Pacific index. All these indices are monthly values from April of the previous year to March of the current year.

Predictor 3. West Pacific index

The West Pacific (WP) pattern is a primary mode of low-frequency variability over the North Pacific in all months (Barnston and Livezey, 1987). During winter and spring, this pattern shows a north-south dipole of 500-hPa geopotential height anomalies, with one center over the Kamchatka Peninsula and another center of opposite sign over the WNP along 30°N.
The WP index in the months March and April of the current year is negatively correlated with TC activity. Positive values of this index indicate the positive phase of the WP pattern, which shows a north-south dipole of 500-hPa geopotential height anomalies, with positive anomalies over the WNP. This pattern is generally associated with a stronger subtropical high and a weaker monsoon trough in the peak TC season. Therefore a less active TC season is expected.

Predictor 4. Index of the westward extent of the subtropical high over the WNP

The index of the westward extent of the subtropical high over the WNP in the months February-May of the current year is positively correlated with TC activity. A lower value of this index indicates that the subtropical high extends more westward and is generally associated with a less active TC season. The values of this index in these months are correlated with the geopotential high anomalies during the peak TC season (July-October). Therefore, this index can represent the spring-time mid-level atmospheric conditions, which are related to subsequent changes of the subtropical high during the TC season which eventually affect the TC activity.

June forecast

The parameters used in the June forecast are similar to those in the April forecast. As mentioned in the Introduction, the June forecast makes use of monthly values in the months April and May of each predictor to provide the more up-to-date information about the atmospheric and oceanographic conditions. Such information is a reflection of these conditions during the TC season. Therefore the June forecast should have a higher skill than the April forecast.

7.5 Tropical Storm Risk seasonal hurricane outlooks

Tropical Storm Risk (TSR) has been issuing public outlooks for seasonal tropical cyclone activity since 2000. These outlooks are provided for the North Atlantic, Northwest Pacific and Australian regions (Table 7.7). The TSR forecasts are available for basin activity and for landfalling activity on the USA, Caribbean Lesser Antilles and Australia. Outlooks are issued in deterministic and tercile probabilistic form. The TSR forecast models are statistical in nature but are underpinned by predictors having sound physical links to contemporaneous tropical cyclone activity. These predictors and their physical mechanisms are described by region in the sections below. TSR provides, as part of their seasonal outlooks, the hindcast precision of each forecast parameter assessed over prior periods of at least 20 years. An example of TSR"s extended hindcast skill as a function of lead time is shown for Northwest Pacific typhoon activity (Figure 7.5).

Table 7.7. Summary of Tropical Storm Risk seasonal tropical cyclone outlooks.

TSR Seasonal Tropical Cyclone Outlooks					
Region	**Parameters forecast**	**Landfalling**	**Forecast issue times**	**Deterministic forecasts**	**Probabilistic forecasts**
North Atlantic	TS, H, IH, ACE (and for sub-regions)	United States TS, H, US ACE	Monthly from Dec to Aug	All parameters(basin and landfalling)	Basin ACE US ACE
Western North Pacific	TS, T, IT, ACE	-	Monthly from Mar to Aug	All parameters(basin and landfalling)	Basin ACE
Australian Region	TS, STC, ACE	Australia TS	Monthly from May to Dec	All parameters (basin and landfalling)	Basin TS Australia TS
TS = number of tropical storms; H = number of hurricanes; IH = number of intense hurricanes; ACE = Accumulated Cyclone Energy Index; US ACE = US Accumulated Cyclone Energy Index; T = number of typhoons; IT = number of intense typhoons; STC = number of severe tropical cyclones.					

Seasonal North Atlantic hurricane activity

TSR divides the North Atlantic into two regions: (a) the "tropical" North Atlantic comprising the North Atlantic south of 20°N, the Caribbean Sea and the Gulf of Mexico, and (b) the "extra-tropical" North Atlantic. 85-90% of the hurricanes and intense hurricanes that made landfall on the United States between 1950 and 2005 originated as tropical depressions in the "tropical" North Atlantic. TSR forecasts tropical cyclone activity in the "tropical" North Atlantic and uses a rolling prior 10-year climatology for tropical cyclone activity in the "extra-tropical" North Atlantic.

TSR outlooks for tropical cyclone activity in the "tropical" North Atlantic employ two predictors (Table 7.8 and Figure 7.4). These are: (1) The forecast speed of the trade winds which blow westward across the tropical Atlantic and Caribbean Sea in July, August and September. These winds influence cyclonic vorticity and vertical wind shear over the main hurricane track region. Cyclonic vorticity either helps or hinders the spinning up of storms depending upon its anomaly sign and magnitude. Vertical wind shear either helps or hinders a vertically coherent storm vortex from developing depending upon its magnitude; (2) The forecast temperature of sea surface waters between west Africa and the Caribbean where many hurricanes develop during August and September. Waters here provide heat and moisture to help power the development of storms within the hurricane main development region.

Seasonal US landfalling hurricane activity

TSR outlooks for US landfalling tropical cyclone activity issued between December and July employ a historical thinning factor between "tropical" North Atlantic activity and US landfalling activity.The TSR outlook issued in early August uses wind patterns (at heights between 750 and 7,500 metres above sea level) from six regions over North America and the east Pacific and North Atlantic oceans during July to predict the US ACE index (effectively the cumulative wind

energy from all US striking tropical storms during the main hurricane season). Wind anomalies in these regions in July are indicative of persistent atmospheric circulation patterns that either favour or hinder evolving hurricanes from reaching US shores during August and September. The model correctly anticipates whether US hurricane losses are above-median or below-median in 74% of the years between 1950 and 2003 (Saunders and Lea 2005). It also performed very well in "real-time" operation in 2004 and 2005.

Table 7.8. Predictor(s) underpinning the Tropical Storm Risk seasonal outlooks by region.

TSR Seasonal Forecast Predictor(s)			
Region	**Basin or Landfalling**	**Predictor(s)**	**References**
North Atlantic	Basin	Forecast July-September trade wind speed over the Caribbean Sea and tropical North Atlantic [region 30°W-100°W, 7.5°N-17.5°N], and the forecast August-September sea surface temperature in the hurricane main development region [20°W-60°W, 10°N-20°N].	Lea and Saunders (2004) Lea and Saunders (2006b) Saunders (2006) Saunders and Lea (2008)
	US Landfalling	Historical thinning factors linking basin to US landfalling activity (Dec to July forecasts). July tropospheric wind anomalies between heights of 925mb and 400mb over North America, the east Pacific and the North Atlantic (Aug US ACE index forecast).	Saunders and Lea (2005)
Western North Pacific	Basin	Forecast August-September Niño 3.75 sea surface temperature [region 140°W-180°W, 5°S-5°N].	Lloyd-Hughes, Saunders and Rockett (2004) Lea and Saunders (2006a)
Australian Region	Basin	Forecast August-September Niño 3.75 sea surface temperature [region 140°W-180°W, 5°S-5°N].	Lloyd-Hughes, Saunders and Rockett (2004) Lea and Saunders (2006a)
	Australia Landfalling	Historical thinning factor linking basin to landfalling activity.	

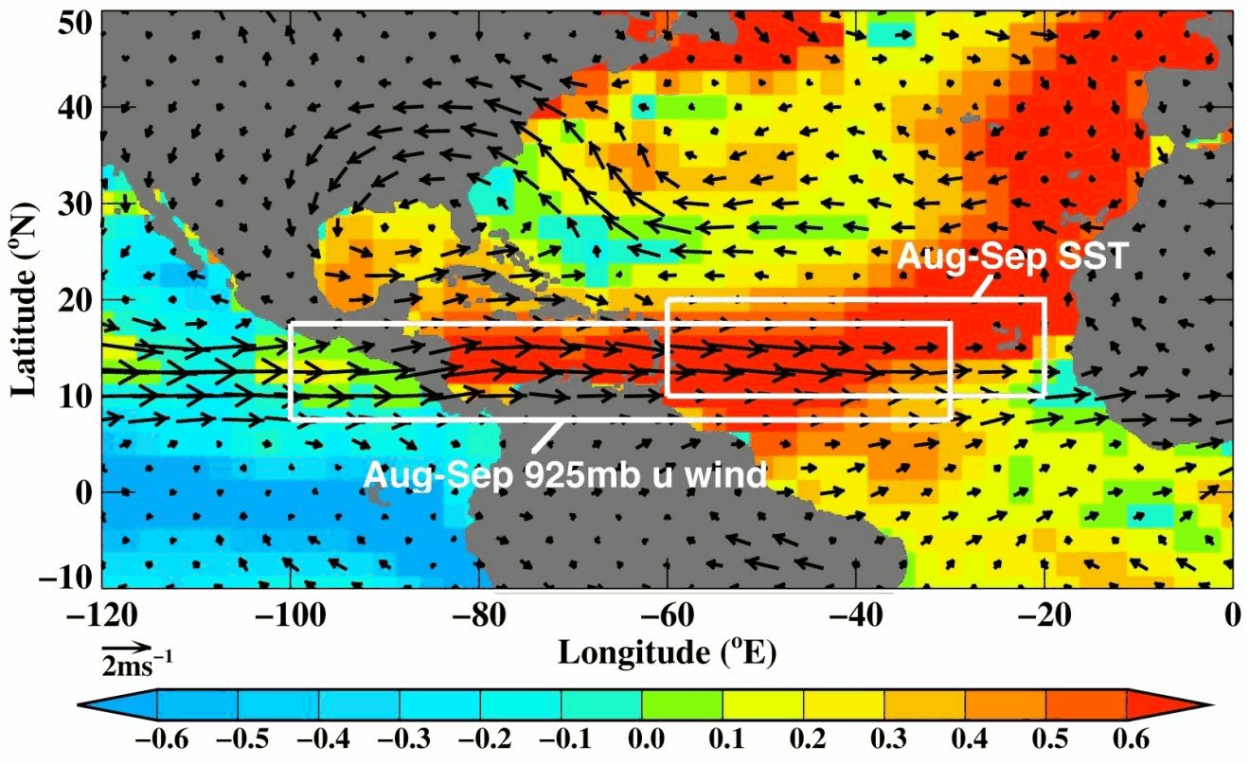

Figure 7.4. Physical nature of the TSR statistical model for "tropical" North Atlantic hurricane activity. The display shows the two August-September environmental field areas that comprise the model and the August-September anomalies in sea surface temperature (color coded in degrees Celsius) and 925mb wind anomalies (arrowed) linked to active Atlantic hurricane years. (Reproduced from Saunders and Lea 2008).

Seasonal Western North Pacific typhoon activity

The TSR predictors for Western North Pacific typhoon activity are as follows. Tropical storm and typhoon numbers are forecast before May using the Niño 3 SST from the prior September; from May they are forecast using April surface pressure over the region 17.5°N-35°N, 160°E-175°W. Intense typhoon numbers and the ACE index are forecast using the forecast value for the August-September Niño 3.75 region (5°S-5°N, 180°W-140°W) SST (Table 7.2). The latter is predicted using the consolidated CLIPER model described in Lloyd-Hughes et al. (2004). Above average (below average) Niño 3.75 SSTs are associated with weaker (stronger)TRADE winds over the region 2.5°N-12.5°N, 120°E-180°E. These in turn lead to enhanced (reduced) cyclonic vorticity over the Western North Pacific region where intense typhoons form.

Figure 7.5 displays the seasonal predictability of the Western North Pacific ACE index for the 41-year period 1965 to 2005. This period starts in 1965 as this marks the beginning of reliable Pacific typhoon wind records (Lea and Saunders 2006a). Hindcast skill is assessed using cross-validation with 5-year block elimination. Confidence intervals are computed using the standard bootstrap method (Effron and Gong 1983) with replacement. The Northwest Pacific ACE index has positive forecast skill to 95% confidence over the 41-year period from early May. Historically 95% of typhoons occur after the 1st May.

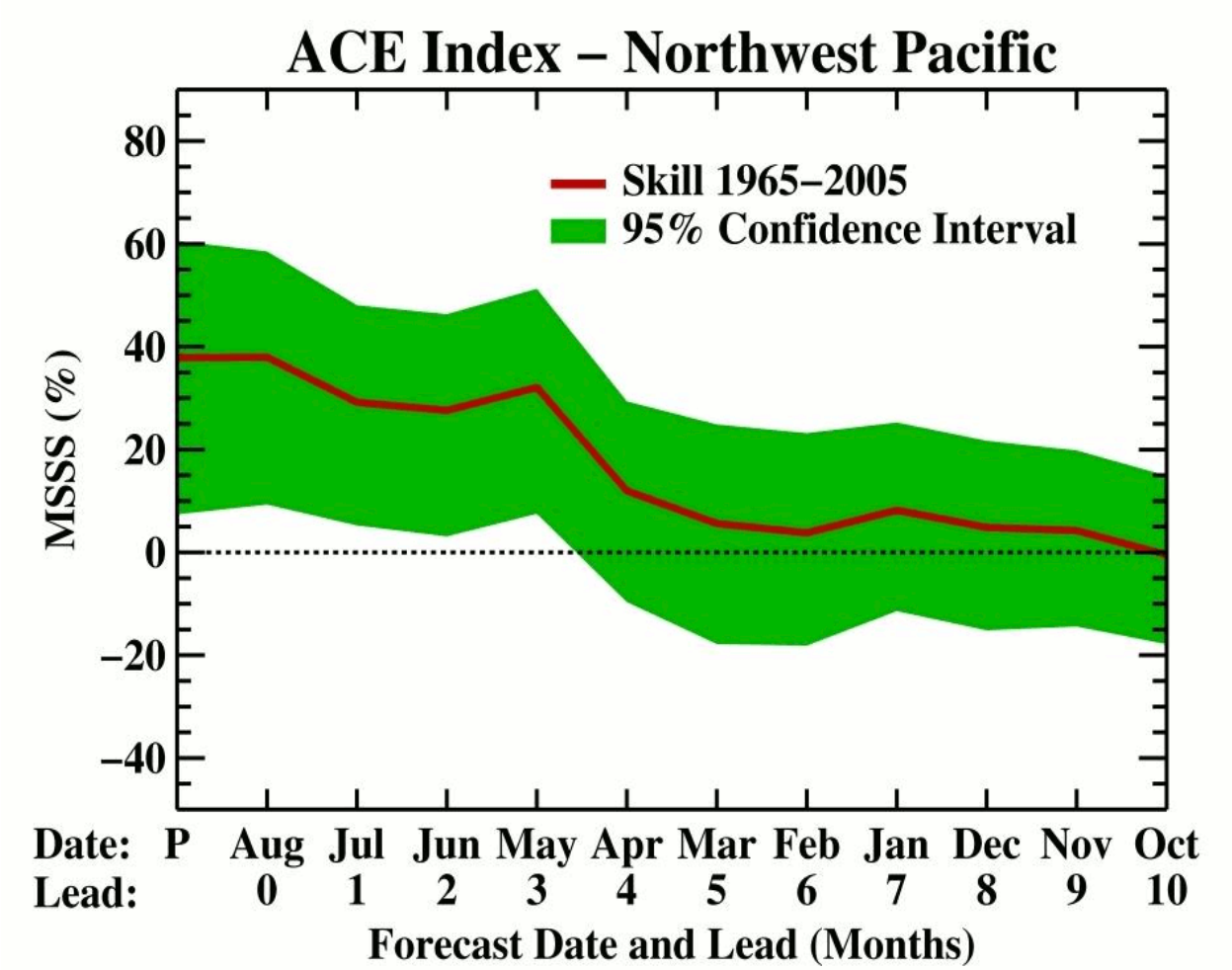

Figure 7.5. TSR hindcast seasonal prediction skill for the Northwest Pacific ACE index 1965-2005 shown for monthly leads from the previous October. Skill is displayed by the mean square skill score (MSSS) with 1965-2005 used as the climatology.

Seasonal Australian-region tropical storm activity

TSR defines the "Australian region" as encompassing the Southern Hemisphere region from 100°E to 170°E (a storm must form as a tropical cyclone within to count).The Australian tropical storm season spans the period from 1st November to 30th April. The TSR predictor for leads up to November is the forecast October-November Niño 4 SST (Table 7.2). The TSR December seasonal outlook employs the observed October-November Niño 4 SST. The Niño 4 SST forecasts are made with the consolidated CLIPER model reported by Lloyd-Hughes et al (2004). Early austral summer SSTs in the Niño 4 region influence Australian-region tropical storm activity by affecting atmospheric vertical wind shear over the Australian region during Austral summer. Cooler (warmer) than normal Niño 4 SST in October-November leads to below-

average (above-average) atmospheric vertical wind shear which, in turn, favours above-average (below-average) tropical storm activity.

7.6 ECMWF seasonal hurricane outlooks

The European Centre for Medium-Range Weather Forecasts (ECMWF) has produced seasonal forecasts of tropical storm frequency since 2001. These forecasts are not publicly available. They are available only to ECMWF member states and World Meteorological Organization (WMO) members. Unlike the NOAA, CSU, City University of Hong Kong, and TSR statistical methods discussed above, the ECMWF seasonal forecasts of tropical storms are based on a dynamical method. They use the outputs of coupled Global Circulation Model (GCM) integrations to predict tropical cyclone activity. This method is based on the ability of GCMs to create tropical storm disturbances that have strong similarities to real-world tropical storms. For example, they develop a warm temperature anomaly over the centre of the vortex, which is a characteristic of observed tropical storms.

The ECMWF seasonal forecasting system 3 (Anderson et al. 2007) is based on a coupled GCM that has been extensively integrated for 7-months forecasts. The atmospheric component has a T159 spectral resolution (about 120 kilometer resolution). The model has 62 vertical levels with a model-top level located at about 5 hPa. The ocean model is the Hamburg Ocean Primitive Equation model (HOPE) with a resolution equivalent to 2° in the extra-tropics, but the resolution increases in the tropics to 0.5°. The ocean model has 29 vertical levels. Ocean initial conditions are provided by the ECWMF operational ocean analysis system (Balmaseda et al. 2007). The ocean and atmosphere are coupled directly, without flux correction, using the Ocean Atmosphere Sea Ice Soil (OASIS) coupler. The coupling frequency is 24 hours. The coupled system is integrated forward for 7 months from the initial conditions. In order to sample the uncertainty in the initial conditions and model formulation, the model is integrated 41 times starting from a control and 40 perturbed initial conditions. The atmospheric perturbations are identical to those applied to ECMWF medium-range forecasts: singular vectors to perturb the atmospheric initial conditions (Buizza and Palmer 1995) and stochastic perturbations during the model integrations (Buizza et al. 1999, Palmer 2001). For each grid point, the stochastic physics perturbs grid point tendencies up to 50%. The tendencies are multiplied by a random factor drawn from a uniform distribution between 0.5 and 1.5. The random factor is constant within a 10°x10° domain for 6 hours. The whole globe is perturbed. The ocean initial conditions are perturbed by adding small perturbations to SST initial conditions. A set of SST perturbations has been constructed by taking the difference between different SST analyses. For each starting date, 20 combinations of SST perturbations are randomly chosen and applied with a + and - sign, creating 40 perturbed states. A set of wind stress perturbations is also calculated by taking the difference between two monthly wind stress analyses. Nine ocean assimilations (one control and four perturbed) are produced by randomly picking two perturbations from the set of wind stress perturbations and adding them with a + and - sign to the analyzed wind. The wind stress and SST perturbations are combined to produce the 40 perturbed oceanic initial conditions. More details can be found in Anderson et al. (2007).

The forecasts are produced once a month with initial conditions from the 1st of each month. These forecasts are then issued on the 15th of each month (the delay allows acquisition of SST fields from the previous month, time to run the forecasts, and a margin to ensure a reliable operational schedule). A problem with long-term integrations is that the model mean climate begins to be different from the analysis climate. The effect of the drift on the model calculations is estimated from integrations of the model in previous years (the re-forecasts). The drift is removed from the model solution during the post-processing. The re-forecasts consist of an ensemble of 11 members starting on the 1st of each month from 1981 to 2007 (the ECMWF seasonal forecasting system 3 became operational in March 2007).

The tropical storms produced by each forecast are tracked using the method described in Vitart and Stockdale (2001). This method identifies the low pressure systems with a warm core in the upper troposphere from the model outputs every 12 hours. Then an algorithm is applied to build the tropical storm trajectories from the low pressure systems with a warm core which have been identified.

The number of tropical storms for each basin is then counted and added over the 7-month period of model integrations, but the first month of the forecast is excluded since it includes the deterministic part of the forecasts. Also, these forecasts are issued with a delay of 15 days. Since the model components have biases, the climatological frequency of model tropical storms can differ from observations. We calibrate the number of model tropical storms in a given year by multiplying the number of model tropical storms by a factor such that the mean of the central distribution (25%-75% distribution) of the model climate equals the mean of the observed central distribution. The calibration of the re-forecasts is performed using cross-validation.

The ECMWF seasonal forecasts of tropical storms are produced each month for all tropical cyclone basins (e.g., the North Atlantic, the eastern North Pacific, the western North Pacific, the North Indian Ocean, the South Indian Ocean, the Australian basin, and the South Pacific). For instance the seasonal forecasts of tropical storms for the Atlantic basin are issued from March to August. These forecasts do not necessarily cover the full season. For instance the 1st March forecasts, which are issued the 15 March, cover only a portion of the Atlantic tropical storm season: the period from June to September. On the other hand, the forecasts starting on 1st May cover the full Atlantic tropical storm season, from June to November. Four times a year (February, May, August, November), the forecasts are extended to 13 months. The tropical storm forecasts produced by those 13 months forecast are still experimental. Current seasonal tropical storm forecast products at ECMWF include:

- The number of named storms
- The mean genesis location (particularly relevant for the western North Pacific, where the genesis location of tropical storms can vary significantly from year to year)
- The number of hurricanes (product available since May 2008)
- The Accumulated Cyclone Energy (ACE) (product available since May 2008).

The forecasts have been evaluated against observed data. Figure 7.6 shows an example of verification of ACE over the Atlantic for the ECMWF seasonal forecasts starting on 1st June.

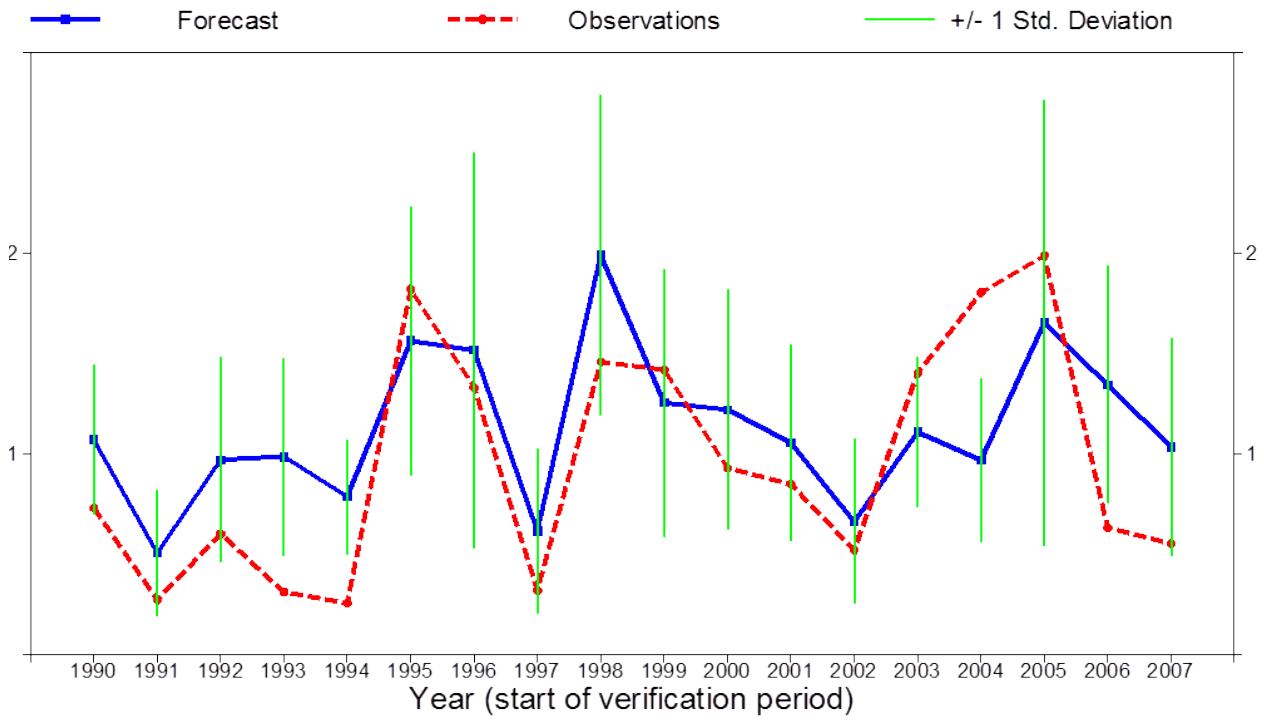

Figure 7.6. Interannual variability of Accumulated Cyclone Energy over the North Atlantic,normalized over its climatological value over the period 1990-2006. The red line represents observations from HURDAT, the blue line represents the interannual variability of the ECMWF ensemble mean forecasts starting on 1st June. The vertical green lines represent 2 standard deviations. The linear correlation between observations and ensemble mean model forecast is 0.72 over the period 1990-1007.

Multi-model prediction

There exist a number of different methods to represent model uncertainty. One method makes use of the so-called multi-model technique. This method consists in combining the forecasts produced by different numerical models. The main idea is that the combination of the different models should filter some of the model error which are specific to one of the model components. The DEMETER project (Palmer et al. 2004) tested this hypothesis by combining the forecasts produced by 7 different coupled ocean-atmosphere seasonal forecasting systems. Vitart (2006) found that the DEMETER multi-model performed better overall than any individual model component. The success of DEMETER, led directly to the development of the operational EUROSIP multi-model ensemble. EUROSIP presently consists of 3 seasonal forecasting systems from the ECMWF, the Met Office and Mé/téo-France. Multi-model seasonal forecasts of tropical storm activity are produced the same way as the ECMWF seasonal forecasts. Each model is calibrated separately and the multi-model tropical storm forecast is the median of the 3 model forecasts. The tropical storm products are the same as for the ECMWF forecast except that we do not issue EUROSIP forecasts of hurricane numbers. This is because some of the model components of EUROSIP do not have enough horizontal resolution to produce hurricanes. As is

the case for the ECMWF forecasts, the EUROSIP multi-model tropical storm forecasts are not public, but are available to ECMWF member states. They may soon become available to WMO members. The skill of the EUROSIP multi-model forecasts of tropical storm frequency is discussed in Vitart et al. (2007).

7.7 IRI seasonal hurricane outlooks

Suspect that the IRI experimental hurricane forecasts have been discontinued. We may need to delete all of Section 7.7.

Since 2003, the International Research Institute for Climate and Society (IRI) has been issuing experimental forecasts for seasonal tropical cyclone (TC) activity in different regions based on climate models. The forecasts are issued in the form of tercile probabilities (above-normal, normal, below-normal) for each of the variables (number of tropical cyclones and accumulated cyclone energy) in each basin for the peak of the TC season and are updated monthly. Here we briefly describe how the forecasts are produced and show their hindcast and real time skill in different regions. This manuscript is strongly based on Camargo and Barnston (2008a, b). The figures and tables shown here appeared originally in Camargo and Barnston (2008, 2009).

Description of forecasts

The possible use of dynamical climate models to forecast seasonal TC activity has been explored by various authors, e.g. Bengtsson et al. (1982). Although the typical low horizontal resolution of climate general circulation models is not adequate to realistically reproduce the structure and behavior of individual cyclones, such models are capable of forecasting with some skill several aspects of the general level of TC activity over the course of a season (Camargo et al. 2005). The skill of dynamical TC forecasts depends on many factors, including the model used, the model resolution, and the inherent predictability of the large-scale circulation regimes, including those related to the ENSO condition.

An important consideration is the dynamical design used to produce the forecasts. Currently, there are two methods for producing dynamical TC forecasts. The first is based on fully coupled atmosphere-ocean models (Vitart and Stockdale 2001; Vitart et al. 2007). At IRI a two-tiered procedure is used (Mason et al. 1999; Goddard et al. 2003; Barnston et al. 2003, 2005),in which SST forecast scenarios are first established, which then are used to force an atmospheric model (Camargo and Barnston 2008, 2009).

The atmospheric model used for the IRI TC forecasts is the ECHAM4.5 model, developed at the Max-Planck Institute for Meteorology in Hamburg (Roeckner et al. 1996), which has been studied extensively for various aspects of seasonal TC activity (Camargo and Zebiak 2002; Camargo and Sobel 2004; Camargo et al. 2005, 2007a). The integrations of this atmospheric model are subject to differing SST forcing scenarios, which are in constant improvement at IRI.

Details of current and past SST scenario methodologies are given in Camargo and Barnston (2008, 2009). In the tropics, multi-model SST forecasts are used for the Pacific, while statistical and dynamical forecasts are combined for the Indian and Atlantic Oceans. In all scenarios, the extra-tropical SST forecasts consist of damped persistence from the previous month's observation (added to the forecast season's climatology), with an anomaly e-folding time of 3 months (Mason et al. 1999). The model skill performance was first examined in model simulations forced with observed SSTs, prescribed during the period 1950 to the present. These runs provide estimates of the upper limit of skill model in forecasting TC activity.

For all types of SST we analyze the output of the ECHAM4.5 global climate model for TC activity. To define and track TCs in the models, we used objective algorithms (Camargo and Zebiak 2002), based in large part on prior studies (Vitart et al. 1997; Bengtsson et al. 1995). The algorithm has two parts: detection and tracking. In the detection part, storms that meet environmental and duration criteria are identified. A model TC is identified when chosen dynamical and thermodynamic variables exceed thresholds calibrated to the observed tropical storm climatology. Most studies (Bengtsson et al. 1982, Vitart et al. 1997) use a single set of threshold criteria globally. However, to take into account model biases and deficiencies, we use basin- and model-dependent threshold criteria, based on analyses of the correspondence between the model and observed climatologies. Thus, we use a threshold exclusive to ECHAM4.5 at a specific horizontal resolution.

Once detected, the TC tracks are obtained from the vorticity centroid, defining the center of the TC, using relaxed criteria appropriate for the weak model storms. These detection and tracking algorithms have been applied to regional climate models (Landman et al. 2005; Camargo et al. 2007b) and to multiple AGCMs (Camargo and Zebiak 2002; Camargo et al. 2005, 2007c).

Following detection and tracking, we count the number of named storms (NS) and compute the model accumulated cyclone energy (ACE) index (Bell et al. 2000) over a TC season. ACE is defined as the sum of the squares of the wind speeds in the TCs active in the model at each 6-hour interval. For the observed ACE, only TCs of tropical storm intensity or greater are included. The model ACE and named storm results are then corrected for bias, based on the historical model and observed distributions of NTC and ACE over the 1971-2000 period, on a per-basin basis. Corrections yield matching values in a percentile reference frame (i.e., a correspondence is achieved non-parametrically). Using 1971-2000 as the climatological base period, tercile boundaries for model and observed NTC and ACE are then defined, since the forecasts are probabilistic with respect to tercile-based categories of the climatology (below, near, and above normal).

For each of the SST forcing designs, we count the number of ensemble members having their named storms and ACE in a given ocean basin in the below-normal, normal and above-normal categories, and divide by the total number of ensembles. These constitute the "raw", objective probability forecasts. In a final stage of forecast production,the IRI forecasters examine and discuss these objective forecasts and develop subjective final forecasts that are issued on the IRI website. The most typical difference between the raw and the subjective forecasts is that the latter have weaker probabilistic deviations from climatology, given the knowledge that the

models are usually too "confident". The overconfidence of the model may be associated with too narrow an ensemble spread, too strong a model signal (deviation of ensemble mean from climatology), or both of these. The subjective modification is intended to increase the probabilistic reliability of the predictions. Another consideration in the subjective modification is the degree of agreement among the forecasts, in which less agreement would suggest greater uncertainty and thus more caution with respect to the amount of deviation from the climatological probabilities.

The raw objective forecasts are available since August 2001. The first subjective forecast for the western North Pacific basin was produced in real-time in April 2003. However, subjective hindcasts were also produced for August 2001 through April 2003 without knowledge of the observed result, making for 6 years of experimental forecasts.

For each ocean basin, forecasts are produced only for the peak TC season, from certain initial months prior to that season (Table 7.9), and updated monthly until the first month of the peak season. The lead time of this latest forecast is defined as being zero, and the lead times of earlier forecasts are defined by the number of months earlier that they are issued. The definitions of the basins' boundaries are given in Fig. 7.7.

Table 7.9. Ocean basins in which IRI experimental TC forecasts are issued: Eastern North Pacific (ENP), Western North Pacific (WNP), North Atlantic (ATL), Australia (AUS) and South Pacific (SP). Date of the first issued forecast; seasons for which TC forecasts are issued (JJAS: June to September, ASO: August-October, JASO: July to October, ASO: August to October, JFM: January to March, DJFM: December to March); months in which the forecasts are issued; and variables forecasted—NS (named storms), ACE (accumulated cyclone energy).

Basin	First Forecast	Season	Months forecasts are issued	Variables
Eastern North Pacific (ENP)	March 2004	JJAS	Mar, Apr, May, Jun	NS,ACE
Western North Pacific (WNP)	April 2003	JASO	Apr, May, Jun, Jul	NS,ACE
North Atlantic (ATL)	June 2003	ASO	Apr, May, Jun, Jul, Aug	NS,ACE
Australia (AUS)	September 2003	JFM	Sep, Oct, Nov, Dec, Jan	NTC
South Pacific (SP)	September 2003	DJFM	Sep, Oct, Nov, Dec	NTC

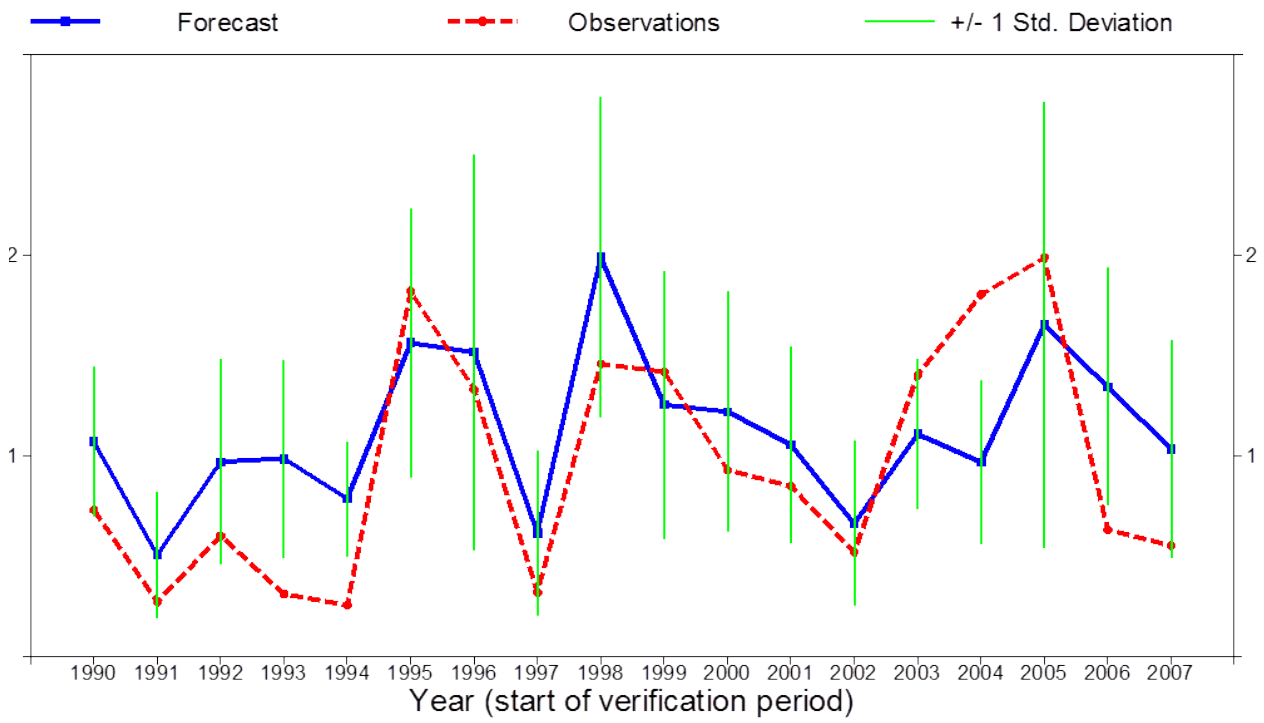

Figure 7.7. Definition of the ocean basin domains used in this study: Australian (AUS),(105°E-165°E); South Pacific(SP), 165°E-110°W; western North Pacific (WNP), 100°E-160°W, eastern North Pacific (ENP), 160°W-100°W; and Atlantic (ATL), 100°W-0°. All latitude boundaries are along the equator and 40°N or 40°S. Note the unique boundary paralleling Central America for ENP and ATL basins.

Forecasts and hindcast skill

In Camargo and Barnston (2008, 2009), a large set of probabilistic and deterministic skill score measures are examined for simulations (forced with observed SST), hindcasts of persisted SSTs and the real-time forecasts.Here we show just a subset of that skill analysis.

Figure 7.8 shows the approximate 6-year record of the model ensemble forecasts of NTC and ACE at all forecast lead times for each of the ocean basins. The vertical boxes show the inter-quartile range among the ensemble members,and the vertical dashed lines ("whiskers") extend to the ensemble member forecasts outside of that range. The asterisk indicates the observation value. Favorable and unfavorable forecast outcomes can be identified, such as, respectively, the ACE forecasts for the western North Pacific for 2002, and the ACE forecasts for the North Atlantic for 2004.

Probabilistic verification using the ranked probability skill score (RPSS) and likelihood scores for NTC and ACE, using the multi-decadal simulations and hindcasts (OSST and HSST), and the real-time forecasts forced by the multiple SST prediction scenarios lead to skills that are mainly near or below zero. This poor result can be attributed to the lack of probabilistic reliability of atmospheric ensemble-based TC predictions as is seen in many predictions made by individual climate models — not just for TC activity but for most climate variables (Anderson 1996; Barnston et al. 2003; Wilks 2006). Climate predictions by atmospheric models have model-

specific systematic biases, and their uncorrected probabilities tend to deviate too strongly from climatological probabilities due to too small an ensemble spread and/or too large a mean shift from climatology. This problem leads to comparably poor probability forecasts, despite positive correlation skills for the ensemble means of the same forecast sets. Positive correlations, but negative probabilistic verification is symptomatic of poorly calibrated probability forecasts — a condition that can be remedied using objective statistical correction procedures.

The actually issued forecasts have better probabilistic reliability than the forecasts of the model output. Likelihood skill scores,and especially RPSS, are mainly positive for the issued forecasts, although modest in magnitude. This implies that the probability forecasts of the atmospheric are potentially useful, once calibrated to correct for overconfidence or an implausible distribution shape. Such calibration could be done objectively, based on the longer hindcast history, rather than subjectively by the forecasters as done to first order here.

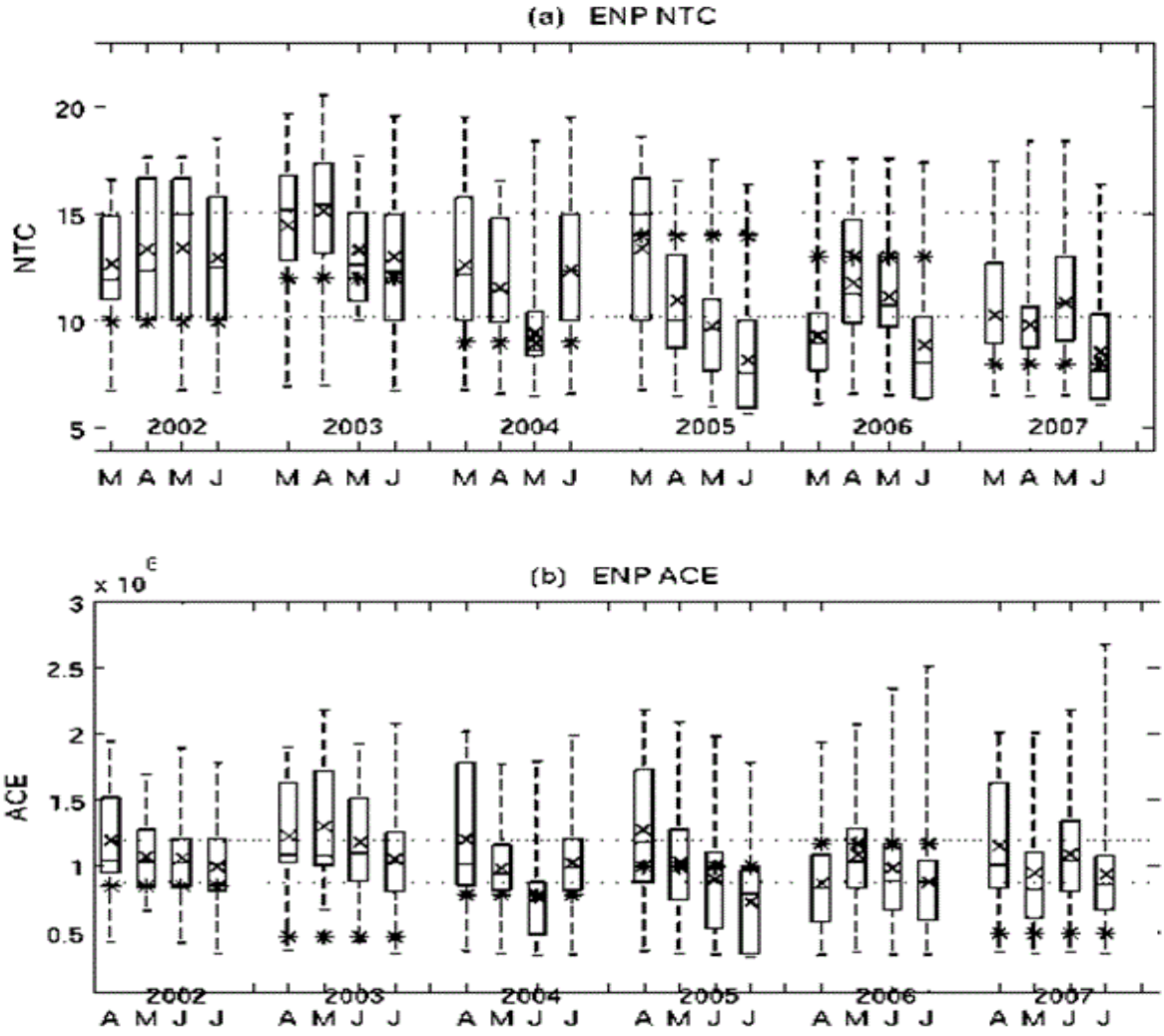

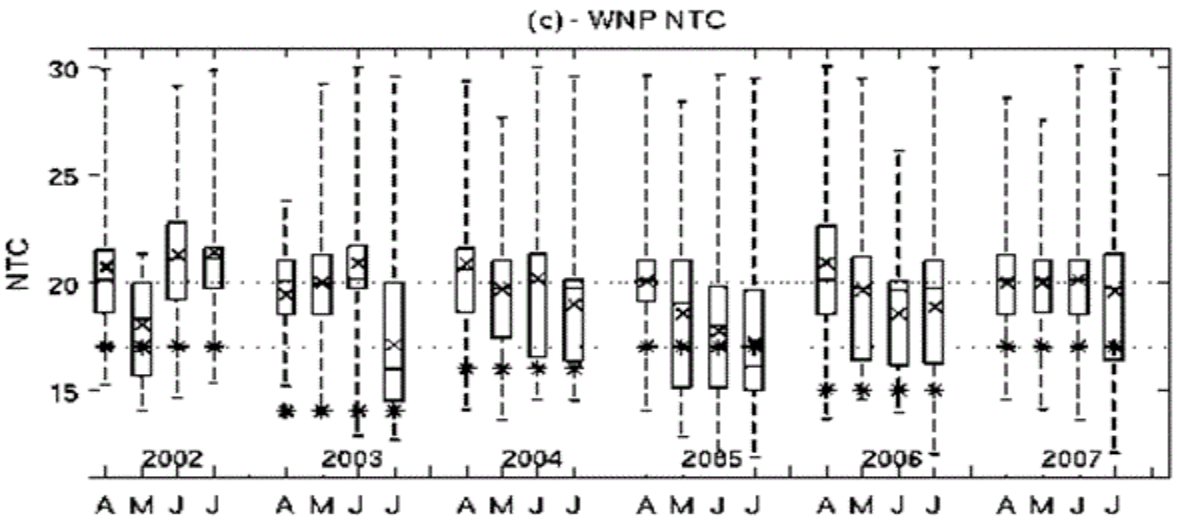
(c) - WNP NTC
NTC
30
25
20
15
2002
2003
2004
2005
2006
2007
A M J J A M J J A M J J A M J J A M J J A M J J

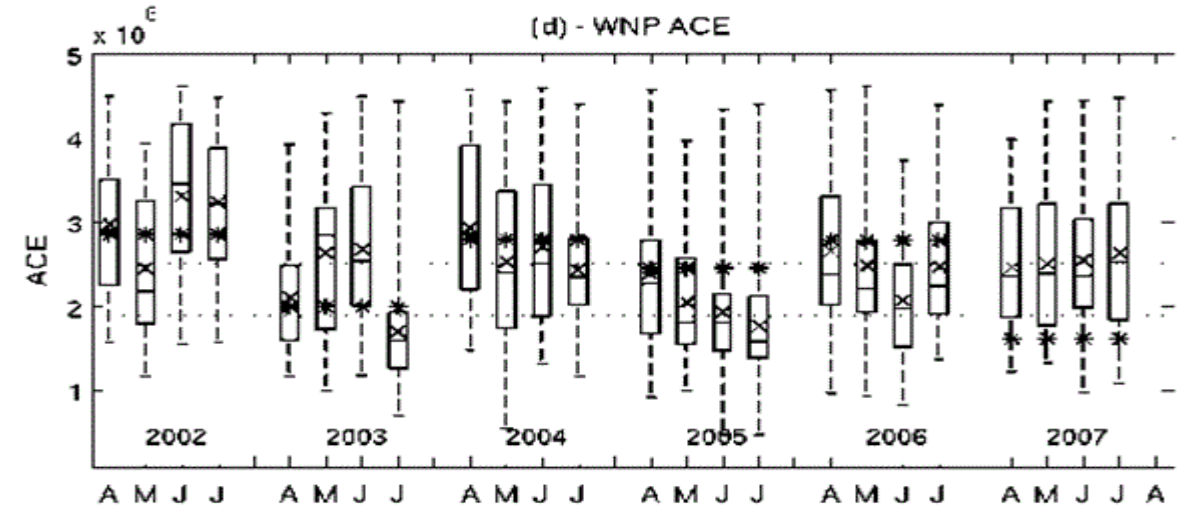
(d) - WNP ACE
x 10^6
ACE
5
4
3
2
1
2002
2003
2004
2005
2006
2007
A M J J A M J J A M J J A M J J A M J J A M J J A

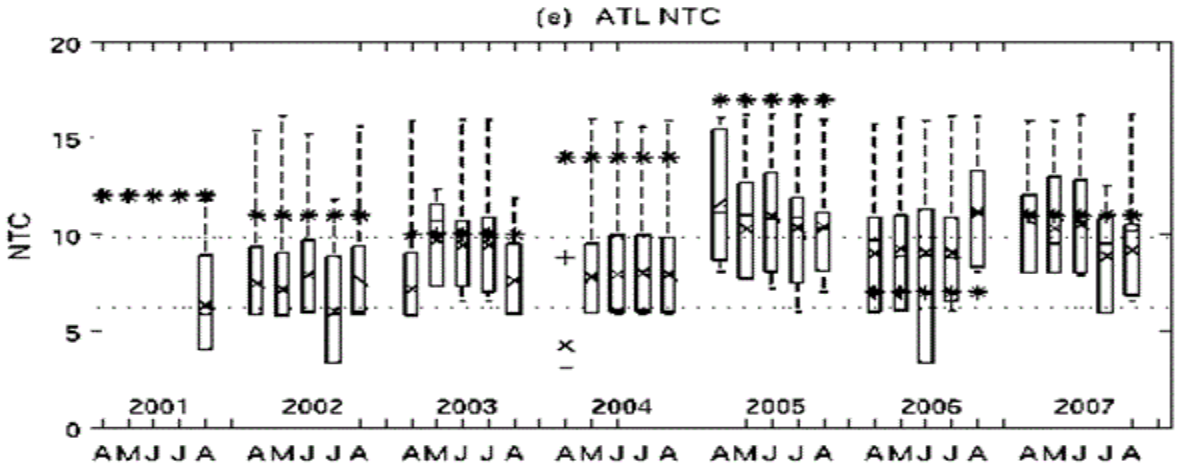
(e) ATL NTC
NTC
20
15
10
5
0
2001
2002
2003
2004
2005
2006
2007
A M J J A A M J J A A M J J A A M J J A A M J J A A M J J A

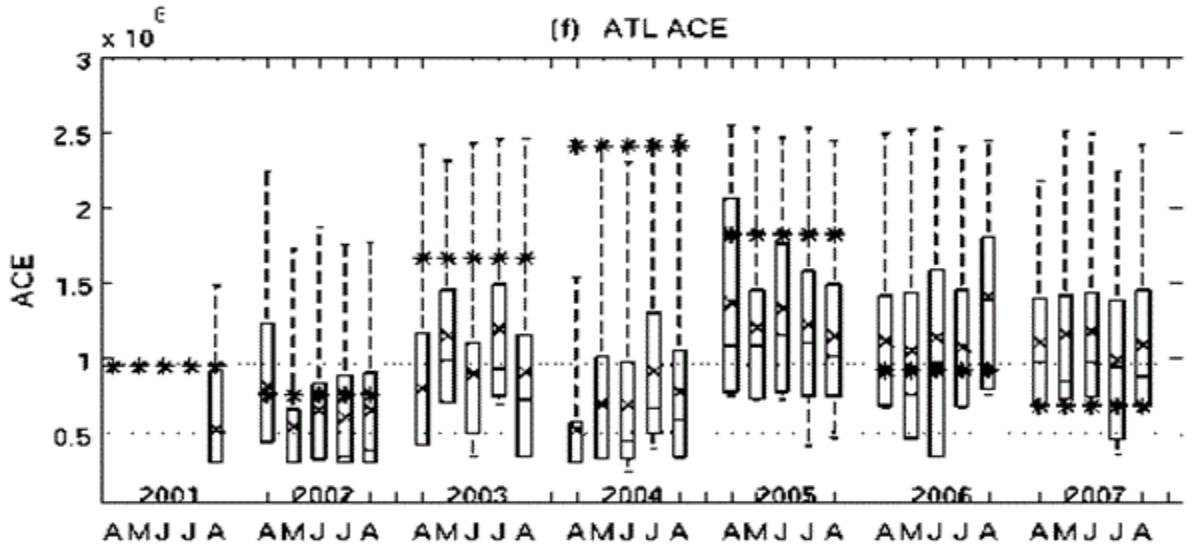
(f) ATL ACE
x 10^5
ACE
3
2.5
2
1.5
1
0.5
2001
2002
2003
2004
2005
2006
2007
A M J J A

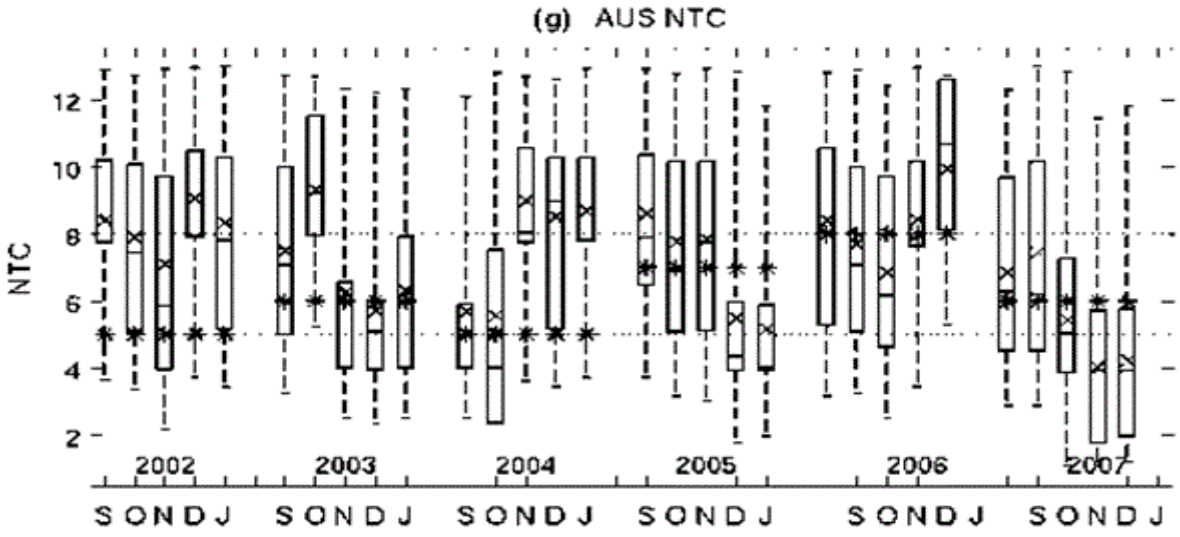
(g) AUS NTC
NTC
12
10
8
6
4
2
2002
2003
2004
2005
2006
2007
S O N D J

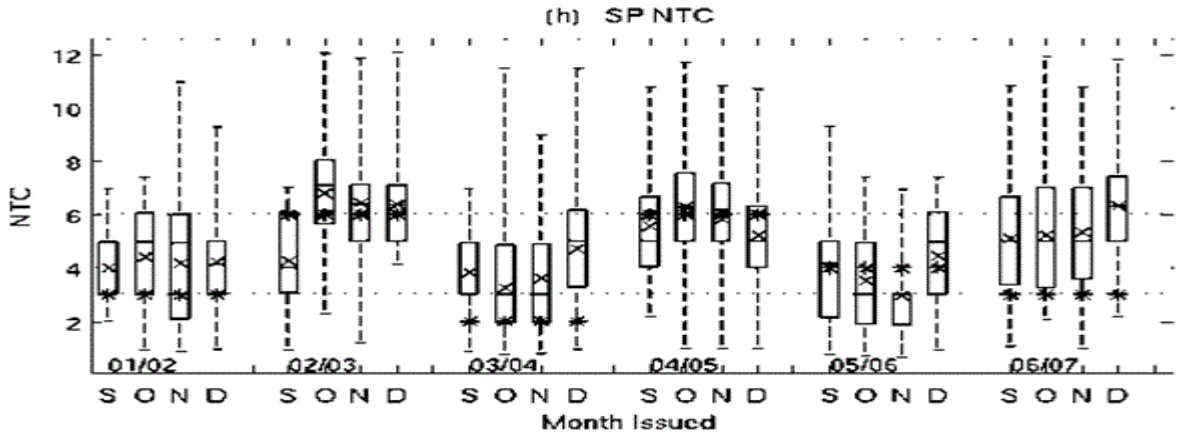
(h) SP NTC
NTC
12
10
8
6
4
2
01/02
02/03
03/04
04/05
05/06
06/07
S O N D
Month Issued

Figure 7.8. Model (raw)forecasts (box plots and whiskers)and observations (asterisks)of number of TCs (NTC)and accumulated cyclone energy (ACE)for all basins and leads. The cross inside the box shows the ensemble mean, and the horizontal line shows the median. Also shown by dotted horizontal lines are the boundaries between the tercile categories. Panels(a)-(f) are for the northern hemisphere basins, with NTC on the left panels and ACE on right panels, for ENP, ATL,W NP in each row, respectively. The two bottom panels are for NTC in the southern hemisphere basins: AUS (g) and SP (h).

7.8 Summary

The International Research Institute for Climate and Society (IRI) has been issuing experimental TC activity forecasts for several ocean basins since early 2003. The forecasts are based on TC-like features detected and tracked in the ECHAM4.5 atmospheric model, at low horizontal resolution (T42). The model is forced at its lower boundary by sea surface temperatures (SSTs) that are predicted first, using several other dynamical and statistical models. Results show that low-resolution model deliver statistically significant, but fairly modest, skill in predicting the inter-annual variability of TC activity. In a 2-tiered dynamical prediction system such as that used in the IRI forecasts, the effect of imperfect SST prediction is noticeable in skills of TC activity compared with skills when the model is forced with historically observed SSTs.

Although prospects for the future improvement of dynamical TC prediction are uncertain,it appears likely that additional improvements in dynamical systems will make possible better TC predictions. As is the case for dynamical approaches to ENSO and near-surface climate prediction, future improvements will depend on better understanding of the underlying physics,more direct physical representation through higher spatial resolution, and substantial increases in computer capacity. Hence, improved TC prediction should be a natural by-product of improved prediction of ENSO, global tropical SST, and climate across various spatial scales.

7.9 Reference

Anderson, J.L., 1996: A method for producing and evaluating probabilistic forecasts from ensemble model integrations. *J. Climate*, **9**, 1518-1530.

Anderson, D., T. Stockdale, M. Balmaseda, L. Ferranti, F. Vitart, F. Molteni, F. Doblas-Reyes, K. Mogensen and A. Vidard, 2007: Development of the ECMWF seasonal forecast system 3, ECMWF Tech. Memo., 503.

Balmaseda, M., A. Vidard and D. Anderson, 2007: The ECMWF system 3 ocean analysis, ECMWF Tech. Memo., 508.

Barnston, A.G., A. Kumar, L. Goddard, and M. P. Hoerling, 2005: Improving seasonal prediction practices through attribution of climate variability. *Bull. Amer. Meteor. Soc.*, **86**, 59-72.

Barnston, A.G., S.J. Mason, L. Goddard, D.G. DeWitt, and S.E. Zebiak, 2003: Multimodel ensembling in seasonal climate forecasting at IRI. *Bull. Amer. Meteor. Soc.*, **84**, 1783-1796.

Bell, G. D., and M. Chelliah, 2006: Leading tropical modes associated with interannual and multi-decadal fluctuations in North Atlantic hurricane activity. *J. Climate*. **19**, 590-612.

Bell, G. D., et al., 2000: Climate assessment for 1999. *Bull. Amer. Meteor. Soc.*, **81**, S1-S50.

Bengtsson, L., H. Böttger, and M. Kanamitsu, 1982: Simulation of hurricane-type vortices in a general circulation model. *Tellus*, **34**, 440-457.

Bengtsson, L., M. Botzet, and M. Esch, 1995: Hurricane-type vortices in a general circulation model. *Tellus* **47A**: 175-196

Buizza, R. and T. Palmer, 1995: The singular-vector structure of the atmospheric global circulation. *J. Atmos. Sci.*, **52**, 1434-2456.

Buizza, R., M. Millter, and T.N. Palmer, 1999: Stochastic representation of model uncertainties in the ECMWF ensemble prediction system. Quart. *J. Roy. Meteor. Soc.*, **125**, 1887-2908.

Camargo, S. J., and A. G. Barnston, 2009: Experimental seasonal dynamical forecasts of tropical cyclone activity at IRI. *Wea. Forecasting*, **24**, 472–491

Camargo, S. J., and A. G. Barnston, 2008: Description and skill evaluation of experimental dynamical seasonal forecasts of tropical cyclone activity at IRI, *IRI Technical Report 08-02*, International Research Institute for Climate and Society, Columbia University, Palisades, NY.

Camargo, S. J., and A. H. Sobel, 2004: Formation of tropical storms in an atmospheric general circulation model. *Tellus*, **56A**, 56-67.

Camargo, S. J., and S. E. Zebiak, 2002: Improving the detection and tracking of tropical cyclones in atmospheric general circulation models. *Wea. Forecasting*, **17**, 1152-1162.

Camargo, S. J., A. G. Barnston, and S. E. Zebiak, 2005: A statistical assessment of tropical cyclone activity in atmospheric general circulation models. *Tellus*, **57A**: 589-604.

Camargo, S.J., A.G. Barnston, P.J. Klotzbach, and C.W. Landsea, 2007a: Seasonal tropical cyclone forecasts. *Bulletin of the World Meteorological Organization*, **56**, 297-307

Camargo, S. J., H. Li, L. Sun, 2007b: Feasibility study for downscaling seasonal tropical cyclone activity using the NCEP regional spectral model. Int. *J. Climate*, **27**, 311-325.

Camargo, S. J., A. H. Sobel, A. G. Barnston, and K. A. Emanuel, 2007c: Tropical cyclone genesis potential index in climate models. *Tellus*, **59A**, 428-443.

Chen, T.C., Yoon, J., Croix, K.J., and Takle, E.S., 2001: Suppressing impacts of Amazonian deforestation by global circulation change. *Bull. Amer. Meteorol. Soc.* **82** 2209-2215.

Chu, P.S., Z.P. Yu, and S. Hastenrath, 1994: Detecting climate change concurrent with deforestation in the Amazon Basin: Which way has it gone? *Bull. Amer. Meteorol. Soc.* **75** 579-583.

Ebisuzaki, W., M. Chelliah, and R. Kistler, 1996: NCEP/NCAR Reanalysis: Caveats. In Proc. First WMO Reanalysis Workshop, Silver Spring, MD.

Efron, B. and G. Gong, 1983: A leisurely look at the bootstrap, the jackknife, and cross-validation. *The American Statistician*, **37**, 36-48.

Goddard, L., A.G. Barnston, and S.J. Mason, 2003: Evaluation of the IRI's "Net Assessment" seasonal climate forecasts: 1997-2001. *Bull. Amer. Meteor. Soc*., **84**, 1761-1781.

Goldenberg, S. B., and L. J. Shapiro, 1996: Physical mechanisms for the association of El Niño and West African rainfall with Atlantic major hurricane activity. *J. Climate*, **9** 1169-1187.

Gray, W. M., 1990: Strong association between West African rainfall and U.S. landfall of intense hurricanes. *Science*, **249**, 1251-1256.

Gray, W. M., J. D. Sheaffer, and C. W. Landsea, 1996: Climate Trends associated with multi-decadal variability of Atlantic hurricane activity.*Hurricanes: Climate and Socioeconomic Impacts*. H. E. Diaz and R. S. Pulwarty, eds., Springer-Verlag, 292 pp.

Gray, W. M., 1984a: Atlantic seasonal hurricane frequency. Part I: El Niño and 30 mb quasi-biennial oscillation influences. *Mon. Wea. Rev*., **112**, 1649-1668.

Gray, W. M., 1984b: Atlantic seasonal hurricane frequency. Part II: Forecasting its variability. *Mon. Wea. Rev.*, **112**, 1669-1683.

Gray, W. M., C. W. Landsea, P. W. Mielke Jr., and K. J. Berry, 1992: Predicting Atlantic seasonal hurricane activity 6-11 months in advance. *Wea. Forecasting*, **7**, 440-455.

Gray, W. M., C. W. Landsea, P. W. Mielke Jr., and K. J. Berry, 1994: Predicting Atlantic basin seasonal tropical cyclone activity by 1 June. *Wea. Forecasting*, **9**, 103-115.

Hastenrath, S., 1990: Decadal-scale changes of the circulation in the tropical Atlantic sector associated with Sahel drought. Int. *J. Climatol*., **10**, 459-472.

Kalnay, E., and Co-authors, 1996: The NCEP/NCAR 4-year Reanalysis project. *Bull. Amer. Meteor. Soc.,* **77,** 437-471.

Kistler, R., and Co-authors, 2001: The NCEP/NCAR 50 year reanalysis: Monthly means CD-ROM and documentation. *Bull. Amer. Meteor. Soc.*, **82**, 247-268

Klotzbach, P. J., 2007: Revised prediction of seasonal Atlantic basin tropical cyclone activity from 1 August. *Wea. Forecasting,* **22**, 937-949.

Klotzbach, P. J., 2008: Refinements to Atlantic basin seasonal hurricane prediction from 1 December. *J. Geophys. Res.*, **113**, D17109, doi:10.1029/2008JD010047.

Klotzbach, P. J., and W. M. Gray, 2004: Updated 6-11 month prediction of Atlantic basin seasonal hurricane activity. *Wea. Forecasting*, **19**, 917-934.

Klotzbach, P. J., and W. M. Gray, 2008a: Extended range forecast of Atlantic seasonal hurricane activity and U.S. landfall strike probability for 2008. Dept. of Atmospheric Science Rep., Colorado State University, Fort Collins, CO, 32 pp.

Klotzbach, P. J., and W. M. Gray, 2008b: Extended range forecast of Atlantic seasonal hurricane activity and U.S. landfall strike probability for 2008. (updated). Dept. of Atmospheric Science Rep., Colorado State University, Fort Collins, CO, 39 pp.

Landman, W. A., A. Seth, and S. J. Camargo, 2005: The effect of regional climate model domain choice on the simulation of tropical cyclone-like vortices in the Southwestern Indian Ocean. *J. Climate*, **18**, 1253-1274.

Landsea, C. W., and W. M. Gray, 1992: The strong association between Western Sahel monsoon rainfall and intense Atlantic hurricanes. *J. Climate*, **5**, 435-453.

Landsea, C. W., W. M. Gray, P. W. Mielke, and K. J. Berry, 1992: Long-term variations of western Sahelian monsoon rainfall and intense U.S. landfalling hurricanes. *J. Climate*, **5**, 1528-1534.

Landsea, C. W., R. A. Pielke, Jr., and A. M. Mestas-Nuñez, 1999: Atlantic basin hurricanes: Indices of climate change. *Climate Change*, **42**, 89-129.

Lea, A. S., and M. A. Saunders, 2004: Seasonal predictability of Accumulated Cyclone Energy in the North Atlantic, Proceedings of the 26th Conference on Hurricanes and Tropical Meteorology, Miami, USA, May 3-7, pp. 419-420.

Lea, A. S. and M. A. Saunders, 2006a: Seasonal prediction of typhoon activity in the Northwest Pacific basin, *27th Conference on Hurricanes and Tropical Meteorology*, Monterey, CA, USA, April 24-28 (poster paper).

Lea, A. S. and M. A. Saunders, 2006b: How well forecast were the 2004 and 2005 Atlantic and US hurricane seasons? *Weather*, **61**, 245-249.

Lloyd-Hughes, B., M. A. Saunders and P. Rockett, 2004: A consolidated CLIPER model for improved August-September ENSO prediction skill, *Wea Forecasting*, **19,** 1089-1105.

Mason, S.J., L. Goddard, N.E. Graham, E. Yulaeva, L.Q. Sun, and P.A. Arkin,1999: The IRI seasonal climate prediction system and the 1997/98 El Niño event. *Bull. Amer. Meteor. Soc.*, **80**, 1853-187.

Palmer, T.N., and coauthors, 2004: Development of a European Multimodel Ensemble System for seasonal to interannual prediction (DEMETER), *Bull. Amer. Meteor. Soc.*, **85**, 853-872.

Palmer, T., 2001: A nonlinear dynamic perspective on model error: A proposal for nonlocal stochastic dynamic parametrization in weather and climate prediction systems. *Quart. J. Roy. Meteor. Soc.*, **127**, 279-304.

Roeckner, E., et al., 1996: The atmospheric general circulation model ECHAM-4: Model description and simulation of present-day climate. Tech. Rep. 218, Max-Planck Institute for Meteorology, Hamburg, Germany. 90 pp.

Saunders, M. A., 2006: Winds of change. *Post Magazine Risk Report*, pp. 28-29, 9 November 2006.

Saunders, M. A. and A. S. Lea, 2005: Seasonal prediction of hurricane activity reaching the coast of the United States. *Nature*, **434**, 1005-1008.

Saunders, M. A. and A. S. Lea, 2008: Large contribution of sea surface warming to recent increase in Atlantic hurricane activity. *Nature*, **451**, 557-560.

Vitart, F., 2006: Seasonal forecasting of tropical storm frequency using a multi-model ensemble. *Quart. J. Roy. Meteor. Soc.*, **132,** 647-666.

Vitart, F., J. L. Anderson, and W. F. Stern, 1997: Simulation of interannual variability of tropical storm frequency in an ensemble of GCM integrations. *J. Climate*, **10**, 745-760.

Vitart, F., M.R. Huddleston, M. Déqué, D. Peake, T.N. Palmer, T.N. Stockdale, M.K. Davey, S. Inenson, A. Weisheimer, 2007: Dynamically-based seasonal forecasts of Atlantic tropical storm activity issued in June by EUROSIP, *Geophys. Res. Lett.*, **34**, L16815, doi:10.1029/2007GL030740.

Vitart F. D. and T. N. Stockdale, 2001: Seasonal forecasting of tropical storms using coupled GCM integrations. *Mon. Wea. Rev.*, **129**, 2521-2537.

Wilks, D. S., 2006: Statistical Methods in the Atmospheric Sciences, 2nd Ed. *International Geophysics Series,* **Vol. 59**, Academic Press, 627 pp.

Chapter Eight

Andrew Burton
Perth Tropical Cyclone Warning Centre
Bureau of Meteorology
Australia

8. Operational Strategy

8.1 Introduction

The aim of this chapter is to suggest an operational strategy to optimise the efficiency and effectiveness of a Tropical Cyclone Warning Centre (TCWC)[1]. The efficiency and effectiveness of TCWC operations is affected by such diverse factors as for example the physical layout of the office, the training of staff, the design and documentation of forecast processes, and business continuity planning. In short it is concerned with all the non-meteorological aspects of delivering a cyclone warning service. In the period since the last edition of the Global Guide to Tropical Cyclone Forecasting (hereafter Global Guide) a number of factors have greatly influenced the TCWC systems and processes.

Tropical cyclone track forecasting skill has improved steadily over the last two decades, aided by improved numerical weather prediction (NWP) and widespread adoption of consensus track forecasting methods that optimise the skill of the available forecast aids. However the increase in forecast skill has lead to an increase in service expectations. Tropical Cyclone Warning Centres (TCWCs) are now typically providing longer lead time forecasts, with an expanded range of products - particularly in graphical formats.

Demands on TCWC forecasters have also grown through an increase in the volume of data to be assimilated during each forecast cycle. Observational data has increased, predominantly as a consequence of a greater number of low earth orbit satellites providing passive and active microwave satellite data that requires additional skills and time to be properly incorporated into the analysis process. The increased number of NWP models available to the forecaster has also imposed a burden on the forecaster to be familiar with the characteristics of a wide range of models and to find the time to diagnose the model forecasts in order to determine where NWP failure may occur and, where different models predict significantly different tracks/intensities, to ascertain what the significant differences are in the model fields.

The rapid advancement of computer technology has offered efficiency dividends to TCWCs, and has helped TCWCs cope with the increased data flows, but it has also raised training overheads for staff, who must now be proficient users of technology in order to meet the demands placed on them.

Operational strategy is important because if TCWC processes are inefficient forecasters find themselves spending the majority of time preparing products and dealing with technological issues and are be unable to devote adequate time to understanding the meteorology of the situation. Operational strategy offers a means by which service improvements can be delivered independent of improvements in forecast accuracy.

Throughout this chapter we will examine how the changes broadly outlined above have affected TCWCs. With the contemporary TCWC in mind we will identify ways in which the available human and technological resources can best be harnessed, and how TCWC processes can be optimally designed to ensure the efficiency and effectiveness of warning operations.

There is considerable diversity in the structure, client focus and funding levels of TCWCs across the globe. Some TCWCs average very few tropical cyclones per season, indeed there are TCWCs that average less than one cyclone per season , whereas others deal with significant numbers (eg. an average of between nineteen and twenty tropical cyclones occur in the Philippines (PAGASA) area of responsibility each season). To ensure that a broad range of perspectives were considered the following TCWCs kindly provided detailed input on current operational strategy: Australian Bureau of Meteorology TCWCs (Brisbane, Darwin and Perth), the Hong Kong Observatory (HKO), Jakarta TCWC, JTWC, RSMC La Reunion, RSMC Tokyo, and the Vietnam National Centre for Hydrometeorological Forecasting (NCHMF).

Given the organisational diversity of TCWCs we cannot take a prescriptive approach to operational strategy, but we can examine the issues which affect operational efficiency and recommend sound strategies for dealing with those issues.

1In referring to TCWCs we include specialised centres (e.g., Regional Specialised Meteorological Centre (RSMC) La Reunion, the US National Hurricane Center (NHC) and the US Department of Defence Joint Typhoon Warning Center (JTWC)) that employ tropical cyclone specialists as well as National Meteorological and Hydrological Services (NMHSs) that generally do not employ specialist tropical cyclone forecasters and which have diverse levels of funding, staffing and training.

8.2 Infrastructure and systems

8.2.1 Physical design of the forecast/warning office

When considering the effectiveness and efficiency of a TCWC some attention should be given to the physical layout of the forecast office. Layout will largely be a function of the available space, and the equipment and people to be accommodated - parameters that will vary considerably between forecast offices - however some general principles can be suggested as guidance.

The TCWC should be located so that outside distractions are minimised. During the forecast cycle there will be times when the TCWC staff are under pressure to make critical warning decisions while meeting tight deadlines. Unnecessary distractions can hamper efficiency.

Sufficient space should be allocated to ensure that during periods of peak work load staff have adequate room and are able to easily move about the area to access equipment and interact with each other.

The layout of equipment should reduce the need for forecasters to move around to access data. The data should be channelled toward the forecaster so that the most commonly accessed data is closest to hand. In the last two decades the use of computer workstations has become ubiquitous and nowadays most data is accessed in this manner. Indeed it is now common for forecasters to use multiple workstations to access additional computing power and “screen real estate” allowing for dedicated radar or satellite displays. Multiple workstations also allow for the use of software with specific operating system requirements. The office layout should ensure that the forecaster can operate frequently used workstations with minimal movement. If a single workstation (perhaps a dedicated radar display for example) is to be shared by a number of forecasters it should be placed closest to the forecasters who need to access it the most as the frequency with which forecasters will refer to data can be influenced by the ease of access.

Ergonomic furniture including adjustable chairs and desks should be stipulated to avoid health problems that can arise from continual use of monitors and keyboards.

Good lighting is also essential, especially in areas used for analysing synoptic charts and other hard copy data. Areas of strong reflection or glare should be minimised as they invariably cause problems with ease of reading computer screens, leading to eye strain.

Noise from equipment such as computers, printers and fax machines should be minimised by the use of sound-absorbent materials, "silent" printers and by placing unavoidably noisy equipment in more unobtrusive places in the office.

Some TCWCs disseminate warnings via a recorded message service and if this is the case some thought should be given to establishing an area separate to the main forecasting area where forecasters can record warning messages without interruption or background noise. A separate area for conducting media interviews is also desirable for some TCWCs and this concept will be considered in more detail later in this chapter.

Manual analysis of hard copy charts is still common and they need to be in an area that is accessible to all forecasters without causing "traffic jams". Although there has been a proliferation of electronic equipment in the forecasting office over the last few decades we have not seen the advent of the "paperless office" and it is still common for many resources to be accessed via hardcopy. The nature of these is varied (standard operating procedures, checklists, Dvorak flowcharts, lists of phone numbers) but invariably the number of such documents grows to be quite large, and it is important that these resources are stored in a logical fashion that facilitates quick retrieval. It is handy to have a fair amount of free wall space for hanging maps and storing these resources. Constructing folders of forecast aids and other resources that are organised in a logical fashion can help ensure efficient retrieval of information under

pressure, but this can also be done electronically and this will be covered in greater detail later in thie chapter.

There are generally three different styles of TCWC accommodation:

1. TCWC incorporated into the main forecasting area: When the TCWC function occurs in an area of the main forecasting operations regular liaison between the two functions is encouraged, however care should be taken to ensure that the two functions do not disrupt each other. An area within the forecast office should be clearly designated as the TCWC (even if it is only on a temporary basis as the need arises) and should contain the equipment necessary to carry out the cyclone forecasting task. Shared facilities should be carefully located to ensure they are easily accessible to both operations.

2. TCWC adjacent to main forecasting area: A TCWC that is separate from the main forecasting area but located adjacent to it offers forecasting staff in both areas greater insulation from the distractions caused by the other operations while still encouraging liaison to maintain consistency between forecast products. Ideally the TCWC will be equipped to run independently of the main forecasting area, however if some facilities need to be shared they should be located close to both operations.

3. Dedicated TCWC: In the case of an office dedicated to the tropical cyclone forecasting function there is generally greater scope to ensure the office design supports the forecast process. The design should channel the information to the forecaster, usually by placing key workstations at the forecasters' fingertips and ensuring synoptic charts are close at hand. The relationship of the shift supervisor to support staff needs to be considered and some thought may need to be given to facilitating the briefing of senior management by the shift supervisor without disrupting support staff.

8.2.2 Technology and data access

A key technological requirement of an efficient TCWC is high speed access to satellite and NWP data through robust information technology (IT) infrastructure. The bandwidth requirements of TCWCs have increased significantly over the last two decades as the variety and resolution of satellite imagery and NWP products has increased. Because of the time constraints in the forecast cycle, forecasters require rapid access to key data sources. Information that may be of value to the decision making process, but which takes time to access, is at high risk of being overlooked by time-poor forecasters. A significant proportion of the TCWCs surveyed reported that the speed of internet connections or of Local/Wide Area Networks (LAN/WAN) occasionally limited data access during operations.

The responsiveness of software used for in the TCWC is also important to operational efficiency. When selecting software for TCWC operations there is often a focus on the functionality and cost, however speed of response should be also be considered a key criterion.

It is also important that the responsiveness of software is tested under operational conditions as response times may increase significantly under the heavy loads that can arise in operations.

The free availability of operationally focused web pages such as:

- the Naval Research Laboratory (NRL) Monterey Marine Meteorology Division Tropical Cyclone Page (http://www.nrlmry.navy.mil/tc_pages/tc_home.html),
- the Cooperative Institute for Meteorological Satellite Studies Tropical Cyclone page (http://cimss.ssec.wisc.edu/tropic2/), and
- the National Environmental Satellite, Data, and Information Service (NESDIS) / Cooperative Institute for Research in the Atmosphere (CIRA) / Regional and Mesoscale Meteorology Branch (RAMMB) Real-Time Tropical Cyclone Products web page (http://rammb.cira.colostate.edu/products/tc_realtime/index.asp)

allows TCWCs sufficient access to satellite data, in a convenient format, without maintenance overheads. Through the provision of resources such as these research centres make significant contributions to the effectiveness and efficiency of tropical cyclone warning centres in a manner that ensures global equity of access.

The Sixth WMO International Workshop on Tropical Cyclones (IWTC-VI) recommended that all tropical cyclone-related Numerical Weather Prediction (NWP) products be made available to all operational centres in real-time. It is hoped that development of GIFS-TIGGE, the Global Interactive Forecast System THORPEX[2] Interactive Grand Global Ensemble will provide the vehicle through which this is achieved. This would mark a similar advance in ensuring equitable global access to NWP products as the above research centres have done for satellite data.

[2] THORPEX is The Observation System Research and Predictability Experiment, a project of the World Meteorological Organisation's World Weather Research Program (WMO/WWRP).

The technological advances described above improve the efficiency and effectiveness of TCWCs through improved data access. Operational strategy also needs to consider the role of technology in streamlining and supporting the forecast process and dissemination of products. Using software in the forecast process can lead to significant improvements in efficiency through automation or partial-automation of tasks; and can lead to improvements in effectiveness through reduction in errors, including errors of logic and transcription. It is not surprising that all the TCWCs surveyed for this chapter use some level of technological support and in many TCWCs the majority of tasks are now either automated, or where subjective judgement is required or desirable (e.g., subjective Dvorak analysis) interactive software is used. The range of technological enhancements being considered here ranges from software specifically designed to support the forecast process (such as the Automated Tropical Cyclone Forecasting System (ATCF) (Miller et al. 1990) or the Australian Bureau of Meteorology Tropical Cyclone Module (TC Module)), to simple technological enhancements, such as the use of a

specially designed spreadsheet to record subjective Dvorak estimates in place of hardcopy recording. (Click here to download an MS Excel spreadsheet for recording Dvorak estimates.)

When considering the incorporation of technology into the operational process the following factors should be considered:

- robustness,
- fitness for purpose,
- future obsolescence,
- maintenance, and
- training requirements

Tropical cyclone warnings services are generally regarded as a critical function for national meteorological services and it is vital that any technology that is relied upon to deliver those services is robust. This applies whether it is hardware or software under consideration. It is important that testing is done under loads as large as might be experienced in operations. For example, when testing operational software on TCWC workstations it is not sufficient to test a software package in isolation. The stability and response times of the software need to be tested when the workstation is running the full complement of operational software, and with the local area network under a load similar to that which will result during significant events - when it is likely that every available workstation will be in use.

Fitness for purpose is another important consideration for TCWC technology infrastructure. Short Message Service (SMS) text messaging is the most widely used data application in the world however its fitness for purpose for the transmission of critical messages to important clients, such as emergency services managers, can be called into question. As a result of its design as a "best effort" service[3] delivery is not guaranteed and there are occasional long delivery times. Hence it cannot be relied upon in situations where a rapid response from the recipient may be vital. Similarly the timeliness of delivery via email cannot be guaranteed so care needs to be taken to explain to recipients the possible risks involved in this method of delivery.

When incorporating new technologies into operations future obsolescence should be considered. In contemporary times it is not uncommon for new technologies to become superseded or functionally obsolete within five to ten years. If it is unlikely that funding will be available to replace the technology within this time frame then its incorporation into the TCWC may cause future problems.

The level of maintenance required to keep the technology operational and prevent obsolescence should also be considered. For example, software designed to incorporate NWP data may require frequent modification to allow for the rapid evolution of NWP models. In this case it will be necessary to ensure that there will be continued access to the expertise required to maintain the software software's functionality.

Finally, the amount of training needed to ensure efficient and effective use is an important consideration when evaluating technology for incorporation into a TCWC. A software package that is designed for "power users" may provide good support to well trained forecasters familiar with its operation while leading to a reduction in efficiency amongst forecasters who are only occasional users of the software. Maintaining the skills of infrequent users at the required level may prove overly burdensome, especially if there is a high level of turnover amongst operational forecasters in the TCWC.

[3] See http://en.wikipedia.org/wiki/Best_effort_delivery for a description of best effort delivery.

8.3 People

8.3.1 Staffing

Due to budgetary constraints, forecast offices are often staffed for "average" weather conditions, with "average" usually meaning "fine" weather conditions. Consequently the extra workload associated with a tropical cyclone often means there are not enough staff to cope with both the routine obligations and the workload specifically related to the tropical cyclone. In many jurisdictions this problem is exacerbated because the workload associated with the routine forecasts (e.g., Terminal Area Forecasts) increases at the same time as the new range of products specifically relating to the tropical cyclone become required. Hence the staff members involved in general forecasting are under increased pressure at the same time that weather service managers are looking to free up staff resources to cope with the extra workload involved in producing tropical cyclone warning services.

It is important that weather service managers give careful consideration to the numbers of staff required to carry out tropical cyclone duties effectively, and the following points need to be considered.

- A TCWC should be manned 24 hours a day once a tropical cyclone poses a significant threat to communities. Ideally the TCWC would be manned 24 hours a day for any tropical cyclone in its area of responsibility, but this is often not possible, particularly if there is the likelihood that the TCWC will be active for a prolonged period causing a strain on available staff resources.
- The level of staffing should increase as the threat level increases. For example, when a cyclone is in the area of responsibility but does not pose a significant threat to communities it may be sufficient to have two 9 or 10-hour shifts with just one person per shift. As the threat to communities increases the staffing should increase to 24-hour coverage; which may require three shifts per day to conform to occupational health and safety guidelines for rostering (see below). It will also likely be necessary to increase the number of staff on each shift as the threat increases.
- The detrimental effects of fatigue on decision making are well documented (eg. Castellan 1993) and it is important that rosters are designed to minimise fatigue. TCWC

managers are urged to consult the available literature when designing shift rosters. Key points to note include:

- The longer the shift length the less consecutive shifts should be worked.
- No shift should exceed 12 hours duration.
- No more than 2 consecutive night shifts should be worked.
- Split shifts should be avoided.

All staff should be assigned clearly defined duties so that there is a minimum of confusion within the office routine during a tropical cyclone event. Care should be taken to limit the other responsibilities of staff assigned to tropical cyclone duties. In high stress situations people tend to focus on the tasks that they are most familiar and comfortable with. Hence if tropical cyclone forecasters are expected to continue to carry out routine tasks not associated with the tropical cyclone, and which they are more familiar with, there is a risk that they will fail to give priority to the TCWC duties.

There are large benefits in having tropical cyclone (or, in general, severe weather) specialist positions established within a TCWC. As well as being able to bolster forecasting staff numbers in cyclone events, cyclone specialists can fulfil a number of other roles which are central to the overall efficient running of a TCWC, including:

- training other forecasters,
- maintaining procedural documentation,
- providing a focal point for tropical cyclone matters throughout the year, and leadership in the TCWC during events,
- conducting applied research and techniques development work for the benefit of the TCWC,
- undertaking seasonal verification work,
- conducting public education campaigns,
- establishing close links with emergency management groups, and
- generally maintaining the TCWC at a high level of efficiency.

8.3.2 Training

The meteorology of tropical cyclones is a specialist area. Consequently the forecasting of tropical cyclones requires specific techniques and skills (e.g., Dvorak analysis) which are not required, or not as heavily relied upon (e.g., analysis of passive microwave data) in general forecasting. It is important that all staff be trained in both the science of tropical cyclone meteorology and in efficient TCWC procedures. The more proficient staff members are in TCWC procedures the more time they will be able to devote to considering the meteorology of the event.

It is beneficial for trainers to themselves be given training in how to most effectively deliver training, but they must also be respected for their knowledge of the science and have

operational experience. Specialist training positions staffed by persons with scientific skills, operational experience and a background in educational theory is an optimal goal that is out of reach of most centres. In the absence of that level of staff resource, the task of delivering training most often falls to the most skilled and experienced forecaster.

Where software is introduced to support the forecasting function forecasters need to be properly trained in its efficient use. The degree to which software can enhance the efficiency of a TCWC is partly a function of its design. It can be extremely beneficial for the programmers writing or updating the software to have an understanding of the forecast processes in the TCWC. If possible they should be encouraged to witness the TCWC in operation and closely examine the workflow in order to be able to design the software to support the process, rather than simply providing a toolbox that includes the necessary functions. Within the Australian Bureau of Meteorology, the occasional deployment of programmers to the TCWC during operations has been recognised as having facilitated a much greater degree of support for the forecast process within the specialist software used in Australian TCWCs (TC Module). This has helped to re-establish sufficient time for meteorological analysis despite an increase in the number of products being issued and in the amount of data being assimilated. Where software is used as a decision support tool it is particularly important that software engineers have an in depth understanding of the forecast decision process.

8.3.3 Roles

Training needs of staff members is best considered in relation to the roles they will fill in the warning centre. The operational functions within the TCWC can be separated into various roles such as:

(a) *scientific officer*: responsible for all meteorological aspects of operations;
(b) *incident manager*: akin to shift supervisor, in charge of overall operations including warning policy decisions, and also acting as primary contact for emergency management;

(c) *logistics officer*: responsible for providing technical and logistical support to the TCWC (for example organising extra observations, maintaining records and checking products prior to dissemination) and

(d) *media/information officer*: primary responsibility for conducting media interviews.

It is very common for one staff member to perform multiple roles in a low-key situation, but as the threat to communities escalates there is generally a need to increase the staff resource in the TCWC and assign one or more staff members to the separate roles. Once the processes and procedures of the TCWC are designed and documented the TCWC supervisor needs to identify which staff members will fill the different roles. Some staff members may need to be trained in all roles, but some will only be brought into the TCWC to fill a specific role. If there is a clear demarcation of roles and the training program is oriented around those roles the efficiency and

effectiveness of the TCWC team can be greatly enhanced during the hectic periods of heightened TCWC activity when communities are under threat.

The TCWC environment can be a high stress and/or high work load environment in which there is little time for explicit coordination strategies. To ensure the cohesion of the TCWC team it is important that the team members not only have clearly defined roles but that they share a common mental model of the operational strategy of the warning centre. One of the goals of training should therefore be to establish a shared mental model of TCWC operational strategy. Providing people with knowledge of the meteorology of tropical cyclones and the principles of good warning strategy is not sufficient to ensure effective performance, either of the individual or of the overall team. Training needs to establish a degree of commonality of understanding of how the TCWC functions, from the application of the science to the resolution of warning policy issues and the communication to clients.

The sharing of a common mental model of operational strategy is also important because the forecast and warning process within a TCWC is a continuous process that extends over many days. The cohesion of the TCWC team needs to extend across the rotation of shifts. If clients perceive that the message being broadcast is regularly changing with the shift changeover it can significantly erode their confidence in the reliability of the forecasts. This is particularly true of emergency services personnel who are in close contact with the forecast centre and are attuned to any sudden changes in forecast policy. On the other hand one of the benefits of the rotation of personnel through the warning centre is the fresh perspective that is brought to bear. Having gone through a complex decision making process, assimilating a myriad of observational and NWP data in order to arrive at a conceptual picture of the meteorology of the tropical cyclone and determine the optimum warning strategy, there is a natural resistance to abandon that model in the light of new information. Instead there is a very human tendency to assimilate new information in the light of the existing conceptual model. The change of shift therefore brings the opportunity for a fresh appraisal. A degree of commonality in the mental model of how the forecast and warning process operates does not prevent the reassessment of operational strategy and in fact this fresh appraisal at the changeover, and the strategies for managing how abrupt changes in forecast policy are managed should all form a part of the shared understanding of operational strategy. A common understanding of the processes by which operational decisions are made can mitigate against fatigue by enabling team members to develop methods of interaction that improve their effectiveness, even when fatigued (Foushee et al. 1986, cited in Canon-Bowers et al. 1993).

8.4 TCWC process and procedures

In this section we will examine a very important component of operational strategy: TCWC process and procedures. The two terms are related and before we proceed some explanation of how we will use them is warranted. In this chapter we will use "process" to denote the higher level sequence involved in transforming a set of inputs (e.g., observations, NWP products, etc.) into outputs (e.g., warning products). We use "procedure" to denote the steps involved in accomplishing a specific task (e.g., performing subjective Dvorak analysis).

8.4.1 A cyclical view of TCWC process

The tropical cyclone warning process can be thought of as comprising the following:

- Gathering meteorological observations and forecast guidance (predominantly Numerical Weather Prediction (NWP) products),
- Presenting the observations and forecast guidance to the forecaster,
- Analysing the observations, diagnosing the forecast guidance and constructing a forecast policy,
- Preparing forecast products
- Disseminating forecast products.

The dissemination of forecast products needs to adhere to a rigid time schedule and hence time management is critical in TCWC operations. TCWC operations typically occur on a six hour cycle where forecast products are updated at a minimum of every six hours (in synchronisation with common NWP cycles), with some products being issued more frequently. Products issued at intermediate intervals typically involve an update to analysis information without a complete reformulation of forecast policy. To simplify the discussion we will consider a forecast

8.4.2 Documenting procedures

The procedures associated with the forecast process need to be documented, and the documentation needs to be: complete, easy to access and up-to-date. Some operational centres use printed reference materials such as a folder of standard operating procedures standard, some use electronic media such as a Wiki page. Many forecasters find a mixture of hard copy and electronic resources most suitable, with hard-copy checklists used in conjunction with electronic reference material. Electronic media generally have the advantage that they can be multi-levelled, outlining a concise high level guide while presenting hyperlinks to more detailed procedural information. A generalised example of this style of process is presented in Appendix 8.1. A procedural checklist can be developed from this list. In an electronic version each section would hyperlink to other web or Wiki pages providing more detailed instructions on how to perform each procedure and links to relevant resources. In this way it can be made as extensive a reference as requirements and resources dictate.

8.4.3 The critical time window

Within the typical six-hourly forecast cycle there is a critical time window between the time of the last observation (the analysis or "fix" time quoted in warning products) and the time the products are issued. This window of time can be expressed as follows:

I – O = L + A + P,

where:

I = warning (I)ssue time
O = time of latest (O)bservation (analysis/fix time)
L = observation (L)atency, the time taken to obtain, process and display the observational data to forecasters
A = time available for (A)nalysis, assessment and incorporation into the forecast policy
P = time taken for message (P)reparation.

The product issue times are fixed, and warning effectiveness is enhanced if the analysis information is recent, so there is an imperative to keep the amount of time between analysis time and issue time **(I – O)** to a minimum. This time window may vary according to product requirements but it is often of the order of 30 to 90 minutes. This is the most hectic time in the TCWC forecast cycle and careful consideration must be given to maximising the efficiency of TCWC processes that impact on this aspect of operations. Every effort should also be made to perform tasks outside this window where possible.

To optimise the accuracy and effectiveness of warnings we need to have **A** (the time devoted to analysis, assessment and the formulation of forecast policy) as large as possible. To achieve this we need to minimise **L** and **P**.

L is the observation latency: the period between the time of an observation and the time that the observation becomes available to the forecaster in a form that they can assess and analyse. Some of the factors affecting data latency are technological and can be addressed at an organisational level by adopting appropriate infrastructure. In the case of satellite data for example, the location of satellite receiving stations and the means of reception by the forecasting office will impact on the time taken for the satellite imagery to arrive at the TCWC. There has been a general trend toward decreased data latency as technological infrastructure has developed. Machine plotting of observations onto synoptic charts is now universal and this has reduced data latency in relation to synoptic observations. The use of computer workstations to process and observations in both tabular and spatial formats further reduces the time taken to make synoptic observations available to forecasters but does not facilitate the manual analysis still valued in most TCWCs.

As a result of the overriding influence of technological infrastructure, reducing data latency often involves decisions at an organisational level. However forecasters can often contribute to reducing data latency by being aware of multiple delivery channels and knowing which channel is likely to provide the earliest access to the observation. For example a forecaster may have a preferred site for viewing scatterometer data but be aware that an alternative site often provides access several minutes earlier. The forecaster will then be sure to check the alternative site during the critical window of time prior to issue if it is expected that a satellite pass will soon become available. This kind of detailed information on data sources needs to be shared amongst forecasters to ensure optimum efficiency, and the best way to do this is to ensure that procedures are thoroughly documented and regularly updated.

We want **A**, the time for analysis and forecasting, to be as large as possible but we must also keep in mind that much of the information that a forecaster must assimilate can be assessed outside of this critical window of time, in the remainder of the six-hourly cycle. For instance, since the NWP models are most commonly run at six to twelve-hourly intervals the diagnosis of NWP fields is best performed outside this window of time. Forecasters should record notes of their synoptic reasoning and NWP diagnosis at the time they perform these tasks. This enables proper documentation of the reasoning behind specific forecast decisions and also makes the construction of comments in technical bulletins more efficient. It is also more effective and efficient to draft the prose elements of public warnings during less pressured parts of the forecast cycle rather than waiting until the high pressure period before issue to perfect the wording of the warning. So for example, it may have become apparent through feedback from others in the forecast office that a particular phrasing in the warning is ambiguous or fails to highlight the greatest risk. It is better to redraft the wording immediately, even if an immediate update is not warranted, rather than leave it to the last minute to try and improve the wording to achieve better communication. When the forecast products are being prepared it is then a simple matter of copying and pasting the prepared prose into the relevant product parts. Efforts such as these can greatly improve the efficiency of product preparation, thus reducing **P**, the time taken for message preparation.

The public's trust in the warning message can be significantly degraded if there are errors within products or inconsistencies between products. It is therefore essential that products are checked before issue, and this can be considered part of the preparation time. When the issue time is imminent it may be tempting to shortcut this step. However the potential damage to the effectiveness of the warnings should not be underestimated and hence this is an important component of operational strategy. Where different products within the product suite are crafted separately and do not share data, the workload associated with this step can be significant. The number of errors in disseminated products and the time taken to check products prior to issue can both be greatly reduced using appropriate software. The Australian Bureau of Meteorology achieved a significant reduction in product errors and inconsistencies through the development of TC Module. TC Module supports product preparation by allowing the forecaster to enter all the components of the forecast policy (including prose components of public warnings) into a database and then feeding the data into products in a structured manner. Because the forecast policy components are error checked and automatically fed from a single source the potential for typographic errors and inconsistencies between products is virtually eradicated. The person asked to check the products prior to dissemination can then concentrate on ensuring that the written communication in the public warnings is of the highest standard. It should be noted that wherever possible products should be checked by people who were not involved in writing them, as a fresh perspective can catch errors of phrasing that are not readily apparent to those involved in the drafting of the product.

8.4.4 Coping with the extraordinary

Every tropical cyclone basin will carry cases of systems that have not satisfied the definition of a tropical cyclone but have still caused flash flooding, landslip, wave damage or local wind

damage with the aftermath criticism of the adequacy of the warning system. When writing procedures for tropical cyclone operations it is necessary to discuss what to do with systems that do not make it through the tropical cyclone threshold and definition but which can nevertheless be quite troublesome from a forecasting and warning sense and sometimes, quite lethal. Operational strategy needs to remain flexible enough to enable forecasters to respond effectively in these atypical situations. The documentation may simply instruct forecasters to consult senior management; however even if this is the case the documentation needs to give a clear indication of the circumstances under which the forecaster should cease to exercise their own discretion and is obliged to consult management.

8.5 Delivering the message

8.5.1 Forecast dissemination

An accurate forecast is of no benefit if it is not received, understood and acted upon in a timely manner. Once the warning is prepared, rapid dissemination is essential. The method of delivery of warnings is a function of the communications infrastructure of individual countries. However rapid change in communications technology has been universal and it is clear that this will continue, so it is important for warning agencies to stay abreast of emerging trends. Dissemination via facsimile (fax) machines is on the decline in many countries while email, social media and social networking has undergone explosive growth. Later in this section we consider the importance of these new communication channels from the viewpoint of operational strategy, but first we examine the forecaster's role in the dissemination process.

Operationally, a forecaster's job does not end when the warning is issued. Forecasters need to be involved in some aspects of the dissemination process; however for the sake of the overall efficiency of the TCWC, the general rule should be that the less human intervention in the sending processes the better. Warnings prepared on a workstation can be interfaced with the office's communications system for direct transmission. However warnings need to be disseminated using multiple channels and some of these will involve forecaster input, such as media interviews on television and radio or perhaps input into social media forums.

The optimum methods of delivery are likely to vary according to the type of hazard and the immediacy of the threat. Television has strong visual impact and is a good channel for disseminating warnings about slowly developing events (Mileti and Sorenson, 1990). Television typically reaches a large number of people in the evening hours and has the advantage that graphic information such as maps or diagrams can be incorporated into the message.

Radio is also a major channel for disseminating warnings during non-sleeping hours because it can quickly reach a large number of people. Radio tends to be able to respond more quickly and is therefore generally a more valuable medium than television in a rapidly changing scenario. Radio also has the advantage that it is inexpensive to buy some sortof radio receiver,

and battery powered radios allow people to stay informed even if their normal power supply has failed.

Networking of both television and radio stations can make it more difficult to break into programming to deliver emergency messages to the public in areas at risk. Program content may be being broadcast across a very large area that includes many people not at risk. Establishing memorandums of understanding (MOUs) with broadcasters can ensure that warning messages are broadcast in a timely fashion, preferably at agreed times. Scheduled broadcasts enable people to know when they can tune in to obtain updates. In Australia, for example, communities in cyclone-prone areas know that warnings are broadcast at set times (in most cases, 15 minutes past the hour) by regional radio stations. The broadcast is preceded by a distinctive alerting sound which draws people's attention to the fact that cyclone information is about to be transmitted. MOUs can also ensure that warning messages are read out word-for-word by the broadcaster.

8.5.2 Interaction with the media

Good tropical cyclone forecasters have a sound scientific knowledge of meteorology combined with experience, but "complete" tropical cyclone forecasters are also excellent communicators. People will react to a warning only if they believe that the information they are hearing is true and is relevant to them. A good communicator will give the cyclone warning this credibility and relevance. There are two major benefits of forecasters interacting directly with the media. Firstly this helps to curtail misinterpretations of a warning message. Secondly, it establishes a direct link between the forecaster and the affected community.

All TCWCs rely on senior management and/or operational forecasters to meet the needs of the media in high impact events. Rather than leave good communication to chance, all staff members who interact with the media should be trained in media presentation. The media do not want a sterile scientific portrayal of the hazard. They want to engage with vibrant personalities who can communicate in plain language the excitement and tension of the tropical cyclone hazard. If forecasters cannot meet the needs of media they will tend to look elsewhere in order to find the "talent" they need. It is in the best interests of warning agencies to ensure they have people who are skilled presenters on both radio and television in order to ensure the organisation maintains a high profile.

There are no hard and fast rules for any particular office about how to interact with the media. It will always be a matter of the circumstances surrounding each cyclone event and the traditions and backgrounds of each individual country. The degree of interaction is very much a function of the sophistication of the media itself. TCWCs should try to develop a protocol which minimises media intrusion on staff already under stress from dealing with the tropical cyclone, but still shows the TCWC as a dynamic, credible organisation. If a separate area can be allocated in the layout of a TCWC specifically for media interviews, then disruption to the office routine can be minimised. However, this should done in consultation with the media - it would be plainly wasting resources to set up a facility that the media would not be happy to use, and

media who have traditionally enjoyed free access to a TCWC may not see any benefit from this at all.

Television (TV) is a visual medium and reporters will want to capture vision of the TCWC as a dynamic and animated place. Even if it is possible to conduct all media interviews in other areas it may be necessary to allow some intrusion into the operational area by TV cameras, despite the annoyance this can cause to staff that are already under pressure from the task at hand.

The U.S. National Hurricane Center has adopted a policy which allows the media to have open access during a hurricane event with free access to the forecasting area and to all staff, particularly senior decision makers. This gives the NHC a high public profile during a hurricane event and creates a path for effective, direct communication. The trade-off for this is a corresponding level of disruption for staff involved in the forecasting process.

In contrast the Hong Kong Observatory uses a specially designed TV studio for conducting all briefings and media are not invited into the operational forecasting centre. However they cater to media needs through the provision of graphics presentations of the typhoon event.
In some Australian TCWCs specially designed media briefing rooms have been built adjacent to operational areas, with glass walls allowing the media to film the operational areas without intruding on operational staff. The media are allowed into the operational areas only with permission of the senior forecaster (usually outside the critical window of time leading up to issue of forecasts).

In each of these cases special technological infrastructure has been put into place to make it easier for media to do direct broadcasts from the forecast office. Media interaction should be integrated into the office routine as a planned, deliberate task rather than left as an ad hoc exercise. With prior coordination it is usually possible to minimise the intrusion into critical periods in the forecast cycle.

8.5.3 Social media

It is important for tropical cyclone warning agencies to acknowledge and incorporate emerging communication trends into common place work practice to facilitate stronger linkages with the community. While radio and television continue to be major communication channels, in the last two decades there has been explosive growth in social media and social networks, collectively referred to as Web 2.0[4]. The uptake of social media and involvement in social networks is particularly high amongst young people.

Email, Short Message Service (SMS) texts, instant messaging, Facebook® and Twitter® have become ubiquitous. When the Global Guide to Tropical Cyclone Forecasting was last published in 1993 commercial deployment of SMS was just beginning. It is now the most widely used data application in the world with particularly high rates of usage in Asian countries (Motlik, 2008). Facebook was only launched in 2004 but has already reached over 400 million active users (Website-Monitoring.com, 2010). Twitter and Facebook are largely becoming functions that

users place on mobile devises and receive "tweets" and messages as they would an SMS. This capability allows people to receive, read, update and pass on information anywhere at anytime. Facebook and Twitter allow people to receive links to warning information in real time. This is particularly relevant for Twitter as the short summary messages of 140 characters or less, allows users to quickly scan information and links of interest.

Many meteorological agencies worldwide are utilising social media and social networks to help achieve their organisational responsibilities. Some of these agencies include NOAA, UK Met Office and the NZ Met Service. Web 2.0 technologies may also be useful as a means of maintaining operational liaison with emergency services, allowing graphical briefings during operations for example.

4 **Web 2.0** is a term describing the broad shift towards online communication platforms and environments characterised by interaction, collaboration and user-generated content. Web 2.0 encompasses social media technologies and social networks.

Social media are built on technological foundations which use highly accessible and scalable publishing techniques that collectively facilitate communication. Types of social media include internet forums, blogs, wikis, podcasts, pictures and picture-sharing, video, music and music-sharing, rating and bookmarking, instant messaging and email.

Social networks are services which build online communities of people who share interests, information and/or activities. Facebook and Twitter are examples of social network services which are widely used globally and provide the platform for individuals, groups and organisations to engage.

8.5.4 Interaction with Emergency Management agencies

Coordination with emergency management agencies is critical to the overall effectiveness of the tropical cyclone warning efforts. Emergency managers make critical decisions during tropical cyclone events based largely on meteorological advice. Forecasters have responsibility for ensuring that emergency managers have the best possible information on which to make decisions and possess a clear understanding of the probabilities and risks associated with the full range of forecast scenarios.

Poor communication can result in poor decision making that will directly affect many in the community. It is advantageous for forecasters to have a basic understanding of the emergency management arrangements in their jurisdiction. There may be multiple levels of operational emergency management during a large scale event. In order to provide relevant and appropriately targeted briefings forecasters need to understand the role of the group they are briefing within the overall emergency response structure. The effectiveness and efficiency of communication is further improved if the forecasters have developed relationships with key emergency managers. The investment in "relationship maintenance" outside the peak of the season can be of great benefit during operations.

8.6 Outreach and public education

A warning service is only effective if it stimulates appropriate action and for this to happen recipients of the warning must understand what is being said. It is essential therefore to embark on a campaign of public education to help overcome ignorance of tropical cyclone hazards. Storm surge is a clear example of an area where many people are unaware of the nature and scale of the risk. Deficiencies in understanding make it much harder to effectively communicate during operations and can be the root cause of criticism after the threat has passed. Put another way, a weather service can achieve a marked increase in its value to the community — even though its actual forecasting skill has remained unchanged, by undertaking to raise awareness of tropical cyclones.

Public education is usually more effective if it is done in collaboration with the country's counter disaster organisations. Senior personnel, and particularly those personnel who will be conducting media interviews during operations, should be closely involved in the public education programme. A cyclone education campaign is valuable in the following ways:

- It presents a face for the public to associate with and to focus on so that the weather service is not seen as just an anonymous organisation from which impersonal information issues;
- It lets weather service people tell the public the risks involved with tropical cyclones, what a cyclone is, how a cyclone forms, how it can behave, and the problems involved in forecasting tropical cyclones;
- It can acquaint people with how a TCWC operates; how it detects and tracks cyclones and how it puts a warning together;
- It can try to curtail complacency, particularly in areas that have not been seriously affected for some time or where there is a transient population;
- Through a strong bias towards local counter-disaster groups it can ensure that key people involved in emergency response at the local level are well informed about cyclones and TCWC operations.

8.7 Continuous improvement

Components of the tropical cyclone warning system are continuously evolving. Consequently it is important to routinely review operational strategy to ensure that the TCWC continues to operate in the most effective and efficient manner.

8.7.1 Immediate post impact assessment

Post impact assessments are important to understanding the effectiveness of tropical cyclone warning systems and hence should be considered as part of the operational strategy.

They can also yield important information regarding track and intensity in areas where observations are sparse. For example, in areas where there are limited numbers of tide gauges

it is often possible to estimate storm tide heights through a field survey. Damage to vegetation or to simple structures such as road signs can also be used to estimate wind speeds.

Assessment of social aspects of the warning system are equally important and is best done while people have recent memories of how they received the warnings, how they understood the messages and the actions they took. Post impact surveys are also a way of building the relationship with the community and can affect the response of the community to subsequent threats.

A wide range of skills is needed to conduct a multi-faceted post impact assessment and they are best conducted by multi-disciplinary teams sourced from relevant agencies. It is necessary to build strong relationships between the agencies in order to be able to organise a post impact assessment in a timely manner following a cyclone impact. To keep the organisation of the field trip to a manageable level, and to prevent unnecessary disruption to communities in recovery, teams should be kept as small as possible. Separating the physical and social aspects can assist in this regard.

8.7.2 Formal review/verification

Continuous improvement is not possible without routine performance review. It is strongly recommended that each weather service should carry out a rigorous evaluation of its forecast ability. A routine validation programme can assess any tangible improvements in forecast skill, and may even be able to suggest where resources could be most economically directed to effect forecast improvements.

The bare minimum of any weather service's validation programme should be an assessment of its forecasts of track position and intensity; at least at 12, 24 and 48 h. Ideally however, an office should validate all of the parameters that it uses in its warnings. Eventually parameters should include position, intensity, size, wind speed and direction (for site specific warnings and/or for islands), rainfall, storm surge, area of land under warning and timing of onset of gales.

Performance validation can be a time consuming process, involving many hours of staff time, which some countries may struggle to afford. However workstations allow the validation process to be automated. With a database management system running in the background of normal operational tasks, forecast data can be efficiently stored, and then used by the verification program to produce the desired results very efficiently and with a minimum of human resources. It is further recommended that weather services also verify the effectiveness of any forecast guidance material that they use to produce their warnings. An analysis of such data will assist in determining the relative usefulness of individual forecast techniques and products.

Debrief meetings following significant impacts can help to establish where existing systems and procedures need improvement. They enable the shiftwork team to gather as one to discuss operational strategy. It is often through meetings such as these that more efficient procedures

identified by one team member are discussed, documented and adopted by other members of the team.

8.7.3 Preseason readiness

As part of a TCWC's operational strategy, it is absolutely necessary that there be planning for the coming cyclone season. Forecasters in particular must be ready and waiting for the first active episode in the season rather than merely reacting to events as they unfold. Managers should be aware of issues such as systems preparedness, staff preparedness and public education, prior to the start of the season.

Systems preparedness

It is important that every piece of equipment that is needed to make a TCWC functional works. This will require a systematic checking and monitoring programme which should also be carefully costed and incorporated into the weather service's annual budget. The following points are noteworthy in a TCWC pre-season schedule:

1. There is an operational plan that is both effective and current. If any deficiencies are identified in the cyclone warning system, then the plan should be amended to correct these;
2. Data acquisition systems are operative, e.g., radars tested, remote AWS serviced, observation sites checked (barometers, hydrometers, anemometers etc), and satellite equipment serviceable;
3. All computer systems are operative, e.g., chart plotters, workstations, etc;
4. Warning proformae are up to date
5. Office equipment is serviceable and in adequate supply;
6. All communications are tested, e.g., data in, communication lines out (fax, SSB radio, etc.), and trial warning messages sent to ensure the recipients of the warnings are ready and that address lists for warnings are current;
7. Contingency plans should be in place. There needs to be fallback positions in case of major failure of equipment so that some level of service can still be maintained. It helps to ask the question "What if this fails?" for every piece of equipment in the TCWC. Ideally a business continuity plan will be drawn up that allows for a full range of contingencies including the building being uninhabitable (due to fire for example);
8. The cyclone season programme must be adequately funded so that it can work properly, e.g., extra funds allowed for supplementary observations and payment for staff callouts (if applicable).

Staff preparedness

All staff should be completely aware of their individual roles in a cyclone event. Pre-season briefing sessions are an effective means of doing this, although it can present problems when

staff are operational shift workers and cannot all make meetings at the same time. Every endeavour should be made to overcome these sorts of problems. The task of ensuring staff preparedness is an important role and emphasises the fact that there should be a designated specialist within the TCWC to accommodate this.

Forecasters should be aware of the office procedures, particularly any new procedures or techniques that have been introduced. Established techniques should be revised (e.g., Dvorak, formation checklists, motion techniques, storm surge calculation, etc.). The normal or expected performance of the TCWC should be pointed out to forecasters (e.g., previous seasons' forecast errors) as well as general climatological trends, and tips/rules from the more experienced staff on features that should be watched for in the coming season.

Procedural checklists should also be in place so that TCWC duties are clear and can be worked through systematically in a cyclone event (refer Appendix 8.1). This can minimise instances where tasks may be forgotten under pressure.

An invaluable means of preparation is the use of training modules and educational videos from experts in various fields. This can be an effective method of overcoming the problems of rotational shift working staff becoming familiar with procedures and techniques.

Support staff must also be aware of their duties in a cyclone event. Check lists should be prepared for all staff so that the performance of peripheral tasks is not neglected or forgotten, to the detriment of overall operations.

8.8 A forecaster's operational strategy

The previous sections have outlined areas where efficiencies could be made in an operational environment. These involved office layout and staffing, observing systems, the use of workstations, warning dissemination systems, validation of forecasts and the need for public education programs. Something that has not been adequately addressed in the chapter so far is what forecasters actually do during a cyclone episode. Much of the rest of this chapter takes the perspective of management responsible for designing the systems and processes of a TCWC. In this section we take a look at operational strategy from the perspective of a forecaster. The following points are intended to serve as general guidance — a checklist of how to prepare and what to do.

8.8.1 Know your operational plan

Your government may be able to justify an inaccurate forecast made with the best intentions and based on all available information a lot easier than trying to justify an inaccurate forecast resulting from a lapse in procedures or indecision that could point to some degree of incompetence. Forecasters should be fully aware of the operational plan and adhere to it.

8.8.2 Know your duties

Have available a checklist of duties on a time schedule. You can then manage your available time more effectively. There is nothing worse than not being able to make a warning deadline, particularly if the delay was avoidable.

8.8.3 Know your equipment

Once upon a time tropical cyclone forecasters required no more technological skill than the ability to keep a pencil sharp. Advances in technology have changed all that and a forecaster must be very familiar with the intricacies of all operational equipment, especially computer based workstations. Although these systems are designed with robustness in mind, one can never eliminate the possibility of "crashing" a system, and this is most likely to occur in a pressure situation. A forecaster will need to be able to quickly restore a system in such an event (assuming the problem is not hardware related). Pre-season familiarisation with equipment is essential.

8.8.4 Try to anticipate cyclogenesis

Refer to Chapter 4 of this manual for techniques to use in assessing cyclone formation. If the suspect area has the potential to produce gales within 24 h[5], act. If the system does not develop, then the warning can be readily cancelled, but as long as there is a recognised potential for cyclone formation, there should be appropriate alerts to users. It is easier and often a lot less painful to cancel a warning for a system that did not develop than to issue a reduced lead time warning for a developing system.

5The trigger points may be longer for some products. Trigger points will be documented in standard operating procedures.

8.8.5 Locate the system centre as effectively as possible

Make sure each position fix is consistent with previous fixes. It may be necessary to revise past locations in the light of more recent data. Always have a consistent track. Know the location errors associated with each technique used (refer to Section 3.2 for position analysis). Make sure you have processed all available information.

8.8.6 Use all available prediction techniques

Refer to Chapter 4 of this Global Guide on intensity change techniques and Chapter 3 on track prediction techniques. Be aware of the techniques and objective aids and of their shortcomings. Forecasters need to know which techniques to favour in certain circumstances. This ability may be acquired after years of working in a TCWC and it may be called "experience", but if it can be documented, this useful knowledge can be passed on to others.

8.8.7 Keep a log

If time permits, keeping a log or diary (for example, of reasons for adopting certain policies, or reasons for discounting a certain track prediction technique or for positioning the centre in a particular location) can be of significant benefit. By documenting everyone's reasoning, someone (your cyclone specialist, for example) can post-analyse why things went right or maybe astray. Forecasters may be squandering vast amounts of experience and knowledge by not documenting their actions.

8.8.8 Issue "now-time" warnings

In a warning message, always give the cyclone position corresponding to the warning issue time or at the most, 1 h before. For example, the last firm cyclone fix may have been at 2100 UTC, prior to the next warning issue time of 2400 UTC. That warning should carry an extrapolated cyclone position for either 2300 UTC or 2400 UTC. The error in the extrapolation will be small overall, but it will have the effect of enhancing the timeliness and the credibility of the whole warning message. Users do not respond well to apparently "hours old" information. Also, make sure the warning carries the time of the next warning issue, so that users will be in no doubt when the next information update will be (and adhere rigorously to that schedule). Warning proformae should help ensure warning fix times are current and the time of the next warning is included, so be familiar with your proformae.

8.8.9 Know the danger zones for possible cyclone impact

Forecasters should be aware of when a cyclone is starting to pose a threat to a community. Local research into the location of cyclones 24 h prior to impacting a community can lead to the identification of "danger zones" to alert forecasters as to what may be occurring. Continually ask yourself: "When might the gale/storm/hurricane force winds reach the coast if the system moves (i) at the most likely speed (your motion forecast)? (ii) at the fastest speed indicated as possible by the available guidance?" Don't fall into the trap of thinking only about when the system centre will cross the coast, conditions may have become dangerous many hours before that time depending on the structure and size of the system.

8.8.10 Keep your message clear

Tell people what you know when you know it, and don't get caught up with your "gut feeling". Be as specific as you can in the information you provide but remember that there will always be uncertainty in forecasting. The trick is in how you convey your knowledge of the forecast so that the community understands the scenario they are faced with. When briefing emergency services and the media always try to focus on the likely time when gale force or stronger winds will commence on the coast, rather than when the system centre will cross the coast. If there is uncertainty about when the strong winds will commence indicate both the range of uncertainty

and why there is uncertainty. For example, rather than saying, "Strong winds are expected to commence some time during Wednesday", it is better to say, "The system is moving very slowly now but is expected to accelerate toward the coast overnight. Depending on just when it begins to move we may see gales commence as early as around sunrise. It's most likely gales will commence around lunchtime but everyone should be prepared before retiring for the evening."

8.8.11 "Double check" warning information

It is easy to make mistakes when working under the stress of a tropical cyclone event — simple mistakes such as putting in the wrong issue time, or the wrong date, or an incorrect position coordinate, or even leaving out an important piece of information about the cyclone. Simple, avoidable errors and omissions like these can have the effect of eroding credibility amongst users. Make it a policy to double check every warning before releasing it. If possible get another staff member to check the warning text, as a fresh eye will usually pick up an error much more effectively. Time taken at this stage for one final check will pay dividends, so make allowances for this step when you reach the critical time window prior to the scheduled issue time.

8.8.12 Be responsive

If there is a major change likely to the forecast (for example, a cyclone changing direction, a significant relocation of centre position or sudden intensification), know the key outside people who need to be contacted and pre-empt the issue of the next warning by informing them of the changes as soon as possible. Time saved at this stage can be invaluable. However don't delay issuing products beyond the scheduled transmission time to incorporate insignificant changes in the analysis position that may have come to light as you were preparing the products.

8.9 Summary

The theme of this chapter is building systems — putting together all the knowledge and techniques presented in the other chapters and moulding it into an effective tropical cyclone warning service. If the system is not effective, or if it is deficient in any one aspect of tropical cyclones, then the price in life and property could be intolerably high.

Ways and means were discussed in which to optimise efficiency and enhance effectiveness within a TCWC, reasoning that real advances made in the organisation of a forecasting office can compensate to some extent for the relatively slow rate of improvement of forecasting performance.

Modification to the general layout of the forecast office should be considered by weather service managers when any deficiencies are found to exist in this area. If information can be channelled into the forecaster rather than the forecaster having to physically search it out, then economies of time could be made which may then translate into improvements in the warning

itself. Occupational health and safety issues also need to be dealt with when planning the layout of a TCWC. Aspects such as the reduction of background noise and the use of appropriate lighting were seen to be important areas for consideration.

Adequate staffing should be made available to cope with a cyclone event. Advantages were seen in the appointment of specialist positions that were capable of concentrating on tropical cyclone issues on a year round basis.

Communications are an integral part of the effective functioning of a TCWC and this was discussed both for incoming data and outgoing warning information. The principle data types were examined and the most effective methods of assimilating these into a TCWC were discussed. The most efficient methods of ingesting data involved the use of workstation technology for most data types. Rapid ingestion of data into a readily accessible form will allow the forecaster more available time to assess the situation. The less rushed a forecaster is, the more likely it is that the forecasting decisions that are made will be better reasoned and the warnings issued will be error-free.

Personal computer-based workstations are rapidly becoming more accessible and more affordable, and will eventually become essential to effective operations. The development of software applications specifically for tropical cyclone forecasting will most likely be at the forefront of any future major advances in TCWC operations. Warning dissemination is an important issue if a TCWC is to be effective. Dissemination systems should be developed so that warnings are issued in a timely manner and reach the user as quickly as possible. This usually means a minimum of human intervention (the fewer links in the warning chain the better). The main methods of sending warnings were identified and discussed. An issue here was the need for forecasters to become involved directly with the media. Good media skills will pay off through an increase in the credibility of a warning and a better reaction to the warning information by the general public.

A TCWC must be prepared well before the cyclone season begins. For a warning system to work, it must be well understood by everybody involved, including forecasters themselves, counter disaster groups and the general community. Forecasters' briefing sessions should be encouraged within the TCWC. Close liaison should be nurtured with disaster management groups, and the participation by weather service personnel in public education programs is essential. Also, equipment and systems should be fully tested prior to the commencement of the tropical cyclone season.

The importance of routinely verifying tropical cyclone warnings was emphasised. Although it was recognised that manual verification techniques are tedious, the advent of a verification package on a tropical cyclone workstation and running off a database management system made the prospect of routine verification highly realisable.

Finally, an attempt was made to list (generally, and without being region specific) the sort of strategy which should be adhered to by an operational tropical cyclone forecaster. The underlying message was to be systematic in one's personal approach to forecasting and be

involved to ensure that the overall warning system is as efficient as possible. The stakes are much too high to be anything else.

8.10 References

Cannon-Bowers, J. A., Salas, E., & Converse, S. A. (1993). Shared mental models in expert team decision making. in N. J. Castellan, Jr. (Ed.), *Current issues in individual and group decision making* (pp. 221-246). Hillsdale, N J: Erlbaum.

Castellan, N. J. Jr. (Ed.) 1993, *Current issues in individual and group decision making*. Hillsdale, N J: Erlbaum.

Mileti, D.S., and Sorensen, J.H., 1990. *Communication of emergency public warnings: A social science perspective and state-of-the-art assessment*. Oak Ridge, TN: Oak Ridge National Laboratory, U.S. Department of Energy.

Miller, R. J., A. J. Schrader, C. R. Sampson, and T. L. Tsui, 1990: The Automated Tropical Cyclone Forecasting System (ATCF). *Wea. Forecasting*, **5** 653-660.

Motlik, S. 2008. *Technical Evaluation Report 63. Mobile Learning in Developing Nations*. The International Review of Research in Open and Distance Learning, Vol 9, No 2 (2008) ISSN:1492-3831 Available from http://www.irrodl.org/index.php/irrodl/article/viewArticle/564/1039 Accessed 16 June 2010.

Website-Monitoring.com, 2010. Facebook Facts and Figures. Available from http://alltechnoblog.com/category/infographic/ (Accessed 14 June 2010).

Appendix

Appendix 8.1 TCWC forecast process time line

This example is intended to be illustrative only, but could be used to build a time line checklist for a specific TCWC scenario.)

At start of each shift:

1. Handover, situational awareness.
2. Review existing products.
3. Assess the broad scale environment (e.g., oceanic heat content, long loops of WV and IR, isobaric and streamline analyses over the entire basin).

Each six-hourly cycle:

1. Analyse synoptic environment. Build a conceptual picture of the dominant synoptic influences on the system. Look for changes in intensity/structure/motion, and changes in the environment (e.g., factors that may affect vertical shear). Take notes to document your synoptic reasoning and for use in technical products.
2. Review current location, intensity and structure (subjective Dvorak, ADT, AMSU intensity estimates, scatterometer data).
3. Review major NWP guidance. Determine consistency with current analyses, consistency between models, variations in timing, amplitude and location of synoptic features, differences in environmental vertical shear. Build a physically consistent conceptual picture of the likely evolution of the system and the spread of possible outcomes arising from different forecast scenarios. Take notes to document your synoptic reasoning and for use in technical products.
4. Check for additional NWP data and ingest/construct NWP guidance forecasts.
5. Locate the system centre. Use all available data and interpreted using the conceptual framework you have built up during your synoptic analysis.
6. Perform Dvorak analysis.
7. Compare against all available intensity guidance (ADT, AMSU estimates, etc.) and assign final estimate of intensity.
8. Assess structure (radius to gales/storm/hurricane winds, eye diameter, radius outer closed isobar, environmental pressure).
9. Create consensus and official forecast tracks. Note the spread of model tracks. Only exclude models if you have a clear rationale for doing so. Check short term forecast speed and direction against recent movement.
10. Determine all forecast parameters (intensity and structure) to the required forecast period (e.g., +120 hrs).
11. Consider warning policy. (Do any communities need their alert status changed?) Determine likely gale/storm onset times at key locations.

12. Determine rainfall forecasts. (Consider eTRAP, NWP forecasts, ensemble products, possible totals under different development scenarios, etc.)
13. Storm surge forecasts (work through probable and worst case scenarios…)
14. Pre-issue liaison with internal stakeholders and emergency management if required.
15. Review latest observational data and update analysis/forecast if significant change implied.
16. Prepare and issue product suite, taking account of priorities and deadlines.
17. Once products issued, check for successful delivery (on publicly available web sites for example).
18. Conduct internal briefings/emergency management briefings/media interviews.
19. Ensure logs (operational diary/Wiki, etc.) are up to date.

Return to beginning of six-hour cycle.

Appendix 8.2 Tropical Cyclone Information Processing System (TIPS) at the Hong Kong Observatory

A decision-support tool named Tropical Cyclone Information Processing System (TIPS) was developed by the Hong Kong Observatory, Hong Kong, China to facilitate decision making in forecasting and warning operations during tropical cyclone (TC) situations. TIPS serves four main functions: (i) integrate all TC related information and data, including satellite/radar fixes and imageries, forecast tracks from warning centres and those derived from NWP models for display; (ii) assimilate track data for computation of an ensemble track for operational forecasting; (iii) compute key parameters for evaluating local impact to facilitate warning decisions; and (iv) generate and dispatch forecast and warning products to the local public and other weather centres. The system has been in operation since 2001 and forecasters at the Hong Kong Observatory find TIPS to be user-friendly and indispensable in TC forecast and warning operations.

A paper which describes the design and features of TIPS is available from the HKO: http://severe.worldweather.org/tcc/document/other/TIPS-final.doc

Appendix 8.3 Some capabilities at the RSMC - Tropical Cyclone Centre New Delhi

Technical capability

Regional Specialized Meteorological Centre (RSMC)-Tropical Cyclones, New Delhi, which is co-located with Cyclone Warning Division of the India Meteorological Department (IMD), has the responsibility of issuing Tropical Weather Outlook and Tropical Cyclone Advisories for the benefit of the countries in the World Meteorological Organization (WMO) / Economic and Social Cooperation for Asia and the Pacific (ESCAP) Panel region bordering the Bay of Bengal and the

Arabian Sea, namely Bangladesh, Pakistan, Maldives, Myanmar, Sultanate of Oman, Sri Lanka and Thailand. It has also the responsibilities to issue Tropical Cyclone Advisories to the designated international airports as per the requirements of the International Civil Aviation Organization (ICAO).

Observational system

Surface observatories

IMD has a network of 559 surface observatories. The data from these stations are used on real time basis for operational forecasting. Recently a number of moored ocean buoys including meteorological buoy (MB), shallow water (SW), deep sea (DS) and ocean thermal (OT) buoys have been deployed over the Bay of Bengal and Arabian Sea. A number of automated weather stations (AWS) are also in operation along the Indian coast and provide surface observations on hourly basis which are utilized in cyclone monitoring and forecasting.

Upper air observatories

IMD's upper air network includes 62 pilot balloon observatories, 39 radiosonde / radiowind observatories and 1 radiosonde observatory.

Cyclone detection radars

There are 11 S-band radars for cyclone detection located at Kolkata, Chennai, Visakhapatnam, Machilipatnam, Sriharikota, Paradip, Karakikal, Kochi, Goa, Mumbai and Bhuj, which provide vital information for forecasting cyclone landfall point and intensity. IMD has plans to augment its network of AWS and cyclone detection radars.

Satellite monitoring

At present IMD is receiving and processing meteorological data from two Indian satellites, namely Kalpana-1 and INSAT-3A. Kalpana-1 was launched on 12th September, 2002 and is located at 74.0°E. INSAT-3A was launched on 10 April, 2003 and is located at 93.50°E. Kalpana-1 and INSAT-3A both have three channel Very High Resolution Radiometer (VHRR) for imaging the Earth in visible (0.55-0.75 µm), infrared (10.5-12.5 µm) and water vapour (5.7-7.1 µm) channels having resolution of 2x2 km in visible, and 8x8 km in water vapour (WV) and infrared (IR) channels. In addition the INSAT-3A has a three channel Charge Coupled Device (CCD) payload for imaging the earth in Visible (0.62-0.69 µm), near IR (0.77-0.86 µm) and shortwave IR (1.55-1.77 µm) bands of the spectrum. The resolution of the CCD payload in all the three channels is 1km x 1km. At present about 48 satellite images are taken daily from Kalpana-1 which is the main operational satellite and 9 images are taken from INSAT-3A. Imaging from CCD is done 5 times during daytime only. All the received data from the satellite are processed and archived in National Satellite Data Centre (NSDC), New Delhi.

The Indian Meteorological Data Processing System (IMDPS) is processing meteorological data from INSAT VHRR and CCD data and supports all operational activities of the Satellite Meteorology Division on a round the clock basis.

Under INSAT-3D programme, a new geostationary meteorological satellite, INSAT-3D, is being designed by ISRO. It will have an advanced imager with six imagery channels (VIS, SWIR, MIR, TIR-1, TIR-2, & WV) and a nineteen channel sounder (18 IR and 1 visible) for derivation of atmospheric temperature and moisture profiles. It will provide 1 km resolution imagery in the visible band, 4 km resolution in IR bands, and 8 km in the water vapour channel. This new satellite was launched in July 2013 and should provide much improved capabilities to the meteorological community and users.

Analysis and Prediction

Cloud imageries from geostationary meteorological satellites INSAT-3A and METSAT (Kalpana-1) are the main sources of information for the analysis of tropical cyclones over the data-sparse region of the north Indian Ocean. Data from ocean buoys also provide vital information. Ship observations are also used critically during the cyclonic disturbance period.

The analysis of synoptic observations is performed four times daily at 00, 06, 12, and 18 UTC. During cyclonic disturbance (depression and above intensity), synoptic charts are prepared and analysed every three hours to monitor the tropical cyclones over the north Indian Ocean.

The direction and speed of the movement of a tropical cyclone are determined primarily from the three hourly displacement vectors of the centre of the system and by analyzing satellite imagery. When the system comes closer to the coastline, the system location and intensity are determined based on hourly observations from CDR and DWR stations as well as coastal observatories. The AWS stations along coast are also very useful as they provide hourly observations on real time basis. The WV and CMV, in addition to the conventional wind vectors observed by radio wind (RW) instruments, are very useful for monitoring and prediction of cyclonic disturbance, especially over the Sea region.

A new weather analysis and forecasting system has been installed at IMD, New Delhi, which has the capability to plot and analyse different weather parameters, INSAT and radar imagery and NWP products using pc software known as Synergie, procured from Météo-France International (MFI). It has a tropical cyclone model, to deal with various aspects of cyclonic disturbances. The experimental run in the system commenced at the end of 2009.

Prediction models in operational use

Quasi-Lagrangian Model (QLM)

The QLM, a multilevel fine-mesh primitive equation model with a horizontal resolution of 40 km and 16 sigma levels in the vertical, is being used for tropical cyclone track prediction in IMD. The integration domain consists of 111x111 grid points centred over the initial position of the

cyclone. The model includes parameterization of basic physical and dynamical processes associated with the development and movement of a tropical cyclone. The two special attributes of the QLM are: (i) merging of an idealized vortex into the initial analysis to represent a storm in the QLM initial state, and (ii) imposition of a steering current over the vortex area with the use of a dipole. The initial fields and lateral boundary conditions are derived based on global model (T-80 and T254) forecasts obtained online from the National Centre for Medium Range Weather Forecasting (NCMRWF), India. The model is run twice a day based on 00 UTC and 12 UTC initial conditions to provide 6 hourly track forecasts valid up to 72 hours. The track forecast products are disseminated as a World Weather Watch (WWW) activity of RSMC, New Delhi.

Limited Area Model (LAM)

The operational forecasting system known as Limited Area Forecast System (LAFS) is a complete system consisting of data decoding and quality control procedures, 3-D multivariate optimum interpolation scheme for objective analysis and a semi-implicit semi-Lagrangian multi-layer primitive equation model. The model is run twice a day based on 00 UTC and 12 UTC observations. The horizontal resolution of the model is 0.75° x 0.75° with 16 sigma levels in the vertical. First guess and boundary conditions for running the LAFS are obtained online from the global forecast model being operated by the NCMRWF. During a cyclone situation, the model is run by including the Holland vortex scheme. The forecast products are disseminated as a WWW activity of RSMC, New Delhi.

Non-hydrostatic Meso-scale Model MM5 (Version 3.6)

The non-hydrostatic model MM5 is being run on operational basis daily once based on 00 UTC initial conditions for the forecast upto 72 hours. The horizontal resolution of the model is 45 km with 23 sigma levels in the vertical. The domain of integration covers the area between latitude 25°S to 45°N and longitude 30°E to 120°E. National Centre for Environmental Prediction (NCEP) analyses and six hourly forecasts are used as initial and boundary conditions to run the model. During cyclone situations, the model is run by including the Holland vortex scheme. The forecast products are disseminated as a WWW activity of RSMC, New Delhi.

Non-hydrostatic mesoscale model WRF

The Weather Research and Forecast (WRF) model has been implemented based on 00 UTC initial and boundary conditions from NCEP model outputs for the forecast up to 72 hours. The model is run with a single forecast domain covering the Indian subcontinent at a horizontal resolution of 27 km. The performance of the model is found to be reasonably skillful for cyclone genesis and track prediction.

Multi-model ensemble (MME) technique

The multi model ensemble (MME) technique is based on a statistical linear regression approach. The predictors selected for the ensemble technique are forecast latitude and

longitude positions at 12-hour interval up to 72-hour of five operational NWP models. In the MME method, forecast latitude and longitude position of the member models are linearly regressed against the observed (track) latitude and longitude position for each forecast time at 12-hour intervals for the forecast up to 72 hours. The model outputs at 12 hourly forecast intervals are first post-processed using the GRIB decoder. The 12 hourly predicted cyclone tracks are then determined from the respective mean sea level pressure fields using a cyclone tracking software. Multiple linear regression technique is used to generate weights (regression coefficients) for each model for each forecast hour (12hr, 24hr, 36 hr, 48hr, 60hr, 72hr) based on the past data. These coefficients are then used as weights for the ensemble forecasts.

Forecast Demonstration Project (FDP) on Landfalling Tropical Cyclones over the Indian Ocean

A Forecast Demonstration Project (FDP) on landfalling tropical cyclones over the Bay of Bengal has been taken up. It will help us in minimizing the error in prediction of tropical cyclone track and intensity forecasts. The programme was divided into three phases:

(i) Pre-pilot phase: Oct-Nov. 2008, 2009
(ii) Pilot phase: Oct-Nov. 2010, 2011
(iii) Final phase: Oct-Nov 2012

Cyclone Warning Dissemination

Cyclone warnings are disseminated to various users through telephone, fax, email, GTS. These warnings/advisories are also put in the website www.imd.gov.in of IMD. Another means to transmit warning is IVRS (Interactive Voice Response system). The requests for weather information and forecasts from general public are automatically answered by this system. For this purpose, the person has to dial a toll free number, "1 800 180 1717" from anywhere in the country. This system has been installed at 26 Meteorological Centres/ Regional Meteorological Centres. High Speed data terminals (HSDT) are installed almost at almost all MCs and RMCs. HSDTs are capable of sending short warning message as SMS and the whole warning message as email. Local weather warnings are put in IMD website for common people. GMDSS message is also put in IMD website as well as transmitted through GTS. Fax is also used extensively for weather warning dissemination.

In addition to the above network, for quick dissemination of warning against impending disaster from approaching cyclones, IMD has installed specially designed receivers within the vulnerable coastal areas for transmission of warnings to the concerned officials and people using the broadcast capacity of the INSAT satellite. This is a direct broadcast service of cyclone warning in the regional languages meant for the areas affected or likely to be affected by the cyclone. There are 352 Cyclone Warning Dissemination System (CWDS) stations along the Indian coast; out of these 101 digital CWDS are located along Andhra coast. The IMD's Area Cyclone Warning Centres (ACWCs) at Chennai, Mumbai, and Kolkata and Cyclone Warning Centres (CWCs) at Bhubaneswar, Visakhapatnam, and Ahmedabad are responsible for originating and disseminating the cyclone warnings through CWDS. The bulletins are generated and

transmitted every hour. The cyclone warning bulletin is up-linked to the INSAT in C band. For this service, the frequency of transmission from ground to satellite (uplink) is 5859.225 MHz and downlink is at 2559.225 MHz. The warning is selective and will be received only by the affected or likely to be affected stations. The service is unique in the world and helps the public in general and the administration, in particular, during the cyclone season. It is a very useful system and has saved millions of lives and enormous amount of property from the fury of cyclones. The digital CWDSs have shown good results and working satisfactorily.

References

These references are provided for further reading related to the material in this appendix

India Meteorological Department, 2003: Cyclone manual. IMD, New Delhi, India.

India Meteorological Department, 2008: Track of storm and depressions over the Indian Seas during 1891-2007. Cyclone e-Atlas of IMD, New Delhi, India.

Kelkar, R.R., 1997: Satellite based monitoring prediction of tropical cyclone intensity and movement. Mausam, 48, 157-168.

Raghavan, S., 1997: Radar observation of Tropical Cyclones over the Indian Seas. Mausam, 48: 169-188.

Prasad, K., and Rama Rao, Y.V., 2003: Cyclone Track Prediction by quasi-Lagrangian limited area model. Meteorology and Atmospheric Physics. 83: 173-185.

Singh, O.P., Khan, T.M.A and Rehman, S., 2000: Changes in the frequency of Tropical Cyclones over the north Indian Ocean. Meteorology and Atmospheric Physics. 75: 11-20.

Singh, O.P., and H. Singh, 2011: Use of scatterometer based surface vorticity fields in forecasting genesis of tropical cyclones over the north Indian Ocean. Mausam 62: 61-72.

Chapter Nine

Charles 'Chip' Guard
US National Oceanic and Atmospheric Administration (Retired)
Science Applications International Corporation
National Weather Service Forecast Office, Guam

Philippe Caroff
Météo-France

S. T. Chan
Hong Kong Observatory

Ryan P. Crompton
Risk Frontiers Macquarie University

Jim Davidson
Australian Bureau of Meteorology

9. Warning Strategies

9.1 Introduction

Some of this Warning Strategy chapter is extracted from the original Warning Strategy chapter by the late Mr. Robert Southern, as much of his basic input is still valid. The remainder of the material is taken from newer studies and presentations provided by various international subject matter experts.

9.1.1 Purpose of strategies

The purpose of strategies, according to management theory (Koontz et al. 1984), is to determine and communicate, through a system of major objectives and policies, a concept of how the main mission of an organization may be accomplished. Emphasis is placed on the acquisition and deployment of resources (physical, human and information). Warning, response, and preparedness strategies thus may be described as:

- Guidelines that promote objective assessments of the current and changing nature of a hazardous weather threat; and,
- Sequences of actions and announcements that provide the most appropriate and timely response by threatened or affected communities.

Thus, the strategies here provide a framework of guidelines to assist decision-making required to counter the threat of an approaching tropical cyclone (TC). For example, as a TC threatens a vulnerable section of coast, initially there is a large degree of uncertainty associated with forecast errors at longer time periods. As the TC approaches, the uncertainty decreases, but so does the available preparation time. Thus, an effective warning and response strategy is to react prudently and alertly at the initial threat, then to marshal the necessary resources to progressively prepare for the developing threat. The type of strategy requires a balance between the costs and the hardship associated with unnecessary response and the consequences of being caught ill-prepared. For extreme risk areas with slow response times, for example, it is prudent to evacuate early to avoid catastrophic loss of life. In other regions, with rapid response facilities, a different strategy could be employed.

9.1.2 Objective of an integrated national warning service

The broader objective or mission of an integrated national warning service therefore is:

to promote effective community response, in order to avoid potential disaster, and thereby reduce the loss of life, property and environmental damage, while holding the community disruption to a realistic and appropriate minimum.

While avoiding potential disaster is a major component of this mission, attention also must be given to reduction of consumption of national resources already scheduled for deployment in national development programs, and consequential triggering of a host of other adverse socio-economic impacts on a nation's prosperity.

In a TC context, the strategies may be sub-divided into three, highly interrelated subcomponents: forecast strategy, warning strategy and response strategy. The first is presented in Chapter 8. The last two are discussed in this chapter. It should be noted that Forecast Strategy and Warning Strategy are highly interrelated, especially in the areas of forecast uncertainty and message formulation and content, and thus, there may be some overlap between the chapters. While the Response Strategy is primarily the responsibility of Emergency Managers, it is imperative that forecasters have a good understanding of Response Strategy in order to effectively support the Emergency Managers and the community. There should be a close working relationship between the TCWC and the Emergency Management community and even closer working relationships between local weather offices and local emergency managers.

9.1.3 Forecast strategy

Includes the strategy for collection of observations, with enhanced collection in the TC vicinity; specialized analysis methods; and the preparation of forecasts using the most appropriate techniques for the situation.

9.1.4 Warning strategy

Includes an explicit understanding of the forecast uncertainties; an appreciation of the most vulnerable and susceptible communities and populations in the potential warning area, the "least regret" approach to ensuring no catastrophes occur; and a sharp sense of timeliness to fit with communication capacities and community cycles.

9.1.5 Response strategy

Includes preparedness activities such as public education and awareness programs aimed at ensuring good community responses; developing an infrastructure capable of handling the threat; ensuring a balanced preparation appropriate to the community under threat, to ensure full response without unnecessary over-reaction; taking contingency action, such as establishing and activating emergency operations centers and implementation of ordered evacuations; deploying available resources to meet the threat and to be available for post-event response; and planning ahead to mitigate the detrimental effects of future events. To ensure the most cost-effective strategy, an all-hazards approach is highly encouraged, where preparedness, response, recovery and mitigation measures can be applied to any one of a large suite of hazards.

9.1.6 Help make critical decisions more effective

A major objective of the TC strategy should be to provide a strong element of innovative oversight to plan and facilitate the effectiveness of the critical decisions made during the event. This planning will vary considerably according to the meteorological conditions, the facilities and communications available to the community, and to its degree of sophistication in responding to the threat. It also will be readily understood that the effectiveness of warning strategies needs examination from the perspective not only of national meteorological/hydrological services, but from the viewpoint of many diverse agencies located in the sequential cycle of disaster response and mitigation functions. This includes, primarily, the host of potential victims at community levels most threatened, and having most to gain from the implementation of effective warning strategies. Thus, experience in one country may or may not be readily translated to another. It may be noted, however, that this chapter incorporates the warning experiences and lessons learned from a number of recent major TCs of global significance.

Warning strategy should not be so focused on principles and definitions as on common sense and practical application. People in responsible agencies and organizations need to observe the response to their warnings, assess the effectiveness of the warnings, and take steps to correct shortfalls. They need to be proactive and flexible.

This chapter draws on published and unpublished sources of information, in addition to the author's own practical experience. Readers not familiar with modern concepts, principles and

practices of data management are invited to refer to two excellent publications by the Asian Development Bank (ADB 1991, Carter 1992). Despite their age, these are still valid and excellent common sense references for emergency managers and for those who support emergency managers.

9.2 The nature of warning and response

Warning and response are interrelated; one is of little effect without the other. They are quantifiable actions consisting of:

Warning: a positive action-oriented stimulus intended to alert people about an impending hazardous event or circumstance in their location, which may threaten their safety and security, and which requires an "adaptive human response";

Adaptive Human Response: the degree of organized reaction to a warning stimulus, which enables rational communication between individuals and communities, and which facilitates avoidance or mitigation of the perceived threat.

To be of maximum effect, a warning must therefore alert the community at risk, clearly communicate the physical nature, potential danger and urgency of the threat, and recommend avoidance/preparedness measures. Such warning and alerting stimuli may take many audio-visual forms and actions, which will vary according to the type and capabilities of a community.

There are basically two primary methods of real-time dissemination of warnings, each with its specific audience. These methods are radio and live or recently recorded television. Warning information is highly perishable, and must be updated frequently. Television is the method of choice, provided it is live or recently recorded. This is usually available in well-developed countries. However, a second and very effective medium is the radio, provided the warnings are frequently updated and well-prepared for the radio medium. The purpose of the warning is to illicit a desired human response to the hazard. The purpose of the media is to clearly spread the warning message to the majority of the threatened population.

9.2.1 Principles for good major hazard warnings

General issue of warnings is made through the mass media, where opportunities for queries and feedback are limited. In such cases the following general principles apply:

- Design messages to attract attention and evoke timely rational response;
- Specify the nature, severity and imminence of the threat, in accordance with relevant officially announced warning stages or phases;
- Specify the location of threatened areas with reference to well-known geographical locations or landmarks;

- Advise optimum avoidance or preparedness measures related to the degree and imminence of the threat;
- Achieve a balance in content between detail and simplicity in terms meaningful to the majority of recipients;
- Allocate the highest priority to the more critical elements in messages, especially those requiring urgent responsive action;
- Increase frequency of issue or updates as the threat increases (warnings are perishable products);
- Take into account pre-event behavioral response studies, the level of community experience, and the vulnerability of threatened areas;
- Advise how, when and where to obtain further information.

It is most important that warnings utilize the selected medium to the best advantage. For example, radio alerts can be preceded by a distinctive siren or melody, television can utilize background footage of typical conditions, and perhaps maps of where to proceed.
According to WMO (2006), below are the characteristics of an effective warning issued by NHMSs:

(i) Accurate — on the onset and intensity of the weather hazard, and the geographic area likely to be affected. It is also important to include discussion of the uncertainties so that the warning recipients will understand how to deal with the warnings effectively.

(ii) Clear and understandable — about the expected phenomenon and the risks to person, community and property. This allows the community to respond in commensurate with the risk involved as the weather situation develops.

(iii) Available to all — the warning must be disseminated to all affected, including those unable to receive television, radio or the Internet.

(iv) Reliable and timely — so as to develop trust in the warnings from the users, who would then be prepared to act when a warning is issued.

(v) Authoritative — the media and partners participating in addressing the hazard must not create or broadcast conflicting information.

(vi) Collaborative — through development of strong partnerships with all levels of decision-makers involved in disaster prevention and mitigation.

9.2.2 Response to warnings: behavioral factors

Response occurs at a spectrum of levels:

(a) individual,
(b) family,

(c) neighbourhood or village,
(d) local autonomous community,
(e) district (e.g., taluk, upazilla, etc.),
(f) province,
(g) region or state,
(h) national,
(i) regional or international (global).

The immediacy of response decreases from (a) to (i) but the availability of resources needed for effective response increases from (a) to (i). Warnings need to be conveyed in languages and modes of communication relevant to the response level required.

Many studies, surveys, and general observations during TC events have identified numerous factors that influence human response to TC warnings. One specific summary freely available is WMO (1983). Each catastrophic TC event reveals a spectrum of causes for major deficiencies in effective community response, some of which may not be closely related to the effectiveness of formal warning messages.

Commonly experienced response factors may be grouped into three overlapping categories:

Human (personal) factors: Age, sex, health, mobility, education and literacy, occupation, comprehension of danger, family and neighbourhood influence, cultural or religious attitudes, previous experience, poverty and economic circumstance, security of house and livestock, urban or rural residence, etc;

Hazard factors: Nature, severity and imminence of hazard(s), hazard frequency, immediate past experience of hazard including warning performance, credibility of warning service, visible evidence of threat, clarity of warnings, vulnerability of the community, etc;

Community aspects: Supporting infrastructure, availability of safe shelter and supporting welfare, extent of published evacuation planning, flood-free road access, confidence in counter-disaster officials, evidence of contingency planning, media collaboration to upgrade information, integrity of community lifeline services, level of community awareness, etc.

9.2.3 Warning strategies in an interdisciplinary perspective

Many TC specialists and forecasters have had limited opportunity to consider their particular roles of providing hazard and warning information in the perspective of a comprehensive sequential cycle of disaster management functions. The same comment applies to most personnel closely involved in natural hazard and disaster reduction and disaster management functions.

Most disaster managers consider the warning function to be a limited, though highly important part, of non-structural preparedness measures that often must proceed in relation to hazards

for which little or no warning is feasible (e.g., an earthquake). In this respect, the availability of warnings for TCs may be considered a special bonus input to the comprehensive function of preparedness, since they usually provide considerable "pre-warning" of the event.

In respect of warning strategies the following quote indicates the varying perceptions, and thus criticisms, with which specialists may view the effectiveness of TC warning systems:

"The perspective from which the basic organisational effectiveness of a TC warning service is examined will depend very much upon the focus of interest of the reviewer or his organisation place in the chain of events in the warning (origination, delivery, utilization) response process. The meteorologist is anxious to see that his geophysical information, obtained by huge investment in science and technology, is usefully deployed. The social scientist will study the behavioural response of communities and individuals to a variety of warning stimuli in varied social, geographic and cultural circumstances. A systems analyst may wish to test organisation theories of human interaction in the crisis situation, which the landfall of a TC presents, while a disaster specialist may compare all aspects of the total warning-response system in the context of other natural hazard occurrences. A politician may take advantage of perceived deficiencies in the system to plead for additional resources for his electorate, and perhaps a government economist may be anxious to compare the cost-effectiveness of various inputs into a warning system with subsequent outputs to rationalise competing demands on his budget. These and many other inter-disciplinary interests are recognised as contributing to the totality of an assessment of the usefulness of a TC warning system." (WMO, 1990).

Among the most compelling factors that influence response to TC warnings are the degree of sustained community awareness of the great dangers of TC hazards, the perception of the credibility of the warning authority, and the degree of confidence in the capacity of community officials to martial resources to implement preparedness measures. Thus, an aim of warning strategies must be to take into account the roles played by the great range of interdisciplinary interests that jointly foster human response to TC warning and mitigation measures.

9.3 Operational strategies for tropical cyclone (TC) warning and response systems

No successful TC warning and response system can be finely tuned and objectively defined to the finest detail. The facts of life are that each TC embedded in its broader environment exhibits a physical eccentricity and predictability generally unlike any of its predecessors, whilst the human and physical geography of the most threatened areas are constantly changing. Warning strategies thus have to be sufficiently flexible to enable forecasters, emergency services and affected communities to respond effectively under conditions in which there is not a precise model and the hazard potential is constantly changing. Unlike many other natural hazards, however, TCs do have a development life cycle and seasonal occurrence, which assists in logical planning and in allocation of required resources. A solid effort devoted to assessment

of demographic and economic vulnerability, and to the community response capacity, will prove to be a very good investment when a TC occurs.

Four Phases of National Action Plans: Preparedness, response, recovery, mitigation.

Levels of warnings of approaching hazards: Advisories, watches, warnings

According to WMO (2006), below are the characteristics of an effective warning issued by NHMSs:

(i) Accurate - on the onset and intensity of the weather hazard, and the geographic area likely to be affected. It is also important to include discussion of the uncertainties so that the warning recipients will understand how to deal with the warnings effectively.

(ii) Clear and understandable - about the expected phenomenon and the risks to person, community and property. This allows the community to respond in commensurate with the risk involved as the weather situation develops.

(iii) Available to all - the warning must be disseminated to all affected, including those unable to receive television, radio or the Internet.

(iv) Reliable and timely - so as to develop trust in the warnings from the users, who would then be prepared to act when a warning is issued.

(v) Authoritative - the media and partners participating in addressing the hazard must not create or broadcast conflicting information.

(vi) Collaborative - through development of strong partnerships with all levels of decision-makers involved in disaster prevention and mitigation.

9.3.1 Warning and response system

The warning and response system objectives are threefold: to *alert* communities of a potential danger, to *identify* areas likely to be affected, and to *call* the community to action through w*arning* messages and recommendations of specific actions. The strategy follows an evolutionary, persuasive process starting with pre-season education and awareness programs. As a threat develops, the strategy evolves to early alerts of potential, but uncertain threats. The strategy further evolves as the TC approaches or develops by increasing the detail and urgency of the information. Finally, the strategy should end with a review of the effectiveness of the warning-response system.

The major components of the warning and response system required to support these objectives are:

Tropical Cyclone Forecast: A scientific prediction of the future location, motion and intensity, and main parameters of a TC. These predictions must be in a form useful for the derivation of warnings for the public and be capable of objective verification.

Tropical Cyclone Warning: An imperative TC forecast that consists of several stages: *Early Alert* of potential threat more than 48 hours away, especially for industrial and emergency service operations; *Watch* for a TC that is likely to affect the community, but not within 24-36 hours; and *Warning* of imminent onset of TC conditions within 24-36 hours. The time designated for a warning is dictated by the time necessary to evacuate vulnerable populations. [Note: For most locations the warning time is 24 hours, but for many United States locations, the warning time is 36 hours.] This graded system consists of messages compiled in meaningful laymen's language, which conveys the personal danger imposed by the destructive elements of an approaching TC, first raising the community awareness of the threat, then inviting and finally demanding active response commensurate with the urgency and severity of the threat.

Utilisation: Adaptation of warnings by recipients into required preparedness measures and announcements in accord with contingency plans for the threatened areas.

Emergency Response: Implementation of community emergency procedures under the coordination of the relevant counter-disaster organisations.

System Evaluation: Review and evaluation of the total system to identify deficiencies and effect improvements in both warning and response functions.

The warning and response system thus consists of several interrelated components, all of which must function effectively and in a complementary manner for effective operation of the whole system. Perfect warnings are of little use if no response organisation exists.

An objective approach is to take the effectiveness of implementation of the warning inputs and of the community response organisation on a scale of 1-10, then multiply these to arrive at the percentage effectiveness of the overall warning-response system. Thus, an excellent warning effectiveness of 9 with a poor community response of 1 would result in a poor 9% effectiveness of the overall system. A very satisfactory result and overall practical objective would be to achieve a 9 for each component giving an 81% measure of effectiveness. This requires a co-ordinated approach, which includes the following essential ingredients:

- Development of official, community and special user awareness of the nature of the threat of TCs and preparedness measures to counter this threat.
- Assessment of hazard risk and vulnerability of the local areas prone to the TC threat, particularly in respect of preservation of community lifeline facilities and services.
- Preparation of contingency plans of action to facilitate decision making during TC crises, covering resources allocation and nomination of agency and individual duties.
- Training and rehearsal of simulated TC exercises to test the effectiveness of plans for deployment of human and physical resources.

- Appropriation of funds and resources to support departmental and community response.
- Development or institution of longer-term mitigation programs to minimise losses, which are difficult to avoid by short-term preparedness measures.

9.3.2 Warning and response phases

Effective warning-response strategies cover all aspects from pre-season review and preparation to post-event evaluation. From the perspective of a forecaster, ten major phases may be identified. (See also Chapter 8.)

(i) The Pre-Season Check Phase: All aspects of the system are checked and reviewed, including: observational and communication equipment, operational procedures, emergency service organisation contacts and revised procedures. Available techniques are updated and forecasters review their own methodologies. Community awareness campaigns are conducted in conjunction with counter-disaster authorities.

(ii) Routine Monitoring Phase: Continuous surveillance by a national meteorological centre, a TC warning centre or preferably both using twice-daily (or more frequent as necessary) scientifically-based procedural checks for signs of potential TC activity.

(iii) Cyclone Information Phase: Media and preparedness authorities are advised that a TC has formed near or within the area of warning responsibility but is not forecast to cause dangerous conditions within a specified time, often 48 hours. The information is contained in low-key statements issued once or twice daily with the aim of arousing initial interest and creating a climate of expectancy should the system move to the next phase. Very specific information may be passed to highly vulnerable areas such as offshore oil operations and fishing fleets.

(iv) Cyclone Watch or Alert Phase: The alert phase commences when an existing or potential cyclone poses a threat within 48 hours, but not within 24-36 hours. The objective is to build public awareness of the increasing threat without making definitive predictions that are beyond the forecast system capacity at this early stage. The frequency of warning advices is increased, generally to 6 hours, but provided only in general terms, for example, potential landfall along extended coastal sectors several times the lateral dimensions of gale or storm force winds and which incorporate the degree of uncertainty in the forecast. This phase may activate costly public counter-disaster plans, such as the setting up of emergency operations centres and initial deployment of resources. Preparedness recommendations include return of fishing craft to home ports and preliminary precautions by residents. In general, this phase means "get ready to get ready"; do the inexpensive preparations and save the most expensive for the warning phase.

(v) Cyclone Warning Phase: This is initiated when TC conditions, in the form of gale-force winds, are expected within at least 24 hours at a vulnerable location (some regions may require

longer lead times). It is usual at the beginning of this phase to have to place at least 600-800 km length of coastline under expectancy of damaging winds, with perhaps another 200 km remaining under a watch stage at the peripheries. For a TC approaching at an acute angle, the warning/watch region may be substantially larger. As a general strategy, discrete coastal sectors between named well-known locations should be identified in warning statements. This is the highest level of operation of the warning system and is accompanied by significant cost impact for all concerned parties. Disaster operations centres are staffed on a 24-hour basis to implement contingency action plans, which will often include opening of shelters and evacuations starting from the more exposed areas. The community is expected to make immediate arrangements for its safety and security, and businesses and industry commence shutdown procedures.

The frequency of warnings is progressively increased to 3 hours. When practical, such as with radar tracking, abbreviated hourly warnings may be issued to media. The warning system is fully extended to enable rapid response to changes in the cyclone motion and structure. Additional persuasive information is martialled and broadcast to heighten the sense of urgency in the community and to hasten public response in the decreasing safe lead time available. As the landfall lead time shortens, more specific information on the destructive power of the TC and general warning of abnormal tides (storm surge) and flash floods are issued, and attention is drawn to unusual features about the storm, such as unusual intensity, speed of approach, or large size of the wind field.

(vi) Imminent-Landfall Phase: At this advanced stage of the warning phase gale or stronger force winds are imminent or have commenced along with heavy rain, rough seas and increasing tides, and the community should be already sheltering in expectation of landfall of the TC within 6-8 hours. Well-equipped emergency services personnel checking on the safety of people in the most vulnerable areas and the continuing operation of community lifeline facilities should be among the few persons not sheltering inside safe refuges.

Broadcast warnings contain highly pertinent information concerning the impact of the cyclone in the most vulnerable areas. The expected landfall region for the destructive cyclone core should be detailed to within an accuracy of 50-100 km, but it is essential to stress the asymmetric extent of destructive winds and rainfall to ensure communities do not concentrate unnecessarily on the TC centre. Preliminary flood warnings may be issued for coastal catchments and river basins. During this phase when increasing gales are being experienced, monitoring and prediction focus on nowcasting. Predictions are usually given on the basis of persistence and current surface synoptic conditions.

Because the track and structure of a TC may change in the hours approaching landfall, Simpson (1971) advocated last-minute warnings on a "course of least regret". This assumes that the most serious impact will occur close to the region or towns of highest vulnerability. If these locations suffer lesser damage then so much the better. If the situation is marginal then the higher rated TC category or public warning signal number should be quoted in warnings. For the same reasons, immediate pre-landfall announcements that the TC is weakening should

generally be avoided, especially as serious misinterpretations may be made with disastrous consequences. At this point, there is nothing to gain by indicating a weakening trend.

It is recommended that the highest priority, *Flash Cyclone Warning* prefix (or the local warning equivalent) be used for the first urgent advice of destructive cyclonic effects within 24-36 hours in areas not previously alerted. Flash warnings (or the local equivalent) also should be used to indicate sudden changes in the TC track or intensity, which could seriously affect vulnerable communities.

(vi) Imminent-Landfall Phase: At this advanced stage of the warning phase gale or stronger force winds are imminent or have commenced along with heavy rain, rough seas and increasing tides, and the community should be already sheltering in expectation of landfall of the TC within 6-8 hours. Well-equipped emergency services personnel checking on the safety of people in the most vulnerable areas and the continuing operation of community lifeline facilities should be among the few persons not sheltering inside safe refuges.

Broadcast warnings contain highly pertinent information concerning the impact of the cyclone in the most vulnerable areas. The expected landfall region for the destructive cyclone core should be detailed to within an accuracy of 50-100 km, but it is essential to stress the asymmetric extent of destructive winds and rainfall to ensure communities do not concentrate unnecessarily on the TC centre. Preliminary flood warnings may be issued for coastal catchments and river basins. During this phase when increasing gales are being experienced, monitoring and prediction focus on nowcasting. Predictions are usually given on the basis of persistence and current surface synoptic conditions.

Because the track and structure of a TC may change in the hours approaching landfall, Simpson (1971) advocated last-minute warnings on a "course of least regret". This assumes that the most serious impact will occur close to the region or towns of highest vulnerability. If these locations suffer lesser damage then so much the better. If the situation is marginal then the higher rated TC category or public warning signal number should be quoted in warnings. For the same reasons, immediate pre-landfall announcements that the TC is weakening should generally be avoided, especially as serious misinterpretations may be made with disastrous consequences. At this point, there is nothing to gain by indicating a weakening trend.

It is recommended that the highest priority, *Flash Cyclone Warning* prefix (or the local warning equivalent) be used for the first urgent advice of destructive cyclonic effects within 24-36 hours in areas not previously alerted. Flash warnings (or the local equivalent) also should be used to indicate sudden changes in the TC track or intensity, which could seriously affect vulnerable communities.

(vii) Post-Landfall Phase: The warning advices continue at 3-hour intervals for about 12 hours after landfall, advising communities of the location of landfall, the subsequent track of the cyclone and rate of weakening, and potential developments, such as movement back offshore. The emphasis now centres on the issue of warnings for rapid riverine and flash floods, and for tornados, where necessary. At this phase, all power (except emergency power) and

communications may be out. In addition, most meteorological instrumentation may be damaged or destroyed.

A Final Cyclone Warning should be issued, in consultation with counter-disaster authorities, to indicate the passage of the TC threat and recommend a gradual resumption of normal community activities, and deployment of medical and engineering crews to badly hit regions. The final warning should not only consider the reduction of the wind danger but also the reduction of the danger of the inundation from the sea.

(viii) Impact Assessment Phase. This phase is entered as soon as a TC has dissipated, or passed into another area of warning responsibility. Meteorological officers, accompanied by disaster personnel, visit the affected areas to gather relevant observational and hazard-related data and discuss warning-response performance with people and officials.

(ix) Documentation Phase: This covers the period from genesis of a TC through the sequential warning phases until dissipation or passage of the TC from an area of warning responsibility. All relevant information about the TC including copies of warnings, press items and damage photographs, criticisms, and a chronology of events, is collected in a substantial case history file for reporting and archival. Selected data are extracted for storage in computer compatible form to facilitate enquiries and research. Supervising meteorologists should keep diaries for strategic planning, remedial training, and procedural improvement purposes.

A summary of each season's TC activity is prepared annually. Special reports on major disaster-impact TCs are given wide distribution to interested parties.

(x) System Review Phase: At the end of the TC season, a review is conducted of the total performance of the warning and response system. This usually culminates in annual review conferences covering internal procedures as well as external liaison with counter-disaster authorities. As noted earlier, each new TC brings unique experience with respect to warning and response aspects, which may need to be incorporated into warning procedures and or preparedness contingency plans.

Major innovations involving the community at large may need to be tested for their feasibility before final adoption into national procedures. In some cases, such as when a TC has not impacted a country or coastal sector for many years and/or there has been a substantial breakdown in the warning and response process, the opportunity should be taken for a thorough appraisal of the system. Annual preparedness and response exercises can reduce the chances that the system will fail when it is needed for an actual hazard event.

9.4 Constraints that challenge warning strategies

Several meteorological, climatological, regional and human perception uncertainties apply to constrain the application of warning strategies. These include the uncertainty in TC forecasts,

regional and seasonal variations in TC characteristics and forecast difficulty, and language and communication ambiguities that lead to misinterpretation of warning content.

Because the atmosphere is non-linear, some level of uncertainty or error is present in all forecasts and must be accounted for in warning strategies. This uncertainty can be quantified by mean forecast errors (Chapter 3) that generally increase in 75 km increments for every 12 hours of the forecast. Pike and Neumann (1987, see Chapter 2) have shown that the degree of uncertainty, as defined by a forecast difficulty index using the CLIPER technique, varies considerably between ocean basins. Marked seasonal and latitudinal variation also is experienced.

In many situations, the forecast errors will prove to be less than indicated by the forecasting difficulty level because the forecaster will use a number of techniques, allied with professional judgment and experience. In addition, there may be much better than normal observations available. In other cases, the warning strategy must account for the worst case scenario, for example, the high degree of uncertainty that can be present when a TC is in a potential recurvature or rapid intensification situation.

The warning strategy, therefore, is to account for regional characteristics and the current situation for the forecast period, and then to provide a prudent margin for error. At the alert or watch stage, a large section of coast will be notified, and this will be reduced and focused as the TC landfall approaches and the forecast confidence level increases.

9.4.1 Forecast uncertainty

Care needs to be taken to maintain realistic and conservative levels of forecast uncertainty in the warnings. Counter-disaster managers tend to regard the occasional instances of excellent forecasts as the basis for routine expectancy of exceptional performance, which if not achieved on subsequent occasions, quickly inspires criticism of apparent monitoring negligence. Forecasters have a natural tendency to overestimate their real predictive skills by making overconfident forecasts of the probable location of landfall in warning announcements several days in advance. This can subsequently lead to substantial amendments, confusion and potential tragedy.

Tropical cyclone (TC) track forecasts have greatly improved in the past several years. Benefiting from the advances of numerical weather prediction and the multi-model consensus technique, reduction in the track forecast errors has been impressive. RSMC La Reunion saw a big step forward in their operational performances in 2006, when a spectacular gain exceeding 30% for forecasts beyond 48 hours was attained. Since then, the track errors have stabilized with a slight downward trend (Fig. 9.1). The improvement in the track forecasting has led to the extension of La Reunion's official forecasts out to 5 days starting from February 2010. Day 3 track forecasts are now better than were the day 2 forecasts before 2006 and the forecasts for day 5 are also better than were the forecasts for day 3 compared with four years ago.

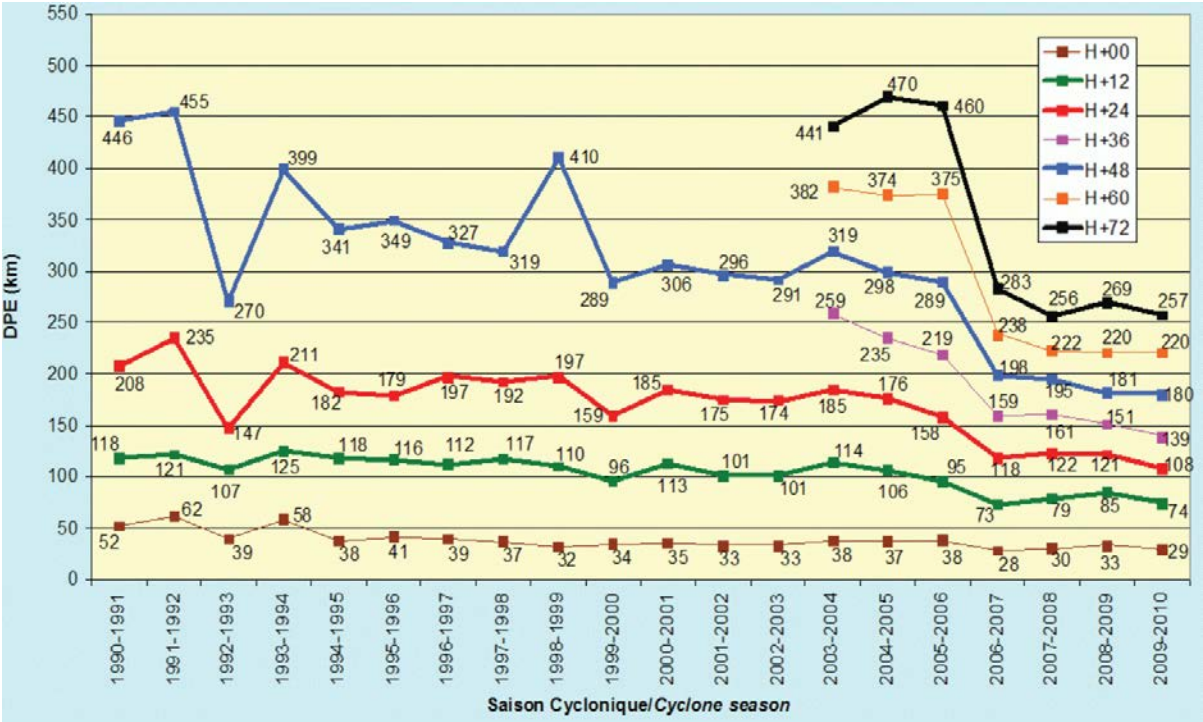

Figure 9.1. Annual mean position errors of TC track forecasts issued by RSMC La Reunion from 1990 onward.

Similar enhancement was also implemented in other centres - RSMC Tokyo extended its TC track forecasts from 3 days to 5 days in April 2009. As a primary basis for TC trackforecasting, JMA refers to the Global Spectral Model (GSM), the horizontal resolution of which was upgraded to approximately 20 km in November 2007, and also to the Typhoon Ensemble Prediction System (TEPS) which became operational in February 2008. The annual mean errors of 24-, 48-, 72-, 96-, and 120-hour forecasts of the TC centre position in 2009 were 122 km, 216 km, 312 km, 415 km and 528 km respectively. China Meteorological Administration (CMA) also followed suit to extend its track forecast from 3 days to 5 days in 2010, based on one-year test in 2009. The annual mean errors of 24-, 48-, 72-, 96-, 120-h track forecast in 2009 were 119 km, 205 km, 299 km, 392 km and 514 km respectively.

While track forecast improvements over the past decade have been substantial, intensity forecast improvements have been virtually flat. Improved track forecast models and new ensemble track forecasting techniques have made it much more difficult for the forecaster to add improvement to the numerically-derived track forecasts. When considered in terms of the increases in coastal populations, intensive coastal land-usage and vulnerable investments, the risk in human and economic terms continues to increase even with the significant track forecast improvements, just at a slower rate. Thus, while the track forecasts may continue to improve, because the number of people or resources at risk continues to grow, the size of the warning zone may not shrink accordingly.

Despite the significant reduction in track forecast errors in recent years, we have not yet reached the point where this could result in a major change in the approach of decision making

for emergency management and warning strategy. With the 24-hour track forecast errors still above 100 km on average, the contingency of being hit or not hit by the core of a TC remains too uncertain to avoid taking preventive measures that may eventually turn out to be excessive or unnecessary. This is especially the case for small islands like La Reunion or the metropolitans like Hong Kong where the issue may amount to an "all or nothing" question when a midget TC passes nearby.

An indication of the best possible forecast skill is provided by that obtained by the United States National Hurricane Center at Miami, staffed by specialist hurricane forecasters who have the best available initial location accuracy and forecast track guidance. The mean errors for the decade 2001-2010 were around:

Table9.1: Track forecast errors for NHC (Miami)

Forecast Period (h)	**12**	**24**	**48**	**72**
Mean Error (nm)	45	90	180	270
Mean Error (km)	83	167	333	500

Whilst current research and model development (Chapter 3) indicates that a substantial improvement in forecast accuracy is occurring, the best forecast performance that can be reasonably expected will result in errors greater than half those listed above. This should be accounted for in planning for future warning strategies.

9.4.2 Strike probability forecasts

One method of quantifying the uncertainties inherent in a particular situation is by the issue of strike probability forecasts (Chapter 3). However, many forecasters are unaware of the practical significance of these statistics, since forecasts are judged correct, partially correct or incorrect according to other criteria. They thus may not appropriately relate hit or miss probabilities to suitable preparedness measures by people living in the threatened areas.

For the purpose of determining hurricane strike probabilities in the U.S.A. a hit is adjudged a successful forecast for appropriate preparedness decision-making if actual landfall occurs within 100 kilometres to left or right of predicted landfall. This is the approximate length of coastline that may be considered liable to the severe destructive power of hurricane-force winds and storm surge encompassed by the central core of an intense tropical cyclone (Carter 1983).

A stricter interpretation would incorporate the left-right asymmetry due to storm motion. The probabilities of successful hit predictions, given the above mean errors for specific forecast validity periods can be shown to be:

Table9.2: Probabilities of successful hit predictions

Forecast Period (h)	72	48	36	24	12
Maximum Probability (%)	10	15-20	25-30	45-55	70-80
Miss to Hit Ratio	8:1	6:1	4:1	2:1	2:3

Thus the odds of a specific location forecast issued more than 36 hours in advance of estimated landfall being assessed as a successful hit prediction are rather slim. An even probability of success is not reached until nearing 18 hours before landfall.

As a caveat to this discussion it should be noted that the narrow assessment used in the U.S.A. for hit and miss criteria, based on the premise that the destructive power of a mature cyclone will be limited to a spread of destruction of about 200 km from the coastal crossing of its centre, may be expanded for the Asian and other regions. Asian cyclones tend to be larger than those in the North Atlantic (Merrill 1984). In developing countries the impact of winds within 300 km or so of the centre of a mature storm may well cause significant damage to modest houses built of traditional materials. Similarly, gale to storm force winds may develop very rough seas sufficient to endanger the huge number of small craft engaged in fishing off most tropical coasts.

9.4.3 Expect the unusual, it is normal

As has been emphasised in Chapter 3, the view of a "normal" TC track extending along a straight or neatly parabolic arc into the subtropics while the TC develops along the standard Dvorak climatological curve is actually the exception. The majority of TCs are associated with some sort of abnormal behaviour. Examples include:

- rapidly changing trends in motion and intensity;
- monitoring difficulties, especially related to the central core of the TC and obscuring effects of wind shear, and unusual asymmetry in the strong wind circulation;
- large potential errors in predicting the track of TCs for longer periods prior to a clear indication of initial movement becoming apparent;
- several TCs interacting (Fujiwhara effect) and simultaneously threatening within the same area of warning responsibility (e.g., Philippines and mainland China);
- quasi-stationary TCs close to landfall (e.g., China, Australia, United States);
- TCs, which develop or intensify close to a populated coastline or island group, sometimes from an origin over land (e.g., Australia, Pacific Islands, Caribbean, Philippines);
- TCs approaching a vulnerable coastline at an acute angle so that minor forecast errors introduce large landfall uncertainty (e.g., India, US Atlantic coast, Western Australia, China NE coast);
- TCs, which occur outside or at the margin of the normal TC season, or in locations not seriously threatened for a decade or more (Gulf of Thailand, Sri Lanka, Hawaii);

- TCs, which threaten communities during a high pitch of seasonal activity such as harvesting, festivals, holidays, often with workers or tourists from non-TC areas;
- TCs, which simultaneously offer a greatly varying threat to adjacent coastal areas in the same country due to irregular coastal configuration of varying physical vulnerability (e.g., Gulf of Thailand, Gulf of Carpentaria);
- extratropical re-intensification accompanying loss of typical TC core structure affecting monitoring (e.g., SW Australia, New Zealand, Japan, NE United States);
- TCs with physical characteristics that vary substantially from their immediate predecessors;

These "unusual" characteristics must be properly accounted for in warning strategies. In particular, communities need to understand that TCs are capable of erratic behaviour and that the uncertainty in warnings is designed to account for such behaviour.

While track forecasts have improved, the main roadblock of TC forecasting remains with the lack of significant improvement in TC intensity and structure change forecast. Limiting factors for TC intensity forecasting include the lack of understanding of rapid changes in storm structure and intensity, routinely available in situ observations, and high-resolution coupled air-sea-land models (Chen et al., 2007). Although forecasters have now integrated some harbinger signals on the microwave imageries (structure of the convection and low level circulation as seen on 36 or 37 GHz — see example in Fig. 3 of the early stage of development of TC Ernest as seen on microwave imageries) that may help anticipate a rapid intensification (RI) to come, this may often be at a rather short notice. A situation of RI can become critical when it occurs close to a populated area with the landfall happening soon after, since the lead time may then become too short for the issue of a proper warning to the public.

An example of a potentially catastrophic rapid intensification event is shown in Figure 9.2. On 20 January 2005 Tropical Cyclone ERNEST developed very rapidly on the northern Mozambique Channel passing from 25 to 65 kt max 10-min average winds in 24 hours' time. This unexpected evolution (all numerical models had failed to predict this RI and even the genesis of this storm — some even hardly seeing a significant low) resulted in gale force winds affecting Mayotte Island (easternmost island of the Comoros Archipelago). As a result no warning had been issued for the island. But would have the island been situated 150 km to the southwest it would have been hit by a stronger storm and would have undergone gusts over 150 km/h by the end of the afternoon. In that situation the 1st warning would have been issued only 8 hours prior to the occurrence of such cyclonic conditions — too short for activating the warning process.

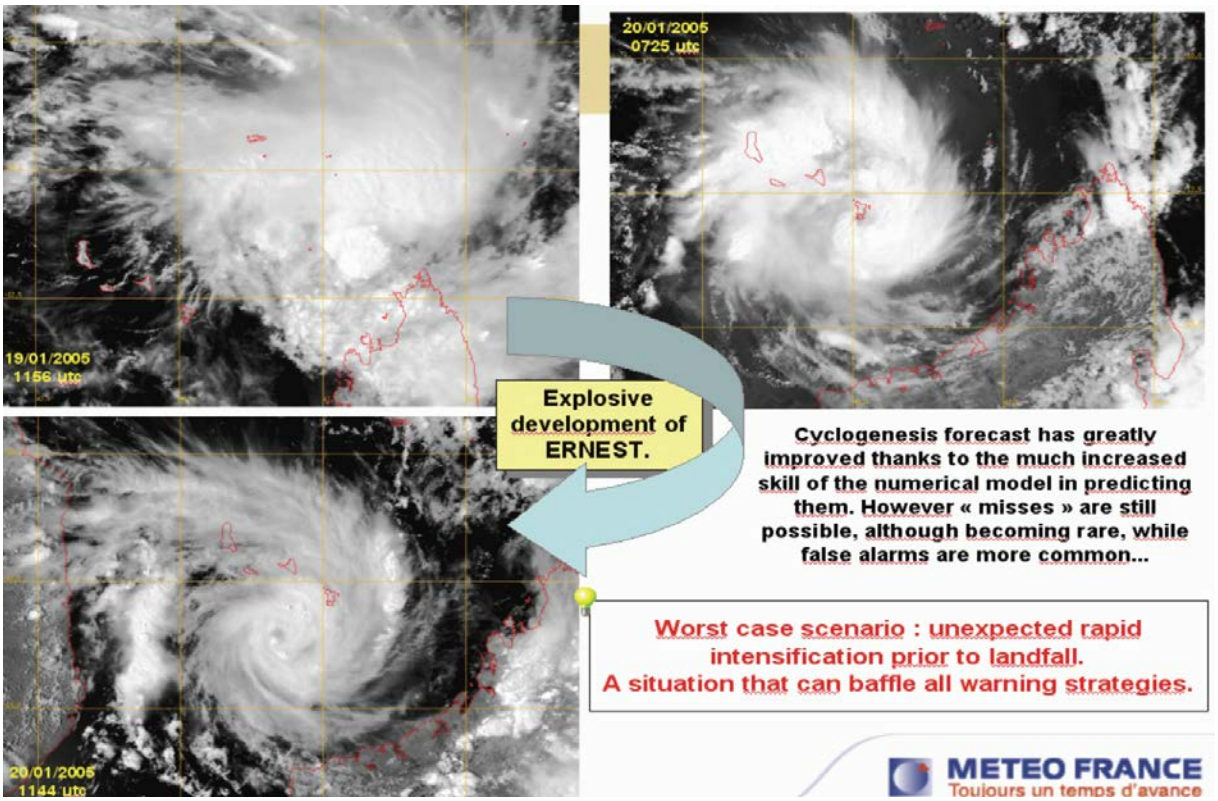

Figure 9.2. 20 January 2005 satellite imagery of Tropical Cyclone ERNEST illustrating very rapid intensification in the northern Mozambique Channel from 18 January 2005 to 20 January 2005. The intensity increased from 25 to 65 kt max 10-min average winds in 24 hours.

9.4.4 Warning content and terminology

The content of a TC warning message is of prime importance in an effective warning system. This information has to be converted into convincing and credible images of the approaching threat, which will create a climate of expectancy and responsive action over a very wide spectrum of people with differing preparedness interests and responsibilities. In countries, which possess a communications and media infrastructure capable of presenting a current visual view aided by expert commentary, the reliance on the technical formulation of a warning message is not so high. In most countries affected by TCs, however, one prime warning message for the general public often carries the responsibility of catering for a vast diversity of user needs. At best a limited number of messages semi-tailored to the needs of major socio-economic groups must suffice. In some cases, the dissemination relies on a series of relays, often by telephone and single-side-band radio, during which the message may be abbreviated or distorted and loses some of its original intent. These dissemination modes tend to degrade and often become inoperable as a TC approaches the area of interest.

The format, content and terminology of warning messages should be determined by the status of the warning phase, category of user, level of public understanding, vulnerability of the threatened areas, particular medium used for dissemination, and regional agreements on standardised procedures. A major difficulty is that the messages are prepared by technical

experts, and even the most obvious technical terms can often cause considerable confusion amongst many members of the community. For this reason, careful use of key words, backed up by public education programs, is essential.

Inspection of recent warnings issued by many different warning services indicates a wide variety in either pragmatic or narrative style, and a seemingly reluctance to introduce new styles of persuasiveness and format to focus on the most critical information. Examples of various styles of messages are shown at the end of this chapter.

The optimum design for TC warning advices, including audio-visual signals, is discussed in detail in WMO (1990). This discussion takes into account the diverse requirements of users and the available communication modes. Special consideration should be given to the limited attention span of most people and their ability to retain the important elements of a message. The essential information may be determined through surveys of disaster specialists, the media and communities. The use of information and communications specialists and social scientists is highly advisable.

9.4.4.1 Forms of presentation

In transforming weather forecasts into warnings, it is essential that the warning messages be clear and understandable, so that the warning recipients know how to incorporate the information into their decision-making process, and most importantly, be prepared to take appropriate actions. The warning messages should be developed so that they take full advantage of the dissemination platforms and target the greatest number of warning recipients to enable effective communication of the warnings. The broadband capacity of the Internet allows detailed information such as real-time observational data, radar and satellite imageries, predicted TC tracks, etc. to be made available to the public. This enables the more sophisticated users to assess, for themselves, the risk associated with their particular circumstances and to devise response actions accordingly.

A lot of work was done by RSMC La Reunion to design a new specialized website in order to provide the best access to the Centre's products (both real-time and archived) and to relevant information such as satellite imageries and NWP outputs. The site is a bilingual (French and English) site, which includes GIS-related facilities for "dynamical" visualization of maps of tracks and related data such as wind radii. It was opened in April 2010.

The NHC in Miami, Florida, USA issues TC watches and warnings in both textual and graphical advisory products. TC watches and warnings for the United States are issued in a coded text product called the Tropical Cyclone Watch-Warning Product (TCV). This product summarizes all new, continued, and cancelled TC watches and warnings for the United States in a coded format that is used by computer plotting programs. Areas under a TC watch or warning in the United States are defined using a list of well-known, recognizable geographical locations along the coast. The NHC also provides a summary of all coastal TC watches and warnings in effect in the TC Public Advisory and Forecast/Advisory. These are text products that include TC forecast information. The NHC also graphically depicts the watch and warning areas for the United

States and foreign countries on the TC Track Forecast Cone and Watch/Warning Graphic (Fig. 9.3) and the Initial Wind Field Graphic. In addition, NHC provides watch/warning information in GIS format with each forecast advisory.

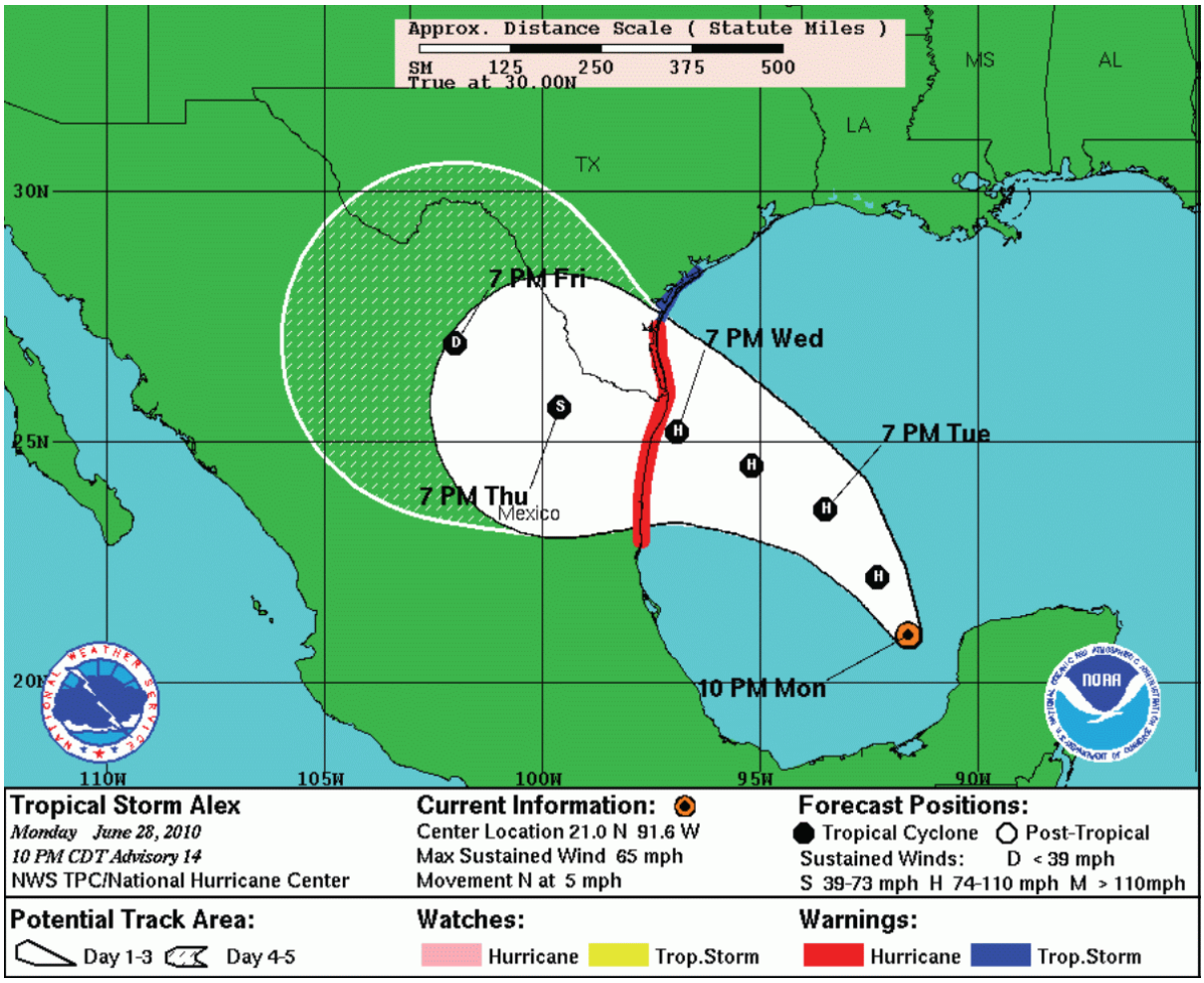

Figure 9.3. Example of the NHC Track Forecast Cone and Watch/Warning Graphic. The graphic depicts the most recent NHC forecast track of the center of a TC with representation of coastal areas under a hurricane warning (red), hurricane watch (pink), tropical storm warning (blue), and tropical storm watch (yellow).

CMA labels 24-hour and 48-hour warning zones within its responsible area. Normally, CMA issues TC track forecasts 4 times a day at 00, 06, 12, 18 UTC. When a TC enters the 48-hour warning zone, CMA provides an additional 4 forecasts at 03, 09, 15, 21 UTC. With a TC further approaching the mainland and entering the 24-hour warning zone, CMA issues TC position and intensity every hour to the meteorological communities and public in a variety of ways. Similar product density is provided by warning centers in the USA (NHC, CPHC, and the Weather Forecast Office in Guam for the US-affiliated islands of Micronesia).

Bulletins of TC advisories are issued by RSMC Tokyo in text and CREX, the table driven codes introduced by WMO to replace the various alphanumeric codes. Those in Extensible Markup Language (XML) format, an Internet-based language format which facilitates the exchange of

data between incompatible systems and applications, were disseminated to domestic users starting in 2011.

9.4.4.2 Communicating forecast uncertainties

As weather forecasting involves an element of probability, it is important that the forecast information provided to emergency services and government decision makers includes a discussion of any uncertainties, so that they can factor that information into their decisions. With increased skill and confidence in the forecast tracks of TCs, there are now situations where we can save resources by not issuing a warning when and where we would have issued one a few years ago. Having a much better idea of the degree of uncertainty of the forecast also helps to convey the degree of confidence of the forecast to the users and decision makers. In 2007, based on the past 5-year mean track forecast errors, CMA introduced the 70% probability circle into their official TC track forecasts. In Hong Kong, uncertainty circles are also presented, the radii of which represent the historical errors of the respective forecast range.

Instead of referring to simple climatological uncertainties, RSMC La Reunion is working on a dynamical approach to convey track forecast uncertainty based on the outputs of the ensemble prediction systems (EPS) - www.wmo.int/pages/prog/arep/wwrp/new/documents/Reunion_TCens.ppt (9MB). The tests using ECMWF EPS data have revealed that the uncertainty of the spread of the ensemble (with 50 members) contains skillful information on the uncertainty in the track forecast at least up to the 72-hour range. A plan was underway at La Reunion to produce the EPS-based dynamical cones of uncertainty with radii of the 75% probability circles and include them in the operational products on the centre's website by the end of 2010.

RSMC Tokyo also issues radii of the 70% probability circles of four and five-day track forecasts determined using the degree of forecast uncertainty derived from the ensemble spread of the JMA's TEPS.

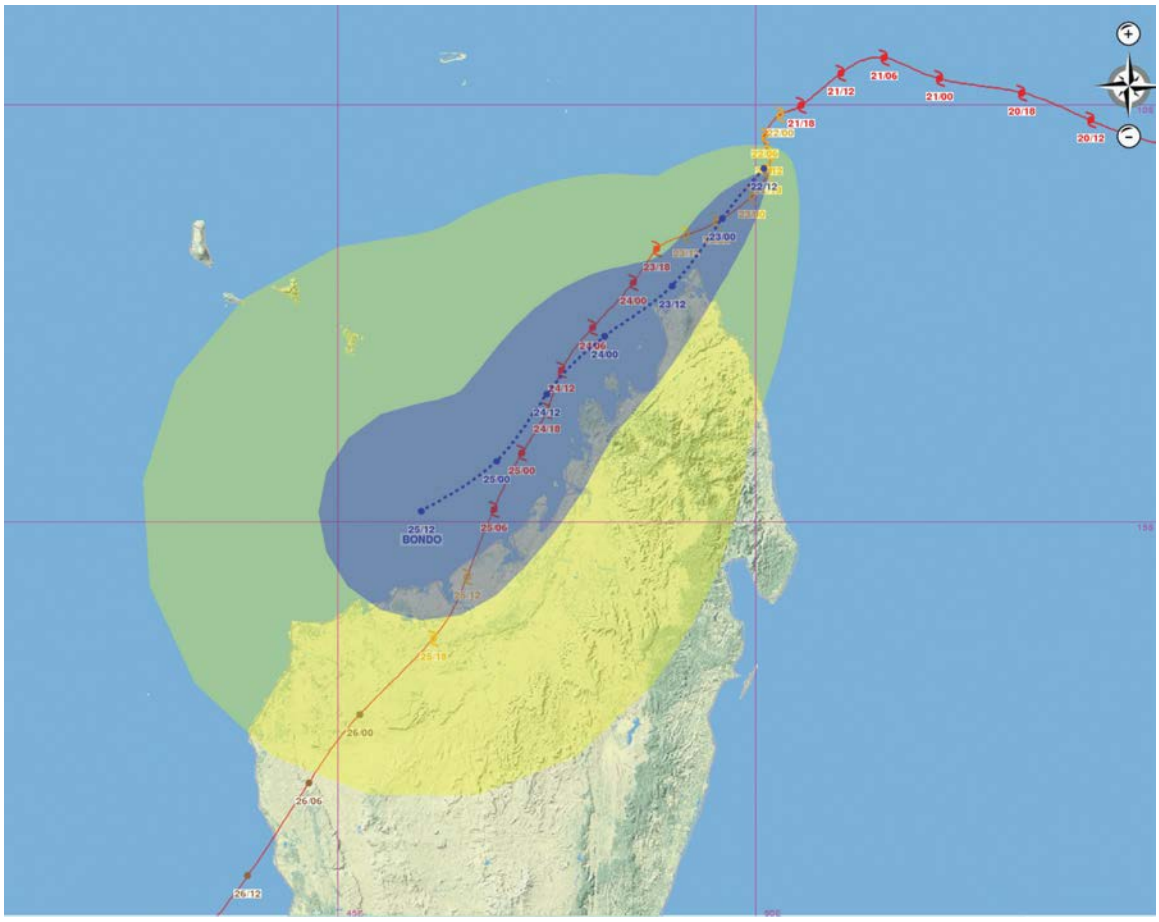

Figure 9.4. An example illustrating the difference between the "cone" of uncertainty based on the spread of the ensemble forecast from ECMWF model (radii of the 75% probability circle in blue) and a climatological "cone" of uncertainty (in yellow) in the case of limited uncertainty in the track forecast for Tropical Cyclone Bondo issued at 12 UTC, 22 December 2006.

In US, when issuing TC watches and warnings, the NHC forecasters take into account the uncertainties in the track, size, and intensity forecasts. Typically, the NHC forecasters determine the watch or warning area by adding the 5-year mean track forecast error to the deterministic forecast track, after accounting for the forecast size of the wind field. Uncertainties in the timing of the arrival of tropical-storm-force winds, and in the size and intensity of the TC are also considered when determining the type of watch or warning (tropical storm vs. hurricane) and the area to be placed under a TC watch or warning. Figure 9.5 illustrates how track uncertainty is incorporated when determining coastal watch and warning areas.

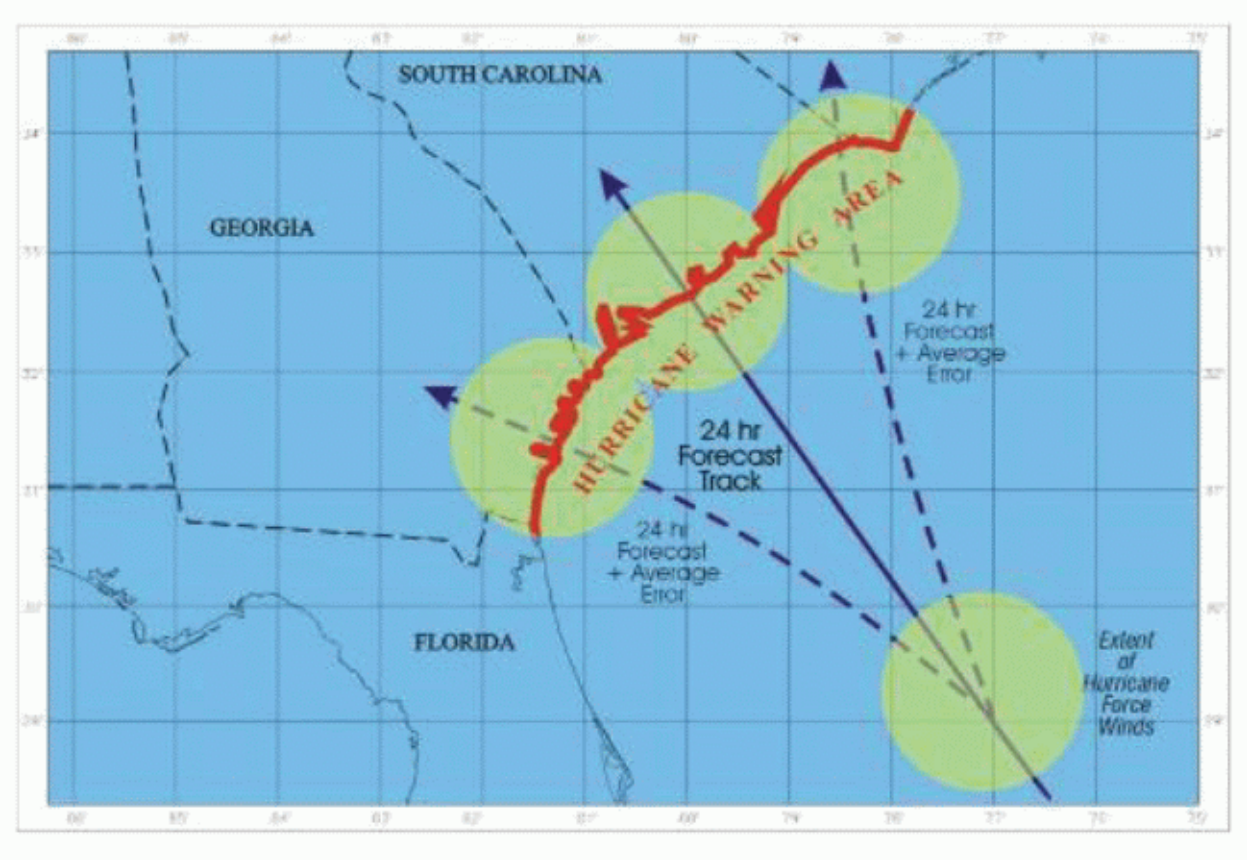

Figure 9.5. Example of how the NHC incorporates forecast uncertainty in the placement of coastal TC watches and warnings. NHC would issue a hurricane warning about 36 hours prior to the expected on-set of hurricane force winds. NHC would also likely issue tropical storm warnings for areas on either side of the hurricane warning where tropical-storm-force winds are expected to occur.

NHC also communicates forecast uncertainty by issuing text and graphic wind speed probability products. These products show the chance of 34-, 50-, and 64-kt or greater winds occurring at individual locations during the 5-day forecast period (Fig. 9.6). The probabilities are calculated using a set of 1000 realizations, or alternate tracks and intensities, that vary around the official forecast based on a Monte Carlo sampling of the previous 5-year errors in NHC track and intensity forecasts (DeMaria et al., 2009). Figure 9.6 shows an example of the hurricane-force-wind probabilities when a hurricane warning was issued for south Texas and northeastern Mexico for Tropical Storm Alex in June 2010. As indicated by the product, the highest probability of hurricane-force-winds at any individual location within the warning area was about 18% (at Brownsville, Texas, located near the Mexico-U.S. border). This example illustrates how emergency planners often deal with small probabilities of hurricane force winds when making evacuation decisions.

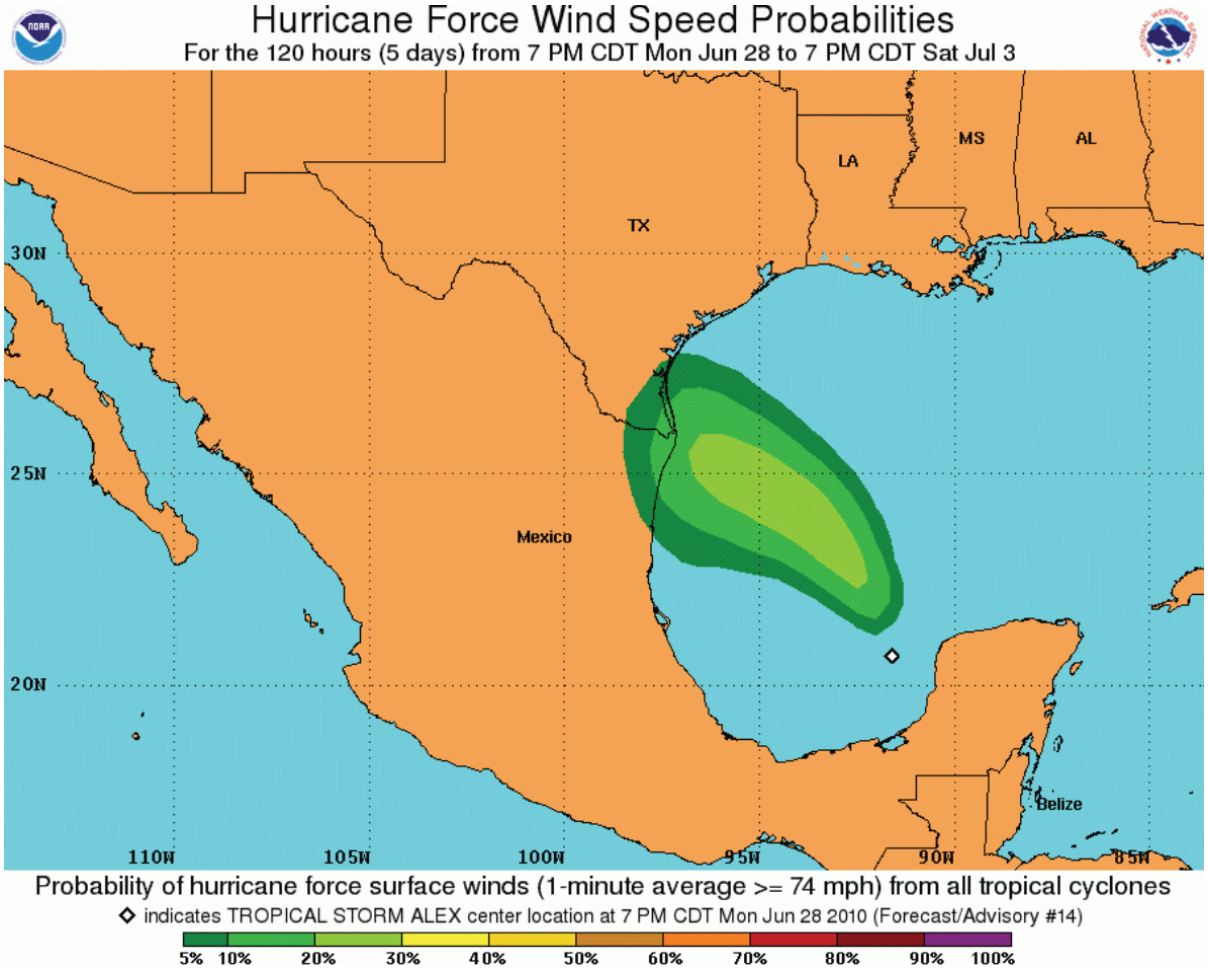

Figure 9.6. The probability of hurricane-force-winds during the next 5 days at individual locations issued by NHC.

9.4.4.3 From weather prediction to weather impacts prediction (National Research Council, 2010)

The atmospheric community has been spending a lot of efforts to improve the accuracy and resolution of the atmospheric quantities predicted by NWP models, such as temperature, wind and precipitation. Users have largely taken these weather predictions and used them in their own decision support and risk management process. However, this approach has not always produced the desired outcome, especially when complex weather forecasts are difficult to understand and yet require public action in response to the forecast. For instance, probabilistic forecasts of a land-falling hurricane's track and intensity, without specific impact information such as timing and location of storm surge, extent of flooding, extreme winds, and power outages, are insufficient for effective responses from emergency managers. A new paradigm is for both the scientists and the end-users to work together to provide explicit weather impact forecasts and warnings. This transition from simple weather prediction to weather impacts prediction demands a full integration of the physical sciences with the socioeconomic sciences. One key component of the prediction of impacts is to more fully exploit the capabilities of ensemble modeling to produce probabilistic forecasts of atmospheric quantities, and for these

to then be used to generate probabilistic forecasts of the weather impacts, thereby enabled improved decision making.

Fig. 9.7 shows an example comparing traditional portrayals of weather forecasting, and the potential for impacts forecasting. The weather services should place priority on providing not only improved weather forecasts but also explicit impact forecasts.

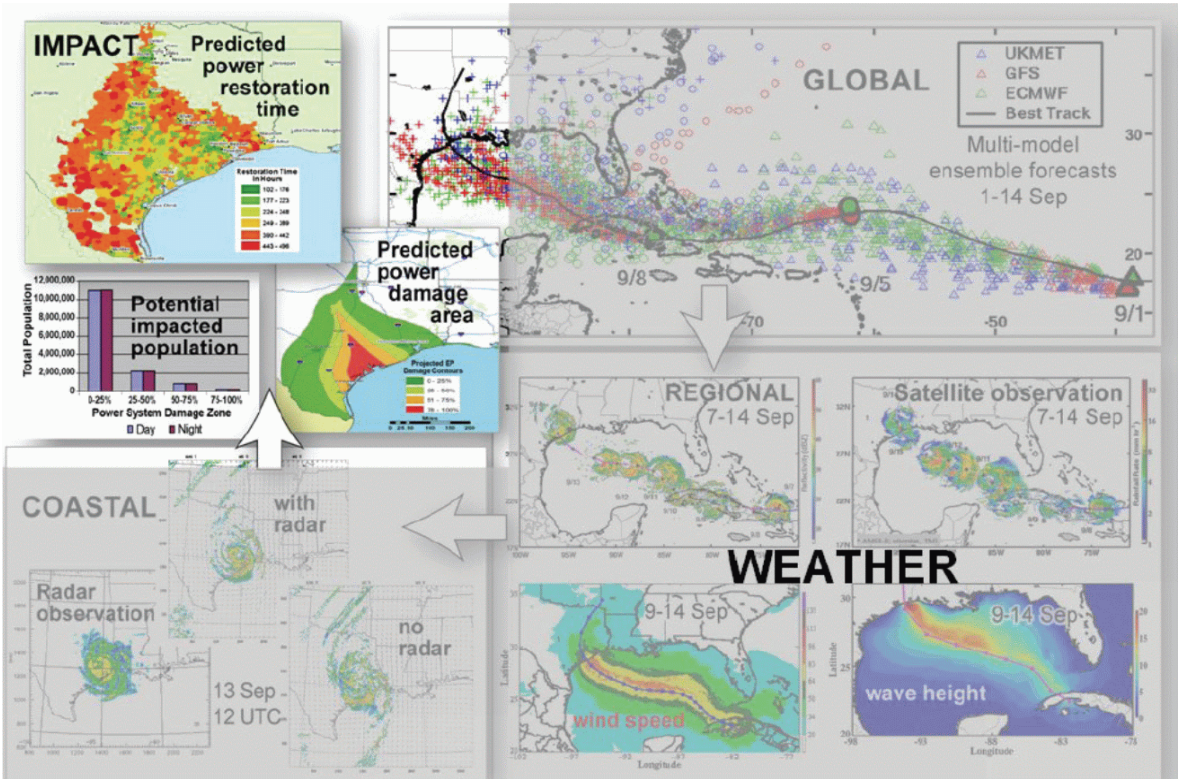

Figure 9.7. Schematic representation of weather impact forecasting. At upper right and lower right are traditional depictions of predicted TC paths, wind and wave height swaths, rain, and satellite observations. At lower left are radar observations and NWP radar renditions of the TC. The figure in the upper left predicts areas of power outages and restoration times. (National Research Council, 2010).

9.4.5 Warning dissemination

9.4.5.1 Various modes of warning dissemination

Timely delivery of warnings to the public is essential for disaster preparedness and mitigation. In India and Vietnam, like most other countries, the TC warnings are disseminated to users through telephone, fax, email and GTS. These warnings/advisories are also put on the website of the Hydro-Meteorological Service of Vietnam (VHMS, www.nchmf.gov.vn) and the Indian Meteorological Department (IMD, www.imd.gov.in). Another means to transmit the warning is through the Voice of Vietnam (VOV) television channel. During TCs, VHMS staff will attend live interviews on VOV to explain to the public the latest weather situation. This kind of warning dissemination is one of the fastest and most direct ways to reach the public. At IMD, one other

effective mode of warning transmission is via IVRS (Interactive Voice Response system). The requests for weather information and forecasts from the general public are automatically answered by this system. Besides, high speed data terminals (HSDT), installed across the whole country, are capable of sending short warning messages as SMS and the whole warning message as email.

Coastal TC watches and warnings issued by the NHC are officially disseminated via the NOAA Weather Wire. Watch/warning information is also available on the NHC Internet website and email. While email is not the official NHC mechanism for warning dissemination, this delivery option has become quite effective for NHC users. External partners such as the media and emergency managers play a critical role in the dissemination process by relaying watch/warning information to the general public.

During hurricane threats, NHC typically makes spokesperson, usually the NHC Director, Deputy Director, Hurricane Specialist Unit Branch Chief, or one of the Hurricane Specialists, available to the media. When hurricane watches or warnings are in effect for the United States, NHC activates a media pool, which allows local and national media to schedule short windows of time to interview the spokesperson. NHC also activates a Hurricane Liaison Team (HLT) to assist in the communication of information with federal and state emergency responders. The HLT is led by the U.S. Federal Emergency Management Agency and is staffed by emergency managers and meteorologists from outside the affected region. Informational briefings, typically led by the NHC Director or Deputy Director, are provided to federal and state emergency managers through the HLT when it is activated. The channels through which the warnings are relayed to the public have indeed, undergone evolvement, in response to user needs and taking advantage of the advancement of communication technology. Television and radio remain the most popular means of dissemination by HKO. This is followed by the HKO web site.

The warning recipients span a wide spectrum, ranging from the little-educated and the underprivileged to sophisticated users capable of assimilating large amount of information themselves. As shown in Fig. 9.8, the rapid rise in internet usage has not diminished the use of telephone calls to get weather information. It illustrates very well the persistent needs of a sector of the community which still relies on simple, cheap technology to access weather information or warnings. While adding advanced technology into their operation, NMHSs should not forget the former category of recipients, otherwise, the most vulnerable sector of the community would be left out in the disaster mitigation effort. In addition to a "pull", the Internet also allows an information "push" to the user. It also makes individual alerting and customization possible. A case in point is the provision of lightning location information by HKO on the Internet. Here a user may pick his/her location of interest and choose the alert range circles for receiving distinct audio and/or visual alarms when lightning occurs within a particular alert range. Coupled with geographic information, user-specific alerts thus set up provide fast and very relevant information, which is conducive to prompt and effective response actions.

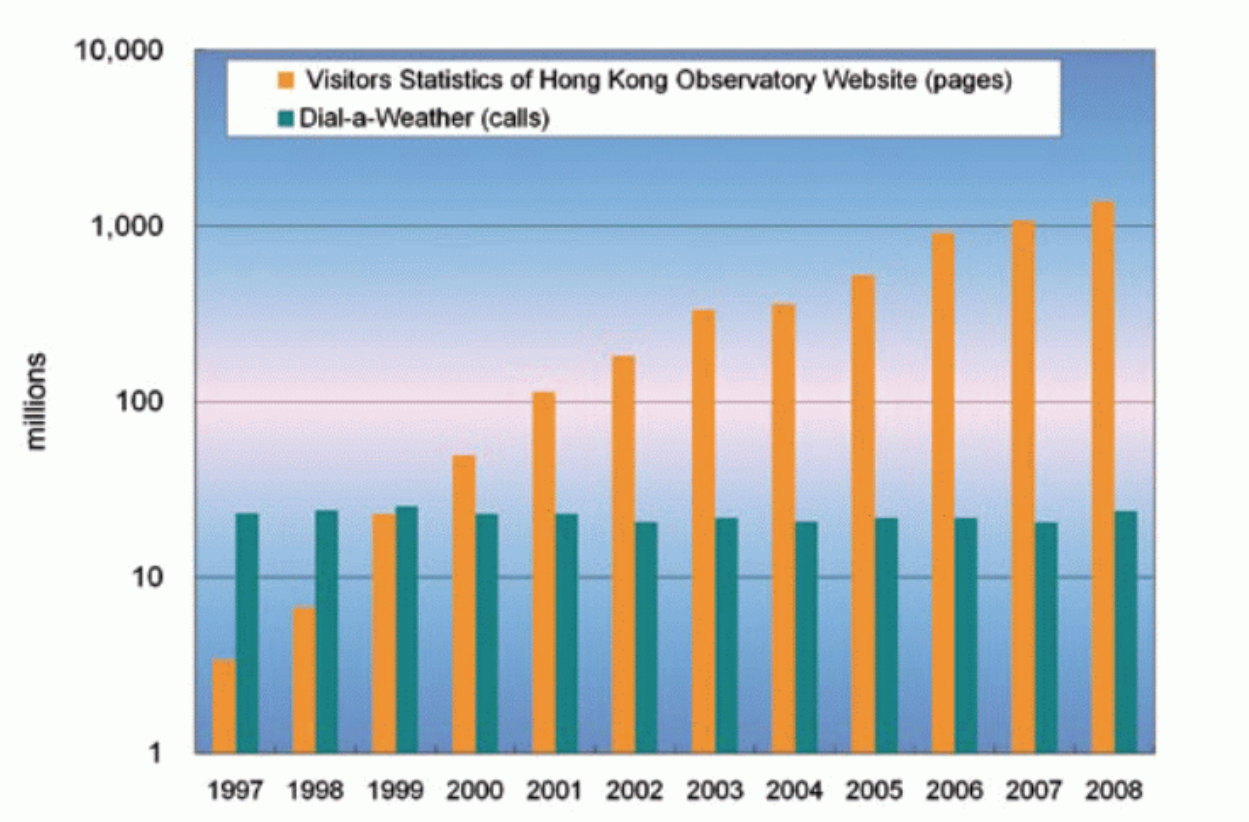

Figure 9.8. The usage of telephone for weather information remained steady in spite of growth in internet usage.

The HKO recently has also started exploring social networking services for warning dissemination. The Twitter service in both PC and mobile setup (Fig. 9.9) is being tried out. Weather warning, in the form of a "Tweet", will be published on the Observatory's Twitter profile and spread to all users. Tweets are text-based messages of up to 140 characters, which are suitable for conveying simple warning messages, in a one-way broadcast mode. The advantage of using Twitter is that it is relatively inexpensive to implement and maintain. The drawback is that the dissemination relies on the proper functioning of the Twitter service. At present, many international and national weather organizations are using Twitter for information dissemination. Examples are: WMO (http://twitter.com/WMOnews), UK Met Office (http://twitter.com/metoffice) and NOAA (http://twitter.com/usnoaagov).

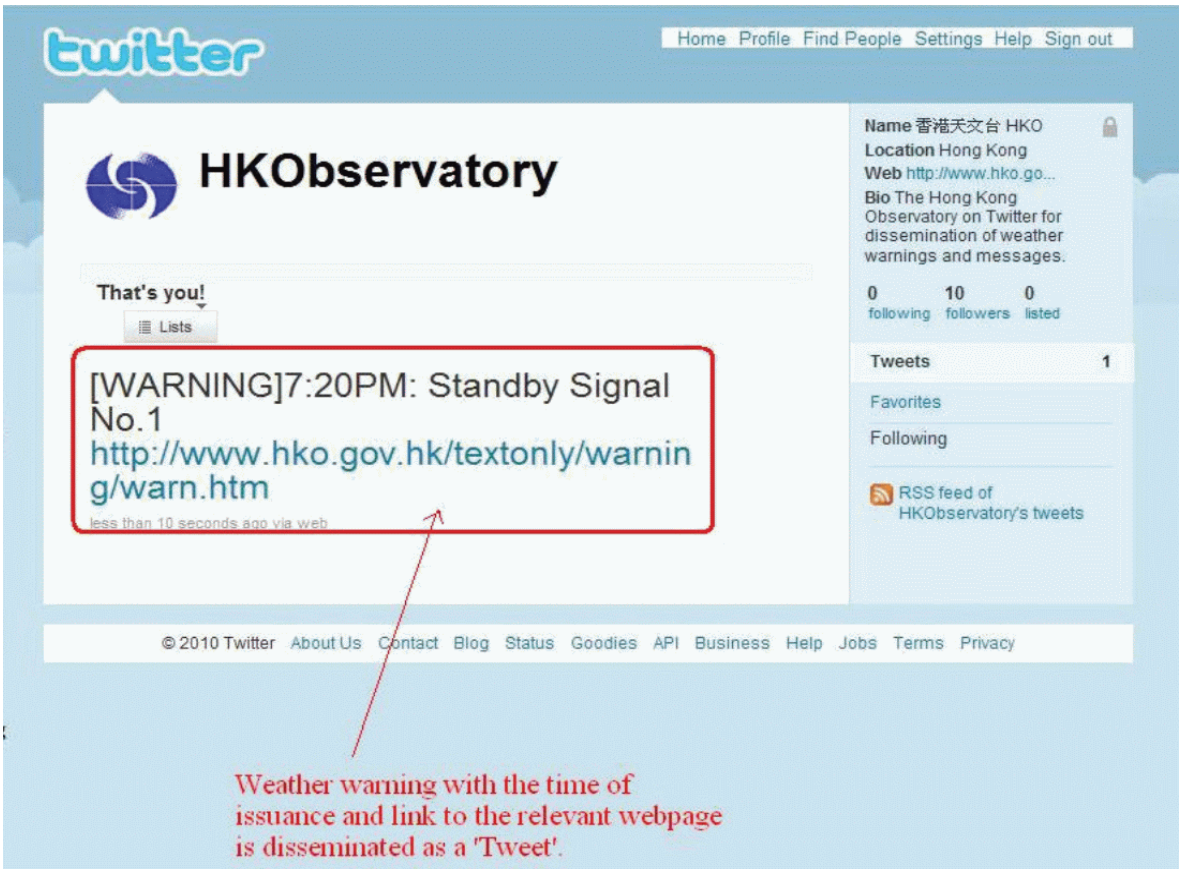

Figure 9.9. Warning message issued via Twitter.

9.4.5.2 Warnings to the last mile

The warning messages must be disseminated to all affected persons and groups, including those unable to receive television, radio or the Internet. This entails the operation of a robust warning dissemination system which could withstand the furious onslaught of TCs and deliver the warning messages through to the "last mile/kilometer".

For quick dissemination of warning against impending disaster from approaching cyclones, IMD has installed specially designed receivers within the vulnerable coastal areas for transmission of warnings to the concerned officials and people using broadcast capacity of INSAT satellite. This is a direct broadcast service of TC warnings in the regional languages meant for the areas affected or likely to be affected by the TC. There are 352 Cyclone Warning Dissemination System (CWDS) stations along the Indian coast; out of these 101 digital CWDS are located along Andhra coast. The warning bulletins are generated and transmitted every hour via the INSAT in C-band. The warning distribution is selective and will be received only by the affected or likely to be affected stations. It is a very useful system which has saved millions of lives and enormous amount of property from the fury of TCs. The advantages of C-band transmission are its bigger footprint, high bandwidth, and less likely to be affected by severe weather.

EMWIN (Emergency Managers Weather Information Network) and RANET (RAdio InterNET) are two communications programs that have had a great impact on advancing the warning capabilities and strategies of many developing countries, especially in the Pacific basin. EMWIN has been discussed at many WMO conferences and workshops, and RANET was discussed in some detail at the International Workshop on Tropical Cyclones (IWTC)-VI in San Jose, Costa Rica by Anderson-Berry (WMO, 2007). Since IWTC-VI, several new capabilities have come on-line or are being tested.

EMWIN has been in use for nearly two decades in the US and for over a decade in the Pacific basin as a low-cost method for passing weather and warning information to emergency managers, weather service offices, and other critical locations such as hospitals and college campuses (http://www.nws.noaa.gov/emwin/). In some cases, EMWIN has been used as a backup system, but for many developing island nations, it has been the primary or only source of reliable weather information. GOES satellites that no longer provide meteorological data but that still have communications capability are sometimes repositioned near the International Date Line to support EMWIN and another US communications program called the Pan-Pacific Education and Communication Experiments by Satellite (PEACESAT) (http://www.peacesat.hawaii.edu/). This program transmits, via satellite from the University of Hawaii and via satellite and HF Radio from the University of Guam, important distance education programs and critical storm and warning information to many isolated islands in the Pacific basin. The program also coordinates search and rescue in the Micronesian islands and passes daily weather information to the remote islands. Occasionally, the operator at the PEACESAT terminal at the University of Guam will call forecasters at the Weather Forecast Office on Guam (WFO Guam) and request them to provide a live, real-time assessment of upcoming weather. In the US, EMWIN has been using the digital Low Rate Information Transmission (LRIT) standard in areas covered by GOES-East and GOES-West. LRIT and EMWIN are now being made available in other parts of the Pacific not in the footprint of the operational GOES-West satellite (http://noaasis.noaa.gov/LRIT/). A High Rate Information Transmission (HRIT) capability is being developed for US users in the future (http://www.goes-r.gov/users/hrit.html). This capability will combine the current LRIT broadcast services with the EMWIN broadcast services and transmit both at a significantly higher data transfer rate.

The purpose of RANET (https://www.wmo.int/pages/prog/www/Planning-Impl/RA-5/2005-APIA/Ranet-Emwin-Doc5-2%284%29.pdf) (Clarke et al, 2010) is to get important information about TCs and other hazards down to the community level. Over the years, RANET has taken on many forms, especially in terms of the types of hardware and communications methods used. In the western Pacific, two new uses of RANET are highlighted. The first is the installation of FM radio stations (Fig. 9.10a) in some island weather facilities, allowing them to pass critical weather and warning information from the weather service office directly to the community level. The second is the development of the "Chatty Beetle" (http://beetle.ranet.mobi/) (Fig. 9.10b), a durable, low-power, easy-to-maintain, two-way communications device designed to get emergency warning information down to the most isolated locations, such as remote atolls and islets. Both of these systems have proved to be very useful, and could be used in many other locations.

In July and August 2008, Mr. Bruce Best of the University of Guam and his team installed an 80-foot FM radio transmitting tower and an FM transmission and recording console at the Weather Service Office (WSO) in Chuuk State, Federated States of Micronesia (FSM) (Best and Marquez 2008). There was no reliable radio station in Chuuk State, and the island State is very vulnerable to numerous natural hazards such as typhoons, flash floods, mudslides, droughts and high surf events. An FM Radio solution was ascertained as the most economical way to pass critical weather information and warnings to the 40,000+ residents living on islands in the Chuuk Lagoon. Special radios, such as the VHF radios that are required with the US NOAA Weather Radio program, are not needed. In fact, simple transistor radios, car radios and "boom boxes" can be used by residents to get the weather and warning information. A repeater was later installed to extend the range and coverage of the signal to more locations in the lagoon. In 2009, a similar FM radio station was installed in Majuro, Republic of the Marshall Islands (RMI). Since there is reliable radio service there, the FM station is used in times of emergency rather than routinely. A repeater is planned to push the signal to the neighbouring atoll of Arno in the RMI. This FM radio concept is an inexpensive, highly reliable, and relatively simple method to pass critical and routine weather information to the public. It could be considered as a potential solution for developing countries with communications challenges, especially those oceanic nations with small islands in close proximity or inside lagoons.

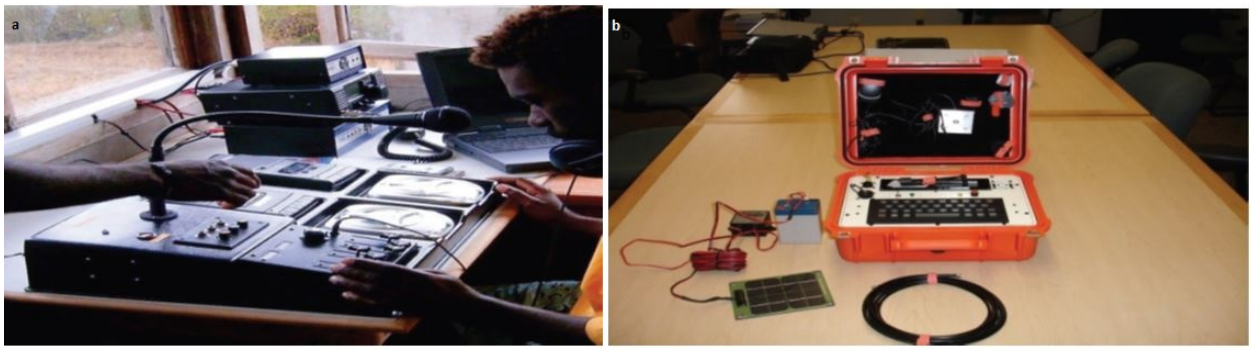

Figure 9.10. (a) Wantok FM radio Station similar to the one installed at the Weather Service Office in Chuuk Lagoon, Federated States of Micronesia; (b) The "Chatty Beetle".

9.5 Hazard, vulnerability and risk assessment

Because of the inherent forecast uncertainty, TCs initially offer a macroscale threat to large areas and significant populations. This condenses to a mesoscale highly destructive impact in which the greatest loss of life and property generally occurs in small areas comprising a small subgroup of the autonomous local government authorities initially under threat. Since the warning task is to persuasively *alert* and to *promote response* to counter this developing threat, it follows that any developments in the warning system should commence with hazard risk and

vulnerability assessments of the elemental local government authority areas. When integrated, these indicate the total vulnerability of all components of the system, districts, provinces, and nations. However, each house has its own vulnerability and only sustained community programs can hope to bridge the gap between the formality of government protection at the higher level and the street -by-street level of the local community.

In several advanced countries, notably the USA, detailed hazard risk and vulnerability assessments, often initiated by meteorologists themselves, have been performed over much of their cyclone-prone coastal zones for many years. This preparedness homework has enabled detailed evacuation planning to be implemented on the basis of operational processing of the SPLASH and SLOSH storm surge models in accord with bathymetric and topographic risk mapping, assisted by community behavioural response studies in the most vulnerable sectors. This capability is incorporated in recommended response activity announced in hurricane local statements issued by national weather service offices around the US coast that follow authoritative national hurricane advisories issued by the NHC. Detailed topographic mapping makes it possible to recommend evacuation on a street-by-street basis in respect of forecast storm surge inundations augmented by heavy rainfall runoff.

Regrettably it is recognised that although most other countries have published information on the frequency of cyclone occurrences, and some have computed return periods for cyclones of stated intensity or cyclone parameter statistics, only a few countries have undertaken comprehensive vulnerability assessments, especially at community or district level. The absence of adequate hazard mapping and skills may have contributed to this situation. A result is the almost complete absence of localised contingency action plans in these countries, which negates many of the benefits of improved warnings and inhibits the deployment of warning strategies.

9.5.1 Quantification of risk

Vulnerability and risk analysis provides a structured analytical procedure to identify and quantify hazards and to estimate the probability and consequences of their occurrence. It must be emphasised that the absolute risk is a complex, multiplicative function of the hazard threat level, the vulnerability of a community and the consequences of the event on the community. In an illustrative sense, this means that:

Disaster Risk = Hazard or Threat x Vulnerability x Consequences.

Say we were to rate the hazard and vulnerability on scales of 1-5, then a community with high vulnerability and hazard levels of 5 would be many times more at risk (25) than would a community with low levels of 1. However, if the consequences are low or negligible, then the risk will be low even with high threat and vulnerability levels. If the consequences of an event to a population are low, that population is said to have high resiliency.

9.5.2 Hazard or threat assessment

Although many countries use designated cyclone warning phases or stages, few have adopted scales which combine a rating of the intensity of cyclone parameters with corresponding estimates of the typical damage that may be expected. Examples of this categorisation include the US Saffir-Simpson Hurricane Scale (Simpson 1974), the US Saffir-Simpson Tropical Cyclone Scale (Guard and Lander 1999), and the Australian Cyclone Severity scale, all of which classify cyclones of hurricane intensity from 1-5, weakest to strongest. The Saffir-Simpson Tropical Cyclone Scale also utilizes two tropical storm categories to include sub-hurricane-force winds. It is recommended that such categorisations be undertaken by all countries with a tropical cyclone threat.

The hazard/threat component can be assessed in terms of the frequency return period or recurrence interval of a particular intensity category for the specified location. This method is particularly useful in countries where detailed observations are not available, and assessment is best made using derived parameters from the known tropical cyclone statistics. These scales are also extremely useful for planning and exercise purposes. Alternatively, return period estimates of particular cyclone parameters, such as maximum wind gusts, storm surge heights, river flood levels or rainfall intensities may be developed or estimated. These latter criteria are favoured for engineered structural mitigation measures. In any case, an estimate is required of the return period frequency of cyclones of each intensity category as guidance to provide an objective indication of the cyclone hazard in each coastal sector.

For the purpose of general community preparedness a worst-case scenario for a period of 30 years may be reasonable. If this is translated into appropriate contingency planning, any cyclone of lesser intensity should not cause major unexpected adverse effects (provided community vulnerability does not increase). Preservation of essential community lifeline facilities (hospitals, power and water supplies, communication systems, meteorological radar tracking stations, cyclone shelters and operations centres etc.) require design criteria for a longer time period.

National standards associations generally determine regional engineering design wind loadings. An indicative example, normalised by Australian Cyclone Severity Scale (or category), for a stretch of coast from Port Douglas to Fraser Island on the Australian East Coast and applicable to 50 km inland is (SAA, 1989):

Table9.3: TC Occurrence rates on Australian east coast

Category	**Cat 2** **<170 km h^{-1}**	**Cat 3** **170-225 km h^{-1}**	**Cat 4** **226-280 km h^{-1}**	**Cat 5** **>280 km h^{-1}**
Occurrence/year	1/3	1/6	1/30	1/100

These statistics refer to cyclones directly impacting coastal areas. Approximately twice as many cyclones in each category threaten the coastal section, without direct impact.

An indication of return periods for tropical cyclone parameters for Andhra Pradesh and West Bengal (which provides a guide for Bangladesh) has been published by Jayanthi and Sen Sarma (1988) based on a 95-year data base. This includes the following statistics for maximum wind speed and storm surge height:

Table9.4: TC Occurrence rates: North Inian Ocean

	Return Period (years)				
	10	**25**	**50**	**100**	**200**
Andhra Pradesh	104 kt 3.8 m	113 kt 4.2 m	119 kt 4.8 m	125 kt 5.2 m	129 kt 5.6 m
West Bengal	90 kt 4.5 m	105 kt 6.3 m	116 kt 7.8 m	125 kt 9.2 m	135 kt 10.9 m

The two cyclones that occurred in nearly the same locations in Andhra Pradesh in 1977 and 1990 and the two that occurred in Bangladesh in 1970 and 1991 were of a similar intensity that lay within the 25-50 year return period in this table. This illustrates the problem with literal use of return period statistics. Although catastrophic, with 300,000 and 140,000 deaths, respectively, in Bangladesh, and 10,000 and 1000 deaths in Andhra Pradesh, these statistics illustrate the advances in warning-response systems in these regions. In 2002, the eye of a Category 2 typhoon and a Category 4 typhoon passed across the 50-km long island of Guam in July and December 2002, respectively. Each typhoon produced 24-hour rainfall amounts (610 mm) that were classified as 100-year events. Again, this points out the problem with using return periods: Were these really 100-year events?

9.5.3 Vulnerability assessment

Vulnerability comprises the people in their environment and their exposure to the cyclone hazard. The geographical and physical components of provincial, district and local level vulnerability are assessed through a combination of hazard risk maps, detailed demographic maps, and information on supporting community infrastructure and facilities. Such assessment can be made by satellite remote sensing, aircraft photography, and on the ground by surveyors, engineers and urban and rural planners. A good survey will provide details of:

- Siting and constructional integrity of community lifeline facilities, including access roads;
- Proportions of flimsy, partly cyclone-resistant, and cyclone resistant residential housing, commercial buildings and markets;
- Existence and state of maintenance of cyclone protective works, river and coastal dykes and embankments, drainage systems and public shelters;
- Degree of protective forestation and mangroves, which can reduce wind, wave and surge energy.

The non-physical social and economic aspects of vulnerability of a community also need to be assessed. These include a measure of the community's capacity for coping with the occurrence of cyclones by martialing resources and organising effective response actions. Readily assessable elements include:

- The existence of a local counter-disaster council, an equipped emergency operations centre, a cyclone contingency plan of action which has been resourced, implemented and rehearsed;
- Evidence of an ongoing community cyclone awareness program.

An obvious indication of the vulnerability of a community may be found from its performance in coping with a previous cyclone, after noting subsequent improvements.

An extensive program of interdisciplinary training courses entitled "Improving Cyclone Warning Response and Mitigation" is now conducted by the Asian Disaster Preparedness Center (ADPC), based at the Asian Institute of Technology in Bangkok. The ADPC has introduced practical experience for participants through the conduct of field vulnerability assessment studies in towns and villages. Such studies take advantage of any available hazard maps and primarily comprise visual inspections of potentially hazardous terrain, community life and facilities, aided by interviews with officials and residents on cyclone and flood hazard experiences and on the current state of preparedness measures, local communications and warning arrangements. The course participants, comprising meteorologists and hydrologists, disaster managers, engineers, planners and technical personnel interacting in workshop sessions. Reports to a workshop plenary session, supported by maps and sketches, are discussed and published and the total exercise takes little more than a day's work.

While these exercises obviously comprise a fair degree of subjectivity they summarise a good deal of human hazard experience of residents in a short time and probably acquire about 80% of the environmental, physical, and socio-economic information needed for a useful vulnerability assessment. An immediate feel for the community's hazard awareness is gained, as well as knowledge of the cyclone-resistant integrity and maintenance standards of the principal lifeline facilities.

In general, a nation's effectiveness in disaster prevention, mitigation and preparedness is related to its level of economic activity (PAHO, 1992). This indicates that current socio-economic indices, such as per-capita income, may provide one objective basis for quantifying vulnerability in the above equation.

A complementary input to the vulnerability index should come from recent disaster experience. For example, damage evidence in relation to 20 categories of socio-economic activity is clearly noted for the April 1991 Bangladesh cyclone in BCAS (1992). This cyclone effected 10,800,000 people with a total damage of US$2.1 billion, or roughly the per-capita GDP of US$210 (FEER, 1993) This simple analysis could be extended to local districts and normalised on a scale of 1-5. Separate quantification could be developed for deaths and casualties.

Where recent damage statistics are not available, the current per-capita income probably provides an objective basis for relating statistics from other regions and quantifying both the economic and social effects of a tropical cyclone.

Vulnerability depends on several factors. These include: the level of preparedness, the efficiency of response, ability to recover, and the implementation of mitigation measures.

9.5.4 Potential disaster risk scales

No objective method has yet been devised to integrate the cyclone hazard and vulnerability into a disaster risk scale similar to the Saffir-Simpson Hurricane (Intensity) Scale. Such a scale would first require the development of a suitable vulnerability scale, as recommended in the previous section, then a method needs to be developed for incorporating this with the hazard scale. It is almost certain that the total risk will be a multiplicative combination of the hazard and vulnerability scales, but research is needed to determine the optimum combination.

Such a scale could markedly simplify the development of warning and response strategies and the allocation of mitigation measures. It could provide a globally consistent indication of disaster risk. The scale could be printed on maps and displayed on computer workstations as indicators of the relative vulnerability of hundreds of autonomous local government areas threatened by an approaching cyclone. National potential disaster risk maps can be prepared and disseminated to indicate an objective measure of the real danger of the threat, compared to previous occurrences, and thus to promote preparedness measures. By agreement an tropical cyclone warning centre could include such information in its advisory warning messages, together with potential disaster risk predictions for each community, in a manner reminiscent of the issue of hurricane strike probabilities in the USA.

9.5.5 Conveying forecast uncertainty

Tropical cyclone prediction involves a great deal of uncertainty. There is uncertainty in the limited input storm data and in the even more limited environmental data, uncertainty in the prediction model physics and due to truncated terms, uncertainty introduced by the time-steps, and other, less obvious, sources of uncertainty. Most of the storm data and the environmental input data are indirectly determined. The numerous algorithms that have been developed to derive that indirect data are also sources of uncertainty.

This uncertainty must be conveyed to the general public so that the users understand that there is error associated with the forecast tracks and intensities. While the errors can be estimated, there is uncertainty in those estimates. So, how do we convey this uncertainty to the customers? This has been a perplexing question that has been addressed by many different methods. These methods include uncertainty swaths based on historical error information such as is shown in the US National Hurricane Center depiction in figure 9.3 and by the Japan

Meteorological Agency (JMA) in Tokyo (not shown). Over the last decade, more sophisticated techniques have been developed employing ensemble methods as shown in figure 9.6.

9.6 Societal impacts of tropical cyclones

9.6.1 Introduction

Despite significant advances in the meteorological science and understanding of tropical cyclones and the associated capacity of sophisticated warning systems, negative impacts upon societies throughout the tropical and subtropical world remain severe. Table 9.5 illustrates the enormous impact of tropical cyclones over the last 110 years. At the beginning of this period, many people died at sea and local communities bore the impact of storms without warning. Yet despite the advances that have been made, losses and impacts of tropical cyclones remain high. In recent years, cyclones such as Katrina's impact upon New Orleans, Jeanne, Ida, Mitch, and Stan in Central America and the Caribbean, and Nargis in Myanmar continued to wreak havoc, destroy structures and cause loss of life.

Table 9.5 Tropical cyclones by continent from 1900 to 2010.

		No. events	Killed	Total affected	Damage (000 US$)
Africa	Tropical cyclone	100	3,400	14,995,592	3,079,430
	average per event		34	149,956	30,794
Americas	Tropical cyclone	537	86,332	46,918,376	402,062,632
	average per event		161	87,371	748,720
Asia	Tropical cyclone	940	1,237,484	560,845,477	151,642,503
	average per event		1,316	596,644	161,321
Europe	Tropical cyclone	22	201	94,682	1,817,360
	average per event		9	4,304	82,607
Oceania	Tropical cyclone	194	1,721	2,294,553	7,461,364
	average per event		9	11,828	38,461
World	Tropical cyclone	1,793	1,329,139	625,148,680	566,063,289
	average per event		741	348,661	315,707

Source: "EM-DAT: The OFDA/CRED International Disaster Database http://www.emdat.be/ - Université Catholique de Louvain - Brussels - Belgium" Created on: Sep-17-2010. - Data version: v12.07

During the last decade alone, from 2000 to 2009, there were 540 tropical cyclone occurrences worldwide (several individual cyclones struck a number of countries, especially in the Caribbean

and Central America — for example Hurricane Michelle in 2001 affected people in 8 countries and Dean in 2007 affected 9 countries). These events of the last decade killed 167,692 people, affected a further 286,222,031 and cost an estimated US$ 385.12 billion (CRED 2009). The impact of these storms was extremely uneven with the Philippines bearing the brunt of 70 cyclones. The Peoples Republic of China was impacted 46 times and Taiwan a further. The next most impacted countries were Mexico 25, Japan 23, USA 22 and Bangladesh 19. In terms of death rates, cyclone Nargis which devastated Myanmar in 2008, killed 138,366 people, followed by Sidr killing 4,234 in Bangladesh, Jeanne's death toll of 2,754 in Haiti, 1,833 killed by Katrina in the USA, 1,619 killed by Winnie in the Philippines, a death toll of 1,513 from Stan in Guatemala and 1,399 killed by Durian in the Philippines (CRED 2009).

Societal risk is formally defined as "the risk of a number of fatalities occurring." (Emergency Management Australia 1998). This can be related directly to the risk equation

risk = hazard X vulnerability

or

risk = hazard X vulnerability X elements at risk

Society's risk is identified with vulnerability, although the elements at risk may seriously impact upon social losses and recovery.

Impact is "a sudden occurrence without prior warning," and the impact area is defined as "any area which is likely to bear, is bearing, or has borne the full impact of any disaster and in which major lifesaving operations are necessary" (Emergency Management Australia 1998). Mitigation consists of "measures taken in advance of a disaster aimed at decreasing or eliminating its impact on society and environment" and prevention which is "regulatory and physical measures to ensure that emergencies are prevented, or their effects mitigated - measures to eliminate or reduce the incidence or severity of emergencies" (Emergency Management Australia 1998). Vulnerability is defined as a function of susceptibility to loss and constraints to the capacity to recover, while the capacity to recover from a disastrous impact is termed resilience. These definitions are necessarily starting points.

Following from these basic definitions, the review is structured into three main areas; physical impacts of tropical cyclones on human beings and their communities, vulnerability and resilience, and mitigation.

9.6.2 Physical impacts of tropical cyclones on people and communities

The physical characteristics of tropical cyclones bring destruction through wind, surge and associated flooding (Chittibabu et al 2004). The loss of life principally results from surge and flooding such as recent examples of the consequences of cyclone Nargis in Myanmar, Sidr in

Bangladesh and Katrina at New Orleans USA (Congleton 2006), but all three characteristics cause damage to structures, dwellings, infrastructure and resources.

Wind damage is affected by both terrain and vegetation, but there is no easy solution to the identification of either protective land features or appropriate vegetation. Valleys may funnel intensive high cyclonic winds and steep hills may act as a buffer or minor protection, but these effects will entirely be dependent on the direction of the wind, which will change direction after the passage of the eye anyway. The sheer size of tropical cyclones easily overcomes most features of the landscape. However, there are classifications for landscape types that acknowledge some impact upon wind damage. Knowledge of vegetation performance capacity during strong winds is well developed and translates into advice from organizations such as local councils on the best trees and shrubs to plant in cyclone prone areas. This may extend to the clearance of vegetation, and pruning of branches, etc., close to buildings and infrastructure such as power lines. Vegetation acts as both a buffer and debris. The speed of passage of the cyclone influences the potential for debris damage as well as the extended battering of structures. Once damage has occurred, debris from both structures and vegetation become missiles that extend the impacts of high winds. Wind damage is additionally exacerbated by precyclonic heavy rain and flooding, that saturates the soil, loosens the root structures of trees, and initiates soil erosion.

Before electronic communications were available to ocean going vessels, cyclones caused significant loss of life at sea, especially in the days of long distance passenger travel by sea. While there has been a decrease in the loss of large vessels, recent cyclones have continued to destroy small fishing boats in developing countries as well as recreational vessels.

Storm surge, and associated flooding from the ocean, heavy rainfall and rivers overtopping their banks, frequently bring about more extensive damage than that caused by cyclonic winds, and it is certainly this aspect of tropical cyclones that causes the greatest loss of life. This was the case in all of the recent tropical cyclones, identified in the introduction, that resulted in extensive loss of life. The most vulnerable locations for tropical cyclone surge and flood impacts are low lying coastal plains and beach frontage that have been the focus of residential development, tourist resorts and coastal resource and fishing settlements. Additionally many estuaries and tidal rivers that have experienced significant development are even more vulnerable to surge and flooding. Many of these areas also have evacuation issues of access and egress.

The recovery and long-term viability of tropical cyclone impacted communities is a consequence of tropical cyclone intensity, on top of related and past disasters, such as previous cyclones and accompanying floods. Recovery is additionally constrained by household and community wealth, resources and infrastructure. Communities in less developed countries face much greater recovery constraints, and some places and regions do not recover from their losses in the medium to long term. Even New Orleans in the world's wealthiest nation had not recovered five years after Katrina's catastrophic impact (fieldwork, King 2009).

An additional wind impact is the variability of wind speeds, bringing gusts and vortices that randomly destroy structures. Building codes and community preparations are inevitably for an average set of expected conditions and will frequently fall short of preparation for severe storms.

Frequent catastrophic tropical cyclones lead to a long-term loss of economy and population. Younger people migrate away from the disaster zone to seek opportunities elsewhere (Hunter 2005), while the elderly become particularly vulnerable to sickness and depression. On the other hand while scientists have questioned whether increasing losses from disasters were due to climate change, and also concluding that there is no global trend in tropical cyclones, many, such as Bruce (1999) stressed that mitigation has to proceed on the cautionary principle.

9.6.3 Physical impacts upon households and communities

Tropical cyclone impacts on houses range from minor repairs to total destruction. Loss of the household dwelling then leads to temporary migration and relocation (that may last for many months or even years), as well as social and community dislocation, isolation, and in many cases (especially in less developed countries) homelessness. A specific developing country problem is tropical cyclone destruction of the local environment which removes accessibility to resources for rebuilding village houses -- timber, palm, bamboo and roofing thatch. In all societies, both dwellings and personal belongings are spoiled or destroyed by water damage. Outside the immediate losses to the household and its dwelling, community facilities, infrastructure and lifelines are equally damaged, compromising the processes of survival and recovery.

The impact of hurricane Ivan in 2004, assessed in a post-disaster study of Orange Beach, Alabama (Picou and Martin 2006), showed that average damage to each home was $36,000, with 81 percent of the residents of Orange Beach having to be evacuated for an average of 11 days absence. There was no power for an average of 12 days, and no telephone for an average of 9 days. The study showed significant social conflict and loss of trust within the community. The following year, these sorts of impacts were repeated on a greater scale after hurricanes Katrina and Rita (Khoury et al. 2006).

9.6.4 Psychological impacts upon households and communities

Psychiatrists and psychologists have developed specific analytical tools to assess the traumatic effects of experiencing a disaster. An extensive range of experiences is involved, both for the victims and responders — fear, shock, bereavement, depression, loss of control, social and psychological isolation which in turn contribute to community and societal impacts which may range from strength, resilience and empowerment to severe loss, disruption and breakdown. Impacts of cyclones and hurricanes generate from enormous losses and widespread disruption to peoples' lives with long term PTSD (Post Traumatic Stress Disorder), relocation and longer

term out-migration, economic disruption and decline and unequal impact on the socio-economically disadvantaged and vulnerable groups within the community.

Stein and Preuss (2008) recorded oral histories amongst the victims of Katrina. There were stories of violence, and of police preventing people entering evacuation centres. Drawing on studies carried out with focus groups, interviews and photo-journalism with narratives from a wide diversity of participants, oral histories captured people's awareness of their own misperceptions. For example the oral histories captured the black story of New Orleans, but while the researchers acknowledge that they missed the white story, the highest impact fell upon African-Americans (Spence et al 2007). While the lessons learned from one disaster help prepare for future events, the experience of the events are probably distorted for each individual, as people select and construct their memories, and prioritize their actions, behavior and responses. Any single individual has an incomplete and personal experience of a disaster, which affects the way in which they will interpret future warnings and information.

9.6.5 Environmental damage

The damage to the natural environment reduces landscape amenity that contributes to non-quantifiable and non economic impacts that influence community well-being, culture and heritage. There are direct and quantifiable effects on agriculture, tourist attractions, fisheries and construction materials. There are also intangible socio-economic environmental impacts where species are lost, weed species invade an area, and time and labor are transferred from economic activities to recovery of the environment.

9.7 Vulnerability and resilience

The vulnerability of people and communities to tropical cyclone risk is measured at levels of the individual, the household and the community. Communities are complex entities, at their simplest consisting of a collection of households at a geographical location — a neighbourhood or a village. In all societies, but especially in urban and industrial settlements, people are members of multiple communities, of family, workplace, educational institution, recreation and interest communities, which include religious, political and cultural groups, and many more. The idea of community also includes intangible networks, like facebook, where relationships and support extend way outside the impact area of a specific tropical cyclone.

Social capital and collective action are central to resilience and will also drive some of the adaptation strategies needed for climate change. Adger (2003) illustrates how social capital operates at different scales from the individual through communities to the state. However, measurements of both vulnerability characteristics and elements and social capital present problems to emergency managers and local governments. Some characteristics of individuals, households and communities can relatively easily be measured from censuses and local government inventories of lifelines and community infrastructure. However, such databases only provide snapshots, or non contextual aspects of human and community characteristics of

either vulnerability or resilience. The lack of data makes it difficult to measure the qualitative and intangible aspects of individuals or of communities — things like knowledge, wisdom, community spirit, sense of place and purpose, all of which are extremely important aspects of the social capital that reduces vulnerability and enhances resilience.

There is a problem for all levels of government in influencing or attempting to reduce vulnerability. In defining such demographic characteristics as the very young of the very old as vulnerable groups, there is little one can do about it. The same applies to many other vulnerability characteristics which are structural and fixed in the short to medium term. Vulnerability assessments at the beginning of the IDNDR identified specific population characteristics or elements of structures and infrastructure. These have proved to be useful indicators, but they left out too many of the qualitative and intangible aspects of communities. Models of vulnerability have more recently emphasised broader issues of governance, resilience and education. For example Gopalakrishnan and Okada (2007) list elements for vulnerability assessment:

1. Awareness and accessibility
2. Autonomy
3. Affordability
4. Accountability
5. Adaptability
6. Efficiency
7. Equity
8. Sustainability

Schroter et al. (2005) also presented five criteria for vulnerability assessment that anticipate climate change adaptation:

1. Flexible knowledge base
2. Place based — local scale
3. Interconnectedness of change
4. Differential adaptive capacity
5. The future draws from the past.

They added eight steps towards the achievement of such a vulnerability assessment:

1. Defining the area along with stakeholders
2. Know the place over time
3. Hypothesise vulnerability
4. Develop a causal model of vulnerability
5. Develop indicators for vulnerable elements
6. Operationalise the model
7. Project future vulnerability
8. Communicate vulnerability clearly.

Myers's et al. (2008) study of migration following Hurricanes Katrina and Rita illustrates issues of disadvantage and social class. Out-migration following the hurricanes was particularly concentrated amongst the disadvantaged and those living in densely populated areas. Motivations for migration are complex but economic loss is strongly related to opportunities that exist elsewhere. Housing loss and damage are prompts to migration, but the socio-economically disadvantaged are less likely to have well maintained or protected properties. The loss for the poor is then exacerbated by the loss of jobs.

Hurricane Katrina led to the loss of 1,833 people's lives, but there were many other social impacts. Immediately following the hurricane, 5,088 children were separated from their families, and many adults remained unaccounted for months after the disaster, leading to a considerable separation anxiety and other psychological distress associated with being orphaned. During the subsequent evacuation after the hurricane, a further 300,000 schoolchildren were moved away from their homes and communities. Out-migration includes the impact upon children and young people (Peek and Fothergill 2006; Casserly 2006). Schools were destroyed and the public education system in New Orleans has not recovered. Peek and Fothergill's study records the importance of school in terms of recovery, but they also point out problems for the socio-economically disadvantaged and people of minorities in dealing with relocation.

After Cyclone Larry struck North Queensland in 2006, there were similar issues among schoolchildren in recovering from the psychological trauma of the event. Children stated the importance of the reopening of their schools in helping them to deal with the event as it brought them back to a state of relative normality (King et al. 2006). Cyclone Larry was as severe as Katrina but communities were spared the flooding. There was no loss of life, although 19,000 building insurance claims and 27,000 domestic contents claims were made in an impact area that contained less than 50,000 people. There was immediate short-term out-migration (King et al. 2006) and longer term migration during the recovery period following disruption to the local economy such as the short-term destruction of the banana industry (Glick 2006).

9.8 Tropical cyclone hazard mitigation

Mitigation of tropical cyclone risk requires preparatory action from a wide range of institutions and organizations — government at all levels, non-government organizations, private enterprise and community groups. The physical prevention of risk will continue to involve the building of protective barriers, such as sea walls and levees, even if these are short-term and contribute to community complacency. More significantly physical protective measures contribute to the strength of buildings to withstand high winds and localized flooding. Building codes exist, but weak enforcement and non compliance are governance issues that continue to put communities at risk. During the last decade land use planning has been targeted to ensure greater responsibility and vigilance over the suitable siting of new urban developments. Planners are directly involved in hazard mitigation efforts but they also face governance, information and legislative constraints that reduce the effectiveness of appropriate hazard zone planning.

For weather agencies and emergency managers the core business of tropical cyclone mitigation is communication, warnings, awareness, preparedness, and education. Communication extends beyond pre-season education campaigns. It takes place at different stages — mitigation, response and recovery. At all of these levels the media is crucial in transmitting information and warnings and informing the community. Engagement with the media, including the important role of media liaison officers, is a specific hazard mitigation role.

Pielke and Sarewitz (2005) argue that the impacts of climate change are social (although environmentalists might take issue), but that while society has a past history of adaptation, it has no experience in successfully modifying climate. This reinforces the argument that mitigation (including carbon trading and emissions reduction) is much less likely to be successful than adaptation to a changing global climate. Initially, adaptation brings high costs, but in the long-term it might transform into a new sustainability. Seasonal mitigation strategies have been put in place to reduce the hazard risk and to lessen the impact of a tropical cyclone. In practice mitigation has been conservative, oriented towards maintenance of the status quo (Handmer et al. 1999). Climate change has added a new vocabulary to hazard mitigation — specifically the concept of adaptation.

Adaptation is neither static nor protective as it requires change to an uncertain future state. It is the uncertainty of future climate change scenarios that makes adaptation a particularly difficult concept to sell to communities. There is a need for much greater clarity and precision of potential climate change scenarios and changing risk. Tropical cyclone awareness and preparedness strategies are in danger of being devalued by imprecise warnings of more intense and possibly more frequent cyclones, which may not transpire in reality. If we are not certain about these trends we should not confuse the mitigation message but should concentrate on sound preparation and enhance governance to support communities.

9.9 Economic impacts of tropical cyclones

Global natural disaster losses have risen dramatically in recent decades and tropical cyclones have contributed significantly to this trend. Tropical cyclones account for nine of the ten most costly inflation-adjusted insurance natural disaster losses (2009 dollars) between 1970 and 2009 (Swiss Re, 2010). Of these nine, eight impacted the US and surrounding areas and one impacted Japan. In original loss values, tropical cyclones account for two of the five most costly economic losses and four of the five most costly insurance losses from natural disasters over the period 1950 to 2009 (Munich Re, 2010). All hurricanes in the top five of both original loss lists impacted the US and Hurricane Katrina tops the original and inflation adjusted loss lists.

The increase in tropical cyclone losses has led to concern that anthropogenic climate change is contributing to this trend. In response to this, numerous studies of databases1 from around the world have been undertaken to examine the factors responsible for this increase. Research has also focused on what role various factors may have in shaping tropical cyclones losses in the future. This report summarizes those efforts.

The significant increase in losses has also made the question of how to better manage tropical cyclones, and natural hazards more generally, even more salient. An important component of catastrophe risk management is the development of adequate and sustainable financial protection for potential victims of future disasters and our report discusses this financial management aspect.

9.9.1 Loss normalization

Before comparisons between the impacts of past and recent tropical cyclones can be made, various societal factors known to influence the magnitude of losses over time must be accounted for. This adjustment process has become commonly known as *loss normalization* (Pielke and Landsea, 1998).

Normalizing losses to a common base year is undertaken primarily for two reasons:

1. to estimate the losses sustained if events were to recur under current societal conditions; and,
2. to examine long term trends in disaster loss records.

In particular, to explore what portion of any trend remaining after taking societal factors into account may be attributed to other factors including climate change (natural variability or anthropogenic).

Climate-related influences stem from changes in the frequency and/or intensity of tropical cyclones whereas socio-economic factors comprise changes in the vulnerability and in the exposure — value of assets at risk — to the natural hazard. Socio-economic adjustments have largely been limited to accounting for changes in exposure, although Crompton and McAneney (2008) adjusted Australian tropical cyclone losses for the influence of improved building standards introduced since the early 1980s.

Bouwer (2011) provides a recent comprehensive summary of loss normalization studies. Table 9.6 has been adapted from that study to include only those relating to tropical cyclones.

Table 9.6. Normalization studies of tropical cyclone disaster loss records (Modified from Bouwer 2010).

location	Period	normalization	Normalized loss	reference
Latin America	**1944-1999**	**Wealth, population**	**No trend**	**Pielke et al. (2003)**
India	**1977-1998**	**Income, population**	**No trend**	**Raghaven and Rajash (2003)**

United States	**1900-2005**	**Wealth, population**	**No trend**	**Pielke et al. (2008)**
United States	**1950-2005**	**Asset values**	**Increase since 1970; no trend since 1950**	**Schmidt et al. (2009)**
China	**1983-2006**	**^GDP**	**No trend**	**Zhang et al. (2009)**
China	**1984-2008**	**^GDP**	**No trend**	**Zhang et al. (2010)**
United States	**1900-2008**	**^GDP**	**Increase since 1900**	**Nordhaus (2010)**
***Australia**	**1967-2006**	**Dwellings, dwelling value**	**No trend**	**Crompton and McAneney (2008)**
***United States**	**1951-1997**	**Wealth, population**	**No trend**	**Choi and Fisher (2003)**
***World**	**1950-2005**	**^GDP per capita, population**	**Increasing since 1970; no trend since 1950**	**Miller et al. (2008)**

***Includes other weather hazards besides tropical cyclones.**

^ Gross domestic product (GDP) is a measure of a country's overall official economic output. It is the market value of all final goods and services produced in a country in a given year.

In what follows we focus on the more recent tropical cyclone loss normalization studies.

a) China

Zhang et al. (2009) examined the direct economic losses and casualties caused by landfalling tropical cyclones in China during 1983-2006 using the data released by the Department of Civil Affairs of China. The economic loss data was estimated by the governments usually at town and county levels and collected by provincial governments and reported to the Department of Civil Affairs. Zhang et al. (2009) show that in an average year, seven tropical cyclones made landfall over the Chinese mainland and Hainan Island, leading to 28.7 billion yuans (2006 RMB) in direct economic losses and killing 472 people. A significant upward trend in the direct economic losses was found over the 24-year period. This trend disappeared after the rapid increase in the annual total Gross Domestic Product (GDP) of China was taken into consideration, a result that

suggested that the upward trend in direct economic losses was a result of Chinese economic development.

More recently, Zhang et al. (2010) updated the earlier analysis to 2008 and also included a consumer price index (CPI) inflation-adjusted time series of direct economic losses. Over the period 1984-2008, tropical cyclones led to 505 deaths and 37 billion yuan in direct economic loss per year accounting for about 0.4% of annual GDP. The annual total direct economic losses increased significantly due to the rapid economic development over the 25-year period, while the percentage of direct economic losses to GDP (the 'normalization') and deaths caused by landfalling tropical cyclones decreased over this period. Both studies concur that economic development is the primary factor responsible for the increasing tropical cyclone damage in China.

Over the past 25 years, tropical cyclones made landfall on the Chinese mainland and Hainan Island with an average landfall intensity of 29.9 m/s and they retained their tropical cyclone intensity for 15.6 hours over land (Zhang et al., 2010). No significant trends in landfalling frequency and intensity have been found. Rainfall associated with landfalling tropical cyclones is a major contributor to damage in China. Chen et al. (2011) shows a significant increase in the time landfalling tropical cyclones spend over land with tropical storm intensity. By separating the tropical cyclone rainfall from other weather systems, Chen et al. (2011) found that the overall rainfall associated with landfalling tropical cyclones was dominated by significant downward trends over the past 25 years. In the extreme rainfall days, Chen et al. (2011) also did not find an overall increasing trend. These results suggest that the significant upward trend in typhoon damage cannot be explained by changes in tropical cyclone activity.

b) US

Schmidt et al. (2009a) discuss two essential differences between their normalization methodology and the Pielke et al. (2008) "PL05" methodology. The first is their use of capital stock at risk (determined from the number of housing units and mean home value) rather than the wealth at risk (determined from population and per capita wealth) employed in Pielke et al. (2008). Secondly, Schmidt et al. (2009a) apply regional figures for mean home value whereas Pielke et al. (2008) use the national average for per capita wealth. Fig. 9.11 shows the different rate of change in these metrics over time (Schmidt et al., 2009a). The wealth at risk factors are higher than the capital stock at risk factors and this difference generally increases back in time.

Green bars show the factors applied based on wealth at risk (population in 177 coastal counties and real wealth per capita). Losses adjusted by wealth at risk will be higher than adjusted by capital stock at risk (source: Schmidt et al. (2009a)).

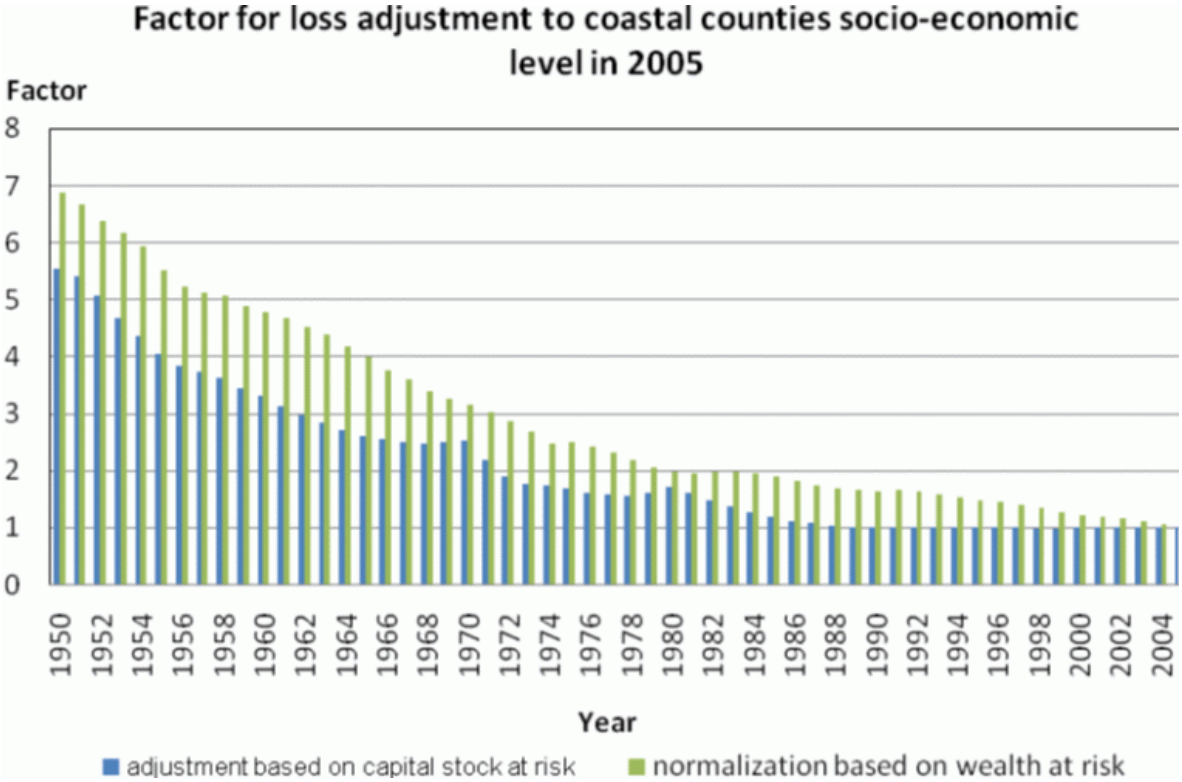

Figure 9.11. Blue bars show the factors applied for adjustment of losses to 2005 socio-economic level based on capital stock at risk (e.g. losses in year 1962 will be multiplied by factor of 3).

Here we update the Pielke et al. (2008) analysis to include US hurricane losses from the 2006 to 2009 seasons with all losses now normalized to 2009 values. Fig. 9.12 shows the normalized US hurricane losses for 1900 to 2009. While it is apparent that there is no obvious trend over the entire time series, our emphasis is on the period 1971-2005 for which Schmidt et al. (2009a) report a statistically significant trend. (This trend in the log-transformed annual normalized losses was significant at the 10% level). Schmidt et al. (2009a) also show what effect a single event can have on the result as the trend was no longer significant when the Hurricane Katrina loss was excluded. In what follows, we investigate the effect that accounting for recent seasons has had on resulting trends beginning in 1971.

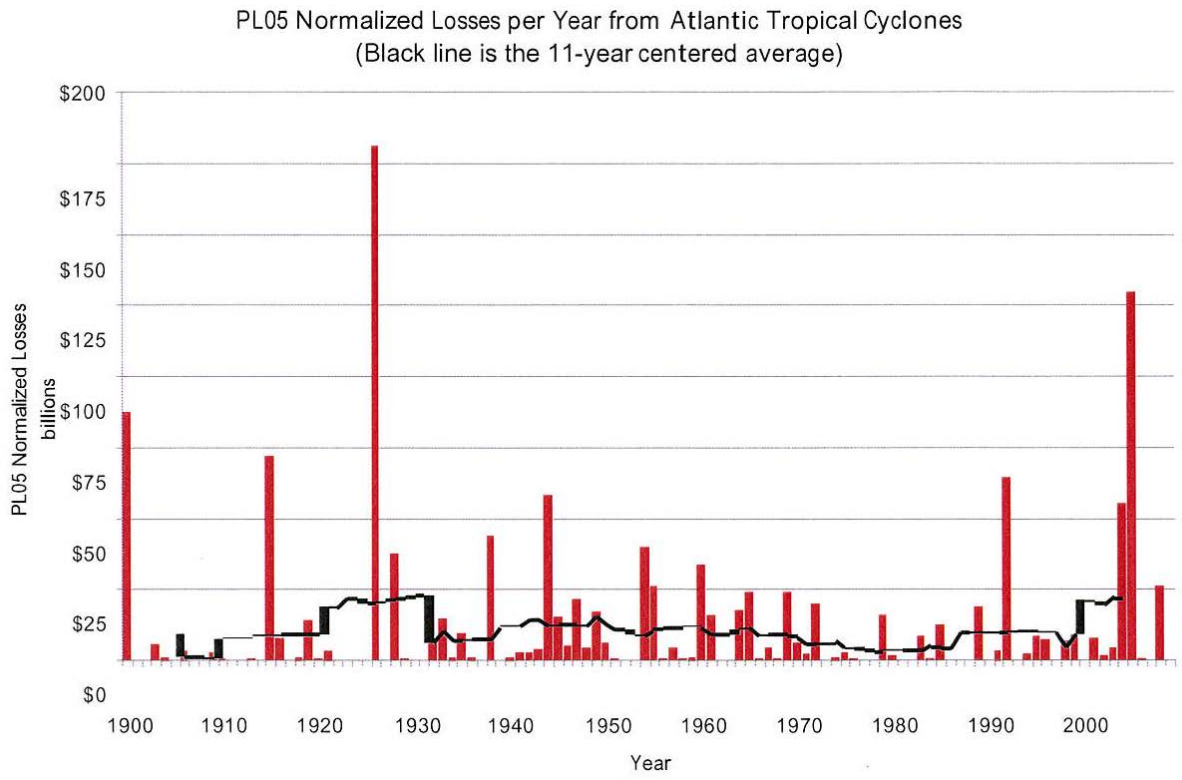

Figure 9.12. U.S. Gulf and Atlantic damage, 1900-2005, for total U.S. tropical cyclone losses normalized with a methodology that focuses on population change. An alternate methodology that focuses on housing units was within 2% of the population change methodology. Although the 2004 and 2005 seasons produced high losses, these years are not unprecedented when considering normalized losses since 1900. (From Pielke et al, (2008))

Similar to Schmidt et al. (2009a) we find a statistically significant (at the 10% level) trend (*Pvalue* = 0.091) in log-transformed annual normalized losses (2009 values) during 1971-2005. However the trend is not statistically significant (at the 10% level) when the time series is extended to any year after 2005 (e.g. 1971-2006, etc.). This highlights the difficulty that the large volatility in the time series of tropical cyclone losses poses when estimating trends over short periods of time.

c) Australia

Crompton and McAneney (2008) normalized Australian weather-related insured losses over the period 1967-2006 to 2006 values. Insured loss data were obtained from the Insurance Council of Australia (http://www.insurancecouncil.com.au/). The methodology adjusted for changes in dwelling numbers and nominal dwelling values (excluding land value). A more marked point of departure from previous normalization studies was an additional adjustment for tropical cyclone losses to account for improvements in construction standards mandated for new construction in tropical cyclone-prone parts of the country.

Crompton and McAneney (2008) found no statistically significant trend in weather-related insured losses once they were normalized in the manner described above. They emphasize the success improved building standards have had in reducing building vulnerability and thus tropical cyclone wind-induced losses. Due to limited data, they did not analyze the losses from any one particular hazard. In total, only 156 event losses were included in their analysis and this relatively small number results from the combined effect of a short data series and sparse population, especially in tropical cyclone-prone locations of the country.

d) World

Miller et al. (2008) compiled a global normalized weather-related catastrophe catalogue covering the principal developed and developing countries and/or regions (Australia, Canada, Europe, Japan, South Korea, United States, Caribbean, Central America, China, India, the Philippines). Various data sources were accessed and losses surveyed from 1950 to 2005, however post-1970 data were more reliable across all countries. Economic losses were normalized to 2005 values by adjusting for changes in wealth (GDP per capita in USD), inflation (national level), and population (national level).

Miller et al. (2008) discuss a number of issues in relation to their methodology including what effect applying a national level population factor has on normalized losses. They state that for those events that impacted certain high growth, coastal regions such as Florida, their national population factor will understate the true population growth rate. A regression of global normalized hurricane losses over the period 1970-2005 found a statistically significant (at the 5% level) trend.

More generally, Miller et al. (2008) found a 2% per year increasing trend in global normalized weather-related losses after 1970. However, their conclusions were heavily weighted by US losses and their removal eliminated any statistically significant trend. Their results were also strongly influenced by large individual events such as Hurricane Katrina. The significance of the post-1970 global trend disappeared once national losses were further normalized relative to per capita wealth (i.e. by multiplying each region's normalized losses by the ratio of US GDP per capita to regional GDP per capita to approximate a homogenous distribution of wealth). They confirm that the principal driver of increasing global disaster losses to date was tropical cyclones in wealthy regions and that there was insufficient evidence to claim any firm link between global warming and disaster losses.

9.10 Future and current loss sensitivity

A number of studies have projected US tropical cyclone losses. This has been done to either quantify the effect of anthropogenic climate change (due to a projected change in tropical cyclone frequency and/or intensity) on its own, or to compare the effect of projected changes in both exposure and climate. Future losses will also be sensitive to changes in vulnerability, but this factor is usually held constant. Table 9.7 (from Schmidt et al. (2009b)) summarizes US

tropical cyclone loss projection studies and Table 9.8 provides a more detailed account of some of the more recent studies as well as that of Schmidt et al. (2009b). The logic usually employed in these studies to examine the effects over a given time horizon is presented below.

Table 9.7: Overview of studies to estimate future storm losses in the USA resulting from global warming (source: Schmidt et al. (2009b)).

Study	Loss function	Assumed change in intensity	Assumed change in frequency	Result
Cline (1992)	Increase in intensity produces a linear increase in losses	Increase of 40–50% with 2.3–4.8°C warming	_	Average loss increases by 50%
Fankhauser (1995)	Increase in intensity triggers a 1.5 increase in losses	Increase of 28% with warming of 2.5°C	_	Average loss (global) increases by 42%
Tol (1995)	Connection is in the quadratic form $f(x)=\alpha x+bx^2$	Increase of 40–50% with warming of 2.5°C	constant	Increase in losses of 300 million US$ (1988 values)
Nordhaus (2006)a	$d= \alpha$ X windspeed^3	Increase of maximum wind speeds of 8.7% with warming of 2.5°C	constant	Average loss increases of 104%
Stern et al. (2006)	$d= \alpha$ X windspeed^3	Increase of 6% with warming of 3°C	_	Average loss increases by 100%
Hallegatte (2007)b	Physical storm model to create synthetic storms; loss function in the form $d= \alpha x(s)$ X windspeed^3	Increase of 10% under the expected climate conditions at the end of the 21st century	no change in absolute number	Increase in landfalls and maximum wind speed (+13%); Average loss increases by 54%
Pielke (2007)	$d= \alpha$ X windspeed^3 (further scenarios with elasticity of 6 and 9)	Increase of 18% by 2050	constant	Increase in loss of 64%c

Notes:

a Losses adjusted for economic development using GDP.
b Losses adjusted for population and wealth trends, s for vulnerability index.
c Additional loss increase of 116% from the combined effect of increase in intensity and socio-economic trend.

Anthropogenic climate change effect:
Emission scenario → tropical cyclone projection (frequency and intensity) → relationship between tropical cyclone normalized damages and intensity (wind speed) (referred to as "loss function") → projected anthropogenic climate change influence on tropical cyclone losses

Exposure effect: (e.g. projected changes in population and wealth)
Total effect:

Anthropogenic climate change effect + Exposure effect + Anthropogenic climate change effect X Exposure effect + 1

Despite the various assumptions made in each of the studies in Table 9.8, the estimated changes in future tropical cyclone losses in the US resulting from anthropogenic climate change fall into two broadly similar pairs of studies. The Pielke (2007) lower estimate extrapolated to 2100 is approximately +128%, a figure comparable to the Nordhaus (2010) central estimate of +113%. On the other hand, linearly extrapolating the Schmidt et al. (2009b) estimate to 2090 results in an approximate +20% change in loss, whereas the Bender et al. (2010) ensemble-mean estimate is +28%.

Both Pielke (2007) and Schmidt et al. (2009b) show that exposure growth will have a greater effect than anthropogenic climate change on future US tropical cyclone losses. Pielke (2007) adopted a conservative approach in deliberately selecting upper end estimates for the anthropogenic climate change effect on tropical cyclone intensity. Schmidt et al. (2009b) note that the anthropogenic climate change-induced increase in loss results in an additional loss of wealth in the sense that it increases loss over and above the proportional increase in exposure (capital stock).

Loss functions have also been used by Nordhaus (2010) and Schmidt et al. (2010) to estimate the climate-induced (i.e., resulting from natural variability and any unquantifiable anthropogenic contribution) increase in mean US tropical cyclone damage since 1950. Nordhaus (2010) estimates an 18.4% increase in mean damages since 1950 based on an elasticity of 9 and a 1.9% increase in intensity. The intensity estimate was calculated using the Knutson and Tuleya (2004) intensity / SST relationship assuming a 0.54°C increase in SST.

Schmidt et al. (2010) examined the sensitivity of storm losses to changes in socioeconomic and climate-related factors over the period 1950-2005. They show losses to be much more

responsive to changes in storm intensity (as estimated by changes in the basin-wide Accumulated Cyclone Energy (ACE) between successive "warm phases") than to changes in capital stock. Nonetheless capital stock had a greater effect on losses due to its far greater increase over the study period. They determine that the increase in losses was approximately three times higher for socio-economic changes (+190%) than for climate-related changes (+75% based on the 27% increase in ACE between the "warm phases" 1926-70 and 1995-2005 — the authors note that the latter "warm phase" had not ended) and state that the extent to which the climate-related changes were the result of natural climate variability, or anthropogenic climate change, remains unanswered.

9.11 Financial management of extreme events

Previous sections have showed that the significant growth in exposure in hazard-prone areas have been the primary reasons for the increase in natural disaster losses (both insured and uninsured) in the US and other parts of the world. This result is consistent with the conclusion from Kunreuther and Michel-Kerjan (2009) that the increase in losses is due to growth in population and assets coupled with a lack of investment in risk reduction measures. Recent catastrophes have highlighted many challenges, including how to best organize systems to pay for the damage caused by natural disasters and how to mitigate their effects.

9.11.1 Catastrophe insurance: how it is changing in the US

In most Organization for Economic Co-operation and Development (OECD) countries, insurance penetration is quite high, so a large portion of the economic damage from natural disasters is covered by public or private insurance. For truly catastrophic risks, many countries have developed some type of private sector — government partnerships for certain risks or certain exposed regions (as is the case for example in the UK, France, Spain or Japan). In the US, cover for damage due to floods and storm surge from hurricanes has been available through the federally managed National Flood Insurance Program (NFIP) since 1968 (Michel-Kerjan, 2010). State government programs supplement private sector cover in many US states; in Florida, the state has set up a reinsurer (the Florida Hurricane Catastrophe Fund) and a direct insurer (Citizens) which absorb a considerable proportion of the state's hurricane risk.

Cover against wind damage in the US has typically been offered in standard homeowners' insurance policies provided by private insurers. A number of extremely damaging hurricanes since the late 1980's (including Hugo, Andrew, and others during the intense hurricane seasons of 2004 and 2005) caused substantial instability in property insurance markets in coastal states. High loss activity prompted most insurers doing business in coastal states to seek major price increases; however, state insurance regulators failed to authorize the full amounts requested. Even with the restricted premium increases, rates doubled or even tripled in the highest risk areas in Florida between 2001 and 2007 (Kunreuther and Michel-Kerjan, 2009). Due to their inability to charge adequate premiums many insurers reduced their exposure in coastal regions

and in December 2009 State Farm, for example, announced that it would discontinue 125,000 of its 810,000 property insurance policies in Florida (State Farm, 2009).

The combined effect of dramatically increased premiums for private residential wind insurance in coastal states and the decline in access to coverage for those in areas most exposed to wind damage has resulted in increased demand for government programs that provide insurance for residents in high-risk areas at highly subsidized rates. While subsidized rates have short term political benefit they do not encourage investment in risk reduction measures. Moreover, inadequate rates lead to large deficits in government pools over time and excessive growth in high risk areas and thus an even greater potential for large losses. Historically inadequate rates fuelled the dramatic exposure accumulation in the southeastern US where large losses have subsequently occurred.

9.11.2 The disaster mitigation challenge

Insurance (public and private) plays a critical role in providing funds for economic recovery after a catastrophe. But insurance merely transfers risks to others with a broader diversification capacity; simply purchasing insurance does not reduce the risk. The insurance system can play a critical role in providing incentives for loss mitigation by sending price signals reflecting risk. Regulatory efforts to limit premium increases in high risk areas can diminish the insurance system's ability to perform this function.

Disaster mitigation measures can offset some of the upward pressure demographic and economic drivers (as discussed in previous sections) exert on tropical cyclone losses. Kunreuther and Michel-Kerjan (2009) shed some light on this aspect by analysing the impact that disaster mitigation would have had on reducing losses from hurricanes in four states in 2005: Florida, New York, South Carolina, and Texas. In their analysis of the impact of disaster mitigation, they considered two extreme cases: one in which no one invested in mitigation and the other in which everyone invested in predefined mitigation measures. A US hurricane loss model developed by Risk Management Solutions (RMS) was used to calculate losses assuming appropriate mitigation measures on all insured properties. The analyses revealed that mitigation has the potential to significantly reduce losses from future hurricanes with reductions ranging from 61% in Florida for a 100-year return period loss to 31% in Texas for a 500-year return period loss. In Florida alone, mitigation is estimated to reduce losses by $51 billion for a 100-year event and $83 billion for a 500-year event.

In a study for the Australian Building Codes Board, McAneney et al. (2007) estimated that the introduction of building code regulations requiring houses to be structurally designed to resist wind loads had reduced the average annual property losses from tropical cyclones in Australia by some two-thirds. Their estimate was based on the likely losses had the building code regulations never been implemented or had they always been in place.

Without regulations, the challenge lies in encouraging residents in hazard-prone areas to invest in mitigation measures and this has been highlighted by many recent extreme events. Even

after the devastating 2004 and 2005 US hurricane seasons, a large number of residents in high-risk areas still had not invested in relatively inexpensive loss-reduction measures, nor had they undertaken emergency preparedness measures. A survey of 1,100 residents living along the Atlantic and Gulf Coasts undertaken in May 2006 revealed that 83% had taken no steps to fortify their home, 68% had no hurricane survival kit and 60% had no family disaster plan (Goodnough, 2006). Homeowners, private businesses, and public-sector organizations often fail to voluntarily adopt cost-effective loss-reduction measures, particularly if regulatory actions inhibit the insurance system from providing sufficient economic incentives to do so. In addition, the magnitude of the destruction following a catastrophe often leads governmental agencies to provide disaster relief to victims — even if prior to the event the government claimed that it would not do so. This phenomenon has been termed the "natural disaster syndrome" (Kunreuther, 1996). This combination of underinvestment in protection prior to a catastrophic event and taxpayer financing of part of the recovery following can be critiqued on both efficiency and equity grounds.

9.11.3 Global risk financing in coming decades

In coming decades, global trends in population distribution, economic development, wealth accumulation and increasing insurance penetration will place significant strain on the ability to absorb economic losses and undertake post-event reconstruction. The problems that Florida is currently experiencing may develop elsewhere. For example, patterns of urbanization in areas of China vulnerable to typhoons resemble those of Florida in years past.

Musulin et al. (2009) analysed the financial implications of future global insurance losses. Future losses were estimated by using projected values of the variables used to normalize losses and an additional adjustment was made for changes in insurance penetration. Their analysis revealed that new peak zones (those locations that have the largest disaster potential globally) are likely to emerge in several developing nations due to the projected changes in demographics, wealth and insurance penetration. They note that the rapid projected exposure accumulation was similar to that experienced in Florida between 1950 and 1990. Musulin et al. (2009) conclude that the future loss levels will have significant ramifications for the cost of financing disasters through the insurance system, both in the new peak zone locations and in the system as a whole. Their results were independent of any anthropogenic climate change effects on future losses.

Musulin et al. (2009) identify an additional factor that must be considered to correctly assess the proper level of investment in loss mitigation. They refer to three lenses through which loss mitigation activities can be viewed: life safety, protection of individual properties, and management of overall economic impact. While building code development traditionally focuses on the first two, the authors argue that consideration also needs to be given to the current and future potential for large disaster losses in the area where the building code applies.

The management of overall economic impact means that current building code design should also reflect the current and future potential impact of large disaster losses on the overall economy (Musulin et al., 2009). The destruction of a single building can be easily absorbed into the normal building capacity of an economy but the destruction of one million homes by a major hurricane cannot — the required diversion of material and labour to post-event reconstruction from other activities would cause massive stress and disruption. The potential economic damage from tropical cyclones can become very significant at a macroeconomic level as exposure grows disproportionately in high risk areas, particularly when there is a dramatic increase in insurance penetration (Musulin et al., 2009).

Musulin et al. (2009) conclude that the economic value of loss mitigation must reflect the expected cost of risk transfer over the lifetime of the building. Since the cost of risk transfer is affected by the aggregate level of risk in an area, it can change if the surrounding area is subject to significant population growth and wealth accumulation. Loss mitigation should therefore also target areas of high potential future growth (Musulin et al., 2009).

9.11.4 Integrating the financial management of disasters as part of a national strategy

In the aftermath of the very destructive 2004/05 US hurricane seasons, increasing the country's resiliency to natural disasters was destined to become a national priority in the US. As other crises occurred locally and abroad, attention was directed away from this issue. The question of how to best organize financial protection and risk reduction against future hurricanes remains largely unanswered.

Other countries that have suffered disasters are faced with similar questions. Outside of the OECD countries, developing countries have started to think about these issues. In many cases, populations are growing fast and assets at risk have increased significantly as a result of decades of economic development. People and businesses are turning to their governments and the private sector for solutions. These solutions will come in the form of micro-insurance (well-developed in India and several African countries today), strong government participation (as is the case in China), traditional insurance, or the transfer of catastrophe exposure directly to investors on the financial markets (e.g. catastrophe bonds of which over 160 have been issued to date) (Michel-Kerjan and Morlaye, 2008).

Each country will have to define and select what solutions make the most sense given its culture, current development of its insurance market, risk appetite and other national priorities. These solutions will also evolve over time as a response to the occurrence of (or absence of) major catastrophes. Higher climate variability and increasing exposure means that the financing of disaster risks and long-term disaster mitigation planning must become a critical element of the national strategy in many countries to assure sustainable development.

9.12 Acknowledgements

The author is indebted to the late Mr. Robert Southern, the author of this corresponding chapter in the previous edition of the Global Guide, whose excellent contribution enabled me to begin the update from a firm foundation. The author is also thankful to the many contributors who provided materials from IWTC-VI and IWTC-VII.

9.13 References

9.13.1 References

ADB, 1991: Disaster Mitigation in Asia and the Pacific. *Asian Development Bank*, Mandaluyang City, Metro Manila, Philippines, pp.391.

Also see updated text at ADB, 2008: Disaster Management: *A Disaster Manager's Handbook, Asian Development Bank*, Mandaluyang City, Metro Manila, Philippines, pp. 391.

Adger, W. N., 2003: Social capital, collective action and adaptation to climate change. *Economic Geography,* **79,** 387-404.

Bangladesh Centre for Advanced Studies (BCAS), 1992: http://pubs.iied.org/pdfs/G00016.pdf

Bender, M.A.,T.R. Knutson, R. E. Tuleya, and J. J. Sirutis, 2010: Modeled Impact of Anthropogenic Warming on the Frequency of Intense Atlantic Hurricanes. *Science,* **327,** 454.

Best,B. and V.B.Marquez,2008: http://www.uog.edu/professional-international-programs/tadeo-peacesat

Bouwer, L. M., 2011: Have Disaster Losses Increased Due to Anthropogenic Climate Change? *Bull. Amer. Meteor. Soc.*, **92,** 39-46. doi: http://dx.doi.org/10.1175/2010BAMS3092.1

Bruce, J. P., 1999: Disaster loss mitigation as an adaptation to climate variability and change.*Mitigation and Adaptation Strategies for Global Change,* **4,** 295-306.

Carter, M. T., 1983: The Probability of Hurricane/Tropical Storm Conditions: *A User's Guide for Local Decision Makers.* National Weather Service, Silver Spring, MD.

Carter, W. N., 1992: Disaster Management: *A Disaster Manager's Handbook, Asian Development Bank,* Mandaluyang City, Metro Manila, Philippines, pp.391.

Casserly, M., 2006: Double jeopardy: Public education in New Orleans before and after the storm. In There is no such thing as a natural disaster: *Race, class and Hurricane Katrina. ed.C. Hartman and G. D. Squires. 197-214. New York: Routledge. Centre for Research on the Epidemiology of Disasters (CRED)*, 2009:

Chen, S. S., J. F. Price, W. Zhou, A. Donelan, and E. J. Walsh, 2007: The C-BLAST-Hurricane Program and the next-generation fully coupled atmosphere-wave-ocean models for hurricane research and prediction. *Bull. Am. Meteor. Soc.*, **88,** 311-317.

Chen, X., L. Wu, and J. Zhang, 2011: Increasing duration of tropical cyclones over China. *Geophysical Research Letters,* **38.**

Chittibabu, P., S. K. Dube, J. B. Macnabb, T. S. Murty, A. D. Rao, U. C. Mohanty, and P. C. Sinha, 2004: Mitigation of Flooding and Cyclone Hazard in Orissa, India. *Natural Hazards,* **31.**

Choi Onelack, and Fisher, A. 2003. The Impacts of Socioeconomic Development and Climate Change on Severe Weather Catastrophe Losses: Mid-Atlantic Region (MAR) and the US Climatic Change 58 (2003): 149-170.

Clarke, G, C. Shultz, and B. Best, 2010: *Chatty Beetle Terminal Operations Manual*. http://iepas.net/wp-content/uploads/2014/01/cbtom.pdf

CRED 2009, EM-DAT, Emergency Events Database. Centre for Resaearch on the Epidemiology of Disasters (CRED), Université catholique de Louvain, Brusse, Belgium. www.emdat.be/

Congleton, R. D., 2006: The Story of Katrina: New Orleans and the Political Economy of Catastrophe.*Public Choice,* **127,** 5-30.

Crompton, R.P., K. J.McAneney, 2008: Normalised Australian insured losses from meteorological hazards: 1967-2006. *Environ. Sci. Policy,* 371-378.

DeMaria, M., J. A. Knaff, R. Knabb, C. Lauer, C. R. Sampson, and R. T. DeMaria, 2009: A New Method for Estimating Tropical Cyclone Wind Speed Probabilities. *Wea. Forecasting,* **24,** 1573-1591.

Emergency Management Australia, 1998: *Australian Emergency Manuals Series Part I: The Fundamentals. Manual 3,* Commonwealth Government of Australia.

Far Eastern Economic Review (FEER), 1993: Reduced death rates from cyclones in Bangladesh: what more needs to be done? *Bull. World Health Organ.,* **90 (2)**, 150-156.http://www.ncbi.nlm.nih.gov/pmc/articles/PMC3302549/

Glick, J., 2006: Banana Farms in the Innisfail Region Eight Months after Cyclone Larry: Dynamics of Farm Level Recovery December 2006. *Townsville: Centre for Disaster Studies Post Disaster Report,*James Cook University.

Goodnough, A., 2006: "As Hurricane Season Looms, State Aim to Scare," *The NewYork Times,* May 31.

Gopalakrishnan, C., and N. Okada, 2007: Designing new institutions for implementing integrated disaster risk management: key elements and future directions. *Disasters,* **31** (4), 353-372.

Guard, C. P., and M. A. Lander, 1999: A Scale Relating Tropical Cyclone Wind Speed to Potential Damage for the Pacific Ocean Region: A User's Manual. *WERI Technical Report* **86**. University of Guam, Mangilao, Guam, pp 60.

Handmer, J. W., S. Dovers, and T. E. Downing, 1999. Societal vulnerability to climate change and variability. *Mitigation and Adaptation Strategies for Global Change,* **4,** 267-281.

Hunter, L. M., 2005: Migration and Environmental Hazards. *Population and Environment,* **26,** 273-302. DOI 10.1007/s11111-005-3343-x
Jayanthi, N. and A. K. Sen Sharma, 1988: *Mausam,* **38,** 193-196.

Khoury, E., G. Warheit, M. Hargrove, R. Zimmerman, W. Vega, and A. Gil, 2006: The impact of Hurricane Andrew on deviant behaviour among a multi-racial/ethnic sample of adolescents in Dade County, Florida: A longitudinal analysis, *Journal of Traumatic Stress,* **10 (1)**, 71-91

King, D., D. Goudie, and D. Dominey-Howes, 2006: Cyclone knowledge and household preparation: Some insights from Cyclone Larry, *Australian Journal of Emergency Management,* **21 (3)**, 52-59.

King, B., 2009: fieldwork

Thomas R. Knutson and Robert E. Tuleya, 2004: Impact of CO2-Induced Warming on Simulated Hurricane Intensity and Precipitation: Sensitivity to the Choice of Climate Model and Convective Parameterization. *J. Climate,* **17**, 3477-3495. doi: http://dx.doi.org/10.1175/1520-0442(2004)017<3477:IOCWOS>2.0.CO;2

Koontz, H. (1984). "Commentary on the management theory jungle - nearly two decades later," in H. Kooontz, C. O'Donnell, and H. Weihrick (eds) *Management: A Book of Readings,* 6th Ed. New York: McGraw-Hill.

Kunreuther, H and E. Michel-Kerjan, 2009: The Development of New Catastrophe Risk Markets.*Annual Review of Resource Economics,* 10.1146/annurev.resource.050708.144302, 119-137. http://ascelibrary.org/doi/abs/10.1061/(ASCE)1527-6988(2008)9:1(29)

Kunreuther, H., 1996: Mitigating disaster losses through insurance. *Journal of Risk and Uncertainty,***12,** 171-187.

9.13.2 References

McAneney, J., K. Chen, and A. Pitman, 2007: 100-years of Australian bushfire property losses: Is the risk significant and is it increasing? *J. Environ. Management,* **90**, 2819-2822.

Merrill, R. T., 1984: A comparison of Large and Small Tropical cyclones. *Mon. Wea. Rev.,* **112**, 1408-1418.

Michel-Kerjan, E. 2010. "Reform of the National Flood Insurance Program: Introducing Long-Term Flood Insurance." *The Huffington Post,* April 28

Michel-Kerjan, E. and F. Morlaye, 2008: Extreme events, global warming, and insurance-linked securities: How to trigger the "tipping point". *The Geneva Papers on Risk and Insurance-Issues and Practice, Palgrave Macmillan,* 33 (1), 153-176.

Miller, S., R. Muir-Wood, and A. Boissonade, 2008: *An exploration of trends in normalized weather-related catastrophe losses.* Edited by H. F. Diaz and R. J. Murnane, pp. 225-247, In Climate Extremes and Society. Cambridge University Press, New York, pp. 356.

Munich Re, 2010: Natural catastrophes 2009. Analyses, assessments, positions. *TOPICS GEO.* http://www.munichre.com/publications/302-06295_en.pdf

Musulin, R., R. Lin, and S. Frank, 2009: Dealing with the axis of financial destruction: demographics, development, and disasters. *Proceedings of a Conference sponsored by Aon Benfield Australia Limited,* 43-58.
http://www.aon.com/attachments/reinsurance/201008_axis_of_financial_destruction.pdf

Myers, C. A., T. Slack, and J. Singelmann, 2008: Social vulnerability and migration in the wake of disaster: the case of Hurricanes Katrina and Rita. *Popul. Environ,* **29**, 271-291. DOI 10.1007/s11111-088-0072-y.

National Hurricane Center (NHC), 2014:
http://www.nhc.noaa.gov/pdf/NHC_Product_Description.pdf

National Research Council, 2010: When Weather Matters: Science and Service to Meet Critical Societal Needs. *The National Academies Press.*

Nordhaus, W. D., 2010: The Economics Of Hurricanes And Implications Of Global Warming. *Clim. Change Econ.,* **01,1** (2010). DOI: 10.1142/S2010007810000054.
http://www.worldscientific.com/doi/abs/10.1142/S2010007810000054

Pan American Health Organization (PAHO), 1992:
http://www.paho.org/hq/index.php?option=com_topics&view=article&id=72&Itemid=40787&lang=en

Peek, L. and A. Fothergill, 2006: Reconstructing childhood: An exploratory study of children in Hurricane Katrina. *Quick Response Report* **No. 186**, Boulder: Natural Hazards Center, University of Colorado, Boulder, CO.

Picou, J. S., and C. G. Martin, 2006: Community Impacts of Hurricane Ivan: A Case Study of Orange Beach, Alabama. *Quick Response Research Report* **190**. Boulder, CO: University of Colorado Natural Hazards Center.

Pielke, Jr., R.A., 2007: Future economic damage from tropical cyclones: sensitivities to societal and climate changes. *Philosophical Transactions of the Royal Society A,* **365** (1860), 2717-2729.

Pielke Jr., R.A., J. Gratz, C. W. Landsea, D. Collins, M. A. Saunders, and R. Musulin, 2008: Normalized hurricane damages in the United States: 1900-2005. *Nat. Hazard. Rev.,* **9 (1)**, 29-42.

Pielke Jr., R.A., and C. W. Landsea, 1998: Normalized hurricane damages in the United States: 1925-1995. *Wea. Forecast.,* 621-631 (September).

Pielke Jr., R. A., J. Rubiera, C. Landsea, M. L. Fernandez, and R. Klein, 2003: Hurricane vulnerability in Latin America and the Caribbean: normalized damage and loss potentials. *Nat. Hazards Rev.*, **4,** 101-114.

Pielke Jr, R. A. and D. Sarewitz, 2005: Bringing Society back into the Climate Debate. *Population and Environment,* **26**, 255-268.

Pike, A. C., and C. J. Neumann, 1987: The Variation of Track Forecast Difficulty among Tropical Cyclone Basins. *Wea. Forecasting,* **2,** 237-241.

Raghavan, S., and S. Rajesh, 2003: Trends in tropical cyclone impact: a study in Andhra Pradesh, India. *Bull. Am. Meteorol. Soc.,* **84 (5),** 635-644.

Schmidt, S., C. Kemfert, and P. Hoppe, 2009a. Tropical cyclone losses in the USA and the impact of climate change - a trend analysis based on data from a new approach to adjusting storm losses.*Environ. Impact Assess. Rev., **29**,* 359-369. http://www.diw.de/sixcms/detail.php?id=diw_02.c.298404.de

Schmidt, S., C. Kemfert, and P. Hoppe, 2010: The impact of socio-economics and climate change on tropical cyclone losses in the USA. *Region. Environ. Change,* **10**, 13-26

Schmidt, S., C. Kemfert, and E. Faust, 2009b: Simulation of economic losses from tropical cyclones in 2050. The effects of anthropogenic climate change and growing capital stock at risk. Submitted to *Global Environmental Change* (and DIW Discussion Paper, 914).

Schroter and 34 Co-authors, 2005: Ecosystem service supply and vulnerability to global change in Europe. *Science,* **310** (2005), pp. 1333-1337.

Simpson, R. H.1971: The decision process in hurricane forecasting. *NOAA Tech. Memo.* **SR-63**, 35 pp.

Simpson, R. H.1974: Saffir-Simpson Hurricane Disaster. *Weatherwise, 27,* **169**.

Spence, P. R., K. A. Lachlan, and D. R. Griffin, 2007: Crisis Communication, Race, and Natural Disasters. *Journal of Black Studies,* **37**, 539-554. doi: 10.1177/0021934706296192.

State Farm, 2009: State Farm Florida and Florida Office of Insurance Regulation Reach Settlement: December. http://www.statefarm.com/florida/20091230.asp

Standards Association of Australia (SAA), 1989: http://www.standards.org.au/Pages/default.aspx

Stein, A. H., and G. B. Preuss, 2008: Oral History, Folklore, and Katrina. *Louisiana Folklore Miscellany,***Vol 16-17** (in 2008).

Swiss Re, 2010: Natural catastrophes and man-made disasters in 2009: catastrophes claim fewer victims, insured losses fall. sigma No 1/2010. http://media.swissre.com/documents/sigma1_2010_en.pdf

World Meteorological Organization (WMO), 1983. Human Response to Tropical Cyclone Warnings and Their Content. *World Meteorological Organization Tropical Cyclone Project* **no.12**, 128 pp.

World Meteorological Organization (WMO), 1990: Tropical Cyclone Warning Systems 1990. *WMO/TD***394**, TCP-26.

World Meteorological Organization (WMO), 2006: Multi-hazard Early Warning Systems (MHEWS). http://www.wmo.int/pages/prog/drr/projects/Thematic/MHEWS/MHEWS_en.html

World Meteorological Organization (WMO), 2007: Sixth WMO International Workshop on Tropical Cyclones (IWTC-VI) (San José, Costa Rica, 21-30 November 2006). *WMO/TD* **1383**, World Weather Research Programme (WWRP) 2007-1.

World Meteorological Organization (WMO), 2008: Guidelines on Communicating Forecast Uncertainty.*WMO/TD* **1422**. Lead author and coordinator Jon Gill; edited by Haleh Kootval. Geneva, Switzerland, pp 25.

Zhang, J., L. Wu, and Q. Zhang, 2010: Tropical cyclone damages in China under the Background of Global Warming. *J. Trop. Meteorol.,* **2011-04,** (in Chinese with English abstract).

Zhang, Q., L. Wu, and Q. Liu, 2009: Tropical cyclone damages in China: 1983-2006. *Bull. Am. Meteorol. Soc.,* **90 (4)**, doi:10.1175/2008BAMS2631.1.

Chapter Ten

Charles 'Chip' Guard
USNR (Retired)
US National Oceanic and Atmospheric Administration
Science Applications International Corporation
National Weather Service Forecast Office Guam

10 Tropical Cyclone Training

Since the original *Global Guide* was written, a tremendous amount of training materials have been developed and made available to the meteorology and hydrology communities. There is absolutely no reason to duplicate these programs and materials in this document. The major sources of training materials come from the WMO, some of the RSMCs and TCWCs, and specific organizations that have their mission as the development of training materials (e. g., UCAR COMET® MetEd). Some of the major sources are listed in this chapter, but this list is in no way exhaustive.

10.1 UCAR, COMET®, MetEd

The University Corporation for Atmospheric Research (UCAR), with its headquarters at Boulder, Colorado, USA, serves as a hub for research, education, and public outreach for the atmospheric and related Earth sciences community. UCAR's mission includes:

- Support, enhance and extend the capabilities of the university community, nationally and internationally
- Understand the behavior of the atmosphere and related systems and the global environment
- Foster the transfer of knowledge and technology for the betterment of life on Earth

A part of UCAR's Community Programs that helps satisfy its advancement of education goals is the COMET® Program ((https://www.meted.ucar.edu/). This Program is a world-wide leader in support of education and training for the environmental sciences, particularly meteorology, but also oceanography, hydrology, space weather and emergency management. COMET is sponsored by NOAA's National Weather Service (NWS) with additional funding from several national and international organizations. COMET offers the following products and services:

- Media-rich, interactive and multi-lingual distance learning
- Internet-based courses
- The MetEd website with a user tracking and assessment system
- Residence courses, workshops and meetings

- Small grants program (outreach)
- Leadership and consultation in science education and training

The MetEd website hosts hundreds of hours of education and training material for the geosciences. The training materials are composed of modules and courses. A **module** is targeted toward one focused subject. A **course** is a collection of modules that pertain to a broader subject area. You can obtain Certificates of Completion for both modules and courses. Courses are entirely self-paced and are available for open enrollment. This is a free service, and those in the tropical cyclone business are highly encouraged to take advantage of it. Pertinent training topic headings are:

- Tropical/Hurricanes
- Satellite Meteorology
- Radar Meteorology
- Oceanography/Marine Meteorology
- Hydrology/Flooding
- Emergency Management
- Numerical Modeling
- Environment and Society
- Aviation Weather

10.1.1 COMET/MetEd: Tropical/Hurricanes

The following sections list COMET courses sorted by subject matter categories. Courses in **bold** are recommended as the most urgent for tropical cyclone forecaster training.

- **Introduction to Tropical Meteorology**
  - **Chapter 1: Introduction**
  - **Chapter 2: Tropical Remote Sensing Applications**
  - **Chapter 3: Global Circulation**
  - **Chapter 4: Tropical Variability**
  - **Chapter 5: The Distribution of Moisture and Precipitation**
  - **Chapter 8: Tropical Cyclones**
  - **Chapter 9: Observations, Analysis and Predictions**
- **Topics in Tropical Meteorology**
- **Conceptual Models of Tropical Waves**
- **Diagnosing and Forecasting Extratropical Transition: A Case Exercise on Hurricane Michael**
- **Hurricanes Canadian Style: Extratropical Transition**

10.1.2 COMET/MetEd: Satellite Meteorology

- **Remote Sensing Using Satellites**
- **Polar Satellite Products for the Operational Forecaster: Microwave Analysis of Tropical Cyclones**
- **Microwave Remote Sensing: Overview**
- **Microwave Remote Sensing: Resources**
- **Microwave Remote Sensing: Clouds, Precipitation and Water Vapor**
- **Microwave Remote Sensing: Land and Ocean Surface Applications**
- Satellite Feature Identification: Atmospheric Rivers
- Satellite Meteorology: GOES Channel Selection
- Satellite Meteorology: Introduction to Using the GOES Sounder
- Atmospheric Dust
- Multispectral Satellite Applications: RGB Products Explained
- Toward an Advanced Sounder on GOES
- Satellite Feature Identification: Blocking Patterns
- Jason 2: Using Satellite Altimetry to Monitor the Ocean
- WMO Regional Satellite Workshop: Regional Training Course on the Use of Environmental Satellite Data in Meteorological Applications for RAIII and RAIV.
- GOES-R: Benefits of Next-Generation Environmental Monitoring
- Advanced Satellite Sounding: The Benefits of Hyperspectral Observation
- Environmental Satellite Resource Center (ESRC)
- Creating Meteorological Products from Satellite Data
- **Remote Sensing of Ocean Wind Speed and Direction: An Introduction to Scatterometry**
- **Advances in Microwave Remote Sensing: Ocean Wind Speed and Direction**

10.1.3 COMET/MetEd: Radar Meteorology

- **Caribbean Radar Cases**
- **Weather Radar Fundamentals**
- Radar Signatures for Severe Convective Weather
- Lectures on Radar Applications in Mesoscale Meteorology

10.1.4 COMET/MetEd: Oceanography/Marine Meteorology

- A Forecaster's Overview of the Northwest Pacific

- **Introduction to Ocean Models**
- Mesoscale Ocean Circulation Models
- **Nearshore Wave Modeling**
- **Operational Use of Wave Watch III**
- North Wall Effects on Winds and Waves
- **Analyzing Ocean Swells**
- Wave Ensembles in the Marine Forecast Process
- **Introduction to Ocean Currents**
- **Winds in the Marine Boundary Layer: A Forecaster's Guide**
- Understanding Marine Customers
- Introduction to Ocean Tides
- Rip Currents: Near Shore Fundamentals
- Rip Currents: Forecasting
- Rip Currents: NWS Mission and Partnerships
- **Shallow Water Waves**
- **Marine Wave Model Matrix**
- Wave Life Cycle I: Generation
- Wave Life Cycle II: Propagation & Dispersion
- Low Level Coastal Jets

10.1.5 COMET/MetEd: Hydrology/Flooding

- ASMET: Flooding in West Africa
- Satellite Precipitation Products for Hydrological Management in South Africa
- Flash Flood Early Warning System Reference Guide
- Flood Forecasting Case Study: International Edition
- **Basic Hydrologic Science Course**
- **Flash Flood Processes: International Edition**
- Introduction to Verification of Hydrologic Forecasts
- Techniques in Hydrological Forecast Verification
- Runoff Processes: International Edition
- Streamflow Routing: International Edition
- Flood Frequency Analysis: International Edition
- Unit Hydrograph Theory: International Edition
- Understanding the Hydrologic Cycle: International Edition
- Introduction to Distributed Hydrologic Modeling
- Distributed Hydrologic Models for Flow Forecasts Part 1
- Distributed Hydrologic Models for Flow Forecasts Part 2
- Precipitation Estimates, Part 1: Measurement
- Precipitation Estimates, Part 2: Analysis
- Quantitative Precipitation Forecasting Overview
- QPF Verification: Challenges and Tools

- An Introduction to Ensemble Streamflow Prediction
- NWS Hydrologic Ensemble Forecast System
- Dams & Dam Failure Module 1: Terminology and Open Channel Hydraulics
- Dams and Dam Failure Module 2: St.Venant Equations, Modeling and Case Study
- **Flash Flood Processes**
- **Flash Flood Case Studies**
- **River Forecasting Case Study**
- **Allison Rains in Houston, Texas**

10.1.6 COMET/MetEd: Emergency Management

- Anticipating Hazardous Weather and Community Risk
- Quality Management Systems: Implementation in Meteorological Services
- Role of the Skywarn Spotter
- Skywarn Spotter Convective Basics
- **Hurricane Strike!**
- **Community Hurricane Preparedness**
- **Urban Flooding: It Can Happen in a Flash!**
- **A Social Science Perspective on Flood Events**

10.1.7 COMET/MetEd: Numerical Modeling

- Gridded Forecast Verification and Bias Correction
- Bias Correction of NWP Model Data
- **Optimizing the Use of Model Data Products**
- **Introduction to Ensemble Prediction**
- **Ensemble Forecasting Explained**
- How Mesoscale Models Work
- **Tropical Storm Allison in the Southeastern US**
- Ten Common NWP Misconceptions
- Interpretation of Global Forecast Model "Flip-Flops"
- Preparing to Evaluate NWP Models
- **Effective Use of NWP in the Forecast Process: Introduction**
- **Impact of Model Structure and Dynamics**
- Understanding Assimilation Systems: How Models Create Their Initial Conditions
- **Influence of Model Physics on NWP Forecasts**
- How Models Produce Precipitation and Clouds
- Effective Use of High Resolution Models
- How NWP Fits into the Forecast Process
- Downscaling of NWP Data

- Adding Value to NWP Guidance
- Determining Plausible Forecast Outcomes
- **Understanding the Role of Deterministic Versus Probabilistic NWP Information**

10.2 WMO-sponsored training

The WMO sponsors tropical cyclone, disaster preparedness and hydrological training at various WMO Training Centers such as the one at the University of Nanjing in China.

10.3 Regional training

10.3.1 National meteorological center-sponsored, RSMC-sponsored, and TCWC-sponsored training

Various National Meteorological Centers, Regional Specialized Meteorological Centers and Tropical Cyclone Warning Centers often sponsor and provide regional tropical cyclone training. Some examples are:

- Region Association I: RSMC-La Reunion (Meteo-France), TCWC Perth;
- The Economic and Social Commission for Asia and the Pacific (ESCAP): Japan Meteorological Agency, RSMC-Tokyo, Korean Meteorological Administration, China Meteorological Administration, Chinese Meteorological Society, Hong Kong Observatory, Weather Forecast Office Guam;
- Central Pacific Hurricane Center Pacific Desk/RSMC-Honolulu;
- Regional Association IV: National Hurricane Center/RSMC-Miami;
- Regional Association V: Australian Bureau of Meteorology (BoM), the New Zealand Met Service, RSMC-Nadi, TCWCs at Darwin and Brisbane.

10.3.2 National and regional disaster risk reduction

Training centres include:

- Asian Disaster Preparedness Center (ADPC), based at the Asian Institute of Technology in Bangkok. The ADPC has introduced practical experience for participants through the conduct of field vulnerability assessment studies in towns and villages.
- National Disaster Risk Reduction Institute Japan;
- Asian Disaster Reduction Center (ADRC) sponsored by the Republic of Korea.

10.4 Internal training programs and certifications

10.4.1 NOAA

In the US, NOAA's National Weather Service (NWS) has its own training program through the NOAA Learning Center. This is an online program that not only includes all of the MetEd modules and courses, but also includes modules and courses that pertain specifically to NWS equipment and methodology. In addition, NWS provides a great deal of on-the-job initial and recurrent training with formalized certification.

10.5 The function of training programs in tropical cyclone centers

There are several functions of formal and informal training programs. While education satisfies the basic level of knowledge for tropical cyclone forecasters, training is what qualifies them to actually issue forecasts as a certified forecaster. Training familiarizes a new forecaster with local and regional knowledge, and with other specialized knowledge. Training programs are part of the overall Forecasting Strategy as discussed in Chapter 8. Every TCWC must have some kind of formal training program that includes initial training, preseason readiness training, and training of opportunity as discussed in the earlier sections of Chapter 10.

10.5.1 Certification training

As pointed out in Chapter 8, training needs of staff members are best considered in relation to the roles they will fill in the warning centre. See Section 8.3 for a more complete discussion of training with respect to staffing and the various TCWC roles.

A Tropical Cyclone Warning Center (TCWC) should have some formalized training program that prepares and ultimately certifies a new forecaster. This is generally conducted as local study and on-the-job-training, and may require several months. In general, the new forecaster should be trained, evaluated by a certified forecaster, and ultimately "signed off" as knowledgeable or proficient in that subject or task. Once the new forecaster has satisfactorily completed the training program, he/she can either be designated as certified or can be required to meet and an evaluation board of management and certified forecasters. That board requires the new forecaster to meet with it in order to address and answer a series of pre-selected questions about forecasting, operations and emergency procedures. Following the session, the board either votes for certification or recommends additional training for the new forecaster.

10.5.2 Recurrent training

Recurrent training is discussed in Chapter 8, in the Continuous Improvement Section (8.7) under the topic of "preseason readiness". Even at the Joint Typhoon Warning Center (JTWC), where tropical cyclone warning is a year-round job, some preseason training is required for the switch between northern and southern hemisphere forecasting. And, at the National Hurricane Center at Miami, where hurricane specialists have year-round tasks, hurricane forecasting is seasonal, and preseason preparation is needed as the season approaches. This may involve something as simple as an annual review of Standing Operating Procedures (SOPs) or

something as complicated as attending a formal course at a training center. The TCWC should have a program that addresses recurrent training needs and tracks them.

10.5.3. Advanced or specialized training

The TCWC program should include WMO and national or regional training opportunities as well. These are usually advanced or specialized courses, and the attendee should be prepared to pass his/her newly acquired knowledge to colleagues. Advanced and specialized training is also available through the multitude of online and *MetEd* training programs. These opportunities should be periodically monitored for new, relevant courses.

10.6 WMO Tropical Cyclone Forecaster's Website

The Hong Kong Observatory hosts the WMO Tropical Cyclone Forecaster's Website at

http://severe.worldweather.wmo.int/TCFW/

This site has a Training Materials module that includes:

- TC RSMC Training Documentations
- E-material and presentations from RSMC Miami
- Web-based training from MetEd
- Advanced Warning Operations Course from US NWS

The website also includes modules for:

- Observations and Products Data
- Advisory and Warning Centres
- WMO Technical Publications
- Tropical Cyclone Research
- TC Data Archive
- Weather Event Discussion

We highly encourage all forecasters to visit and use this site.

Chapter Eleven

Greg Holland
Formerly Bureau of Meteorology
Melbourne, Australia

11. Ready Reckoner

11.1 Introduction

This chapter provides a ready reference for various parameters and information related to tropical cyclones.

11.2 Unit conversion

Multiply the line unit by the indicated number to get the column unit; for example, on the first line inches multiplied by 12 gives 1 ft in the second column. Only conversions to higher values are shown. Take care to convert to the degree of accuracy of the original observation only; for example a ship estimate of 20 kt based on sea state should convert to 10 ms^{-1}, a literal transformation to 10.256 ms^{-1} is incorrect.

SI length units are identified by an asterisk

Length								
	mm*	**in**	**ft**	**m***	**km***	**mi**	**nm**	**°lat**
mm*	1	25.4	304.8	1000	10^6	$1.61x10^6$	$1.85x10^6$	$1.11137x10^8$
in		1	12	39.37	39370	63360	72913	$4.38x10^6$
ft			1	3.28	3281	5280	6080	364320
m*				1	1000	1609	1853	$1.11137x10^5$
km*					1	1.609	1.853	111.137
mi						1	1.15	69
nm							1	60

Time				
	sec	**min**	**hour**	**day**
sec	1	60	$3.6x10^3$	$8.64x10^4$

min		1	60	$1.44x10^3$
hour			1	24

Speed				
	km h^{-1}	**mph**	**kt**	**ms^{-1}**
km h^{-1}	1	1.61	1.85	3.6
mph		1	1.15	2.24
kt			1	1.95

Conversion from °C to °F

$$°F = (1.8 \times °C) + 32$$

Conversion from °K to °C

$$°C = °K - 273.15$$

11.3 Beaufort scale

Several versions of the Beaufort wind scale exist. They mostly vary by small degrees. The following is adapted from Pielke (1991) and Dunn and Miller (1964) following work by Black and Adams (personal communication), and using information provided by R. Simpson (personal communication).

Beaufort Force	**Estimated 10-min averaged wind (kt) at 19m*.**	**Description**
0	Calm	Sea glassy. Appearance of being covered by oil.
1	1-3	Slight ripple.
2	4-6	Slight ripple. Isolated brief whitecaps. Unable to determine direction.
3	7-10	Gentle Breeze: Surface like wrinkled paper. Small. well defined whitecaps of uniform size but few in number. White crests disappear quickly. First able to tell direction but with difficulty.
4	11-16	Moderate Breeze: Small foam patches. Number of breaking crests increase slightly and are a little larger. First able to tell direction with confidence. Wrinkle

		texture of surface is very evident.
5	17-21	Fresh Breeze: Size and number of whitecaps and foam patches increase significantly. Whitecaps on most wave crest. Very short streaks may appear in foam patches.
6	22-27	Strong Breeze: Well defined short streaks in foam patches. Small whitecaps on most wave crests. Occasional medium-size foam patch or breaker. Isolated green patches of short duration. Foam patches, short streaks, and whitecaps (white water) cover 5-7% of sea surface.
7	28-33	Moderate Gale: Medium-size breaking crest. Dense foam patches and accompanying short streaks are numerous. Average length of streaks equal to diameter of average foam patch. Small green patches occasionally visible.
8	34-40	Fresh Gale - Tropical Cyclone: Streaks more numerous and occasionally longer. Some streaks may appear unassociated with breaking waves or foam patches. Area covered by whitecaps stabilises at 7-10%. Occasional large foam patch. Small green patches continually visible with occasional moderate-size green patch.
9	41-47	Strong Gale: Streaks readily apparent between foam patches. Streak length varies from patch size to occasional regions of long, nearly continual streaking. Streaks, patches, and breaking waves cover 15-20% of sea. 50% of foam patches are green.
10	48-55	Storm Force: Wind streaks become the most obvious surface feature and are continuously or nearly so. Well-defined, thinly breaking waves form on long crestlines, often preceded by short breaking wavelets giving a step-like appearance. Occasional large foam patches are quickly fragmented and elongated into streaks. Sea covered 2-25% by white water.
11	56-63	Streaks are well-defined, parallel, thin, close together, and continuous with very short capillary wavelets cutting across and perpendicular to streaks, giving sea surface a 'shattered glass' effect in certain areas. Some large breaking crests may take on 'rolling' or 'tumbling' appearance. Sea covered 30-40% by white water.

12	64-69	Hurricane Force: Sea may occasionally be obscured by spray and take on a murky appearance. Large, curved, breaking crests have undulating effect on steaks, giving churning appearance. Streaks appear to thicken and become milky or pale green.
13	70-75	Surface features generally become murky. Streaks and foam patches begin to sole their sharp definition and appear to smudge, thicken, or merge together. Frequent, extremely large, almost semicircular crests outlined by thinly breaking waves with occasional groups of large foam patches after entire crest breaks.
14	76-80	Quantity of spray increases. Streaks thicken and appear to have more depth. Previous crisp, shattered glass appearance now appears blurred. Most features appear to be a submerged rather than a surface phenomenon, owing to obscuration. Very short capillary wavelets which cut across streaks give surface a stressful appearance as though undergoing compression. Sea surface 50% white.
15	81-85	Sea appears flatter and entire surface takes on a whitish/greyish cast. Streaks organise somewhat into broader, diffuse bands. All features lose some definition and appear submerged. Surface 50-55% white.
16	86-90	Many thin streaks are partially obscured and those which can be seen may appear as bands spaced farther apart. Occasional cloud below aircraft blots out or obscures surface. Sea appears almost flat. Whitish cast covers 60-65% of surface.
17	91-95	Breaking waves and foam patches appear as diffuse, white, puffy areas. Streaks become fuzzy bands. Surface 70-80% white.
18	96-100	Cloud, spray, and foam patches merge into large, white, indefinable areas historically referred to as 'white sheets'. Surface features have only rough boundary definition.
19	101-105	Isolated large, white puffs. Only strongest features of previously seen thick streaks remain to be observed and result gives impression of only a very few widely scattered and non-parallel streaks or wide bands. Whitish and greenish cast covers 100% of surface.

20	106-110	Foam patches, bands, and whitecaps merge into large indefinable areas or white sheets. Variations in brightness are less distinct but still result in churning appearance.
21	>110	Sea 100% white and green. Only slight variation in whiteness is apparent.

* The standard height for ship observations is 19m, rather than the 10m used for land.

11.4 Useful tropical cyclone parameters

11.4.1 Tropical cyclone severity scales

The **Saffir Simpson Hurricane Scale** (Simpson and Riehl, 1981) was developed to provide a sliding scale of damage potential for hurricanes, including that arising from storm surge. A similar scale, though adapted for local conditions is used in Australia. Global adoption of such scales is strongly recommended.

Hurricane or Severe Tropical Cyclone	**Maximum Sustained Winds**	
	Saffir-Simpson	**Australian Scale**
	Level (1-min mean, kt)	**(10 min mean, km h^{-1})**
1	64-83	63-90
2	84-96	91-125
3	97-113	126-165
4	114-135	166-225
5	>135	>225

Some of the tables from the main text are also listed on the following pages for convenience.

11.4.2 Gust factors

Gust factors defined by the ratio of peak 2-s wind to the mean wind at 10 m elevation for various exposures and averaging times and in wind speeds of at least hurricane force. Parentheses give an indication of the range in gust factors. From Atkinson (1974), Spillane and Dexter (1976) and Padya (1975).

	OCEAN	FLAT GRASSLAND	WOODS/CITY
1-min Mean	1.25 (1.17-1.29)	1.35 (1.29-1.45)	1.65 (1.61-1.77)
10-min Mean	1.41 (1.37-1.51)	1.56 (1.51-1.70)	2.14 (1.89-2.14)
10-min Mean over Ocean	1.41	1.31	1.11

11.4.3 Dvorak intensity relationship

Empirical relationship between the current intensity number (CI), the Maximum sustained 1-min Wind Speed (MWS, kt), and the central pressure (hPa) in tropical cyclones. The central pressure values for the western North Pacific are from Shewchuk and Weir (1980).

		Central Pressure	
CI	**MWS (kt)**	**(Atlantic)**	**(NW Pacific)**
0.0	<25		
0.5	25		
1	25		
1.5	25		
2	30	1009	1000
2.5	35	1005	997
3	45	1000	991
3.5	55	994	984
4	65	987	976
4.5	77	979	966
5	90	970	954
5.5	102	960	941
6	115	948	927
6.5	127	935	914
7	140	921	898

7.5	155	906	879
8	170	890	858

11.5 Useful constants

9.6.1 Universal constants

Avogadro's Number,	N_A	6.02247×10^{26} kmol^{-1}
Base of Natural Logarithms,	e	2.71828
Boltzmann's Constant,	k	1.381×10^{-23} J K^{-1} molecule^{-1}
Gravitational Constant		6.673×10^{-11} Nm^2 kg^{-1}
Pi	π	3.1415927
Planck's Constant,	h	6.6262×10^{-34} J s^{-1}
Speed of Light,	c	2.998×10^{8} ms^{-1}
Speed of Sound in Air at 0°C		340 ms^{-1}
Stefan-Boltzmann Constant,	σ	5.6696×10^{-8} W m^{-2} K^{-4}
Universal Gas Constant,	R	8.3143×10^{3} J K^{-1} kmol^{-1}

9.6.2 The Earth

Angular Velocity,	Ω	7.292×10^{-5} s^{-1}
Gravitational Acceleration at the surface,	g	9.81 ms^{-2}
Radius: Mean, Equatorial Polar	R_E	 6370 km 6379 km 6357 km
Volume		1.083×10^{21} m^3
Surface Area		5.1×10^{12} m^2
Mass		5.988×10^{24} kg
Mean Density		5.529×10^{3} kg m^{-3}

Mean Distance to Moon		3.8×10^5 km
Mean Distance to Sun		1.49×10^8 km
Orbital Speed around Sun		2.977×10^4 ms^{-1}
Azimuthal Speed at Equator		465 ms^{-1}
Solar Irradiance		1.38×10^3 W m^{-2}

9.6.3 The Atmosphere

Density of dry air at 0°C and 1000 hPa		1.29 kg m^{-3}
Gas Constant:		
Universal		8.31436×10^3 J K^{-1} $kmol^{-1}$
For Dry Air,	R_d	287 J K^{-1} kg^{-1}
Mass of Atmosphere		5.3×10^{18} kg
Molecular Weight of Dry Air		28.966 kg $kmole^{-1}$
Specific Heat of Dry Air:		
at Constant Pressure,	c_p	1004 J K^{-1} kg^{-1}
at Constant Volume,	c_v	717 J K^{-1} kg^{-1}
Standard Sea Level:		
Pressure,	p_s	1013.28 hPa
Temperature,	T_s	288.16K
Density,	ρ_s	2.225 kg m^{-3}
Speed of Sound,	c_s	331.3 ms^{-1}

9.6.4 Water

Density of Water	(0°C)	1.0×10^3 kg m^{-3}
Density of Ice	(0°C)	0.917×10^3 kg m^{-3}
Gas Constant for Vapour,	R_v	461.5 J K^{-1} kg^{-1}
Molecular Weight of Water Vapor		18.016 kg $kmol^{-1}$
Specific Heat:		
Water Vapour:		
Constant Pressure		1810 J K^{-1} kg^{-1}
Constant Volume		1350 J K^{-1} kg^{-1}
Liquid Water at 0°C		4218 J K^{-1} kg^{-1}
Ice at 0°C		2106 J K^{-1} kg^{-1}
Latent Heat:		2.5×10^6 J kg^{-1}

Vaporisation at 0°C	2.25×10^6 J kg^{-1}
Vaporisation at 100°C	3.34×10^5 J kg^{-1}
Fusion at 0°C	2.83×10^6 J kg^{-1}
Sublimation at 0°	

11.6 Derived parameters

11.6.1 Definition of terms

b	empirical constant
c_g	gravity wave phase speed
c_p	specific heat of dry air at constant pressure
c_1, c_2	empirical constants
e	base of natural logarithm
f	Coriolis parameter
h, H	atmospheric scale height
I	inertial frequency
k	unit vector perpendicular to the earth surface
L	latent heat of condensation
L_r	Rossby radius of deformation
ln	natural logarithm
M_a	absolute angular momentum
N	Brunt Vaisala frequency, total number in population sample
p	air pressure
p_c	central (minimum) pressure of a tropical cyclone
p_n	representative environmental pressure for a tropical cyclone
q	specific humidity
R	universal gas constant
R_d	gas constant for dry air
R_o	Rossby number
r	radius

r_m	radius of maximum winds
T	temperature
t	time
u	wind component, either zonal or radial
V	velocity
v	wind component, either meridional or azimuthal
v_g	geostrophic wind
v_m	maximum wind speed
x	empirical parameter
z	height above the earth surface
∂	gradient operator
∂	partial derivative
!	factorial
ζ	relative vorticity
θ	potential temperature
θ_e	equivalent potential temperature
λ	latitude, azimuthal angle
ρ	air density
Σ	summation convention
σ	standard deviation
Ω	earth angular velocity

11.6.2 Derived parameters

Angular Momentum:

$$M_a = rv + \frac{f_o r^2}{2}$$

where f_0 is evaluated at the cyclone centre (Holland, 1983)

Brunt Vaisala Frequency (Static Stability):

$$N^2 = g\frac{\partial ln\theta}{\partial z}$$

Coriolis Parameter:

$$f = 2\Omega sin(\lambda)$$
$$= 14.584 sin(\lambda)\ s^{-1}$$

Divergence:

$$\text{General: } D = \nabla.\mathbf{v}$$

$$\text{Cartesian: } D = \frac{\partial u}{\partial x} + \frac{\partial v}{\partial y}$$

$$\text{Cylindrical: } D = \frac{1}{r}\left(\frac{\partial ru}{\partial r} + \frac{\partial v}{\partial \lambda}\right)$$

Equation of State:

$$\rho = pRT$$

Equivalent Potential Temperature:

$$\theta_E \approx T_E\left(\frac{1000}{p}\right)^{R_d/C_p}$$

$$T_E = T\, e^{L_q/c_p T}$$

Inertial Frequency (Inertial Stability):

$$I^2 = (f_o + \zeta)\left(f_o + \frac{2v}{r}\right)$$

Mean:

$$\bar{x} = \frac{\sum x}{N}$$

Poisson Distribution: The discrete probability distribution

$$p(x) = \frac{\lambda^x\, e^{-\lambda}}{x!}$$

which has the properties of mean = λ and standard deviation, $\sigma = \lambda^{1/2}$

Potential Temperature:

$$\theta = T\left(\frac{p_o}{p}\right)^{R/C_p}$$

Rossby Number:

$$R_o = \frac{v}{fr}$$

Rossby Radius of Deformation:

$$L_R = \frac{c_g}{\zeta + f}$$

$$= \frac{\sqrt{gh}}{\zeta + f}$$

$$= \frac{NH}{I}$$

Standard Deviation:

$$\sigma = \sqrt{(\overline{x^2} - \bar{x}^2)}$$

Thermal Wind:

Geostrophic: $$f\frac{\partial v_g}{\partial lnp} = -R\nabla T$$

Cylindrical: $$\left(\frac{2v}{r} + f\right)\frac{\partial v}{\partial lnp} = -R\frac{\partial T}{\partial r}$$

Vorticity:

General: $$\zeta = k.\nabla \text{ x } \boldsymbol{V}$$

Cartesian: $$\zeta = \frac{\partial v}{\partial x} - \frac{\partial u}{\partial y}$$

Cylindrical: $$\zeta = \frac{1}{r}\left(\frac{\partial rv}{\partial r} - \frac{\partial u}{\partial \lambda}\right)$$

Wind Balance:

Gradient: $$v = \frac{-fr}{2} \pm \sqrt{\left(\frac{r\partial p}{\rho \partial r} + \frac{f^2r^2}{4}\right)}$$

Cyclostrophic: $$v = \pm\sqrt{\frac{1}{\rho r}\frac{\partial p}{\partial r}}$$

For cyclones, the positive (negative) root is used in the northern (southern) hemisphere

Wind Profiles: (Holland, et al, 2010)

Knowledge of radial wind profiles has become quite complex. This is best understood by consulting the reference at:http://nldr.library.ucar.edu/repository/assets/osgc/OSGC-000-000-001-080.pdf

Wind/Pressure Relationships:

Recent research into wind-pressure relationships have shown involvement of storm motion, size & latitude. The following equations are taken from (Knaff and Zehr, 2007):

$$\mathrm{MSLP} = 23.286 - 0.483V_{\mathrm{srm}} - \left(\frac{V_{\mathrm{srm}}}{24.254}\right)^2 - 12.587S - 0.483\phi + P_{\mathrm{env}}, \quad (7)$$

where V_{srm} is the maximum wind speed adjusted for storm speed, S (i.e., = V_{500}/V_{500c}) is the normalized size parameter (see below), and φ is latitude (in degrees). V_{500} is the mean tangential wind at 500km from the cyclone centre and V_{500c} is defined below.

$$V_{500c} = V_{\max}\left(\frac{R_{\max}}{500}\right)^x, \quad (4)$$

where x, the shape factor, and $R_{\max}$, the radius of maximum winds in kilometers, are functions of latitude (ϕ) in degrees and intensity ($V_{\max}$) in knots:

$$x = 0.1147 + 0.0055V_{\max} - 0.001(\phi - 25) \quad \text{and} \quad (5)$$

$$R_{\max} = 66.785 - 0.09102V_{\max} + 1.0619(\phi - 25). \quad (6)$$

11.7 Tropical cyclone records

Recording records is a difficult task, because of the extreme nature of the event and the tendency for observing equipment to break. The following records are backed up by good analysis methods and are considered to be reasonably reliable.

11.7.1 Global records

These records have been taken from http://wmo.asu.edu/#cyclone and from tropical cyclone records. Visit the page for the sources for these records and also any recent updates.

Tropical Cyclone Characteristic	Value	Date (D/M/Y)	Length of Record	Tropical Cyclone	Latitude/ Longitude
Most Intense - by Central Pressure (World and Eastern Hemisphere)	870mb (25.69")	12/10/1979	1951-present	Typhoon Tip in the Northwest Pacific Ocean	16°44'N, 137°46'E
Most Intense - by Central Pressure (western hemisphere)	882mb (26.05")	19/10/2005	1951-present	Hurricane Wilma in Caribbean Sea	17°18'N, 82°48'W
Most Intense - by Maximum Sustained Surface Wind	95m/s (185 kt, 215 mph)	12/9/1961	1945-present	Typhoon Nancy in the Northwest Pacific Ocean	15°30'N, 137°30'E
Maximum Surface Wind Gust for Tropical Cyclone	113.2 m/s (253mph; 220 kt	1055 UTC, 10/4/1996	1949-present	Barrow Island, Australia	20°49'S, 115°23'E
Northern Hemispheric Maximum Surface Wind Gust for Tropical Cyclone	94.4 m/s (211.3 mph; 183.5 kt	2235 UTC, 30/9/2008	1949-present	Pinar del Rio, Cuba	22°34'N, 83°40'W
Fastest Intensification	100mb (976 to 876 mb) in just under 24 hours	22-23/9/1983	1951-present	Typhoon Forrest in Northwest Pacific Ocean	18°0'N, 136°0'E
Highest Storm Surge	13m (42 feet)	5/3/1899		Tropical Cyclone Mahina; Bathurst Bay, Queensland, Australia	14°15'S, 144°23'E
First Identified South Atlantic Hurricane		28/3/2004	1966-present	Tropical Cyclone Catarina; state of Santa Catarina, Brazil	approximately 27°S, 48°W
Largest Tropical Cyclone (winds from center)	Gale winds [17m/s, 34 kt, 39mph] extending 1100km (675 mi) from center	12/10/1979	1945-present	Typhoon Tip in Northwest Pacific Ocean	16°44'N, 137°46'E
Smallest Tropical Cyclone (winds from center)	Gale winds [17m/s, 34kt, 39mph] extending 50km (30 mi) from center	24/12/1974	1956-present	Tropical Cyclone Tracy near Darwin, Australia	12°12'S, 130°00'E
Longest Lasting Tropical Cyclone	31 days	10/8/1994-10/9/1994	1945-present	Hurricane / Typhoon John in Northeast & Northwest Pacific	

				Basins	
Longest Distance Traveled by Tropical Cyclone	13280 km (7165 st. mi.)	10/8/1994-10/9/1994	1961-present (satellite era)	Hurricane / Typhoon John in Northeast & Northwest Pacific Basins	
Smallest eye	6.7km (4 mile)	24/12/1974	1956-present	Tropical Cyclone Tracy at Darwin Australia	12°12'S, 130°00'E
Largest eye	90km (56 mile)	21/2/1979	1956-present	Tropical Cycle Kerry, Coral Sea	17°30'S, 154°06'W

Largest Rainfall of Tropical Cyclones	Value	Date (D/M/Y)	Length of Record	Tropical Cyclone	Latitude/ Longitude
12 hr	1.144m (45.0")	7-8/1/1966	1966-1990	Tropical Cyclone Denise in South Indian Ocean	21°14'S, 55°41'E
24 hr	1.825m (71.8")	7-8/1/1966	1966-1990	Tropical Cyclone Denise in South Indian Ocean	21°14'S, 55°41'E
48 hr	2.467m (97.1")	7-9/4/1958	1952-1980 & 2004-present	Unnamed Tropical Cyclone In South Indian Ocean	21°00'S, 55°26'E
72 hr	3.930m (154.7")	24-27/2/2007	1968-present	Tropical Cyclone Gamede in South Indian Ocean	21°12'S, 55°39'E
96 hr	4.869m (191.7")	24-27/2/2007	1968-present	Tropical Cyclone Gamede in South Indian Ocean	21°12'S, 55°39'E
10-day	5.678m (223.5")	18-27/1/1980	1968-present	Tropical Cyclone Hyacinte in South Indian Ocean	21°12'S, 55°39'E

11.7.2 Regional Records

When printing this file include your regional records here.

11.8 Trivia corner

Hurricane Rubble: Surge and waves from Hurricane Bebe at Funafuti Atoll (8°S, 179°E) during 21 October, 1972 raised a permanent rubble rampart 3.5 m high, 37 m wide and 18 km long (Maragos et al., 1973).

Hot Air: A localised region of extremely warm stratospheric air with 240 hPa temperature anomaly of 18° attained over a distance of 13 km at the end of a cloud band *outside* the eye of Tropical Cyclone Kerry, February 1979, Coral Sea (Holland et al., 1984); measured by 747 with meteorologist in the cockpit, caused a major scare as the jet engines lost substantial power; in a similar incident in Western Australia a jet descended to 3 km altitude before regaining engine power.

Best Ship Observations: Caught in a typhoon in the western North Pacific during 26 September 1935, officers of the Japanese Imperial Navy collected the first, and possibly still the most comprehensive set of observations of the surface structure of a tropical cyclone (Arakawa and Suda, 1953).

Best Book Title: "An Attempt To Develop The Law of Storms By Means of Facts, Arranged According To Place and Time; and Hence To Point Out A Cause For The Variable Winds With The View To Practical Use In Navigation" (Reid, 1838).

Meteorology: This word seems to have been introduced to the language by Rear Admiral FitzRoy (1862), who begged his readers to accept the "abbreviation" from the then accepted meteorologic or meteorological.

Cyclone=Coiled Snake: Piddington (1855) first coined the term cyclone based on the Greek word, *κυκλοζ* or coil of a snake, which indicated the characteristic circular and centripetal air flow.

Typhoon=Big Wind: The derivative of the word typhoon seems to have arisen from very appropriate Mandarin word *t'ai fung* for great wind.

Hurricane=Angry God: The derivative of the word hurricane comes from *Huracan*, or "God of Evil" used by the Central American Tainos tribe (Anthes, 1982).

Cock-Eyed Bobs: Contrary to popular belief, tropical cyclones are not referred to as Willy Willys in Australia. This name refers to dust devils. However, old timers on the Australian west coast often used the colourful name Cock-Eyed Bob to refer to severe tropical cyclones.

Divine Wind: In the 13th century, a Mongol fleet, possibly the largest fleet ever assembled up to that time, was destroyed by a typhoon on its way to what would have been a successful invasion of Japan. This great fortune for Japan gave rise to the term *kamikaze*, for Divine Wind.

Friend or Foe: Clement Wragge, the Australian forecaster who started the convention of naming tropical cyclones, occasionally named a particularly severe one after politicians with whom he was displeased.

Coincidences? The TCM-90 Field experiment was initiated following a less than good series of forecasts for Typhoon Abby; the Project Manager was Bob Abbey. The Director of the field experiment in Guam was Russ Elsberry; several months later Guam was badly damaged by Supertyphoon Russ.

11.9 References

Anthes, R. A., Tropical Cyclones: Their Evolution, Structure and Effects, *American Meteorological Society*, Boston, MA, 1982.

Arakawa H., and Suda K., 1953, Analysis of winds, wind waves, and swell over the sea to the east of Japan during the typhoon of September 26, 1935. *Mon. Wea. Rev.,* **81,** 31-37.

Atkinson G.D., 1974, Investigation of gust factors in tropical cyclones. *U.S. Fleet Weather Central Tech. Note.* JTWC **74-1**, 9pp

Battan, L. J., 1973: Radar observations of the atmosphere. The University of Chicago Press, 324 pp.

Dunn, G. E., Miller B. I., 1964, Atlantic Hurricanes, Louisiana State University Press, Baton Rouge, Louisiana.

Dvorak, V.F. 1984. Tropical cyclone intensity analysis using satellite data. *NOAA Technical Report NESDIS 11,* NTIS, Springfield, VA 22161, 45 pp

FitzRoy R. 1862. The weather book: a manual of practical meteorology. Longman, Green: London.

Fujiwhara, S. (1921): The natural tendency towards symmetry of motion and its application as a principle in meteorology. *Q. J. Roy. Meteor. Soc.*, **47**, 287-292.

Guard C., Lander M.A., 1999. A scale relating tropl=ical cyclone wind speed to potential damage for the tropical Pacific Ocean region: A user's manual. *WERI Tech. Report* **86** (2nd Edition) 60pp

Greg J. Holland. (1983) Angular momentum transports in tropical cyclones. *Q. J. Roy. Meteor. Soc.***109** 187-209.

Holland, G. J., T. D. Keenan, and G. D. Crane (1984), Observations of a phenomenal temperature perturbation in Tropical Cyclone Kerry (1979), *Monthly Weather Review,* **112,** 1074-1082.

Holland, G. , Belanger, J. I. and Fritz, A., 2010, A Revised Model for Radial Profiles of Hurricane Winds.*Mon. Wea. Rev.*, **138**, 4393-4401

Knaff, J. and Zehr, R. M., 2007: Reexamination of Tropical Cyclone Wind-Pressure Relationships. *Wea. Forecasting,* **22,** 71-88.

Leslie, L. M., Hess, G. D., Holland, G. J., Morison, R. P., Fraedrich, K., 1992. Predicting changes in intensity of tropical cyclones using a Markov chain technique. *Aust. Met. Mag.* **40(1)**, 41-46.

Maragos, J.E., Baines, G.B.K., Beveridge, P.J., 1973. Tropical Cyclone Bebe Creates a New Land Formation on Funafuti Atoll. *Science,* **181(4105)**, 1161-1164.

Padya, B.M., 1975: Spatial variability and gustiness of cyclone winds: Gervaise, Mauritius, February, 1975. *Aust. Met. Mag.,* **23,** 61-69.

Piddington H., 1864, "The Sailor's Horn-Book for the Law of Storms"

(Pielke (1991)) -- (11.4 Beaufort Scale - this reference cannot be sourced)

Shewchuk, J. D., and R. C. Weir, 1980: An evaluation of the Dvorak technique for estimating TC intensities from satellite imagery. *JTWC Tech. Note 80-2*, JTWC, Pearl Harbor, HI, 16 pp

Simpson, R.H. (1974). The hurricane disaster potential scale. *Weatherwise,* **27**, 169-186.

Simpson, R.H. and H. Riehl (1981): The Hurricane and Its Impact. Louisiana State Univ. Press, Baton Rouge (IBSN 0-8071-0688-7), 398 pp.

Spillane K.T. and Dexter P.E. 1976: Design waves and wind in the Australian tropics. *Aust. Met. Mag.,***24,** 37-48.

Glossary

Adiabatic Process:

A process in which there is no diabatic heating and temperature changes arise solely from expansion and contraction.

Analogue:

A tropical cyclone from the climatological archive that has features similar to that of the cyclone under consideration.

Assimilation:

Any means of incorporating observations, or analyses into the prediction cycle of a numerical model.

Australian Tropical Cyclone Severity Scale:

Five categories indicating the damage potential of severe tropical cyclones.

Best Track:

A subjectively-smoothed representation of a tropical cyclone's location and intensity over its lifetime. The best track contains the cyclone's latitude, longitude, maximum sustained surface winds, and minimum sea-level pressure at 6-hourly intervals. Best track positions and intensities, which are based on a post-storm assessment of all available data, may differ from values contained in storm advisories. They also generally will not reflect the erratic motion implied by connecting individual center fix positions. (NHC Glossary)

Baroclinic:

Has vertical structure, in the form of variable density, temperature and winds. Baroclinic numerical models have a number of layers in the vertical in addition to a horizontal grid (Chapter 3, Section 3.3).

Barotropic:

Single level, with no vertical structure. Current numerical models tend to use either the barotropic vorticity equation (non-divergent models) or the shallow-water equations (free surface, allows divergence).

Basin:

Either an oceanic region with coherent features (eg, the north Indian Ocean Basin), or a set of bathymetric data for use in numerical models of storm surge.

Beaufort Number:

Categorization of wind speed based on visual state of the sea or land effects (see section 4 of this chapter).

Binary Tropical Cyclones:

Two tropical cyclones co-existing in sufficiently close proximity for each to effect the motion of the other (see also Fujiwhara effect).

Bogus Cyclone:

A preconstructed vortex inserted into analyses to provide a numerical model with a reasonable approximation of a tropical cyclone in data sparse areas.

Bogus Observation:

Any pseudo observation derived from indirect means, such as human interpretation, or empirical relationships with, for example, cloud fields. Used to provide additional information for analysis in data-void regions.

Boundary Conditions:

The means of specifying the forcing at boundaries of numerical models.

Central Dense Overcast:

The region of very high and cold cirrus cloud covering the core of a tropical cyclone (Dvorak, 1984).

Centre of a Tropical Cyclone:

Varies according to the analysis method; typically one of geometric centre of eye, minimum pressure, zero wind, or end of a spiral band.

Complex Extratropical Transition:

A tropical cyclone moves into high latitudes, merges with and intensifies a pre-existing baroclinic cyclone.

Compositing Forecast Technique:

A technique in which a tropical cyclone forecast track is constructed by averaging the tracks from different forecast models. The averaging scheme may treat each forecast model the same or may weight specific models according to their past performance under similar conditions.

Compound Extratropical Transition:

A tropical cyclone moves into high latitudes and induces a new development, such as waving on a frontal zone.

Cost-Loss:

An objective method of taking strike probability forecasts and calculating the ratio of expected cost of ameliorating action with the potential loss from taking no action; a ratio of less than one means that no ameliorating action should be taken on economical grounds alone.

Deep/Shallow Water:

Used in the context of gravity waves, water that is several wavelengths deep; thus greater than 100 m constitutes deep water for a ocean swell (wavelength tens of meters), but a storm surge (wavelength several tens of kilometres) is in shallow water anywhere on a continental shelf.

Diabatic Heating:

Externally imposed heating; for example solar radiation or latent heat release in a cloud.

Direct observation:

In situ measurements of meteorological elements at weather stations, from ships and aircraft, and with instrumented probes such as rawinsondes.

Doppler Effect:

Change in frequency of an electromagnetic or sound wave resulting from differential movement, for example, raindrops moving towards a Doppler radar will cause the reflected microwave beam to move towards higher frequency, enabling calculation of the raindrop speed.

Embedded Cloud Top:

Regions of very cold, overshooting cloud tops in a cirrus overcast.

Ensemble Forecasting:

Ensemble forecasting is a numerical prediction method that is used to generate a representative sample of the future states of a dynamical system, such as a tropical cyclone track. Ensemble forecasting is a form of Monte Carlo analysis, where multiple numerical predictions are conducted using slightly different initial conditions that are all plausible given the past and current set of observations, or measurements. Sometimes the ensemble of forecasts may use different forecast models or different formulations of a forecast model. (modified from *Wikipedia*)

Eulerian Coordinate System:

A coordinate system located on the earth surface.

Extratropical:

A term used in advisories and tropical summaries to indicate that a cyclone has lost its "tropical" characteristics. The term implies both poleward displacement of the cyclone and the conversion of the cyclone's primary energy source from the release of latent heat of condensation to baroclinic (the temperature contrast between warm and cold air masses) processes. It is important to note that cyclones can become extratropical and still retain winds of hurricane or tropical storm force. (NHC Glossary)

Extratropical Cyclone:

A synoptic scale low pressure system which derives its energy primarily from available potential energy in a pre-existing horizontal temperature gradient.

Eye:

The roughly circular area of comparatively light winds that encompasses the center of a severe tropical cyclone. The eye is either completely or partially surrounded by the eyewall cloud.

Eyewall / Wall Cloud:

An organized band or ring of cumulonimbus clouds that surround the eye, or light-wind center of a tropical cyclone. Eyewall and wall cloud are used synonymously. (NHC Glossary)

Fetch:

The area of sea, especially along the direction of the wind, over which winds are relatively constant and wave generation occurs.

Fujiwhara Effect:

Interaction of two binary cyclones in which both orbit cyclonically about their geometric centre; named after the pioneering laboratory experiments of Fujiwhara (1921).

Fully Developed Sea:

Sea in a quasi-steady state in which the energy gained by waves from the wind is approximately equal to that lost to wave breaking and other mechanisms.

Gravity Wave:

A perturbation along a vertical density discontinuity, or gradient, which has gravity as its restoring force; for example ocean waves, storm surges. In the atmosphere, gravity waves are generated whenever an imbalance between the mass and wind fields develops. This can be a major problem for the initial integration of numerical models.

Habitation Layer:

The thin layer of the atmospheric boundary layer in which humans live (Simpson and Riehl, 1981).

Hazard:

An event of occurrence that has the potential for causing injury to life or damage to property or the environment.

Hazard Risk Map:

Detailed demographic maps, including local community facilities, storm surge lines, etc, to provide a ready reference of people and facilities at risk when a tropical cyclone is threatening.

Hurricane / Typhoon:

A tropical cyclone in which the maximum sustained surface wind (using the U.S. 1-minute average) is 64 kt (74 mph or 119 km/hr) or more. The term hurricane is used for Northern Hemisphere tropical cyclones east of the International Dateline to the Greenwich Meridian. The term typhoon is used for Pacific tropical cyclones north of the Equator and west of the International Dateline. (NHC Glossary)

Indirect observation:

A remotely sensed but quantitative estimate of a meteorological element. The estimated variable is physically related to the observed quantity, though the estimate is often made by statistical means in practice. Examples are retrievals of temperature and

humidity from satellite sounders, estimates of winds made by tracking clouds in satellite imagery, and estimates of rainfall rates from radar or microwave radiometers.

Inferred estimate:

An estimate of a meteorological element based on remote observations of other quantities which are empirically related but not physically related in any direct sense. Tropical cyclone central pressure and wind speed estimated from satellite observed cloud top temperatures using the Dvorak method are examples of inferred estimates.

Intensity:

The maximum low-level sustained winds or the minimum sea level pressure of a tropical cyclone.

Inundation:

The flooding of normally dry land, primarily caused by severe weather events along the coasts, estuaries, and adjoining rivers. These storms, which include hurricanes and "winterstorms", bring strong winds and heavy rains. The winds drive large waves and storm surge on shore, and heavy rains raise rivers. (A tsunami - a giant wave caused by earthquakes or volcanic eruptions under the sea or landslides into the sea - is another kind of coastal inundation, but should not be confused with storm surge.) (NHC Glossary)

Inverted Barometer Effect:

The uplift of water in the centre of a tropical cyclone as a dynamic adjustment to the low air pressure there, roughly 1 cm sea level rise for every 1 hPa drop in sea level pressure, but substantial enhancement may occur from interactions with local bathymetry.

Isodrosotherm:

Line of constant specific humidity.

Lagrangian Coordinate System:

A coordinate system located on and moving with the feature of interest, for example centred on and moving with a tropical cyclone.

Landfall:

The intersection of the surface center of a tropical cyclone with a coastline. Because the strongest winds in a tropical cyclone are not located precisely at the center, it is possible for a cyclone's strongest winds to be experienced over land even if landfall does not

occur. Similarly, it is possible for a tropical cyclone to make landfall and have its strongest winds remain over the water. (NHC Glossary)

Leading Edge Band:

The first convective band on the front of a tropical cyclone.

Markov Chain:

Technique used to estimate the transition probabilities between various ranges or categories in a time series; for example the probability that a cyclone moving in the speed range 5-10 ms-1 will accelerate to 15-20 ms-1 in the next 12 hours (see Leslie et al., 1992).

Marsden Square:

Any region on earth with sides comprised of equal degrees of latitude and longitude.

Meander:

Quasi-oscillatory motion of a tropical cyclone centre about a longer-term mean track; see also trochoidal motion.

Mesoscale Convective System:

A small, long-lived cloud cluster, typically a few hundred kilometres in diameter.

Monte Carlo Method:

In the context of this volume, many forecasts made by a numerical model, each with a small change in the initial conditions; useful for indicating regions of rapid growth of errors in the initial conditions.

Multivariate Analysis:

Analysis utilising more than one variable in combination, for example maintaining the wind and pressure fields in balance.

Murphy's Law:

Anything that cannot possibly go wrong, will go wrong. There are two useful corollaries:
1. The chance of something going wrong is directly proportional to the amount of damage that will ensue;
2. Murphy was an optimist.

Outer Band Areas:

The edge of all outer convective cloud regions in a tropical cyclone.

Parameterisation:

A means of incorporating unresolved atmospheric features into numerical model forecasts. For example cumulus parameterisation incorporated the sub-grid forcing by convective clouds into a numerical model.

Partially Developed Sea:

Sea which has not reached a steady state for the imposed wind conditions and is still developing.

Poisson Distribution:

Used in the description of discrete cyclone occurrence in limited domains.

Potential Intensity:

The theoretical maximum possible intensity that can be sustained for the current environmental conditions; normally related to ocean temperature and tropopause height and temperature (Emanuel, 1986).

Radar:

Radio Direction And Ranging, a conical beam of pulsed electromagnetic energy in the microwave range transmitted outward from a rotating antenna. Backscattered energy from hydrometeors and other atmospheric scatterers, is collected by the same antenna and displayed either as a horizontal Plan Position Indicator (PPI) plot, or a vertical Range Height Indicator (RHI) slice. Some radar display systems also have the capacity to integrate volumetric data collected from several scans at different beam elevations. One such method is to display a Constant Altitude PPI (CAPPI).

Radius of Maximum Winds:

The radial distance from a cyclone centre to the mean position of the band of maximum winds.

Rankine Vortex:

A special type of vortex, which has zero vorticity outside the radius of maximum winds. Also called a potential vortex, or vortex patch. A modified Rankine vortex is sometimes used as an analytic approximation to tropical cyclones.

Repetitive Strain Injury:

Injury, generally sustained to wrists elbows and shoulders, arising from repetitive activities, such as keyboard operation.

Rapid Intensification:

An increase in the maximum sustained winds of a tropical cyclone of at least 30 kt in a 24-hour period. An earlier definition required a pressure fall of at least 42-hPa in a 24-hour period.

Relocated:

A term used in an advisory to indicate that a vector drawn from the preceding advisory position to the latest known position is not necessarily a reasonable representation of the cyclone's movement. (NHC Glossary)

Return Period:

The projected period of recurrence of a particular event, such as a tropical cyclone of a particular intensity, severe flooding, or a defined wind gust; derived using either empirical or Monte Carlo methods and assumed distributions of extreme events. Great care needs to be taken in interpretation this statistical result; in particular a return period of, say, 50 years does not mean that the next event will occur in 50 years, it could occur next year, albeit with a low probability.

Risk:

A probability that injury to life or damage to property and the environment will occur.

Rossby Number:

(also called Kibble Number in Russia); indicates the relative magnitude of centrifugal and Coriolis accelerations; an approximate breakdown of regimes is:

R_o<1 Geostrophic Flow,
R_o>1 Gradient Flow,
R_o>50 Cyclostrophic Flow.

Rossby Radius of Deformation:

The ratio of the speed of the relevant gravity wave mode and the local vorticity, or, equivalently, the ratios of the Brunt Vaisala and inertial frequencies. This scale indicates the amount of energy that goes into gravity waves compared to inertial acceleration of the wind. For a local length scale, L, and Rossby Radius, L_R:

Relative Magnitude	Response to a Mass Perturbation	Response to a Wind Acceleration
$L \ll L_R$	Mostly gravity waves	Mass adjusts largely to the winds.
$L \geq L_R$	Inertial accelerations become dominant	Mass adjusts only partially to wind acceleration
$L \gg L_R$	Almost no gravity waves	Inertial oscillations with no mass adjustment.

Saffir/Simpson Hurricane Scale (Simpson 1974):

A Scale that defines five categories for indicating the damage potential of tropical cyclones. The Scale originally included storm surge estimates, but these estimates were removed from the scale circa 2010.

Saffir/Simpson Tropical Cyclone Scale (Guard & Lander 1999):

A Scale adapted from the Saffir/Simpson Hurricane Scale that defines two tropical storm categories and five typhoon categories for indicating the wind and storm surge damage potential of tropical cyclones. The Scale considers tropical building materials and practices, tropical plants, the weakening effects of salt spray, termites and wood rot, and the damaging potential of sub-hurricane force winds.

σ-coordinate:

A special vertical coordinate, used in numerical models, which "smooths out" variable topography by using surface pressure as the baseline.

Size:

The extent of the tropical cyclone's circulation, typically given by the extent of gale force winds, or ROCI, although this is arbitrary.

Spectral Function:

A means of representing a variable field, such as horizontal winds or a time-series of temperatures, as a series of sine waves or polynomials. A spectral model (Chapter 3, Section 3) holds the required atmospheric variables in the form of spectral functions.

Spherics:

Shortened from atmospherics, the crackle heard on radio from lightning discharges in the atmosphere.

Statistical Interpolation:

A method of analysing random observations onto a regular grid, using their known errors and spatial correlation characteristics in a statistically optimal way.

Steering Current:

Imprecise term used to designate the flow in which a tropical cyclone is embedded.

Storm Surge:

An abnormal rise of sea water associated with a tropical cyclone. It is described as the still water elevation above the local astronomical tide, uncontaminated by high frequency, short gravity wind waves.

Storm Tide:

The total ocean elevation, including the astronomical tide, above or below a standard datum resulting from the passage of a tropical cyclone.

Strike Probability:

The probability that a particular region will be directly affected by a current tropical cyclone; currently calculated from climatological and persistence forecasts, though Monte Carlo forecasts with numerical models now provide an alternative approach (see Cost-Loss).

Subtropical Cyclone:

A non-frontal low-pressure system that has characteristics of both tropical and extratropical cyclones. Like tropical cyclones, they are non-frontal, synoptic-scale cyclones that originate over tropical or subtropical waters, and have a closed surface wind circulation about a well-defined center. In addition, they have organized moderate to deep convection, but lack a central dense overcast. Unlike tropical cyclones, subtropical cyclones derive a significant proportion of their energy from baroclinic sources, and are generally cold-core in the upper troposphere, often being associated with an upper-level low or trough. In comparison to tropical cyclones, these systems generally have a radius of maximum winds occurring relatively far from the center (usually greater than 60 nm), and generally have a less symmetric wind field and distribution of convection. (NHC Glossary)

Subtropical Storm:

A subtropical cyclone in which the maximum sustained surface wind speed (using the U.S. 1-minute average) is 34 kt (39 mph or 63 km/hr) or more. (NHC Glossary)

Trochoidal Motion:

Short-term, oscillatory motion of a cyclone centre, which can be approximated by the equations for trochoidal motion.

Tropical Cyclone:

A warm-core non-frontal synoptic-scale cyclone, originating over tropical or subtropical waters, with organized deep convection and a closed surface wind circulation about a well-defined center. Once formed, a tropical cyclone is maintained by the extraction of heat energy from the ocean at high temperature and heat export at the low temperatures of the upper troposphere. In this they differ from extratropical cyclones, which derive their energy from horizontal temperature contrasts in the atmosphere (baroclinic effects). (NHC Glossary)

A synoptic-scale to meso-scale low pressure system which derives its energy primarily from: 1. evaporation from the sea in the presence of high winds and low surface pressure; and 2. condensation in convective clouds concentrated near its centre.

Tropical Depression:

A tropical cyclone in which the maximum sustained surface wind speed (using the U.S. 1-minute average) is 33 kt (38 mph or 62 km/hr) or less. (NHC Glossary)

Tropical Disturbance:

A discrete tropical weather system of apparently organized convection -- generally 100 to 300 nm in diameter -- originating in the tropics or subtropics, having a nonfrontal migratory character, and maintaining its identity for 24 hours or more. It may or may not be associated with a detectable perturbation of the wind field. (NHC Glossary)

Tropical Storm:

A tropical cyclone in which the maximum sustained surface wind speed (using the U.S. 1-minute average) ranges from 34 kt (39 mph or 63 km/hr) to 63 kt (73 mph or 118 km/hr). (NHC Glossary)

Tropical Wave:

A trough or cyclonic curvature maximum in the trade-wind easterlies. The wave may reach maximum amplitude in the lower middle troposphere. (NHC Glossary)

Univariate Analysis:

Analysis of each variable, such as pressure or zonal wind component independently of all other variables.

Vulnerability:

A set of prevailing or consequential conditions composed of physical, geographic, demographic, socio-economic and/or political factors which increase a community's susceptibility to calamity, or which adversely affects its ability to respond to events.

Wall Cloud:

The region of deep cloud surrounding a mature cyclone eye.(Also see eyewall / wall cloud.)

Wave

Height: The vertical distance between a wave crest and trough;
Length: The horizontal distance between two wave crests;
Period: The time taken for two wave crests to pass a fixed point;
Set-Up: Water forced inshore by breaking waves;
Significant Wave Height/Period: The average height/period of the highest third of all waves in a sample of wind-waves;
Swell: Smooth, regularly spaced waves that have propagated long distances from their initial generation region;
Wind Waves: Choppy and chaotic waves generated locally by the wind.

Weibull Distribution:

Used in the estimation of extreme events, such as cyclone return periods.

Wind

Mean, Average or Sustained: Taken as the 10-min mean wind, except in the USA and North Atlantic, where 1-min means are used; conversion factor from 1 to 10-min mean is approximately 0.871;
Maximum Sustained: Highest mean wind in the tropical cyclone;
Gust: The highest wind burst, generally taken as the 1 s value.

Z-R Relationship:

Empirical relationship between the power of the reflected signal from a radar (Z), in units of dBZ, and rainfall at the ground (R); after Battan (1973); many relationships exist, depending on the degree of convection, presence of ice and assumed rain drop distribution.

Acknowledgements

The original basis for the Guide has been the materials prepared by participants in the first two International Workshops on Tropical Cyclones. A very substantial revision was made following the 6th and 7th International Workshops on Tropical Cyclones held in 2006 and 2010.

In addition to WMO resources, the United Nations Development Program, the US Office of Foreign Disaster Assistance, the Australian International Development Assistance Bureau and others provided support for these workshops. Each of the major contributors to the Guide was supported by their organisation. Additional support was provided by the US Office of Naval Research, the US National Science Foundation and by other organizations. Special recognition is also given to UCAR COMET for allowing the publication of several figures from COMET modules and to the Naval Research Laboratory in Monterrey, CA, for the use of archived microwave imagery for several TCs. The contributions from the many people who made inputs directly to the Guide or through the series and support provided by organizations and agencies are acknowledged with appreciation.

Particular thanks are due to Charles "Chip" Guard (USA), Chief Editor, for his leadership and scientific contributions, and the chapter authors for their time, dedication, and expertise.

Many others kindly provided their advice and assistance, including Jeff Hawkins, Jim Goerss, James Franklin, Jack Beven, Richard Pasch, Dan Brown, Eric Blake, Robbie Berg, John Cangialosi, Chris Landsea, David P. Roberts, Colin McAdie, Patrick Chan, Michael Ziobro, Philippe Caroff, Duong Lien Chau, Ed Fukada, Hilda Lam, Kiichi Sasaki, Alipate Waqaicelua, Gary Foley, and the late Mr. Robert Southern.

Technical assistance in updating the Global Guide was ably provided by Joan David, Fareez Ahmed, Libby Paynter, Thurai Sivasaththivel, David Scurrah, Mey Manickam, Alan Sharp, Anu Arora, Tong Yu Fai, and Andrew Ebert.

The Global Guide to Tropical Cyclone Forecasting website is sponsored by the World Meteorological Organization.